Évolution de la virulence et infections multiples

Mircea T Sofonea

THÈSE POUR OBTENIR LE GRADE DE DOCTEUR DE L'UNIVERSITÉ DE MONTPELLIER

En Évolution des Systèmes Infectieux

École doctorale GAIA

Unité de recherche MIVEGEC – CNRS, IRD, UM

Évolution de la virulence et infections multiples

Présentée par Mircea SOFONEA

Le 14 septembre 2017

Sous la direction de Yannis MICHALAKIS et Samuel ALIZON

Devant le jury composé de

Ophélie RONCE, DR, CNRS	Président du jury
Fabrice VAVRE, DR, CNRS	Examinateur
Elisabeta VERGU, CR, INRA	Examinateur
Samuel ALIZON, CR, CNRS	Co-directeur
Bernard CAZELLES, PR, UPMC	Rapporteur
Amaury LAMBERT, PR, UPMC	Rapporteur
Yannis MICHALAKIS, DR, CNRS	Directeur

UNIVERSITÉ DE MONTPELLIER

Évolution
de la virulence et infections multiples

Mircea T. Sofonea

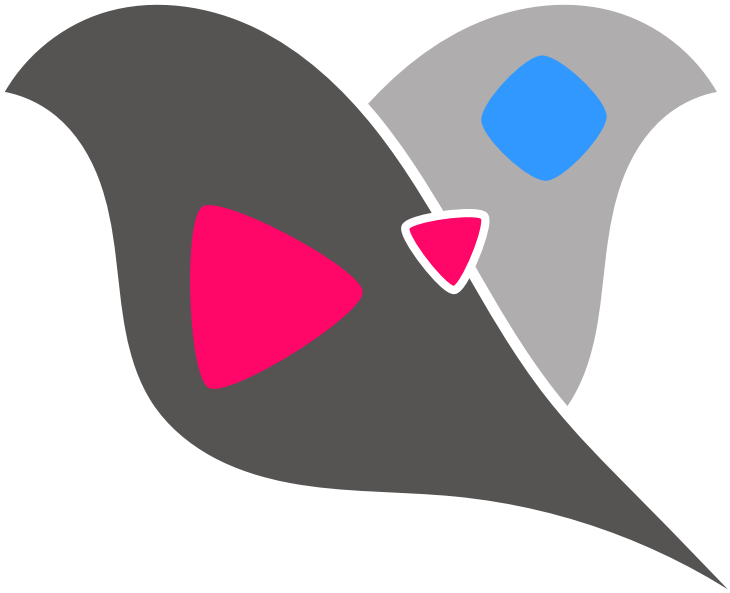

sous la direction de

Yannis Michalakis & Samuel Alizon

2017

Évolution de la virulence et infections multiples

par Mircea T. SOFONEA,
sous la direction de Yannis MICHALAKIS & Samuel ALIZON

thèse pour l'obtention du grade de Docteur
délivré par l'Université de Montpellier

champ disciplinaire : Évolution des systèmes infectieux

préparée au sein de l'unité mixte de recherche Maladies Infectieuses et Vecteurs - Écologie, Génétique, Évolution et Contrôle – Centre national de la recherche scientifique, Institut de Recherche pour le Développement, Université de Montpellier, école doctorale Biodiversité, Agriculture, Alimentation, Environnement, Terre, Eau,

soutenue publiquement le 14·IX·2017 à Montpellier,
devant le jury composé de :

· Amaury LAMBERT (UPMC) · Bernard CAZELLES (UPMC)	rapporteurs
· Elisabeta VERGU (INRA) · Ophélie RONCE (CNRS), président du jury · Fabrice VAVRE (CNRS)	examinateurs
· Yannis MICHALAKIS (CNRS) · Samuel ALIZON (CNRS)	directeurs de thèse

Contact :

MIVEGEC - SEE - ETE, Centre IRD de Montpellier France-Sud,
911 av. Agropolis, BP 64501, 34394 Montpellier Cedex 5, FRANCE

mircea.sofonea@normalesup.org

Évolution de la virulence et infections multiples

Mircea T. SOFONEA

Résumé

Au sein des populations naturelles d'êtres vivants circulent une diversité de parasites, qu'il s'agisse de plusieurs espèces, souches ou plus généralement types. Si certains modèles d'épidémiologie évolutive intègrent déjà le polymorphisme des parasites, rares sont ceux pour lesquels la dynamique épidémiologique dépend de la croissance intra-hôte et des interactions que les parasites entretiennent lorsqu'ils infectent le même hôte. Les complexité combinatoire et dynamique explique pourquoi il n'y a pour l'heure pas de prédiction générale de l'évolution de la virulence dans de tels contextes d'infections multiples. À la recherche d'une tendance générale d'évolution de la virulence, nous modélisons chaque niveau de dynamique sur lequel l'évolution des parasites repose. En particulier, nous étudions explicitement les interactions et l'issue de la compétition au sein des hôtes, les dynamiques épidémiologique et enfin adaptative. Sur l'exemple des infections chroniques causées par des micro-parasites transmis horizontalement, nous employons les approches propres aux systèmes dynamiques et aux probabilités pour emboîter cette suite de dynamiques afin d'en explorer les conséquences évolutives. Nous introduisons notamment le concept de patron d'infection, à savoir l'ensemble des issues intra-hôte associées à chaque configuration d'inoculation et décrivons cinq patrons jusqu'ici non décrits, lesquels échappent à la dichotomie classique entre super- et coinfection. Cette typologie nous permet par la suite d'envisager l'évolution de la virulence dans un cadre général. Nous observons en particulier une inéluctable mais bornée croissance évolutive de la virulence.

Champs : épidémiologie évolutive, biomathématiques, systèmes dynamiques, dynamique adaptative

Mots-clés : virulence, infections multiples, adaptation, polymorphisme, coinfection, superinfection, patron d'infection, interactions intra-hôte

Citation : SOFONEA, M. T. 2017, *Évolution de la virulence et infections multiples*, thèse de doctorat, Université de Montpellier (FRANCE).

Virulence evolution and multiple infections

Mircea T. SOFONEA

Abstract

Natural populations of living beings are exposed to a diversity of parasites, be they several species, strains or more generally types. While some evolutionary epidemiology models already incorporate parasite polymorphism, few make the connection between between-host dynamics and within-host parasite growth. As parasite polymorphism can even occur within the same host, distinct parasite types can interact in various ways and thus interfere with their transmission and therefore their evolution. The combinatorial and dynamical complexity explains why we still lack general predictions regarding the evolution of virulence in such multiple infection contexts. Seeking for a general trend in virulence evolution, we model each dynamical level on which parasite evolution relies. In particular, we explicitly investigate the within-host interactions and competition outcomes, the epidemiological and adaptive dynamics. Focusing on chronic infections caused by horizontally-transmitted microparasites, we apply both dynamical systems and probabilistic approaches to this nested sequence of dynamics to explore the evolutionary outcomes. We notably define the concept of infection pattern, that is the set of within-host outcomes of all inoculation challenges and identify five yet undescribed patterns that escape from the classical super/coinfection dichotomy. This typology then allows us to address virulence evolution under a general framework. We in particular observe an unavoidable but bounded evolutionary increase in virulence.

Subject areas : evolutionary epidemiology ; biomathematics ; dynamical systems ; adaptive dynamics

Keywords : virulence ; multiple infections ; adaptation ; polymorphism ; coinfection ; superinfection ; infection pattern ; within-host interactions

Citation : Sofonea M. T. 2017. Virulence evolution and multiple infections. *PhD thesis*, University of Montpellier (FRANCE).

Adevărul este o eroare exilată în eternitate.

La vérité est une erreur exilée dans l'éternité.

Emil CIORAN,
Amurgul gândurilor, 1940.

Remerciements

Ma profonde gratitude s'exprime en premier lieu auprès de Yannis et de Samuel dont l'implication a largement dépassé le simple encadrement de cette thèse. D'une indéfectible bienveillance mâtinée de sage exigence, Yannis et Samuel m'ont accordé leur confiance dès nos premiers échanges – il y a de cela six années, alors désorienté à la fin de ma licence. Ils m'ont appris, guidé et poussé scientifiquement, soutenu et inspiré humainement (y compris sur les plans éthique et politique), en permanence avec justesse et raison – et très souvent avec humour. Je les remercie de m'avoir confié le projet à l'origine de cette thèse, un défi de longue haleine aux allures de poupées russes, en m'autorisant une liberté considérable dont j'apprécie aujourd'hui la chance et le bénéfice pour la recherche et la vie à venir.

Je mesure l'immense honneur que me font Amaury LAMBERT et Bernard CAZELLES – loin d'être étrangers à ma passion pour les biomathématiques, j'aimerais qu'ils sachent ici à quel point je la leur dois –, en acceptant de rapporter cette thèse, ainsi qu'Elisabeta VERGU, Ophélie RONCE et Fabrice VAVRE, en acceptant de l'examiner. Je les remercie ici chaleureusement de porter leur regard d'expert sur ce travail.

Enfin, je suis très reconnaissant envers ceux qui ont constitué mon comité de thèse : François ROUSSET, Gaël THÉBAUD et Sébastien LION, dont l'opinion et les conseils avisés ont permis de cadrer mon travail et su me redonner confiance lors des inévitables périodes maigres en résultats.

Le présent document aurait été bien mince et confus s'il n'avait connu de nombreuses suggestions, commentaires ou relectures extérieures. Les salutaires contributions aux différents chapitres sont détaillés ci-après :

$\boldsymbol{i}$: Samuel, Yannis et Sébastien – **0** : Virginie RAVIGNÉ, François BLANQUART et Hans METZ – $\boldsymbol{\iota}$: Samuel, Yannis – **1** : Yannis, Samuel, Yves DUMONT et Alain RAPAPORT – **2** : Andrea GRAHAM et deux relecteurs anonymes – **3** : Gaël, Rémy FROISSART, Stéphane BLANC, Yves DUMONT, Matthieu HILLAIRET, Alain RAPAPORT, Nicole MIDEO, Ben ALTHOUSE et un relecteur anonyme – **4** : Sébastien, Eva KISDI, Yves DUMONT, Alain RAPAPORT et Hans METZ – $\boldsymbol{\delta}$: Yannis, Samuel et Gaël – **D** : Yannis, Samuel et Sébastien.

En outre, je n'oublie pas ceux auprès de qui j'ai pu aborder des approches alternatives non présentées ici : Lorenzo PELLIS, Meir SHILLOR, Jacques GAUTRAIS, Stéphane BLANCO, Richard FOURNIER, Ovidiu RADULESCU.

Je tiens à remercier tous les collègues (et ex-collègues) de recherche pour nos innombrables et inénarrables échanges passionnés autour du déjeuner ou d'un café, et en particulier Eva et Emma, mes demi-sœurs de thèse et de labeur, Rémy (avec qui refaire le monde est un plaisir renouvelé), Nacho (l'incollable *xiquet*), Carmen-Lia, Phil, Matthew (*whose problem of the week is missed*), Eugene, Tsukuchi, Lafi et Luis (qui ont, malheureusement dû essuyer les plâtres de mon rôle d'encadrant), sans oublier les autres membres du MIVEGEC (théoricien ne veut pas dire ermite) dont Taissa, Daniel, Romain, Manon, Marlène, Jessie, Fréd T., Valérie, Mallorie, Franck, Virginie, Jean-François (dont les interventions parisiennes ont été fructueuses), Fréd S.

J'éprouve une vive reconnaissance pour ceux qui ont osé me confier des interventions, leurs cours, voire de me laisser concevoir des épreuves, bref, ceux qui m'ont tendu la main pour mes premiers pas d'enseignant : Sylvain, Thomas, Sylvie, Sandrine, Fleurice, Karen, Christine, Céline, Benjamin, Benoît, Pascale, Daniel. De l'Université, de je n'oublierai pas la générosité de Colin, Olivier, Nicolas, Catherine, Georges.

Bien entendu, je remercie tous ceux qui se reconnaîtront parmi mes amis, les parisiens et les roussillonais – de naissance ou d'adoption –, qu'ils sachent que nos retrouvailles me sont chères ; je remercie affectueusement mes proches, ma famille *l.s.* qui s'est montrée si attentive et encourageante.

Je pense enfin à ceux qui auraient aimé me voir soutenir cette thèse ; je pense à mes parents, pour lesquels ma reconnaissance est indicible ; je pense aux deux personnes qui donnent à chaque aube leur sourire.

À Milan et Marina,
et leur contagieuse joie de vivre

Avant-propos

Ce document présente ma production scientifique réalisée entre septembre 2013 et juin 2017 au sein de l'unité mixte de recherche (UMR 5290) *Maladies Infectieuses et Vecteurs - Écologie, Génétique, Évolution et Contrôle* (MIVEGEC, directeurs : Didier FONTENILLE puis Frédéric SIMARD) – affiliée au Centre national de la recherche scientifique (CNRS), à l'Institut de recherche pour le développement (IRD) et à l'Université de Montpellier (UM) –, dans l'équipe *Santé, Écologie, Évolution* (SEE, responsable : François RENAUD), entité scientifique fonctionnelle *Évolution Théorique et Expérimentale* (ETE, coordonateur : Samuel ALIZON), sous la direction de Yannis MICHALAKIS et de Samuel ALIZON. Ce travail a été financé par les émoluments de la scolarité normalienne puis par une allocation spécifique de l'École normale supérieure (ENS, Paris), avec l'appui logistique du CNRS, de l'IRD et de l'UM.

Cette thèse sur articles est composée de neufs chapitres groupés en trois parties à la méthodologie progressive et emboîtée. Les chapitres 0, 1, 2, 3, 4 et δ correspondent à des articles de recherches indépendants ayant pour vocation d'être publiés dans des revues scientifiques internationales à comité de lecture, d'où leur rédaction en langue anglaise (seuls les résumés sont traduits en français). Deux de ces articles sont d'ores et déjà parus – les chapitres 2 et 3 correspondent respectivement aux références SOFONEA *et al.* (2017b) et SOFONEA *et al.* (2015) – et sont ici reproduits à l'identique de leur version acceptée pour publication, ce qui explique les légères différences de terminologie et de notations avec le reste du document. Le chapitre 0, au rôle introductif, est quant à lui prépublié SOFONEA *et al.* (2017a) et recommandé (voir RAVIGNÉ & BLANQUART (2017)). Au contraire, les chapitres introductifs i et ι, ainsi que le chapitre conclusif et les transitions entre chapitres (*i.e.* les sections de prologues et d'épilogues, respectivement désignées par α et ω) sont rédigés en français, conformément aux attendus et à la portée vernaculaire de ce document.

L'essentiel du travail présenté ici résidant davantage dans les détails de modélisation et les preuves que dans les interprétations biologiques elles-mêmes, il est apparu raisonnable d'adosser les annexes des articles de recherches à la suite de chaque texte principal (sections désignées par des lettres latines) afin de préserver l'unité de la démarche plutôt que compiler l'ensemble du matériel additionnel, et ce, malgré la redondance évidente de certains calculs (que le lecteur ennuyé ou pressé pourra esquiver sans craindre de passer à côté d'une subtilité cruciale).

Le texte a été composé en LaTeXet en LyX, les calculs et simulations ont été exécutés sous Mathematica (WOLFRAM RESEARCH INC., 2014) et R (R CORE TEAM, 2013) – les scripts étant disponibles sur demande. L'ensemble des figures sont originales et réalisées avec Inkscape.

De quoi les biomathématiques sont-elles le nom ? On dira, bien sûr, qu'elles sont trop abstraites pour être de la biologie et à la fois trop concrètes pour être des mathématiques. Mon opinion toute objective est que ces deux disciplines jalousent les biomathématiques pour leur généralité -- la généralité des cas des systèmes étudiés d'un côté, et la généralité des approches employées de l'autre... Amateurs du moyen ou amateurs de la fin, réjouissons-nous ensemble que l'Évolution des entités biologiques nous posent des questions aussi disposées à être énoncées dans la langue de la Nature.

Table des matières

Notations

symbole	signification	remarque
	relations et opérateurs logiques	
$:$	tel que	
$:=$	égalité par définition (du membre de gauche)	introduit/rappelle une notation
$\triangleq$	égalité par compréhension	emploie une propriété
$\equiv$	équivalence entre objets	
$\Leftrightarrow$	équivalence entre propositions	*i.e.*, ssi ou *iff* dans le texte
$\top$	tautologie	
$\bot$	antilogie	
$\neg$	négation	
$\wedge$	conjonction logique	« et »
$\vee$	disjonction logique	« ou » inclusif
	ensembles	
$\varnothing$	ensemble vide	
$\cap$	intersection	
$\cup$	union	
$\setminus$	différence ensembliste	
$\mathcal{A}^{\complement}$	complémentaire de l'ensemble $\mathcal{A}$	
$\subset$	inclusion	
$\subsetneq$	inclusion stricte	
$\wp(\mathcal{A})$	ensemble des parties (sous-ensembles) de $\mathcal{A}$	
$\times$	produit cartésien	
$\mathrm{Card}\mathcal{A}$ $\lvert\mathcal{A}\rvert$	cardinal de $\mathcal{A}$	
$\mathbb{N}$	ensemble des entiers naturels	
$\aleph_0$	cardinal de tout ensemble infini dénombrable	$(\aleph_0 := \mathrm{Card}\mathbb{N})$
$\mathbb{R}$	ensemble des nombre réels	
$\overline{\mathbb{R}}$	droite réelle achevée	$(\overline{\mathbb{R}} := \mathbb{R} \cup \{-\infty\} \cup \{\infty\})$
$\mathbb{R}_+$	ensemble des nombres réels positifs	
$\mathbb{C}$	ensemble des nombres complexes	
$\mathbb{K}^\star$	ensemble privé de 0 (si $\mathbb{K} \equiv \mathbb{N}$ ou $\mathbb{R}$) ou de $\{\varnothing\}$ (si $\mathbb{K}$ une famille de parties)	
$[a;b[$ $[a,b)$	intervalle fermé à gauche et ouvert à droite	$((a,b) \in \overline{\mathbb{R}}^2, a \leq b)$
$[\![a;b]\!]$ $\{a,\ldots,b\}$	ensemble des nombre entiers entre a et b	$((a,b) \in \mathbb{N}^2, a \leq b)$

symbole	signification	remarque
	objets mathématiques	
a	scalaire constant	
A	scalaire variable du temps ou variable/évènement aléatoire	
$\mathbf{a}$ $\begin{bmatrix} a_1 & \cdots & a_n \end{bmatrix}$ $(a_1,\ldots,a_n)$	vecteur	
$\boldsymbol{a}$	partie finie de $\mathbb{N}$	
$\mathcal{A}$	ensemble	
$\mathbf{A}$ $\begin{bmatrix} a_{1,1} & \cdots & a_{1,p} \\ \vdots & \ddots & \vdots \\ a_{n,1} & \cdots & a_{n,p} \end{bmatrix}$	matrice	
	algèbre	
$\mathfrak{M}_{n,p}(\mathbb{K})$	ensemble des matrices $n \times p$ à coefficients dans $\mathbb{K}$	
$\mathbf{A}^{\mathrm{T}}$, $\mathbf{A}^{\mathbf{T}}$	matrice transposée	(s'applique aussi aux vecteurs)
$\mathbf{A} \prec a$	relation d'ordre $<$ vis-à-vis de a pour tous les coefficients de $\mathbf{A}$	(*id.* $\preceq$ pour $\leq$, s'applique aussi aux vecteurs)
det$\mathbf{A}$	déterminant d'une matrice carrée $\mathbf{A}$	(parfois noté $\lvert\mathbf{A}\rvert$)
tr$\mathbf{A}$	trace d'une matrice carrée $\mathbf{A}$	
.	produit matriciel usuel	
$\odot$	produit d'HADAMARD	(coefficient par coefficient)
$\otimes$	produit de KRONECKER	(coefficient par matrice)
diag$\mathbf{A}$	vecteur des coefficients diagonaux de $\mathbf{A}$	
diag$\mathbf{a}$	matrice diagonale à coefficients diagonaux $\mathbf{a}$	
$\mathbf{0}_n$	vecteur de n coefficients égaux à 0	(*id.* $\mathbf{1}_n$ pour 1)
$\mathbf{0}_{n,p}$	matrice $n \times p$ de coefficients égaux à 0	(*id.* $\mathbf{1}_{n,p}$ pour 1)
$\mathbf{I}_n$	matrice identité $n \times n$	
$\mathbf{e}_i^{(d)}$	i-ème vecteur de la base canonique de $\mathbb{R}^d$	
Sp$\mathbf{A}$	spectre (ensemble des valeurs propres) d'une matrice carrée $\mathbf{A}$	

symbole	signification	remarque
	analyse	
$\log$	logarithme népérien	(ln en français)
$\log_{10}$	logarithme décimal	
sgn	fonction signe	
$\lvert a \rvert$	valeur absolue ($a \in \mathbb{R}$) ou module ($a \in \mathbb{C}$)	
$\mathrm{Re}(a)$ $\Re a$	partie réelle de a	
$\lVert \mathbf{a} \rVert$	norme euclidienne du vecteur $\mathbf{a}$	
$\mathcal{F}(\mathcal{X}, \mathcal{Y})$	ensemble des fonctions de $\mathcal{X}$ dans $\mathcal{Y}$	
$\mathcal{A}(\mathcal{X}, \mathcal{Y})$	ensemble des applications de $\mathcal{X}$ dans $\mathcal{Y}$	
$\mathscr{C}^k(\mathcal{X}, \mathcal{Y})$	ensemble des fonctions C^k de $\mathcal{X}$ dans $\mathcal{Y}$	
$\frac{\mathrm{d}\cdot}{\mathrm{d}t}$ $\dot{\cdot}$	dérivée temporelle	
$\partial_i F$	dérivée partielle par rapport à l'i-ème argument de F	
$\frac{\partial \mathbf{a}}{\partial \mathbf{b}}$	matrice des dérivées $\left(\frac{\partial a_i}{\partial b_j}\right)_{i,j}$	
$o(x)$	fonction négligeable devant x pour $x \to 0$ $(f(x) = o(x) \iff \frac{f(x)}{x} \underset{x \to 0}{\longrightarrow} 0)$	
$\underset{x \to a}{\sim}$	équivalence de fonctions dans un voisinage pointé de $a \in \overline{\mathbb{R}}$ $(f(x) \underset{x \to a}{\sim} g(x) \iff \frac{f(x)}{g(x)} \underset{x \to a}{\longrightarrow} 1)$	
$\hat{\cdot}$ $\tilde{\cdot}$	scalaire ou vecteur relatif à un point fixe (solution stationnaire)	

symbole	signification	remarque
	arithmétique, dénombrement et fonctions binaires	
$\propto$	relation de proportionnalité	
$\mathrm{mod}_m a$	reste de la division euclidienne de a par m	
$\lfloor a \rfloor$	partie entière (par défaut) de a	
$a!$	factorielle de l'entier a	
$\binom{a}{b}$	coefficient binomial	($\binom{a}{b} \coloneqq \frac{a!}{(a-b)!b!}, (a,b) \in \mathbb{N}^2, a \geq b$)
$\mathbb{I}_{\{A\}}$ $[A]$	fonction indicatrice de A	(égale 1 si A est satisfait, 0 sinon)
$\delta_{i,j}$	delta de KRONECKER	($\delta_{i,j} = [i = j]$)
	probabilités et statistiques	
$\mathbb{P}[A]$	probabilité de l'événement A	
$\mathbb{P}[A\|B]$	probabilité conditionnelle de l'événement A sachant l'événement B	
$\mathcal{N}$	loi normale	
iid	indépendantes et identiquement distribuées	
$a_\bullet$	sommation sur un indice	
$\overline{a}$	moyenne arithmétique	
var	variance statistique	
cov	covariance statistique	
	biologie	
$a \ll b$	négligeabilité de a devant b	($a \leq b/10$)
$a \approx b$	approximation de a par b	($\lvert b-a \rvert \ll \lvert a \rvert$)
$\cdot_0, \dot{\cdot}, \mathring{\cdot}$	relatif à un état sans infection	
$\cdot^\star$	relatif à une stabilité évolutive	
$\mathcal{R}$	nombre de reproduction	
β	relatif à la transmission	
μ	relatif à la mortalité (naturelle)	
θ	relatif à la guérison	
α	relatif à la virulence	

I

Des questions et des outils

i Du parasitisme

i.1. Tétralogie parasitaire

Dans la Grèce antique, l'adjectif παράσιτος, littéralement « qui mange auprès de », désignait entre autres les citoyens déjeunant au Prytanée, *i.e.* au siège – donc aux frais – de la cité (Bailly, 1895). De nos jours, la biologie qualifie de **parasite** une entité biologique [*] qui vit et se reproduit aux dépens d'une autre [†], l'**hôte**, au sens où il l'exploite comme ressource de son vivant (Combes, 2010).

Dans son acception la plus générale, le parasitisme est devenu au cours des dernières décennies, un remarquable objet d'études multidisciplinaires, dont les quatre principaux prismes sont exposés ci-après.

i.1.1. Écologie

Qu'il soit facultatif – tel celui des rhinanthes (*Rhinanthus sp.,* angiospermes de la famille des *Orobanchaceae*), des armillaires (*Armillaria sp.*, champignons basidiomycètes), du percolozoaire *Naegleria fowleri* – ou obligatoire – comme celui des sacculines (*Sacculina sp.*, crustacés cirripèdes), du tréponème pâle (*Treponema pallidum*, bactérie spirochète), du virus bactériophage λ (*Siphoviridae*) –, le parasitisme est représenté au sein de tous les grands groupes du monde vivant (bactéries, archées [‡], métazoaires, végétaux, champignons et autres eucaryotes unicellulaires [§] (De Meeûs & Renaud, 2002)), ainsi que par l'intégralité du monde viral. En outre, aucun grand groupe d'entités biologiques n'est épargné par le parasitisme, virus compris (La Scola *et al.*, 2008).

Comme il est vraisemblable que chaque espèce libre (*i.e.* non parasite) héberge en

*. Nous préférons ici ce terme à celui d'être vivant car il nous permet d'inclure les virus, dont les formes extra-cellulaires sont dépourvues de métabolisme et ne peuvent, à ce titre, répondre à la définition du vivant largement acceptée (*i.e.* confinement, auto-maintien et auto-réplication (Thomas *et al.*, 2016)).

†. À ce titre, nous distinguerons l'**inoculation**, qui est la mise en contact ou l'introduction du parasite dans l'hôte, de l'**infection**, qui correspond à l'établissement et à la reproduction du parasite au sein de l'hôte (Willey, 2008).

‡. *Nanoarchaeum equitans* (Huber *et al.*, 2002) étant toutefois, à ce jour, l'unique espèce parasite recensée dans cet empire (Abedon, 2013).

§. Noter ici que la définition écologique des parasites est plus large que la définition médicale qui comprend les seuls eucaryotes.

moyenne une espèce parasitaire qui lui est propre, et qu'*a fortiori* certains parasites sont eux-mêmes parasités (les parasites dont les hôtes sont eux-mêmes des parasites sont appelés hyperparasites, *e.g.* les bactéries du genre *Borrelia* véhiculés par les tiques), on dénombre en réalité plus d'espèces parasites que d'espèces libres (Price, 1980; Windsor, 1998). S'il est évident que cela se vérifie aussi en termes de nombre d'individus, il est moins trivial de réaliser que les parasites peuvent concentrer autant de biomasse que les prédateurs de sommet (Kuris *et al.*, 2008). Son impact sur les écosystèmes (Thomas *et al.*, 2005), de l'extinction (Kilpatrick *et al.*, 2010) à la coexistence d'espèces d'hôtes (Schall, 1992), sous-tendus par les mécanismes de la relation inter-spécifique entre un parasite et son hôte (Thomas *et al.*, 2000), fait du parasitisme une interaction centrale de la recherche en écologie (Begon *et al.*, 2005).

i.1.2. Physiopathologie

Du point de vue de l'hôte exploité, l'interaction parasitaire représente nécessairement un coût qui s'exprime comme une réduction de la durée de vie et/ou une réduction de la reproduction, voire s'accompagne d'autres formes de morbidité. L'interaction peut ainsi se voir sous le prisme physiopathologique et porter le nom de **maladie**[*]. L'infection, lorsqu'elle ne devient pas chronique (Virgin *et al.*, 2009), se solde soit par la guérison de l'hôte (lequel survit à l'exploitation du parasite, éliminé, au prix d'éventuelles séquelles) soit par sa mort, potentiellement plus précoce.

L'Homme a identifié relativement tôt dans son histoire le risque que certains parasites font peser sur sa santé, à commencer par les plus visibles d'entre eux, les helminthes. Daté du XVI^{ème} siècle AEC , le papyrus Ebers est à ce jour la plus ancienne mention du parasitisme (Bryan, 1930; Miller, 1989), par la description de la méthode d'extraction, encore pratiquée de nos jours, du ver de Guinée (le nématode *Dracunculus medinensis*). À noter que ce parasite est l'une des toutes premières espèces nommées et classées par Linné (1735). Mais il faudra attendre le développement de la microscopie et l'avènement de la théorie des germes (Pasteur et Koch) au XIX^{ème} pour identifier l'étiologie microbienne des principales maladies humaines dites infectieuses (Lederberg, 2000; Cox, 2002). Nous savons à présent que l'Homme est susceptible d'être infecté par 1400 espèces d'« agents pathogènes » (Taylor *et al.*, 2001), responsables de maladies dont certaines peuvent être prévenues (prophylaxie, dont vaccination), diagnostiquées, atténuées voire guéries par la médecine moderne (Bennett *et al.*, 2014), s'appuyant principalement sur les récentes découvertes en immunologie (Owen *et al.*, 2013).

i.1.3. Épidémiologie

Un hôte infecté peut transmettre ses parasites à plusieurs autres hôtes qui ne le sont pas encore. De l'état dit susceptible, ces hôtes deviennent infectés et peuvent à leur tour transmettre la descendance parasitaire à d'autres hôtes et ainsi de suite. Il en résulte que la proportion d'hôtes infectés dans la population, ou prévalence, augmente : c'est l'**épidémie**. Du grec ancien ἐπιδήμιος, littéralement « qui est de passage dans un pays », ce terme déjà employé dans le sens de diffusion d'une maladie par Hipprocrate (Littré, 1839) à la fin du V^{ème} siècle AEC. L'épidémie retombe généralement sous l'effet d'une rétro-action épidémiologique induite par la faible proportion d'hôtes susceptibles restants.

*. À noter que le point de vue clinique du parasitisme présente d'intéressants prolongements philosophes au premier rang desquels figurent le concept de normalité (Canguilhem, 1966) et celui du soi (Pradeu & Carosella, 2006).

Sous certaines conditions, le parasite peut néanmoins continuer à circuler dans la population d'hôtes et ainsi se maintenir : c'est l'**endémie**, d'ἔνδημος, littéralement « qui reste dans son pays ». Déterminer si l'introduction d'un hôte infecté (le cas index) dans une population (dite naïve) composée d'individus tous susceptibles sera à l'origine d'une épidémie, prédire l'éventuelle persistance de la maladie et envisager des stratégies de contrôle caractérise le volet épidémiologique (May & Anderson, 1979).

i.1.4. Évolution

Il ne faut attendre que le cinquième paragraphe de l'ouvrage fondateur de la théorie unificatrice de la biologie moderne, l'Origine des Espèces (Darwin, 1859), pour y lire le terme de parasite. S'appuyant sur l'exemple du gui (*Viscum album*, *Santalaceae*), Darwin s'interroge ainsi sur les processus naturels ayant conduit à l'adéquation apparente entre le cycle de vie particulier et la morpho-anatomie de cette angiosperme. Mais c'est au sujet de l'isopode *Proteolepas binvicta* que Darwin, se demandant pourquoi le plan d'organisation adulte de ce parasite de cirripèdes est si réduit par comparaison aux autres crustacés, écrit que « *l'économie d'une conformation complexe et développée, devenue superflue, constitue un grand avantage pour chaque individu de l'espèce ; car, dans la lutte pour l'existence, à laquelle tout animal est exposé, chaque* Proteolepas *a une meilleure chance de vivre, puisqu'il gaspille moins d'aliments* ». Cette explication, qui rappelle naturellement la perte des organes inutilisés de Larmack (1809), constitue probablement l'un des premiers **scénarios adaptatifs** relatifs aux parasites.

La biologie de l'évolution, tout en gagnant en rigueur au moyen des bases théoriques portées par la génétique des populations (Fisher, 1930), n'a dès lors cessé de poser des questions au sujet des parasites – de l'organisation de leur génome (Sicard *et al.*, 2016), à leur dispersion (McCoy *et al.*, 1999), en passant par leur rôle dans l'émergence de la sexualité (Frada *et al.*, 2008), sans oublier leur virulence (Méthot, 2012), sujet central du présent travail – et tenter d'y apporter des réponses d'ordre évolutif (Schmid Hempel, 2011), composant ainsi le quatrième et dernier point de vue sur la biologie parasitaire.

Dans la suite, la biologie parasitaire sera exclusivement abordée sous les prismes épidémiologique et évolutif. Les pages à venir tenteront de faire converger ces points de vue au sujet des parasites dont l'évolution est la plus sensible, les **micro-parasites** (*i.e.* tous les parasites à l'exception des végétaux et animaux), et en particulier ceux à transmission directe (*i.e.* infectant une unique espèce d'hôte et ne possédant pas de stade de vie libre)[*].

*. Cette limitation fréquente (Keeling & Rohani, 2008) exclut notamment, pour ce qui est des parasitoses humaines, les helminthiases et les maladies dites à vecteur (p.ex. le paludisme ou la dengue), mais inclut la majorité des cas de maladies infectieuses humaines (Lozano *et al.*, 2013; WHO, 2016d) et l'essentiel des parasites en général (Suttle, 2007).

i.2. Maladies infectieuses et temps court

i.2.1. Risque infectieux

Bien que la diversité des hôtes parasités reflète celle de l'ensemble du vivant, c'est évidemment lorsqu'il affecte l'Homme que le parasitisme, qui prend alors le nom de maladies infectieuses, est le plus étudié et documenté (et s'ensuivent les animaux domestiques et les plantes cultivées)[*]. De par leur cause insaisissable, leur issue – à l'échelle individuelle – imprévisible et potentiellement fatale, et leur diffusion – à l'échelle collective – parfois foudroyante et massive, les maladies infectieuses ont longtemps constitué une crainte majeure pour l'Homme (Kiple, 1993). Certaines épidémies, aussi meurtrières sinon plus que les deux guerres mondiales, sont devenues des événements historiques à part entière : l'épidémie de peste (bactérie *Yersinia pestis*), entre 1346 et 1353, et l'épidémie de grippe A (virus H1N1), entre 1918 et 1919, décimèrent chacune environ 50 millions de personnes (Hays, 2005).

Le développement qu'a connu la médecine au cours de la dernière centaine d'années, de l'étiologie (identification microbiologique) à la thérapeutique (antiobiotiques) et la santé publique (mesures hygiénistes, vaccination), a laissé penser que l'Homme allait finir par s'affranchir du risque infectieux (Spellberg & Taylor-Blake, 2013). S'il est vrai qu'au cours du XX$^{\text{ème}}$ siècle, le poids relatif des maladies infectieuses dans la mortalité globale a baissé (Jones *et al.*, 2012), que l'espérance de vie a presque doublé, que certains pathogènes ont été quasiment (virus de la poliomyélite (WHO, 2016c)) ou définitivement éradiqués (virus de la variole (Breman & Arita, 1980)), les maladies infectieuses ont entraîné en 2010 la mort de 13 millions de personnes[†] dans le monde et représenté près de 60 % de la mortalité totale des pays les plus déshérités (Dye, 2014). La persistance des pandémies de SIDA, tuberculose et paludisme (près de 4 millions de décès en 2010 (Lozano *et al.*, 2013)) d'un côté, l'émergence de nouvelles maladies infectieuses (SRAS (2005), Ebola (2014), Zika (2016)), l'expansion de souches bactériennes résistantes (au premier rang desquelles les staphylocoques dorés résistants à la méthicilline) couplée à un manque de nouvelles molécules antibiotiques de l'autre (Jones *et al.*, 2008; Silver, 2011), montrent que les maladies infectieuses demeurent un enjeu humanitaire de premier plan et justifient que leur étude dépasse le seul champ médical. Par la suite, nous nous focalisons sur l'approche mathématique de l'épidémiologie et discutons plus généralement de la démarche de modélisation dans l'encadré **[a]** (p.29).

∗. Ceci explique l'anthropocentrisme malheureux des exemples, données et motivations de modèles présentés dans ce travail, sans que cela ne dénote une restriction du parasitisme étudié aux seules infections humaines et nous en profitons pour rappeler ici la riche littérature de parasitologie végétale (van der Plank, 1963; Hull, 2013) et vétérinaire (Timoney *et al.*, 1988), ainsi que deux exemples d'actualité en région Occitanie, respectivement le chancre coloré (l'ascomycète *Ceratocystis platani*) décimant les populations de platanes (*Platanus* ×*hispanica*) (Tsopelas *et al.*, 2017) et le virus de la grippe aviaire H5N8, les élevages de volailles (Lycett *et al.*, 2016).

†. En réalité, ce chiffre prend aussi en compte la mortalité due à des causes maternelles, périnatales ou nutritionnelles, qui ne sont en général pas distinguées dans les données de l'OMS pour des raisons pratiques de collecte dans certains pays , mais en excluant les cancers secondaires à une infection (*e.g.* cancers cervicaux ou hépatiques) (WHO, 2015; Lozano *et al.*, 2013).

[a] de la modélisation

Un modèle est une représentation d'un phénomène réel qui le rend compréhensible au point de pouvoir en prédire les variations. On peut distinguer trois groupes épistémologiques de modèles, par degré croissant de compréhension : heuristique (une réponse qui convient), phénoménologique (qui reproduit les patrons), mécanistique (qui explique les processus à partir d'un niveau d'organisation inférieur) (Haefner, 2012). Il en résulte un cadre de travail plus ou moins fourni comprenant un formalisme et des **hypothèses constitutives** (supposées vraies, dans le sens anglais d'*assumption*) qui lui sont propres et qui permet de tester certaines **conjectures** (à confirmer ou infirmer, au sens anglais d'*hypothesis*).

La démarche de modélisation procède d'un triple objectif (Keeling & Rohani, 2008). Le premier est de rendre compte formellement de l'ensemble du système étudié afin de pouvoir prédire au moins qualitativement l'état du système au bout d'un temps donné partant d'un état donné, c'est le **réalisme**.
Les niveaux d'organisation caractérisant les systèmes biologiques sont cependant difficilement réductibles, de par leur intrication et leur complexité, tant dynamique (non-linéarité) que combinatoire (grand nombre d'entités en interactions). Une modélisation de ces systèmes qui ne serait guidée que par le seul réalisme est donc une entreprise prétentieuse et essentiellement vaine à l'heure actuelle, tant notre connaissance fine et exhaustive des processus aussi bien endogènes qu'exogènes au système est parcellaire (May, 2004). De plus, rien ne garantit que nous soyons en mesure de comprendre un modèle formalisant un système biologique dans ses moindres détails. Ainsi, l'excès de réalisme s'oppose au second objectif, l'**intelligibilité** : un modèle doit pouvoir être compris au point de saisir l'influence sur sa dynamique de chacune de ses composantes et les interdépendances qu'elles entretiennent (ce qui, dans le cas des phénomènes non-linéaires, est loin d'être trivial et porte parfois le nom de rétro-actions (Heino *et al.*, 1998)).
Un modèle trop détaillé est difficile à appréhender, à modifier, à paramétrer, et dans les cas des modèles mathématiques, l'étude analytique (*i.e.* purement littérale) restreinte. Aussi, le troisième objectif de la modélisation est celui de la **généralité**. Un modèle général est un modèle dont la portée est grande : sa validité embrasse une diversité de cas, son étude une variété de questions, et ses résultats stimulent l'émergence de concepts. La généralité intervient par ailleurs dans la sélection de modèles concurrents : dans une certaine mesure, parmi deux modèles équivalents, celui aux hypothèses constitutives les plus faibles explique préférablement le phénomène considéré – il s'agit du **principe de parcimonie**[a] (Stoica & Söderström, 1982).

a. Principe toutefois discutable pour bâtir des modèles généraux lorsque la causalité est multiple, cf Pigliucci (2008).

Étant donné que les trois objectifs qui guident la modélisation – réalisme, intelligibilité et généralité – sont relativement antagonistes, le modèle idéal n'existe pas et on ne peut au mieux qu'aboutir à un compromis ne satisfaisant que partiellement ces trois objectifs [a]. Mais il convient de traiter ce modèle, aussi bien dans sa conception que dans son analyse, comme le système le plus simple vérifiant les propriétés d'intérêt du phénomène focal. Le modèle est certes un système théorique mais il doit être appréhendé avec la même objectivité qu'une observation naturaliste du phénomène dont il est la représentation et donc être contemplé à part, c'est-à-dire sans nécessairement faire de leur brute ressemblance le premier critère de pertinence du modèle. Dès lors, les résultats fournis par l'analyse du modèle ne relèvent pas de la prédiction quantitative mais de la potentialité qualitative du phénomène focal, sur le principe que si un système minimaliste génère tel patron alors tout système plus complexe dont il est un cas très particulier en est aussi capable. L'intérêt de la modélisation réside alors dans l'éclairage qu'apportent le formalisme (comme ici, les équations mathématiques) qui sous-tendent le patron observé : la modélisation propose une représentation concise, explicite et manipulable du phénomène étudié. D'aucuns voient ainsi le modèle mathématique comme la **validation logique** (preuve de concept) du raisonnement verbal (Servedio *et al.*, 2014).

Une fois établi, le modèle est l'outil privilégié pour exploiter les données, orienter leur acquisition, tester des hypothèses et en formuler de nouvelles, proposer des pistes de contrôle et d'optimisation, prédire et conceptualiser (Ezanno *et al.*, 2012). Et au-delà de son utilisation proximale, le modèle participe aussi bien à la diffusion de la connaissance [b], qu'à l'édification d'une théorie future (Shou *et al.*, 2015).

a. Parfois, le réalisme est volontairement sacrifié dans le but d'identifier un principe général, indépendant du reste du modèle (p.ex. le modèle d'une population haploïde de taille infinie uniquement soumise à la sélection naturelle et le théorème fondamental de Fisher), cf Masel & Trotter (2010).

b. Rôle dont le modélisateur ne saurait s'affranchir, au même titre que tout autre chercheur ainsi que le rappelle P. Tort sur le ton de l'humour : « *un scientifique qui ne s'adresserait qu'à ses pairs serait comme le facteur qui ne distribuerait le courrier qu'aux employés de la Poste* » (Regards – journal de La Courneuve, n°298, 2009).

i.2.2. Épidémiologie mathématique

Si la thérapeutique peut faire l'objet d'essais préliminaires à son application, il n'en est pas de même en ce qui concerne la prophylaxie, pour des raisons pratiques et éthiques évidentes, et en particulier la prévention primaire dont le but est de minimiser le nombre d'individus infectés. L'usage de modèles mathématiques où les calculs remplacent les expériences dans l'aide à la prise de décision en matière de santé publique remonte au XVIII$^{\text{ème}}$ siècle. À cette époque, l'Europe découvre la variolisation, *i.e.* l'inoculation volontaire du virus de la variole à partir de survivants à cette maladie, importée d'Asie où cette pratique est attestée depuis le X$^{\text{ème}}$ siècle (Gross & Sepkowitz, 1998). La question est alors de savoir si cet acte, précurseur de la vaccination, doit être encouragé dans le but d'assurer une protection collective (Anderson & May, 1985) malgré une mortalité collatérale non négligeable (et une mortalité naturelle par ailleurs élevée). En estimant, à partir de l'étude d'équations différentielles ordinaires, un gain de trois ans d'espérance de vie par variolisation systématique, le travail D. Bernoulli (1760) est considéré comme le point de départ de l'épidémiologie mathématique (Dietz & Heesterbeek, 2002; Bacaër, 2011).

La modélisation de D. Bernoulli reposait sur une hypothèse forte : l'**incidence**, la probabilité qu'un individu susceptible, *i.e.* non infecté et non immunisé, contracte la maladie, était supposée constante. Or, au cours d'une épidémie, la **prévalence**, *i.e.* la fréquence d'individus infectés (sous-entendu infectieux/contagieux), croît au cours du temps, et, avec elle, l'incidence. En rendant l'incidence proportionnelle au nombre d'individus infectés dans la population, à l'image de la loi d'action de masse qui régit les rencontres aléatoires entre réactifs chimiques (McCallum *et al.*, 2001; Voit *et al.*, 2015), Ross (1911), dans le cas du paludisme, McKendrick (1926) et Kermack (Kermack & McKendrick, 1927, 1932), dans celui de la peste, introduisent la non-linéarité dans les modèles épidémiologiques et jettent les bases du plus connu d'entre eux, le modèle *SIR* (pour *Susceptible - Infected - Recovered*, où ce dernier compartiment représente les immunisés définitifs).

À titre de référence, la figure i.2.1 présente de façon détaillée le modèle SIS^* (une variante du modèle *SIR* où l'éventuelle guérison n'octroie aucune immunité) sur lesquels les modèles épidémiologiques développés par la suite sont bâtis. De fait, tous les modèles traités ici, qu'ils soient épidémiologiques ou démographiques (cf. croissances parasitaires intra-hôte du chapitre 1) relèvent d'un champ mathématique circonscrit, documenté et prolifique (Wiggins, 2003) : les **systèmes dynamiques autonomes d'équations différentielles ordinaires du premier ordre non linéaires**. Dans de tels systèmes, le temps et les variables sont continus et la dynamique déterministe et sans mémoire. Les éléments théoriques relatifs à leur étude sont brièvement exposés dans l'encadré **[b]** (p.i.2.2), tandis que leurs limites seront discutées à la fin du présent document (section D.3).

∗. Le modèle *SIS* a l'avantage de ne présenter que deux compartiments tout en étant équivalent au modèle *SIR*, sauf dans le cas où les immunisés participent explicitement à la reproduction.

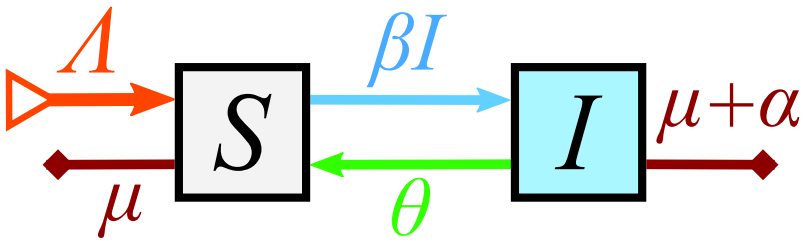

$$\begin{cases} \frac{\mathrm{d}S}{\mathrm{d}t} &= \Lambda - (\beta I + \mu) S, \\ \frac{\mathrm{d}I}{\mathrm{d}t} &= (\beta S - \theta - \mu - \alpha) I. \end{cases} \tag{i.2.1}$$

FIGURE i.2.1. – Modèle *SIS* : diagramme de flux et équations.
Soit t une grandeur temporelle et ind une grandeur de densité d'individus, pouvant être un nombre brut, soit une concentration (linéaire, surfacique, ou volumique) d'individus. Le compartiment des individus **susceptibles**, *i.e.* non infectés non immunisés, S (en ind) est alimenté par un **influx** Λ (natalité, immigration, en ind.t^{-1}, quantité positive possiblement fonction de S et de I), et connaît un efflux d'individus sortant soit par décès, au taux de **mortalité** de cause autre que l'infection focale (souvent appelée naturelle) μ (en t^{-1}), soit par infection, à l'incidence βI. Cette dernière est le produit du **taux de transmission** β (en ind^{-1}.t^{-1}) par la densité d'individus **infectés** I (en ind). Le compartiment constitué par ces individus présente une première sortie par décès au taux $\mu + \alpha$ (en t^{-1}), somme du **taux de mortalité naturelle** μ et de la **virulence** α, *i.e.* ici la mortalité additionnelle due à l'infection focale. La seconde sortie correspond à la **guérison**, au taux θ (en t^{-1}), laquelle ne confère pas d'immunité, d'où le retour de ces individus dans le compartiment susceptible. Noter que la transmission est ici densité-dépendante, c'est-à-dire que l'incidence est linéaire vis-à-vis de la densité I (cas des maladies transmises par contacts réguliers ou aérosols), à distinguer de la transmission fréquence-dépendante, pour laquelle l'incidence est linéaire vis-à-vis de la prévalence $I/(S+I)$ (cas des maladies transmises sexuellement) (KEELING & ROHANI, 2008).

Nous exposons ci-après des notions classiques d'épidémiologie mathématique, sur la base du modèle *SIS* détaillé dans la figure i.2.1 et des méthodes de l'encadré **[b]** mais aisément transposables à des modèles plus complexes. On appelle **équilibre sans infection** (ou *DFE*, pour *Disease Free Equilibrium*) l'état démographique $(S,I) = (S^\circ, 0)$ de la population d'hôte dépourvue de parasites, et donc d'hôtes infectés. La quantité S°est souvent décrite comme la taille initiale de la population au sens où une épidémie se propage dans une population uniquement composée d'individus susceptibles ayant déjà atteint, par hypothèse, l'équilibre démographique *. Considérons à présent l'introduction d'un individu infecté, dit **cas index**, dans cette population complètement susceptible. Avant de guérir ou de mourir (que la cause soit infectieuse ou non), le cas index aura eu en moyenne $(\mu+\theta+\alpha)^{-1}$ unités de temps pour transmettre le parasite, transmission qui s'effectue au taux β par unité de temps et d'individu susceptible. Étant donné la densité initiale S° des individus susceptibles, le nombre total d'individus infectés par le cas index au cours de sa vie vaut la quantité adimensionnelle

$$\mathcal{R}_0 = \frac{\beta S^\circ}{\mu+\theta+\alpha}, \tag{i.2.2}$$

*. $S^\circ > 0$ vérifie $\Lambda(S^\circ) = \mu S^\circ$ et $\frac{\partial \Lambda}{\partial S}(S^\circ) < \mu$.

appelée **nombre de reproduction de base** * (Diekmann *et al.*, 1990).

La maladie infectieuse se propage à partir du cas index si et seulement si l'équilibre sans infection est instable. On montre aisément par analyse de stabilité que cet équilibre est instable si et seulement si $\mathcal{R}_0 > 1$. Ainsi, $\mathcal{R}_0 = 1$ est le seuil épidémiologique au-delà duquel toute maladie infectieuse se propage (épidémie) et persiste (endémie) † (Anderson & May, 1981; Diekmann *et al.*, 1990; van den Driessche & Watmough, 2002). Au contraire, une maladie infectieuse de $\mathcal{R}_0$ sous-unitaire introduite dans une population non infectée est vouée à l'extinction ‡.

Outre son intérêt prédictif du risque épidémique (estimable par les premiers temps d'une épidémie (Dietz, 1993; Champagne *et al.*, 2016)), le nombre de reproduction de base apparaît aussi dans plusieurs autres applications d'intérêt . Lorsque le modèle est suffisamment simple, l'effort de contrôle nécessaire à l'éradication d'une maladie infectieuse fait directement appel au $\mathcal{R}_0$ – p.ex. la couverture vaccinale requise est de $1 - \mathcal{R}_0^{-1}$ (Anderson & May, 1983) –, *idem* pour la probabilité d'extinction par stochasticité (Allen & Burgin, 2000), ou la densité limite de susceptibles ($\widehat{S} = S^\circ/\mathcal{R}_0$, en population « ouverte » comme ici). L'ensemble de ces propriétés ont fait du $\mathcal{R}_0$ le descripteur privilégié de l'épidémiologie classique.

Toutefois, les propriétés autres que celle de seuil épidémiologique ne se généralisent pas à des modèles plus complexes (Roberts, 2007), en particulier lorsque le cycle de vie contient un vecteur ou implique des infections multiples (cf. chapitre 3). Dans ces cas, le calcul du $\mathcal{R}_0$ ne peut plus être effectué intuitivement et requiert l'utilisation de la méthode dite de la génération suivante (cf. encadré **[b]** et Diekmann *et al.* (1990); van den Driessche & Watmough (2002)).

Pour un aperçu de la diversité des modèles compartimentaux et d'autres développements en épidémiologie mathématique, voir Hethcote (2000); Keeling & Rohani (2008); Ezanno *et al.* (2012) ainsi qu'Heesterbeek *et al.* (2015) pour une revue des enjeux actuels de la modélisation des maladies infectieuses.

∗. L'historique de cette notion, qui puise ses origines dans la démographie, est relaté dans Heesterbeek (2002).

†. À noter que la propriété de seuil épidémiologique est bien une conséquence de la définition du $\mathcal{R}_0$, comme le montre Diekmann *et al.* (1990), mais ne devrait pas être prise pour sa définition elle-même (Ezanno *et al.*, 2012). De fait, le $\mathcal{R}_0$ n'est pas l'unique seuil épidémiologique – il est possible d'en trouver d'autres – mais il est le seul à s'interpréter biologiquement comme le nombre initial d'infectés secondaires (Roberts & Heesterbeek, 2003; Roberts, 2007; Hurford *et al.*, 2010).

‡. Le problème de l'extinction par mesures de contrôle d'une maladie déjà établie est toutefois plus délicat à traiter car des effets d'hystérèse peuvent survenir. Il en est en effet possible que la système soit bistable et que, partant d'un équilibre endémique, l'extinction ne se produise pas pour tout $\mathcal{R}_0 < 1$, voir Hadeler & Van den Driessche (1997); Brauer (2004) et l'épilogue du chapitre 3.

[b] éléments de systèmes dynamiques

Les systèmes dynamiques tels que ceux étudiés ici (déterministes, autonomes, continus en temps et en espace, non-linéaires et du premier ordre) peuvent être vus comme un mobile dont la position $\mathbf{x}$ dans un espace à $d \in \mathbb{N}^\star$ dimensions, $\mathbf{x} \in \mathbb{R}^d$, satisfait le **système d'équations différentielles ordinaires** $(\mathcal{S})$ $\left\{\frac{\mathrm{d}}{\mathrm{d}t}\mathbf{x} = \mathbf{f}(\mathbf{x})\right\}$, où $\mathbf{f}$ est le **champ de vecteurs** qui détermine le système dynamique[a]. Plus précisément, la vitesse instantanée du mobile dépend uniquement de sa position actuelle, car le champ $\mathbf{f}$ associe à chaque point de l'espace un vecteur vitesse. Une **solution** du système dynamique est une **trajectoire** $\mathbf{x}(t)$ qui, partant d'une **condition initiale** $\mathbf{x}(0) = \mathbf{x}_0$, satisfait $(\mathcal{S})$ pour tout $t \in [0, T[$, avec T éventuellement infini. L'existence et l'unicité d'une solution maximale est garantie par le théorème de CAUCHY-LIPSCHITZ, sous réserve que $\mathbf{f}$ soit localement lipschitzienne. (Par la suite, et dans les modèles considérés, $\mathbf{f}$ sera toujours aussi régulière que nécessaire.)

Une partie $\mathcal{A}$ de l'espace $\mathbb{R}^d$ est dite **invariante** si toute trajectoire initiée dans $\mathcal{A}$ n'en sort jamais. $\mathcal{A}$ est un **attracteur** si, en plus d'être invariant, $\mathcal{A}$ est fermé et s'il existe un voisinage $\mathcal{U}$ de $\mathcal{A}$ tel que toute trajectoire initiée dans $\mathcal{U}$ décrit $\mathcal{A}$ à l'infini. Les attracteurs représentent donc les formes limites vers lesquelles la dynamique tend sur le long cours. Les attracteurs peuvent être des cycles ou tores limites, des attracteurs étranges ou bien de simples points, dits fixes[b].
Un **point fixe** $\widehat{\mathbf{x}}$, aussi appelé équilibre ou état stationnaire, est un point de l'espace dans lequel le mobile est à l'arrêt, il vérifie donc le système algébrique $\{\mathbf{f}(\widehat{\mathbf{x}}) = \mathbf{0}\}$, dont chaque équation définit une **isocline**. La résolution de ce système (au moyen, par exemple, de l'intersection des isoclines (SIMONYI & KASZÁS, 1968)) identifie tous les points fixes du système mais certains d'entre eux peuvent se révéler biologiquement non pertinents : si une des coordonnées est négative alors que la grandeur associée n'a de sens que positive, le point est dit infaisable – sinon, il est dit **faisable** et noté $\mathbf{x} \geq 0$ (la comparaison porte sur chaque composante).

Le comportement à long terme des trajectoires aux abords d'un point fixe dépend de sa stabilité. On dit qu'un point fixe est **stable** si, pour tout voisinage $\mathcal{B}$ de ce point fixe, il existe un second voisinage $\mathcal{C}$ tel que toute trajectoire initiée dans $\mathcal{C}$ reste dans $\mathcal{B}$ – sinon, il est dit instable. Il est par ailleurs **asymptotiquement stable** lorsqu'il est non seulement stable mais si de plus toutes les trajectoires initiées dans un certain voisinage y convergent – ce voisinage porte alors le nom de **bassin d'attraction**. Lorsque le bassin d'attraction contient l'ensemble des conditions initiales faisables, le point fixe est dit **globalement** asymptotiquement stable (GAS) et toutes les trajectoires biologiquement pertinentes tendent vers ce point. Si le bassin d'attraction est en revanche plus restreint, le point fixe est seulement **localement** asymptotiquement stable (LAS).

a. Nous adoptons ici une formulation volontairement simpliste dans l'unique but de rappeler dans les grandes lignes les définitions et les méthodes relatives aux systèmes dynamiques qui seront employées par la suite. Pour une introduction complète et mathématiquement rigoureuse aux systèmes dynamiques, se référer, au choix, à HIRSCH & SMALE (1974); GLENDINNING (1994); WALTER (1998); WIGGINS (2003); ROUSSARIE & ROUX (2014).

b. Dans le présent travail, les seuls attracteurs rencontrés seront des points fixes.

La **matrice jacobienne J** du système $(\mathcal{S})$ est la matrice $d \times d$ des dérivées partielles du premier ordre du champ **f** par rapport à chacune de ses variables, $\mathbf{J} = \partial\mathbf{f}/\partial\mathbf{x}$. Le développement limité au premier ordre du champ au voisinage d'un point fixe $\widehat{\mathbf{x}}$ donne alors $\mathbf{f}(\mathbf{x}) = \mathbf{J}(\widehat{\mathbf{x}}).(\mathbf{x}-\widehat{\mathbf{x}}) + o\left(\|\mathbf{x}-\widehat{\mathbf{x}}\|_{\mathbb{R}^d}\right)$. Si aucune des valeurs propres de $\mathbf{J}(\widehat{\mathbf{x}})$ n'est imaginaire pure, alors $\widehat{\mathbf{x}}$ est dit **hyperbolique** et, par le **théorème d'HARTMAN-GROBMAN** (GROBMAN, 1959; HARTMAN, 1960), le comportement du système au voisinage de $\widehat{\mathbf{x}}$ est qualitativement identique au système linéarisé (c'est-à-dire en remplaçant **f** par $\mathbf{x} \mapsto \mathbf{J}(\widehat{\mathbf{x}}).(\mathbf{x}-\widehat{\mathbf{x}})$) dans un voisinage du point fixe. Il en découle [a] que $\widehat{\mathbf{x}}$ est LAS si et seulement si les parties réelles de toutes les valeurs propres de $\mathbf{J}(\widehat{\mathbf{x}})$ sont strictement négatives [b], condition notée $\max\{\Re\lambda : \lambda \in \mathrm{Sp}(\mathbf{J}(\widehat{\mathbf{x}}))\} < 0$. Il est instable sinon.
Le théorème de la **génération suivante** (*next-generation theorem*) (DIEKMANN *et al.*, 1990; VAN DEN DRIESSCHE & WATMOUGH, 2002; HURFORD *et al.*, 2010) fournit une formulation alternative de cette condition : soient des matrices **F** et **V** satisfaisant $\mathbf{F}-\mathbf{V} = \mathbf{J}(\widehat{\mathbf{x}})$, $\mathbf{F} \succeq 0$, $\det\mathbf{V} \neq 0$, $\mathbf{V}^{-1} \succeq 0$, $\max\{\Re\ell : \ell \in \mathrm{Sp}(\mathbf{V})\} > 0$, alors $\widehat{\mathbf{x}}$ est LAS si et seulement si le module maximal des valeurs propres de $\mathbf{F}.\mathbf{V}^{-1}$ est sous-unitaire, condition notée $\max\left\{\left|\mu\right| : \mu \in \mathrm{Sp}\left(\mathbf{F}.\mathbf{V}^{-1}\right)\right\} < 1$.
La seconde méthode de LYAPUNOV (1992) généralise l'analyse de stabilité à tous les points fixes (et non plus seulement hyperboliques) et précise le voisinage maximal, autrement dit, elle permet d'appréhender la stabilité globale : s'il existe une **fonction**, dite **de LYAPUNOV**, $V \in \mathcal{C}^1\left(\mathbb{R}^d\right)$ telle que $V(\widehat{\mathbf{x}}) = \frac{\mathrm{d}V}{\mathrm{d}t}(\widehat{\mathbf{x}}) = 0$, et, pour tout $\mathbf{x} \in \mathcal{B} \setminus \{\widehat{\mathbf{x}}\}$, $V(\mathbf{x}) > 0$ et $\frac{\mathrm{d}V}{\mathrm{d}t}(\mathbf{x}) < 0$, alors $\widehat{\mathbf{x}}$ est asymptotiquement stable sur le voisinage $\mathcal{B}$.

Enfin, il peut arriver que toutes les composantes du système dynamique étudié ne varient pas à la même vitesse, le système présentant alors des temporalités multiples. Si $(\mathcal{S})$ peut s'écrire sous la forme $\left\{\varepsilon\frac{\mathrm{d}}{\mathrm{d}t}\mathbf{y} = \mathbf{g}(\mathbf{x}), \frac{\mathrm{d}}{\mathrm{d}t}\mathbf{z} = \mathbf{h}(\mathbf{x})\right\}$, où ε est une petite quantité positive ($0 < \varepsilon \ll 1$), alors $(\mathcal{S})$ est un système **lent-rapide** avec **y** regroupant les variables dites rapides, **z** les variables lentes et ε est le ratio des temps caractéristiques des dynamiques rapide et lente. D'après la théorie géométrique des perturbations singulières (KUEHN (2015), p.53), le comportement au temps long de $(\mathcal{S})$ peut s'approximer par celui du sous-système lent $\left\{\mathbf{g}(\mathbf{x}) = 0, \frac{\mathrm{d}}{\mathrm{d}t}\mathbf{z} = \mathbf{h}(\mathbf{x})\right\}$, en vertu du théorème de FENICHEL-TIKHONOV (LOBRY *et al.*, 1998), sous réserve que la variété critique caractérisée par $\{\mathbf{g}(\mathbf{x}) = 0\}$ soit un attracteur hyperbolique. Ce résultat justifie la **séparation des échelles de temps** opérée dans la modélisation des systèmes à temporalités multiples (et utilisée par la suite à de nombreuses reprises).

a. Au moyen notamment d'un lemme d'algèbre linéaire stipulant que $\forall\mathbf{A} \in \mathfrak{M}_{d,d}(\mathbb{R}), \forall(a,b) \in \mathbb{R}^2 : \forall\lambda \in \mathrm{Sp}(\mathbf{A}), \Re\lambda \in]a;b[\Longrightarrow \exists\mathscr{B}$ base de $\mathbb{R}^d : \forall\mathbf{x} \in \mathbb{R}^d, \mathbf{x}^{\mathbf{T}}.\mathbf{A}.\mathbf{x} \in \|\mathbf{x}\|^2_{\mathscr{B}}\,]a;b[$ (HIRSCH & SMALE, 1974, p.147).

b. À noter que dans les chapitres, écrits en anglais, les adjectifs *positive* et *negative* seront à comprendre au sens anglais, *i.e.* respectivement strictement positifs et strictement négatifs.

i.3. Parasites et temps long

i.3.1. Coût du parasitisme

En vivant aux dépens de leurs hôtes (De Meeûs & Renaud, 2002) – par occupation, exploitation, détournement de ressources et reproduction – les parasites leur nuisent [*]. On considère ainsi que le parasitisme induit un double coût [†] pour l'hôte : le premier est proximal – l'altération de sa physiologie –, le second distal – il s'agit de la réduction du nombre total de descendants. Selon que l'étude relève de la microbiologie, de l'infectiologie, de l'immunologie d'un côté, ou de l'écologie et de l'évolution de l'autre, le coût considéré sera respectivement soit proximal soit distal. Malgré une confusion terminologique rémanente due à la diversité des disciplines impliquées, ainsi qu'au clivage entre zoologie et botanique, il convient d'appeler **pathogénicité** le coût proximal et **virulence** le coût distal (Shaner *et al.*, 1992; Read, 1994; Poulin & Combes, 1999).

La pathogénicité est relativement facile à mettre en évidence à partir des symptômes de la maladie – d'où son caractère parfois purement qualitatif – et repose sur des déterminants génétiques identifiés chez le parasite (Rahme *et al.*, 1995; Miller *et al.*, 2002), ce qui l'inscrit dans le phénotype étendu du parasite (Dawkins, 1999). La pathogénicité peut toutefois être modulée par le génotype de l'hôte lui-même (Carius *et al.*, 2001) – elle se révèle être un trait partagé entre le parasite et son hôte – voire par d'autres éléments du contexte infectieux (Nathan, 2015), ce qui en fait le résultat d'une interaction génotype - environnement (Ferguson & Read, 2002).

La pathogénicité étant une condition nécessaire à la virulence, cette dernière hérite des propriétés sus-citées (dépendance aux génotypes du parasite, de l'hôte et à l'environnement). Mais si tous les parasites sont pathogènes, tous ne sont pas virulents. En effet, un parasite infectant un hôte après la période de reproduction de ce dernier ne réduit pas le nombre de descendants de l'hôte. Il existe même des exemples de parasitisme à effets pléiotropes pour lesquels la descendance des hôtes infectés est favorisée vis-à-vis de celle des non infectés (Michalakis *et al.*, 1992). De plus, la virulence étant définie comme la diminution de valeur sélective [‡] de l'hôte (Read, 1994), elle est difficile à mesurer (Poulin & Combes, 1999; Alizon *et al.*, 2009). Dans la littérature expérimentale, certaines mesures de virulence se confondent ainsi avec des mesures de pathogénicité (de Roode *et al.*, 2005b; Doumayrou *et al.*, 2013).

Pour ces raisons et malgré des effets identifiés du parasitisme sur la fécondité des hôtes (Price, 1980), nous faisons le choix, impulsé par l'écrasante majorité des travaux théoriques (Alizon *et al.*, 2013; Cressler *et al.*, 2015), de restreindre notre étude de la virulence à sa composante de survie (d'autant plus que nous ignorerons l'hétérogénéité spatiale de la population d'hôte (O'Keefe & Antonovics, 2002)). Autrement dit, la virulence sera désormais entendue au sens de mortalité additionnelle due à l'infection.

*. Ou tout du moins dans une proportion représentative des conditions où le parasitisme s'établit – autrement, le parasite devrait être considéré comme commensal ou mutualiste (Thomas *et al.*, 2000).

†. Voir Sélosse & Gouyon (2011) pour une justification du vocabulaire anthropomorphe en biologie.

‡. La valeur sélective (ou succès reproducteur, *fitness* en anglais) quantifie la propension à contribuer génétiquement à la génération suivante – hors mutation et biais d'échantillonnage (dérive) – et résulte du produit entre survie et fécondité intégré à tous les âges (Lenormand *et al.*, 2016).

i.3.2. Épidémiologie évolutive

La virulence est un des traits parasitaires les plus étudiés (Schmid Hempel, 2011). En particulier, elle apparaît paradoxale pour l'intuition évolutionniste (Smith, 1887; Méthot, 2012) : **pourquoi les parasites écourtent-ils la vie des hôtes qui assurent pourtant leur transmission ?** La virulence étant en partie héritable d'une génération de parasites à l'autre (Hale, 1991; Rahme *et al.*, 1995; Ferguson & Read, 2002; Fraser *et al.*, 2014), les souches épargnant leurs hôtes devraient être sélectivement avantagées puisque profitant de plus d'occasions pour se transmettre [*]. D'après cette « sagesse conventionnelle » (May & Anderson, 1983), les parasites devraient évoluer vers une virulence nulle, ou avirulence. On pourrait penser que certains parasites sont virulents car non « encore » adaptés à leurs hôtes. Mais les observations de Fenner (1983) contredisent cette hypothèse.

En 1950, l'Homme a volontairement introduit le virus de la myxomatose dans le but de réguler les populations australiennes invasives de lapin de garenne (*Oryctolagus cuniculus*). Initialement très virulent, le virus fait place à des souches mutantes moins létales. Mais au bout de 30 ans, c'est une souche de virulence intermédiaire qui persiste majoritairement, comme le montre la Figure i.3.1.

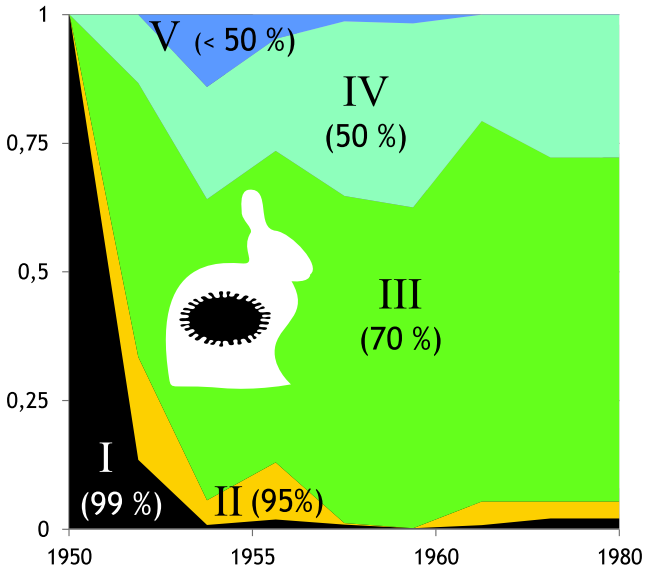

Figure i.3.1. – Prévalences relatives de cinq souches de Myxoma Virus dans les populations australiennes d'*Oryctolagus cuniculus*, entre 1950 et 1980.
Les souches du virus sont numérotées de I à V, de la plus virulence à la moins virulente, la proportion de létalité étant indiquée entre parenthèses. Données d'après Fenner (1983).

De plus, nous savons aujourd'hui que *Plasmodium falciparum* infectait déjà les humains il y a plus de 3000 ans comme l'atteste la momie de Toutânkhamon (Hawass *et al.*, 2010), le virus de la variole ou de la rougeole causaient déjà des épidémies à Athènes au V$^{\text{ème}}$ siècle AEC (Hays, 2005). Étant donné que les micro-parasites présentent des temps de génération au moins mille fois inférieurs à ceux de leur hôtes (Kwiatkowski & Nowak, 1991; Perelson *et al.*, 1996), et que l'évolution des micro-organismes est observable en seulement quelques milliers de générations (Lenski *et al.*, 1991), le maintien de la virulence n'est vraisemblablement pas une maladaptation en cours d'atténuation.

∗. Notons ici que, malgré une biologie analogue, les espèces parasitoïdes, *i.e.* qui ne peuvent se transmettre sans tuer leur hôte, ne sont pas considérées ici puisque relevant en fait de la prédation.

Un trait partagé par tous les individus, ou presque, d'une espèce peut être le résultat de trois causes : des contraintes développementales, un héritage phylogénétique, et/ou une évolution adaptative (Seilacher, 1970). Dans le présent travail, nous nous limitons à la seule évolution adaptative, mais notons que les deux premières causes caractérisent l'approche *evo-devo* (Maynard Smith *et al.*, 1985) et que des approches unificatrices commencent à émerger (Manceau *et al.*, 2016). La question de l'évolution adaptative de la virulence est à l'origine d'un champ hybride jeune d'une trentaine d'années, l'épidémiologie évolutive (Anderson & May, 1979; Ewald, 1988; Restif, 2009), dont la Figure i.3.2 détaille les influences.

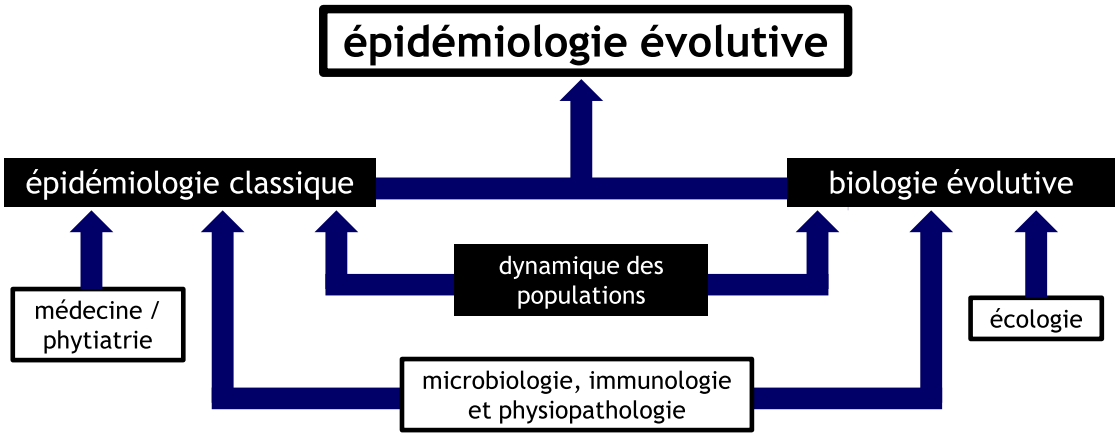

Figure i.3.2. – Origines et fondations disciplinaires de l'épidémiologie évolutive.
L'épidémiologie évolutive repose essentiellement sur l'interdisciplinarité entre l'épidémiologie classique et la biologie évolutive, lesquelles présentent des apports indépendants de la recherche médicale (pour les animaux) ou phytiatriques (pour les végétaux) et respectivement de l'écologie, tout en partageant les méthodes développées par la dynamique des populations et les observations fournies par l'étude des micro-organismes (microbiologie) et leurs relations avec leurs hôtes (immunologie et physiopathologie) (Dieckmann, 2002). Le fond noir signifie la présence de techniques mathématiques majeures dans le développement de l'épidémiologie évolutive.

Tandis que l'épidémiologie suit la fréquence des individus infectés et s'inscrit dans le temps court d'une épidémie, la biologie évolutive s'intéresse aux variations de fréquences alléliques au cours des générations (Gouyon & Henry, 1998), donc sur un temps long. Et c'est au moyen du nombre de reproduction de base (et de ses dérivés) que l'épidémiologie évolutive réussit à coupler ces deux types de fréquences et ces deux échelles de temps. En effet, calculé comme le nombre de fois qu'un parasite boucle son cycle de vie à partir d'une infection isolée, le $\mathcal{R}_0$ est non seulement un seuil épidémiologique, mais aussi un pertinent quantificateur de la valeur sélective des parasites (Dieckmann, 2002; Alizon & Michalakis, 2015).

Une première approche fructueuse consiste à considérer que l'évolution des parasites tend à maximiser leur $\mathcal{R}_0$, ainsi que le prédit le théorème fondamental de la sélection naturelle de Fisher (1930). Reprenant son expression (i.2.2), il est évident que $\mathcal{R}_0 = \beta S^\circ / (\mu + \theta + \alpha)$ est maximisé pour $\alpha = 0$ si aucun autre trait ne varie avec la virulence, s'accordant ainsi avec la sagesse conventionnelle. Mais si l'on considère à présent que, sur un certain intervalle, le taux de transmission est une fonction croissante de la virulence, alors, à partir d'un certain niveau de dépendance ($\frac{\mathrm{d}\mathcal{R}_0}{\mathrm{d}\alpha} > 0 \iff \frac{\mathrm{d}\beta}{\mathrm{d}\alpha} \geq \frac{\beta}{\mu+\theta+\alpha}$), la virulence est favorisée au moins jusqu'à un certain point. S'il existe une virulence finie $\alpha^\star > 0$ telle que $\beta(\alpha^\star) = (\mu + \theta + \alpha^\star)\frac{\mathrm{d}\beta}{\mathrm{d}\alpha}(\alpha^\star)$ et $\frac{\mathrm{d}^2\beta}{\mathrm{d}\alpha^2}(\alpha^\star) < 0$, alors $\alpha^\star$ maximise localement

$\mathcal{R}_0$ et sa valeur est une ESS de la virulence (van Baalen & Sabelis, 1995). Ce résultat est la transposition épidémiologique en théorie optimale de la recherche de nourriture (Charnov, 1976), ainsi que l'illustre son interprétation géométrique en Figure i.3.3, et constitue la fondation théorique de l'hypothèse du **compromis entre transmission et virulence**.

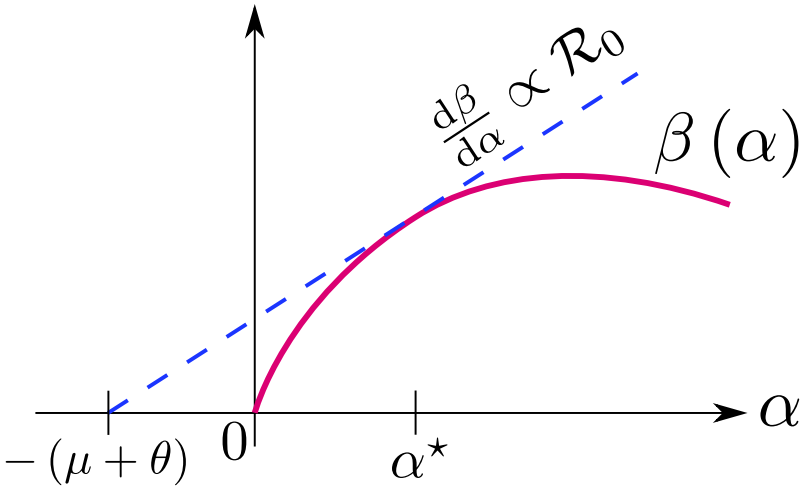

Figure i.3.3. – Interprétation géométrique de la virulence optimale en dépendance avec la transmission.
S'il existe $\alpha^\star \in \mathbb{R}_+^\star$ telle que $\beta(\alpha^\star) = (\mu+\theta+\alpha^\star)\frac{d\beta}{d\alpha}(\alpha^\star)$ et $\frac{d^2\beta}{d\alpha^2}(\alpha^\star) < 0$, alors il existe au moins une droite passant par le point $(-\mu-\theta, 0)$ qui intersecte $\mathcal{C}_\beta := \{(x,y) \in \mathbb{R}_+^2 : y = \beta(x)\}$ avec une pente maximale. La droite tangente alors $\mathcal{C}_\beta$ au point d'abscisse $\alpha^\star$. D'après van Baalen & Sabelis (1995).

L'hypothèse du compromis transmission - virulence suppose ainsi que la perte en durée de transmission engendrée par la virulence est compensée par le gain en intensité de transmission et qu'il existe une virulence optimale maximisant le nombre de reproduction de base (Levin & Pimentel, 1981; Anderson & May, 1982; van Baalen & Sabelis, 1995; Alizon & van Baalen, 2005; Alizon *et al.*, 2009). Cette hypothèse, ainsi que celle analogue du compromis guérison - virulence, a reçu un soutien empirique dans quelques systèmes biologiques (Fraser *et al.*, 2007; de Roode *et al.*, 2008; Doumayrou *et al.*, 2013) (voir Alizon *et al.* (2009); Schmid Hempel (2011) pour une revue des preuves expérimentales).

Cependant, tout comme les dépendances à la fréquence et à la densité échappent au théorème fondamental de la sélection naturelle, les situations garantissant l'optimisation évolutive du nombre de reproduction de base sont marginales (Metz *et al.*, 2008). L'expression du $\mathcal{R}_0$ se complexifiant avec celle du cycle de vie (Alizon, 2013a; Alizon & Michalakis, 2015; Champagne *et al.*, 2016), la valeur sélective d'invasion d'un mutant dans une population d'hôtes déjà infectée par une souche résidente (voir encadré **[c]** p.41) peut ne plus être égale au rapport des nombres de reproduction de base (Dieckmann, 2002). En conséquence, l'attracteur évolutif de la virulence peut être différent de la virulence maximisant le $\mathcal{R}_0$. Ceci se vérifie en particulier dans le cas où les parasites sont en compétition au sein des hôtes (Bremermann & Pickering, 1983).

La virulence sélectionnée pour sa corrélation positive avec la **compétitivité** est une autre hypothèse avancée pour expliquer son maintien : dès lors qu'un parasite plus virulent exploite aussi plus rapidement son hôte, toute compétition intra-hôte devrait conduire à une tragédie des biens communs, dont la virulence n'est que la conséquence épidémiologique (Levin & Pimentel, 1981; Bremermann & Pickering, 1983; van Baalen

& Sabelis, 1995; Alizon *et al.*, 2013). Soutenue par de rares preuves empiriques (de Roode *et al.*, 2005b), cette hypothèse est aussi contredite dans d'autres systèmes (Pollitt *et al.*, 2014). Dans la mesure où la compétition fait appel au polymorphisme parasitaire, elle sera plus longuement abordée dans la deuxième partie de l'introduction.

Enfin, il a aussi été proposée que la virulence soit un **sous-produit** d'une évolution intra-hôte à court-terme, par pléiotropie d'une adaptation locale résultant de l'infection (Levin & Bull, 1994). Cette hypothèse, qui n'a toutefois pas été démontée par un travail d'évolution expérimentale, n'exclut pas les deux précédentes. À noter que d'autres explications à l'existence de la virulence impliquent cette fois-ci non pas le parasite mais l'hôte, et plus exactement son système immunitaire, dont la réponse à l'infection peut constituer la cause même de la maladie et donc la virulence observée (Graham *et al.*, 2005).

[c] de la génétique des populations à la dynamique adaptative

Soit une espèce à reproduction asexuée (chaque individu est issu d'un parent unique) dont la population est homogène[a] et catégorisable en $m \in \mathbb{N}^\star$ morphes (types, génotypes, variétés...) selon leur capacité à se reproduire. Pour un instant $t \in \mathbb{R}_+$ donné, les individus appartenant au morphe i sont en nombre n_i et se reproduisent tous au même taux de croissance individuel w_i, *i.e.* $\dot{n}_i = w_i n_i$ (où $\dot{}$ désigne la dérivation par rapport au temps, dont la dépendance est par ailleurs sous-entendue pour toutes les variables). Il découle alors que la fréquence du morphe i notée $f_i := \frac{n_i}{N}$, où $N := \sum_{i=1}^{m} n_i$ est le nombre total d'individus, satisfait l'**équation du réplicateur**[b] (Hofbauer & Sigmund, 1998)

$$\dot{f}_i = (w_i - \overline{w}) f_i, \tag{i.3.1}$$

avec $\overline{w} := \sum_{i=1}^{m} w_i f_i$ le taux de croissance individuel moyen dans la population. Cette équation différentielle, à la fois triviale et d'une grande généralité[c], est la formalisation du raisonnement de Darwin (par ailleurs étendue à toutes les démographies, la compétition intra-spécifique n'étant pas une condition nécessaire de l'évolution) : les formes les plus représentées sont celles dont la reproduction est supérieure à la moyenne de l'espèce, autrement dit, ce qui se reproduit le plus s'observe le plus.
Considérons à présent un trait quantitatif x, dont la valeur pour chaque morphe i est x_i, lequel n'est pas nécessairement constant (il peut par exemple dépendre de l'environnement). Il est aisé de montrer que la valeur moyenne de ce trait dans la population, $\overline{x} := \sum_{i=1}^{m} x_i f_i$ satisfait l'**équation de Price**[d] (Price *et al.*, 1970),

$$\dot{\overline{x}} = \overline{\dot{x}} + \mathrm{cov}(x, w), \tag{i.3.2}$$

qui décompose formellement la variation de la valeur moyenne du trait dans la population au cours des générations comme la moyenne des variations propres du trait (p.ex. par mutation, terme $\overline{\dot{x}}$) additionnée du biais induit par la corrélation (terme $\mathrm{cov}(x,w)$) entre la valeur du trait et le taux de reproduction individuel, lequel est une mesure de la valeur sélective.
Il est intéressant de noter que si le trait focal est la valeur sélective elle-même et supposée invariante ($x \equiv w$ = constante), alors $\dot{\overline{w}} = \mathrm{var} w \geq 0$. Il s'agit du **théorème fondamental de la sélection naturelle de Fisher** (Fisher, 1930), qui énonce que si la valeur sélective est indépendante de l'environnement, alors la valeur sélective moyenne ne peut qu'augmenter (voir Grafen (2015) pour une étude récente de ce théorème).

---

a. Pour des raisons de concision nous ne considérons ici que le cas le plus simple. La prise en compte de la sexualité et de l'hétérogénéité spatiale continuent de faire l'objet de recherches actives (voir p.ex. Collet *et al.* (2013); Lion & Gandon (2016)).

b. Preuve : $\dot{f}_i = \left(\frac{\dot{n}_i}{N}\right) = \frac{w_i n_i}{N} - \frac{n_i}{N^2}\left(\sum_{j=1}^{m} \dot{n}_j\right) = \frac{n_i}{N}\left(w_i - \frac{1}{N}\sum_{j=1}^{m} w_j n_j\right) = (w_i - \overline{w}) f_i$.

c. Voir Page & Nowak (2002) au sujet de la place centrale occupée par l'équation du réplicateur dans la biologie évolutive théorique.

d. Preuve : $\dot{\overline{x}} = \sum_{i=1}^{m} (\dot{x}_i f_i) = \sum_{i=1}^{m} \dot{x}_i f_i + \sum_{i=1}^{m} x_i \dot{f}_i = \overline{\dot{x}} + \sum_{i=1}^{m} x_i (w_i - \overline{w}) f_i$ or $\sum_{i=1}^{m} x_i (w_i - \overline{w}) f_i = \underbrace{\sum_{i=1}^{m} (x_i - \overline{x})(w_i - \overline{w}) f_i}_{=:\mathrm{cov}(x,w)} + \overline{x} \underbrace{\sum_{i=1}^{m} (w_i - \overline{w}) f_i}_{=0 \text{ (variable centrée)}}$, *cqfd*.

Dans la Nature, le nombre de descendants est toutefois modulé par les interactions entre individus de la même espèce, qu'elles soient directes (compétition pour la reproduction) ou indirectes (compétition pour les ressources). Réduisons la diversité de la population considérée à un dimorphisme ($m = 2$) dont les valeurs du trait focal sont x et y, en proportion respectives p et $1-p$. Les valeurs sélectives $w(x)$ et $w(y)$ de ces deux morphes peuvent alors s'écrire comme des fonctions affines des gains g issus des rencontres entre deux individus [a], supposée aléatoirement uniformes (sous l'hypothèse d'homogénéité),

$$\begin{cases} w(x) &= w_0 + pg(x,x) + (1-p)g(x,y), \\ w(y) &= w_0 + pg(y,x) + (1-p)g(y,y), \end{cases} \tag{i.3.3}$$

où w_0 est la composante de valeur sélective indépendante du trait focal et $g(a,b)$ le gain en reproduction induit par la rencontre d'un individu de trait de valeur a avec un individu de trait de valeur b [b].

En posant $y = x + \varepsilon$, les valeurs sélectives de (i.3.3) peuvent se réécrire sous la forme de développement limités par rapport à la valeur de référence du trait (x) :

$$\begin{cases} w(x) &= w_0 + g(x,x) + (1-p)\varepsilon\partial_2 g(x,x) + o(\varepsilon), \\ w(x+\varepsilon) &= w_0 + g(x,x) + (\partial_1 g(x,x) + (1-p)\partial_2 g(x,x))\varepsilon + o(\varepsilon). \end{cases} \tag{i.3.4}$$

Ainsi, la valeur sélective moyenne de la population, $\overline{w} \coloneqq pw(x) + (1-p)w(x+\varepsilon)$, s'écrit

$$\overline{w} = w_0 + g(x,x) + (1-p)(\partial_1 g(x,x) + \partial_2 g(x,x))\varepsilon + o(\varepsilon). \tag{i.3.5}$$

De plus, par application de (i.3.1), la variation des fréquences des morphes est régie par

$$\dot{p} = -(1-p)p\varepsilon\partial_1 g(x,x) + o(\varepsilon)p. \tag{i.3.6}$$

Considérons à présent que la population modélisée est monomorphe et que le morphe dit résident a pour valeur de trait x. Supposons de plus qu'un morphe de valeur de trait alternative $x + \varepsilon$ y apparaît par mutation. Si l'effet phénotypique de cette mutation ou celui de la sélection (portée par les variations de g), ce qui revient au même par normalisation, est suffisamment faible (Taylor, 1989), alors $0 < |\varepsilon| \ll 1$ et en découle les deux résultats fondamentaux de la **dynamique adaptative** suivants(Geritz *et al.*, 1998; Dieckmann, 2002; Lion, 2017).

1) en comparant les vitesses caractéristiques des dynamiques écologique et évolutive, par exemple en divisant le taux de croissance de la population totale par celui de la fréquence d'un morphe, il vient d'après (i.3.5) et (i.3.6),

$$\frac{\dot{N}/N}{\dot{p}/p} = \frac{\overline{w}}{w(x) - \overline{w}} \xrightarrow[\varepsilon \to 0]{} \infty,$$

c'est-à-dire que la **dynamique évolutive est négligeable devant la dynamique écologique**, ce qui, d'après la théorie des systèmes lents-rapides (voir encadré **[b]**), appelle à séparer les deux échelles de temps (l'équilibre écologique étant atteint bien avant la fixation d'un morphe).

a. La fréquence des rencontres à plus de deux individus étant négligeable.

b. Une extension multidimensionnelle de l'approche développée ci-après est donnée par Leimar (2009).

2) d'après (i.3.6), le sens de la sélection est donné par

$$\operatorname{sgn}\left(\dot{p}\right) \underset{\varepsilon\to 0}{\sim} -\operatorname{sgn}\left(\varepsilon\partial_1 g(x,x)\right), \tag{i.3.7}$$

c'est-à-dire qu'il n'est régi que par le sens de la mutation ($\operatorname{sgn}\varepsilon$) et le signe de la quantité $\partial_1 g(x,x)$ appelée **gradient de sélection** et ci-après notée $\Delta(x)$, et est en particulier indépendant de la fréquences des morphes. En conséquence, toute mutation de même sens que le gradient de sélection croît jusqu'à exclure le morphe résident. Autrement dit, **l'invasion implique la fixation** (Geritz *et al.*, 2002). Dans le cas contraire, le mutant disparaît.

Une valeur de trait x qui annule le gradient de sélection ($\Delta(x)=0$) est appelée **stratégie**[a] **évolutivement singulière**. Comme nous le verrons ci-après, ces stratégies occupent une place centrale dans la dynamique adaptative et leur étude requiert le développement limité à un ordre supérieur. En se plaçant à l'instant initial où le mutant est rare, $p\approx 1$, il vient

$$w(x+\varepsilon) \approx w_0 + g(x,x) + \frac{\varepsilon^2}{2}\partial^2_{1,1} g(x,x) + o\left(\varepsilon^2\right).$$

Une stratégie x est dite **évolutivement stable** (*ESS*, (Maynard Smith & Price, 1973)) si et seulement si aucun mutant (phénotypiquement proche ici, mais le qualificatif initial se réfère à l'ensemble des stratégies possibles, voir Maynard Smith (1982)) ne peut envahir la population résidente. On montre que x est *ESS* si et seulement si elle est singulière et $\partial^2_{1,1} g(x,x) < 0$ [b].
Par ailleurs, une stratégie x est dite **évolutivement convergente** (Eshel, 1983) si et seulement si toute population monomorphe de trait avoisinant y converge graduellement par cycles de mutation-sélection (en faisant l'hypothèse que les mutations phénotypiques sont rares et surviennent toujours après fixation) (Geritz *et al.*, 1998; Dieckmann, 2002). D'après le point **2)** discuté précédemment, la convergence évolutive survient dès lors que le gradient de sélection est positif (resp. négatif) pour des valeurs de trait inférieures (resp. supérieures) à x. Ainsi, x est évolutivement convergente si et seulement si elle est singulière et $\Delta'(x)<0$.
Enfin, une stratégie évolutivement convergente et stable est un **attracteur évolutif**[c], au sens où le trait converge évolutivement vers cette valeur et s'y stabilise.

a. Terme hérité de la théorie (économique) des jeux où les traits sont des comportements.

b. Preuve : d'après (i.3.1), le mutant disparaît de la population ssi $w(x+\varepsilon)-\overline{w}<0$, or $\overline{w}=w(x)=w_0+g(x,x)$ puisque la population est monomorphe. Ainsi, $\operatorname{sgn}\left(w(x+\varepsilon)-\overline{w}\right) \underset{\varepsilon\to 0}{\sim} \operatorname{sgn}\left(\partial^2_{1,1} g(x,x)\right)$, *cqfd*.

c. Étant donnée l'objectif de vulgarisation de cet encadré, nous évitons volontairement d'employer la terminologie historique mais peu intuitive de la dynamique adaptative (Diekmann, 2004).

0 Modéliser l'évolution de la virulence, un exemple

0.α. Prologue

Les méthodes usuelles d'épidémiologie évolutive ayant été brièvement présentées, ce chapitre introductif se veut une illustration de leur application à une maladie infectieuse documentée : la fièvre hémorragique à virus Ébola. Découverte en 1976, il s'agit d'une des maladies infectieuses humaines les plus mortelles avec une proportion de létalité observée jusqu'à 90 % (moins d'un mois après contamination) lors de certaines épidémies (WHO Ebola Response Team, 2015; WHO, 2016b). Si l'extrême virulence de cette zoonose* émergente à l'égard de l'Homme peut s'expliquer par l'impasse épidémiologique que représente l'hôte humain pour lequel ce virus (*Filoviridae*) n'est *a priori* pas adapté (Wolfe *et al.*, 2007), l'épidémie récente (2014-2016) en Afrique de l'Ouest (en particulier au Sierra Léone, au Libéria et en Guinée (WHO, 2016a)), de par ses proportions inédites comparées aux précédentes épidémies†, soulève la légitime interrogation de l'évolution de la virulence de ce pathogène manifestement capable de se maintenir dans la population humaine.

Plus précisément, nous avons identifié trois temporalités relatives à l'évolution de la virulence du virus Ébola : l'initiation de la zoonose (qui peut filtrer certains niveaux de virulence), la dynamique initiale (les premiers mois durant lesquels l'intervention sanitaire n'est pas encore opérationnelle), l'attraction évolutive (l'évolution au long cours sous hypothèse d'endémie), ainsi que l'illustre la Figure 0.α.1.

∗. Maladie infectieuse transmise à l'Homme à partir d'un réservoir d'animaux sauvages.

†. Plus de 28000 cas en deux ans contre au plus quelques centaines de cas limités à quelques mois (CDC, 2016).

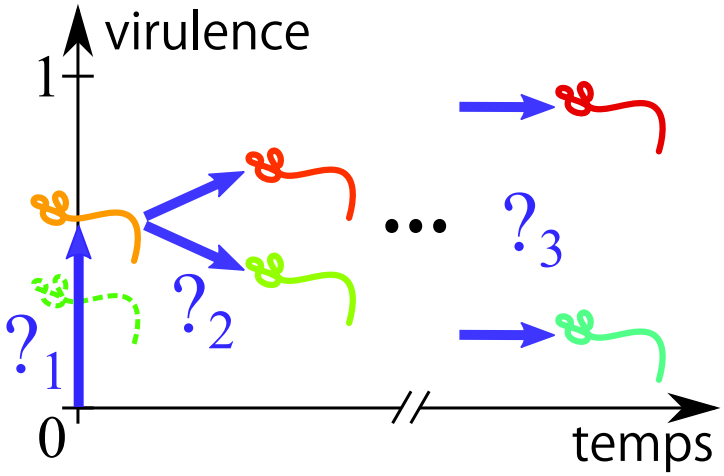

FIGURE 0.α.1. – Les trois questions posées au sujet de la virulence d'EBOV.
Chaque question explore une temporalité distincte de l'épidémiologie évolutive du virus. 1) Quelle est la virulence nécessaire au déclenchement d'une épidémie ? 2) Comment la virulence moyenne varie-t-elle dans les premiers temps d'une épidémie (ici, quelques mois) ? 3) Dans quel sens la virulence est-elle susceptible d'évoluer une fois l'état endémie atteinte ?

Sur la base commune d'un modèle épidémiologique inédit incluant les trois voies de transmission du virus Ébola – contact régulier avec l'hôte infecté vivant, contact rituel avec un cadavre infecté et rapport sexuel avec un survivant de guérison récente – et calibré d'après l'épidémie récente au Libéria, nous traitons chacune des questions illustrées en Figure 0.α.1 par une approche spécifique : respectivement par l'étude du nombre de reproduction de base (cf. équation (i.2.2)), par des équations de PRICE (cf. (i.3.2)) et par l'étude du gradient de sélection de la virulence (cf. (i.3.7)).

Nous montrons pour une large gamme de paramètres que les épidémies humaines de virus Ébola seront vraisemblablement toujours virulentes, quelle que soit la temporalité. Ceci s'explique par la possibilité pour le virus de boucler son cycle de vie comme parasitoïde ainsi qu'une transmission sexuelle limitée. Nous estimons au passage la proportion d'enterrements hygiéniques minimale requise pour induire une contre-sélection de la virulence. De manière générale, nous mettons en évidence l'importance d'une intervention sanitaire précoce, notamment par le biais du contrôle des enterrements.

Le virus Ébola peut-il devenir moins virulent pour l'Homme ?

Mircea T. Sofonea, Lafi Aldakak, Luis F.V.V. Boullosa, Samuel Alizon

Résumé

Comprendre l'évolution de la virulence du virus Ebola est non seulement urgent mais soulève des questions spécifiques dans la mesure où il s'agit de l'un des pathogènes humains les plus virulents et qu'il est capable de se transmettre après la mort de son hôte. En utilisant un modèle épidémiologique à compartiments qui capture les trois voies de transmission du virus Ebola (par contact régulier, via les cadavres et par voie sexuelle), nous inférons la dynamique évolutive de son ratio de létalité de l'initiation de l'épidémie jusqu'au temps long. Nous montrons notamment que le cycle de vie particulier de ce virus impose une sélection pour un niveau de virulence élevé et que ce patron est vérifié sur la gramme biologique des valeurs de paramètres. Outre l'éclairage apporté sur les causes ultimes de la virulence élevée du virus Ebola, ces résultats formulent des prédictions testables et contribuent à l'information des politiques de santé publique. En particulier, la gestion sanitaire des enterrements apparaît comme le mode d'intervention le plus approprié en diminuant le $\mathcal{R}_0$des épidémies tout en sélectionnant pour des souches moins virulentes.

Mots-clés : ratio de létalité, virulence, EBOV, transmission, épidémiologie évolutive, santé publique, compromis évolutifs, épidémie, adaptation

Can Ebola Virus evolve to be less virulent in humans?

Mircea T. Sofonea, Lafi Aldakak, Luis Fernando Boullosa, Samuel Alizon

Abstract

Understanding Ebola Virus (EBOV) virulence evolution is not only timely but also raises specific questions because it causes one of the most virulent human infections and it is capable of transmission after the death of its host. Using a compartmental epidemiological model that captures three transmission routes (by regular contact, via dead bodies and by sexual contact), we infer the evolutionary dynamics of case fatality ratio (CFR) on the scale of an outbreak and on the long term. Our major finding is that the virus's specific life cycle imposes selection for high levels of virulence and that this pattern is robust to parameter variations in biological ranges. In addition to shedding a new light on the ultimate causes of EBOV's high virulence, these results generate testable predictions and contribute to informing public health policies. In particular, burial management stands out as the most appropriate intervention since it decreases the $\mathcal{R}_0$ of the epidemics, while imposing selection for less virulent strains.

Keywords : case fatality ratio ; virulence ; EBOV ; transmission ; evolutionary epidemiology ; public health ; trade-offs ; outbreak ; adaptation

Citation: Sofonea MT, Aldakak L, Boullosa LFVV, Alizon S. 2017. Can Ebola Virus evolve to be less virulent in humans? *bioRxiv* 108589, ver. 3 of 19th May 2017; doi: 10.1101/108589, (peer-reviewed and recommended by Peer Community In Evolutionary Biology (Ravigné & Blanquart, 2017))

Impact Summary

The severe haemorrhagic fever caused by Ebola Virus (EBOV) usually kills more than one infected individual out of two in the absence of treatment, which makes this pathogen one of the most virulent known to humans. The recent outbreak in West Africa (2013-2016) revealed that the virus is able to spread and persist for months across countries. It is often thought that virulence could be due to the fact that the virus is adapted to its reservoir host. Given that microbes evolve rapidly, it is important to determine whether EBOV virulence is likely to decrease as the virus adapts to its human host. To address this problem, we developed a novel mathematical model tailored to EBOV's life cycle, notably by capturing its three main transmission routes (by regular contact, sexual contact and via dead bodies). We investigated the evolutionary trends of EBOV's virulence on different time scales (outbreak initiation, short term and long term). Our results reveal that the virulence of EBOV might not be due to the maladaptation of the virus, but could rather originate from its unique life cycle. These results are robust to the parameter values chosen. From a public health perspective, burial management stands out as the main leverage to fight the virulence of EBOV, both on the short and long terms.

0.1. Introduction

Ebola Virus (EBOV) has been a major source of fear since its discovery in 1976. Until 2013, all outbreaks could be traced to spillover from reservoir hosts (Leroy *et al.*, 2005) and were limited in size. This was attributed to EBOV's extremely high case fatality ratio (CFR), that is the ratio of infected hosts who die from the infection, which we use here as a measure of infection virulence. The dramatic 2013-2016 epidemic in West Africa, which caused more than 28,000 infections and claimed at least 12,000 lives, showed that the virus can persist in the human population for months, therefore raising the question: 'How will the virulence of Ebola Virus evolve in humans?' (Kupferschmidt, 2014).

Being an RNA virus, Ebola is prone to rapid evolution (de La Vega *et al.*, 2015) and *in vitro* analyses suggest that the virus has evolved during the outbreak towards an increased tropism for human cells (Urbanowicz *et al.*, 2016). It was first thought that host-parasite interactions should always evolve towards benignity because mild strains seem to have a transmission advantage over strains that kill their hosts rapidly (Méthot, 2012). Since the 1980s, evolutionary biologists have shown that parasite virulence can be adaptive because it may correlate with transmissibility or within-host competitiveness (for a review, see Alizon & Michalakis (2015)). The avirulence theory does remain prevalent in many fields. For instance, some envisage a decrease in EBOV virulence due to host adaptation Kupferschmidt (2014), even though we know the virulence of some human infectious diseases such as HIV or tuberculosis has followed an increasing trend since their emergence (Gagneux, 2012; Herbeck *et al.*, 2012).

Studying virulence as a potentially adaptive trait for the parasite requires encompassing the whole epidemiological life cycle of the infectious agent (Alizon & Michalakis, 2015). In the case of Ebola Virus, most individuals acquire the infection after direct contact with blood, bodily secretions or tissues of other infected humans whether alive or dead (Bausch *et al.*, 2007). This *post-mortem* transmission route cannot be neglected in Ebola Virus epidemics (Chan, 2014), although its magnitude is likely to be low compared to direct transmission (Weitz & Dushoff, 2015). From an evolutionary standpoint, this route might be crucial as well since the timing of life-history events can dramatically affect virulence evolution (Day, 2003). Intuitively, if the virus is still able to transmit after host death, virulence will have a smaller effect on the parasite's transmission potential. Moreover, there is an increasing evidence that EBOV might also be transmitted through sexual contact even long after the clinical 'clearance' of the infection since the virus can persist in the semen for months (Eggo *et al.*, 2015; Thorson *et al.*, 2016; Uyeki *et al.*, 2016).

Will EBOV become more virulent by adapting to humans? To address this question, we use mathematical modelling to determine how case fatality ratio affects the risk of emergence, how it evolves on the long and on the short term. To this end, we introduce an original epidemiological model that captures all three transmission routes of the virus in human populations. We parametrize our model with data from the well-documented 2013-2016 epidemics. We also perform sensitivity analyses on conservative biological ranges of parameter values to verify the robustness of our conclusions.

We find that EBOV undergoes selection for higher case fatality ratios due to its life cycle that includes transmission from hosts after death. This result is robust to most parameter values within biological ranges. We also show that short-term evolutionary dynamics of virulence are more variable but consistently depend on the duration of the incubation period. Finally, we investigate how public health interventions may affect EBOV virulence evolution. We find a direct, but limited, effect of safe burials that may decrease the spread of the virus, while favouring less virulent strains over more virulent ones.

0.2. Methods

For clarity, most of the technical details are shown in Supplementary materials and this section contains verbal description of the model, Figures illustrating the life cycle and a list of parameter values.

0.2.1. Epidemiological model

Our original compartmental model is based on the classical Susceptible-Exposed-Infected-Recovered ($SEIR$) model, which we enhanced by adding a convalescent class (C) that allows for sexual transmission (Abbate *et al.*, 2016) and an infected dead body class (D) that allows for *post-mortem* transmission (Legrand *et al.*, 2007; Weitz & Dushoff, 2015). The model is deterministic and does not include additional host heterogeneity, spatial structure or public health interventions.

We incorporated demography through a host inflow term λ and a baseline mortality rate μ. Susceptible individuals (S) can become infected by regular contact with symptomatic infected individuals (I) (WHO Ebola Response Team, 2014), by sexual contact with convalescent individuals (C) (Mate *et al.*, 2015) and by contact with the dead body of EVD victims, mostly during ritual practices (D) (Chan, 2014). The rates at which these events occur are proportional to β_I, β_C and β_D respectively. As in most models (Keeling & Rohani, 2008), we assumed sexual transmission to be frequency-dependent. For non-sexual transmission, we assumed density-dependent transmission following an analysis of the 2013-2016 epidemic (Leander *et al.*, 2016), although performed at a smaller scale than ours. The total population size of live hosts is denoted N.

Upon infection, susceptibles move to the so-called 'exposed' class (E), meaning they are infected but not yet infectious. For Ebola Virus infections, this latency period is also the incubation period, i.e. the time from the contamination to the onset of the symptoms. These symptoms arise at a rate ω.

At the end of this latency/incubation period, individuals move to the symptomatic infected compartment (I). They leave this compartment at a rate γ, which we calibrated using the average time elapsed from the onset of the symptoms to death or recovery. We hereafter refer to this as the 'symptomatic period'. The probability that an infected individual survives the infection is $1-\alpha$. The case fatality ratio (CFR), α, is our measure of virulence (we hereafter assume uncorrelated with the symptomatic infectious period γ).

We assumed that infected individuals who survive the infection clear the virus from their bloodstream but not from other fluids such as semen and may therefore still transmit EBOV through sexual contacts (Deen *et al.*, 2015). These convalescent individuals (C) completely eliminate EBOV at a rate σ. Notice that given the severity of the symptoms (Feldmann & Geisbert, 2011) and the fact that the convalescence period is one order of magnitude greater than the symptomatic period, we neglected the sexual transmission from symptomatic infected individuals (I).

Based on the current immunological data (Sobarzo *et al.*, 2013), we assumed that full elimination of EBOV from convalescent hosts confers lifelong immunity to recovered individuals (R), who do not contribute to the epidemiology.

On the contrary, infected individuals who die from the disease may continue to transmit EBOV if their burial is performed in unsafe conditions, which occurs at a probability θ. There is little data from which to estimate this parameter. However, the proportion of EBOV-positive dead bodies has been estimated to decline from 35% to 5% by the end of 2014 in the most populous county of Liberia (Nyenswah *et al.*, 2016). We therefore set the

default value $\theta = 0.25$. In the analysis, we strongly vary this parameter since it represents an important leverage public health policies have on the epidemics. In the absence of burial team intervention, body fluids from dead bodies remain infectious for a period ε^{-1} which is known to be less than 7 days in macaques (PRESCOTT *et al.*, 2015).

Our model, pictured in Figure 0.2.1, consists in a set of Ordinary Differential Equations (ODEs) shown in Supplementary Material 0.a.

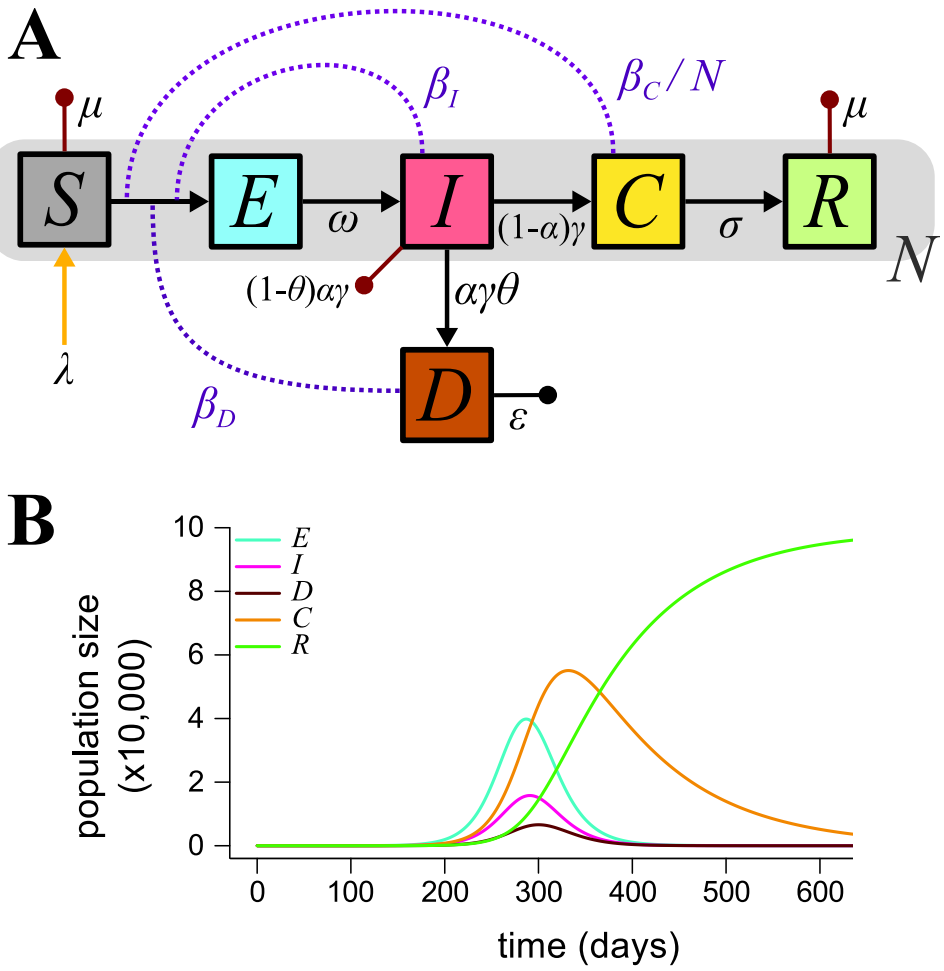

Figure 0.2.1. – Epidemiology of Ebola Virus in humans.
A) Epidemiological life cycle of Ebola Virus in humans and B) Population dynamics for default parameters. S, E, I, C, R and D are host densities that correspond to the following compartments: susceptible, exposed (infected but not yet infectious), symptomatic infected, convalescent, recovered (immunised) and dead bodies respectively. N is the total living population size. Lower-case letters are rate and flow parameters, the description of which is given in Table 0.2.1.

Table 0.2.1 lists the 11 model parameters. Their values were calibrated using data from the 2013-2016 epidemic in West Africa. We worked at a country level and preferentially chose estimates from the Liberia outbreak, because with approximately 10,000 cumulative cases (WHO, 2016a), its magnitude lies in between that of Sierra Leone and Guinea. Demography data from Liberia were obtained from publicly available data from the Central Intelligence Agency (CIA, 2016). The newborn inflow was set such that the disease free equilibrium matches the country's population size.

Notation	Description	Default value	Reference or inference
λ	Host inflow	$2 \cdot 10^2$ ind.day^{-1}	such that $\lambda/\mu \approx 4 \cdot 10^6$, (CIA, 2016)
μ	Host baseline mortality rate	$4.5 \cdot 10^{-5}$ day^{-1}	
b_I	Regular contact transmission factor (from infectious hosts)	10^{-7} ind^{-1}.day^{-1}	with the constraint $\mathcal{R}_{0,I} \approx 10\mathcal{R}_{0,D}$, $\mathcal{R}_{0,I} \approx 10^2\mathcal{R}_{0,C}$ and $\mathcal{R}_0 \approx 1.8$ (WHO Ebola Response Team, 2014; Weitz & Dushoff, 2015; Abbate *et al.*, 2016)
b_C	Sexual transmission factor (from convalescent hosts)	10^{-4} day^{-1}	
b_D	*Post- mortem* transmission factor (from dead hosts)	10^{-8} ind^{-1}.day^{-1}	
ω	Inverse of latency period	10^{-1} day^{-1}	(WHO Ebola Response Team, 2014)
α	Case fatality ratio	0.7	
γ	Inverse of symptomatic infectious period	0.25 day^{-1}	(Abbate *et al.*, 2016)
θ	Unsafe burial proportion	0.25	(Nyenswah *et al.*, 2016)
ε	Inverse of *post mortem* infectious period	10^{-1} day^{-1}	(Prescott *et al.*, 2015)
σ	Elimination rate of convalescent hosts	10^{-2} day^{-1}	(Uyeki *et al.*, 2016; Abbate *et al.*, 2016)

Table 0.2.1. – Parameter list, description and default values.
See the main text for further details about the calibration of the transmission constants. Note that the sexual transmission constant is higher because it involves frequency-dependent transmission. ind stands for individuals. When used in the main text or in the appendix, these estimated values are denoted by a hat.

In Supplementary Material 0.c, we calculate the basic reproduction number of EBOV (denoted $\mathcal{R}_0$), which is the average number of secondary infections caused by a single infected individual in a fully susceptible population (Diekmann *et al.*, 1990). By studying the local stability of the system (0.a.1) at the disease free equilibrium, we found that

$$\mathcal{R}_0 = \frac{\beta_I}{\gamma} S_0 + \frac{\alpha\theta\beta_D}{\varepsilon} S_0 + \frac{(1-\alpha)\beta_C}{\sigma}, \tag{0.2.1}$$

where $S_0 = \lambda/\mu$ is the total population size before the epidemic. The three terms in $\mathcal{R}_0$ correspond to each transmission route: from symptomatic individuals ($\mathcal{R}_{0,I} := \beta_I S_0/\gamma$), infectious bodies ($\mathcal{R}_{0,D} := \alpha\theta\beta_D S_0/\varepsilon$), and convalescent individuals ($\mathcal{R}_{0,C} := (1-\alpha)\beta_C/\sigma$). Notice that the incubation period does not affect $\mathcal{R}_0$.

0.2.2. Transmission-virulence trade-off and estimated values

Trade-offs are a central component of evolutionary model and, without them, predictions tend to be trivial (e.g. viruses should evolve to maximise their transmission rates and minimise their virulence). Although the EBOV life cycle generates constraints that may lead to non-trivial evolutionary outcomes, we do also allow for an explicit trade-off between CFR and transmission rates. Such a relationship has been shown in several host-parasite systems (Alizon & Michalakis, 2015). The case of HIV is particularly well documented (Fraser *et al.*, 2014): viruses causing infections with higher viral loads have increased probability to be transmitted per sexual contact, while causing more virulent (shorter) infections. As a result, there exists an optimal intermediate viral load that balances the virus benefits of transmission with the costs of virulence, thus maximising the number of secondary infections.

In the case of EBOV, there is indirect evidence that viral load is positively correlated with case fatality ratio (CFR) since survivor hosts tend to have lower viral loads than non-survivors (Towner *et al.*, 2004; Crowe *et al.*, 2016). Viral load is thought to correlate with transmission (Osterholm *et al.*, 2015) but demonstrating a clear link is challenging (for HIV, it has required identifying sero-discordant couples in cohorts).

We assumed an increasing relationship between transmission rates and CFR (α) such that:

$$\beta_H(\alpha) := b_H \alpha^p, \tag{0.2.2}$$

where b_H is a constant factor, $p \in \mathbb{R}_+$ is a parameter capturing the concavity of the trade-off curve and H stands for one of the compartment I, D or C. The exact value of p results from within-host interactions (Alizon & van Baalen, 2005) but one can identify four kinds of trade-offs: $p > 1$ corresponds to an amplifying transmission benefit from increasing CFR, $p = 1$ corresponds to a linear relationship between transmission and CFR, $0 < p < 1$ corresponds to a saturating transmission benefit from increasing CFR and $p = 0$ is the degenerate case without trade-off. From a biological standpoint, we could expect different transmission routes to have different trade-off shapes (p) but, as we show here, our results are largely independent of p.

Transmission rates being difficult to estimate (Leander *et al.*, 2016), we indirectly infer the order of magnitudes of b_I, b_C and b_D by setting the $\mathcal{R}_0$ close to 2, that is its approximate value for the 2014 epidemic (WHO Ebola Response Team, 2014). Since $\mathcal{R}_0$ is the sum of the epidemiological contributions of each transmission route (see equation (0.2.1)), we added the constraint that, according to previous studies, transmission from symptomatic individuals contributes about ten times more than transmission from dead bodies (WHO Ebola Response Team, 2014; Weitz & Dushoff, 2015) and one hundred times more than transmission from convalescent individuals (Abbate *et al.*, 2016). Straightforward calculations (analogous to those done for sensitivity analysis in Supplementary Material 0.e) resulted in attributing the orders of magnitude shown in Table 0.2.1.

In the following, the exponent p was left undetermined, but its value was set to 0 for the estimation of b_H in the null hypothesis. This leads to $\mathcal{R}_0 \approx 1.86$, which is very close to the WHO mean estimation for the Liberia epidemic, namely 1.83 (WHO Ebola Response Team, 2014).

0.2.3. Long term evolution

We used the adaptive dynamics framework (Geritz *et al.*, 1998), which assumes that evolution proceeds by rare and small phenotypic mutations occurring in a monomorphic population that has reached ecological stationarity. Polymorphism is therefore limited to transient dimorphic phases where the ancestor (hereafter called the 'resident') and its mutant compete. Depending on the outcome of the competition, the system either goes back to the previous endemic equilibrium or reaches a new monormophic equilibrium. The corresponding dynamical system is shown in Supplementary Material 0.a (system (0.a.2) applied to $n = 2$).

Given the focus of this study, we assumed that the resident and the mutant only differ in their CFR (and in their transmission traits if there was a transmission-virulence trade-off). We denoted the virulence of the mutant and the resident by α' and α respectively. α' was assumed to be close to α. Since the mutant is rare by definition, its emergence can be assumed not to affect the resident system. We therefore investigated the local stability of the related endemic equilibrium. This only depended on the local stability of the mutant

sub-system (E_2, I_2, D_2, C_2) to which we applied the next-generation theorem (Diekmann *et al.*, 1990; Hurford *et al.*, 2010). This eventually led (see Supplementary Material 0.c.3) to the mutant relative reproduction number

$$\mathcal{R}(\alpha', \alpha) = \frac{\frac{\beta_I(\alpha')}{\gamma} + \frac{x\theta\beta_D(\alpha')}{\varepsilon} + \frac{(1-\alpha')\beta_C(\alpha')}{\sigma\widetilde{N}(\alpha)}}{\frac{\beta_I(\alpha)}{\gamma} + \frac{\alpha\theta\beta_D(\alpha)}{\varepsilon} + \frac{(1-\alpha)\beta_C(\alpha)}{\sigma\widetilde{N}(\alpha)}}, \tag{0.2.3}$$

where there total host population size can be approximated (see Supplementary Material 0.b) by

$$\widetilde{N}(\alpha) \approx (1-\alpha)S_0 + \frac{\alpha}{\frac{\beta_I(\alpha)}{\gamma} + \frac{\alpha\theta\beta_D(\alpha)}{\varepsilon}}. \tag{0.2.4}$$

We then calculated the selection gradient by differentiating the relative reproduction number (equation (0.2.3)) with respect to the mutant's trait (Otto & Day, 2007). Equating the mutant and resident trait value we eventually found

$$\Delta(\alpha) = \frac{p}{\alpha} + \frac{\frac{\theta b_D}{\varepsilon}\widetilde{N}(\alpha) - \frac{b_C}{\sigma}}{(1-\alpha)\frac{b_C}{\sigma} + \left(\frac{b_I}{\gamma} + \frac{\theta b_D}{\varepsilon}\alpha\right)\widetilde{N}(\alpha)}. \tag{0.2.5}$$

The sign of Δ indicates the way natural selection acts on the trait depending on the resident's trait.

0.2.4. Short term evolution

Viruses evolve so rapidly that evolutionary and epidemiological dynamics may overlap. The epidemiological Price equation framework is designed to predict short-term evolution based on standing genetic variation (Day & Proulx, 2004; Day & Gandon, 2006).

Practically, we assumed that the parasite population is initially diverse and consists of n different genotypes, each genotype i being defined by a specific value for several phenotypic traits of interest: the case mortality (α_i), the rate of end of latency (ω_i), the rate of end of the infectious period (γ_i), the rate at which dead bodies cease to be infectious (ε_i), the rate at which convalescent hosts clear the infection (σ_i) and the transmission rates ($\beta_{D,i}$, $\beta_{I,i}$ and $\beta_{C,i}$).

The dynamics of the populations of interest are described by $4n+1$ ODEs that are shown in Supplementary Material 0.a.

After thorough calculations (in Supplementary Material 0.f) we find that, if we neglect mutational bias, mean traits in each compartment vary according to a system of ODEs that involves statistical covariances and variances of traits in the different compartments. The equations involving average CFR are shown in the Results section.

An important assumption of this Price equation approach is that covariance terms are assumed to be constant, which implies that predictions are only valid on the short term. Given that the main limitation of the adaptive dynamics framework relies in its assumption that epidemiological dynamics are fast compared to evolutionary dynamics, combining the two frameworks allows us to get a broader picture.

0.3. Results

0.3.1. Virulence and emergence

We first consider the risk for an epidemic to occur as a function of EBOV virulence, trade-off shape and burial management. A disease spreads in a fully susceptible population if its reproduction number ($\mathcal{R}_0$) is greater than unity (Anderson & May, 1981). Using our default parameters values (Table 0.2.1), we show in Figure 0.3.1 that the most virulent EBOV strains are almost always the most likely to emerge, independently of the trade-off exponent p and of proportion of unsafe burials θ. To have $\mathcal{R}_0$ decrease with α, one needs to have neither trade-off nor unsafe burials ($\theta = p \approx 0$). However, with our default parameter values this decrease is limited.

If we focus on the lowest virulence that may lead to an epidemic (denoted $\alpha_{\min}$), we find that with our default parameter values burial management can prevent emergence (that is bring $\mathcal{R}_0$ below unity by moving vertically in Figure 0.3.1) only if the transmission-virulence trade-off is strong enough (the green, blue and cyan curves).

In the following, we will generally assume that EBOV is adapted enough to persist in the human population ($\mathcal{R}_0 > 1$). Since outbreak originates via spillover from reservoir hosts (Leroy *et al.*, 2000), it is likely that the virus is maladapted in the first human infections. However, to capture these dynamics, an evolutionary rescue formalism would be more appropriate given the importance of stochastic events and this is outside the scope of this study (for a review, see Gandon *et al.* (2013)).

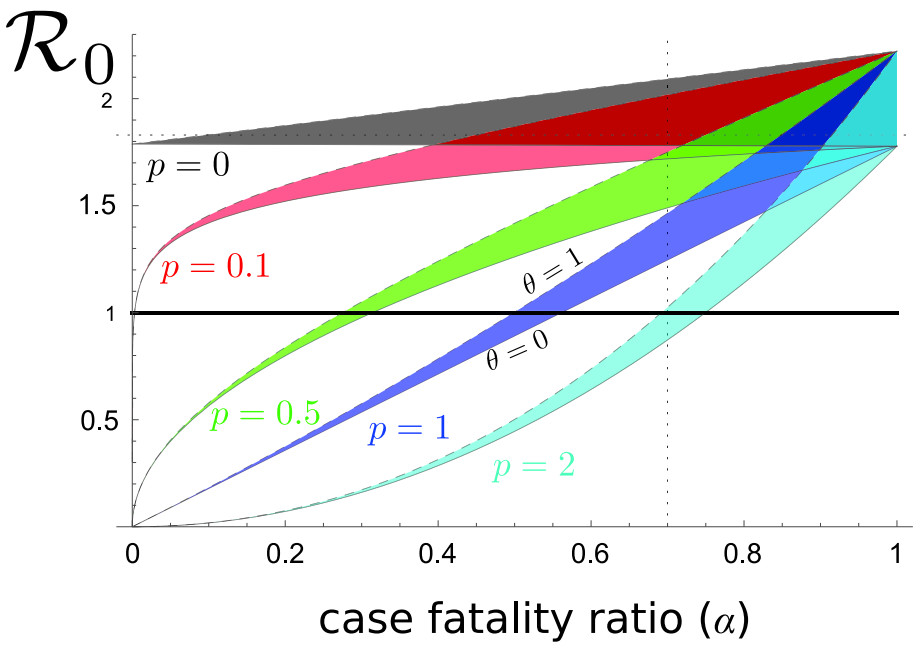

Figure 0.3.1. – Basic reproduction number as a function case fatality ratio (α), unsafe burial ratio and trade-off shape.
Colors indicate five trade-off scenarios: absence ($p = 0$, in grey), very weak ($p = 0.1$, in red), concave ($p = 0.5$, in green), linear ($p = 1$, in dark blue), and convex ($p = 2$, in light blue). The width of the coloured regions corresponds to variations in the unsafe burial ratio from completely unsafe ($\theta = 1$, dashed upper bound) to completely safe ($\theta = 0$, solid lower bound). The intersection between the horizontal line and the colored areas indicates the range of $\alpha_{\min}$ for each scenario. The dotted gridlines show the α and $\mathcal{R}_0$ estimates from the literature. Other parameter values are in Table 0.2.1. See Supplementary Material 0.d.4 for more details.

0.3.2. Long-term virulence evolution

If the selection gradient in equation (0.2.5) is negative for any CFR ($\Delta(\alpha) < 0$), then the virus population evolves towards its lowest virulence that allows persistence (that is $\alpha_{\min}$). If the gradient is always positive ($\Delta(\alpha) > 0$), the CFR evolves towards 1. Intermediate levels of virulence can only be reached if there exists $\alpha^\star$ such that $\Delta(\alpha) \geq 0$ for $\alpha \leq \alpha^\star$, $\Delta(\alpha) \leq 0$ for $\alpha \geq \alpha^\star$ and $\mathcal{R}(\alpha, \alpha^\star) < 1$ for any $\alpha \neq \alpha^\star$. We show in Supplementary Material 0.d.4 that this occurs only if the proportion of unsafe burials (θ) and the trade-off parameter (p) are lower than the following boundaries

$$\theta < \frac{b_I b_C \varepsilon}{\gamma \sigma b_D} \text{ and } p < \frac{b_C}{\sigma}, \tag{0.3.1}$$

Unless these two conditions are met, the selection gradient is always positive and EBOV is expected to always evolve towards higher case fatality ratios ($\alpha^\star = 1$). Rewriting the first inequality as $\frac{\theta b_D S_0}{\varepsilon} < \frac{b_I S_0}{\gamma} \times \frac{b_C}{\sigma}$ highlights that virulence is favoured by natural selection as soon as the *post mortem* transmission component is greater than the product of the symptomatic and convalescent transmission components.

Figure 0.3.2 shows how $\alpha^\star$ is numerically affected by a change in burial management (θ) and trade-off strength (p). Unless the proportion of safe burials is brought below 4%, and unless there is a weak trade-off ($p < 0.01$), CFR will remain high. Intuitively, this double condition can be understood in the following way. If the trade-off is negligible,

the CFR is weakly linked to transmission by regular contact and therefore selection on α only weakly depends on this component of the life cycle. As a consequence, the value of θ governs the relative importance of the two transmission routes that matter. *Post mortem* transmission always favours higher CFR, whereas the sexual transmission route can be maximised for intermediate levels of virulence (see Supplementary Material 0.h).

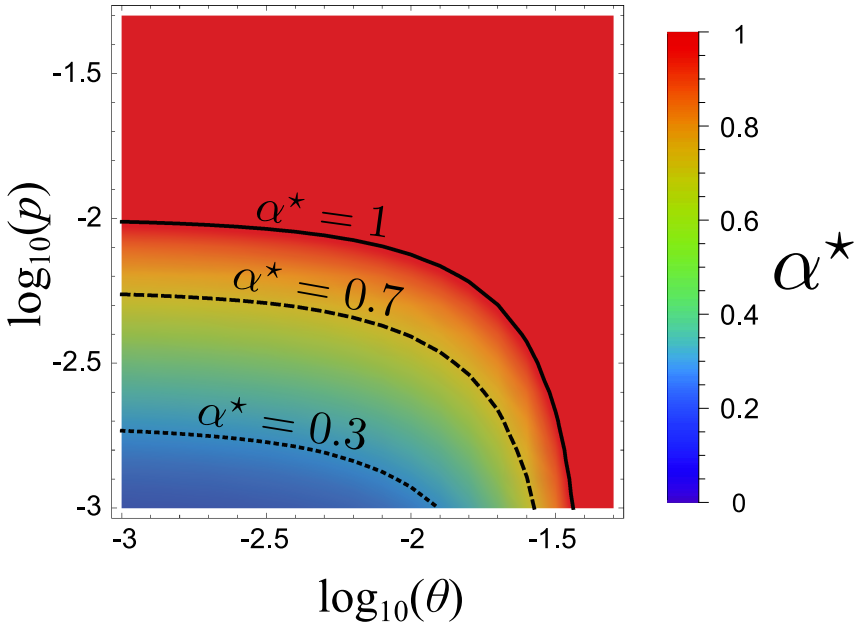

Figure 0.3.2. – Evolutionary stable virulence ($\alpha^\star$) as a function of unsafe burial ratio (θ) and trade-off exponent (p).
The solid, dashed and dotted lines correspond to $\alpha^\star = 1$, 0.7 and 0.3 respectively. Parameter vlaues are shown in Table 0.2.1. See Supplementary Material 0.d.4 for more details.

It was not possible to find an explicit expression for the long-term equilibrium virulence ($\alpha^\star$), but we found it lies in the following interval (Supplementary Material 0.d.5):

$$\alpha^\star \in \left[\frac{p}{\frac{b_C}{\sigma} - \frac{\theta\frac{b_D}{\varepsilon}}{\frac{b_I}{\gamma}+\theta\frac{b_D}{\varepsilon}}}, \frac{\left(\left(\frac{b_I}{\gamma}+\theta\frac{b_D}{\varepsilon}\right)S_0 + \frac{b_C}{\sigma}\right)p}{(1+p)\frac{b_C}{\sigma} - \theta\frac{b_D}{\varepsilon}S_0} \right]. \tag{0.3.2}$$

The lower bound of this interval increases with trade-off strength (p) and intensity of the *post mortem* transmission route ($\theta b_D/\varepsilon$). If *post mortem* transmission is strongly reduced, owing to a safer burial management ($\theta \to 0$), the lower bound simplifies to $p\sigma/b_C$. The long-term virulence then appears to be a balance between trade-off strength and sexual transmission intensity, which is consistent with our intuitive explanation of the condition for an intermediate virulence to be selected. In particular, any decrease in the time for convalescent hosts to clear the virus (i.e. increase in σ) will increase the lower bound for CFR.

To further assess the robustness of these results, we performed a sensitivity analysis by varying the relative importance of each transmission route (regular contact, sexual transmission and transmission from dead bodies), while keeping the total value of $\mathcal{R}_0$ constant. As shown in Figure 0.3.3, unless the values of p are extremely low, variations in the relative transmission routes is unlikely to be sufficient to move our default value (dotted lines) to the region where low virulences (e.g. $\alpha < 50\%$) are favored (green

area). To give a quantitative estimate, the relative importance of transmission via sexual contact (on the vertical axis) would need to be about 40 times greater than the current estimates to bring the current estimate above the blue separatrix, which already assumes a low trade-off and a perfect burial management.

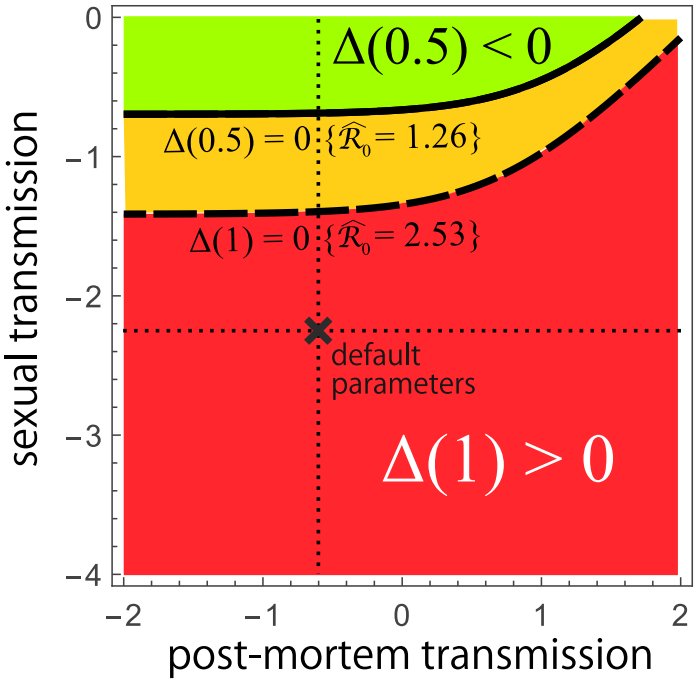

Figure 0.3.3. – Sensitivity analysis of long-term virulence evolution.
The graphic shows the sign of the selection gradient for virulence when varying the relative weight (in orders of magnitude) of the *post-mortem* transmission component ($\log_{10}(\delta)$, on the x-axis) and the sexual transmission component ($\log_{10}(\kappa/S_0)$, on the y-axis) in the overall transmission of EBOV. When the basic reproduction number is set at its upper bound ($\widehat{\mathcal{R}_0} = 2.53$, dashed line), the selection gradient at the maximum virulence ($\alpha = 1$) is positive below the dashed line (red area). When the basic reproduction number is set at its lower bound ($\widehat{\mathcal{R}_0} = 1.26$, plain line), the selection gradient is also positive for a range of virulence higher than one half ($\alpha \geq 50\%$) in the orange area. It is negative for lower virulences ($\alpha < 50\%$) above the dashed line (green area). The unsafe burial proportion and the trade-off exponent are low ($\theta = 0$ and $p = 0.1$). See Supplementary Material 0.e for more details.

0.3.3. Short term evolutionary dynamics

Reaching an evolutionary equilibrium may take time (especially if strains have similar trait values) and the transient dynamics can be non-trivial because the system is non-linear. The Price equation framework provides a way to qualitatively address the initial trends of average trait values, by considering the initial diversity in the virus population.

If we denote by $\overline{x}^H$ the average value of trait x in compartment H and by $\mathrm{cov}_H(x, y)$ the statistical covariance between traits x and y in compartment H (which becomes the statistical variance $\mathrm{var}_H(x)$ if $x \equiv y$), the dynamics of average virulence in the four infected compartments satisfy the following ODEs (see Supplementary Material 0.f for further

details):

$$\frac{\mathrm{d}\overline{\alpha}^I}{\mathrm{d}t} = -\mathrm{cov}_I\left(\alpha,\gamma\right) + \left(\mathrm{cov}_E\left(\alpha,\omega\right) + \left(\overline{\alpha}^E - \overline{\alpha}^I\right)\overline{\omega}^E\right)\frac{E_\bullet}{I_\bullet}, \tag{0.3.3}$$

$$\frac{\mathrm{d}\overline{\alpha}^E}{\mathrm{d}t} = -\mathrm{cov}_E\left(\alpha,\omega\right) + \frac{S}{E_\bullet}\sum_{H\in\{I,D,C\}}\left(\mathrm{cov}_H\left(\beta_H,\alpha\right) + \left(\overline{\alpha}^H - \overline{\alpha}^E\right)\overline{\beta_H}^H\right)H_\bullet, \tag{0.3.4}$$

$$\frac{\mathrm{d}\overline{\alpha}^D}{\mathrm{d}t} = -\mathrm{cov}_D\left(\alpha,\varepsilon\right) + \left(\mathrm{var}_I\left(\alpha\right) + \overline{\alpha}^I\left(\overline{\alpha}^I - \overline{\alpha}^D\right)\right)\theta\gamma\frac{I_\bullet}{D_\bullet}, \tag{0.3.5}$$

$$\frac{\mathrm{d}\overline{\alpha}^C}{\mathrm{d}t} = -\mathrm{cov}_C\left(\alpha,\sigma\right) + \left(\mathrm{cov}_I\left(\alpha,\gamma\right) - \gamma\mathrm{var}_I\left(\alpha\right) + \left(1-\overline{\alpha}^I\right)\left(\overline{\alpha}^I - \overline{\alpha}^C\right)\overline{\gamma}^I\right)\frac{I_\bullet}{C_\bullet}, \tag{0.3.6}$$

where $H_\bullet := \sum_{i=1}^{n} H_i$ denotes the total size of compartment $H \equiv E,I,D,C$.

Focusing on the compartment on which virulence acts, namely the symptomatic individuals, indicates that the short-term evolution of the average virulence $\overline{\alpha}^I$ is mainly governed by the correlations between this trait and the symptomatic and latency periods. More explicitly, equation (0.3.3) states that if the most virulent strains induce the longest symptomatic period and/or the shortest latency periods, the average virulence in I can be expected to increase at the beginning of the epidemic. Intuitively, newly symptomatic individuals are more likely to have been infected with a highly virulent strain.

Equation (0.3.3) contains a third term proportional to $\overline{\alpha}^E - \overline{\alpha}^I$, which is more difficult to apprehend. Indeed, $\overline{\alpha}^E$ varies as well and follows a complicated ODE that involves not only the correlation with the latency period but also correlations with the transmission rates (equation (0.3.4)). This diversity of components make both $\overline{\alpha}^E$ and $\overline{\alpha}^I$ difficult to predict early in the epidemics.

We therefore simulated epidemics numerically according to system (0.a.2). We considered nine scenarios of increasing complexity, three of which are shown in Figure 0.3.4 (see Supplementary Material 0.g for more details). During the first six months of an (unmanaged) epidemic, average virulence exhibits wide variations. In most scenarios (panels A and B), it tends to evolve towards the maximum of the range provided by its initial polymorphism. Transient evolution for further virulence in an expanding epidemic have been highlighted by previous models (Day & Proulx (2004), e.g.) and studies (Berngruber *et al.*, 2013) but this effect was due to a positive correlation between virulence and transmission rates, which is here not required (Figure 0.3.4A). Unsurprisingly, the addition of such correlation amplifies the transient increase in virulence observed during the approximately first 300 days after the onset of the epidemic (Figure 0.3.4B).

A scenario where average virulence decreases initially is when it is positively correlated with the latency period (Figure 0.3.4C). This occurs because less virulent strain have an advantage early in the epidemics by reaching the infectious class earlier. More virulent strains become more frequent again when the value of D begins to take off (Figure 0.3.4B).

A secondary result shown in these figures is that dead bodies (in brown) always carry more virulent strains on average.

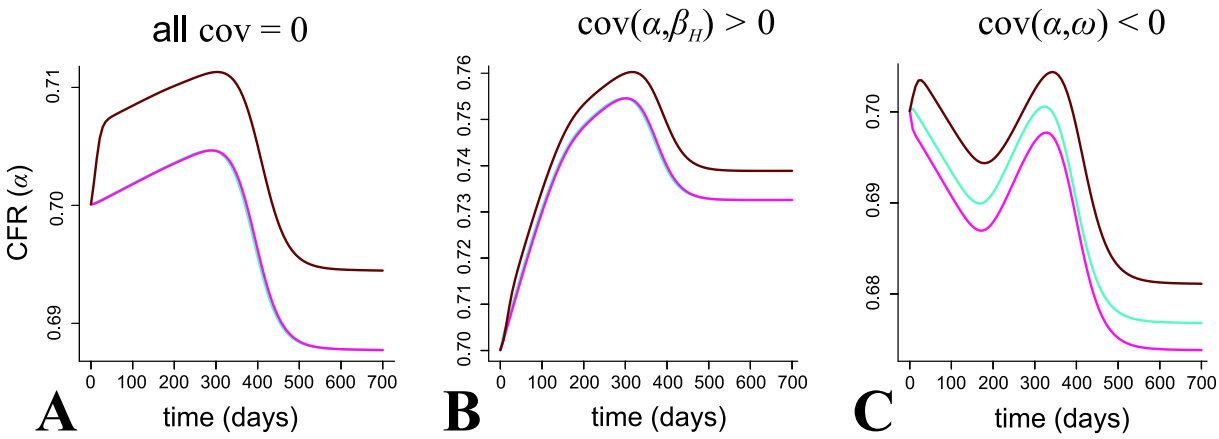

Figure 0.3.4. – Short-term evolution of CFR with standing genetic variation in three scenarios.

A) Without correlations between traits, B) with a positive correlation between CRF and transmission rate and C) with a negative correlation between CRF and latency period. The CFR averaged over the exposed individuals ($\overline{\alpha}^E$) is depicted in cyan, over the symptomatic individuals ($\overline{\alpha}^I$) in pink and over the infectious dead bodies ($\overline{\alpha}^D$) in brown. Parameter values are shown in Table 0.2.1. See Supplementary Material 0.g for details about the simulations.

0.4. Discussion

0.4.1. Virulence could be adaptive for EBOV

Ebola Virus is one of the deadliest human pathogen (Feldmann & Geisbert, 2011). The recent epidemic in West Africa has shown that it can transmit for months months among humans throughout entire countries. As any microbe (especially RNA viruses), it is likely exposed to fast evolution during the course of the epidemic. From a public health standpoint, it is important to predict Ebola virus' next move and the current hope is that the shift from an emerging to an endemic lifestyle could favour less virulent strains (Kupferschmidt, 2014).

Predicting virulence evolution is usually challenging because we tend to lack details about correlations between epidemiological parameters. Furthermore, even when there is data to estimate a trade-off relationship, its exact shape can have huge quantitative and even qualitative effects on the evolutionary dynamics of the trait (Alizon & van Baalen, 2005; Svennungsen & Kisdi, 2009). Our results stand out because they are robust both to parameter variation in wide biological ranges (WHO Ebola Response Team, 2014, 2015) and also to the type of trade-off assumed. Importantly, the numerical analysis of the model show that our results still hold even if there is no transmission-virulence trade-off at all, as long as the burial management is not perfect ($\theta > 5\%$).

In addition to the strong selection on EBOV virulence due to its transmission via dead bodies, another striking result is that decreasing the ratio of unsafe burials is triply effective. First, it decreases the spread of the virus (i.e. its $\mathcal{R}_0$). Second, in the short term, it can help limit a transitory increase in virulence. Indeed, in the first weeks of an epidemic, the sexual transmission route is negligible compared to the other routes that are maximised for the highest CFR values. Third, in the long term, decreasing the proportion of unsafe burials is necessary to shift the selective pressure in favour of less virulent strains.

Overall, EBOV is unlikely to evolve to become less virulent because that would require two conditions. First, the proportion of unsafe burials must be brought to a very low value, which we estimate to be lower than 4%. Second, there must be very little or no genetic relationship between EBOV case fatality ratio and transmission rate. This latter condition is particularly frustrating because it cannot directly be addressed by public health policies. Finally, even if these conditions are met, the level of virulence reached in the long term may still be high, especially if sexual transmission is limited. On a more positive note, results from the Price equation approach show that the virus may experience transitory lower levels of virulence before reaching this maximum via a positive genetic correlation between virulence and incubation period. This is somehow unexpected because this latter parameter does not appear in the calculations related to long-term evolutionary or emergence.

In addition to the strong selection for maximum virulence of EBOV, another striking result is that decreasing the ratio of unsafe burials is triply effective. First, it decreases the spread of the virus (i.e. its $\mathcal{R}_0$). Second, in the short term, it can help limit a transitory increase in virulence. Indeed, in the first weeks of an epidemic, the sexual transmission route is negligible compared to the other routes that are maximised for maximum CFR. Third, in the long term, decreasing the proportion of unsafe burials is necessary to shift the selective pressure in favour of less virulent strains.

0.4.2. Virulence is a shared trait

In evolutionary biology, virulence is defined as the decrease in host fitness due to the infection (Alizon & Michalakis, 2015). Given the speed at which a pathogen kills its host, EBOV's virulence can neither be measured as a decrease in instantaneous fecundity (which would be almost zero) nor as an increase of instantaneous mortality rate (which would tend towards infinity or zero depending on the infection outcome). The case fatality ratio (CFR) therefore appears to be the only measurable and epidemiologically relevant proxy for EBOV's virulence.

We focused on the virus side but, like any infection trait, virulence is also determined by the host and its environment. To predict how virulence will change in the future, we should also consider how hosts may change. In the case of EBOV, it was known before the recent epidemics that some people can become immune to the virus without exhibiting any symptoms (Leroy *et al.*, 2000). The question remains to know if they can also be infectious. More generally, our assumption of life-long protection could be oversimplifying.

Finally, to make predictions on the long term evolution, we need to factor in how the virus population will evolve in response to the variation in the host population's immune status. Since the immunological status of the host population is determined by that of the virus population, this *de facto* qualifies as a coevolutionary interaction. Earlier models shows that host heterogeneity in resistance and tolerance can lead to a variety of outcomes (Miller *et al.*, 2006; Cousineau & Alizon, 2014). Overall, introducing realistic host heterogeneity, in particular age-dependent or sex-dependent mortality, appears like a relevant extension of this model.

0.4.3. Spatial structure

Trait evolution is shaped by contact patterns between hosts (Lion & van Baalen, 2008). Regarding the recent Ebola epidemic, the lack of medical personnel and infrastructure in the affected countries played an key role in the spread of the disease as, for example, according to the World Health Organisation, in 2008 Liberia and Sierra Leone had only a density of 0.015 physicians per 1000 inhabitants, when at the same time France had a density of 3.5 and the United States of America 2.4. This was further exacerbated by historical, political and sociological factors (Ali *et al.*, 2016).

It is difficult to predict how explicitly accounting for spatial structure would affect the results. Indeed, it is generally thought that the more 'viscous' the population, the more virulence is counter-selected (Boots & Sasaki, 1999). However, the life cycle of the parasite and the host demography can create epidemiological feedbacks that alter this prediction by causing virulence to be maximised for intermediate levels of population structures (Lion & Boots, 2010). This is why predicting virulence evolution in a fully spatially structured model is beyond the scope of this study.

0.4.4. Testable predictions

One of the underlying assumptions of our model, which could be tested is that the variation we observe in virulence is at least partially controlled by the virus genetics. This could be done by combining virus sequence data with infection traits (virus load or infection outcome) through a phylogenetic comparative approach (Alizon *et al.*, 2010) or a genome wide association study on the virus genome (Power *et al.*, 2017). If virus load is confirmed to be partially controlled by the virus genetics and if, as current evidence suggests, it is correlated with virulence (Towner *et al.*, 2004; Crowe *et al.*, 2016), then

studying variations in virus load throughout the 2013-2016 epidemics can help us understand the evolutionary dynamics of virulence. On that note, an experiment consisting in generating pseudovirions based on ancestral or recent EBOV sequences suggests that some of the substitutions observed during the 2013-2016 epidemics may confer increased tropism for human cells (Urbanowicz *et al.*, 2016).

Another result of the short-term evolutionary dynamics analysis is that individuals who contract EBOV from dead bodies should have a higher probability of dying than those infected by contact with living infectious individuals. This could be tested by collecting data from individuals where the transmission route is well documented.

Finally, the remote possibility that lower virulence strains will evolve depends on the existence of a transmission-virulence trade-off. Assessing the shape of this trade-off may be, therefore, very valuable. Note that in the case of EBOV, it is not the exact shape that matters but rather the general trend.

0.4.5. Conclusion

This evolutionary epidemiology work shows that EBOV's high virulence, whether it is about emergence, short-term or long-term dynamics, can be explained by its particular life cycle that mixes parasitism and parasitoidism (*post mortem* transmission). Unfortunately, any long term decrease in virulence is unlikely for West African strains at any time scale, although increasing the safe burial proportion appears to be an optimal response in both the short and long terms.

Appendix

0.a. Equation systems

0.a.1. Epidemiology

The epidemiological dynamics are governed by the following set of ODEs:

$$\begin{cases} \frac{\mathrm{d}S}{\mathrm{d}t} &= \lambda - \left(\mu + \beta_I I + \beta_D D + \beta_C \frac{C}{N}\right) S, \\ \frac{\mathrm{d}E}{\mathrm{d}t} &= \left(\beta_I I + \beta_D D + \beta_C \frac{C}{N}\right) S - \omega E, \\ \frac{\mathrm{d}I}{\mathrm{d}t} &= \omega E - \gamma I, \\ \frac{\mathrm{d}D}{\mathrm{d}t} &= \alpha\theta\gamma I - \varepsilon D, \\ \frac{\mathrm{d}C}{\mathrm{d}t} &= (1-\alpha)\gamma I - \sigma C, \\ \frac{\mathrm{d}R}{\mathrm{d}t} &= \sigma C - \mu R, \end{cases} \tag{0.a.1}$$

where $N \coloneqq S + E + I + C + R$ is the total living population size, which varies with time. Notice that since life expectancy is several orders of magnitudes greater than the latency, the symptomatic and the convalescent periods, mortality rate μ can be neglected when summed with ω, γ or σ.

0.a.2. Price equation

The dynamics of the populations of interest are described by $4n + 1$ ODEs, for all $i \in \{1, \dots, n\}$:

$$\begin{cases} \frac{\mathrm{d}S}{\mathrm{d}t} &= \lambda - \sum_{i=1}^{n} \left(\beta_{I,i} I_i + \beta_{D,i} D_i - \mu\right) S, \\ \frac{\mathrm{d}E_i}{\mathrm{d}t} &= \left(\beta_{I,i} I_i + \beta_{D,i} D_i\right) S - \omega_i E_i, \\ \frac{\mathrm{d}I_i}{\mathrm{d}t} &= \omega_i E_i - \gamma_i I_i, \\ \frac{\mathrm{d}D_i}{\mathrm{d}t} &= \alpha_i \theta \gamma_i I_i - \varepsilon_i D_i, \\ \frac{\mathrm{d}C_i}{\mathrm{d}t} &= (1-\alpha_i)\gamma_i I_i - \sigma_i C_i. \end{cases} \tag{0.a.2}$$

The total density of each compartment is denoted by a bullet index ($\bullet$) and its dynamics satisfy

$$\begin{cases} \frac{\mathrm{d}S}{\mathrm{d}t} &= \lambda - \left(\overline{\beta_I}^{I} I_\bullet + \overline{\beta_D}^{D} D_\bullet - \mu\right) S, \\ \frac{\mathrm{d}E_\bullet}{\mathrm{d}t} &= \left(\overline{\beta_I}^{I} I_\bullet + \overline{\beta_D}^{D} D_\bullet\right) S - \overline{\omega}^{E} E_\bullet, \\ \frac{\mathrm{d}I_\bullet}{\mathrm{d}t} &= \overline{\omega}^{E} E_\bullet - \overline{\gamma}^{I} I_\bullet, \\ \frac{\mathrm{d}D_\bullet}{\mathrm{d}t} &= \theta \overline{\alpha\gamma}^{I} I_\bullet - \overline{\varepsilon}^{D} D_\bullet, \\ \frac{\mathrm{d}C_\bullet}{\mathrm{d}t} &= \overline{\gamma}^{I} I_\bullet - \overline{\alpha\gamma}^{I} I_\bullet - \overline{\sigma}^{D} D_\bullet, \end{cases} \tag{0.a.3}$$

where the bars indicate average values and the superscripts indicate the compartment in which the trait is averaged. We can already notice that the CFR and the rate at which the infectious period ends are difficult to disentangle in this system because we have second order terms (i.e. an average of the product $\alpha_i \gamma_i$).

0.b. Stationary dynamics

0.b.1. Endemic equilibrium

At equilibrium, all time derivatives of system (0.a.1) cancel out. If we denote by $\widetilde{H}$ the corresponding value of density H at this equilibrium, we get $\widetilde{S} = S_0 = \frac{\lambda}{\mu}$ and $\widetilde{E} = \widetilde{I} = \widetilde{D} = \widetilde{C} = \widetilde{R} = 0$ for the disease free equilibrium (DFE).

The endemic equilibrium (EE), on the other hand, is found by assuming non zero values for all $\widetilde{H}$. We thus first get that,

$$\begin{cases} \frac{\mathrm{d}I}{\mathrm{d}t} = 0 & \iff \widetilde{I} = \frac{\omega}{\gamma}\widetilde{E}, \\ \frac{\mathrm{d}D}{\mathrm{d}t} = 0 & \iff \widetilde{D} = \frac{\alpha\theta\gamma}{\varepsilon}\widetilde{I} = \frac{\alpha\theta\omega}{\varepsilon}\widetilde{E}, \\ \frac{\mathrm{d}C}{\mathrm{d}t} = 0 & \iff \widetilde{C} = \frac{(1-\alpha)\gamma}{\sigma}\widetilde{I} = \frac{(1-\alpha)\omega}{\sigma}\widetilde{E}, \\ \frac{\mathrm{d}R}{\mathrm{d}t} = 0 & \iff \widetilde{R} = \frac{\sigma}{\mu}\widetilde{C} = \frac{(1-\alpha)\omega}{\mu}\widetilde{E}. \end{cases} \tag{0.b.1}$$

Hence,

$$\begin{aligned} \frac{\mathrm{d}E}{\mathrm{d}t} = 0 &\iff \left(\beta_I\widetilde{I} + \beta_D\widetilde{D} + \beta_C\frac{\widetilde{C}}{\widetilde{N}}\right)\widetilde{S} - \omega\widetilde{E} = 0, \\ &\iff \left(\beta_I\frac{\omega}{\gamma}\widetilde{E} + \beta_D\frac{\alpha\theta\omega}{\varepsilon}\tilde{E} + \beta_C\frac{(1-\alpha)\omega}{\sigma\widetilde{N}}\widetilde{E}\right)\widetilde{S} - \omega\widetilde{E} = 0, \\ &\iff \widetilde{S} = \left(\frac{\beta_I}{\gamma} + \frac{\alpha\theta\beta_D}{\varepsilon} + \frac{(1-\alpha)\beta_C}{\sigma\widetilde{N}}\right)^{-1}, \end{aligned} \tag{0.b.2}$$

and

$$\begin{aligned} \frac{\mathrm{d}S}{\mathrm{d}t} = 0 &\iff \lambda - \left(\mu + \beta_I\widetilde{I} + \beta_D\widetilde{D} + \beta_C\frac{\widetilde{C}}{\widetilde{N}}\right)\widetilde{S} = 0, \\ &\iff \mu + \beta_I\frac{\omega}{\gamma}\widetilde{E} + \beta_D\frac{\alpha\theta\omega}{\varepsilon}\tilde{E} + \beta_C\frac{(1-\alpha)\omega}{\sigma\widetilde{N}}\widetilde{E} = \frac{\lambda}{\widetilde{S}}, \\ &\iff \frac{\omega\widetilde{E}}{\widetilde{S}} = \frac{\lambda}{\widetilde{S}} - \mu, \\ &\iff \widetilde{E} = \frac{\lambda - \mu\widetilde{S}}{\omega}. \end{aligned} \tag{0.b.3}$$

It follows that

$$\begin{aligned} \widetilde{N} \coloneqq \widetilde{S} + \widetilde{E} + \widetilde{I} + \widetilde{C} + \widetilde{R} &= \widetilde{S} + \left(1 + \frac{\omega}{\gamma} + \frac{(1-\alpha)\omega}{\sigma} + \frac{(1-\alpha)\omega}{\mu}\right)\widetilde{E}, \\ &= \widetilde{S} + \left(\frac{1}{\omega} + \frac{1}{\gamma} + \left(\frac{1}{\sigma} + \frac{1}{\mu}\right)(1-\alpha)\right)\left(\lambda - \mu\widetilde{S}\right). \end{aligned} \tag{0.b.4}$$

By combining (0.b.2) and (0.b.4), we can find the exact solution for $\widetilde{N}$. This closed form is excessively large and therefore not shown here. It is however possible to find a approximation of $\widetilde{N}$ as a simple function of the model's parameters with some simplifications that are shown hereafter, with a particular treatment of the $\alpha = 1$ case.

0.b.2. Stationary total population size approximation for $\alpha \neq 1$

In this subsection, we assume that $\alpha < 1$ (the case where $\alpha = 1$ is treated in the next subsection).

Given that life expectancy is several orders of magnitude greater than the convalescent period, i.e. $\frac{1}{\mu} \gg \frac{1}{\sigma}$, we have

$$\frac{1}{\omega} + \frac{1}{\gamma} + \left(\frac{1}{\sigma} + \frac{1}{\mu}\right)(1-\alpha) \approx \left(\frac{1}{\omega} + \frac{1}{\gamma} + \frac{1}{\mu}\right) - \frac{\alpha}{\mu},$$

Furthermore, since life expectancy is also several orders of magnitude greater than the latency and symptomatic period, i.e. $\frac{1}{\mu} \gg \frac{1}{\omega} + \frac{1}{\gamma}$, and since $\alpha \neq 1$, we finally have

$$\begin{aligned} \widetilde{N} &\approx \widetilde{S} + (1-\alpha)\left(S_0 - \widetilde{S}\right), \\ \widetilde{N} &\approx (1-\alpha)S_0 + \alpha\widetilde{S}. \end{aligned} \tag{0.b.5}$$

The virulence of EBOV is usually high and its sexual transmission low compared to the two other transmission route (Abbate *et al.*, 2016), which is why we can approximate $\widetilde{S}$ by its value by neglecting the third term in equation (0.b.2), which leads to

$$\widetilde{S} \approx \frac{\gamma\varepsilon}{\varepsilon\beta_I + \alpha\gamma\theta\beta_D}. \tag{0.b.6}$$

This then results in

$$\widetilde{N} \approx (1-\alpha)S_0 + \frac{\alpha\gamma\varepsilon}{\varepsilon\beta_I + \alpha\gamma\theta\beta_D}. \tag{0.b.7}$$

Numerical comparisons performed on positive and stable equilibria for realistic parameter sets show that this approximation differs from the exact value by less than 10,000 individuals, which corresponds to a relative error of less than 1%, thus validating the accuracy of this approximation.

0.b.3. Stationary total population size approximation for $\alpha = 1$

Here we assume that $\alpha = 1$ (notice that in this case the trade-off exponent p vanishes).

We then get back to equation (0.b.2) that becomes such that

$$\widetilde{S} = \left(\frac{\beta_I}{\gamma} + \frac{\theta\beta_D}{\varepsilon}\right)^{-1} = \frac{\gamma\varepsilon}{\varepsilon\beta_I + \gamma\theta\beta_D},$$

which shows that the exact value of $\widetilde{S}$ coincides with its equation (0.b.6) approximation for $\alpha = 1$.

As for equation (0.b.4), we get

$$\widetilde{N} = \left(1 - \frac{(\gamma+\omega)\mu}{\gamma\omega}\right)\widetilde{S} + \frac{(\gamma+\omega)\lambda}{\gamma\omega},$$

it is straightforward to show numerically (using parameters from Table 0.2.1) that, since $\widetilde{S}$ and $\frac{\lambda}{\mu} = S_0$ are of the same order of magnitude and that, as already mentioned, life expectancy is several orders of magnitude greater than the latency and symptomatic period, i.e. $\frac{1}{\mu} \gg \frac{1}{\omega} + \frac{1}{\gamma}$, which is equivalent to $\frac{(\gamma+\omega)\mu}{\gamma\omega} \ll 1$, we have

$$\widetilde{N} \approx \widetilde{S} = \frac{\gamma\varepsilon}{\varepsilon\beta_I + \gamma\theta\beta_D}, \tag{0.b.8}$$

which shows the consistency of equation (0.b.7) even for $\alpha = 1$.

This approximation shows a relative error of about 10^{-3} with Table 0.2.1 parameters values.

0.c. Reproduction number derivation

The basic reproduction number, $\mathcal{R}_0$, and the relative reproduction number, $\mathcal{R}_m$, are two epidemiological quantifications of the invasion potential of an infectious agent in a fully susceptible population and in an population already infected by an alternative strain, respectively. They emerge from the stability analysis of the disease free equilibrium (DFE) and the endemic equilibrium (EE) respectively. Their threshold value is 1.

The next-generation method (Diekmann *et al.*, 1990; Hurford *et al.*, 2010) is the most efficient derivation of these reproduction numbers and proceeds as follows.

0.c.1. General reproduction number

First, we isolate the ODEs of the infected compartments from the rest of the system (here system (0.a.1)) to obtain

$$\begin{cases} \frac{\mathrm{d}E}{\mathrm{d}t} &= \left(\beta_I I + \beta_D D + \beta_C \frac{C}{N}\right) S - \omega E, \\ \frac{\mathrm{d}I}{\mathrm{d}t} &= \omega E - \gamma I, \\ \frac{\mathrm{d}D}{\mathrm{d}t} &= \alpha\theta\gamma I - \varepsilon D, \\ \frac{\mathrm{d}C}{\mathrm{d}t} &= (1-\alpha)\gamma I - \sigma C. \end{cases} \tag{0.c.1}$$

Second, we write the Jacobian matrix $\mathbf{J}$ that corresponds to this sub-system (0.f.2), by deriving each time-derivative ($\frac{\mathrm{d}E}{\mathrm{d}t}, \frac{\mathrm{d}I}{\mathrm{d}t}, \frac{\mathrm{d}D}{\mathrm{d}t}, \frac{\mathrm{d}C}{\mathrm{d}t}$) with respect to each infected compartment density (E, I, D, C):

$$\mathbf{J} = \begin{bmatrix} -\beta_C \frac{CS}{N^2} - \omega & \left(\beta_I + \beta_C \frac{C}{N^2}\right) S & \beta_D S & \left(1 - \frac{C}{N}\right) \beta_C \frac{S}{N} \\ \omega & -\gamma & 0 & 0 \\ 0 & \alpha\gamma\theta & -\varepsilon & 0 \\ 0 & (1-\alpha)\gamma & 0 & -\sigma \end{bmatrix},$$

reminding that $N := S + E + I + R + C$.

Third, we arbitrarily decompose $\mathbf{J}$ as a sum of an 'inflow' matrix $\mathbf{F}$ and an 'outflow' matrix $-\mathbf{V}$ provided that $\mathbf{V}$ is non-singular (that is $\mathbf{V}^{-1}$ exists), $\mathbf{F}$ and $\mathbf{V}^{-1}$ are non-negative elementwise and the real parts of all eigenvalues of $-\mathbf{V}$ are negative. Here, we conveniently choose two matrices that fulfil these requirements:

$$\mathbf{F} = \begin{bmatrix} 0 & \left(\beta_I + \beta_C \frac{C}{N^2}\right) S & \beta_D S & \beta_C \frac{S}{N} \\ 0 & 0 & 0 & 0 \\ 0 & 0 & 0 & 0 \\ 0 & 0 & 0 & 0 \end{bmatrix} \text{ and } \mathbf{V} = \begin{bmatrix} -\beta_C \frac{CS}{N^2} - \omega & 0 & 0 & -\beta_C \frac{CS}{N^2} \\ \omega & -\gamma & 0 & 0 \\ 0 & \alpha\gamma\theta & -\varepsilon & 0 \\ 0 & (1-\alpha)\gamma & 0 & -\sigma \end{bmatrix}.$$

Finally, the general reproductive number $\mathcal{R}$ is given by the largest modulus of all eigenvalues of the $\mathbf{F}.\mathbf{V}^{-1}$ matrix. Elementary calculations result in the following general result

$$\mathcal{R} = \frac{\left((1-\alpha)\gamma\varepsilon\beta_C + \left(\varepsilon\beta_I + \alpha\gamma\theta\beta_D\right) N\right) \omega S N}{\left(\gamma\sigma\beta_C CS + \left((1-\alpha)\gamma\beta_C CS\left(\beta_C CS + N^2\gamma\right)\sigma\right)\omega\right)\varepsilon}. \tag{0.c.2}$$

0.c.2. Basic reproduction number

The basic reproduction number $\mathcal{R}_0$ is obtained from $\mathcal{R}$ by setting the densities to their values at the disease free equilibrium (DFE), namely $S = N = \frac{\lambda}{\mu}$ and $C = 0$, hence

$$\mathcal{R}_0 = \left(\frac{\beta_I}{\gamma} + \frac{\alpha\theta\beta_D}{\varepsilon}\right) S_0 + \frac{(1-\alpha)\beta_C}{\sigma}, \tag{0.c.3}$$

Any strain introduced in a fully susceptible host population spreads if and only if $\mathcal{R}_0 > 1$.

0.c.3. Relative reproduction number

As for the relative reproduction number $\mathcal{R}_\mathrm{m}$, it is obtained from $\mathcal{R}$ by setting the densities to their values at an alternative strain endemic equilibrium (EE), namely $S = \widetilde{S}$, $N = \widetilde{N}$ and $C = 0$ (notice that in such setting $N = S + R + E_\mathrm{r} + I_\mathrm{r} + C_\mathrm{r} + E + I + C$ where the r index denotes compartments of individuals infected by the previously established ('resident'), which may not be empty at EE, making $\widetilde{S} < \widetilde{N}$), hence

$$\mathcal{R}_\mathrm{m} = \left(\frac{\beta_I}{\gamma} + \frac{\alpha\theta\beta_D}{\varepsilon} + \frac{(1-\alpha)\beta_C}{\sigma\widetilde{N}}\right)\widetilde{S}.$$

It follows that a rare mutant strain of CFR x that appears in a host population endemically infected by a resident strain of CFR y spreads and persists if and only if

$$\mathcal{R}(x,y) \coloneqq \left(\frac{\beta_I(x)}{\gamma} + \frac{x\theta\beta_D(x)}{\varepsilon} + \frac{(1-x)\beta_C(x)}{\sigma\widetilde{N}(y)}\right)\widetilde{S}(y) > 1. \tag{0.c.4}$$

Moreover, it is possible to eliminate $\widetilde{S}(y)$ using equation (0.b.2), leading to

$$\mathcal{R}(x,y) = \frac{\frac{\beta_I(x)}{\gamma} + \frac{x\theta\beta_D(x)}{\varepsilon} + \frac{(1-x)\beta_C(x)}{\sigma\widetilde{N}(y)}}{\frac{\beta_I(y)}{\gamma} + \frac{y\theta\beta_D(y)}{\varepsilon} + \frac{(1-y)\beta_C(y)}{\sigma\widetilde{N}(y)}}. \tag{0.c.5}$$

This formula shows in particular that, because of the two occurrences of $\widetilde{N}(y)$, the relative reproduction number is not the ratio between the two basic reproduction numbers, as it is in simpler models (Dieckmann, 2002).

We can finally apply approximation (0.b.7) $\widetilde{N}(y) \approx (1-y)S_0 + \frac{\gamma\varepsilon y}{\varepsilon\beta_I(y)+\gamma\theta y\beta_D(y)}$ to obtain a closed-form expression for $\mathcal{R}(x,y)$ (not shown here).

0.d. Evolutionary analysis of virulence

Investigating the evolutionary trends require to consider trade-offs. From now on, we will then always apply the transmission-virulence trade-off assumed in equation (0.2.2) and keep in mind that the β_H constant case can be retrieved if $p = 0$.

0.d.1. Virulence effect on basic reproduction number

It is worth noticing that unless $p = 0$, we have $\mathcal{R}_0 = 0$ when $\alpha = 0$. Therefore not all CFR/virulence levels are able to give rise to an epidemic and persist in the population. Indeed, $\mathcal{R}_0(\alpha)$ may not be greater than 1 for all $\alpha \in [0;1]$. First, let us then study how $\mathcal{R}_0$ is affected by α, by calculating its derivative

$$\begin{aligned}\frac{\mathrm{d}\mathcal{R}_0}{\mathrm{d}\alpha}(\alpha) &= \frac{\mathrm{d}}{\mathrm{d}\alpha}\left(\left(\left(\frac{b_I}{\gamma}+\frac{\alpha\theta b_D}{\varepsilon}\right)S_0+\frac{(1-\alpha)b_C}{\sigma}\right)\alpha^p\right),\\ &= \left(\left(\frac{\theta b_D S_0}{\varepsilon}-\frac{b_C}{\sigma}\right)\alpha+p\left(\left(\frac{b_I}{\gamma}+\frac{\alpha\theta b_D}{\varepsilon}\right)S_0+\frac{(1-\alpha)b_C}{\sigma}\right)\right)\alpha^{p-1},\end{aligned}$$

which cancels only if $\alpha = 0$ or

$$\alpha = \frac{\frac{b_C}{\sigma}+\frac{b_I S_0}{\gamma}}{\frac{b_C}{\sigma}-\frac{\theta b_D S_0}{\varepsilon}}\times\frac{p}{1+p} =: \alpha^\circ,$$

which lies in $]0,1[$ if and only if $\theta < \frac{\varepsilon b_C}{\sigma b_D S_0} \approx 2.3\%$ and $p < \frac{\frac{b_C}{\sigma S_0}-\frac{\theta b_D}{\varepsilon}}{\frac{b_I}{\gamma}+\frac{\theta b_D}{\varepsilon}} \underset{\theta=0}{\approx} 5.6\cdot 10^{-3}$ (numerical values are given according to Table 0.2.1 calibration). If these conditions are not fulfilled, then $\mathrm{d}\mathcal{R}_0/\mathrm{d}\alpha$ is positive for all CFR.

Given these conditions, the value of α° can be approximated by

$$\alpha^\circ \underset{\theta\to 0}{\approx} \frac{\sigma b_I S_0}{\gamma b_C} p.$$

The basic reproduction number at this value is

$$\mathcal{R}_0(\alpha^\circ) = \left(\left(\frac{b_I}{\gamma}+\frac{\alpha\theta b_D}{\varepsilon}\right)S_0+\frac{(1-\alpha)b_C}{\sigma}\right)\left(\frac{\sigma b_I S_0}{\gamma b_C}p\right)^p \underset{\theta\to 0}{\approx} \frac{b_I S_0}{\gamma},$$

which is a maximum on $]0,1[$ (inequality $\frac{\mathrm{d}^2\mathcal{R}_0}{\mathrm{d}\alpha^2}(\alpha^\circ) < 0$ has been checked after calculations not shown).

Besides, evaluating $\mathcal{R}_0$ for $\alpha = 1$ leads to

$$\mathcal{R}_0(1) = \left(\frac{b_I}{\gamma}+\frac{\theta b_D}{\varepsilon}\right)S_0 \geq \frac{b_I S_0}{\gamma},$$

the lower bound being greater than one according to Table 0.2.1 estimates, and this holds even with almost half of the b_I value and smaller values of γ.

To conclude, for any given values of p and θ, there is always a CFR interval $[\alpha_{\min}, 1]$ in which any strain can spread.

Notice also that for $\alpha = 0$ and $p = 0$,

$$\mathcal{R}_0 = \frac{b_I S_0}{\gamma} + \frac{b_C}{\sigma} \geq \frac{b_I S_0}{\gamma},$$

and likewise this is greater than one for estimated parameters. Consequently, all CFR values can spread in absence of trade-off.

0.d.2. Minimum spreadable CFR approximation

$\alpha_{\min} \in [0,1]$ is the minimum CFR of EBOV required to spread, i.e. $\mathcal{R}_0(\alpha_{\min}) := 1$. However, it is not possible to find the exact closed form of $\alpha_{\min}$ (as the equation $\mathcal{R}(x) = 1$ involves irreducible terms of both x^p and x). It is nonetheless possible to analytically find a lower bound for $\alpha_{\min}$, which we denote by α_- ($0 \leq \alpha_- \leq \alpha_{\min} \leq 1$). First, notice that

$$\mathcal{R}_0(\alpha) := \left(\frac{\beta_I}{\gamma} + \frac{\alpha\theta\beta_D}{\varepsilon}\right) S_0 + \frac{(1-\alpha)\beta_C}{\sigma} \leq \left(\frac{\beta_I}{\gamma} + \frac{\theta\beta_D}{\varepsilon}\right) S_0 + \frac{\beta_C}{\sigma} =: \mathcal{R}_{0,+}(\alpha), \tag{0.d.1}$$

where $\mathcal{R}_{0,+}(\alpha)$ is an over-estimate of $\mathcal{R}_0(\alpha)$. Applying the trade-off from equation (0.2.2), we get

$$\mathcal{R}_{0,+}(\alpha) = \left(\left(\frac{b_I}{\gamma} + \frac{\theta b_D}{\varepsilon}\right) S_0 + \frac{b_C}{\sigma}\right) \alpha^p.$$

Let α_- be the CFR such that $\mathcal{R}_{0,+}(\alpha_-) = 1$, that is

$$\alpha_- = \left(\left(\frac{b_I}{\gamma} + \frac{\theta b_D}{\varepsilon}\right) S_0 + \frac{b_C}{\sigma}\right)^{\frac{-1}{p}}. \tag{0.d.2}$$

From equation (0.d.1) and as $\mathcal{R}_0$ and $\mathcal{R}_{0,+}$ are increasing functions of α, it follows that

$$\mathcal{R}_0(\alpha_-) \leq \mathcal{R}_{0,+}(\alpha_-) = 1 = \mathcal{R}_0(\alpha_{\min}) \leq \mathcal{R}_{0,+}(\alpha_{\min}),$$

thus α_- is an analytical under-estimate of $\alpha_{\min}$.

Notice that in absence of trade-off, the closed form $\alpha_{\min}$ can be easily found as

$$\alpha_{\min} = \frac{1 - \frac{b_I S_0}{\gamma} - \frac{b_C}{\sigma}}{\frac{\theta b_D S_0}{\varepsilon} - \frac{b_C}{\sigma}}. \tag{0.d.3}$$

0.d.3. Virulence effect on stationary densities

From now one, we will assume that $\alpha \in [\alpha_{\min}, 1]$.

We apply definition from equation (0.2.2) to equation (0.b.6), that is

$$\widetilde{S} \approx \frac{\gamma\varepsilon}{\left(\varepsilon b_I + \gamma\theta b_D \alpha\right) \alpha^p}.$$

Its derivative with respect to α is

$$\frac{\mathrm{d}\widetilde{S}}{\mathrm{d}\alpha}(\alpha) \approx \frac{-\left(\gamma\theta b_D \alpha + p\left(\varepsilon b_I + \gamma\theta b_D \alpha\right)\right)\gamma\varepsilon\alpha^{p-1}}{\left(\varepsilon b_I + \gamma\theta b_D \alpha\right)^2} < 0.$$

Thus, it comes from equation (0.b.5), that

$$\frac{\mathrm{d}\widetilde{N}}{\mathrm{d}\alpha}(\alpha) = -S_0 + \widetilde{S}(\alpha) + \alpha\frac{\mathrm{d}\widetilde{S}}{\mathrm{d}\alpha}(\alpha).$$

Since $\widetilde{S}(\alpha) < S_0$ for $\alpha \geq \alpha_{\min}$ (any EBOV strain that spreads decreases the number of susceptible individuals), $\frac{\mathrm{d}\widetilde{N}}{\mathrm{d}\alpha}(\alpha) < 0$, that is $\widetilde{N}(\alpha)$ is a decreasing function of α, we have

$$\widetilde{N}(\alpha) \geq \widetilde{N}(1) = \frac{\gamma\varepsilon}{\varepsilon b_I + \gamma\theta b_D}.$$

0.d.4. Virulence selection gradient

We can finally investigate the virulence selection gradient, Δ, by deriving the relative reproduction number from equation (0.c.5) with respect to the first argument (i.e. the mutant's virulence), which leads to $\partial_1\mathcal{R}$, and equalizing the mutant and resident's virulence. After some calculations, we find that

$$\Delta(y) \coloneqq \partial_1\mathcal{R}(y,y) = \frac{p}{y} + \frac{\frac{\theta b_D}{\varepsilon}\widetilde{N}(y) - \frac{b_C}{\sigma}}{(1-y)\frac{b_C}{\sigma} + \left(\frac{b_I}{\gamma} + \frac{\theta b_D}{\varepsilon}y\right)\widetilde{N}(y)}.$$

Since the CFR is bounded by 1, it is expected to evolve towards lower values if and only if $\Delta(1) < 0$, that is

$$\Delta(1) \approx p + \frac{\theta b_D\gamma}{\varepsilon b_I + \gamma\theta b_D} - \frac{b_C}{\sigma} < 0.$$

By investigating burial control under the most favourable trade-off, which is no trade-off ($p = 0$), we find that this condition is equivalent to (for $b_C \ll \sigma$):

$$\theta < \frac{b_I b_C \varepsilon}{\gamma\sigma b_D} \approx 4\%.$$

By investigating trade-off shape under the most favourable burial control ($\theta = 0$), we find that the condition is equivalent to

$$p < \frac{b_C}{\sigma} \approx 10^{-2}.$$

Moreover, investigating the selection gradient at the lowest spreadable CFR $y = \alpha_{\min}$, we notice that the following lower bound

$$\Delta(\alpha_{\min}) \geq \frac{\frac{\theta b_D}{\varepsilon}\widetilde{N}(1) - \frac{b_C}{\sigma}}{(1-\alpha_{\min})\frac{b_C}{\sigma} + \left(\frac{b_I}{\gamma} + \frac{\theta b_D}{\varepsilon}\alpha_{\min}\right)\widetilde{N}(1)}$$

is positive if $\theta > \frac{b_I b_C \varepsilon}{\gamma\sigma b_D}$. Therefore a necessary condition for having a negative selection gradient on the lowest spreadable CFRs is $\theta < \frac{b_I b_C \varepsilon}{\gamma\sigma b_D}$.

0.d.5. Evolutionary attracting virulence estimation

Unless it is equal to the 0 or 1 boundaries (the determination of which only requires the invariant sign of the selection gradient), the evolutionary attracting virulence $\alpha^\star$ is an intermediate CFR value in $]0,1[$ such that $\Delta\left(\alpha^\star\right) = 0$ (singularity condition), $\partial_{1,1}\mathcal{R}\left(\alpha^\star,\alpha^\star\right) < 0$ (evolutionary stability condition) and $\frac{\mathrm{d}\Delta}{\mathrm{d}\alpha}\left(\alpha^\star\right) < 0$ (convergent stability

condition), according to the adaptive dynamics framework (Geritz *et al.*, 1998). We therefore investigate the singularity condition that provides an equation $\alpha^\star$ has to satisfy.

By writing the selection gradient under a condensed form and defining $\eta := \frac{b_I}{\gamma}, \phi := \frac{b_D}{\varepsilon}, \psi := \frac{b_C}{\sigma}$, we find that

$$\begin{aligned} \Delta\left(\alpha^\star\right) = \frac{p}{\alpha^\star} + \frac{\theta\phi\widetilde{N}\left(\alpha^\star\right) - \psi}{(1-\alpha^\star)\psi + \left(\eta + \theta\phi\alpha^\star\right)\widetilde{N}(\alpha^\star)} &= 0, \\ \iff \left(p - (1+p)\,\alpha^\star\right)\psi + \left(p\eta + \left(p+\alpha^\star\right)\theta\phi\right)\widetilde{N}\left(\alpha^\star\right) &= 0. \end{aligned} \tag{0.d.4}$$

As noticed in the previous subsection, this equation has a solution only if p is small enough (for the first term to be negative) and θ is small enough (for the second term not to be too positive). Hereafter, and because we are seeking for an intermediate evolutionary attracting virulence, we assume that p and θ are small enough such that this equation has a solution in $]0,1[$.

The complexity of $\widetilde{N}\left(\alpha^\star\right)$ prevents us from having a closed-form expression of $\alpha^\star$. However, $\alpha^\star$ can be bounded by an underestimate $\alpha^\star_-$ on the one hand, and an overestimate $\alpha^\star_+$ on the other hand.

First, notice that the left hand side of equation (0.d.4) has the following upper bound, replacing $\widetilde{N}\left(\alpha^\star\right)$ by its maximum $S_0 = \frac{\lambda}{\mu}$,

$$\left(p - (1+p)\,\alpha^\star\right)\psi + \left(p\eta + \left(p+\alpha^\star\right)\theta\phi\right)S_0,$$

which cancels out only if $\alpha^\star$ is replaced by a greater value we denote by $\alpha^\star_+$ (since the first term is a decreasing function of the CFR). This leads to

$$\alpha^\star_+ = \frac{\left(\left(\eta+\theta\phi\right)S_0 + \psi\right)p}{(1+p)\,\psi - \theta\phi S_0}. \tag{0.d.5}$$

Notice that $\alpha^\star_+ > 0$ requires that $\psi(1+p) > \theta\phi S_0$ that is θ small.

Second and analogously, the left hand side of equation (0.d.4) has the following lower bound, replacing $\widetilde{N}\left(\alpha^\star\right)$ by its minimum $\widetilde{N}(1) = \frac{1}{\eta+\theta\phi}$,

$$\left(p - (1+p)\,\alpha^\star\right)\psi + \frac{p\eta + \left(p+\alpha^\star\right)\theta\phi}{\eta+\theta\phi},$$

which cancels out only if $\alpha^\star$ is replaced by a smaller value we denote $\alpha^\star_-$ (since the first term is a decreasing function of the CFR). This leads to

$$\alpha^\star_- = \frac{\left(1+\psi\right)p}{(1+p)\,\psi - \frac{\theta\phi}{\eta+\theta\phi}}. \tag{0.d.6}$$

Notice that $\alpha^\star_- < 1$ requires that $p < \psi - \frac{\theta\phi}{\eta+\theta\phi}$. Since $\frac{\widehat{b_C}}{\widehat{\sigma}} = 10^{-2}$, the approximations $1+\psi \approx 1$ and $1+p \approx 1$ holds, which makes this expression even simpler:

$$\alpha^\star_- \approx \frac{p}{\psi - \frac{\theta\phi}{\eta+\theta\phi}},$$

which in turn is positive only if $\theta < \frac{\psi\eta}{(1+\psi)\phi} \approx \frac{\psi\eta}{\phi}$. Therefore, the two conditions on p and θ related to the cancellation of Δ are retrieved.

As one can see by comparing Figure 0.d.1 with Figure 0.3.2, $\alpha^\star_+$ but moreover $\alpha^\star_-$ are accurate estimates of $\alpha^\star$.

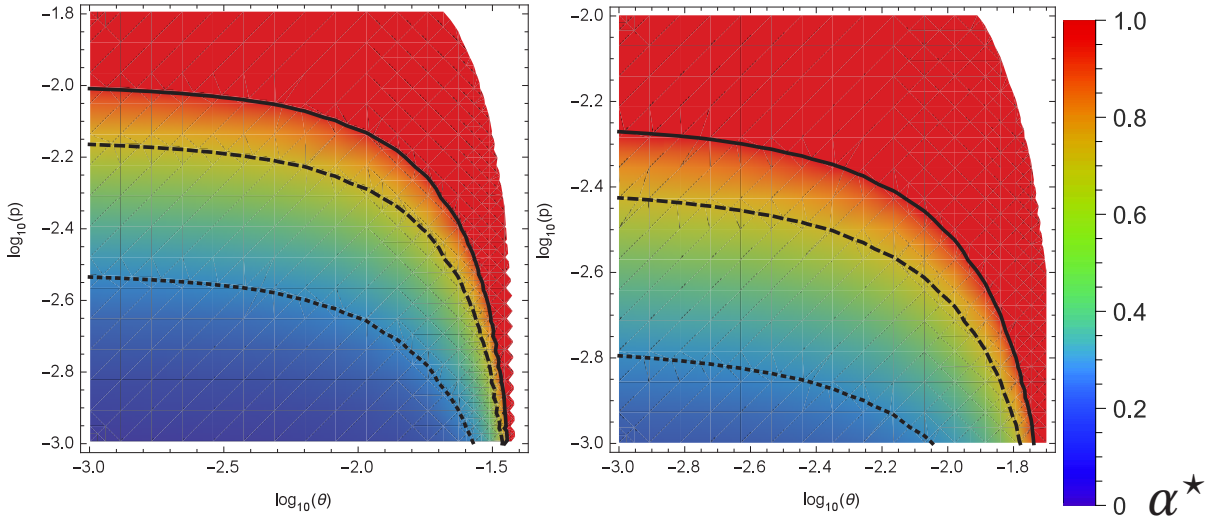

Figure 0.d.1. – Boundaries of the evolutionary attracting values of CFR.
Underestimate ($\alpha^\star_-$, left) and the overestimate ($\alpha^\star_+$, right) values of the evolutionary attractor $\alpha^\star$ as a function of unsafe burial ratio θ and trade-off exponent p. The solid, the dashed and the dotted lines correspond to $\alpha^\star = 1, 0.7$ and 0.3 respectively. Other parameter values are default (Table 0.2.1).

0.e. Sensitivity analysis

For the sake of both generality and graphical readability, we reduced the dimensionality of the parameter space by defining:

$$\eta := \frac{b_I}{\gamma}, \delta := \frac{b_D}{\varepsilon} \cdot \frac{\gamma}{b_I}, \kappa := \frac{b_C}{\sigma} \cdot \frac{\gamma}{b_I}, \tag{0.e.1}$$

where η is the average number of infectious contacts between one susceptible and one symptomatic individual over the symptomatic individual's symptomatic period, δ is the ratio between the equivalent of η for dead bodies and η itself, and κ is the ratio between the equivalent of η for convalescent individuals and η itself. Quantity η is equal to the symptomatic individual relative (that is normalised by S_0) contribution to the basic reproduction number, and is used for defining both δ and κ. Therefore, η is a primary scaling factor that can be eliminated through any estimated value of the $\mathcal{R}_0$. δ and κ are secondary scaling factors that can be studied independently.

First, the basic reproduction number can be rewritten using definitions (0.e.1),

$$\mathcal{R}_0 = ((1 + \alpha\theta\delta)S_0 + (1 - \alpha)\kappa)\eta\alpha^p.$$

Therefore, any given a set of estimated epidemiological data $(\widehat{\alpha}, \widehat{\theta}, \widehat{S_0}, \widehat{\mathcal{R}_0})$ can be used to scale η, while keeping undetermined the trade-off exponent p, that is to say

$$\widehat{\eta} = \frac{\widehat{\mathcal{R}_0}\widehat{\alpha}^{-p}}{\left(1 + \widehat{\alpha}\widehat{\theta}\delta\right)\widehat{S_0} + (1 - \widehat{\alpha})\kappa}. \tag{0.e.2}$$

Rewriting the selection gradient at $\alpha = 1$ with definitions (0.e.1),

$$\Delta(1) \approx p + \frac{\theta\delta}{1 + \theta\delta} - \kappa\eta,$$

and imputing estimated data with equation (0.e.2),

$$\Delta(1) \approx p + \frac{\theta\delta}{1+\theta\delta} - \frac{\widehat{\mathcal{R}_0}\widehat{\alpha}^{-p}\kappa}{\left(1+\widehat{\alpha}\widehat{\theta}\delta\right)\widehat{S_0} + (1-\widehat{\alpha})\kappa},$$

we find that

$$\begin{aligned}\Delta(1) < 0 &\Longleftrightarrow ((1+\theta\delta)p+\theta\delta)\left(\left(1+\widehat{\alpha}\widehat{\theta}\delta\right)\widehat{S_0} + (1-\widehat{\alpha})\kappa\right) < (1+\theta\delta)\widehat{\mathcal{R}_0}\widehat{\alpha}^{-p}\kappa,\\ &\Longleftrightarrow ((1+\theta\delta)p+\theta\delta)\left(1+\widehat{\alpha}\widehat{\theta}\delta\right)\widehat{S_0} < \left((1+\theta\delta)\widehat{\mathcal{R}_0}\widehat{\alpha}^{-p} - ((1+\theta\delta)p+\theta\delta)(1-\widehat{\alpha})\right)\kappa.\end{aligned}$$

Further investigation requires to study the inequality

$$\widehat{\mathcal{R}_0} \gtrless \left(p + \frac{\theta\delta}{1+\theta\delta}\right)(1-\widehat{\alpha})\widehat{\alpha}^p.$$

Elementary calculus then shows that for any couple $(p,\widehat{\alpha}) \in \mathbb{R}_+ \times [0,1]$, we have the following upper bound

$$\left(p + \frac{\theta\delta}{1+\theta\delta}\right)(1-\widehat{\alpha})\widehat{\alpha}^p \leq (p+1)(1-\widehat{\alpha})\widehat{\alpha}^p \leq 1,$$

By definition, epidemiological data originate from outbreaks for which $\widehat{\mathcal{R}_0} > 1$, therefore we get the inequality used to plot our figure

$$\Delta(1) < 0 \Longleftrightarrow \frac{\kappa}{\widehat{S_0}} > \frac{((1+\theta\delta)p+\theta\delta)\left(1+\widehat{\alpha}\widehat{\theta}\delta\right)}{(1+\theta\delta)\widehat{\mathcal{R}_0}\widehat{\alpha}^{-p} - ((1+\theta\delta)p+\theta\delta)(1-\widehat{\alpha})}, \tag{0.e.3}$$

with values $\widehat{\alpha} = 0.7$, $\widehat{\theta} = 0.25$, $\widehat{S_0} = 4.44444 \cdot 10^6$ and $\widehat{\mathcal{R}_0} \in [1.26, 2.53]$, according to reference (WHO Ebola Response Team, 2014; Nyenswah *et al.*, 2016; Abbate *et al.*, 2016) respectively.

0.f. Application of the Price equation

Introducing a diversity of $n \in \mathbb{N}^\star$ non-coinfecting strains of EBOV, system (0.a.1) becomes a set of $4n+1$ ordinary differential equations, where for all $i \in \{1,\dots,n\}$,

$$\begin{cases} \frac{\mathrm{d}S}{\mathrm{d}t} &= \lambda - \mu S - \sum_{i=1}^{n} \left(\beta_{I,i} I_i + \beta_{D,i} D_i + \beta_{C,i} C_i\right) S, \\ \frac{\mathrm{d}E_i}{\mathrm{d}t} &= \left(\beta_{I,i} I_i + \beta_{D,i} D_i + \beta_{C,i} C_i\right) S - \omega_i E_i, \\ \frac{\mathrm{d}I_i}{\mathrm{d}t} &= \omega_i E_i - \gamma_i I_i, \\ \frac{\mathrm{d}D_i}{\mathrm{d}t} &= \alpha_i \theta \gamma_i I_i - \varepsilon_i D_i, \\ \frac{\mathrm{d}C_i}{\mathrm{d}t} &= (1-\alpha_i)\gamma_i I_i - \sigma_i D_i. \end{cases} \tag{0.f.1}$$

The total population size of each class, denoted by $H_\bullet \coloneqq \sum_{i=1}^{n} H_i$, therefore satisfies

$$\begin{cases} \frac{\mathrm{d}S}{\mathrm{d}t} &= \lambda - \mu S - \left(\overline{\beta_I}^I I_\bullet + \overline{\beta_D}^D D_\bullet + \overline{\beta_C}^C C_\bullet\right) S, \\ \frac{\mathrm{d}E_\bullet}{\mathrm{d}t} &= \left(\overline{\beta_I}^I I_\bullet + \overline{\beta_D}^D D_\bullet + \overline{\beta_C}^C C_\bullet\right) S - \overline{\omega}^E E_\bullet, \\ \frac{\mathrm{d}I_\bullet}{\mathrm{d}t} &= \overline{\omega}^E E_\bullet - \overline{\gamma}^I I_\bullet, \\ \frac{\mathrm{d}D_\bullet}{\mathrm{d}t} &= \theta \overline{\alpha\gamma}^I I_\bullet - \overline{\varepsilon}^D D_\bullet, \\ \frac{\mathrm{d}C_\bullet}{\mathrm{d}t} &= \overline{\gamma}^I I_\bullet - \overline{\alpha\gamma}^I I_\bullet - \overline{\sigma}^D D_\bullet. \end{cases} \tag{0.f.2}$$

By definition, an average value of a trait x in a compartment H is given by $\overline{x}^H = \sum_{i=1}^{n} x_i \frac{H_i}{H_\bullet}$.

If we assume that the trait value of a strain is constant and neglect mutational variance (i.e. $\frac{\mathrm{d}x_i}{\mathrm{d}t} = 0$), the dynamics of any trait x in the I compartment are thus given by

$$\begin{aligned} \frac{\mathrm{d}\overline{x}^I}{\mathrm{d}t} &= \sum_{i=1}^{n} \left(\frac{1}{I_\bullet} \frac{\mathrm{d}I_i}{\mathrm{d}t} - \frac{I_i}{I_\bullet^2} \frac{\mathrm{d}I_\bullet}{\mathrm{d}t} \right) x_i, \\ &= \sum_{i=1}^{n} \left(\left(\omega_i E_i - \gamma_i I_i\right) \frac{1}{I_\bullet} - \left(\overline{\omega}^E E_\bullet - \overline{\gamma}^I I_\bullet\right) \frac{I_i}{I_\bullet^2} \right) x_i, \\ &= \sum_{i=1}^{n} \left(\omega_i \frac{E_i}{E_\bullet} - \overline{\omega} \frac{I_i}{I_\bullet} \right) x_i \frac{E_\bullet}{I_\bullet} - \sum_{i=1}^{n} \left(\gamma \frac{I_i}{I_\bullet} - \overline{\gamma} \frac{I_i}{I_\bullet} \right) x_i, \\ &= \frac{E_\bullet}{I_\bullet} \sum_{i=1}^{n} \left(\omega_i \frac{E_i}{E_\bullet} - \overline{\omega} \frac{E_i}{E_\bullet} + \overline{\omega} \frac{E_i}{E_\bullet} - \overline{\omega} \frac{I_i}{I_\bullet} \right) x_i - \sum_{i=1}^{n} \left(\gamma - \overline{\gamma}\right) x_i \frac{I_i}{I_\bullet}, \\ \frac{\mathrm{d}\overline{x}^I}{\mathrm{d}t} &= \left(\mathrm{cov}_E(x,\omega) + \left(\overline{x}^E - \overline{x}^I\right) \overline{\omega}^E \right) \frac{E_\bullet}{I_\bullet} - \mathrm{cov}_I(x,\gamma), \end{aligned} \tag{0.f.3}$$

where cov indicates a genetic covariance between two traits, $\overline{x}^H$ is the average value of trait x in host compartment X and $\overline{xy}^H$ is the average value of the product xy in the same compartment. This illustrates that it might be difficult to disentangle a trait of interest x with the duration of the latent period ($1/\omega$) if this latter trait varies for different virus genotypes.

Similarly, in the E compartment we have

$$\begin{aligned}
\frac{\mathrm{d}\overline{x}^E}{\mathrm{d}t} &= \sum_{i=1}^{n}\left(\frac{1}{E_\bullet}\frac{\mathrm{d}E_i}{\mathrm{d}t} - \frac{E_i}{E_\bullet^2}\frac{\mathrm{d}E_\bullet}{\mathrm{d}t}\right)x_i,\\
&= \sum_{i=1}^{n}\left(\left(\left(\beta_i^I I_i + \beta_i^D D_i + \beta_i^C C_i\right)S - \omega_i E_i\right)\frac{1}{E_\bullet}\right.\\
&\qquad \left. - \left(\left(\overline{\beta^I}^I I_\bullet + \overline{\beta^D}^D D_\bullet + \overline{\beta^C}^C C_\bullet\right)S - \overline{\omega}E_\bullet\right)\frac{E_i}{E_\bullet^2}\right)x_i,\\
&= \frac{S}{E_\bullet}\sum_{i=1}^{n}\left(\left(\beta_i^I I_i + \beta_i^D D_i + \beta_i^C C_i\right) - \left(\overline{\beta^I}^I I_\bullet + \overline{\beta^D}^D D_\bullet + \overline{\beta^C}^C C_\bullet\right)\frac{E_i}{E_\bullet}\right)x_i\\
&\qquad - \sum_{i=1}^{n}(\omega_i - \overline{\omega})x_i\frac{E_i}{E_\bullet},\\
&= \frac{S}{E_\bullet}\left(\sum_{H\in\{I,D,C\}} H_\bullet \sum_{i=1}^{n}\left(\beta_i^H\frac{H_i}{H_\bullet} - \overline{\beta_H}^H\frac{H_i}{H_\bullet} + \overline{\beta_H}^H\frac{H_i}{H_\bullet} - \overline{\beta_H}^H\frac{E_i}{E_\bullet}\right)x_i\right) - \mathrm{cov}_E(x,\omega),\\
\frac{\mathrm{d}\overline{x}^E}{\mathrm{d}t} &= \frac{S}{E_\bullet}\left(\sum_{H\in\{I,D,C\}}\left(\mathrm{cov}_H\left(x,\beta_H\right) + \left(\overline{x}^H - \overline{x}^E\right)\overline{\beta_H}^H\right)H_\bullet\right) - \mathrm{cov}_E(x,\omega). \qquad (0.f.4)
\end{aligned}$$

If we now focus on the dead hosts, we have

$$\begin{aligned}
\frac{\mathrm{d}\overline{x}^D}{\mathrm{d}t} &= \sum_{i=1}^{n}\left(\frac{1}{D_\bullet}\frac{\mathrm{d}D_i}{\mathrm{d}t} - \frac{D_i}{D_\bullet^2}\frac{\mathrm{d}D_\bullet}{\mathrm{d}t}\right)x_i,\\
&= \sum_{i=1}^{n}\left(\left(\alpha_i\theta\gamma_i I_i - \varepsilon_i D_i\right)\frac{1}{D_\bullet} - \left(\theta\overline{\alpha\gamma}^I I_\bullet - \overline{\varepsilon}D_\bullet\right)\frac{D_i}{D_\bullet^2}\right)x_i,\\
&= \theta\frac{I_\bullet}{D_\bullet}\sum_{i=1}^{n}\left(\alpha_i\gamma_i\frac{I_i}{I_\bullet} - \overline{\alpha\gamma}^I\frac{D_i}{D_\bullet}\right)x_i - \sum_{i=1}^{n}(\varepsilon_i - \overline{\varepsilon})x_i\frac{D_i}{D_\bullet},\\
&= \theta\frac{I_\bullet}{D_\bullet}\sum_{i=1}^{n}\left(\alpha_i\gamma_i\frac{I_i}{I_\bullet} - \overline{\alpha\gamma}^I\frac{I_i}{I_\bullet} + \overline{\alpha\gamma}^I\frac{I_i}{I_\bullet} - \overline{\alpha\gamma}^I\frac{D_i}{D_\bullet}\right)x_i - \sum_{i=1}^{n}(\varepsilon_i - \overline{\varepsilon})x_i\frac{D_i}{D_\bullet},\\
\frac{\mathrm{d}\overline{x}^D}{\mathrm{d}t} &= \left(\mathrm{cov}_I\left(x,\alpha\gamma\right) + \left(\overline{x}^I - \overline{x}^D\right)\overline{\alpha\gamma}^I\right)\theta\frac{I_\bullet}{D_\bullet} - \mathrm{cov}_D(x,\varepsilon). \qquad (0.f.5)
\end{aligned}$$

Finally, in the convalescent hosts, we have

$$\begin{aligned}
\frac{\mathrm{d}\overline{x}^C}{\mathrm{d}t} &= \sum_{i=1}^{n}\left(\frac{\mathrm{d}C_i}{\mathrm{d}t}\frac{1}{C_\bullet} - \frac{\mathrm{d}C_\bullet}{\mathrm{d}t}\frac{C_i}{C_\bullet^2}\right)x_i,\\
&= \sum_{i=1}^{n}\left(\left((1-\alpha_i)\gamma_i I_i - \sigma_i C_i\right)\frac{1}{C_\bullet} - \left(\left(\overline{\gamma}^I - \overline{\alpha\gamma}^I\right)I_\bullet - \overline{\sigma}^C C_\bullet\right)\frac{D_i}{D_\bullet^2}\right)x_i,\\
&= \frac{I_\bullet}{C_\bullet}\sum_{i=1}^{n}\left(\gamma_i\frac{I_i}{I_\bullet} - \alpha_i\gamma_i\frac{I_i}{I_\bullet} - \left(\overline{\gamma}^I - \overline{\alpha\gamma}^I\right)\frac{C_i}{C_\bullet}\right)x_i - \sum_{i=1}^{n}\left(\sigma_i - \overline{\sigma}^C\right)x_i\frac{C_i}{C_\bullet},\\
&= \frac{I_\bullet}{C_\bullet}\sum_{i=1}^{n}\left(\frac{I_i}{I_\bullet}\left(\gamma_i - \overline{\gamma}^I - \alpha_i\gamma_i + \overline{\alpha\gamma}^I\right) + \overline{\gamma}^I\frac{I_i}{I_\bullet} - \overline{\gamma}^I\frac{C_i}{C_\bullet} + \overline{\alpha\gamma}^I\frac{C_i}{C_\bullet} - \overline{\alpha\gamma}^I\frac{I_i}{I_\bullet}\right)x_i - \sum_{i=1}^{n}\left(\sigma_i - \overline{\sigma}^C\right)x_i\frac{C_i}{C_\bullet},\\
\frac{\mathrm{d}\overline{x}^C}{\mathrm{d}t} &= \frac{I_\bullet}{C_\bullet}\left(\mathrm{cov}_I\left(x,\gamma\right) - \mathrm{cov}_I\left(x,\alpha\gamma\right) + \left(\overline{x}^I - \overline{x}^C\right)\overline{\gamma}^I - \left(\overline{x}^I - \overline{x}^C\right)\overline{\alpha\gamma}^I\right) - \mathrm{cov}_C(x,\sigma). \qquad (0.f.6)
\end{aligned}$$

0.g. Numerical simulations

We explored 8 scenarios. For each, we assume that we have $n = 100$ EBOV strains. The standing genetic variation for the CFR α_i ($i \in \{1,\dots n\}$) is drawn from a Gaussian distribution with mean $\widehat{\alpha} = 0.7$ and standard deviation $\varsigma = 0.1$

We only explored positive correlations between CFR and transmissions rates, consistently with our trade-off hypothesis. We also did not investigate correlations between CFR and *post mortem* elimination rate because we assume that the period over which an unsafe buried body is still a suitable environment for virion survival is independent from the initial number of virions. Finally, we ignored convalescent-related variables received since this component of EBOV transmission is much smaller than the others two.

The description of the 9 scenarios is as follows:

1. No genetic correlation between the CFR α and other traits ("all constant" panel, also shown in the main text).
2. Addition of a negative correlation between α and the rate of end of latency period ω.
3. Addition of a positive correlation between α and the transmission rates β_H ("+bH" panel) that will be kept for the next six scenarios.
4. Addition of a positive correlation between α and the inverse of the latency period ω ("+bH+O" panel).
5. Reversing the correlation between α and ω ("+bH-O" panel).
6. positive correlations between α and β_H, α and ω and α and the inverse of the symptomatic period γ ("+bH+O+G" panel)
7. positive correlations between α and β_H and between α and γ, negative correlation between α and ω ("+bH-O+G" panel)
8. positive correlations between α and β_H and between α and ω, negative correlation between α and γ ("+bH+O-G" panel)
9. positive correlation between α and β_H, negative correlations between α and ω and between α and γ ("+bH-O-G" panel)

Positively and negatively correlated traits were drawn according to the formulas $x_i = \left(\varrho\frac{\alpha_i}{\widehat{\alpha}} + \left(1-\varrho\right)\xi_i\right)\widehat{x}$ and $x_i = \left(\left(-(\max(\alpha)-\widehat{\alpha})\frac{\alpha_i}{\widehat{\alpha}} + \max(\alpha) - \min(\alpha)\right)\frac{\varrho}{\widehat{\alpha}-\min(\alpha)} + \left(1-\varrho\right)\xi_i\right)\widehat{x}$ respectively, where $\widehat{x}$ the estimated value of $x \equiv \beta_H, \omega, \gamma$ according to Table 0.2.1, $\varrho = 0.5$ denotes the strength of the correlation and ξ_i a Gaussian random variable with mean 1 and standard deviation $\varsigma = 0.1$. Initial conditions are given by $S(0) = \frac{\lambda}{\mu} \approx 4.4 \cdot 10^6$ ind and $H_i(0) = 1$ ind for all $i \in \{1,\dots,n\}$ and all $H \equiv E, I, D, C$.

Results for 8 of the scenarios are shown in Figure 0.g.1 (scenario 2 is only shown in the main text for space constraint reasons).

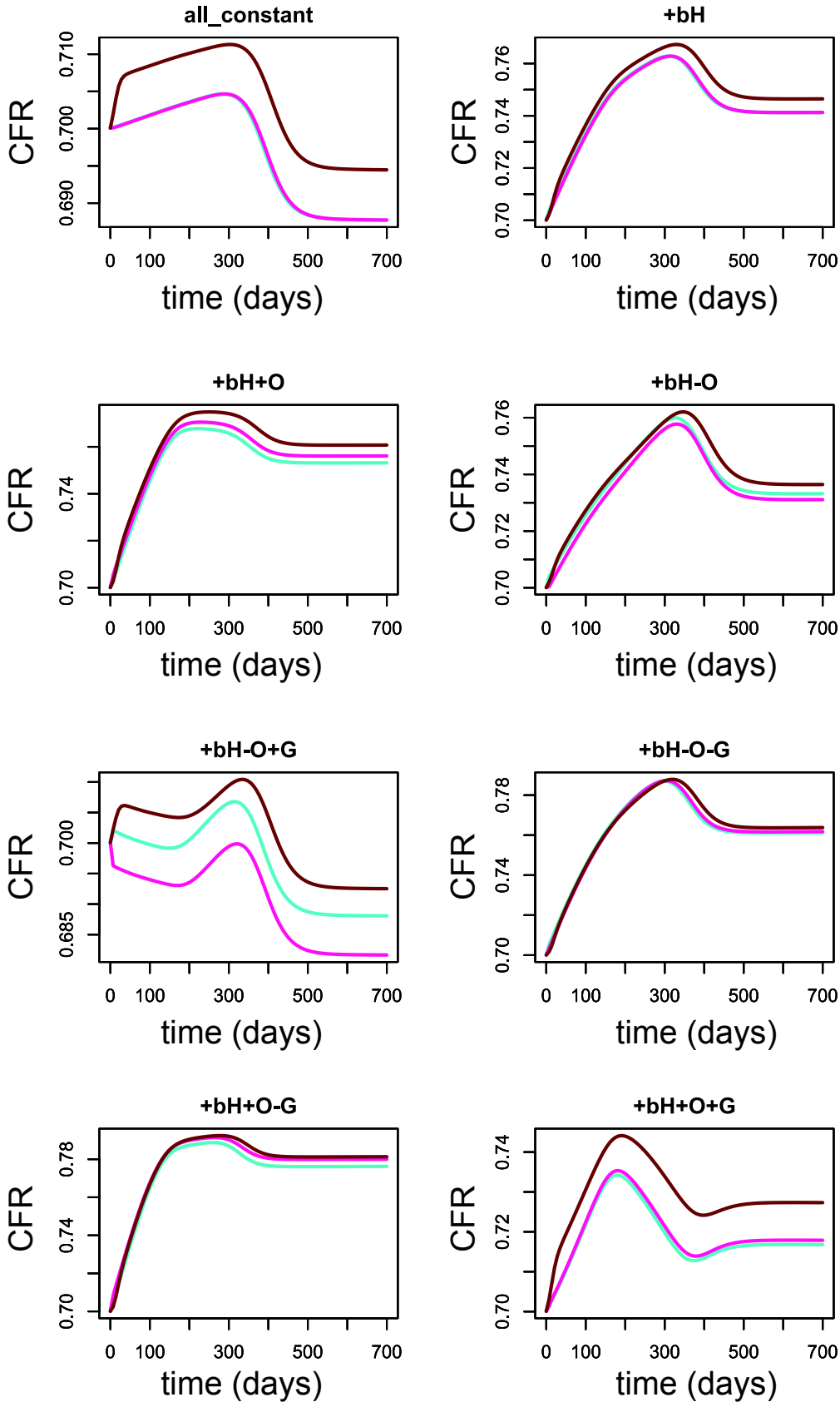

Figure 0.g.1. – Short-term evolution of CFR with standing genetic variation.
The CFR averaged over the exposed individuals ($\overline{\alpha}^E$) is depicted in cyan, over the symptomatic individuals ($\overline{\alpha}^I$) in pink and over the infectious dead bodies ($\overline{\alpha}^D$) in brown.

0.h. Virulence and transmission routes

We have showed that EBOV' reproduction numbers can be split into three additive components that correspond to each of the three transmission routes namely symptomatic (through regular contact with symptomatic individuals), *post mortem* (through contact with unsafe buried infectious dead bodies) and sexual (through sexual contact with convalescent individuals). According to our trade-off assumption, the intensity of each of these components is modulated by virulence: both symptomatic and *post mortem* components always increase with virulence while sexual component is maximum for an intermediate virulence level (unless there is no trade-off, in which case the symptomatic component is constant and the sexual component decreases with virulence), as in Figure 0.h.1.

This come from the fact that virulence increases all transmission rates and infectious bodies inflows, while decreasing the convalescent individuals inflow. Virulence then also acts as an investment cursor between the exclusive *post mortem* and sexual transmission routes. It thus appears that the cost of virulence is strictly limited to loss in sexual transmission. Therefore, it is only if the sexual component is the dominant route of the virus' life cycle that this cost can really balances with the overall transmission

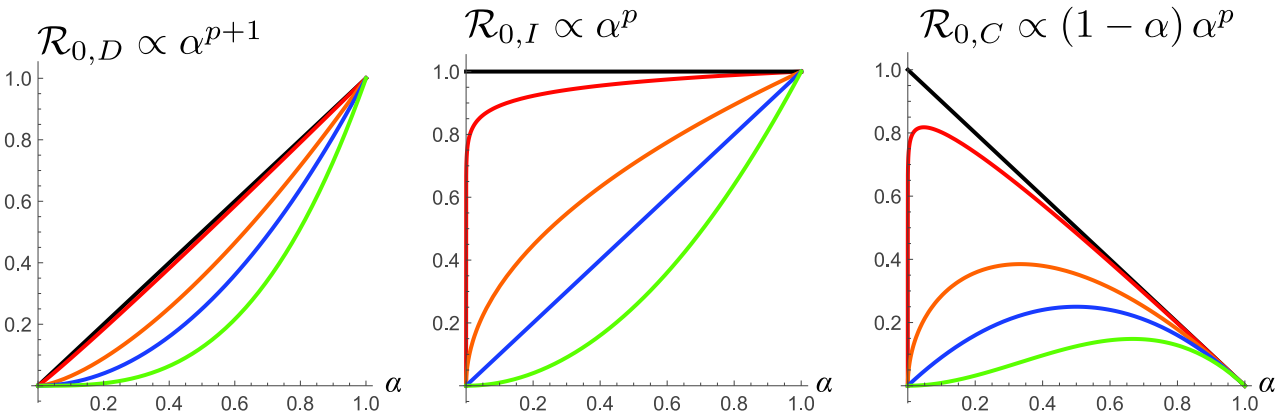

Figure 0.h.1. – Relative variation of transmission route component intensity as a function of virulence and trade-off shape.
Post mortem (left), symptomatic (middle), and sexual (right) transmission components as a function of virulence and trade-off shape ($p = 0$ in black, 0.05 in red, 0.5 in orange, 1 in blue and 2 in green).

0.ω. Épilogue

Ainsi que montré au cours de ce chapitre, l'étude de l'évolution de la virulence ne pose pas de problème théorique majeur lorsque la dynamique épidémiologique est relativement simple et se suffit à elle-même. La co-circulation de plusieurs souches a bien été envisagée (tantôt n souches initiales pour l'évolution au temps cours, tantôt un dimorphisme transitoire pour l'évolution au temps long), mais sur l'unique mode de voies d'infections parallèles et indépendantes. Il s'agit d'une hypothèse forte qui suppose qu'une souche déjà établie exclut toutes les autres et qu'il existe une parfaite immunité croisée.

Ci-après, la seconde partie de l'introduction montre l'importance naturelle des infections multiples, qu'il s'agisse de polymorphisme inter-hôte ou intra-hôte. Ce dernier cas soulève alors le problème des interactions intra-hôtes, dont l'étude est la seule à pouvoir justifier de l'issue d'une co-inoculation. En particulier, nous montrerons dans le chapitre 2, que le polymorphisme d'Ébola a ici été traité sous l'angle de ce que nous formaliserons par la *priorinfection*, qui n'est qu'une modalité parmi d'autres d'infections multiples.

ι Des infections multiples

ι.1. Polymorphisme parasitaire

Le paradigme considérant le parasitisme comme une relation asymétrique entre deux agents, le parasite et son hôte, s'est révélé fécond pour la compréhension de ce mode de vie majoritaire au sein du monde vivant (qu'il s'agisse de concepts généraux ou de diversité des mécanismes impliqués) (Combes, 2010). Néanmoins, il est aujourd'hui établi que les parasites circulant dans les populations naturelles d'hôtes se limitent rarement à une unique souche ou espèce (ci-après simplement **type**, ou génotype) (Petney & Andrews, 1998; Lord *et al.*, 1999; Cox, 2001). Ce **polymorphisme parasitaire** (au sens large, *i.e.* incluant diversité intra- et inter-spécifique) réside avant tout entre les hôtes – plus de 1400 espèces de parasites sont recensées chez l'Homme (Taylor *et al.*, 2001) – mais peut aussi survenir au sein d'un même hôte lorsque plusieurs types l'infectent simultanément. Souvent appelées **coinfections**, elles sont chez l'Homme aussi bien le fait de plusieurs souches d'une même espèce de parasite (Balmer & Tanner, 2011), citons en premier lieu le cas du paludisme (plus d'une dizaine de souches de *Plasmodium falciparum* chez certains individus (Juliano *et al.*, 2010)), que de plusieurs espèces, en particulier les coinfections VIH - *Mycobacterium tuberculosis* (Sharma *et al.*, 2005) ou VIH - HBV ou HCV (Alter, 2006). Une analyse méta-génomique a même révélé qu'en moyenne 5,5 genre de virus sont représentés dans le microbiome de chaque être humain (Wylie *et al.*, 2014).

Le pluralisme de référentiels est une source d'ambigüité courante dans la nomenclature biologique. Ainsi, le qualificatif botanique d'hermaphrodite s'applique aussi bien à la fleur, à l'individu ou à l'espèce d'angiosperme (Gouyon *et al.*, 1996). De même, une infection se réfère à la persistence d'un micro-organisme aussi bien dans une cellule (Syverton & Berry, 1947) – pour les virologistes –, dans un organisme (Keeling & Rohani, 2008) – pour les épidémiologistes –, ou dans une population (van Baalen & Sabelis, 1995) – pour les écologues et évolutionnistes. Dans le présent travail, nous choisissons d'appeler **infections multiples** le polymophisme parasitaire à l'échelle de la population d'hôtes, sans présumer de la possible coexistence de plusieurs types parasitaires au sein d'un même hôte, qui sera, le cas échéant, explicitement mentionnée *.

*. On recense dans la littérature un nombre pléthorique de termes désignant les infections poly-

Parce que le polymorphisme parasitaire affecte l'épidémiologie ainsi que la virulence effective (Griffiths *et al.*, 2011), les infections multiples constituent un sujet d'étude de premier plan en biomédecine humaine (Harries *et al.*, 2004; Balmer & Tanner, 2011; de Oliveira *et al.*, 2015; Verma, 2015) en médecine vétérinaire et zoologie (Battilani *et al.*, 2011; Ybañez *et al.*, 2016; Cassle *et al.*, 2016) et en phytopathologie et biologie végétale (van der Plank, 1963; Sanz *et al.*, 2000; Roossinck, 2012; Hull, 2013). Elles soulèvent par ailleurs de nouvelles questions en écologie microbienne (Read & Taylor, 2001; Riley & Wertz, 2002; Pedersen & Fenton, 2007; Hellard *et al.*, 2015; Bashey, 2015; Bose *et al.*, 2016) et biologie évolutive (Brown, 1999; Alizon & Lion, 2011; Alizon *et al.*, 2013; Pollitt *et al.*, 2014; Cressler *et al.*, 2015), spécialement du fait des interactions qui surviennent entre types parasitaires à l'intérieur des hôtes qu'ils se partagent.

morphes à l'échelle de l'hôte : (dans le désordre) infections concomitantes (Cox, 2001), concourantes (Reddy *et al.*, 2017), mélangées (Moore, 1898), poly-microbienne (Brogden *et al.*, 2005), poly-parasitaires (Pullan & Brooker, 2008), génétiquement variées (Read & Taylor, 2001), à souches multiples (Penn *et al.*, 2002), à génotypes multiples (Rigaud *et al.*, 2010), multi-infections (Radomyos *et al.*, 1994), poly-infections (Lancastre *et al.*, 1989), pluri-infections (Demaerschalck *et al.*, 1995), *mix-infections* (Chen *et al.*, 2003) et bien sûr coinfection (Damasio *et al.*, 2015). Dans le chapitre 2, nous reviendrons en détail sur ces appellations et montrons en quoi elles ne sont pas pertinentes pour appréhender la diversité épidémiologique des infections multiples.

ι.2. Interactions intra-hôte

Lorsque plusieurs types parasitaires circulent dans une population d'hôtes, ils ne concourent pas seulement pour les hôtes susceptibles, mais aussi pour les hôtes déjà infectés et, en leur sein, leurs ressources limitées (Mideo, 2009). Une fois inoculé dans un hôte, les parasites interagissent : ces interactions peuvent être directes (Costerton *et al.*, 1999) (de parasite à parasite) ou indirectes (via d'autres agents, inertes voire vivants), et leurs effets sur la croissance négatifs comme positifs (Hellard *et al.*, 2015). De fait, ces interactions concernent aussi bien les parasites appartenant à des types différents (interactions inter-typiques, ou croisées) que des parasites du même type (interactions intra-typiques ou auto-interactions) (Bashey, 2015). La figure ι.2.1 présente certaines de ces interactions sur l'exemple de deux types bactériens infectant un hôte vertébré.

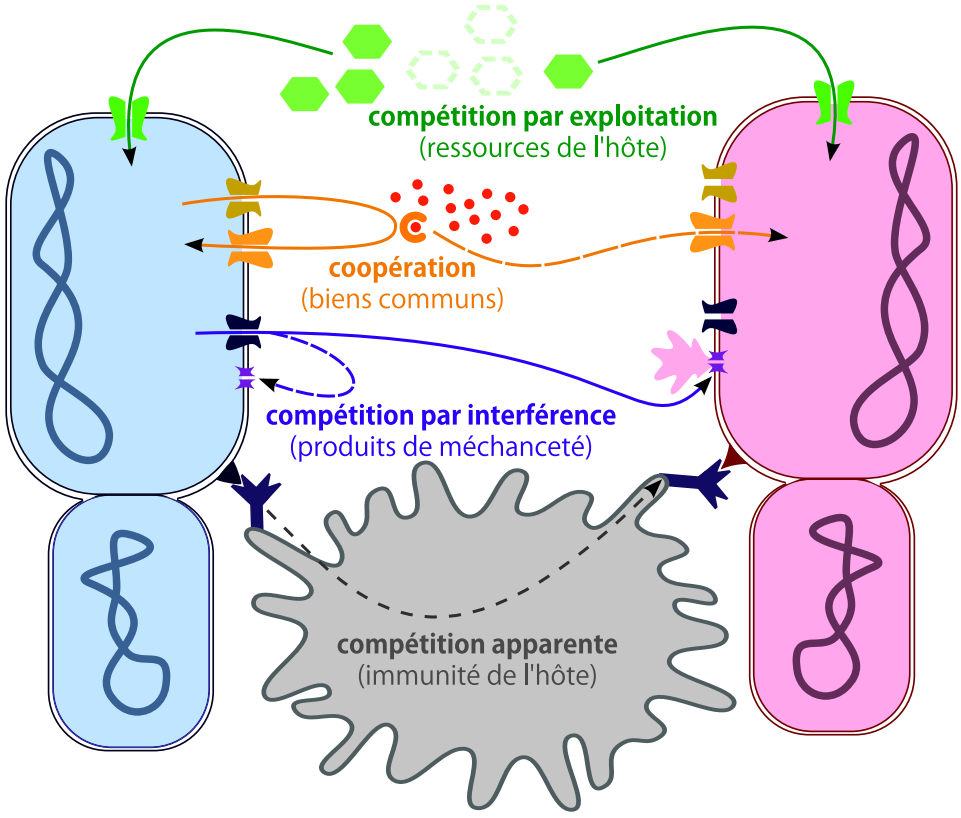

Figure ι.2.1. – Illustration schématique des différentes catégories d'interactions possibles entre deux types de bactéries au sein d'un même hôte.
Les bactéries sont représentées par des cellules oblongues, leur couleur indiquant leur lignée. Les bactéries sont en compétition par exploitation lorsqu'elles se partagent une même ressource présentes dans l'hôte, comme le glucose(Wilson & Perini, 1988). Elles coopèrent au moyen de biens communs (Brown *et al.*, 2002) qui peuvent aussi bénéficier aux bactéries qui n'en produisent pas, comme ici un sidérophore chélatant les ions ferriques (Wandersman & Delepelaire, 2004). Les produits de méchanceté (Gardner *et al.*, 2004), quant à eux, caractérisent une compétition par interférence, à l'image de bactériocines perforant la paroi bactérienne (Riley & Chavan, 2007). Enfin, le système immunitaire de l'hôte, sur l'exemple du macrophage, médie une compétition apparente entre bactéries (Owen *et al.*, 2013).

Une interaction est l'effet d'un individu émetteur A sur un individu récepteur B. Elle peut éventuellement être réciproque (B influence A) voire réflexive (A s'influence lui-

même). Nous appelons coopération * une interaction qui bénéficie (en terme de survie ou de fécondité) aux deux individus impliqués et compétition une interaction qui nuit à l'individu récepteur (l'individu émetteur peut quant à lui en retirer un bénéfice ou en payer un coût). La compétition se décline en trois principales modalités selon le type de médiation : apparente (via un prédateur commun), par exploitation (via les ressources) et par interférence (via des sécrétions nuisibles) (Bashey, 2015). Nous appliquons ces termes aux interactions parasitaires intra-hôte indépendamment des types auxquels appartiennent les parasites, contrairement à la littérature écologique dont s'inspire ce vocabulaire, qui emploie des nomenclatures distinctes selon si l'interaction est intra- ou inter-spécifique. Le tableau ι.2.1 résume ces correspondances terminologiques tout en illustrant chacune de ces interactions par des exemples documentés dans le monde bactérien † et viral. (Des interactions intra-hôtes impliquant des micro-parasites eucaryotes ont aussi été mises en évidence, en particulier chez *Plasmodium sp.*, voir Råberg *et al.* (2006); Antia *et al.* (2008), y compris en relation avec des parasites bactériens et viraux, voir la revue de Cox (2001)).

	terminologie		exemples	
générique	intra-spécifique	inter-spécifique	bactériens	viraux
coopération	bénéfices mutuels ou altruisme	mutualisme	sidérophores (West & Buckling, 2003)	réplicases (Huang & Baltimore, 1970)
compétition par exploitation	égoïsme	compétition par exploitation	via les ressources de l'hôte (Wilson & Perini, 1988)	(Turner & Chao, 1998)
compétition par interférence	égoïsme ou méchanceté	compétition par interférence	bactériocines (Gardner *et al.*, 2004)	régulateurs[a] (Nethe *et al.*, 2005)
compétition apparente	égoïsme	compétition apparente	via le système immunitaire de l'hôte (Lysenko *et al.*, 2005)	(Cao *et al.*, 1997)

Table ι.2.1. – Typologie des interactions entre micro-organismes.
a : il s'agit de facteurs intracellulaires régulant l'expression génétique de récepteurs d'entrée du virus dans la cellule-hôte.
La terminologie générique est celle employée au cours de ce travail sans distinction de parenté entre acteurs, tandis que les termes intra- et inter-spécifiques se réfèrent respectivement à West *et al.* (2006) et à Smith & Smith (2012). D'autres exemples d'interactions sont référencés dans Hellard *et al.* (2015) et Bashey (2015).

∗. Nous employons ici ce terme dans un sens différent de West *et al.* (2007), pour qui une coopération est une interaction intra-spécifique à effet positif sur l'individu récepteur (*i.e.* bénéfices mutuels ou altruisme) qui résulte d'une adaptation de l'individu émetteur.

†. Dans le présent travail, nous mettrons néanmoins de côté la détection du quorum, importante communication et modulation inter-bactérienne (Miller & Bassler, 2001; Brown *et al.*, 2002), qui mériterait un traitement particulier.

ι.3. Évolution parasitaire sous polymorphisme : faits et modèles

À l'image d'une population de plantes occupant un site dont l'intégrité est compromise par le temps (Ronce, 2007), la survie des micro-parasites repose (sauf exceptions, voir p.ex. Dwyer (1994)) sur la transmission d'un hôte à l'autre de propagules, fruits de la reproduction intra-hôte. En affectant cette reproduction, les interactions qui ont lieu au sein des hôtes ont donc des répercussions majeures sur l'écologie et l'évolution des parasites.

Si la transmission d'un parasite peut demeurer inchangée voire être favorisée* par la présence d'un autre type parasitaire à l'intérieur du même hôte (cas respectivement illustrées par les souches *Israel* et *Mild* du *Tomato yellow leaf curl Virus* (Péréfarres *et al.*, 2014)), elle peut aussi être considérablement diminuée du fait de la compétition (p.ex. entre clones de *Plasmodium chabaudi* (de Roode *et al.*, 2005a), le virus de la dengue (Pepin *et al.*, 2008), ou bien *Borrelia burgdorferi* (Rynkiewicz *et al.*, 2017)). La coexistence intra-hôte peut parfois même être rendue impossible, en vertu de la relative instabilité des communautés écologiques (Tilman, 1982; Mihaljevic, 2012; Barabás *et al.*, 2016). C'est en particulier le cas de l'exclusion mutuelle, où le premier type infectant empêche les infections secondaires, comme par exemple entre souches de bactériophages (Delbrück, 1945) ou de virus de plantes (Ratcliff *et al.*, 1997). Il en résulte qu'en contexte d'infections multiples, la survie au sein d'un hôte fraîchement inoculé, ou tout du moins sa transmission future à partir de celui-ci, n'est plus garantie, à la différence des infections simples (sauf dans le cas où le parasite a besoin d'une autre espèce de parasite pour infecter, voir chapitre 2). Comme tout comportement héritable, les traits qui sous-tendent ces interactions devraient évoluer dans le sens de la maximisation de la transmission parasitaire et donc (hors effets synergiques) de l'exclusion des autres types inoculés. Ces intuitions sont soutenues par les travaux expérimentaux listés dans le tableau ι.3.1.

∗. Cette favorisation est même indispensable dans les cas où l'un des types parasitaires a besoin de l'autre pour se reproduire et/ou se transmettre, à l'image des virus satellites, familiers des phytologues (Francki, 1985).

interaction	trait	sélection	référence expérimentale	système biologique
coopération	production de bien commun	$\searrow^{a}$	Köhler *et al.* (2009)	*Pseudomonas aeruginosa in Homo sapiens*
compétition par exploitation	efficacité d'exploitation des ressources de l'hôte	$\nearrow$	de Roode *et al.* (2005b)	*Plasmodium chabaudi in Mus musculus*
compétition par interférence	méchanceté	$\curvearrowright^{b}$	Riley & Gordon (1999)	*Escherichia coli in Mus musculus*
compétition apparente	activation et résistance à la réponse immunitaire	$\nearrow$	Bae *et al.* (2006)	*Staphylococcus aureus in Mus musculus*

Table ι.3.1. – Prédictions d'évolution adaptative des interactions et preuves empiriques.
a : la coopération est contre-sélectionnée car elle expose la population de parasites à l'invasion par un tricheur avantagé par le bien commun et l'absence du coût de sa production (Turner & Chao, 1999).
b : le paysage adaptatif de la compétition par interférence est vraisemblablement non monotone puisqu'une surproduction peut s'avérer plus coûteuse que bénéfique (Gardner *et al.*, 2004).
Pour plus de détails, voir Bashey (2015).

L'idée que la compétition intra-hôte façonne l'évolution de la virulence est naturellement apparue avec les premiers modèles théoriques considérant le polymorphisme parasitaire (Levin & Pimentel, 1981; Bremermann & Pickering, 1983), renforcés par la suite par les modèles épidémiologiques de Nowak & May (1994); May & Nowak (1995); van Baalen & Sabelis (1995) d'un côté, et les modèles de sélection de parentèle de Frank (1992; 1994; 1996) de l'autre (l'idée de ces derniers fait l'objet de l'encadré **[d]** p.90). Bien que certaines observations empiriques corroborent cette hypothèse (de Roode *et al.*, 2005b; Bell *et al.*, 2006), plusieurs expériences ont en revanche montré une contre-sélection de la virulence en présence de polymorphisme intra-hôte (Turner & Chao, 1999; Pollitt *et al.*, 2014), ainsi que prédit par des modèles alternatifs plus récents (Brown *et al.*, 2002; West & Buckling, 2003) qui mettent en avant la dépendance de l'infection à une action collective (telle la production de biens communs). Le tableau ι.3.2 met en avant les principales modalités d'évolution de la virulence en contexte d'infection multiples, exposant, quand cela est possible, une référence théorique et une validation expérimentale, mais le lecteur intéressé pourra avec profit lire les revues de Gandon & Michalakis (2002); Alizon *et al.* (2013); Alizon (2013a); Cressler *et al.* (2015) sur ce vaste sujet. La figure ι.3.1 illustre quant à elle les principes que partagent les travaux théoriques prédisant une sélection de la virulence d'un côté, et une contre-sélection de l'autre.

Au bout du compte, cela révèle que, jusqu'à présent, la recherche théorique sur l'évolution des infections multiples n'a pas réussi à apporter une réponse unificatrice relative aux pressions de sélections qui pèsent sur la virulence. Cet échec partiel peut s'expliquer par la tendance à complexifier les couches superficielles du modèles (Alizon, 2013a) tout en évitant de s'attaquer à la cause des issues d'inoculation et à la virulence, à savoir la dynamique intra-hôte elle-même (mais voir Alizon & van Baalen (2005)).

contexte	sélection de la virulence	référence théorique	référence empirique	système
compétition par exploitation	↗	Bremermann & Pickering (1983)	de Roode *et al.* (2005b)	*Plasmodium ch. in Mus musculus*
action collective	↘	Brown *et al.* (2002)	Turner & Chao (1999)	Phage Φ6 *in Pseudomonas sp.*
transmission assurée	↗	Lipsitch & Nowak (1995)	Mangin *et al.* (1995)	*Tuzetia sp. in Daphnia magna*
stade libre	↗	Gandon (1998)	Walther & Ewald (2004)	Variola virus *in Homo sapiens*
plasticité, immunité altérée	↘	Choisy & de Roode (2010)		
vaccination, hôte hétérogène	↘	Nowak & May (1994)		

Table ι.3.2. – Prédictions théoriques et validations expérimentales de l'évolution de la virulence en contexte d'infections multiples.

d) évolution de la virulence et apparentement

Considérons un hôte infecté par plusieurs parasites. La valeur sélective w d'un parasite focal peut être vue comme une fonction de sa virulence propre $\alpha \in]0;1[$ ainsi que de la virulence moyenne des parasites coinfectant $\overline{\alpha}$ selon $w(\alpha,\overline{\alpha}) = (\alpha/\overline{\alpha})\cdot(1-\overline{\alpha})$. En faisant l'hypothèse que la virulence est positivement corrélée avec l'exploitation de l'hôte, le premier facteur s'interprète comme le bénéfice individuel à être plus virulent que les autres parasites, tandis que le second facteur représente le coût collectif de la virulence.

Par définition, la virulence évolutivement stable $\alpha^\star$annule le gradient de sélection. Mais ici, la deuxième variable n'est pas indépendante de la première : en effet, si la population de parasite est clonale, alors la virulence focale ne peut varier sans que la virulence moyenne fasse de même (ou alors la structure génétique ne serait plus respectée). Le gradient de sélection se calcule donc comme $\frac{\mathrm{d}w}{\mathrm{d}\alpha} = \partial_1 w + \partial_2 w \frac{\partial\overline{\alpha}}{\partial\alpha}$ où $\frac{\partial\overline{\alpha}}{\partial\alpha}$ s'interprète comme l'apparentement moyen r de la population de parasites (ainsi, lorsque les individus ne sont pas du tout apparentés ($r = 0$), le changement de virulence de l'un n'impacte pas du tout les autres ($\frac{\partial\overline{\alpha}}{\partial\alpha} = 0$) et inversement pour une population clonale ($r = \frac{\partial\overline{\alpha}}{\partial\alpha} = 1$)). Le gradient de sélection s'écrit alors simplement $\frac{\mathrm{d}w}{\mathrm{d}\alpha}(\alpha,\overline{\alpha}) = \left(\overline{\alpha} - \overline{\alpha}^2 - r\alpha\right)/\overline{\alpha}^2$ et on a $\frac{\mathrm{d}w}{\mathrm{d}\alpha}\left(\alpha^\star,\alpha^\star\right) = 0 \Longleftrightarrow \alpha^\star = 1-r$.

Ce modèle phénoménologique simple, d'après Frank (1994, 1996); Gandon & Michalakis (2002), montre ainsi que lorsque l'exploitation est positivement corrélée à la virulence, alors la virulence évolutivement stable l'est négativement avec l'apparentement moyen dans les hôtes coinfectés. Cette modélisation suppose néanmoins que tous les hôtes sont infectés identiquement, or la prise en compte des rétro-actions épidémiologiques peut, selon la paramétrisation des interactions, aboutir à une évolution de la virulence qualitativement différente de celle prédite par la seule modélisation intra-hôte (Alizon & Lion, 2011).

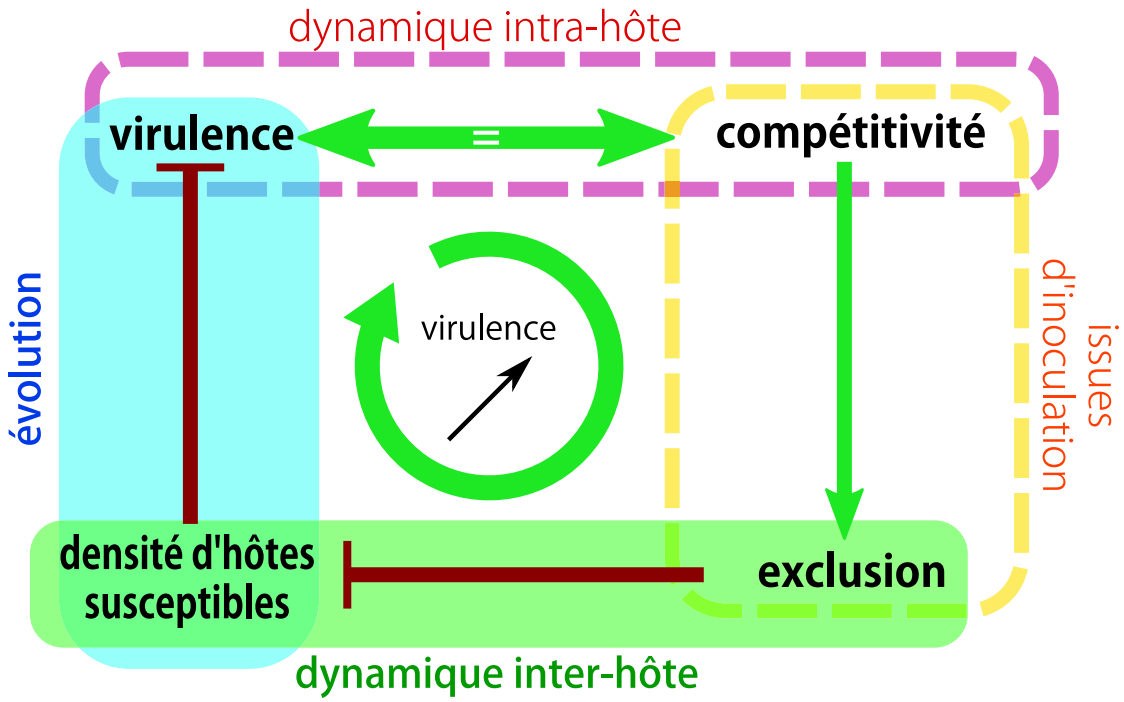

FIGURE ι.3.1. – Deux grandes classes de modèles d'évolution de la virulence.
L'évolution adaptative de la virulence repose sur l'intégration de quatre niveaux biologiques déterminants : la dynamique intra-hôte, l'issue de l'inoculation (*i.e.* la donnée de persistance ou d'extinction de chaque type inoculé au sein d'un hôte – dans la plupart des modèles, l'ordre d'inoculation n'a pas d'incidence sur cette issue, généralement unique et arbitraire (VAN BAALEN & SABELIS, 1995; MAY & NOWAK, 1995; LION, 2013)), la dynamique inter-hôte, et enfin l'évolution. Ces niveaux sont symbolisés par les cadres se chevauchant aux charnières de l'interprétation des modèles. Le cadre est plein lorsque le niveau biologique est explicitement traité par les modèles. Il est creux et tireté lorsqu'il est seulement implicite et fortement contraint (noter qu'aucune classe de modèle ne s'attarde sur l'issue de l'inoculation). Les flèches vertes indiquent une influence positive (la croissance de l'élément de départ induit celle de l'élément d'arrivée). Les flèches rouges indiquent une influence négative (la croissance de l'élément de départ induit la décroissance de l'élément d'arrivée). La dynamique écologique (trois premiers niveaux) influence la dynamique évolutive (dernier niveau) et réciproquement : la rétro-action éco-évolutive (FERRIÈRE & LEGENDRE, 2013) ainsi obtenue est soit positive (en vert) soit négative (en rouge) vis-à-vis de la virulence.
A) Modèles du type « tragédie des biens communs » (HARDIN *et al.*, 1968) : la virulence est supposée positivement corrélée avec la compétitivité intra-hôte, laquelle permet d'envahir des hôtes déjà infectés et d'en exclure les autres types parasitaires. Les hôtes disponibles à l'infection pour les autres types se font donc plus rares, ce qui élimine les stratégies d'exploitation prudentes et provoque une fuite en avant de la virulence. (Remarque : cette classe de modèle peut aussi être formulée au moyen de la sélection de parentèle : en envahissant les hôtes déjà infectés, les types compétitifs diminuent l'apparentement moyen au sein des hôtes, ce qui favorise la virulence, cf encadré **[d]**. Des modèles représentatifs de cette classe sont : LEVIN & PIMENTEL (1981); BREMERMANN & PICKERING (1983); NOWAK & MAY (1994); VAN BAALEN & SABELIS (1995); MAY & NOWAK (1995); FRANK (1996); GANDON (1998).
Voir suite page suivante.

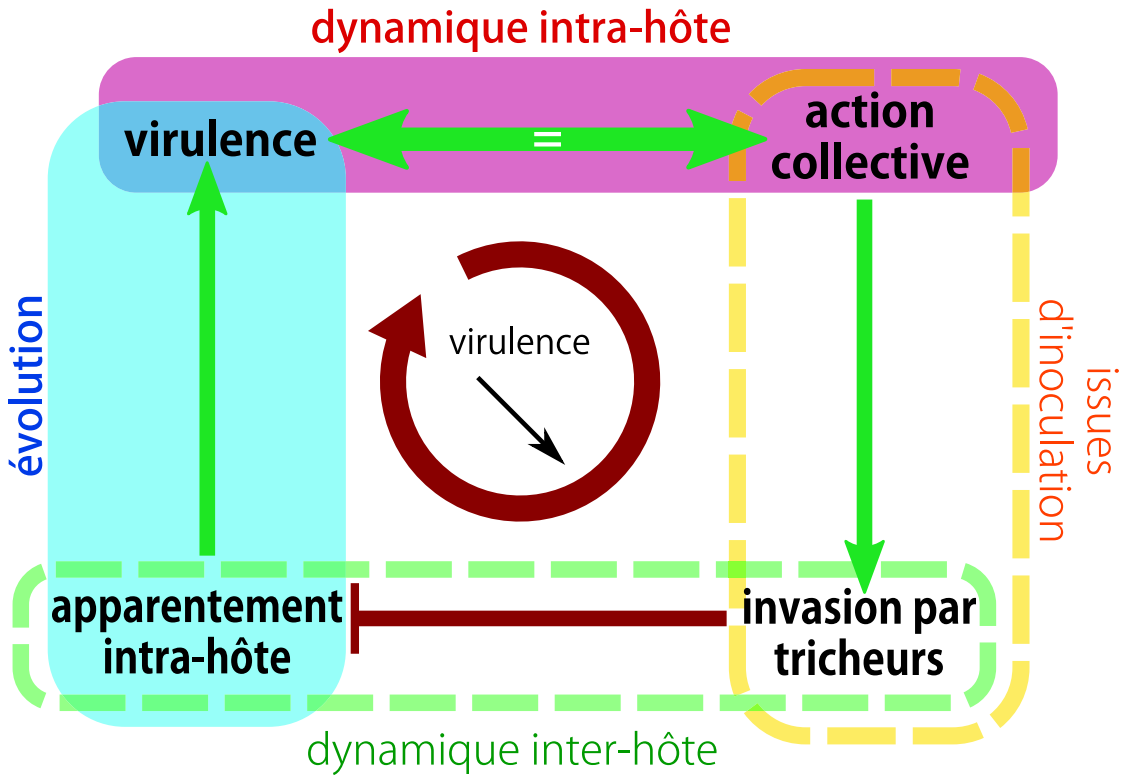

(suite de la Figure ι.3.1)

B) Modèles du type « action collective » (Brown *et al.*, 2002) : ici, l'exploitation et donc l'infection de l'hôte reposent sur une action collective telle la production d'un bien commun. Cette action collective expose la communauté parasitaire de l'hôte à l'invasion par un tricheur qui bénéficie du bien commun sans en payer le coût de production. La reproduction des tricheurs diminue l'apparentement moyen au sein de l'hôte ce qui accroît le coût de production du bien commun au point où le trait d'exploitation collective responsable de la virulence devient contre-sélectionné, d'où une baisse de cette dernière. Les modèles représentatifs de cette classe sont : Brown (1999); Brown *et al.* (2002); West & Buckling (2003).
Notons que ces modèles omettent la dynamique inter-hôte, et que le résultat peut être renversé lorsque celle-ci est considérée sous certaines formes de compromis épidémiologiques (Alizon & Lion, 2011).

ι.4. Présente démarche

S'il est établi que les interactions intra-hôte influencent la croissance des parasites au sein d'un même hôte (Hellard *et al.*, 2015; Bashey, 2015), que la virulence est en partie la conséquence de cette croissance (Dormans *et al.*, 2004; de Roode *et al.*, 2008) (et qu'elle est même héritable (Fraser *et al.*, 2007)), au même titre que l'issue des inoculations (Kinnula *et al.*, 2017), il n'existe pour le moment aucun consensus sur le lien entre virulence et résultat de la compétition intra-hôte. Malgré sa suggestion précoce par les théoriciens (Levin & Pimentel, 1981; Nowak & May, 1994) (davantage pour des raisons de simplification calculatoire que par support mécanistique selon toute vraisemblance), cette corrélation a été tantôt supportée (de Roode *et al.*, 2005b), infirmée (Kell *et al.*, 2013) ou renversée (Pollitt *et al.*, 2014). Cette disparité peut s'expliquer par la différence entre systèmes biologiques mais aussi par les avatars mesurés de la virulence ou de la compétitivité.

Ainsi que l'encourage Cressler *et al.* (2015), la recherche d'une tendance générale dans l'évolution de la virulence en infections multiples requiert inévitablement la construction d'un nouveau cadre théorique fondé sur les traits de croissance des parasites, s'affranchissant ainsi des limitations arbitraires des précédents modèles, dont les résultats devraient être inclus et enrichis par cette approche ascendante (Lambert, 2010).

Au moyen d'un formalisme approprié à la complexité combinatoire des infections multiples et l'étude mathématique de modèles classiques d'écologie et d'épidémiologie, adaptés pour l'occasion, nous tentons d'apporter des éléments de réponse à la question suivante : **existe-t-il une tendance générale à l'évolution de la virulence en contexte d'infections multiples ?**

La figure ι.4.1 illustre le principe de la présente démarche.

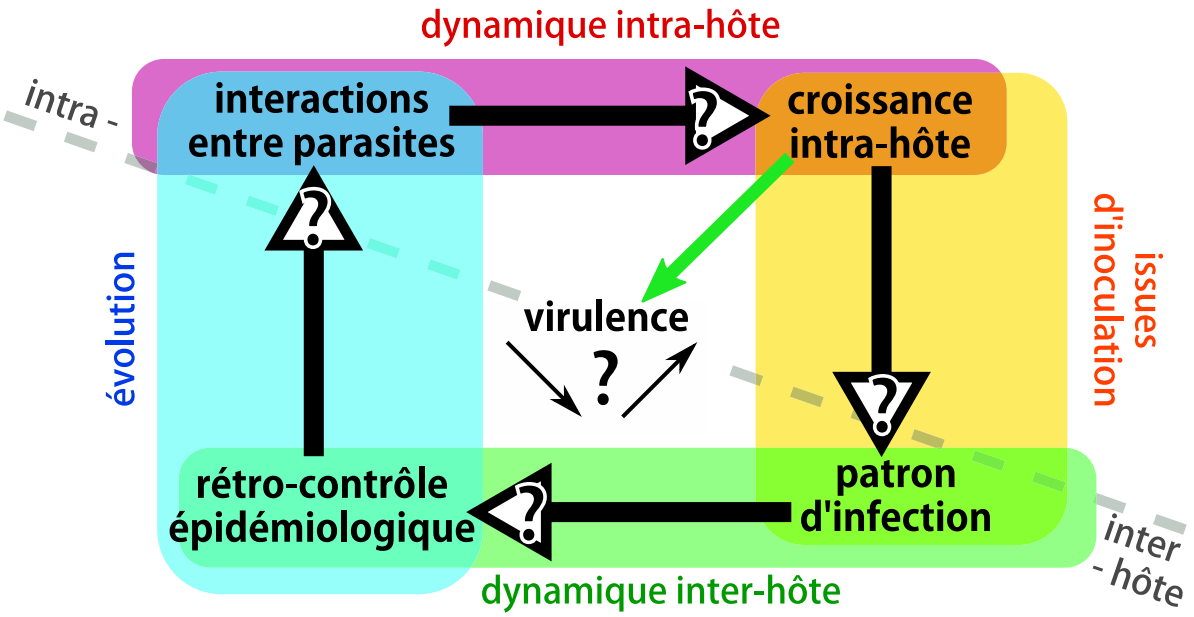

FIGURE ι.4.1. – Schématisation de la démarche adoptée pour aborder l'évolution de la virulence en contexte d'infections multiples.

Cette illustration reprend les codes de la figure ι.3.1. Les flèches marquées d'un point d'interrogation représentent des causalités inconnues dans le cas général et non soumises ici à des hypothèses contraignantes. La démarche ici adoptée se fixe pour objectifs *a*) de n'ignorer aucun niveau biologique déterminant (en particulier celui des issues d'inoculation) – chacun fait l'objet d'un chapitre du présent document dont le numéro est indiqué à côté de leur nom, *b*) d'identifier les charnières pertinentes du modèle (en particulier la définition des patrons d'infection, cf. chapitre 2), *c*) de faire reposer indépendamment la virulence et l'ensemble des issues d'inoculation (*i.e.* les patrons d'infection) sur la croissance intra-hôte, elle-même conséquence des interactions parasitaires.

II

De nouveaux outils

1 Dynamique intra-hôte

1.α. Prologue

Nous avons vu que l'étude des infections multiples ne peut s'affranchir de celle de la dynamique parasitaire se déroulant au sein des hôtes. En regardant le polymorphisme parasitaire intra-hôte comme une communauté écologique classique, notre démarche modélisatrice s'inscrit dans un champ théorique bien documenté.

Le subtil équilibre entre simplicité de formulation et richesse des dynamiques produites (il s'agit du plus petit système dynamique quadratique en nombre de paramètres) des équations de LOTKA-VOLTERRA (LOTKA, 1925; VOLTERRA, 1928), *i.e.* tout système dynamique de la forme

$$\forall N \in \mathbb{N}^\star, \forall i \in [\![1;N]\!], \frac{\mathrm{d}X_i}{\mathrm{d}t} = \left(\varrho_i + \sum_{k=1}^{N} m_{i,k} X_k\right) X_i, \tag{1.α.1}$$

en ont fait le modèle phénoménologique de référence pour la dynamique de populations en interaction (GOH, 1977; HOFBAUER & SIGMUND, 1998; MURRAY, 2001). D'une part, les propriétés mathématiques de ces équations sont aujourd'hui bien documentées, y compris pour un nombre quelconque d'espèces et certaines extensions (TAKEUCHI, 1996; HOFBAUER & SIGMUND, 1998; HOU *et al.*, 2013). D'autre part, leur étude dans une perspective biologique fait encore l'objet de travaux actuels, comme en témoignent COYTE *et al.* (2015) et BARABÁS *et al.* (2016) sur le lien entre interactions et stabilité des communautés écologiques à grand nombre d'espèces, une question initiée par MAY (1972).

Si les termes quadratiques des équations de LOTKA-VOLTERRA correspondent aux interactions directes entre individus se rencontrant uniformément, ils ne sont *a priori* pas suffisants pour rendre compte des interactions indirectes telles que celles véhiculées par les biens communs ou les produits de méchanceté. Afin de modéliser la dynamique parasitaire intra-hôte, nous avons donc amendé le modèle de LOTKA-VOLTERRA en ajoutant un nombre quelconque de composés produits collectivement au système.

Ce chapitre met ainsi en évidence les propriétés de ce nouveau modèle (limité au cas dimorphe, $N = 2$) utiles pour son emboîtement futur dans la dynamique épidémiologique (chapitres 2 et 3) – à savoir ses points fixes, des conditions de stabilité locale asymptotique ainsi qu'une condition de stabilité globale asymptotique, cette dernière relevant plus de l'exercice mathématique que de la compréhension biologique.

Une condition de stabilité globale asymptotique pour un modèle de LOTKA-VOLTERRA dimorphe avec interactions indirectes explicites

Mircea T. SOFONEA

Résumé

Ce travail présente un modèle de LOTKA-VOLTERRA à deux espèces auxquelles s'ajoutent un nombre arbitraire d'interactions indirectes véhiculées par des composés diffusibles et renouvelables, dans un cadre de modélisation de communautés microbiennes. Après la détermination des points fixes du système et une courte discussion au sujet de leur stabilité locale asymptotique, nous appliquons la seconde méthode de LYAPUNOV dans le but de déterminer une condition suffisante de stabilité globale asymptotique. Biologiquement, cette condition indique la nécessité qu'un type microbien inhibe fortement sa propre croissance et que le renouvèlement des composés soit élevé.

Mots-clés : stabilité globale, seconde méthode de LYAPUNOV, modèle compétitif de LOTKA-VOLTERRA, compétition par exploitation, bien commun, méchanceté

A global asymptotic stability condition for a dimorphic Lotka-Volterra model with explicit indirect interactions

Mircea T. Sofonea

Abstract

A two-species Lotka-Volterra model extended with an arbitrary number of indirect interactions through diffusible and renewable compounds is presented according to its relevance in microbial community modelling. After the determination of the system's fixed points and a short discussion over their local asymptotic stability, Lyapunov's second method is applied to derive a sufficient condition of global asymptotic stability. Biologically, this condition indicates the necessity for one microbial type to show strong self-inhibition and the compounds to be fastly replaced.

Keywords: global stability; Lyapunov's Second Method; competitive Lotka-Volterra model; exploitative competition; public goods; spite

1.1. Introduction

Non-linear dynamical systems hardly ever show closed-form solutions. Usually, their behaviour is investigated by determining their fixed points and studying their stability after linearisation in their neighbourhood (Grobman, 1959; Hartman, 1960). This straightforward method, however, cannot be applied to non hyperbolic fixed points and is usually inefficient to investigate the dynamics far from and between fixed points. Linearisation is especially unable to predict which locally asymptotically stable (LAS) fixed point the solution will eventually converge to or to detect non fixed point attractors such as limit cycles or chaos. These questions can be addressed using a global stability analysis, for which a suitable approach is known as Lyapunov's Second Method (Lyapunov, 1992). This method is based on the definiteness properties of a so-called Lyapunov function that needs to be identified for each fixed point of the dynamical system under study. The existence of such a function thus provides a sufficient condition for the global stability of the system.

Lyapunov functions have been widely used in mathematical biology and especially to model ecological communities (Goh, 1977; Hofbauer & Sigmund, 1990) for two reasons. The first one is that the dynamics of these systems emerge from the interactions between numerous individuals hence, assuming a well-mixed community, the encounters follow the classical non-linear mass action law (Waage & Guldberg, 1986; McCallum *et al.*, 2001). The second reason is that biologists seek for global asymptotic stability because it guarantees the convergence of the systems towards the same point whatever the initial conditions (which are poorly known in natural phenomena). Moreover, if a closed-form value of this globally asymptotically stable (GAS) fixed point can be found, the focal dynamics can be nested into long-term processes such as evolution, by means of a timescale separation assumption (Geritz *et al.*, 1998; Metz *et al.*, 2016).

Since their first formulations (Lotka, 1925; Volterra, 1928), the Lotka-Volterra equations have been a fruitful source of models and generalizations and constitute undoubtedly one of the most studied theoretical frameworks in population biology and even beyond (Hofbauer & Sigmund, 1990; Hernández-Bermejo & Fairén, 1997). Nowadays, Lotka-Volterra equations continue to receive a strong interest in the study of the stability of ecological communities (Barabás *et al.*, 2016) and are especially investigated within the popular topic of microbiome (Pepper & Rosenfeld, 2012; Coyte *et al.*, 2015).

In contrast with macroscopic free living organisms that often interact directly by contact (predation, competition or mutualism) (Begon *et al.*, 2005), an important part of the interactions between symbiotic micro-organisms, may they be commensal, mutualist or parasitic, is carried through soluble compounds secreted in the medium which may have negative as well as positive effects on their growth (Mideo, 2009; Hellard *et al.*, 2015; Bashey, 2015).

Some bacteria for instance, secrete siderophores chelating molecules that harvest iron in the medium, which can be then imported within the cell provided that the bacterium possesses the matching receptor (Neilands, 1995; Wandersman & Delepelaire, 2004). Cheating bacteria may not produce siderophores but still benefit from the siderophores produced by other bacteria (Ghoul *et al.*, 2016). On the other side, bacteriocins are secreted enzymes that break the bacterial wall. This detrimental compound may even affect the producing bacteria (Riley & Chavan, 2007). If pathogenic, the reproduction of the bacteria elicits the production of host defense molecules such as lactoferrin and siderocalin (Skaar, 2010). Analogous examples can be found for other microbes such as virus and protozoans (Hellard *et al.*, 2015). It results from here that the dynamics of microbial communities are not shaped by simple direct competitive interactions but by a great set

of indirect interactions with various effects on each microbe type (Rath & Dorrestein, 2012; Dobson *et al.*, 2012). Such indirect interactions are lacking in the Lotka-Volterra equations, which would need structural modifications to fit to microbial dynamics.

In this article, we consider the classical Lotka-Volterra equations to which we add an arbitrary number of indirect interactions through diffusible compounds, for which we seek a sufficient global stability condition and biologically interpret its closed-form expression. We restrict the model to two microbe types in order to derive the less stringent condition suited for major theoretical ecology and evolutionary biology frameworks that rely – by virtue of their game theory origins (Maynard Smith, 1982; Geritz *et al.*, 1998).

1.2. Model formulation

Let us consider two microbe types (may they be strains or species) labeled 1 and 2. Hereafter, unless stated otherwise, i will indifferently refer to 1 or 2 and k to the other type – that is the quantification $\forall (i,k) \in \{1,2\}^2, i \neq k$ will be implied or simply reminded as $i = 1,2; k = 2,1$.

The microbial densities are non-negative variables $X_i \in \mathbb{R}_+$ that vary through time $t \in \mathbb{R}_+$ according to several processes. The first is an intrinsic growth quantified by the rate $\varrho_i \in \mathbb{R}$, which can be negative if the microbe is unable to grow without collective help. The second is the self density dependent effect emerging from direct interactions between individuals that belong to the same type and is quantified by $\eta_{i,i} \in \mathbb{R}$. Likewise, a cross density dependent effect can be defined as describing the consequences of the inter-type direct interactions and is quantified by $\eta_{i,k} \in \mathbb{R}$ where the first index indicates the type that undergoes the interaction and the second index the one that produces it.

Finally, we consider that an arbitrary number $n \in \mathbb{N}$ of diffusible compounds modulate microbial growth according to their non-negative concentration $Y_p \in \mathbb{R}_+$ and their respective effect $\gamma_{i,p} \in \mathbb{R}$ on microbial type i's growth. Whether they are microbial or host secretions, these compounds are likely to be produced at non-negative rates that are proportional to microbial densities through a positive factor denoted by $u_{i,p} \in \mathbb{R}_+$. Note that $u_{i,p} = 0$ if microbial type i does not contribute to compound p production. We moreover assume that these compounds are mostly removed from the medium through processes that are not related to their activity, such as self-denaturation, host degradation, dilution – which is the case of a large class of secreted molecules namely those with a renewable activity such as enzymes (bacteriocins) or chelates (siderophores, lactoferrin). Their clearance is therefore proportional to their concentration through a positive factor denoted by $v_p > 0$ (Alizon & Lion, 2011). In the end, the microbial growth of the two types conforms to the following set of ODEs, with $i = 1,2; k = 2,1; p = 1,\dots,n$:

$$\begin{cases} \frac{\mathrm{d}X_i}{\mathrm{d}t} = \left(\varrho_i + \eta_{i,i}X_i + \eta_{i,k}X_k + \sum_{p=1}^{n} \gamma_{i,p}Y_p\right)X_i & =: f_i(\mathbf{w}), \\ \frac{\mathrm{d}Y_p}{\mathrm{d}t} = u_{i,p}X_i + u_{k,p}X_k - v_pY_p, & =: g_p(\mathbf{w}), \end{cases} \tag{1.2.1}$$

where $\mathbf{w} \coloneqq \begin{bmatrix} X_1 & X_2 & Y_1 & \cdots & Y_n \end{bmatrix}^{\mathrm{T}}$. For the sake of concision, we hereafter denote by $R_i(\mathbf{w})$ the quotient $f_i(\mathbf{w})/X_i$ which can be interpreted as the instantaneous *per capita* growth rate of microbial type i. The Jacobian matrix associated to (1.2.1) is

$$\begin{aligned} \mathbf{J}(\mathbf{w}) &\coloneqq \frac{\partial}{\partial \mathbf{w}} \begin{bmatrix} f_1 & f_2 & g_1 & \cdots & g_n \end{bmatrix}(\mathbf{w}), \\ &= \begin{bmatrix} R_1(\mathbf{w}) + \eta_{1,1}X_1 & \eta_{1,2}X_1 & \gamma_{1,1}X_1 & \cdots & \gamma_{1,n}X_1 \\ \eta_{2,1}X_2 & R_2(\mathbf{w}) + \eta_{2,2}X_2 & \gamma_{2,1}X_2 & \cdots & \gamma_{2,n}X_2 \\ u_{1,1} & u_{2,1} & -v_1 & \mathbf{0}_{p-2}^{\mathrm{T}} & 0 \\ \vdots & \vdots & \mathbf{0}_{p-2} & \ddots & \mathbf{0}_{p-2} \\ u_{1,n} & u_{2,n} & 0 & \mathbf{0}_{p-2}^{\mathrm{T}} & -v_p \end{bmatrix}, \end{aligned} \tag{1.2.2}$$

where $\mathbf{0}_d$ denotes the zero vector of $\mathbb{R}^d$.

Because of the biological meaning of variables X_i and Y_i, we restrict the initial conditions (considered at $t = 0$) of (1.2.1) to the positive orthant $\mathcal{W} \equiv (\mathbb{R}_+)^{p+2}$. It is straightforward to see that $\mathcal{W}$ is positively invariant. Indeed, $X_i(t) = X_i(0)\exp\left(\int_0^t R_i \mathrm{d}\tau\right)$, therefore $X_i(t) \geq 0, \forall t \geq 0$. Therefore, $\frac{\mathrm{d}Y_p}{\mathrm{d}t} \geq -v_p Y_p$, from which it follows that $Y_p(t) \geq Y_p(0)\exp\left(-v_p t\right) \geq 0, \forall t \geq 0$. Hereafter, global properties are understood with respect to $\mathcal{W}$.

1.3. Fixed point determination

The sets $\mathcal{X}_i \coloneqq \{\mathbf{w} \in \mathbb{R}^{p+2} : f_i(\mathbf{w}) = 0\}$ and $\mathcal{Y}_p \coloneqq \{\mathbf{w} \in \mathbb{R}^{p+2} : g_p(\mathbf{w}) = 0\}$ define the i-th microbial density nullcline and the p-th compound concentration nullcline respectively. A fixed point $\mathbf{w}$ of (1.2.1) is such that $\forall (i,p) \in \{1,2\} \times \{1,\dots,n\}, f_i(\mathbf{w}) = 0 = g_p(\mathbf{w})$. The set of fixed points $\mathcal{F}$ is thus the intersection of all nullclines (Simonyi & Kaszás, 1968), $\mathcal{F} = \mathcal{X}_1 \cap \mathcal{X}_2 \cap \bigcap_{p=1}^{n} \mathcal{Y}_p$.

On one hand, all points of $\mathcal{F}$ satisfy

$$Y_p = \frac{1}{v_p}\left(u_{1,p}X_1 + u_{2,p}X_2\right), \qquad p = 1,\dots,n \tag{1.3.1}$$

which allows us to rewrite R_i on $\mathcal{F}$ such as

$$\mathbf{w} \in \mathcal{F} \Longrightarrow R_i(\mathbf{w}) = \varrho_i + m_{i,i}X_i + m_{i,k}X_k, \qquad i = 1,2, k = 2,1, \tag{1.3.2}$$

with

$$m_{i,j} \coloneqq \eta_{i,j} + \sum_{p=1}^{n} \frac{\gamma_{i,p}u_{j,p}}{v_p}. \tag{1.3.3}$$

On the other hand, all points of $\mathcal{F}$ satisfy $(X_i = 0) \vee (R_i = 0)$ for $i = 1,2$, where $\vee$ denotes the logical disjunction (or). By canceling either X_i or R_i for each type, it follows that there exist at most four different fixed points hereafter denoted by $\mathbf{w}_h, h = 0,1,2,3$. Note that here and below we denote by $\mathcal{X}_i$ the microbial density i nullcline ($X_i = 0$).

The origin $\mathbf{0}_{p+2}$ is the trivial null fixed point $\mathbf{w}_0$. The monomorphic fixed point 1, $\mathbf{w}_1$, is given by solving the system $(R_1 = 0) \wedge (X_2 = 0)$, where $\wedge$ denotes the logical conjunction (and). Hence, $\mathbf{w}_1 = \left[x_1 \quad 0 \quad \frac{u_{1,1}x_1}{v_1} \quad \cdots \quad \frac{u_{1,n}x_1}{v_n}\right]^{\mathrm{T}}$, where $x_1 \coloneqq -\frac{\varrho_1}{m_{1,1}}$ is the stationary i-th monomorphic microbial density, provided that $m_{1,1} \neq 0$ (hereafter assumed). Analogously, the monomorphic fixed point 2 is $\mathbf{w}_2 = \left[0 \quad x_2 \quad \frac{u_{2,1}x_2}{v_2} \quad \cdots \quad \frac{u_{2,n}x_2}{v_n}\right]^{\mathrm{T}}$, where $x_2 \coloneqq -\frac{\varrho_2}{m_{2,2}}$, provided that $m_{2,2} \neq 0$ (hereafter assumed). The fourth fixed point is the dimorphic fixed point $\mathbf{w}_3$, which satisfies $(R_1 = 0) \wedge (R_2 = 0)$. These two equations represent the linear system

$$\begin{bmatrix} m_{1,1} & m_{1,2} \\ m_{2,1} & m_{2,2} \end{bmatrix} \cdot \begin{bmatrix} X_1 \\ X_2 \end{bmatrix} = -\begin{bmatrix} \varrho_1 \\ \varrho_2 \end{bmatrix}, \tag{1.3.4}$$

the solutions of which is $\begin{bmatrix} \xi_1 & \xi_2 \end{bmatrix}^{\mathrm{T}}$ with $\xi_i \coloneqq \frac{m_{i,k}\varrho_k - m_{k,k}\varrho_i}{m_{1,1}m_{2,2} - m_{1,2}m_{2,1}}$, provided that $m_{1,1}m_{2,2} \neq m_{1,2}m_{2,1}$ (hereafter assumed). It results from above that

$$\mathbf{w}_3 = \left[\xi_1 \quad \xi_2 \quad \frac{1}{v_1}\left(u_{1,1}\xi_1 + u_{2,1}\xi_2\right) \quad \cdots \quad \frac{1}{v_n}\left(u_{1,n}\xi_1 + u_{2,n}\xi_2\right)\right]^{\mathrm{T}}.$$

We say that a fixed point is feasible when it belongs to $\mathcal{W}$. While $\mathbf{w}_0$ is always feasible, the three other fixed points may not. Their feasibility conditions are $\mathrm{sgn}\varrho_1 \neq \mathrm{sgn}m_{1,1}$, $\mathrm{sgn}\varrho_2 \neq \mathrm{sgn}m_{2,2}$ and $\mathrm{sgn}\left(m_{1,2}\varrho_2 - m_{2,2}\varrho_1\right) = \mathrm{sgn}\left(m_{2,1}\varrho_1 - m_{1,1}\varrho_2\right) = \mathrm{sgn}\left(m_{1,1}m_{2,2} - m_{1,2}m_{2,1}\right)$ respectively, where sgn is the sign function.

1.4. Local asymptotic stability

Fixed point local asymptotic stability is addressed, as classically, through the sign of the real parts of the eigenvalues of the Jacobian matrix evaluated at the given point. In the case of the null fixed point, $\mathbf{J}(\mathbf{w}_0)$ is a lower triangular matrix the diagonal of which is simply $\begin{bmatrix}\varrho_1 & \varrho_2 & -v_1 & \cdots & -v_p\end{bmatrix}^{\mathrm{T}}$ hence $\mathbf{w}_0$ is LAS whenever $\big(\varrho_1 < 0\big) \wedge \big(\varrho_2 < 0\big)$.

One can also derive the necessary and sufficient condition of local asymptotic stability of the monomorphic fixed points $\mathbf{w}_1$ and $\mathbf{w}_2$ provided that they are LAS in their respective monomophic space $\mathcal{W}_i' \coloneqq \big(\mathcal{W} \cap \mathcal{X}_k\big) \setminus \mathcal{X}_i$. (Note that $\mathcal{W}_i'$ is the subspace of $\mathcal{W}$ where the focal microbial density is positive while the other microbial type is constrained to zero.) Indeed, $\mathbf{J}(\mathbf{w}_2)$ is a lower triangular block matrix of the form

$$\begin{bmatrix} R_1(\mathbf{w}_2) & \mathbf{0}_{p+1} \\ \mathbf{u}_1 & \mathbf{J}_{1,1}(\mathbf{w}_2) \end{bmatrix}$$

where $\mathbf{u}_1 = \begin{bmatrix}u_{1,1} & \cdots & u_{1,p}\end{bmatrix}^{\mathrm{T}}$ and $\mathbf{J}_{1,1}(\mathbf{w}_2)$ is the sub-matrix of $\mathbf{J}(\mathbf{w}_2)$ without the first row and the first column. Therefore, assuming that $\mathbf{w}_2$ is LAS in $\mathcal{W}_2'$ (which is equivalent to the statement that $\mathbf{J}_{1,1}(\mathbf{w}_2)$ has only negative real part eigenvalues), $\mathbf{w}_2$ is LAS in $\mathcal{W} \setminus \mathcal{X}_2$ as well if and only if $R_1(\mathbf{w}_2) < 0$ that is equivalent to $\varrho_1 < -m_{1,2}x_2$. Likewise and by permutation, $\mathbf{w}_1$ is LAS in $\mathcal{W} \setminus \mathcal{X}_1$ provided that is LAS in $\mathcal{W}_1'$ if and only if $\varrho_2 < -m_{2,1}x_1$.

It is straightforward that (1.2.1) can show bistability in $\mathcal{W}$. Indeed, in the simplest case of $n = 0$, the matrices $\mathbf{J}(\mathbf{w}_1)$ and $\mathbf{J}(\mathbf{w}_2)$ become

$$\begin{bmatrix} -\varrho_1 & -\frac{\eta_{1,2}}{\eta_{1,1}}\varrho_1 \\ 0 & \varrho_2 - \frac{\eta_{2,1}}{\eta_{1,1}}\varrho_1 \end{bmatrix} \text{ and } \begin{bmatrix} \varrho_1 - \frac{\eta_{1,2}}{\eta_{2,2}}\varrho_2 & 0 \\ -\frac{\eta_{2,1}}{\eta_{2,2}}\varrho_2 & -\varrho_2 \end{bmatrix}$$

respectively. Therefore, $\mathbf{w}_1$ and $\mathbf{w}_2$ are both feasible and LAS whenever $\left(0 < \varrho_2 < \frac{\eta_{2,1}}{\eta_{1,1}}\varrho_1\right) \wedge \left(0 < \varrho_1 < \frac{\eta_{1,2}}{\eta_{2,2}}\varrho_2\right)$. (Note that for $n \geq 1$, bistability in $\mathcal{W}$ can easily be found numerically.)

Nonetheless, the necessary and sufficient condition for the non-trivial fixed points to be LAS cannot be determined in the most general case. For this reason, given an intial condition, the long term behaviour of the solution of system (1.2.1) cannot be predicted in the general case unless an identified global asymptotic stability condition is satisfied.

1.5. Global asymptotic stability condition

If deriving the global asymptotic condition for the Lotka-Volterra model for two competing species to be globally stable is a classical textbook exercise (Zeeman, 1993), one cannot extrapolate this condition to the present model as the arbitrary number of compounds do influence the dynamics of the system. Following (Lyapunov, 1992), it is well known that a feasible fixed point $\mathbf{w}^\star \in \mathcal{F} \cap \mathcal{W}$ is GAS in $\mathcal{W}^\star := \mathcal{W} \setminus (\mathcal{X}_1 \cup \mathcal{X}_2)$ (to be understood as its attraction basin equals $\mathcal{W}^\star$) if there is a Lyapunov function $V \in \mathscr{C}^1\left(\mathcal{W}^\star, \mathbb{R}_+\right)$ such that

$$\begin{cases} (\alpha) & V\left(\mathbf{w}^\star\right) = 0 \text{ and } \forall \mathbf{w} \in \mathcal{W}^\star \setminus \left\{\mathbf{w}^\star\right\}, V(\mathbf{w}) > 0, \\ (\beta) & \frac{\mathrm{d}V}{\mathrm{d}t}\left(\mathbf{w}^\star\right) = 0 \text{ and } \forall \mathbf{w} \in \mathcal{W}^\star \setminus \left\{\mathbf{w}^\star\right\}, \frac{\mathrm{d}V}{\mathrm{d}t}(\mathbf{w}) < 0. \end{cases}$$

For the sake of concision, we refer to these properties using their respective labels α and β from now on.

In the following, we focus on the case of the dimorphic fixed point $\mathbf{w}_3$ and show in the appendix that the global asymptotic stability condition that emerges also applies to the three other fixed points.

Inspired by the previous works (Goh, 1977; Takeuchi, 1996), we define V as

$$\begin{aligned} V(\mathbf{w}) := a_1 \left(X_1 - \left(1 + \log \frac{X_1}{\xi_1}\right) \xi_1 \right) + a_2 \left(X_2 - \left(1 + \log \frac{X_2}{\xi_2}\right) \xi_2 \right) \\ + \frac{1}{2} \sum_{p=1}^{n} b_p \left(Y_p - \frac{1}{v_p} \left(u_{1,p} \xi_1 + u_{2,p} \xi_2 \right) \right)^2, \end{aligned} \tag{1.5.1}$$

where a_1, a_2, b are arbitrary positive real numbers.

The function V is obviously continuously differentiable on $\mathcal{W}^\star$. Moreover, its first two terms are of the form $h(x) := x - c - c(\log x - \log c)$ with $c > 0$. Given that the first derivative of h is $h'(x) = 1 - \frac{c}{x}$ and its second derivative is $f''(x) = \frac{c}{x^2} > 0$, it follows that $\underset{\mathbb{R}_+^\star}{\operatorname{argmin}}(f) = c$ and $\min_{\mathbb{R}_+^\star}(f) = 0$. Therefore, and since V is a separable function in each component of $\mathbf{w}$, it follows that $V(\mathbf{w}) > 0$ for all $\mathbf{w} \in \mathcal{W}^\star \setminus \{\mathbf{w}_3\}$ and $V(\mathbf{w}_3) = 0$, condition(α) holds.

Before calculating the time derivative of V, let us remind that $R_i(\mathbf{w}_3) = 0$ for $i = 1, 2$. Therefore, the following holds for all $\mathbf{w} \in \mathcal{W}$, and $i = 1, 2$,

$$\begin{aligned} R_i(\mathbf{w}) &= R_i(\mathbf{w}) - R_i(\mathbf{w}_3), \\ &= \eta_{i,1}(X_1 - \xi_1) + \eta_{i,2}(X_2 - \xi_2) + \sum_{p=1}^{n} \gamma_{i,p} \left(Y_p - \frac{1}{v_p} \left(u_{1,p} \xi_1 + u_{2,p} \xi_2 \right) \right). \end{aligned} \tag{1.5.2}$$

It follows from here that

$$\begin{aligned}\frac{\mathrm{d}V}{\mathrm{d}t}(\mathbf{w}) &= a_1(X_1-\xi_1)R_1(\mathbf{w})+a_2(X_2-\xi_2)R_2(\mathbf{w})\\ &\quad+\sum_{p=1}^{n} b_p\left(Y_p-\frac{1}{v_p}\left(u_{1,p}\xi_1+u_{2,p}\xi_2\right)\right)\left(u_{1,p}X_1+u_{2,p}X_2-v_pY_p\right),\\ &=\sum_{i=1}^{2} a_i\eta_{i,1}(X_i-\xi_i)(X_1-\xi_1)+a_i\eta_{i,2}(X_i-\xi_i)(X_2-\xi_2)\\ &\quad+\sum_{p=1}^{n}\left(\left(a_1\gamma_{1,p}+b_pu_{1,p}\right)\left(Y_p-\frac{1}{v_p}\left(u_{1,p}\xi_1+u_{2,p}\xi_2\right)\right)(X_1-\xi_1)\right.\\ &\quad+\left(a_2\gamma_{2,p}+b_pu_{2,p}\right)\left(Y_p-\frac{1}{v_p}\left(u_{1,p}\xi_1+u_{2,p}\xi_2\right)\right)(X_2-\xi_2)\\ &\quad\left.-b_pv_p\left(Y_p-\frac{1}{v_p}\left(u_{1,p}\xi_1+u_{2,p}\xi_2\right)\right)^2\right),\end{aligned}$$

which is equivalent to the following quadratic form

$$\frac{\mathrm{d}V}{\mathrm{d}t}(\mathbf{w})=\frac{1}{2}(\mathbf{w}-\mathbf{w}_3)^{\mathrm{T}}.\left(\mathbf{D}.\mathbf{P}+\mathbf{P}^{\mathrm{T}}.\mathbf{D}\right).(\mathbf{w}-\mathbf{w}_3), \tag{1.5.3}$$

where $\mathbf{D}$ is the diagonal matrix $\mathrm{diag}\left(a_1,a_2,b_1,\ldots,b_p\right)$ and

$$\mathbf{P}=\begin{bmatrix}\eta_{1,1} & \eta_{1,2} & \gamma_{1,1} & \cdots & \gamma_{1,n}\\ \eta_{2,1} & \eta_{2,2} & \gamma_{2,1} & \cdots & \gamma_{2,n}\\ u_{1,1} & u_{2,1} & -v_1 & \mathbf{0}_{p-2}^{\mathrm{T}} & 0\\ \vdots & \vdots & \mathbf{0}_{p-2} & \ddots & \mathbf{0}_{p-2}\\ u_{1,n} & u_{2,n} & 0 & \mathbf{0}_{p-2}^{\mathrm{T}} & -v_p\end{bmatrix}.$$

It follows from (1.5.3) that property (β) holds if and only if $\mathbf{D}.\mathbf{P}+\mathbf{P}^{\mathrm{T}}.\mathbf{D}$ is negative definite (which is equivalent to the negativity of its associated quadratic form).

A theorem from Berman & Plemmons (1979)(p. 137) allows the existence of such a positive diagonal matrix $\mathbf{D}$ provided that the matrix $\mathbf{P}$ is strictly row diagonally dominant. It formally states that

$$\begin{aligned}&\forall q\in\mathbb{N}^{\star},\forall\mathbf{A}=\left(a_{i,j}\right)_{(i,j)\in\{1,\ldots,q\}^2},\\ &(\mathrm{diag}(\mathbf{A})\succ 0)\wedge\left(\exists\left(k_j\right)_{j\in\{1,\ldots,q\}}>0:\forall i\in[\![1;q]\!],k_ia_{i,i}>\sum_{j\in\{1,\ldots,q\}\setminus\{i\}}k_j\left|a_{i,j}\right|\right)\\ &\Longrightarrow\exists\mathbf{C}=\mathrm{diag}\left(c_j\right)_{j\in\{1,\ldots,q\}}>0:\left(\mathbf{C}.\mathbf{A}+\mathbf{A}^{\mathrm{T}}.\mathbf{C}\right)\text{ is positive definite.}\end{aligned} \tag{1.5.4}$$

Applying this theorem to $-\mathbf{P}$ with the particular set of positive real numbers $\left(k_j\right)_{j\in\{1,\dots,p+2\}} := (\kappa, 1, \kappa, \dots, \kappa)$ (the biological relevance of which is exposed in the discussion), it results that if there exists a scaling quantity $\kappa > 0$ such that

$$\begin{cases} -\eta_{1,1} & > \frac{1}{\kappa}\left|\eta_{1,2}\right| + \sum\limits_{p=1}^{n}\left|\gamma_{1,p}\right|, \\ -\eta_{2,2} & > \kappa\left|\eta_{2,1}\right| + \kappa\sum\limits_{p=1}^{n}\left|\gamma_{2,p}\right|, \\ v_p & > u_{1,p} + \frac{1}{\kappa}u_{2,p}, \qquad \forall p \in \{1,\dots,n\}, \end{cases} \tag{1.5.5}$$

then there exists $\left(a_1, a_2, b_1, \dots, b_p\right) \in \left(\mathbb{R}_+^\star\right)^{p+2}$ that ensures property (β).

Overall, provided that $\mathbf{w}_3 \in \mathcal{W}^\star$, the set of inequalities (1.5.5) represents a sufficient condition for V to be a Lyapunov function hence a sufficient condition for $\mathbf{w}_3$ to be GAS on $\mathcal{W}^\star$. In the appendix, we show that this condition also guarantees the global asymptotic stability of the three other fixed points in relevant subspaces of $\mathcal{W}$ provided that they are LAS in these spaces.

1.6. Discussion

In this work we present an extension of the two-species Lotka-Volterra equations that captures indirect interactions through a potentially large number of diffusible and renewable compounds which are relevant for investigating microbial communities (Bashey, 2015).

As the classical Lotka-Volterra model without compounds ($n = 0$), the vector field shows four fixed points that identify to no microbial persistence ($\mathbf{w}_0$), two monomorphic equilibria ($\mathbf{w}_1$ and $\mathbf{w}_2$) and one dimorphic equilibrium ($\mathbf{w}_3$), the closed form expressions of which can be found (which is not the case for a higher number of microbial types). However, accounting for compounds increases the dimensionality of the system hence it prevents the derivation of closed form expressions for local asymptotic stability conditions of the fixed points in the general case. These conditions are, moreover, not enough to prove their global asymptotic stability as in the without compound model (Zeeman, 1993).

Using an argument of generalized row diagonal dominance, we here identify a region of the parameter space in which global asymptotic stability of the extended model is achieved. In this region, all attractors are fixed points and there is at most one attracting fixed point. Moreover, the identification of the globally attracting fixed point reduces to at most two simple algebraic conditions (related to feasibility, see section 1.3, or local asymptotic stability, see appendix).

The sufficient condition for global asymptotic stability provided here has a clear biological interpretation. Indeed, considering a small positive scaling quantity κ ($0 < \kappa \ll 1$), the three conditions in (1.5.5) read as first, microbial type 1 undergoes a strong self density-dependent inhibition and is hardly affected by external interactions, second, microbial type 2 undergoes a self density-dependent inhibition that may be very low and third, the turn-over of the diffusible compounds is high and the microbial type 2 contributes less to their production. This result conforms to the rule that the geometric mean of the intra-type competition has to be greater than the geometric mean of the inter-type competition to insure the global stability of the coexistence equilibrium in the classical Lotka-Volterra model (Barabás *et al.*, 2016). Here, microbial type 1 is responsible for the high intra-type and the low competition geometric means, thus leaving a certain freedom to the traits of microbial type 2.

1.a. Appendix

Here, we show that if conditions (1.5.5) are satisfied, then $\mathbf{w}_0$, $\mathbf{w}_1$ and $\mathbf{w}_2$ are GAS in their relevant spaces, namely $\mathcal{W}\cap\mathcal{X}_2, \mathcal{W}\cap\mathcal{X}_1$ and $\mathcal{W}$ for $\mathbf{w}_0$, and $\mathcal{W}_i'$ and $\mathcal{W}\setminus\mathcal{X}_i$ for $\mathbf{w}_i$, $i=1,2$, as long as they belong and are LAS in these spaces. A distinct Lyapunov function has to be defined for each fixed point and the global asymptotic stability has to be separately investigated on each space.

Let us start by the null fixed point, for which one can consider the following function defined on $\mathbb{R}^{p+2}$

$$V_0(\mathbf{w}) \coloneqq a_1X_1 + a_2X_2 + \frac{1}{2}\sum_{p=1}^{n} b_pY_p^2 \tag{1.a.1}$$

Property α clearly holds on $\mathcal{W}_1', \mathcal{W}_2'$ and $\mathcal{W}$. As for property β, the calculation of $\frac{\mathrm{d}V_0}{\mathrm{d}t}$ gives

$$\begin{aligned}\frac{\mathrm{d}V_0}{\mathrm{d}t}(\mathbf{w}) &= a_1R_1(\mathbf{w})X_1 + a_2R_2(\mathbf{w})X_2 \\ &\quad + \sum_{p=1}^{n} b_pY_p\left(u_{1,p}X_1 + u_{2,p}X_2 - v_pY_p\right), \\ &= \sum_{i=1}^{2} a_i\varrho_iX_i + a_i\eta_{i,i}X_i^2 + a_i\eta_{i,k}X_iX_k \\ &\quad + \sum_{p=1}^{n}\Big(\left(a_1\gamma_{1,p} + b_pu_{1,p}\right)Y_pX_1 \\ &\quad + \left(a_2\gamma_{2,p} + b_pu_{2,p}\right)Y_pX_2 \\ &\quad - b_pv_pY_p^2\Big),\end{aligned}$$

hence $\frac{\mathrm{d}V_0}{\mathrm{d}t}(\mathbf{w})$ can be written as

$$\frac{\mathrm{d}V_0}{\mathrm{d}t}(\mathbf{w}) = \frac{1}{2}\mathbf{w}^{\mathrm{T}}.\left(\mathbf{D}.\mathbf{P} + \mathbf{P}^{\mathrm{T}}.\mathbf{D}\right).\mathbf{w} + a_1\varrho_1X_1 + a_2\varrho_2X_2.$$

Now, let us recall from section 1.4 that $\mathbf{w}_0$ is LAS on $\mathcal{W}$ iff $\left(\varrho_1<0\right)\wedge\left(\varrho_2<0\right)$. Therefore, if $\mathbf{w}_0$ is LAS on $\mathcal{W}$, $\frac{\mathrm{d}V_0}{\mathrm{d}t}(\mathbf{w}) < \frac{1}{2}\mathbf{w}^{\mathrm{T}}.\left(\mathbf{D}.\mathbf{P} + \mathbf{P}^{\mathrm{T}}.\mathbf{D}\right).\mathbf{w}$, hence if (1.5.5) then V_0 is a Lyapunov function than proves the global asymptotic stability of $\mathbf{w}_0$ on $\mathcal{W}$.

If stability is investigated on $\mathcal{W}\cap\mathcal{X}_k$, then all occurrences of X_k vanish, only $\varrho_i<0$ is required for local asymptotic stability and the quadratic form reduces to dimension $p+1$. The application of theorem (1.5.4) then provides sufficient conditions of the form

$$\exists\kappa'>0 : \left(-\eta_{i,i} > \kappa'\sum_{p=1}^{n}\left|\gamma_{i,p}\right|\right)\wedge\left(\kappa'v_p > u_{i,p}, p=1,\ldots,n\right) \tag{1.a.2}$$

with $\kappa'>0$. It is straightforward to see that these conditions are weaker than, and therefore implied by, (1.5.5).

As for the monomorphic fixed points $\mathbf{w}_i, i=1,2$, one can consider the following function defined on $\mathcal{W}_i'\setminus\mathcal{X}_i$

$$V_i(\mathbf{w}) \coloneqq a_i\left(X_i - \left(1+\log\frac{X_i}{x_i}\right)x_i\right) + a_kX_k + \frac{1}{2}\sum_{p=1}^{n} b_p\left(Y_p - \frac{u_{i,p}}{v_p}x_i\right)^2. \tag{1.a.3}$$

It is straightforward to see that property α holds on $\mathcal{W}_i'$ and $\mathcal{W}\setminus\mathcal{X}_i$.

The derivation of V_i with respect to time leads to

$$\frac{\mathrm{d}V_i}{\mathrm{d}t}(\mathbf{w}) = a_i(X_i - x_i)R_i(\mathbf{w}) + a_k R_k(\mathbf{w})X_k + \sum_{p=1}^{n} b_p\left(Y_p - \frac{u_{i,p}}{v_p}x_i\right)\left(u_{1,p}X_1 + u_{2,p}X_2 - v_p Y_p\right).$$

Restricting the investigation to $\mathcal{W}_i'$, and applying relation (1.5.2) to $R_i(\mathbf{w})$, it follows that

$$\frac{\mathrm{d}V_i}{\mathrm{d}t}(\mathbf{w}) = a_i\eta_{i,i}(X_i - x_i)^2 + \sum_{p=1}^{n}\left(\left(a_i\gamma_{i,p} + b_p u_{i,p}\right)\left(Y_p - \frac{u_{i,p}}{v_p}x_i\right)(X_i - x_i) - b_p v_p\left(Y_p - \frac{u_{i,p}}{v_p}x_i\right)^2\right),$$

which is analogous to the aforementioned reduced quadratic form of dimension $p+1$. Hence, V_i satisfies property β on $\mathcal{W}_i'$ under the conditions (1.a.2) which are implied by (1.5.5), that is $\mathbf{w}_i$ is GAS in $\mathcal{W}_i'$, provided $\mathbf{w}_i \in \mathcal{W}_i'$.

Finally, coming back to $\mathcal{W}\setminus\mathcal{X}_i$ leads to $\frac{\mathrm{d}V_i}{\mathrm{d}t}(\mathbf{w}) = \frac{1}{2}(\mathbf{w}-\mathbf{w}_i)^{\mathrm{T}}.\left(\mathbf{D}.\mathbf{P}+\mathbf{P}^{\mathrm{T}}.\mathbf{D}\right).(\mathbf{w}-\mathbf{w}_i) + a_k R_k(\mathbf{w}_i)X_k$. Now recalling that $\mathbf{w}_i$ is LAS in $\mathcal{W}\setminus\mathcal{X}_i$ if and only if $\mathbf{w}_i$ is LAS in $\mathcal{W}_i'$ and $R_k(\mathbf{w}_i) < 0$, it results that if conditions (1.5.5) hold and $R_k(\mathbf{w}_i) = \varrho_k - \frac{m_{k,i}}{m_{i,i}}\varrho_i < 0$, then $\frac{\mathrm{d}V_i}{\mathrm{d}t}(\mathbf{w}) < \frac{1}{2}(\mathbf{w}-\mathbf{w}_i)^{\mathrm{T}}.\left(\mathbf{D}.\mathbf{P}+\mathbf{P}^{\mathrm{T}}.\mathbf{D}\right).(\mathbf{w}-\mathbf{w}_i) < 0$, hence $\mathbf{w}_i$ is GAS in $\mathcal{W}\setminus\mathcal{X}_i$ as well.

1.ω. Épilogue

Dans le cas général, la stabilité locale asymptotique des équations de LOTKA-VOLTERRA dimorphe augmentée d'un nombre quelconque de productions publiques ne peut être déterminée pour tous les points fixes. La condition suffisante de stabilité globale asymptotique mis en évidence ici est une solution à ce problème. Toutefois, les hypothèses qu'elle requiert sont si fortes qu'elles limitent la portée biologique des analyses qui en découleraient.

Au cours des prochains chapitres, la croissance intra-hôte des parasites sera modélisée au moyen de systèmes d'équations plus restreints (et dans un espace des paramètres parfois contraint) que celui ici présenté – les différences résultant de simplifications ou de contingences historiques. De fait, de nombreux paragraphes méthodologiques apparaîtront redondants, et leur lecture pourra être épargnée à profit.

Dans le chapitre 2, seule productions publiques sont considérées : un bien commun et un produit de méchanceté par type parasitaire, dont la production est exclusive. Dans le chapitre 3, le modèle est étendu pour un nombre quelconque de types parasitaires. En revanche, nous supposons que les taux de croissance intrinsèque sont positifs ($\rho_i \geq 0$), que chaque type parasitaire ne produit qu'un unique type de bien commun et un unique type de composé d'animosité (pour lequel nous formulons l'hypothèse d'absence d'effet délétère pour son producteur, *i.e.* $\sigma_{i,i} = 0$). Enfin, les chapitres 4 et δ reprennent le modèle simple de LOTKA-VOLTERRA (cf. équation (i.2.2) avec respectivement $N = 2$ et $N \in \mathbb{N}^\star$), les productions publiques étant absorbées, sous couvert d'un argument de séparation des échelles de temps entre la reproduction microbienne et les cinétiques enzymatiques (voir l'annexe 4.b.1), par des termes généraux d'interaction $m_{i,k}$, sur lesquels aucune contrainte ne pèse, de même que pour les taux de croissance intrinsèques (*i.e.* $\rho_i \in \mathbb{R}, m_{i,k} \in \mathbb{R}$).

Dans ce dernier cas (équation (i.2.2) avec espace des paramètres égal à $\mathbb{R}^{N(N+1)}$ tout entier), notre modèle se distingue du travail de BARABÁS *et al.* (2016) qui se limite aux matrices d'interactions symétriques et à coefficients négatifs, *i.e.* à des communautés écologiques où l'unique interaction est la compétition équilibrée, condition à laquelle les communautés microbiennes ne se conforment pas.

En outre, notre étude des équations de LOTKA-VOLTERRA sans contrainte sur les paramètres (qu'elles contiennent ou non des productions publiques), adopte une approche orthogonale au travail de COYTE *et al.* (2015) traitant pourtant des interactions stabilisant les communautés microbiotiques. En premier lieu, COYTE *et al.* (2015) n'autorisent pas des interactions intra-typiques positives ($m_{i,i} \geq 0$) ni un taux de croissance intrinsèque négatif ($\rho_i \leq 0$), ce qui exclut des cas, certainement marginaux mais néanmoins intéressants, de types nécessitant un ou plusieurs types auxiliaires pour être maintenus dans la communauté. De fait, toutes interactions intra-typiques se voient imposer la même valeur -1 sans justification. Mais le plus important est que l'approche principale du travail de COYTE *et al.* (2015) utilise des théorèmes de propriétés asymptotiques sur la matrice d'interaction $\mathbf{M}$ pour $N \to \infty$. Or la proportion de points fixes faisables (ici de densités strictement positives) décroît géométriquement avec le nombre de types considérés ainsi que le montre la Figure 1.ω.1 (courbe en trait plein bleue). Il en résulte que les conclusions de COYTE *et al.* (2015) ne sont valables que sur une fraction infinitésimale de l'espace des paramètres, ce qui contrevient à l'objectif de réalisme minimal requis pour un modèle. Au contraire, notre approche ne repose pas sur des théorèmes asymptotiques et nous cherchons à identifier les conditions générales de faisabilité et de stabilité locale des points fixes pour un faible nombre de types, dont la proportion n'est pas encore in-

signifiante, y compris dans le cas général (bien qu'inférieure à son équivalent contraint, comme en témoignent les courbes roses de la Figure 1.ω.1).

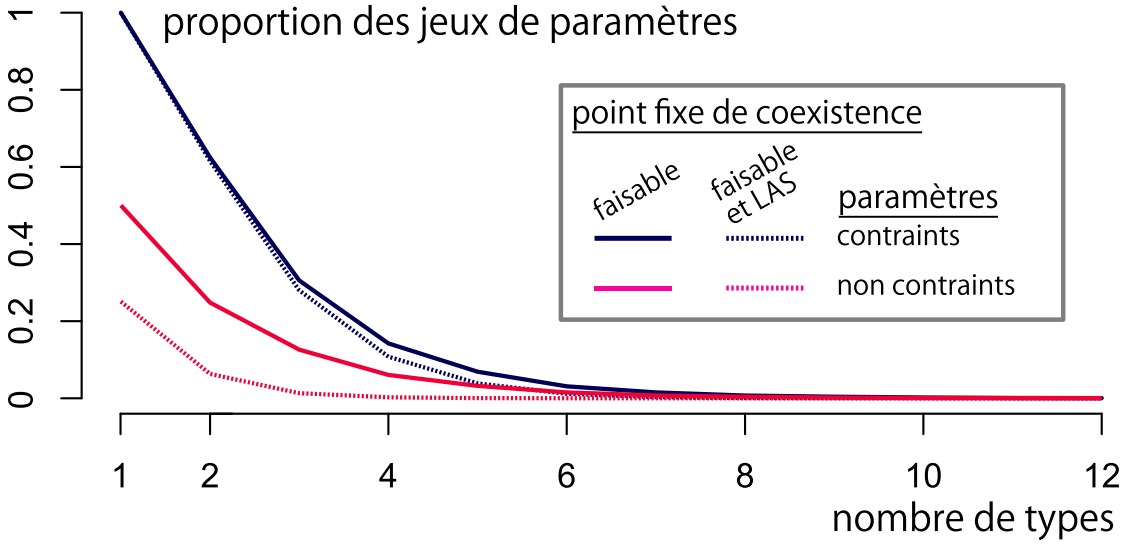

FIGURE 1.ω.1. – Faisabilité et stabilité du polymorphisme en fonction du nombre de types considérés.
Pour chaque nombre de types N, de 1 à 12 (en abscisses), 10^5 jeux de paramètres (le vecteur $\boldsymbol{\rho}$ et la matrice $\mathbf{M}$) ont été tirés aléatoirement : la moitié selon une procédure non contrainte (courbes roses), l'autre selon une procédure contrainte (courbes bleues). Dans la procédure non contrainte, les $N(N+1)$ paramètres sont tirés dans des lois normales centrées réduites indépendantes. La procédure contrainte est identique à ceci près que les taux de croissance intrinsèques ne peuvent être négatifs (ils suivent donc une loi normale repliée), et tous les termes diagonaux de la matrice d'interaction sont fixés à -1. Les courbes indiquent pour chaque procédure la proportion de jeux de paramètres dont le point fixe de coexistence des N types, $\widehat{\mathbf{x}} = -\mathbf{M}^{-1}.\boldsymbol{\rho}$, est faisable (traits pleins), et en outre localement asymptotiquement stable (pointillés).

Notons enfin que des protocoles expérimentaux suggèrent que les équations de LOTKA-VOLTERRA peuvent être améliorées en profondeur dans leur représentation des dynamiques microbiennes (bactérienne tout du moins), par exemple par l'introduction de taux de croissance fréquence-dépendants (LI *et al.*, 2015).

2 Patrons d'infection

2.α. Prologue

Au précédent chapitre, nous avons observé que le système dynamique modélisant phénoménologiquement une communauté microbienne dimorphe par des équations de LOTKA-VOLTERRA (modulo une extension aux productions publiques) présente quatre points fixes et que, dans le cas général, sa stabilité globale n'est pas garantie. Autrement dit, le système peut avoir des comportements au temps long différents selon les conditions initiales.

S'agissant d'espèces parasitaires, cela traduit des infections diverses – aucun type parasitaire ne persiste au sein de l'hôte (l'infection est seulement aiguë), un seul persiste (infection chronique monomorphe) ou les deux coexistent (infection chronique dimorphe) – dont l'issue dépend du contexte d'inoculation (inoculation monomorphe ou co-inoculation dimorphe dans un individu susceptible, inoculation secondaire dans un individu déjà infecté...).

Dans le travail suivant, nous essayons de caractériser et de donner un sens biologique à cette combinatoire en faisant émerger la notion de patron d'infection, qui peut se définir comme l'information de toutes les issues d'infection selon tous les contextes d'inoculation. Après un dénombrement purement formel de ces patrons d'infection indépendamment du modèle de dynamique intra-hôte choisi, nous les caractérisons pour une version réduite du modèle présenté au chapitre 1 (chaque type parasitaire ne produisant exclusivement qu'une sorte de bien commun et qu'une sorte de produit de méchanceté).

Mise en évidence de la diversité des patrons d'infection

Mircea T. SOFONEA, Samuel ALIZON, Yannis MICHALAKIS

Résumé

Les populations naturelles font souvent face à des parasites génétiquement distincts, qui peuvent coexister ou non au sein des mêmes hôtes. Les modèles théoriques d'évolution de la virulence ont souvent considéré deux issues à une inoculation multipe, à savoir superinfection et coinfection. Cette dichotomie a quelque peu limité ce champ de recherche sans correspondre à une réalité empirique, puisque d'autres patrons d'infection, c'est-à-dire les ensembles des issues d'inoculation, sont possibles. Nous montrons en effet qu'il existe plus d'une centaine de patrons d'infection pour les seules infections chroniques guérissables causées par des micro-parasites transmis horizontalement. Par la suite, nous mettons en évidence huit patrons d'infection en utilisant une modélisation explicite des dynamiques intra-hôte qui capturent une large gamme d'interactions écologiques, parmi lesquels cinq ont été négligés jusqu'à présent. Afin de clarifier la terminologie relative aux infections multiples, nous introduisons des termes décrivant ces nouveaux patrons pertinents et nous les illustrons avec des systèmes biologiques existants. Ces patrons d'infection constituent un nouveau cadre de travail pour lier les dynamiques intra et inter-hôte, ce qui est un passage obligé pour parfaire notre compréhension de l'épidémiologie et l'évolution des parasites.

Mots-clés :

superinfection, coinfection, interactions intra-hôte, coopération, bien commun, méchanceté, épidémiologie, patron d'infection

Exposing the diversity of multiple infection patterns

Mircea T. Sofonea, Samuel Alizon, Yannis Michalakis

Abstract

Natural populations often have to cope with genetically distinct parasites that can coexist, or not, within the same hosts. Theoretical models addressing the evolution of virulence have considered two within host infection outcomes, namely superinfection and coinfection. The field somehow became limited by this dichotomy that does not correspond to an empirical reality as other infection patterns, namely sets of within-host infection outcomes, are possible. We indeed formally prove there are over one hundred different infection patterns solely for recoverable chronic infections caused by two genetically distinct horizontally-transmitted microparasites. We afterwards highlight eight infection patterns using an explicit modelling of within-host dynamics that captures a large range of ecological interactions, five of which have been neglected so far. To clarify the terminology related to multiple infections, we introduce terms describing these new relevant patterns and illustrate them with existing biological systems. These infection patterns constitute a new framework for linking within-host and between-host dynamics, which is a requirement to forward our understanding of the epidemiology and the evolution of parasites.

Keywords:

superinfection; coinfection; within-host interactions; cooperation; public goods; spite; epidemiology; infection pattern

Citation: Sofonea MT, Alizon S, Michalakis Y. 2017. Exposing the diversity of multiple infection patterns. *Journal of Theoretical Biology* **419:** 278–289.
doi: 10.1016/j.jtbi.2017.02.011

2.1. Introduction

Parasitism has long been considered as a one-to-one interspecific interaction (Combes, 2001). This vision is gradually changing due to increasing evidence of the multiplicity of genotypes (Rigaud *et al.*, 2010) (in its broadest sense, i.e. including strains and species) infecting the same species of plant, animal or bacterial host (Petney & Andrews, 1998; Lord *et al.*, 1999; Juliano *et al.*, 2010; Balmer & Tanner, 2011). Though they have indirectly been studied through microbiological experiments for decades (Weigle & Delbrück, 1951), multiple infections are nowadays an active research topic in human (Garland *et al.*, 2009; Verma, 2015) and veterinary (Battilani *et al.*, 2011) medicine and in phytopathology (van der Plank, 1963). This recent shift in focus is stimulated by new technologies that make it easier to detect within-host parasitic diversity (see e.g. Juliano *et al.* (2010)).

The current state of the epidemiology and evolution of multiple infections has two caveats that we wish to address in this paper. The first pertains to terminology: interactions among several parasites and hosts are complicated enough but confusion is added by the proliferation and/or ambiguous use and misuse of terms characterizing them. The second issue pertains to a limited theoretical context that only considers two epidemiological scenarios known as coinfection and superinfection. This has led researchers in the field to force any experimental outcome in this binary reference frame. This inevitably results in even more confusion (and frustration). Below, we first expose in more details these two caveats before addressing them. Limiting ourselves to chronic recoverable infections caused by horizontally-transmitted microparasites, we first list all possible epidemiological scenarios using an appropriate formalism. We then show how an explicit model of within-host interactions can help us explore the diversity of these scenarios.

The great diversity of terms related to multiple infections reflects their growing importance in several fields of biological and medical sciences. One can indeed find different names in the literature for the same phenomenon but also the same name for different phenomena, starting with the term 'multiple infection' itself. If not used to qualify the clinical diversity of an infection (Moore, 1898), 'multiple infection' is often restrained to cases where several genetically distinct parasites simultaneously infect the same host (Brown *et al.*, 2002). Such within-host coexistence of distinct parasite genotypes can be referred to using a variety of terms amongst which 'concomitant infections' (Cox, 2001), 'multiple-strain infection' (Penn *et al.*, 2002), 'multiple genotype infection' (Rigaud *et al.*, 2010), 'multi-infection' (Radomyos *et al.*, 1994), 'mixed infection' (Moore, 1898), 'mix-infection' (Chen *et al.*, 2003), 'pluri-infection' (Demaerschalck *et al.*, 1995), 'polyinfection' (Lancastre *et al.*, 1989), 'polymicrobial infection' (Brogden *et al.*, 2005), 'genetically diverse infection' (Read & Taylor, 2001), but also 'coinfection' (Damasio *et al.*, 2015) and 'superinfection' (Sheward *et al.*, 2015) (understood as 'secondary infection'). Conversely, situations where several parasite genotypes present in the population that cannot coexist in the same individual host can be referred to as 'superinfection' (Nowak & May, 1994) (here understood as 'within-host replacement') or 'mutual exclusion' (Delbrück, 1945).

Confusion in the frame of reference is a common source of ambiguity in biological nomenclature. In botany for instance, 'hermaphroditic' can either refer to the flower, to the individual plant or to the species. Although 'infection' usually means "the invasion of a host by a microorganism with subsequent establishment and multiplication of the agent" (Willey, 2008), it can denote the persistence of a parasite at any of the following three levels: the cell (Syverton & Berry, 1947) (in the case of intracellular parasites, mostly used by virologists), the organism (Bundy *et al.*, 1991) (mostly used by clinicians and epidemiologists) and the population (van Baalen & Sabelis, 1995) (mostly used by

ecologists). For the sake of both clarity and generality, we here use 'multiple infection' in its broadest sense only, that is the circulation of several parasite genotypes in a host population.

Once inoculated (that is introduced) into a host, a parasite genotype either survives or goes extinct. Hence, there are only two different inoculation outcomes per genotype. The outcome may nevertheless depend on the presence of other genotypes inoculated previously or simultaneously and we define a multiple infection pattern as the set of outcomes over all possible inoculation challenges.

Classical epidemiological models such as *S-I-R* (for Susceptible-Infected-Recovered (Kermack & McKendrick, 1932)) have naturally been extended to multiple infections, usually by allowing for only two different genotypes (Levin & Pimentel, 1981; van Baalen & Sabelis, 1995). The vast majority of these extensions explicitly modelled the between-host dynamics only and made assumptions on within-host processes. Therefore the within host infection pattern was a modelling assumption and in most models (Hood, 2003) it was either coinfection (van Baalen & Sabelis, 1995; May & Nowak, 1995), where inoculations are always infectious and thus distinct parasite genotypes coexist in the long term within the host, or superinfection (Levin & Pimentel, 1981; Nowak & May, 1994; Boldin & Diekmann, 2008), where within host coexistence never occurs but one genotype always outcompetes the others whatever the inoculation order.

The use of the 'co-' prefix added to the term 'infection' when more than one parasite genotype is involved is now widely used (see references in Alizon *et al.* (2013)). A coinfection can originate from a 'coinoculation' (Saeed *et al.*, 2007), when the genotypes are introduced simultaneously into a susceptible (uninfected) host and can both develop an infection. It may also originate from the infection of a host already infected by a different parasite genotype that neither excludes nor is excluded by the first one. It seems preferable to see this latter case as a particular coinfection rather than using a different designation such as 'superinfection' (Hughes *et al.*, 2011; Sheward *et al.*, 2015), 'sequential infection' (Gorman *et al.*, 2006; Syller & Grupa, 2015) or 'secondary infection' (Dean *et al.*, 1978).

The predominance of super- and coinfection as basic assumptions in models has confined theoretical studies of multiple infections into a binary perspective, while few experimental studies have succeeded in settling the nature of the infection pattern for a given biological system (Alizon *et al.*, 2013). Some models have tried to escape from this dichotomy by nesting an underlying within-host process in the epidemiology (Coombs *et al.*, 2007; Alizon & van Baalen, 2008; Boldin & Diekmann, 2008; Alizon & Lion, 2011) but eventually failed to capture other infection patterns than the canonical two. We explain this by the maintenance of two strong assumptions in these models: parasite survival in single infections and virulence-based genotype replacement, virulence being defined as the decrease in host fitness due to infection.

Empirical studies of multiple infections are usually based on coinoculations, the outcomes of which are then compared to single inoculation outcomes. However, the interpretation of these data remains hindered by the lack of a framework identifying patterns specific to multiple infections, patterns that should rely on the combination of all within-host dynamics endpoints and the conditions that lead to them. For instance, Rigaud *et al.* (2010) clearly emphasise the direct benefit for empirical parasitology to be gained from theoretical investigations on what they call "multi-parasite hosts" but they restrict the scope of their investigations by considering that the super/coinfection dichotomy captures all the "interactions" that parasites sharing a host may have. The aim of our work is thus to push back the limits of the multiple infection world, while rationally mapping it. To do so, instead of assuming that infection outcomes are a biological constraint of

the given host-parasite system (as in the super/coinfection dichotomy), we model them as the aftermath of within-host parasite growth. This allows us to consider novel situations, for instance when two parasite genotypes require each other's presence to survive, which gives rise to the description of new infection patterns. Most importantly, the identification of infection patterns provides a helpful typology for linking within-host and between-host dynamics. Further, it is essential in formulating the appropriate epidemiological model when parasite polymorphism is taken into account. Hence, infection patterns provide the necessary framework to study parasite evolution, in particular with respect to within host interactions.

Drawing up an exhaustive list of infection patterns can be done by an abstract identification of infection patterns to mathematical discrete maps (see section 2.2). The problem is that some of the patterns identified using this logical method may have no biological support, be it experimental or theoretical. Another approach consists in focusing on within-host dynamics and all the kind of ecological interactions parasites exhibit inside their host: cooperation, exploitation competition, interference competition and apparent competition, both within and between genotypes (Mideo, 2009). In practice, the within-host outcomes are determined by the stationary parasite load each genotype reaches inside the host. Given the number of possible interactions in the model, these are non trivial to predict. They may even depend on the initial conditions, that is here the inoculation context. Indeed, an inoculation is not necessarily followed by an infection as the presence of an already established parasite genotype may prevent the growth of the newly inoculated one.

We thereafter investigate these within-host dynamics with a general model for two parasite genotypes that allows several types of interactions, especially those through public goods and spite, which are mutually beneficial and mutually detrimental products respectively (West *et al.*, 2007). After presenting the model and identifying the eight infection patterns it generates, we provide biological interpretations and illustrations of each of these. Importantly, these infection patterns do not depend on the specific assumptions of the model. It is only the conditions under which they may arise that do. The generality and the flexibility of our typological result opens new perspectives for both epidemiological modelling and theoretical parasite evolution. In the latter field, it has indeed been shown that the choice of the infection pattern impacts the evolution of virulence, regarding the range of persisting virulence polymorphism (wider in superinfection than in coinfection (Nowak & May, 1994; May & Nowak, 1995)) and the way selection acts on virulence (coinfection that relies on collective action favours prudent host exploitation (Brown *et al.*, 2002)). However, no general conclusion on virulence evolution has been drawn so far since these models do not share the same assumptions on within-host parasite growth. In our framework, infection patterns are not assumed but, instead, result from within-host interactions (parameter variations in the within-host model may lead to different outcomes). This allows us to progress toward a unified theory of virulence evolution in the context of multiple infections.

Our framework also allows for an unambiguous categorization of empirical multiple infection patterns that should greatly help to clarify the field. The mathematical details of the model and its thorough analysis are provided in the appendix and readers only interested in the biological implications can skip directly to the description of the infection patterns and the Discussion, where their relevance and biological examples are presented without any mathematical requirement.

2.2. Infection pattern diversity: a logician's approach

With two parasite genotypes, there are four qualitatively different host types, depending on the presence/absence of each genotype: the susceptible (uninfected) hosts, the hosts singly infected by genotype 1, the hosts singly infected by genotype 2 and the doubly infected hosts. We call these types "classes" and label them 0, 1, 2 and 3 respectively. We extend this class formalism to the composition of the inocula as well, which are the set of parasite individuals newly introduced into a host. In some epidemiological settings, the two genotypes may not play the same role (for example one of the genotypes may always be outcompeted within a host). However, since we are interested in enumerating scenarios that differ in quality and not in genotype labelling, we hereafter also use the dummy couple of indices (i,k) that indifferently stands for $(1,2)$ or $(2,1)$.

Merely asking whether the two genotypes can chronically infect the same host or not greatly under-estimates the complexity of such an apparently simple setting. For instance, let us assume that the genotypes cannot coexist within one host. Both for clinical, epidemiological or evolutionary investigations, it is still worth knowing what the outcome of the inoculation of a class 1 host by a class 2 inoculum is. Indeed, this challenge can result in a class 1 host (genotype 2 is eliminated), or a class 2 host (genotype 1 is eliminated), or even lead to recovery or death of the host. Knowing this result provides a key argument to initiate (or not) a prophylaxis against genotype 2 from a clinical point of view. It gives necessary information to design the mathematical model that best fits the epidemiological network. Finally, it accurately describes the selective pressure acting on both parasite genotypes from an evolutionary point of view.

Formally, an infection pattern is the set of outcomes of all possible inoculation challenges. It contains the information about all the host classes and inoculum classes involved (e.g. whether the doubly infected host class exists or not). It also contains additional information because the same host classes can be observed with different sets of outcomes. For instance, doubly infected hosts can result from the inoculation of one or both singly infected host classes but it can also result from the double inoculation of susceptible hosts. Therefore, the diversity of infection patterns for two genotypes cannot be reduced to a raw coinfection/superinfection dichotomy.

How many chronic infection patterns are there for two genotypes only? The answer to this question clearly depends on a myriad of biological details such as parasite transmission mode, host recovery ability and heterogeneity in host sensitivity to parasites. To show that the infection pattern diversity is unexpectedly large, we choose a simple setting where both parasite genotypes are exclusively horizontally transmitted, recovery of one genotype at a time is always possible and the host class alone fully determines the outcome of an inoculation challenge. The latter assumption implies that there is a unique inoculation outcome for each couple of host class and inoculum class. With this determinism, infection patterns can be seen as mathematical discrete maps, the principle of which is explained in Figure 2.2.1 along with its graphical convention used throughout this article.

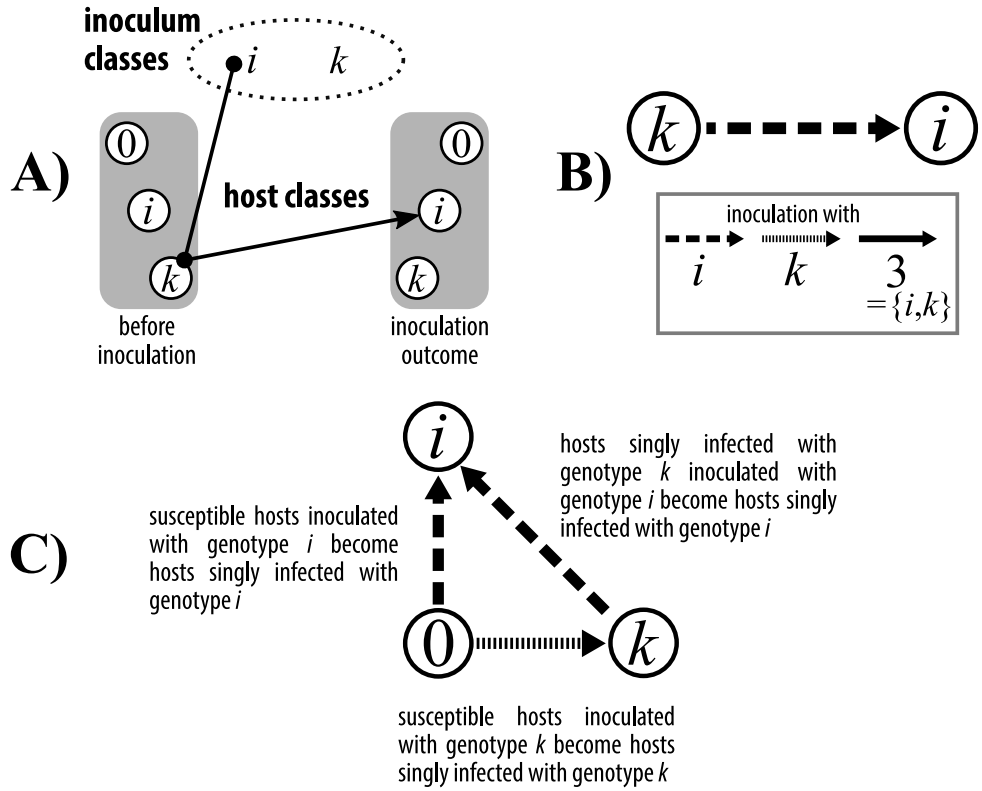

Figure 2.2.1. – Mapping formulation and associated representation in the dimorphic case.

We provide here a mapping example that illustrates the graphical method we use to construct infection maps. This example fulfils the infection pattern requirements related to superinfection i (see text below and figure 4). Under this pattern both single genotype inocula can infect susceptible hosts and turn them to hosts of their respective classes (e.g. inoculum i turns them to i-hosts). Inoculum i always successfully takes over k-hosts while inoculum k is always eliminated from i-hosts. As a consequence, doubly-infected hosts do not exist, and thus inoculum and host classes 3 are not depicted.

A) A mapping example. We show the situation where, following the superinfection i pattern, an i-inoculum always turns a k-host into a i-host. Notice the uniqueness of the inoculation outcome. **B)** Graphical equivalence of the mapping example in **A** and convention. In order to facilitate the mapping representation, we adopt the following graphical conventions: host classes are depicted as circled numbers corresponding to host class labels (0 for susceptible hosts, i for hosts singly infected by genotype i, k for hosts singly infected by genotype k and 3 for hosts infected by both genotypes). They are connected with an inoculation arrow whose style depends on the inoculum class (dashed for genotype i inoculations, striped for genotype k inoculations and solid for 1, 2 double inoculations). The figure represents the mapping example of **A**. **C)** Example of an infection pattern map. The entire map is given by all analogous to **A** and **B** associations between a (before inoculation) host class - inoculum class couple and a unique (inoculation outcome) host class. Only the possible host classes are depicted. Graphical conventions are those introduced in **B**. For the sake of simplicity, recovery arrows (from i-hosts and k-hosts to susceptible hosts) are not depicted. Likewise, the inoculations that do not change the host class are not shown; for example, because k-inoculations of i-hosts are ineffective they are not depicted.

The number of mathematically correct maps involving two parasite genotypes exceeds 4 billions, most of them being biologically irrelevant. Therefore we identify a set of rules a map has to satisfy in order to be an infection pattern candidate, namely type coherence, host class stability, infecting type insensitivity and epidemiological connectivity. These rules are detailed and formalised in Appendix A.3 and illustrated in Figure 2.2.2 (**a - d**). Maps that fulfill all these rules are potential infection patterns. Examples of such maps are given in Figure 2.2.2 (**e - g**).

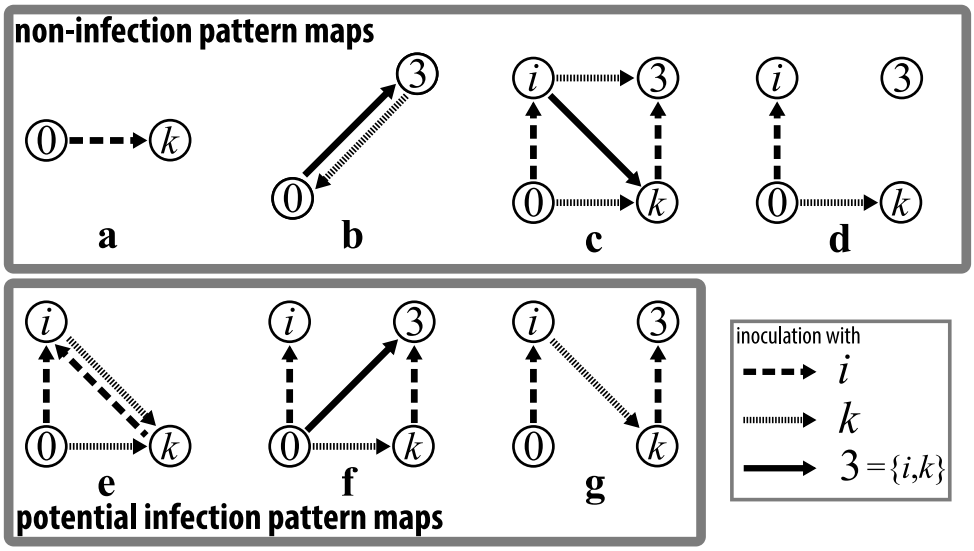

Figure 2.2.2. – Non biologically relevant maps (**a - d**) *versus* potential infection patterns (**e - g**).

Maps **a** - **d** are mathematically correct but biologically unsatisfying. They do not represent potential infection patterns because each of them violates one of the required rules. Map **a** violates type coherence as the inoculation outcome contains a parasite genotype (k) that was present neither in the host nor in the inoculum. Map **b** violates host class stability as the inoculation with an already infecting type induces a host class change: here, hosts of class 3, which are infected by both parasite genotypes are cured when inoculated by a type i inoculum. Map **c** violates infecting type insensitivity: inoculation of i-hosts by k-inoculum can lead to either k- or 3-hosts . Map **d** violates epidemiological connectivity because the doubly infected host class belongs to the set of possible host classes, and hence it is depicted, while it cannot be reached through any sequence of infection event from the susceptible hosts – which contradicts its necessary origin. Maps **e** - **g** are mathematically correct and do satisfy all rules for potential infection patterns. Map **e** is a mutual invasibility with genotypic replacement infection pattern. Map **f** is an infection pattern with inoculation order dependent within-host coexistence: if genotype k infects first then both genotypes can coexist in a co-infected host, but if genotype i infects first it excludes genotype k. Map **g** is an infection pattern with order dependent within-host coexistence: genotype k cannot infect susceptible hosts; when it is inoculated in i-hosts it excludes i, but both genotypes can coexist in initially k-hosts. This is a complicated pattern that perhaps does not exist in the real world, but it nevertheless satisfies all four criteria. Symbols and arrow styles as in Figure 1. For the sake of clarity, looping inoculation and recovery arrows are not shown.

In appendix 2.a, we provide all the mathematical details on the mapping formalism and the infection pattern rules, as well as an exhaustive enumeration of all potential infection patterns in our simple dimorphic setting. It turns out there are 114 such patterns (see Supplementary Figure 2.a.1 for the whole list).

This heuristic approach reveals and quantifies a previously undocumented diversity of infection patterns. However, even if they all formally satisfy biological feasibility, not all of them may have theoretical or empirical support. Indeed, the infection pattern shown in Figure 2.2.2**e** would require both negative frequency-dependence (as the newly inoculated genotype always invades) and unstable coexistence (as invasion by one genotype always leads to extinction of the other), while negative frequency-dependence usually implies the stability of the polymorphic equilibrium. Likewise, the infection patterns shown in Figure 2.2.2 **f** and **g** would require some kind of parasite niche construction to occur since the within-host coexistence of both parasite genotypes depends on the order of inoculation and infection respectively. These three examples illustrate that many potential infection patterns can only occur under very particular settings that involve specific within-host processes that depart from Lotka-Volterra - like dynamics. These dynamics are often used for modelling microbial growth and rather well supported experimentally (Li *et al.*, 2015), which is why we focus on them hereafter.

2.3. Within-host modelling

Infection patterns are not all equally biologically relevant, as some of them require the invocation of rare and very specific within-host processes to be observed. In order to determine infection patterns that have an established mechanistic explanation, we develop a general model for the within-host dynamics. Our goal is to refrain from making any *a priori* assumptions on the outcome of an inoculation, that is the long-term persistence of either none, one or both parasite genotypes (Mideo *et al.*, 2008). This approach allows us to confirm previously described infection patterns but also reveals new patterns, while giving further insight on how parasites interact. To do so we use a modelling framework often used to study microbial communities (Mougi & Kondoh, 2012; Coyte *et al.*, 2015), the competitive Lotka-Volterra model (Lotka, 1925; Volterra, 1928).

Here this continuous-time deterministic model is extended by adding public production kinetics. It thus incorporates many types of ecological interactions within and between genotypes (cooperation, exploitative competition, interference competition and apparent competition).

In particular, cooperation and interference competition processes are referred to as public goods and spite production respectively (Bashey, 2015). Inspired by the case of bacteria, we develop a within-host model where public goods correspond to siderophores and spite to bacteriocins. Siderophores are excreted compounds that harvest extracellular Fe^{3+} ions, which are vital for metabolic processes (Neilands, 1995). Provided a receptor compatibility, the iron-siderophore complex can be imported by a bacterium, even if it was not produced by its own species (Ovaa *et al.*, 1995). The empty siderophore is then released back in the environment (Wandersman & Delepelaire, 2004). As for bacteriocins, they cover a large and diversified family of compounds with a bacteriocidal mode of action (Riley & Wertz, 2002). Some of them are for instance bacteriolytic enzymes that specifically hydrolyse the pentaglycine cross-bridge in peptidoglycan, leading to cell lysis of sensitive strains (Riley & Chavan, 2007). Depending on their type, bacteriocins may affect the producing bacteria or not.

We consider two parasite genotypes labelled 1 and 2. For the sake of concision, i still indifferently refers to 1 or 2 and k to the other genotype (2 or 1) unless stated otherwise. For a given genotype i, X_i, Y_i and Z_i are its parasite load, the concentration of public goods it produces (*e. g.* siderophores (Neilands, 1995)) and the concentration of spite molecules it produces (*e. g.* bacteriocins (Riley & Wertz, 2002)) respectively. These three variables vary with time following a system of ODEs motivated by classical modelling assumptions such as the mass action laws (see Sofonea *et al.* (2015) for more details):

$$\begin{cases} \frac{\mathrm{d}X_i}{\mathrm{d}t} = \left(\rho_i + \eta_{i,i}X_i + \eta_{i,k}X_k + \gamma_{i,i}Y_i + \gamma_{i,k}Y_k - \sigma_{i,i}Z_i - \sigma_{i,k}Z_k\right)X_i \quad , \\ \frac{\mathrm{d}Y_i}{\mathrm{d}t} = \upsilon(u_iX_i - Y_i), \\ \frac{\mathrm{d}Z_i}{\mathrm{d}t} = \upsilon(v_iX_i - Z_i). \end{cases} \tag{2.3.1}$$

In (2.3.1), the lower case Greek letters and u_i and v_i refer to time-independent parameters. Singly indexed parameters denote a given genotype's trait while doubly indexed parameters denote an interaction effect. In this latter case, the first index refers to the genotype that undergoes the effect, while the second index refers to the genotype from which the effect originates. For self effects, the indices are identical. We denote by j and ℓ couples of indices that can be identical.

The basic growth rate ρ_i is the coefficient of the only linear term in the parasite load time derivative. It represents the rate at which the parasite population grows in the absence of all other effects, including self parasite-load dependence. It includes part of

the exploitative competition through the parasite efficiency to exploit host resources and reproduce, but also all the costs of constitutive processes such as public goods and spite production.

The parasite-load dependent effects $\eta_{j,\ell}$ are the coefficients of the parasite load quadratic terms in the parasite load time derivative. These include several interactions, namely exploitative competition , apparent competition (through host immune response elicitation and resistance) and direct cooperation. Note that if $\eta_{i,i} < 0$, then $-\frac{1}{\eta_{i,i}}$ is proportional to the carrying capacity of genotype i in the absence of public goods and spite.

The public goods effects $\gamma_{j,\ell}$ are the coefficients of the parasite load - public goods concentration quadratic terms in the parasite load time derivative. They represent the benefits of public goods on parasite growth. The (standardised) public goods production rate u_i weights the secretion of public goods in the host medium. The combination of public goods effects and production rates captures indirect cooperation. Their spite counterparts are denoted by $\sigma_{j,\ell}$ and v_i respectively, and capture interference competition. Finally, v is the standard clearing rate of the public productions, which we assume to be independent from their nature or origin. As public productions are often catalytic compounds which are not degraded by their recipient (Neilands, 1995; Riley & Chavan, 2007), we further assume that the rate at which they are withdrawn from the host medium is essentially due to dilution, self-denaturing, host counteraction or host excretion, that is parasite load independent processes

This model is the adaptation for two genotypes of the within-host part of a general two-level model for multiple infections (Sofonea *et al.*, 2015) used to quantify epidemiological feedbacks due to genotype diversity. Here, the focus on the within-host interactions between two parasite genotypes allows us to go deeper in the qualitative analysis of the model and investigate the support for co- and superinfection along with the number and nature of potential other infection patterns. Note that three assumptions made in Sofonea *et al.* (2015) are relaxed here: self-spiting is possible, parasites can have a negative basic growth rate and a genotype does not always reach the single infection steady state. This increases the diversity of biological situations this model captures. Finally, our within-host model was designed to be as general as possible and, as such, captures several existing models that only include one or two types of interaction between genotypes (Bremermann & Pickering, 1983; Brown *et al.*, 2002; Gardner *et al.*, 2004; Buckling & Brockhurst, 2008; Mideo *et al.*, 2008).

The flow diagram in Fig. 2.3.1 illustrates the links between variables and parameters according to the set of equations (2.3.1).

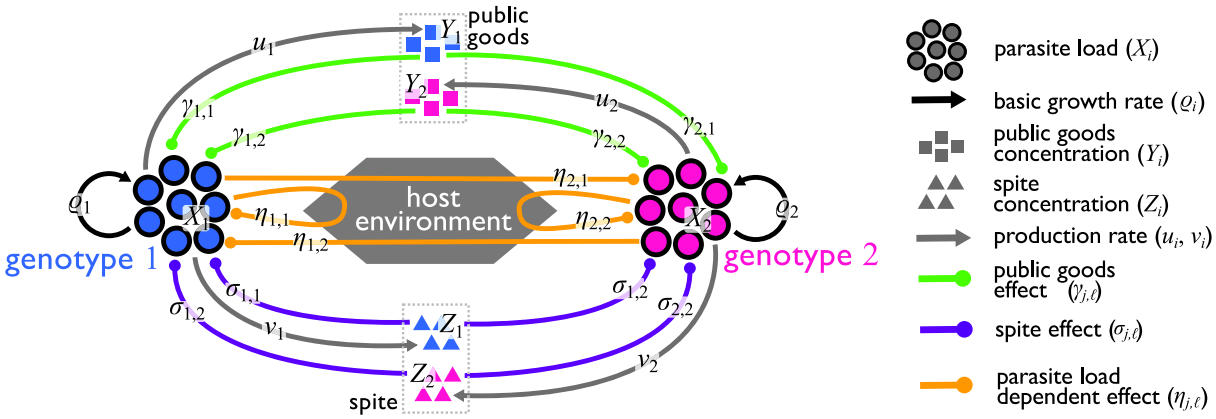

Figure 2.3.1. – The within-host interaction model.
Each genotype produces one kind of public goods and one kind of spite, proportionally to their parasite load. Public productions have beneficial (cooperation – green arrows) and detrimental (interference competition – purple arrows) effects on both genotypes' growth. The remaining interactions (exploitative and apparent competitions, potentially mediated by the host environment) are captured by the parasite load dependent effects (orange arrows). Note that public production rates are proportional to the same constant v, which is the rate at which the public productions are cleared (not shown).

If there is only one parasite genotype in the host, system (2.3.1) is characterized only by the three variables related to the inoculated genotype, while it is characterized by six variables when the host is inoculated by both. For this reason, we shall consider two distinct spaces in which (2.3.1) can take place (see the appendix 2.b for the vectorial formulation of the model). These spaces are the single inoculation space (SIS) and the double inoculation space (DIS) respectively.

The nonlinearity of system (2.3.1) prevents us from finding a general solution. However, the fixed points of the system (i.e. its stationary solutions) can capture its long-term behaviour. For each fixed point, there exists a range of parameters and initial conditions for which the system converges to it. The system has exactly four different fixed points (see appendix 4.b.2 for their derivation): the uninfected fixed point (UFP, where the host is uninfected, none of the parasites can establish an infection), the two singly infected fixed points (SIFP_1 and SIFP_2, where the host is infected by only one of the two genotypes), and the doubly infected fixed point (DIFP, where the host is infected by both genotypes). Notice the DIFP is the only fixed point to exclusively lie in the DIS.

Importantly, these theoretical fixed points do not always correspond to biologically relevant situations. A fixed point is biologically relevant if the system can reach it without taking negative values. Mathematically this requires the conjunction of two properties: feasibility and local asymptotic stability (hereafter in the main text termed simply as 'stability', but see the appendix for details). Feasibility means that the corresponding steady-state values of the variables are non-negative, while stability refers to the property of the system to converge to this point if close enough at some timepoint. If a fixed point is stable, then small perturbations of the system do not affect it on the long run.

Since the variables of a non-inoculated genotype are equal to 0, feasibility in the SIS implies feasilibity in the DIS and vice versa. This is however not true for stability, which can be valid in the SIS and not in the DIS. An interesting biological consequence of this is that the inoculation by genotype j in a host already singly infected by genotype i can result in the persistence of genotype j and in the elimination of genotype i from the host.

Feasibility and stability conditions of each fixed point are derived in appendices 2.c.2 and 2.c.2 respectively. The combination of both conditions (appendix 2.c.4) shows that within-host parameter values govern the outcome of within-host growth in a non-trivial way. The combinatorial complexity that arises when considering each kind of inoculation challenge and asymmetry between genotypes is now to be categorised into infection patterns.

2.4. A biological identification of infection patterns

The previously introduced model provides us with a mechanistic insight of the infection patterns it can generate. Interpreting the within-host outcomes of the model at the host population level requires making some classical assumptions in order to link the two levels of dynamics (Mideo *et al.*, 2008). Importantly, this does not require to specify an epidemiological model, which ensures the generality of our approach. In particular, we assume that epidemiological routes of transmission only depend on the long-term behaviour of the within-host dynamics (i.e. the within-host parasite growth is fast compared to the transmission/inoculation processes occurring at the between-hosts level). This assumption is common in multilevel models and is justified for chronic infections in which hosts transmit the genotypes that have persisted to the within-host steady state substantially longer than the genotypes that vanished during the transient dynamics (Gilchrist & Coombs, 2006; Mideo *et al.*, 2008). Within-host outcomes can be predicted from the feasibility and the stability of the fixed points of (2.3.1). Thus, deciphering all the infection patterns the model can generate is equivalent to characterising all the combinations of fixed points the within-host dynamics can reach.

Before going any further, we need to address a peculiar output of the model when written as (2.3.1), which is explosive infection. Indeed, we show in appendix 2.d that some parameter sets can drive parasite loads to infinity in finite time. One way of dealing with such a biologically unrealistic behaviour of the infection is to assume that there exists a fixed parasite load threshold related to host physiology such that when the total parasite load reaches this threshold all the parasites die. This can either be due to the elicitation of an immune response that kills all parasites or to host death. Similar assumptions have been made in other nested models (see for instance Antia *et al.* (1994)). From an epidemiological standpoint, given our assumption that explosive infections lead to recovery, these have to be interpreted differently depending on the host inoculation status. An explosive infection in singly inoculated hosts should be considered as a non-inoculation because the susceptible host remains susceptible, while an explosive infection caused by a secondary inoculation of singly infected hosts should be considered as a recovery since the initially infecting genotype also vanishes.

This rule to handle explosive infections adds to a set of rules that governs the diversity of the sets of feasible and stable fixed points of the three inoculation spaces (SIS_1, SIS_2 and DIS). The feasibility and stability conditions constrain the existence of feasible and stable fixed point sets and also their combination. The set of feasible and stable fixed points of a given inoculation space (the first three columns in Table 2.4.1) completely determines the biologically relevant outcome of any host inoculation. The combination of these sets over all inoculation spaces (the lines in Table 2.4.1) then determines infection patterns, that is the way both genotypes can circulate through the host population. In appendix 2.e.1, we derive and combine these rules so that all the possible combinations of feasible and stable fixed points sets are explored, leading to the infection pattern list showed in Table 2.4.1.

feasible and stable fixed points in			host	pattern	pattern
SIS_i	SIS_k	DIS	classes	interpretation	name
none or UFP	none or UFP	none or UFP UFP & DIFP	0	no infection is possible	**no infection**
		DIFP	0, 3	genotypes infect only if together	***ambinfection***
$SIFP_i$		none or $SIFP_i$	0, i	one genotype never infects	***latinfection*** (k)
		DIFP	0, i, 3	one genotype needs the other to infect	***suprainfection*** (k)
	$SIFP_k$	none	0, 1, 2	co-inoculation causes explosive infection	***ultrainfection***
		$SIFP_i$	0, 1, 2	one genotype excludes the other	**superinfection** (i)
		$SIFP_i$ and $SIFP_k$	0, 1, 2	secondary inoculated genotype is excluded	***priorinfection***
		DIFP	0, 1, 2, 3	all inoculations lead to infection	**coinfection**

Table 2.4.1. – Exhaustive list of infection patterns generated by a multiple infection model, with respect to the sets of feasible and locally asymptotically stable fixed points.
Previously unnamed patterns are written in italic letters. For the sake of concision, twin infection patterns (*latinfection* i, *suprainfection* i and *superinfection* k) are not shown.

We find 8 patterns, 5 of which have so far never been studied theoretically. We describe each pattern and suggest an adapted terminology when needed. Links with existing experimental studies are given in the discussion.

No infection This pattern arises when no parasite genotype can reach a stable infection state starting from few individuals, neither alone nor in combination. Note that this includes the case where the DIFP is virtually possible but never reached. This pattern is obviously biologically uninteresting and we only mention it for the sake of completeness.

Ambinfection This pattern is characterised by the impossibility of single infections: an infection can only originate from a coinoculation of genotypes. We therefore suggest to call it *ambinfection*, from the latin *ambo* meaning "both".

Latinfection In this pattern, only one parasite genotype is observed, while the other is absent from all within-host outcomes. We call this pattern *latinfection*, from the latin *latere* meaning "to hide", because the latter genotype is never observed at steady states of infections. Note that we label the two latinfections according to the apparently absent genotype ("latinfection i" thus means that genotype i is the "hiding" one).

Suprainfection This pattern is characterised by the impossibility of one genotype to infect without the other. One type singly infected host class is therefore never observed. We call this pattern *suprainfection*, from the latin *supra* meaning "over", since one genotype can only infect if the other is already present. Note that we label the two suprainfections

according to the double infection restricted genotype ("suprainfection i" thus means that genotype i is the "extra" one in double infections).

Superinfection This well known pattern in ecology and evolution arises when one genotype always out-competes the other in doubly inoculated hosts, whatever the inoculation timings. Note that we label the two symmetric superinfections according to the most competitive genotype ("superinfection i" thus means that genotype i always outcompetes genotype k). Parasite dynamics within a doubly-inoculated host in a superinfection pattern are illustrated in Figure 2.4.1A.

Ultrainfection This pattern arises when both genotypes steadily infect singly inoculated hosts but the infection becomes explosive in doubly inoculated hosts leading to an absence of doubly infected hosts. We call this pattern *ultrainfection*, from the latin *ultra* meaning "beyond", since double inoculation here causes immediate death or recovery. Parasite dynamics within a doubly-inoculated host in an ultrainfection pattern are illustrated in Figure 2.4.1B.

Priorinfection This pattern arises when the first genotype infecting a host always excludes the newly inoculated one. Again, doubly infected hosts are never observed. Unlike superinfection, the order of inoculation matters. We call this pattern *priorinfection*, from the latin *prior* meaning "the first of two", since one genotype can never infect if the other is already present.

Coinfection The last pattern is already defined in ecology and evolution. It arises when the two genotypes can infect both alone and together. This is the only case where all four host classes are observed as steady states. Parasite dynamics within a doubly-inoculated host in a coinfection pattern are illustrated in Figure 2.4.1C.

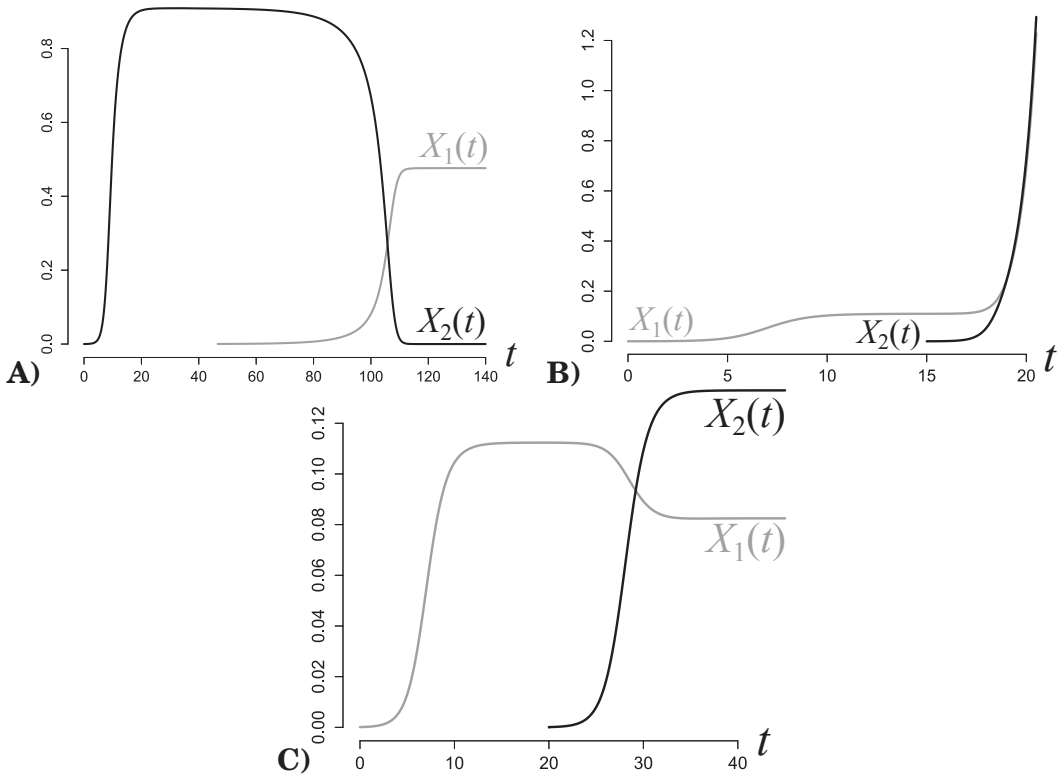

Figure 2.4.1. – Within-host dynamics of parasite genotype loads in superinfection (A), ultrainfection (B) and coinfection (C).

These are the results of numerical integrations of system (2.3.1) in *R* R Core Team (2013) using the *lsoda* function from the *deSolve* package (Soetaert *et al.*, 2010).

A) Superinfection 1. At $t = 0$, a host is inoculated with 10^{-4} PLU (parasite load units) of genotype 2. At $t = 45$, the parasite load of genotype 2 (X_2, in black) has reached its stationary value ($x_2^\circ \approx 0.91$) and 10^{-4} PLU of genotype 1 are introduced (X_1, in grey). At $t = 150$, genotype 2 has almost vanished (X_2 has fallen below 10^{-6} PLU) while genotype 1 has reached its stationary value ($x_1^\circ \approx 0.48$) and so even if $x_1^\circ < x_2^\circ$, indicating that stationary parasite loads in single infections do not predict competitiveness. Parameter values are $\eta_{1,1} = \eta_{2,1} = -3$, $\eta_{2,2} = \eta_{1,2} = -2$, $\gamma_{2,1} = 0.5$, $\gamma_{1,2} = \sigma_{2,1} = 2$, $\sigma_{1,1} = \sigma_{2,2} = 0.1$ and the others are equal to 1. **B) Ultrainfection**. At $t = 0$, a host is inoculated with 10^{-4} PLU of genotype 1. At $t = 15$, the parasite load of genotype 1 has reached its stationary value ($x_1^\circ \approx 0.11$) and 10^{-4} PLU of genotype 2 are introduced. Five time units later, the total parasite load has increased over tenfold. The parameters are the same as in panel A but $\sigma_{1,1} = \sigma_{2,2} = 0.1$, $\sigma_{1,2} = \sigma_{2,1} = 0{,}5$, $\eta_{1,1} = \eta_{2,2} = -10$, $\eta_{1,2} = 9$, $\eta_{2,1} = 10$. **C) Coinfection**. At $t = 0$, a host is inoculated with 10^{-4} PLU of genotype 1. At $t = 20$, the parasite load of genotype 1 has reached its stationary value ($x_2^\circ \approx 0.11$) and 10^{-4} PLU of genotype 2 are introduced. At $t = 45$, both genotype steadily coexist at their stationary values ($x_1 \approx 0.08$ and $x_2 \approx 0.13$). The parameters are the same as in panel A but $\eta_{1,1} = -10$, $\eta_{2,2} = -8$, $\eta_{1,2} = -4$, $\eta_{2,1} = -3$, $\sigma_{1,1} = \sigma_{2,2} = 0.1$.

Finally one can easily remark that any deterministic model assumed with global stability (that is in each space there is at most one fixed point that attracts all trajectories) would not generate other infection patterns than these (and priorinfection would not be generated at all for it requires that two fixed points are local attractors in the same space).

2.5. Discussion

The great number of fields for which multiple infections are a subject of interest, added to time and spatial scale confusions, has lead to a diversified but ambiguous terminology. This terminology essentially relies on the existence (or not) of multiply infected hosts, which is problematic. For instance, the absence of detection of coinfected hosts in a natural population does not imply that parasite genotypes cannot coexist within the same host because it can also be due to between-host limitations such as low contact rates, high recovery rates or high death rates. Another reason why the absence of doubly infected hosts is not sufficient to define superinfection is because an already infecting genotype could exclude the newly inoculated genotype with no absolute competitive hierarchy between genotypes (i.e. a precedence dominance situation, also known as priority effect). Thus coinfection, superinfection, and what we more generally call "infection patterns", are within-host level specific terms that cannot be directly inferred from between-host observations. Nevertheless, empirical and theoretical epidemiology of multiple infections rely on knowing the appropriate pattern for determining what must be measured and modelled respectively. Indeed, avoiding a fully open model greatly reduces the complexity of the investigated system in terms of number of expected host classes, compartments, flows and parameters thus allowing for a greater focus on the relevant processes (but see Sofonea *et al.* (2015) for dealing with this combinatorial complexity).

Modelling epidemiological phenomena, e.g. the spread of an infectious disease or host-parasite co-evolution, is essentially about determining the appropriate equations that well describe the dynamics of these phenomena; these can often be seen as flows between compartments. It is obvious that the flows that govern the between-host dynamics are intrinsically related to the infection pattern. Our logician's approach however reveals that, even in the simple case of two genotypes, the diversity of infection patterns exceeds by far the dichotomy between coinfection and superinfection that most epidemiological models have considered. Designing a different framework for each of the more than a hundred infection patterns, however, would quickly lead to an impractical pile of models, especially since many of the potential infection patterns are biologically unlikely to occur. The modelling initiative must thus go beyond the choice of the infection pattern and consider the processes that generate it, that is the underlying within-host dynamics. We therefore advocate that nested modelling, which considers both within and between-host dynamics, is the most appropriate theoretical approach to understand epidemiological phenomena involving parasite diversity, because it provides a unified framework that is able to generate a biologically relevant diversity of infection patterns.

The model presented here captures several within-host interactions between microparasites, notably cooperation and interference competition through explicitly modelled enzymatic productions. It highlights seven non trivial infection patterns, illustrated in Figure 2.5.1, that are thus supported by common microbiological mechanisms. Consequently, we have shown that the super/coinfection dichotomy is easily overcome without making any *a priori* assumptions. We show below that the typology exposed in Table 2.4.1 accurately captures different within-host processes realised in natural biological systems. It is also worth noting that the list of infection patterns is exhaustive for this model: incorporating other processes than the ones considered here (e.g. types of interactions among parasite genotypes) in the model would not alter the number of infection patterns; only the conditions of their existence.

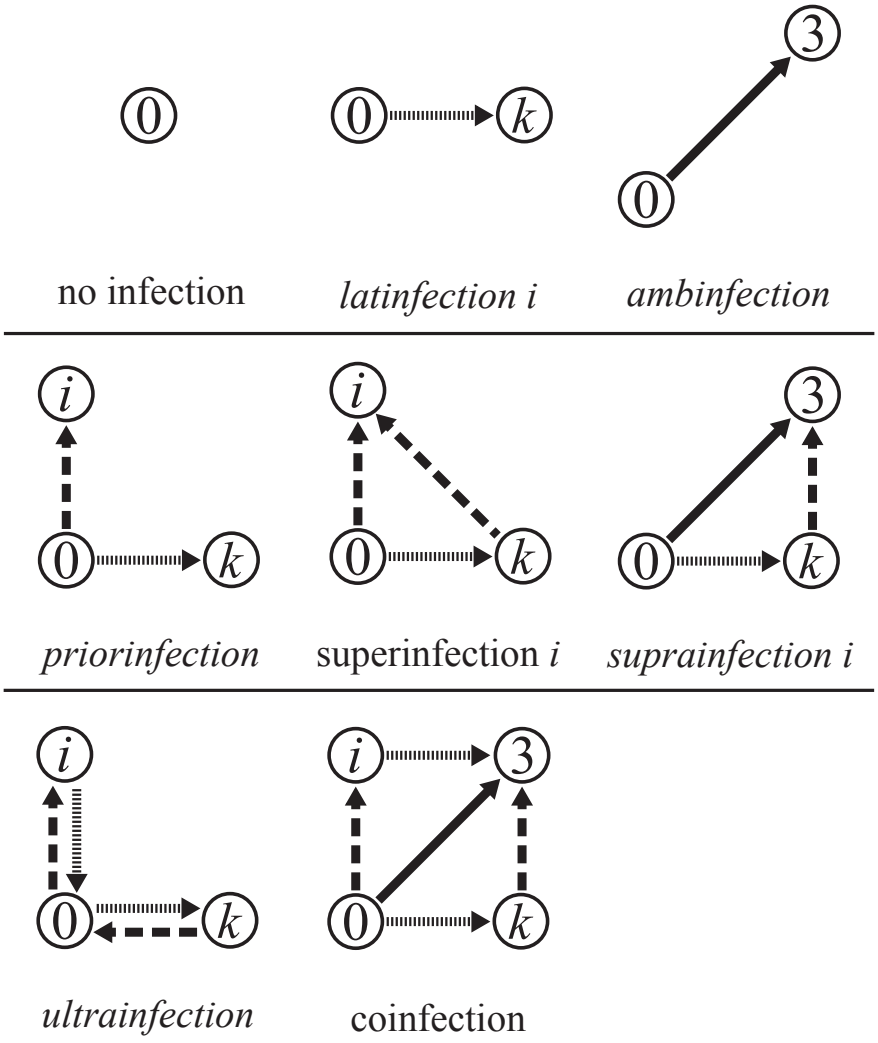

Figure 2.5.1. – Infection patterns for two parasite genotypes.
Circled numbers correspond to host class labels: 0 for susceptible (uninfected) hosts, i for hosts singly infected by genotype i, k for hosts singly infected by genotype k and 3 for hosts infected by both genotypes 1 and 2. Dashed arrows stand for a genotype i inoculation, striped arrows for a genotype k inoculation and solid arrows for a 1, 2 double inoculation.

Coinfection Two parasite genotypes define a coinfection when they can infect together *and* alone. More precisely, these genotypes are able to cause single infections in distinct hosts and double infections when inoculated within the same host. In the literature, 'coinfection' is indeed almost always defined as the "stable coexistence of different parasites in the same hosts" (May & Nowak, 1995). This leaves the outcome of single genotype inoculation in susceptible hosts unspecified. Yet, all theoretical works assume the effectiveness of single infections for each parasite (May & Nowak, 1995; van Baalen & Sabelis, 1995; Mosquera & Adler, 1998; Alizon & van Baalen, 2008; Alizon & Lion, 2011; Lion, 2013). Therefore, our definition of coinfection clarifies a previously implicit condition. At the same time, it enables the unambiguous definition of other patterns that share the double infection condition but not the single infection one (i.e. suprainfection and ambinfection).

Some experimental articles apply the adjective 'coinfected' to hosts that are infected by potentially non self-sufficient parasites, such as satellite viruses (see the discussion part on ambinfection below and Saeed *et al.* (2007)). These studies are usually interested in the interactions between parasites and search for synergistic or antagonistic effects

that may affect epidemiological traits such as virulence or transmission (Péréfarres *et al.*, 2014). However, they do not focus on qualitative properties of the outcome, such as one genotype being rescued by the other. This confusion between models that assume the single infection condition and experimental studies that do not (Aaskov *et al.*, 2006) is an additional reason to clarify the definition of 'coinfection' and its derived words. As a consequence, when dealing with two genotypes within the same host without information about single infections, we recommend to use the term 'double infection'.

By analysing the parameter conditions that lead to the coinfection pattern, we find that it occurs when each genotype inhibits its own growth more than that of the other. This is similar to the famous ecological principle of limiting similarity (MacArthur & Levins, 1967). Nonetheless coexistence within the host does not imply complete neutrality between genotypes. Indeed, as shown in Fig 2.4.1B, parasite loads can be impacted positively or negatively by the presence of the other genotype, which can have dramatical consequences on the total parasite load and the overall virulence (but see below and Alizon *et al.* (2013)).

In nature, coinfection is a common pattern: *Mycobacterium tuberculosis* and the *Human immunodeficiency virus* (HIV) in humans (Harries *et al.*, 2004), or the two strains of the *Tomato yellow leaf curl virus*, TYLCV-Mld and TYLCV-IL, in tomato plants (Péréfarres *et al.*, 2014), are two examples of coinfections, since parasites can infect their host both together and alone. Furthermore, results from metagenomics suggest that coinfection is commonplace (Roossinck, 2012).

Superinfection Superinfection occurs when two parasites can infect alone *and* one always outcompetes the other when together (independently of the order of the inoculations). In the literature, 'superinfection' often implies "the exclusion of the less virulent strain" (Lion, 2013; Nowak & May, 1994; Gandon, 1998). Note that, as for coinfection, the single infection condition is usually implicit. The fact that it may not be satisfied makes the latinfection pattern possible (see below). Contrary to ours, the definition found in the literature relies on a trait, usually virulence, that characterises each genotype. In its broadest sense, virulence is a shared trait between the host and the parasite and is measured as the host's fitness loss due to infection (Read, 1994). Since there are no doubly infected hosts in a superinfection setting, virulence is necessarily measured in single infections. This is problematic because how could the comparison between two environment-dependent traits, quantified in two distinct environments (the singly infected hosts), rule the outcome of a competition that takes place in a third environment (the doubly inoculated host)? This question still holds if the hosts are clonal, because the parasites themselves shape their environment. The nonlinearity of these processes, including apparent competition, makes the infection outcome of the doubly inoculated host impossible to predict just from virulences quantified (whatever the way) in single infections. Our explicit modelling of the within-host dynamics allows us to overcome this problem and to define superinfection as the exclusion of the same genotype in any context.

We have seen that coinfection arises when parasite genotypes satisfy the classical ecological two-species coexistence conditions: they inhibit themselves more strongly than they inhibit the coinfecting genotype. Superinfection arises when the interaction between the two genotypes becomes asymmetrical: while one genotype obeys the "coinfection rule", inhibiting the other genotype less than it inhibits itself, the opponent genotype breaks this rule and inhibits the former genotype more than itself. This confirms that the exclusion of a genotype does not simply depend on growth rate and stationary parasite load, which are potential proxies for virulence, but also on competitiveness.

To further illustrate the risk of defining superinfection through virulence, let us first make the assumption that, for a given parasite genotype, a greater parasite load decreases host fitness. Let us further assume that for two similar genotypes, the relationship between parasite load and virulence approximately follows the same monotonically increasing function. Figure 2.4.1A shows that it is possible for a less virulent genotype to outcompete a more virulent genotype, even when inoculated afterwards. As a conclusion, our model and definition of superinfection capture a greater diversity of asymmetric exclusions freed from the assumption that virulence and competitive ability are positively correlated.

The evidence of competitive exclusion in doubly inoculated hosts has been shown for instance for two strains of the rodent malaria *Plasmodium chabaudi* in mice (DE ROODE *et al.*, 2004, 2005a), where it has been reported that secondary inoculated strains decreased the resident strain loads up to six fold and below detectable levels.

Priorinfection Priorinfection occurs when both parasite genotypes infect alone *and* when the first genotype inoculated always excludes the other. Unlike superinfection, the infection outcome in a doubly inoculated host depends on the sequence of the inoculations (i.e. the excluded genotype is not always the same).

This pattern is reached if each genotype inhibits its own growth less than it inhibits that of the other. A biological interpretation of this result is that the first genotype in a host modifies the within-host environment, for instance through high spite concentrations of immune system elicitation, so much that any newly inoculated genotype rapidly goes extinct.

The impact of priority on the within-host infection outcome has been noticed for a long time. In 1945, Delbrück showed that *Escherichia coli* (strain "B") infected with either α or δ bacteriophages cannot be infected by the other phage if inoculated within four minutes after the first inoculation. He called this the "mutual exclusion effect" (DELBRÜCK, 1945). The use by plants of RNA interference as an antiviral defence mechanism, spite in our model, notoriously gives rise to priorinfection of plant viruses, sometimes referred to as "cross-protection" (RATCLIFF *et al.*, 1999) or "super-infection exclusion" (SYLLER & GRUPA, 2015). Finally, priorinfection echoes vaccination as it prevents secondary infections.

Ultrainfection Two parasite genotypes define an ultrainfection when they can infect alone *and* provoke explosive infection when together. Ultrainfection is due to excessive cooperation between the two genotypes. High concentrations of highly beneficial public goods and/or cross facilitation through the alteration of the host's immune system compensate for the negative density-dependence, which induces explosive infections. In this case, double infections are transient and do not contribute much to the epidemiological dynamics; this may explain why this pattern has been neglected so far. Two honeybee parasites illustrate this pattern: the parasitic mite *Varroa destructor* indeed triggers the replication of the initially cryptic *Deformed wing virus* (DWV) within the bee up to lethal levels, while none of these parasites kills their host alone (NAZZI *et al.*, 2012).

More generally, this pattern should be regarded as a limit case of coinfection, where strong mutual benefits destabilises the within-host dynamics so that parasite loads rise to levels way greater than the ones reached in single infections.

Latinfection Latinfection first requires that one genotype succeeds in infecting hosts alone, while the other fails to do so. Second, in doubly inoculated hosts, the former genotype does not help or actively excludes the latter or both grow beyond the total parasite load the host can bear, as the conditions in Table 2.c.2 suggest (the associated inequality

involves trait values of both genotypes). This should not be seen as a classical "single infection" because two kinds of parasite genetic diversities would be missed: transient diversity at the within-host level (both genotypes are present before reaching the single infection fixed point, or the load threshold) and cryptic diversity at the between-host level (if the second genotype appears from deleterious mutations).

Because of lack of both interest (cryptic genotypes have no epidemiological impact) and data (transient within-host diversity is not easy to detect), this pattern is poorly documented. Yet the case of the *Cucumber mosaic virus* (CMV, *Bromoviridae* family) that infects tomato, zucchini squash and muskmelon is a possible illustration of latinfection. Because of deletion and recombination, this RNA virus generates defective RNAs which are not able to infect systemically (Hull, 2013).

Latinfection finally plays a major role in parasite evolution, since it corresponds to stable monomorphism, thus denoting purifying and stabilizing selection.

Suprainfection Suprainfection is an asymmetric pattern where one genotype successfully infects the host only in the presence of the other. It captures a diversity of microbial systems and evolutionary scenarios.

This pattern occurs if one of the two genotypes does not cause single infections, either because parasite load explodes or because it vanishes. In the first case, suprainfection occurs only if the second genotype slows down the growth of the first when they come about within the host. The second case is more familiar and compelling because if the first genotype fails to reproduce alone, then suprainfection only occurs if it benefits from the presence of the so-called self-sufficient genotype (Nee, 2000). Suprainfection differs from latinfection by the fact that the self-sufficient genotype facilitates or is exploited by the other genotype instead of outcompeting it.

The biology of virus-dependent entities (or subviral agents) is typically based on these two relationships between parasites and thus provides many examples of suprainfection. There are two kinds of virus-dependent entities: virus satellites (Francki, 1985) (including virophages (Krupovic & Cvirkaite-Krupovic, 2011)), which are unrelated to their 'helper' virus, and defective viral particles (Huang & Baltimore, 1970), which are replication and recombination by-products of a parent virus from which they derive. In both cases the helper/parent virus drives at least the replication of the virus-dependent entity, thus allowing it to infect the host as well.

For instance one can find tomato plants doubly infected by the begomovirus *Tomato leaf curl virus* (ToLCV) and its satellite (ToLCV-sat) but the latter is not required for ToLCV infectivity, while it depends on ToLCV for its replication and encapsidation (Briddon & Stanley, 2006). In 2001, defective dengue-virus type 1 (DENV-1) strain originated from a stop-codon mutation in the surface envelope (E) protein gene. This strain nevertheless achieved long-term transmission in nature thanks to the use of the functional proteins generated by regular DENV-1 strains (complementation) within both humans and *Aedes* mosquitoes (Aaskov *et al.*, 2006). Lastly, a well-known example of suprainfection is hepatitis delta virus (HDV), a defective RNA virus the virion coat of which is the one of hepatitis B virus (HBV), thus making HDV unable to infect a human if HBV is not already established or co-inoculated (Hughes *et al.*, 2011).

Suprainfection has strong implications in evolutionary biology. First, it supports the study of complementation in experimental evolution (Froissart *et al.*, 2004). Second, it raises the question of the origin of the dependence: is the dependent genotype the descendent of a defective mutant of the self-sufficient genotype or is it a fully functional mutant that has become parasitic of another genotype? Finally, one can consider the evolution of suprainfection towards ambinfection if, for instance, the self-sufficient genotype

undergoes deleterious mutations that are complemented by the other genotype.

Ambinfection Two parasite genotypes define an ambinfection when they can only infect together. This can result from an association between a genotype that does not grow when alone and another genotype that provokes explosive infections when alone: once together, the latter facilitates the reproduction of the former, while the former inhibits the growth of the latter. It can also derive from the association between two genotypes that provoke explosive infections when alone but inhibit each other when together so that their parasite loads become bounded. Finally, it can result from the cross-facilitation of two genotypes that cannot grow alone otherwise, that is obligate mutualism.

This last situation often occurs in multipartite plant viruses. These viruses, such as the bipartite *Tomato golden mosaic virus* (TGMV) (Hamilton *et al.*, 1983), have a fragmented genome; they encapsidate each fragment in a separate capsid and, typically, all genomic fragments need to be inoculated in the same host to produce a viable infection.

Plasmids causing bacteria to be virulent offer another example of ambinfection. For instance, the bacterial agent of bubonic plague, *Yersinia pestis,* relies on a set of 12 proteins encoded by a 70-kb plasmid (called pYV) to inhibit phagocytosis and hence proliferate inside lymph nodes in humans (Cornelis *et al.*, 1998). The competitive Lotka-Volterra framework is however less relevant in these cases because it relies on the physical independence between competing individuals and may not suit to intracellular molecules such as plasmids (nor hyperparasitism).

The fact that parasites causing ambinfections cannot be detected separately may lead researchers to consider such organisms as a single infectious agent and perhaps explains why this pattern is rarely found.

Perspectives

We argue that it is necessary to challenge the coinfection/superinfection dichotomy for several reasons. First, the inoculation outcome can also depend on the initial conditions and not only on the parasite traits (the difference between superinfection and priorinfection). Second, parasite load explosion in finite time does not fall in either of these two patterns nor 'in between'. Third, even if priorinfection and ultrainfection are added to the dichotomy, there remains an ambiguity between 'coinfection' with the two single infections (what we call coinfection) and 'coinfection' with one or no single infection (ambinfection and suprainfections) for instance. The typology we introduce is less ambiguous and manages to capture infection patterns of actual biological systems (see examples above) that are otherwise unclassifiable.

Our results stress that if only prevalence data are available, it may be difficult to distinguish between infection patterns because this requires knowledge about the within-host dynamics (or at least the outcome of cross-inoculations). As shown in Table 2.e.2 and formalised in appendix 2.e.2, priorinfection, ultrainfection and the two superinfections are epidemiologically equivalent as all the classes can be observed except for the doubly infected one. Leaving aside the epidemiology and observed prevalences, these patterns are shaped by different underlying mechanisms and may therefore have distinct evolutionary pathways.

Synergy between field or experimental work and theoretical analysis emerges as a necessity for studying multiple infections. Models inspire new hypotheses to test on natural systems, such as shifts of infection patterns (see e.g. Péréfarres *et al.* (2014)), and direct observations help to improve frameworks, as in the case of phage mutual exclusion (Delbrück, 1945), which does not fit in the super/coinfection dichotomy. In this sense, our within-host model could be tailored to a particular biological system by integrating specific mechanisms and explicit host immune response in order to better delineate the infection pattern conditions. A particular improvement would be to introduce frequency-dependence, which notably arises in non-enzymatic and consumable public productions, and therefore look for the new infection patterns the model generates but also the lost ones. Nonetheless we believe that the present typology of infection patterns for two genotypes is sufficient to describe most natural situations.

The outcome of a particular inoculation experiment could also be altered by environmental effects, host heterogeneity or stochasticity. Environmental effects and host heterogeneity can be addressed by splitting the host population into as many groups as needed for having constant environmental conditions and host homogeneity within these groups. Then the infection pattern has to be independently identified in each group to determine whether it is environment or host dependent. For example the above procedure could be used to determine whether the outcome of a given set of inoculation experiments depends on an environmental factor, such as temperature, or on host genotype. Stochasticity will not affect the nature of infection patterns, only the probability under which each may be observed. The frequency of each outcome could thus be used to draw a probability distribution of the infection patterns.

Our results may help to identify the infection pattern of a natural system but also to better model the associated epidemiological dynamics by choosing the right flows between compartments and write the appropriate equations according to the underlying within-host interactions. We acknowledge that this approach is still limited because it assumes there are at most two genotypes, while genotypic diversity is often higher (Juliano *et al.*, 2010). Fully determined models of within-host growth with multiple interactions are rare. First, because of obvious practical constraints (Sofonea *et al.*, 2015) but also because it is already possible to draw key qualitative conclusions, as attested by the

popularity of coinfection models. Note that these are still of interest and challenging in quantitative epidemiological modelling once differential host behaviour or heterogeneous transmission networks are taken into account, since the structure of such networks plays a major role on the epidemiological dynamics of coinfections (Hébert-Dufresne & Althouse, 2015). Furthermore, most evolutionary frameworks such as adaptive dynamics consider no more than two different genotypes, the resident and one mutant (Geritz *et al.*, 1998).

Multiple infections are highly polymorphic and polyspecific in nature, where we expect to find many more infection patterns than those listed here. A third genotype could for instance allow two genotypes that are otherwise in a priorinfection setting to coexist by inhibiting both of them. Our typology is helpful to start investigating higher rank infection patterns. Indeed, if we consider three genotypes, there are exactly four possible partitions of the set of genotypes ($\{1,2,3\}$ & $\{\emptyset\}$,$\{1\}$ & $\{2,3\}$,$\{1,2\}$ & $\{3\}$ and $\{1,3\}$ & $\{2\}$). Within each of these partitions, non empty sets of genotypes can be seen as "supergenotypes". The superinfection pattern associated to the supergenotype - genotype couple (or supergenotype alone in the case of the first partition) can then be determined as in our model, with the additional convention that for a supergenotype to be considered as having reached stationary infection, all genotypes that belong to it must have done so. The whole infection pattern is finally provided by the complementary analysis of these four supergenotype - genotype infection patterns plus the three infection patterns of the genotype-genotype couples. Therefore, higher rank infection patterns can be iteratively described by the infection patterns given for two genotypes only.

We have drawn a map of multiple infections along with a clear formalism, thus filling a gap left by previous frameworks and shedding new light on patterns that are observed empirically. Our infection patterns framework can easily be used to study the genetic diversity of microbiota and other commensal and/or mutualistic communities. Furthermore, if we consider non parasitic species and patches of habitat instead of hosts, our results can be extended to the field of meta-community ecology.

Appendix

This appendix provides all the technical background and mathematical analyses that support the formal infection pattern definition and counting (section 2.a), the investigated within-host model (sections 2.b, 2.c and 2.d) and the identification of the infection patterns it generates (section 2.e).

As we consider two parasite types we label 1 and 2, we often have to deal with label-dependent quantities or objects for which the general form can be advantageously given using dummy indices. Thus, unless stated otherwise, i represents 1 and 2 while k respectively represents 2 and 1, and holds for their corresponding bold labels. j and ℓ are instead used for all couples of $\{1,2\}^2$. Hence, unless stated otherwise, the quantifications $\forall (i,k) \in \{1,2\}^2, i \neq k$ and $\forall (j,\ell) \in \{1,2\}^2$ are most often implied.

2.a. Formal infection patterns

2.a.1. Host and inoculum classes

We define a host class as the set of parasite genotypes that steadily infect a host. With two parasite genotypes, there are four host classes: susceptible $\emptyset$ (uninfected host), singly infected by either genotype, $\{1\}$ and $\{2\}$, and doubly infected $\{1,2\}$, which we denote by $\mathbf{0}, \mathbf{1}, \mathbf{2}$ and $\mathbf{3}$ respectively.

We define an inoculum class as a set of parasite genotypes an infected host can simultaneously transmit. The inoculum classes associated to each infected host class are given in Table 2.a.1. Note that contrary to most studies on multiple infections we allow hosts to transmit any non-empty subset of the set of genotypes they are infected with, namely the doubly infected host can transmit genotype 1 alone, genotype 2 alone and both genotypes at the same time (which is inoculum class **3**).

infected host class	**1**	**2**	**3**
potential inoculum classes	**1**	**2**	**1**, **2**, **3**

Table 2.a.1. – Infected host classes and subsequent inoculum classes.

Note that for further formal completeness, we also consider the empty inoculum class **0** that denotes the absence of inoculum.

2.a.2. Mapping

Formally, an infection pattern is a discrete map that associates inoculation outcomes to all the couples of host and inoculum classes. Importantly, for the following mapping framework to apply, we need to assume that the inoculation outcome is unique (an inoculation can only result in one host class). We denote by $\mathfrak{n}_2$ the number of infection patterns for 2 genotypes. Let ϕ be a map from the domain $\mathcal{D}_\phi$ that contains all possible couples of host and inoculum classes to the codomain of all possible host classes $\mathcal{H}_\phi$ ($\phi : \mathcal{D}_\phi \to \mathcal{H}_\phi$). The domain $\mathcal{D}_\phi$ can be seen as the product set of a host class set $\mathcal{H}_\phi$ and an inoculum class set I_ϕ, that is $\mathcal{D}_\phi = \mathcal{H}_\phi \times I_\phi$ where $\times$ denotes the Cartesian product. The biological meaning of a map ϕ is such that $\forall (\boldsymbol{h}, \boldsymbol{p}) \in \mathcal{D}_\phi, \phi(\boldsymbol{h}, \boldsymbol{p})$ is the outcome host class of the inoculation of a host of class $\boldsymbol{h}$ by an inoculum of class $\boldsymbol{p}$. Importantly, ϕ may not be surjective.

If the domain and the codomain of each map are assumed to be as large as possible, then an upper bound for $\mathfrak{n}_2$ can easily be found. Indeed, the set of all classes $\mathcal{A} = \{0,1,2,3\}$ contains all host and inoculum classes so that for any map ϕ, $\mathcal{H}_\phi \subset \mathcal{A}$, $I_\phi \subset \mathcal{A}$ and $\mathcal{C}_\phi \subset \mathcal{A}$. Using classical combinatorial formula, we have

$$\mathfrak{n}_2 \leq \mathrm{Card}\left\{\phi : \mathcal{A} \times \mathcal{A} \to \mathcal{A}\right\} = (\mathrm{Card}\mathcal{A})^{\mathrm{Card}\mathcal{A}\cdot\mathrm{Card}\mathcal{A}} = 4^{16} = 4,294,967,296.$$

This calculation is certainly very rough but it nevertheless shows that listing all possible maps and checking their biological relevance as an infection pattern is not an option. Therefore, we need to define necessary conditions for a map $\phi : \mathcal{D}_\phi \to \mathcal{C}_\phi$ to be an infection pattern.

Before proceeding, we need to mention the infection pattern where no parasite genotype ever reaches a stable within-host steady state. As chronic infection then never occurs, this map ϕ_0 is degenerate (with $= \mathcal{H}_{\phi_0} = \{\mathbf{0}\}$, $I_{\phi_0} = \emptyset, \phi_0(\mathbf{0},\mathbf{0}) = \boldsymbol{h}$). Because one can see this case as the trivial *no* infection pattern, it should be counted as one, but it will be ignored in the rules and counting shown hereafter and only added in the final sum.

2.a.3. Infection pattern requirements

The following rules stem from commonplace biological conceptions of inoculation and infection processes.

Rule 1 (type coherence). The inoculation of a host cannot result in an outcome class containing genotypes that belong neither to the inoculated host class nor to the inoculum class. Formally, $\forall(\boldsymbol{h},\boldsymbol{p}) \in \mathcal{D}_\phi, \phi(\boldsymbol{h},\boldsymbol{p}) \subset \boldsymbol{h} \cup \boldsymbol{p}$. This may seem trivial (genotypes do not come out of nowhere) but note that it implies that we do not allow for within host mutation alone to modify the class a host belongs to.

Rule 2 (host class stability). The inoculation of a host with parasite genotypes it is already infected with results in no change in the host class. Formally, $\forall \boldsymbol{h} \in \mathcal{H}_\phi, \forall \boldsymbol{p} \subset \boldsymbol{h}, \phi(\boldsymbol{h},\boldsymbol{p}) = \boldsymbol{h}$. This is justified by the assumptions that inoculum sizes are at least one order of magnitude below parasite loads and that the dynamics within the inoculated host are at stable equilibrium (otherwise the host class would not be an argument of ϕ). As $\forall \boldsymbol{h} \in \mathcal{H}_\phi, \mathbf{0} \subset \boldsymbol{h}$, a remarkable consequence of this rule is that $\forall \boldsymbol{h} \in \mathcal{H}_\phi, \phi(\boldsymbol{h},\mathbf{0}) = \boldsymbol{h}$.

Rule 3 (infecting type insensitivity). The outcomes of inoculations with or without genotypes that are already infecting the host must be identical. Formally, $\forall(\boldsymbol{h},\boldsymbol{p}) \in \mathcal{D}_\phi, \phi(\boldsymbol{h},\boldsymbol{p}) = \phi(\boldsymbol{h},\boldsymbol{p} \setminus \boldsymbol{h})$. As in rule 2, adding few individuals to an already-established parasite genotype does not qualitatively change the system, but the introduction of a previously absent genotype does.

Rule 4 (epidemiological connectivity). There has to be at least one sequence of inoculation and/or recovery events initiated from the susceptible host class that leads to each infected host class. The recovery process only matters here if singly infected hosts can be generated only through the recovery of doubly infected hosts and not by an inoculation event. We assume that a doubly infected host can always become singly infected through recovery if the corresponding singly infected class belongs to the host class set. It is straightforward that, due to the uniqueness of inoculation outcomes, any inoculation/recovery sequence starting from the susceptible class can lead to any infected host class in one, two or three steps. Therefore, by considering all sequences, one can easily show that this rule is formally equivalent to

$\forall (\boldsymbol{i},\boldsymbol{k}) \in \{\mathbf{1},\mathbf{2}\}^2, \boldsymbol{i} \neq \boldsymbol{k}$,
for singly infected hosts: $\boldsymbol{i} \in \mathcal{H}_\phi \iff \big(\phi(\mathbf{0},\boldsymbol{i}) = \boldsymbol{i}\big) \vee \big(\phi(\mathbf{0},\mathbf{3}) = \boldsymbol{i}\big) \vee \big(\phi(\mathbf{0},\mathbf{3}) = \mathbf{3}\big)$
$\vee \Big(\big(\big(\phi(\mathbf{0},\boldsymbol{k}) = \boldsymbol{k}\big) \vee \big(\phi(\mathbf{0},\mathbf{3}) = \boldsymbol{k}\big)\big) \wedge \big(\big(\phi(\boldsymbol{k},\boldsymbol{i}) = \boldsymbol{i}\big) \vee \big(\phi(\boldsymbol{k},\boldsymbol{i}) = \mathbf{3}\big)\big)\Big)$,
for doubly infected hosts: $\mathbf{3} \in \mathcal{H}_\phi \iff \big(\phi(\mathbf{0},\mathbf{3}) = \mathbf{3}\big)$
$\vee \Big(\big(\big(\phi(\mathbf{0},\boldsymbol{i}) = \boldsymbol{i}\big) \vee \big(\phi(\mathbf{0},\mathbf{3}) = \boldsymbol{i}\big)\big) \wedge \big(\big(\phi(\boldsymbol{i},\boldsymbol{k}) = \mathbf{3}\big) \vee \big(\big(\phi(\boldsymbol{i},\boldsymbol{k}) = \boldsymbol{k}\big) \wedge \big(\phi(\boldsymbol{k},\boldsymbol{i}) = \mathbf{3}\big)\big)\big)\Big)$,

where $\wedge$ and $\vee$ stand for logical conjunction (and) and logical disjunction (or) respectively. A remarkable consequence of this rule is that there has to be at least one inoculum that induces infection in susceptible hosts. Formally, $\exists \boldsymbol{p} \in I_\phi : \phi(\mathbf{0},\boldsymbol{p}) \neq \mathbf{0}$. This makes sense because parasites are not vertically transmitted.

We call the number of determining images of a map ϕ the lowest number of images $\phi(\boldsymbol{a},\boldsymbol{b})$ that completely determine a map that satisfies all infection pattern requirements. Combining these four rules allows us to reduce the number of determining images to five, namely $\phi(\mathbf{0},\mathbf{1}), \phi(\mathbf{0},\mathbf{2}), \phi(\mathbf{0},\mathbf{3}), \phi(\mathbf{1},\mathbf{2}), \phi(\mathbf{2},\mathbf{1})$. According to rule 1, $\phi(\mathbf{0},\mathbf{1}) \in \{\mathbf{0},\mathbf{1}\}$, $\phi(\mathbf{0},\mathbf{2}) \in \{\mathbf{0},\mathbf{2}\}$ and $\phi(\mathbf{0},\mathbf{3}), \phi(\mathbf{1},\mathbf{2}), \phi(\mathbf{2},\mathbf{1}) \in \mathcal{A}$. Therefore, there are "only" $2 \cdot 2 \cdot 4^3 = 256$ different maps left to consider (including the trivial infection pattern discussed above).

2.a.4. Redundancies

The count based on the maps that follow all 4 rules suffers from two kinds of redundancy. The first one is due to unnecessary distinction of maps according to their epidemiological meaning. The previous calculation indeed assumes that $\mathcal{H}_\phi = I_\phi = \mathcal{A}$, that is all hosts and inoculum classes are possible, which may not be true for all biological settings. For example, if genotype 1 requires the presence of genotype 2 to infect, then $\phi(\mathbf{1},\mathbf{2})$ is not defined. Therefore, maps that only differ from other maps because of this particular value which has no epidemiological relevance should be discounted (see Sofonea *et al.* (2015) for more details about "epidemiological classes"). The second kind of redundancy is induced by the symmetry between genotypes. We say that maps ϕ and ϕ' are twins if one can build ϕ' from ϕ by swapping 1 and 2 in both $\mathcal{H}$ and I, and conversely. More precisely, let us define the swapping function $\chi : \{\mathbf{0},\mathbf{1},\mathbf{2},\mathbf{3}\} \to \{\mathbf{0},\mathbf{1},\mathbf{2},\mathbf{3}\}$ such that $\chi(\mathbf{0}) = \mathbf{0}$, $\chi(\mathbf{3}) = \mathbf{3}$, $\chi(\mathbf{1}) = \mathbf{2}$ and $\chi(\mathbf{2}) = \mathbf{1}$. Then, ϕ and ϕ' are twins if and only if $\forall (\boldsymbol{h},\boldsymbol{p}) \in \mathcal{D}_\phi = \mathcal{D}_{\phi'}, \phi(\boldsymbol{h},\boldsymbol{p}) = \chi\big(\phi'\big(\chi(\boldsymbol{h}),\chi(\boldsymbol{p})\big)\big)$. A map ϕ that is its own twin is said label-symmetric. Note that if a map is not label-symmetric, then there always exists a distinct twin map $\phi' \neq \phi$ (one can simply build it using the χ function). If ϕ is an infection pattern, then it is not relevant to count ϕ' as well as an infection pattern since their difference only lies in the contingency of the genotype labelling.

2.a.5. Constrained counting

In the following, we introduce a way of counting all maps that satisfies the infection pattern requirements and takes care of these redundancies. The first kind of redundancy is managed through partitioning according to the possible domains $\mathcal{D}_\phi$, while the second kind is avoided through the use of $\boldsymbol{i}$ and $\boldsymbol{k}$ indices, with $(\boldsymbol{i},\boldsymbol{k}) \in \{\mathbf{1},\mathbf{2}\}^2, \boldsymbol{i} \neq \boldsymbol{k}$.

As defined above, the domain $\mathcal{D}_\phi$ of a map ϕ is the product set of the possible host class and the possible inoculum sets $\mathcal{H}_\phi$ and I_ϕ. Because the contents of $\mathcal{H}_\phi$ completely determine the contents of I_ϕ and consequently $\mathcal{D}_\phi$ (Table 2.a.1), a partition is given by the possible host class sets $\mathcal{H}_\phi$, as shown in Table 2.a.2. Note that for the sake of generality, we also considered simultaneous inoculations to occur which explains why the inoculum set in the case where $\mathcal{H}_\phi = \{\mathbf{0},\boldsymbol{i},\boldsymbol{k}\}$ is $I_\phi = \{\boldsymbol{i},\boldsymbol{k},\mathbf{3}\}$ and not just $\{\boldsymbol{i},\boldsymbol{k}\}$ (this is only the consequence of relaxing the assumption of non-overlapping inoculations). In Table 2.a.2,

we list the determining images that are left in each case after eliminating those whose argument does not belong to $\mathcal{D}_\phi$ and those constrained by rule 4 to a single value.

host class set $\mathcal{H}_\phi$	$\{\mathbf{0},\boldsymbol{i}\}$	$\{\mathbf{0},\mathbf{3}\}$	$\{\mathbf{0},\boldsymbol{i},\mathbf{3}\}$	$\{\mathbf{0},\boldsymbol{i},\boldsymbol{k}\}$	$\{\mathbf{0},\boldsymbol{i},\boldsymbol{k},\mathbf{3}\}$
inoculum class set I_ϕ	$\{\boldsymbol{i}\}$	$\{\boldsymbol{i},\boldsymbol{k},\mathbf{3}\}$			
$\phi(\mathbf{0},\boldsymbol{i})$ set	$\{\boldsymbol{i}\}$	$\{\mathbf{0}\}$	$\{\mathbf{0},\boldsymbol{i}\}$	$\{\mathbf{0},\boldsymbol{i}\}$	$\{\mathbf{0},\boldsymbol{i}\}$
$\phi(\mathbf{0},\boldsymbol{k})$ set	$\varnothing$	$\{\mathbf{0}\}$	$\{\mathbf{0}\}$	$\{\mathbf{0},\boldsymbol{k}\}$	$\{\mathbf{0},\boldsymbol{k}\}$
$\phi(\mathbf{0},\mathbf{3})$ set		$\{\mathbf{3}\}$	$\{\mathbf{0},\boldsymbol{i},\mathbf{3}\}$	$\{\mathbf{0},\boldsymbol{i},\boldsymbol{k}\}$	$\{\mathbf{0},\boldsymbol{i},\boldsymbol{k},\mathbf{3}\}$
$\phi(\boldsymbol{i},\boldsymbol{k})$ set		$\varnothing$	$\{\mathbf{0},\boldsymbol{i},\mathbf{3}\}$	$\{\mathbf{0},\boldsymbol{i},\boldsymbol{k}\}$	$\{\mathbf{0},\boldsymbol{i},\boldsymbol{k},\mathbf{3}\}$
$\phi(\boldsymbol{k},\boldsymbol{i})$ set			$\varnothing$	$\{\mathbf{0},\boldsymbol{i},\boldsymbol{k}\}$	$\{\mathbf{0},\boldsymbol{i},\boldsymbol{k},\mathbf{3}\}$

Table 2.a.2. – Host class set partition and associated inoculum class set and determining image sets.

2.a.5.1. $\mathcal{H}_\phi = \{\mathbf{0},\boldsymbol{i}\}$ and $\mathcal{H}_\phi = \{\mathbf{0},\mathbf{3}\}$

If $\boldsymbol{i}$ or $\mathbf{3}$ is the only infected host class, their determining images are already determined so that there is only one infection pattern for each case.

2.a.5.2. $\mathcal{H}_\phi = \{\mathbf{0},\boldsymbol{i},\mathbf{3}\}$

If one single infection type (let us say $\boldsymbol{k}$) is impossible, then there are three free determining images, namely $\phi(\mathbf{0},\boldsymbol{i}) \in \{\mathbf{0},\boldsymbol{i}\}, \phi(\mathbf{0},\mathbf{3}) \in \{\mathbf{0},\boldsymbol{i},\mathbf{3}\}, \phi(\boldsymbol{i},\boldsymbol{k}) \in \{\mathbf{0},\boldsymbol{i},\mathbf{3}\}$. Table 2.a.3 explores all combinations for these free images and checks the infection pattern requirements.

$\phi(\mathbf{0},\boldsymbol{i})$	$\phi(\mathbf{0},\mathbf{3})$	$\phi(\boldsymbol{i},\boldsymbol{k})$	is ϕ an infection pattern?
$\mathbf{0}$	$\mathbf{0}$	$\mathbf{0},\boldsymbol{i},\mathbf{3}$	no
	$\boldsymbol{i}$	$\mathbf{0},\boldsymbol{i}$	no (double infected hosts cannot be generated)
		$\mathbf{3}$	yes
	$\mathbf{3}$	$\mathbf{0},\boldsymbol{i},\mathbf{3}$	yes
$\boldsymbol{i}$	$\mathbf{0}$	$\mathbf{0},\boldsymbol{i}$	no (double infected hosts cannot be generated)
		$\mathbf{3}$	yes
	$\boldsymbol{i}$	$\mathbf{0},\boldsymbol{i}$	no (double infected hosts cannot be generated)
		$\mathbf{3}$	yes
	$\mathbf{3}$	$\mathbf{0},\boldsymbol{i},\mathbf{3}$	yes

Table 2.a.3. – Free determining image combinations and satisfaction of the infection pattern requirements in the case of $\mathcal{H}_\phi = \{\mathbf{0},\boldsymbol{i},\mathbf{3}\}$.

It follows from Table 2.a.3 that there are 9 different infection patterns produced by this host class set.

2.a.5.3. $\mathcal{H}_\phi = \{\mathbf{0},\boldsymbol{i},\boldsymbol{k}\}$

If double infection is impossible, there are five free determining images, namely $\phi(\mathbf{0},\boldsymbol{i}) \in \{\mathbf{0},\boldsymbol{i}\}, \phi(\mathbf{0},\boldsymbol{k}) \in \{\mathbf{0},\boldsymbol{k}\}, \phi(\mathbf{0},\mathbf{3}) \in \{\mathbf{0},\boldsymbol{i},\boldsymbol{k}\}, \phi(\boldsymbol{i},\boldsymbol{k}) \in \{\mathbf{0},\boldsymbol{i},\boldsymbol{k}\}, \phi(\boldsymbol{k},\boldsymbol{i}) \in \{\mathbf{0},\boldsymbol{i},\boldsymbol{k}\}$.

Let us first count the number of label-symmetric infection patterns in this case. This implies that $\phi(\mathbf{0},\boldsymbol{i}) = \chi\big(\phi(\mathbf{0},\boldsymbol{k})\big), \phi(\boldsymbol{i},\boldsymbol{k}) = \chi\big(\phi(\boldsymbol{k},\boldsymbol{i})\big)$ and $\phi(\mathbf{0},\mathbf{3}) = \chi\big(\phi(\mathbf{0},\mathbf{3})\big)$. Moreover, from the last condition it comes that $\phi(\mathbf{0},\mathbf{3})$ has to be one of the two fixed points of the χ function which are $\mathbf{0}$ and $\mathbf{3}$, but since $\mathbf{3} \notin \mathcal{H}_\phi$, $\phi(\mathbf{0},\mathbf{3}) = \mathbf{0}$ necessarily. Table 2.a.4 explores

all possible combinations for these free determining images and checks the infection pattern requirements.

$\phi(\mathbf{0},\boldsymbol{i})$	$\Leftrightarrow \phi(\mathbf{0},\boldsymbol{k})$	$\phi(\boldsymbol{i},\boldsymbol{k})$	$\Leftrightarrow \phi(\boldsymbol{k},\boldsymbol{i})$	is ϕ an infection pattern?
$\mathbf{0}$	$\mathbf{0}$	$\mathbf{0},\boldsymbol{i},\boldsymbol{k}$	$\mathbf{0},\boldsymbol{k},\boldsymbol{i}$	no (susceptible hosts never get infected)
$\boldsymbol{i}$	$\boldsymbol{k}$	$\mathbf{0}$	$\mathbf{0}$	yes
		$\boldsymbol{i}$	$\boldsymbol{k}$	yes
		$\boldsymbol{k}$	$\boldsymbol{i}$	yes

Table 2.a.4. – Free determining image combinations and satisfaction of the infection pattern requirements for label-symmetric maps in the case of $\mathcal{H}_\phi = \{\mathbf{0},\boldsymbol{i},\boldsymbol{k}\}$.

Thus, there are 3 label-symmetric infection patterns for $\mathcal{H}_\phi = \{\mathbf{0},\boldsymbol{i},\boldsymbol{k}\}$.

With computational help, we listed all non label-symmetric maps sharing this host class set and found that 60 of them satisfy rule 4 (data not shown). Hence, there are 30 distinct non label-symmetric infections patterns for $\mathcal{H}_\phi = \{\mathbf{0},\boldsymbol{i},\boldsymbol{k}\}$.

2.a.5.4. $\mathcal{H}_\phi = \{\mathbf{0},\boldsymbol{i},\boldsymbol{k},\mathbf{3}\}$

If all host classes are possible, there are five free determining images, namely $\phi(\mathbf{0},\boldsymbol{i}) \in \{\mathbf{0},\boldsymbol{i}\}, \phi(\mathbf{0},\boldsymbol{k}) \in \{\mathbf{0},\boldsymbol{k}\}, \phi(\mathbf{0},\mathbf{3}) \in \{\mathbf{0},\boldsymbol{i},\boldsymbol{k},\mathbf{3}\}, \phi(\boldsymbol{i},\boldsymbol{k}) \in \{\mathbf{0},\boldsymbol{i},\boldsymbol{k},\mathbf{3}\}, \phi(\boldsymbol{k},\boldsymbol{i}) \in \{\mathbf{0},\boldsymbol{i},\boldsymbol{k},\mathbf{3}\}$.

Let us first count the number of label-symmetric infection patterns in this case. This implies that $\phi(\mathbf{0},\boldsymbol{i}) = \chi\big(\phi(\mathbf{0},\boldsymbol{k})\big), \phi(\boldsymbol{i},\boldsymbol{k}) = \chi\big(\phi(\boldsymbol{k},\boldsymbol{i})\big)$ and $\phi(\mathbf{0},\mathbf{3}) = \chi\big(\phi(\mathbf{0},\mathbf{3})\big)$. Moreover, the last condition implies that $\phi(\mathbf{0},\mathbf{3})$ has to be one of the two fixed points of the χ function, which are $\mathbf{0}$ and $\mathbf{3}$.

Table 2.a.5 explores all possible combinations for these free determining images and checks the infection pattern requirements.

$\phi(\mathbf{0},\boldsymbol{i})$	$\Leftrightarrow \phi(\mathbf{0},\boldsymbol{k})$	$\phi(\mathbf{0},\mathbf{3})$	$\phi(\boldsymbol{i},\boldsymbol{k})$	$\Leftrightarrow \phi(\boldsymbol{k},\boldsymbol{i})$	is ϕ an infection pattern?
$\mathbf{0}$	$\mathbf{0}$	$\mathbf{0}$	$\mathbf{0},\boldsymbol{i},\boldsymbol{k},\mathbf{3}$	$\mathbf{0},\boldsymbol{k},\boldsymbol{i},\mathbf{3}$	no (susceptible hosts never get infected)
		$\mathbf{3}$	$\mathbf{0},\boldsymbol{i},\boldsymbol{k},\mathbf{3}$	$\mathbf{0},\boldsymbol{k},\boldsymbol{i},\mathbf{3}$	yes
$\boldsymbol{i}$	$\boldsymbol{k}$	$\mathbf{0}$	$\mathbf{0},\boldsymbol{i},\boldsymbol{k}$	$\mathbf{0},\boldsymbol{k},\boldsymbol{i}$	no (double infected hosts cannot be generated)
			$\mathbf{3}$	$\mathbf{3}$	yes
		$\mathbf{3}$	$\mathbf{0},\boldsymbol{i},\boldsymbol{k},\mathbf{3}$	$\mathbf{0},\boldsymbol{k},\boldsymbol{i},\mathbf{3}$	yes

Table 2.a.5. – Free determining image combinations and satisfaction of the infection pattern requirements for label-symmetric maps in the case of $\mathcal{H}_\phi = \{\mathbf{0},\boldsymbol{i},\boldsymbol{k},\mathbf{3}\}$.

Thus, there are 9 label-symmetric infection patterns for $\mathcal{H}_\phi = \{\mathbf{0},\boldsymbol{i},\boldsymbol{k},\mathbf{3}\}$.

With computational help, we listed all non label-symmetric maps sharing this host class set and found that 120 of them satisfy rule 4 (data not shown). Hence, there are 60 distinct non label-symmetric infections patterns for $\mathcal{H}_\phi = \{\mathbf{0},\boldsymbol{i},\boldsymbol{k},\mathbf{3}\}$.

2.a.5.5. Counting summary and total

Table 2.a.6 sums up all the infection patterns we found for each host class set.

$\mathcal{H}_\phi$	$\{\mathbf{0}\}$	$\{\mathbf{0},\boldsymbol{i}\}$	$\{\mathbf{0},\mathbf{3}\}$	$\{\mathbf{0},\boldsymbol{i},\mathbf{3}\}$	$\{\mathbf{0},\boldsymbol{i},\boldsymbol{k}\}$	$\{\mathbf{0},\boldsymbol{i},\boldsymbol{k},\mathbf{3}\}$
label-symmetric	1	0	1	0	3	9
non label-symmetric	0	1	0	9	30	60
total number of infection patterns	**114**					

Table 2.a.6. – Summary of the infection pattern counting.

To conclude, we find that, following our definition and related assumptions presented above, there are exactly 114 different infection patterns, all represented below (Figure 2.a.1).

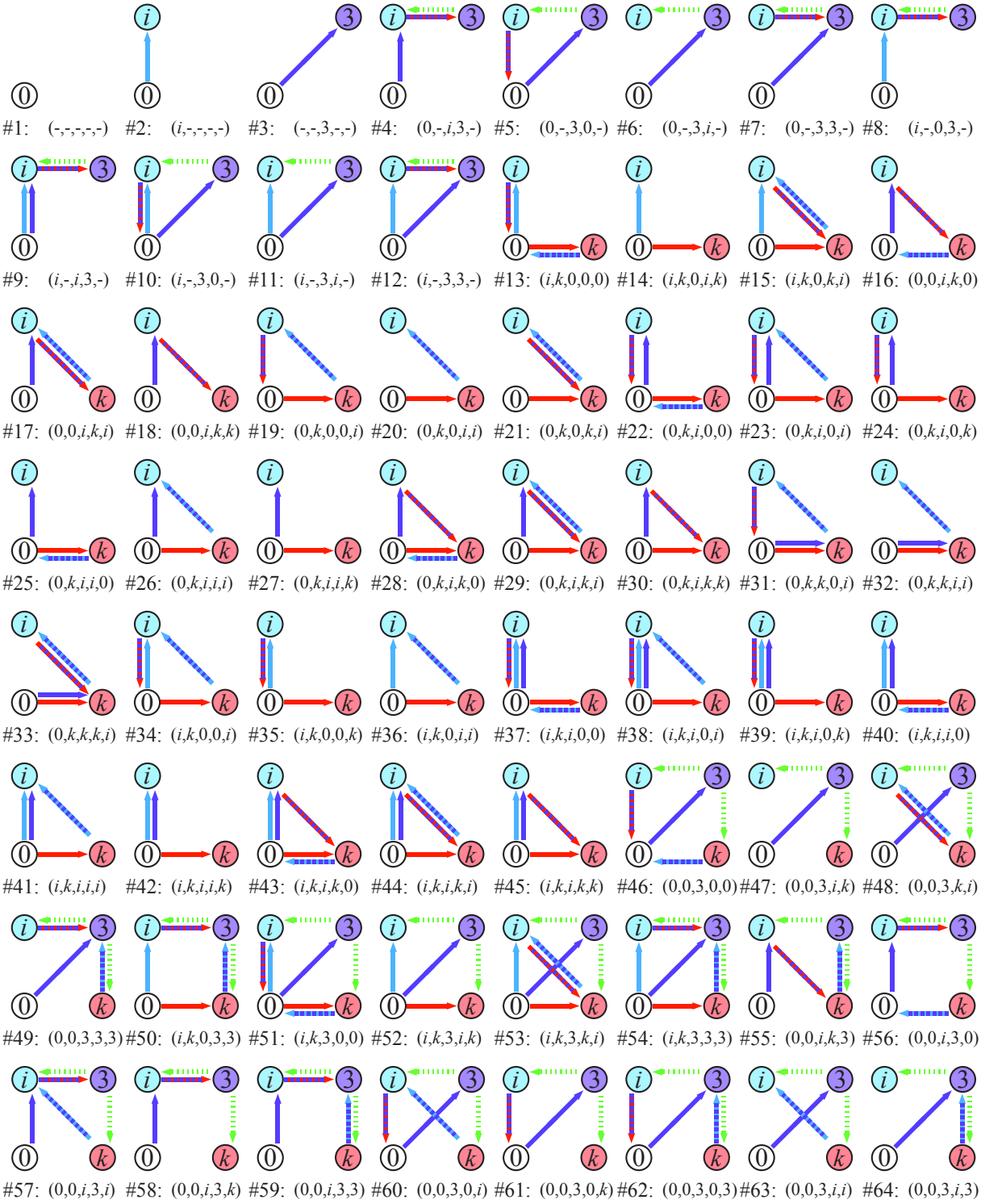

(panel 1/2 ; see panel 2/2 and legend on next page)

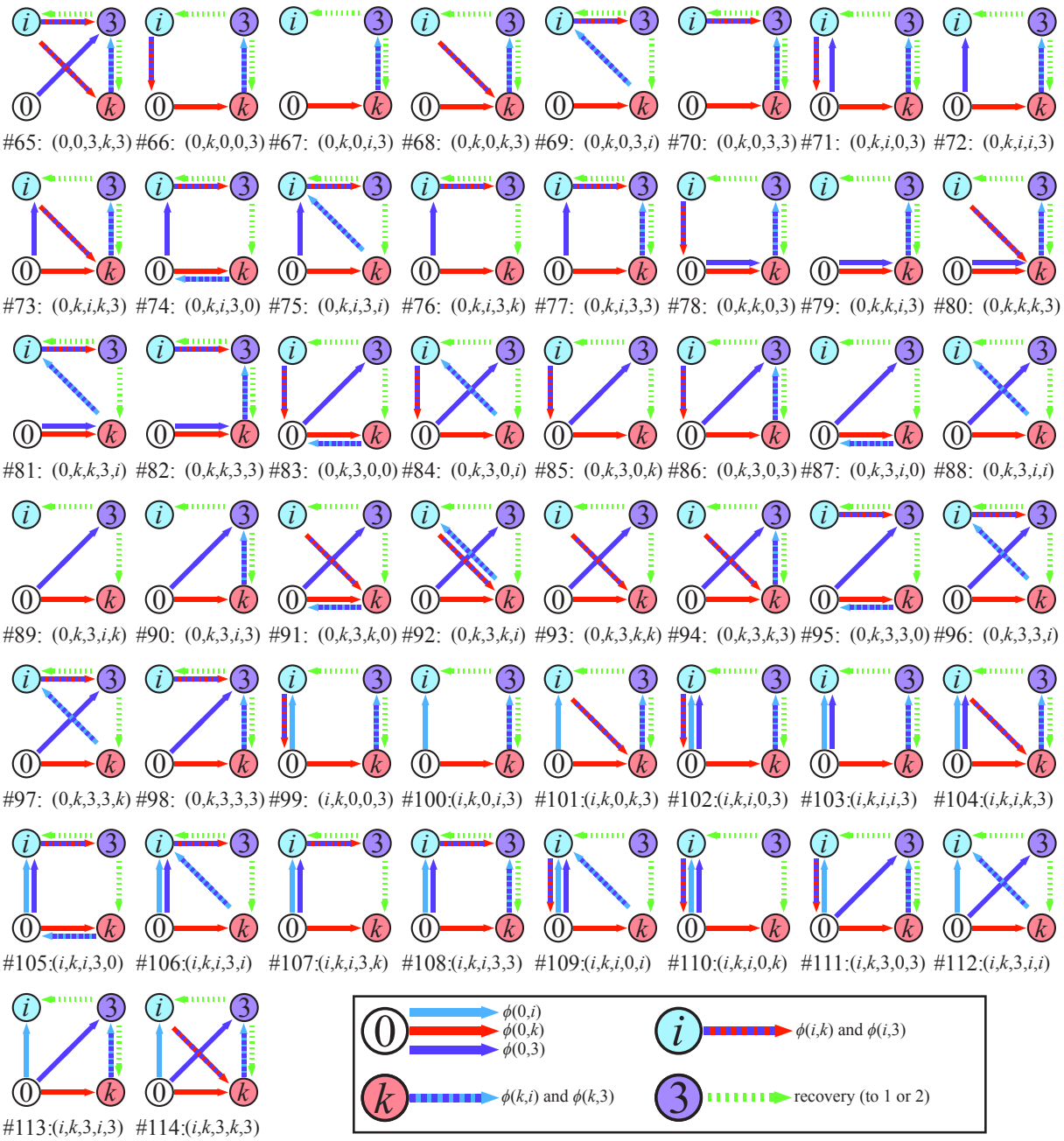

(panel 2/2)

Figure 2.a.1. – Exhaustive list of infection patterns for two parasite genotypes (according to requirements given in 2.a.3).

The quintuple below each infection pattern graph gives the associated values of $\big(\phi(\mathbf{0},\boldsymbol{i}),\phi(\mathbf{0},\boldsymbol{k}),\phi(\mathbf{0},\mathbf{3}),\phi(\boldsymbol{i},\boldsymbol{k}),\phi(\boldsymbol{k},\boldsymbol{i})\big)$, and is denoted by – if undefined. Circled labels represent host classes and arrows transitions between host classes through inoculation or recovery. Full blue arrows represent inocula of genotype $\boldsymbol{i}$ alone, full red arrows represent inocula of genotype $\boldsymbol{k}$ alone, full purple arrows represent inocula of both genotypes, blue and purple dashed arrows represent inocula of genotype $\boldsymbol{i}$ and possibly genotype $\boldsymbol{k}$, and red and purple dashed arrows represent inocula of genotype $\boldsymbol{k}$ and possibly genotype $\boldsymbol{i}$. Green dashed arrows represent recovery from the doubly infected host class to singly infected host classes. For the sake of clarity, recovery arrows from infected host classes to the susceptible host class and looping inoculation arrows (when $\phi(\boldsymbol{h},\boldsymbol{p})=\boldsymbol{h}$) are not shown.

2.b. The within-host dynamics

2.b.1. Vectorial formulation

We recall the equations of the within-host dynamics for the focal genotype i:

$$\begin{cases} \frac{\mathrm{d}X_i}{\mathrm{d}t} = \left(\varrho_i + \eta_{i,i}X_i + \eta_{i,k}X_k + \gamma_{i,i}Y_i + \gamma_{i,k}Y_k - \sigma_{i,i}Z_i - \sigma_{i,k}Z_k\right)X_i \quad , \\ \frac{\mathrm{d}Y_i}{\mathrm{d}t} = \upsilon(u_iX_i - Y_i), \\ \frac{\mathrm{d}Z_i}{\mathrm{d}t} = \upsilon(v_iX_i - Z_i). \end{cases} \tag{2.3.1}$$

Let us denote by $\mathcal{W} \coloneqq \left\{\mathbf{w} \in \mathbb{R}^6\right\}$ the space where all possible variable vectors lie, hereafter referred to as the "double inoculation space" (DIS). Any variable vector in the DIS can also be seen as a concatenated vector $\mathbf{w} = \begin{bmatrix} \mathbf{w}_i & \mathbf{w}_k \end{bmatrix}$, where $\mathbf{w}_i$ is the genotype i restricted variable vector of the form $\mathbf{w}_i = \begin{bmatrix} X_i & Y_i & Z_i \end{bmatrix}$.

The single inoculation case is characterised by the absence of genotype k, that is $X_k = Y_k = Z_k = 0$ for all times $t \in \mathbb{R}_+$. Therefore the variable vector is restrained to the following subspace of the DIS, $\mathcal{W}_i \coloneqq \left\{\mathbf{w} \in \mathcal{W} : X_k = Y_k = Z_k = 0\right\}$, which we call the "single inoculation space i" (SIS_i), $\mathcal{W}_i \subsetneq \mathcal{W}$.

For the sake of concision, r_i hereafter denotes the instantaneous growth rate defined such that $f_{\mathrm{x},i}(\mathbf{w}) = r_i(\mathbf{w})X_i$, that is $r_i(\mathbf{w}) \coloneqq \varrho_i + \sum\limits_{j\in\{1,2\}} \left(\eta_{i,j}X_j + \gamma_{i,j}Y_j - \sigma_{i,j}Z_j\right)$. Moreover, defining concatenated functions as $\mathbf{f}_i \coloneqq \begin{bmatrix} f_{\mathrm{x},i} & f_{\mathrm{y},i} & f_{\mathrm{z},i} \end{bmatrix}^{\mathbf{T}}$ and $\mathbf{f} \coloneqq \begin{bmatrix} \mathbf{f}_i & \mathbf{f}_k \end{bmatrix}^{\mathbf{T}}$, system (2.3.1) can be written under the vectorial form as $\forall t \in \mathbb{R}_+$,

$$\frac{\mathrm{d}\mathbf{w}^{\mathbf{T}}}{\mathrm{d}t}(t) = \mathbf{f}(\mathbf{w}(t)). \tag{2.b.1}$$

We call solution of (2.3.1) the set of values taken by the variables $X_1, Y_1, Z_1, X_2, Y_2, Z_2$ through time, from $t = 0$ to a potentially infinite $T > 0$. Except on a set of measure zero, such a solution always exists and is unique for a given initial condition. Consequently, for any initial condition $\mathbf{a} \in \mathcal{W}$, $\mathbf{w}^{[\mathbf{a}]}$ denotes the solution of (2.3.1) that started in $\mathbf{a}$. Note that in most biologically relevant parameter sets, the solution is defined for all $T > 0$. Nonetheless, for the sake of completeness, we also address cases where parasite loads explode (see section 2.d).

2.b.2. Jacobian matrices

The Jacobian matrix associated to (2.3.1) in single infection, denoted by $\mathbf{J}_i$, is only evaluated in $\mathcal{W}_i$ and is equal to

$$\begin{aligned} &\forall \mathbf{w} \in \mathcal{W}_i, \\ &\quad \mathbf{J}_i(\mathbf{w}) = \frac{\partial \mathbf{f}_i}{\partial \mathbf{w}_i}(\mathbf{w}), \\ &\qquad = \begin{bmatrix} \varrho_i + \gamma_{i,i}Y_i - \sigma_{i,i}Z_i + 2\eta_{i,i}X_i & \gamma_{i,i}X_i & -\sigma_iX_i \\ \upsilon u_i & -\upsilon & 0 \\ \upsilon v_i & 0 & -\upsilon \end{bmatrix}, \end{aligned} \tag{2.b.2}$$

while its double infection counterpart, denoted by $\mathbf{J}_3$, is evaluated in $\mathcal{W}$ and is equal to

$$\forall \mathbf{w} \in \mathcal{W}, \mathbf{J}_3(\mathbf{w}) = \frac{\partial \mathbf{f}}{\partial \mathbf{w}}(\mathbf{w})$$

$$= \begin{bmatrix} r_i(\mathbf{w}) + \eta_{i,i} X_i & \gamma_{i,i} X_i & -\sigma_{i,i} X_i & \eta_{i,k} X_i & \gamma_{i,k} X_i & -\sigma_{i,k} X_i \\ v u_i & -v & 0 & 0 & 0 & 0 \\ v v_i & 0 & -v & 0 & 0 & 0 \\ \eta_{k,i} X_k & \gamma_{k,i} X_k & -\sigma_{k,i} X_k & r_k(\mathbf{w}) + \eta_{k,k} X_k & \gamma_{k,k} X_k & -\sigma_{k,k} X_k \\ 0 & 0 & 0 & v u_k & -v & 0 \\ 0 & 0 & 0 & v v_k & 0 & -v \end{bmatrix}. \quad (2.b.3)$$

All the notations related to the within-host dynamics and their vectorial formalism are given in Table 2.b.1.

2.b.3. Notation table

symbol	set or value	meaning
	time-dependent variables	
X_i	$\in \mathcal{A}(\mathbb{R}_+, \mathbb{R})$	parasite load
Y_i	$\in \mathcal{A}(\mathbb{R}_+, \mathbb{R})$	public goods concentration
Z_i	$\in \mathcal{A}(\mathbb{R}_+, \mathbb{R})$	spite concentration
	constant parameters	
ϱ_i	$\in \mathbb{R}^\star$	basic growth rate
u_i	$\in \mathbb{R}_+^\star$	public goods production rate
v_i	$\in \mathbb{R}_+^\star$	spite production rate
$\eta_{j,\ell}$	$\in \mathbb{R}^\star$	parasite-load dependent effect
$\gamma_{j,\ell}$	$\in \mathbb{R}_+^\star$	public goods effect
$\sigma_{j,\ell}$	$\in \mathbb{R}_+^\star$	spite effect
υ	$\in \mathbb{R}_+^\star$	public production standard clearing rate
	vectorial notations	
$\mathbf{w}_i$	$= \left[\begin{array}{ccc} X_i & Y_i & Z_i \end{array}\right]$	genotype restricted variable vector
$\mathbf{w}$	$= \left[\begin{array}{cccccc} X_1 & Y_1 & Z_1 & X_2 & Y_2 & Z_2 \end{array}\right]$	variable vector
$\mathcal{W}_i$	$= \{\mathbf{w} \in \mathcal{W} : \mathbf{w}_k = \mathbf{0}_3\}$	single inoculation space i (SIS$_i$)
$\mathcal{W}$	$= \{\mathbf{w} \in \mathbb{R}^6\}$	double inoculation space (DIS)
	system dynamics notations	
$\mathbf{w}^{[\mathbf{a}]}$	$\in \mathcal{A}(\mathbb{R}_+, \mathcal{W}) : \mathbf{w}(0) = \mathbf{a}$	within-host dynamics solution for initial condition $\mathbf{a}$
$f_{\mathrm{x},i}, f_{\mathrm{y},i}, f_{\mathrm{z},i}$	$\in \mathcal{A}(\mathcal{W}, \mathbb{R})$	within-host dynamics functions
r_i	$= \varrho_i + \sum_{j\in\{1,2\}} \eta_{i,j} X_j + \gamma_{i,j} Y_j - \sigma_{i,j} Z_j$	Malthusian growth rate
$\mathbf{f}_i$	$= \left[\begin{array}{ccc} f_{\mathrm{x},i} & f_{\mathrm{y},i} & f_{\mathrm{z},i} \end{array}\right]^{\mathbf{T}} \in \mathcal{A}(\mathcal{W}, \mathbb{R}^3)$	genotype restricted within-host dynamics function vector
$\mathbf{f}$	$= \left[\begin{array}{cc} \mathbf{f}_i & \mathbf{f}_k \end{array}\right]^{\mathbf{T}} \in \mathcal{A}(\mathcal{W}, \mathbb{R}^6)$	within-host dynamics function vector
$\mathbf{J}_i$	$= \frac{\partial \mathbf{f}_i}{\partial \mathbf{w}_i} \in \mathcal{A}(\mathcal{W}, \mathfrak{M}_3(\mathbb{R}))$	single infection Jacobian matrix
$\mathbf{J}_3$	$= \frac{\partial \mathbf{f}}{\partial \mathbf{w}} \in \mathcal{A}(\mathcal{W}, \mathfrak{M}_6(\mathbb{R}))$	double infection Jacobian matrix

Table 2.b.1. – Within-host dynamics notations.
$\mathbb{R}$ denotes the set of real numbers $(-\infty, +\infty)$ while $._+$, $._-$ and $.^\star$ and their combination denote restriction to non-negative, non-positive and non-zero numbers respectively. Note that $\mathcal{F}$ denotes the set of functions over the argument sets.

2.c. Fixed point analysis

Although we could not prove it analytically for all parameter sets, the within-host dynamics of our model seems not to generate behaviours such as sustained oscillations or chaos. All simulations done so far show either asymptotic convergence to fixed point or finite time explosions (see next section). Because they govern the long-term behaviour of the system, the analysis of these fixed points is thus the unavoidable step to investigate the within-host outcomes.

2.c.1. Determination

The set of fixed points of (2.3.1) is the intersection set of the nullclines, or zero-growth isoclines, that is the parts of the space over which a variable is stationary (Simonyi & Kaszás, 1968)). In our within-host model, respectively these are

$$\begin{cases} \mathcal{X}_i & := \{\mathbf{w} \in \mathcal{W} : f_{\mathrm{x},i}(\mathbf{w}) = 0\}, \\ \mathcal{Y}_i & := \{\mathbf{w} \in \mathcal{W} : f_{\mathrm{y},i}(\mathbf{w}) = 0\}, \\ \mathcal{Z}_i & := \{\mathbf{w} \in \mathcal{W} : f_{\mathrm{z},i}(\mathbf{w}) = 0\}. \end{cases} \tag{2.c.1}$$

It is straightforward that the public production nullclines can be expressed as

$$\begin{cases} \mathcal{Y}_i : & (Y_i = u_i X_i), \\ \mathcal{Z}_i : & (Z_i = v_i X_i). \end{cases} \tag{2.c.2}$$

Then,

$$\mathbf{w}_i \in \mathcal{Y}_i \cap \mathcal{Z}_i \Longleftrightarrow \mathbf{w}_i = X_i \mathbf{c}_i, \tag{2.c.3}$$

where $\mathbf{c}_i := \begin{bmatrix} 1 & u_i & v_i \end{bmatrix}$ is the direction vector of the the $\mathcal{Y}_i \cap \mathcal{Z}_i$ space.

Since $f_{\mathrm{x},i}(\mathbf{w}) = r_i(\mathbf{w}) X_i$, the parasite load nullcline $\mathcal{X}_i$ can be partitioned into two subsets: $\mathcal{X}_i = \mathcal{X}_i^\circ \cup \mathcal{X}_i^\star$, with $\mathcal{X}_i^\circ \cap \mathcal{X}_i^\star = \emptyset$, where they respectively correspond to the absence, $\mathcal{X}_i^\circ : (X_i = 0)$, and presence,

$$\mathcal{X}_i^\star : \left(X_i = \frac{-1}{\eta_{i,i}} \left(\varrho_i + \gamma_{i,i} Y_i + \gamma_{i,k} Y_k - \sigma_{i,i} Z_i - \sigma_{i,k} Z_k + \eta_{i,k} X_k \right) \neq 0 \right), \tag{2.c.4}$$

of genotype i. Note that $\mathcal{W}_i = \mathcal{X}_k^\circ \cap \mathcal{Y}_k \cap \mathcal{Z}_k$.

Because of (2.c.3), the stationary parasite loads constrain the stationary values of public productions. Owing to the partition of the parasite load nullcline, the set of all fixed points is thus

$$\begin{aligned} \widehat{\mathcal{W}} &:= \mathcal{X}_i \cap \mathcal{Y}_i \cap \mathcal{Z}_i \cap \mathcal{X}_k \cap \mathcal{Y}_k \cap \mathcal{Z}_k, \\ &= \left(\mathcal{X}_i^\circ \cup \mathcal{X}_i^\star\right) \cap \left(\mathcal{X}_k^\circ \cup \mathcal{X}_k^\star\right) \cap (\mathcal{Y}_i \cap \mathcal{Z}_i \cap \mathcal{Y}_k \cap \mathcal{Z}_k), \\ &= \left(\left(\mathcal{X}_i^\circ \cap \mathcal{X}_k^\circ\right) \cup \left(\mathcal{X}_i^\star \cap \mathcal{X}_k^\circ\right) \cup \left(\mathcal{X}_i^\circ \cap \mathcal{X}_k^\star\right) \cup \left(\mathcal{X}_i^\star \cap \mathcal{X}_k^\star\right)\right) \cap (\mathcal{Y}_i \cap \mathcal{Z}_i \cap \mathcal{Y}_k \cap \mathcal{Z}_k). \end{aligned}$$

It is straightforward that there are exactly four different fixed points.

The first one is simply the origin of $\mathbb{R}^6$ and corresponds to the absence of infection. We denote it by $\widehat{\mathbf{w}}_0$ and call it the "uninfected fixed point" (UFP),

$$\widehat{\mathbf{w}}_0 = \mathbf{0}_6.$$

The next two correspond to the case where only one genotype persists, while the other

vanishes. The "singly infected fixed point i" (SIFP$_i$), denoted by $\widehat{\mathbf{w}}_i$, is thus the fixed point for which genotype i infects alone. It is easy to show that

$$\widehat{\mathbf{w}}_i = \begin{bmatrix} x_i^\circ \mathbf{c}_i & \mathbf{0}_3 \end{bmatrix}, x_i^\circ := \frac{-\varrho_i}{\eta_{i,i} + \gamma_{i,i} u_i - \sigma_{i,i} v_i} \in \mathbb{R}^\star, \tag{2.c.5}$$

where x_i° denotes the non-zero stationary parasite load of the SIFP$_i$.

The last fixed point corresponds to the stationary coexistence of both parasite genotypes within the host, so we call it the "doubly infected fixed point" (DIFP). Let us denote by x_i the parasite load of genotype i associated to this fixed point. Finding a non-zero solution $(x_i, x_k) \neq (0,0)$ comes down to solving the following linear system

$$\begin{cases} r_1(\widehat{\mathbf{w}}) = 0, \\ r_2(\widehat{\mathbf{w}}) = 0, \end{cases} \overset{(2.c.2)}{\iff} \begin{cases} \varrho_1 + \gamma_{1,1} u_1 x_1 + \gamma_{1,2} u_2 x_2 - \sigma_{1,1} v_1 x_1 - \sigma_{1,2} v_2 x_2 + \eta_{1,1} x_1 + \eta_{1,2} x_2 = 0, \\ \varrho_2 + \gamma_{2,1} u_1 x_1 + \gamma_{2,2} u_2 x_2 - \sigma_{2,1} v_1 x_1 - \sigma_{2,2} v_2 x_2 + \eta_{2,1} x_1 + \eta_{2,2} x_2 = 0, \end{cases}$$

$$\iff \mathbf{M} \begin{bmatrix} x_1 \\ x_2 \end{bmatrix} = - \begin{bmatrix} \varrho_1 \\ \varrho_2 \end{bmatrix}, \tag{2.c.6}$$

where $\mathbf{M} = \left(m_{j,\ell}\right)_{(j,\ell)\in\{1,2\}^2}$. We call $\mathbf{M}$ the stationary interaction matrix. Its elements, the stationary interaction effects, are defined as

$$m_{j,\ell} := \eta_{j,\ell} + \gamma_{j,\ell} u_\ell - \sigma_{j,\ell} v_\ell. \tag{2.c.7}$$

More precisely, $m_{j,\ell}$ is the sum of the interaction effects over genotype j from genotype ℓ, where the parasite loads of genotypes j and ℓ (j might be equal to ℓ) are at their non-zero stationary values.

The linear system (2.c.6) has a unique solution almost everywhere over the parameter space and it is given by

$$\begin{bmatrix} x_1 \\ x_2 \end{bmatrix} = -\mathbf{M}^{-1}. \begin{bmatrix} \varrho_1 \\ \varrho_2 \end{bmatrix} = \frac{1}{m_{1,1} m_{2,2} - m_{1,2} m_{2,1}} \begin{bmatrix} m_{1,2}\varrho_2 - m_{2,2}\varrho_1 \\ m_{2,1}\varrho_1 - m_{1,1}\varrho_2 \end{bmatrix}.$$

The DIFP is therefore the following vector

$$\widehat{\mathbf{w}}_3 = \begin{bmatrix} x_i \mathbf{c}_i & x_k \mathbf{c}_k \end{bmatrix}, x_i = \frac{m_{i,k}\varrho_k - m_{k,k}\varrho_i}{m_{i,i} m_{k,k} - m_{i,k} m_{k,i}} \in \mathbb{R}^\star. \tag{2.c.8}$$

Finally, note that the $\widehat{\mathbf{w}}_0$ and $\widehat{\mathbf{w}}_i$ belong to $\mathcal{W}_i'$ while $\widehat{\mathbf{w}}_j$ and $\widehat{\mathbf{w}}_3$ do not.

As a conclusion, the stationary values of the parasite loads in single infection, x_i°, and in double infection, x_i, are governed by the elements of the stationary interaction matrix $\mathbf{M} = \left(m_{j,\ell}\right)_{(j,\ell)\in\{1,2\}^2}$.

2.c.2. Feasibility

Hereafter, the comparison symbols $\geq$ and $>$ are the element-wise versions of $\geq$ and $>$, that is for instance $\mathbf{A} = \left(a_{j,\ell}\right) \geq b \iff \forall (j,\ell), a_{j,\ell} \geq b$. Due to the biological meaning of its components, a variable vector $\mathbf{w}$ is said to be "feasible" if none of its elements is negative, that is $\mathbf{w} \geq 0$. The subset of feasible variable vectors is denoted by $\mathcal{W}_+ = \left\{\mathbf{w} \in \mathcal{W} : \mathbf{w} \geq 0\right\}$.

Let us show that $\mathcal{W}_+$ is positively invariant, that is $\mathbf{a} \in \mathcal{W}_+ \Longrightarrow \forall t \in \mathbb{R}_+, \mathbf{w}^{[\mathbf{a}]}(t) \in \mathcal{W}_+$. From $\frac{\mathrm{d}X_i}{\mathrm{d}t} = r_i X_i$, it comes that

$$X_i(t) = X_i(0)\, e^{\int_0^t r_i X_i(\tau)\mathrm{d}\tau},$$

so $X_i(0) \geq 0 \Longrightarrow \forall t \in \mathbb{R}_+, X_i(t) \geq 0$.

Applying this result to $\frac{\mathrm{d}Y_i}{\mathrm{d}t} = v(u_i X_i - Y_i)$, we get the following inequality

$$\frac{\mathrm{d}Y_i}{\mathrm{d}t} \geq -vY_i.$$

Let $\underline{Y_i}$ be the solution of $\begin{cases} \frac{\mathrm{d}\underline{Y_i}}{\mathrm{d}t} = -v\underline{Y_i} \\ \underline{Y_i}(0) = Y_i(0) \geq 0 \end{cases}$, that is $\underline{Y_i}(t) = Y_i(0)e^{-vt} \geq 0$. Thus, $\frac{\mathrm{d}Y_i}{\mathrm{d}t} \geq \frac{\mathrm{d}\underline{Y_i}}{\mathrm{d}t}$ implies $Y_i(t) \geq \underline{Y_i}(t) \geq 0, \forall t \in \mathbb{R}_+$. The same holds for Z_i. By symmetry with j, we conclude that $\mathcal{W}_+$ is positively invariant.

Using the same reasoning, it is straightforward that $\mathcal{W}_+ \cap \mathcal{W}_i'$ is positively invariant as well. As a consequence, the within-host variables always have feasible values if they start from a feasible value and we ignore solutions that do not lie in $\mathcal{W}_+$.

For the sake of simplicity and biological relevance, we do not consider subsets of the parameter space with measure zero, meaning that x_i° and x_i cannot be equal to 0. Since v represents a clearing rate and u_i and v_i production rates, these parameters are positive. We therefore have the following feasibility condition on the non trivial fixed points owing to the fact that $\mathbf{c}_i \succ 0$,

$$\begin{aligned} (\widehat{\mathbf{w}}_i \geq 0) &\iff x_i^\circ > 0, \\ &\iff \operatorname{sgn}(\rho_i) \neq \operatorname{sgn}(m_{i,i}), \end{aligned} \tag{2.c.9}$$

and

$$\begin{aligned} \widehat{\mathbf{w}}_3 \geq 0 &\iff (x_i > 0) \wedge (x_k > 0), \\ &\iff \operatorname{sgn}(m_{i,i}m_{k,k} - m_{i,k}m_{k,i}) = \operatorname{sgn}(m_{i,k}\rho_k - m_{k,k}\rho_i) = \operatorname{sgn}(m_{k,i}\rho_i - m_{i,i}\rho_k), \end{aligned} \tag{2.c.10}$$

where sgn is the sign function ($\operatorname{sgn}(x) := \frac{x}{|x|}, \forall x \neq 0$ and $\operatorname{sgn}(0) := 0$) and $\wedge$ is the logical conjunction (and). Condition (2.c.9) states that in order for one genotype to show a feasible stationary parasite load in single infection, either reproduction can be achieved without any public good ($\rho_i > 0$) and is restrained by some density-dependence effects ($m_{i,i} < 0$), or reproduction is public-good dependent ($\rho_i < 0, m_{i,i} > 0$). Condition (2.c.10) has no straightforward interpretation.

2.c.3. Local asymptotic stability

A fixed point $\widehat{\mathbf{w}}$ is said to be locally asymptotically stable (LAS, but simply 'stable' in the main text) in a given space Ω if any trajectory $\mathbf{w}^{[\mathbf{a}]}(t)$ on Ω, with $\mathbf{a}$ close enough to $\widehat{\mathbf{w}}$, remains close to $\widehat{\mathbf{w}}$ for all later times and $\mathbf{w}^{[\mathbf{a}]}(\infty) := \lim_{t\to\infty} \mathbf{w}^{[\mathbf{a}]}(t) = \widehat{\mathbf{w}}$ (see Wiggins (2003) for a more formal definition). A necessary and sufficient condition for a fixed point to be LAS in a given space Ω is that all the eigenvalues of its associated Jacobian matrix evaluated in Ω have a negative real part (Wiggins, 2003). Otherwise, the fixed point is unstable in Ω.

Local asymptotic stability is a useful property to predict the behaviour of the system in a close neighbourhood of one of its fixed points. After a small perturbation, the system returns to the fixed point if stable and moves away from it if unstable.

Local asymptotic stability of a fixed point may be effective in one space but not in another. An interesting biological consequence of this is that the inoculation by genotype j of a host already singly infected by genotype i can result in the persistence of genotype j and in the elimination of genotype i from the host. Recall that the UFP and the SIFP

belong to $\mathcal{W}_i' \subsetneq \mathcal{W}$; we thus have to distinguish between being LAS in $\mathcal{W}_i'$ and being LAS in $\mathcal{W}$.

2.c.3.1. Necessary and sufficient condition for UFP to be LAS in $\mathcal{W}$ and $\mathcal{W}_i'$

Let us study the the stability of the UFP $\widehat{\mathbf{w}}_0$ in $\mathcal{W}$. The Jacobian matrix evaluated in this point is

$$\mathbf{J}_3(\widehat{\mathbf{w}}_0) = \begin{bmatrix} \varrho_i & 0 & 0 & 0 & 0 & 0 \\ \upsilon u_i & -\upsilon & 0 & 0 & 0 & 0 \\ \upsilon v_i & 0 & -\upsilon & 0 & 0 & 0 \\ 0 & 0 & 0 & \varrho_k & 0 & 0 \\ 0 & 0 & 0 & \upsilon u_k & -\upsilon & 0 \\ 0 & 0 & 0 & \upsilon v_k & 0 & -\upsilon \end{bmatrix},$$

the eigenvalues of which are simply $\mathrm{Sp}(\mathbf{J}_3(\widehat{\mathbf{w}}_0)) = \{\varrho_i, \varrho_k, -\upsilon\}$, because it is a lower triangular matrix. Therefore, we have

$$\widehat{\mathbf{w}}_0 \text{ is LAS in } \mathcal{W} \Longleftrightarrow \big(\varrho_1 < 0\big) \wedge \big(\varrho_2 < 0\big). \tag{2.c.11}$$

Obviously, $\mathbf{J}_i(\widehat{\mathbf{w}}_0)$ is equal to the upper left 3×3 block of $\mathbf{J}_3(\widehat{\mathbf{w}}_0)$ and is also a lower triangular matrix, so

$$\widehat{\mathbf{w}}_0 \text{ is LAS in } \mathcal{W}_i' \Longleftrightarrow \varrho_i < 0. \tag{2.c.12}$$

2.c.3.2. Necessary and sufficient condition for SIFP$_i$ to be LAS in $\mathcal{W}_i'$

Let us study the stability of the SIFP$_i$ $\widehat{\mathbf{w}}_i$ in $\mathcal{W}_i'$, that is when there is only one genotype in the system. The Jacobian matrix evaluated at this point is

$$\mathbf{J}_i(\widehat{\mathbf{w}}_i) = \begin{bmatrix} \eta_{i,i}x_i^\circ & \gamma_{i,i}x_i^\circ & -\sigma_i x_i^\circ \\ \upsilon u_i & -\upsilon & 0 \\ \upsilon v_i & 0 & -\upsilon \end{bmatrix},$$

the eigenvalues of which are the roots of the following polynomial

$$\begin{aligned} |\mathbf{J}_i(\widehat{\mathbf{w}}_i) - \lambda I_3| &= \begin{vmatrix} \eta_{i,i}x_i^\circ - \lambda & \gamma_{i,i}x_i^\circ & -\sigma_{i,i}x_i^\circ \\ \upsilon u_i & -\upsilon - \lambda & 0 \\ \upsilon v_i & 0 & -\upsilon - \lambda \end{vmatrix}, \\ &= (-\upsilon - \lambda)^2\big(\eta_{i,i}x_i^\circ - \lambda\big) - \big(-\sigma_{i,i}x_i^\circ\big)(-\upsilon - \lambda)\upsilon v_i - (-\upsilon - \lambda)\gamma_{i,i}x_i^\circ \upsilon u_i, \\ &= -(\upsilon + \lambda)\big((\lambda + \upsilon)\big(\lambda - \eta_{i,i}x_i^\circ\big) + \upsilon\sigma_{i,i}v_i x_i^\circ - \upsilon\gamma_{i,i}u_i x_i^\circ\big). \end{aligned}$$

A first obvious eigenvalue is $\lambda_0 = -\upsilon < 0$. The remaining eigenvalues are the roots of the polynomial

$$\lambda^2 + \big(\upsilon - \eta_{i,i}x_i^\circ\big)\lambda - \upsilon x_i^\circ\big(\eta_{i,i} + \gamma_{i,i}u_i - \sigma_{i,i}v_i\big) \overset{(2.c.5)}{=} \lambda^2 + \left(\upsilon + \frac{\varrho_i\eta_{i,i}}{\eta_{i,i} + \gamma_{i,i}u_i - \sigma_{i,i}v_i}\right)\lambda + \upsilon\varrho_i,$$

the discriminant of which is

$$\begin{aligned}
\Delta &= \left(v+\frac{\varrho_i\eta_{i,i}}{\eta_{i,i}+\gamma_{i,i}u_i-\sigma_{i,i}v_i}\right)^2-4v\varrho_i,\\
&= v^2+\frac{2v\varrho_i\eta_{i,i}}{\eta_{i,i}+\gamma_{i,i}u_i-\sigma_{i,i}v_i}+\left(\frac{\varrho_i\eta_{i,i}}{\eta_{i,i}+\gamma_{i,i}u_i-\sigma_{i,i}v_i}\right)^2-4v\varrho_i,\\
&= v^2-\frac{-2v\varrho_i\eta_{i,i}}{\eta_{i,i}+\gamma_{i,i}u_i-\sigma_{i,i}v_i}+\left(\frac{\varrho_i\eta_{i,i}}{\eta_{i,i}+\gamma_{i,i}u_i-\sigma_{i,i}v_i}\right)^2-\frac{4v\varrho_i\left(\gamma_{i,i}u_i-\sigma_{i,i}v_i\right)}{\eta_{i,i}+\gamma_{i,i}u_i-\sigma_{i,i}v_i},\\
&= \left(v-\frac{\varrho_i\eta_{i,i}}{m_{i,i}}\right)^2-\frac{4v\varrho_i\left(\gamma_{i,i}u_i-\sigma_{i,i}v_i\right)}{m_{i,i}}.
\end{aligned}$$

In order to simplify the calculus, we make two assumptions without significant loss of biological relevance. First, we assume that the public goods production rate (u_i) has the same order of magnitude than the spite production rate (v_i). Note that otherwise the slowest public production dynamics could be assumed constant. Second, we assume that a parasite genotype benefits much more from its own public good than it is affected by its own spite, in absolute value ($\gamma_{i,i} \gg \sigma_{i,i}$). By formally combining these two assumptions, we assume from now on that

$$\gamma_{i,i}u_i > \sigma_{i,i}v_i. \tag{2.c.13}$$

If we use this inequality and (2.c.9) (we are only interested in the stability of feasible fixed points), it is straightforward that $\Delta > 0$. The remaining two eigenvalues are then the following real numbers

$$\lambda_{1,2} = -\frac{1}{2}\left(v+\frac{\varrho_i\eta_{i,i}}{m_{i,i}}\pm\sqrt{\left(v+\frac{\varrho_i\eta_{i,i}}{m_{i,i}}\right)^2-4v\varrho_i}\right).$$

Two cases must be considered according to (2.c.9) because either $\varrho_i < 0 \wedge m_{i,i} > 0$ or $\varrho_i > 0 \wedge m_{i,i} < 0$.

In the first case,

$$\begin{aligned}
\varrho_i < 0 &\iff -4v\varrho_i > 0,\\
&\iff \left(v+\frac{\varrho_i\eta_{i,i}}{m_{i,i}}\right)^2-4v\varrho_i > \left(v+\frac{\varrho_i\eta_{i,i}}{m_{i,i}}\right)^2 > 0,\\
&\iff \sqrt{\left(v+\frac{\varrho_i\eta_{i,i}}{m_{i,i}}\right)^2-4v\varrho_i} > \left|v+\frac{\varrho_i\eta_{i,i}}{m_{i,i}}\right| > 0,\\
&\iff -\left|v+\frac{\varrho_i\eta_{i,i}}{m_{i,i}}\right|+\sqrt{\left(v+\frac{\varrho_i\eta_{i,i}}{m_{i,i}}\right)^2-4v\varrho_i} > 0,\\
&\implies -\frac{1}{2}\left(v+\frac{\varrho_i\eta_{i,i}}{m_{i,i}}-\sqrt{\left(v+\frac{\varrho_i\eta_{i,i}}{m_{i,i}}\right)^2-4v\varrho_i}\right) > 0,
\end{aligned}$$

so one of the eigenvalues is positive, meaning that $\widehat{\mathbf{w}}_i$ is unstable in $\mathcal{W}_i$.

In the second case,

$$\begin{aligned}
m_{i,i} < 0 &\iff \eta_{i,i}+\gamma_{i,i}u_i-\sigma_{i,i}v_i < 0,\\
&\overset{(2.c.13)}{\implies} \eta_{i,i} < 0,
\end{aligned} \tag{2.c.14}$$

and

$$
\begin{aligned}
\varrho_i > 0 \quad &\Longleftrightarrow \quad -4\upsilon\varrho_i < 0,\\
&\Longleftrightarrow \quad 0 < \left(\upsilon + \frac{\varrho_i\eta_{i,i}}{m_{i,i}}\right)^2 - 4\upsilon\varrho_i < \left(\upsilon + \frac{\varrho_i\eta_{i,i}}{m_{i,i}}\right)^2,\\
&\Longleftrightarrow \quad 0 < \sqrt{\left(\upsilon + \frac{\varrho_i\eta_{i,i}}{m_{i,i}}\right)^2 - 4\upsilon\varrho_i} < \left|\upsilon + \frac{\varrho_i\eta_{i,i}}{m_{i,i}}\right|,\\
&\Longleftrightarrow \quad \left|\upsilon + \frac{\varrho_i\eta_{i,i}}{m_{i,i}}\right| - \sqrt{\left(\upsilon + \frac{\varrho_i\eta_{i,i}}{m_{i,i}}\right)^2 - 4\upsilon\varrho_i} > 0,\\
&\Longleftrightarrow \quad -\left|\upsilon + \frac{\varrho_i\eta_{i,i}}{m_{i,i}}\right| - \sqrt{\left(\upsilon + \frac{\varrho_i\eta_{i,i}}{m_{i,i}}\right)^2 - 4\upsilon\varrho_i} < -\left|\upsilon + \frac{\varrho_i\eta_{i,i}}{m_{i,i}}\right| + \sqrt{\left(\upsilon + \frac{\varrho_i\eta_{i,i}}{m_{i,i}}\right)^2 - 4\upsilon\varrho_i} < 0,\\
&\overset{(2.c.14)}{\Longleftrightarrow} \quad -\frac{1}{2}\left(\upsilon + \frac{\varrho_i\eta_{i,i}}{m_{i,i}} + \sqrt{\left(\upsilon + \frac{\varrho_i\eta_{i,i}}{m_{i,i}}\right)^2 - 4\upsilon\varrho_i}\right) < -\frac{1}{2}\left(\upsilon + \frac{\varrho_i\eta_{i,i}}{m_{i,i}} - \sqrt{\left(\upsilon + \frac{\varrho_i\eta_{i,i}}{m_{i,i}}\right)^2 - 4\upsilon\varrho_i}\right) < 0,
\end{aligned}
$$

that is both eigenvalues are negative.

To conclude on the local asymptotic stability in $\mathcal{W}_i'$ of the SIFP$_i$,

$$\widehat{\mathbf{w}}_i \text{ is LAS in } \mathcal{W}_i' \Longleftrightarrow \left(\varrho_i > 0\right) \wedge \left(m_{i,i} < 0\right). \tag{2.c.15}$$

2.c.3.3. Necessary and sufficient condition for SIFP$_i$ to be LAS in $\mathcal{W}$

Let us study the local stability of the SIFP$_i$ $\widehat{\mathbf{w}}_i$ in $\mathcal{W}$, that is when there are two parasite genotypes in the system.

The Jacobian matrix evaluated at this point is

$$\mathbf{J}_3(\widehat{\mathbf{w}}_i) = \begin{bmatrix} \eta_{i,i}x_i^\circ & \gamma_{i,i}x_i^\circ & -\sigma_{i,i}x_i^\circ & \eta_{i,k}x_i^\circ & \gamma_{i,k}x_i^\circ & -\sigma_{i,k}x_i^\circ \\ \upsilon u_i & -\upsilon & 0 & 0 & 0 & 0 \\ \upsilon v_i & 0 & -\upsilon & 0 & 0 & 0 \\ 0 & 0 & 0 & r_k(\widehat{\mathbf{w}}_i) & 0 & 0 \\ 0 & 0 & 0 & \upsilon u_k & -\upsilon & 0 \\ 0 & 0 & 0 & \upsilon v_k & 0 & -\upsilon \end{bmatrix}.$$

It appears that this matrix can be written as a block matrix using the single infection Jacobian matrices the definition of which can be extended to $\mathcal{W}$ as follows:

$$\mathbf{J}_3(\widehat{\mathbf{w}}_i) = \begin{bmatrix} \mathbf{J}_i(\widehat{\mathbf{w}}_i) & \mathbf{A} \\ \mathbf{0} & \mathbf{J}_k(\widehat{\mathbf{w}}_i) \end{bmatrix}.$$

Thus, the eigenvalues λ of this matrix cancel

$$\det(\mathbf{J}_3(\widehat{\mathbf{w}}_i) - \lambda\mathbf{I}_6) = \det(\mathbf{J}_i(\widehat{\mathbf{w}}_i) - \lambda\mathbf{I}_3)\det(\mathbf{J}_k(\widehat{\mathbf{w}}_i) - \lambda\mathbf{I}_3).$$

By definition, the roots of $\det(\mathbf{J}_i(\widehat{\mathbf{w}}_i) - \lambda\mathbf{I}_3)$ are the eigenvalues of $\mathbf{J}_i(\widehat{\mathbf{w}}_i)$. From the previous results, we know that these roots are all negative iff $\varrho_i > 0 \wedge m_{i,i} < 0$. Put differently, the stability of $\widehat{\mathbf{w}}_i$ in $\mathcal{W}_i'$ is a necessary condition of the stability of $\widehat{\mathbf{w}}_i$ in $\mathcal{W}$.

By definition, the roots of $\det(\mathbf{J}_k(\widehat{\mathbf{w}}_i) - \lambda\mathbf{I}_3)$ are the eigenvalues of

$$\mathbf{J}_k(\widehat{\mathbf{w}}_i) = \begin{bmatrix} r_k(\widehat{\mathbf{w}}_i) & 0 & 0 \\ \upsilon u_k & -\upsilon & 0 \\ \upsilon v_k & 0 & -\upsilon \end{bmatrix}.$$

This matrix is a lower triangular matrix so its spectrum is straightforwardly $\mathrm{Sp}(\mathbf{J}_k(\widehat{\mathbf{w}}_i)) = \{-\upsilon, r_k(\widehat{\mathbf{w}}_i)\}$. Expliciting the instantaneous growth rate, we find that

$$\begin{aligned} r_k(\widehat{\mathbf{w}}_i) &= \varrho_k + \gamma_{k,i} u_i x_i^\circ - \sigma_{k,i} \upsilon_i x_i^\circ + \eta_{k,i} x_i^\circ, \\ &= \varrho_k + m_{k,i} x_i^\circ, \\ &= \varrho_k - \frac{m_{k,i}}{m_{i,i}} \varrho_i, \end{aligned}$$

which is negative iff $m_{i,i}\varrho_k > m_{k,i}\varrho_i$.

In conclusion, and owing to symmetry, the necessary and sufficient condition for the EFPs to be LAS is the following

$$\widehat{\mathbf{w}}_i \text{ is LAS in } \mathcal{W} \Longleftrightarrow \big(\varrho_i > 0\big) \wedge \big(m_{i,i} < 0\big) \wedge \big(m_{i,i}\varrho_k > m_{k,i}\varrho_i\big). \tag{2.c.16}$$

Note that $\big(\varrho_i > 0\big) \wedge \big(m_{i,i} < 0\big) \wedge \big(m_{i,i}\varrho_k > m_{k,i}\varrho_i\big) \Longrightarrow \big(\varrho_k < 0\big) \vee \big(m_{k,i} < 0\big)$. A consequence of this result, which proves to be useful later on, is that

$$\widehat{\mathbf{w}}_i \text{ LAS in } \mathcal{W} \Longrightarrow r_k(\widehat{\mathbf{w}}_i) < 0. \tag{2.c.17}$$

2.c.3.4. Necessary and sufficient condition for DIFP to be LAS in $\mathcal{W}$

The double infection Jacobian matrix evaluated in $\widehat{\mathbf{w}}_3$ is

$$\mathbf{J}_3(\widehat{\mathbf{w}}_3) = \begin{bmatrix} \eta_{i,i}x_i & \gamma_{i,i}x_i & -\sigma_{i,i}x_i & \eta_{i,k}x_i & \gamma_{i,k}x_i & -\sigma_{i,k}x_i \\ \upsilon u_i & -\upsilon & 0 & 0 & 0 & 0 \\ \upsilon v_i & 0 & -\upsilon & 0 & 0 & 0 \\ \eta_{k,i}x_k & \gamma_{k,i}x_k & -\sigma_{k,i}x_k & \eta_{k,k}x_k & \gamma_{k,k}x_k & -\sigma_{k,k}x_k \\ 0 & 0 & 0 & \upsilon u_k & -\upsilon & 0 \\ 0 & 0 & 0 & \upsilon v_k & 0 & -\upsilon \end{bmatrix},$$

the eigenvalues of which are too large to be shown and no parametric condition for local asymptotic stability can easily be extracted from them. Therefore, stability of the DIFP has to be addressed either numerically, either through a more restrictive condition that provides its global stability.

2.c.4. Summary

Table 2.c.1 sum ups the notations and results related to fixed points analysis.

symbol	**value**	**meaning**
$\mathbf{c}_i$	$= \begin{bmatrix} 1 & u_i & v_i \end{bmatrix}$	public productions nullcline direction vector i
$m_{j,\ell}$	$= \eta_{j,\ell} + \gamma_{j,\ell} u_\ell - \sigma_{j,\ell} v_\ell,$	stationary interaction effect of ℓ over j
x_i°	$= -\frac{\varrho_i}{m_{i,i}}$	stationary parasite load in single infection
x_i	$= \frac{m_{i,k}\varrho_k - m_{k,k}\varrho_i}{m_{i,i}m_{k,k} - m_{i,k}m_{k,i}}$	stationary parasite load in double infection
$\widehat{\mathbf{w}}_0$	$= \mathbf{0}_6$	uninfected fixed point (UFP)
$\widehat{\mathbf{w}}_i$	$= \begin{bmatrix} x_i^\circ \mathbf{c}_i & \mathbf{0}_3 \end{bmatrix}$	singly infected fixed point i (SIFP$_i$)
$\widehat{\mathbf{w}}_3$	$= \begin{bmatrix} x_i \mathbf{c}_i & x_k \mathbf{c}_k \end{bmatrix}$	doubly infected fixed point (DIFP)
$\widehat{\mathcal{W}}$	$= \{\widehat{\mathbf{w}}_0, \widehat{\mathbf{w}}_1, \widehat{\mathbf{w}}_2, \widehat{\mathbf{w}}_3\}$	fixed point set

Table 2.c.1. – Fixed points analysis notations and result summary.

The results of the local stability analysis in both spaces are given in Table 2.c.2 along with the feasibility conditions.

fixed point	**feasibility condition**	**local asymptotic stability condition if feasible**	
		in $\mathcal{W}_i'$	**in** $\mathcal{W}$
$\widehat{\mathbf{w}}_0$ (UFP)	always	$\varrho_i < 0$	$(\varrho_1 < 0) \wedge (\varrho_2 < 0)$
$\widehat{\mathbf{w}}_i$ (SIFP$_i$)	$\operatorname{sgn}(\varrho_i) \neq \operatorname{sgn}(m_{i,i})$	$(\varrho_i > 0) \wedge (m_{i,i} < 0)$	$(\varrho_i > 0) \wedge (m_{i,i} < 0)$ $\wedge (m_{k,i}\varrho_i < m_{i,i}\varrho_k)$
$\widehat{\mathbf{w}}_3$ (DIFP)	$\operatorname{sgn}(m_{i,i}m_{k,k} - m_{i,k}m_{k,i})$ $= \operatorname{sgn}(m_{i,k}\varrho_k - m_{k,k}\varrho_i)$ $= \operatorname{sgn}(m_{k,i}\varrho_i - m_{i,i}\varrho_k)$	none ($\widehat{\mathbf{w}}_3 \notin \mathcal{W}_i'$)	not shown

Table 2.c.2. – Fixed points analysis notations and result summary.

2.d. Finite time explosion solutions

2.d.1. Preliminary result

Let us define the following quantity $P_i \coloneqq v_i Y_i - u_i Z_i$, the time derivative of which is

$$\begin{aligned}\frac{\mathrm{d}P_i}{\mathrm{d}t} &= v_i \frac{\mathrm{d}Y_i}{\mathrm{d}t} - u_i \frac{\mathrm{d}Z_i}{\mathrm{d}t},\\ &= v v_i (u_i X_i - Y_i) - v u_i (v_i X_i - Z_i),\\ &= -v Y_i - v Z_i,\\ &= -v P_i.\end{aligned}$$

It follows from this that $\forall t \in \mathbb{R}_+, P_i(t) = P_i(0) e^{-vt}$. Two cases are then to be distinguished. Either genotype i is newly inoculated in the host, which means no public production of its kind is already present, that is $Y_i(0) = Z_i(0) = 0$, yielding $P_i(0) = 0$. Or genotype i is already present in the host when the dynamics are followed up and it is usually at some fixed point, where $Y_i = u_i X_i$ and $Z_i = v_i X_i$, also yielding $P_i(0) = v_i u_i X_i - u_i v_i X_i = 0$. In both cases, $P_i(t) = 0$ yielding a time independent correlation between public production concentrations,

$$\forall t \in \mathbb{R}_+, v_i Y_i = u_i Z_i. \tag{2.d.1}$$

Note that even if different initial conditions than the above are taken, this correlation is reached exponentially (all the more fast as the standard clearing rate v is high).

2.d.2. In singly inoculated hosts

Here we show that when there is no feasible and LAS fixed point in the SIS_i, formulated as $\varpi_i = \emptyset$ (see definition in next section), genotype i parasite load explodes in finite time in a singly inoculated host.

From Table 2.c.2, assuming the emptiness of ϖ_i implies that $\varrho_i > 0$ and $m_{i,i} > 0$, that is $\eta_{i,i} + \gamma_{i,i} u_i > \sigma_{i,i} v_i$ hence $\eta_{i,i} > 0$. Considering a newly singly inoculated host, we have $X_i(0) = \varepsilon > 0$, all other variables being 0 at $t = 0$. Using (2.d.1), it follows that

$$\begin{aligned}\frac{\mathrm{d}X_i}{\mathrm{d}t} &= \left(\varrho_i + \eta_{i,i} X_i + \gamma_{i,i} Y_i - \sigma_{i,i} Z_i\right) X_i,\\ &= \left(\varrho_i + \eta_{i,i} X_i + \left(\gamma_{i,i} - \sigma_{i,i} \frac{v_i}{u_i}\right) Y_i\right) X_i,\end{aligned}$$

yet $\gamma_{i,i} - \sigma_{i,i} \frac{v_i}{u_i} > 0$ because of assumption (2.c.13), the following inequality holds

$$\frac{\mathrm{d}X_i}{\mathrm{d}t} \geq \left(\varrho_i + \eta_{i,i} X_i\right) X_i > 0.$$

Let $\underline{X_i}$ satisfy $\frac{\mathrm{d}\underline{X_i}}{\mathrm{d}t} = \left(\varrho_i + \eta_{i,i} \underline{X_i}\right) \underline{X_i}$, $\underline{X_i}(0) = X_i(0) = \varepsilon$. Defining $f \coloneqq \frac{1}{\underline{X_i}}$, f satisfies the following ODE,

$$\frac{\mathrm{d}f}{\mathrm{d}t} = -\varrho_i f - \eta_{i,i},$$

the solution of which is

$$\begin{aligned} f(t) &= \left(f(0)+\frac{\eta_{i,i}}{\varrho_i}\right)e^{-\varrho_i t}-\frac{\eta_{i,i}}{\varrho_i}, \\ \textit{i.e.}\ \frac{1}{\underline{X_i}(t)} &= \left(\frac{1}{\varepsilon}+\frac{\eta_{i,i}}{\varrho_i}\right)e^{-\varrho_i t}-\frac{\eta_{i,i}}{\varrho_i}, \end{aligned}$$

yielding

$$\underline{X_i}(t)=\frac{\varrho_i\varepsilon}{\left(\varrho_i+\eta_{i,i}\varepsilon\right)e^{-\varrho_i t}-\eta_{i,i}\varepsilon}.$$

But $\underline{X_i}(t)$ is not defined for t^* such that

$$\left(\varrho_i+\eta_{i,i}\varepsilon\right)e^{-\varrho_i t^*}-\eta_{i,i}\varepsilon = 0,$$

i. e.

$$t^*=\frac{1}{\varrho_i}\log\left(1+\frac{\varrho_i}{\eta_{i,i}\varepsilon}\right)\in\mathbb{R}_+^\star.$$

Therefore $\lim_{t\to t^*}\underline{X_i}(t)=+\infty$.

Because $\frac{\mathrm{d}X_i}{\mathrm{d}t}\geq\frac{\mathrm{d}\underline{X_i}}{\mathrm{d}t}$ and $\underline{X_i}(0)=X_i(0)=\varepsilon>0$, it follows that $\lim_{t\to t^*}X_i(t)=+\infty$ as well. To conclude, if the parasite traits are such that neither the UFP nor the SIFP$_i$ are feasible and LAS in the SIS$_i$, then the parasite load of genotype i explodes in finite time.

2.d.3. In doubly inoculated hosts

Here we show the existence of scenarios when both parasite genotypes reach their SIFP in singly inoculated hosts but their parasite load explodes in finite time when they occur together in doubly inoculated hosts.

First, this requires that the two SIFPs are feasible and LAS in their respective SIS, $\varpi_1=\{\widehat{\mathbf{w}}_1\},\varpi_2=\{\widehat{\mathbf{w}}_2\}$ and that there is no feasible and LAS fixed point in the DIS, that is $\varpi=\emptyset$ (see notations in next section). From Table 2.c.2, it follows that $\forall(j,\ell)\in\{1,2\}^2, j\neq\ell, \varrho_j>0, m_{j,j}<0, m_{\ell,j}\varrho_j>m_{j,j}\varrho_\ell$.

Let us follow the total parasite load in the host ($X:=X_1+X_2$), starting from the moment when both parasite genotypes are present (either due to a co-inoculation or to a secondary inoculation). We have

$$\frac{\mathrm{d}X}{\mathrm{d}t} = \frac{\mathrm{d}X_1}{\mathrm{d}t}+\frac{\mathrm{d}X_2}{\mathrm{d}t}=r_1X_1+r_2X_2.$$

Let us focus on the instantaneous growth rate

$$r_1=\varrho_1+\eta_{1,1}X_1+\eta_{1,2}X_2+\gamma_{1,1}Y_1-\sigma_{1,1}Z_1+\gamma_{1,2}Y_2-\sigma_{1,2}Z_2.$$

Applying (2.d.1) on both genotypes, we have

$$r_1=\varrho_1+\eta_{1,1}X_1+\eta_{1,2}X_2+\left(\gamma_{1,1}-\sigma_{1,1}\frac{v_1}{u_1}\right)Y_1+\left(\gamma_{1,2}-\sigma_{1,2}\frac{v_2}{u_2}\right)Y_2.$$

Because of assumption (2.c.13), $\gamma_{1,1}-\sigma_{1,1}\frac{v_1}{u_1}>0$. If we assume as well that $\gamma_{1,2}-\sigma_{1,2}\frac{v_2}{u_2}>0$, the following inequality holds:

$$r_1\geq\varrho_1+\eta_{1,1}X_1+\eta_{1,2}X_2.$$

Using the same arguments for r_2, we have

$$\begin{aligned}\frac{\mathrm{d}X}{\mathrm{d}t} &\geq \left(\varrho_1+\eta_{1,1}X_1+\eta_{1,2}X_2\right)X_1+\left(\varrho_2+\eta_{2,2}X_2+\eta_{2,1}X_1\right)X_2,\\ &= \varrho_1X_1+\varrho_2X_2+\eta_{1,1}X_1^2+\eta_{2,2}X_2^2+\left(\eta_{1,2}+\eta_{2,1}\right)X_1X_2.\end{aligned}$$

By defining $\underline{X} := \min(X_1, X_2) \geq 0$ (which is a continuous function of time), $\underline{\varrho} := \min\left(\varrho_1, \varrho_2\right) > 0$ and $\underline{\eta} := \min\left(\eta_{1,1}, \eta_{2,2}\right) < 0$ and noticing that $X_1^2 + X_2^2 = X^2 - 2X_1X_2$, it follows that

$$\frac{\mathrm{d}X}{\mathrm{d}t} \geq \left(\underline{\varrho}+\left(\eta_{1,2}+\eta_{2,1}+2\underline{\eta}\right)\underline{X}\right)\underline{X}.$$

Let $\underline{X}$ satisfy $\frac{\mathrm{d}\underline{X}}{\mathrm{d}t} = \left(\underline{\varrho}+\left(\eta_{1,2}+\eta_{2,1}+2\underline{\eta}\right)\underline{X}\right)\underline{X}$, $\underline{X}(0) = \varepsilon < X(0) \geq 2\varepsilon > 0$. Defining $f := \frac{1}{\underline{X}}$, f satisfies the following ODE,

$$\frac{\mathrm{d}f}{\mathrm{d}t} = -\underline{\varrho}f - \left(\eta_{1,2}+\eta_{2,1}+2\underline{\eta}\right),$$

the solution of which is

$$f(t) = \left(f(0)+\frac{\left(\eta_{1,2}+\eta_{2,1}+2\underline{\eta}\right)}{\underline{\varrho}}\right)e^{-\underline{\varrho}t} - \frac{\left(\eta_{1,2}+\eta_{2,1}+2\underline{\eta}\right)}{\underline{\varrho}},$$

yielding

$$\underline{X}(t) = \frac{\underline{\varrho}\varepsilon}{\left(\underline{\varrho}+\left(\eta_{1,2}+\eta_{2,1}+2\underline{\eta}\right)\varepsilon\right)e^{-\underline{\varrho}t} - \left(\eta_{1,2}+\eta_{2,1}+2\underline{\eta}\right)\varepsilon}.$$

But $\underline{X_i}(t)$ is not defined for t^* such that

$$\left(\underline{\varrho}+\left(\eta_{1,2}+\eta_{2,1}+2\underline{\eta}\right)\varepsilon\right)e^{-\underline{\varrho}t^*} - \left(\eta_{1,2}+\eta_{2,1}+2\underline{\eta}\right)\varepsilon = 0,$$

i. e.

$$t^* = \frac{1}{\underline{\varrho}}\log\left(1+\frac{\underline{\varrho}\varepsilon}{\left(\eta_{1,2}+\eta_{2,1}+2\underline{\eta}\right)}\right).$$

Assuming that $\min\left(\eta_{1,1}, \eta_{2,2}\right) \leq -\frac{\eta_{1,2}+\eta_{2,1}}{2}$ makes $t^* \in \mathbb{R}_+^\star$. Therefore $\lim_{t\to t^*}\underline{X}(t) = +\infty$.

Because $\frac{\mathrm{d}X}{\mathrm{d}t} \geq \frac{\mathrm{d}\underline{X}}{\mathrm{d}t}$ and $\underline{X}(0) < X(0)$, it follows that $\lim_{t\to t^*}X(t) = +\infty$ as well under the previous assumptions. Moreover we have numerically checked that the dynamics behave similarly for cases where $\varpi = \emptyset$ and relaxed assumptions on the parameters.

To conclude, if the parasite traits are such that no fixed point is feasible and LAS in the DIS, the total parasite load blows up in finite time.

2.d.4. Threshold adaptation to explosive infections

In order to take into account explosive infections and keep the model outputs biologically relevant for all parameter sets or to avoid numerical complications, one should add the following rule to the dynamical system:

$$\exists T \in \mathbb{R}_+^\star : X_1(T) + X_2(T) = x_{\max} > 0 \Longrightarrow \forall t > T, X_1(t) = X_2(t) = 0,$$

where $x_{\max}$ is a new parameter of the model defined as the total parasite load threshold a host can bear before either dying or triggering an acute immune response that leads to recovery.

2.e. Generated infection pattern identification

2.e.1. Compatible sets of FLAS fixed points

Let $\boldsymbol{\omega}_i$ and $\boldsymbol{\omega}$ be the set of feasible and LAS ('FLAS') fixed points in the SIS ($\mathcal{W}_i'$) and the DIS ($\mathcal{W}$) respectively.

$$\boldsymbol{\omega}_i := \left\{ \widehat{\mathbf{w}} \in \widehat{\mathcal{W}_i'} : (\widehat{\mathbf{w}} \geq 0) \wedge \left(\widehat{\mathbf{w}} \text{ LAS in } \mathcal{W}_i' \right) \right\},$$

$$\boldsymbol{\omega} := \left\{ \widehat{\mathbf{w}} \in \widehat{\mathcal{W}} : (\widehat{\mathbf{w}} \geq 0) \wedge \left(\widehat{\mathbf{w}} \text{ LAS in } \mathcal{W} \right) \right\}.$$

From the results obtained in section 2.c and summarised in table 2.c.2, one can derive four rules satisfied by these sets:

$$\widehat{\mathbf{w}}_i \in \boldsymbol{\omega} \implies \widehat{\mathbf{w}}_i \in \boldsymbol{\omega}_i, \tag{2.e.1}$$

$$\widehat{\mathbf{w}}_0 \in \boldsymbol{\omega} \implies \widehat{\mathbf{w}}_0 \in \boldsymbol{\omega}_1 \cap \boldsymbol{\omega}_2, \tag{2.e.2}$$

$$\widehat{\mathbf{w}}_0 \in \boldsymbol{\omega} \implies \{\widehat{\mathbf{w}}_1, \widehat{\mathbf{w}}_2\} \not\supseteq \boldsymbol{\omega}, \tag{2.e.3}$$

$$\widehat{\mathbf{w}}_3 \in \boldsymbol{\omega} \implies \{\widehat{\mathbf{w}}_1, \widehat{\mathbf{w}}_2\} \not\supseteq \boldsymbol{\omega}. \tag{2.e.4}$$

Rule (2.e.1) states that if the SIFP_i is FLAS in the DIS then it is also FLAS in the SIS. Its proof is obvious from (2.c.15) and (2.c.16). Rule (2.e.2) states that if the UFP is FLAS in the DIS then it is also FLAS in the SIS and its proof is obvious from (2.c.11) and (2.c.12). Rule (2.e.3) states that if the UFP is FLAS in the DIS, then none of the SIFPs are FLAS in the DIS and its proof is obvious from (2.c.11) and (2.c.16).

Rule (2.e.4) states that if the DIFP is FLAS in the DIS, then it is the only FLAS fixed point in the DIS. We could not prove this rule analytically because of the size of the local asymptotic stability conditions. However, numerical explorations always satisfied this rule.

A consequence of (2.e.4) is that if any fixed point other than the DIFP is both feasible and LAS in the DIS, then the DIFP is not FLAS in the DIS.

We want to reveal the infection patterns this model generates. This requires enumerating all the $(\varpi_i, \varpi_k, \varpi)$ triplets that satisfy rules (2.e.1) to (2.e.4), with the addition that explosive single infections should be treated as failed infections (that is $\boldsymbol{\omega}_i = \emptyset$ is epidemiologically equivalent to $\boldsymbol{\omega}_i = \{\widehat{\mathbf{w}}_0\}$). The resulting list is given in Table 2.e.1, each combination corresponding to a distinct infection pattern.

$\boldsymbol{\omega}_i =$	$\boldsymbol{\omega}_k =$	$\boldsymbol{\omega} =$	pattern
$\{\widehat{\mathbf{w}}_0\}$ or $\emptyset$	$\{\widehat{\mathbf{w}}_0\}$ or $\emptyset$	$\{\widehat{\mathbf{w}}_0\}$ or $\{\widehat{\mathbf{w}}_0, \widehat{\mathbf{w}}_3\}$ or $\emptyset$	**no infection**
		$\{\widehat{\mathbf{w}}_3\}$	***ambinfection***
$\{\widehat{\mathbf{w}}_i\}$		$\{\widehat{\mathbf{w}}_i\}$ or $\emptyset$	***latinfection*** (k)
		$\{\widehat{\mathbf{w}}_3\}$	***suprainfection*** (k)
	$\{\widehat{\mathbf{w}}_k\}$	$\emptyset$	***ultrainfection***
		$\{\widehat{\mathbf{w}}_i\}$	**superinfection** (i)
		$\{\widehat{\mathbf{w}}_1, \widehat{\mathbf{w}}_2\}$	***priorinfection***
		$\{\widehat{\mathbf{w}}_3\}$	**coinfection**

Table 2.e.1. – FLAS fixed points set combination and corresponding infection patterns. For the sake of concision, twin infection patterns (*latinfection* i, *suprainfection* i and *superinfection* k) are not shown.

2.e.2. Logical viewpoint

If the steady presence of genotype 1 in a given host is denoted by the logical proposition p, and if q denotes the same for genotype 2, then the host classes S, I_1, I_2, I_3 are equivalent to $\{\neg p, \neg q\}$, $\{p, \neg q\}$, $\{\neg p, q\}$, $\{p, q\}$ respectively. If we attribute to each class a value 1 if epidemiologically observed or 0 if not, there exists an application that associates one binary operator (also called logical connective) to each infection pattern. Because the susceptible class is, by definition, always observed (the value of $\{\neg p, \neg q\}$ is always 1), only half of the sixteen different binary operators do match. Restrained to this set, this application is surjective, as shown in Table 2.e.2.

infection pattern	S $\{\neg p, \neg q\}$	I_1 $\{p, \neg q\}$	I_2 $\{\neg p, q\}$	I_3 $\{p, q\}$	**logical connective equivalence**	
no infection	1	0	0	0	$p \downarrow q$	joint denial
ambinfection	1	0	0	1	$p \leftrightarrow q$	biconditional
latinfection 1	1	0	1	0	$\neg p$	negation of p
suprainfection 1	1	0	1	1	$p \rightarrow q$	material implication
latinfection 2	1	1	0	0	$\neg q$	negation of q
suprainfection 2	1	1	0	1	$p \leftarrow q$	converse implication
ultrainfection, priorinfection, superinfection 1, superinfection 2	1	1	1	0	$p \uparrow q$	alternative denial
coinfection	1	1	1	1	$\top$	tautology

Table 2.e.2. – Infection patterns and their binary operators (logical connectives) equivalents.

However, the infection pattern-to-logical connective map is not injective since ultrainfection, priorinfection and the two superinfections match with the alternative denial. This yields two lessons. The first one is that the world of (formal) infection patterns is richer than the logical one. The second is that if only prevalence data is available for a host-parasite system, then it is impossible to distinguish between these four infection patterns. This requires the knowledge of the within-host dynamics or, at least, the outcome of cross-inoculations.

2.ω. Épilogue

La notion de patron d'infection introduite ici formalise le lien entre la dynamique intra-hôte et la dynamique inter-hôte, ou épidémiologique, quels que soient les modèles qui caractérisent chacun de ces niveaux (pourvu qu'il s'agisse d'infections chroniques – dans le cas des infections aiguës, la séparation des échelles de temps est moins réaliste et il convient de recourir aux équations aux dérivées partielles, voir Mideo *et al.* (2008); Day *et al.* (2011)).

En nous limitant au seul dimorphisme parasitaire, nous avons montré qu'un unique modèle intra-hôte relativement simple est en mesure de générer sept patrons d'infection interprétables biologiquement et par ailleurs observés dans la nature. Il apparaît dorénavant nécessaire pour tout modèle épidémiologique à polymorphisme parasitaire (y compris purement transitoire, à l'instar des cycles de remplacements de la dynamique adaptative, et/ou la dynamique intra-hôte implicite comme dans de nombreuses approches exposées dans l'introduction ι) d'être justifié et discuté quant au choix du patron d'infection. Non seulement les patrons d'infection mis en avant se distinguent par des épidémiologies qualitativement différentes (en terme de classes d'hôtes et de transitions entre celles-ci, voir les diagrammes de flux en Figure 2.ω.1), mais, en outre, chacun repose sur des conditions bien précises portant sur les interactions intra-hôte (p.ex. la coexistence requiert une compétition intra-typique plus importante que la compétition inter-typique ; en revanche le paradigme de l'exclusion compétitive par le type le plus virulent est critiquable ainsi que le montre la Figure 2.4.1**A**). Dès lors, la modélisation épidémiologique d'un système biologique réel implique soit d'identifier empiriquement le patron d'infection, soit d'en formuler explicitement l'hypothèse en s'efforçant de la motiver, autrement l'on s'expose à une interprétation fautive des résultats générés, quand bien même certains paramètres seraient justement estimés (voir Spicknall *et al.* (2013) pour une typologie et le choix des modèles dans le cadre la résistance aux antibiotiques).

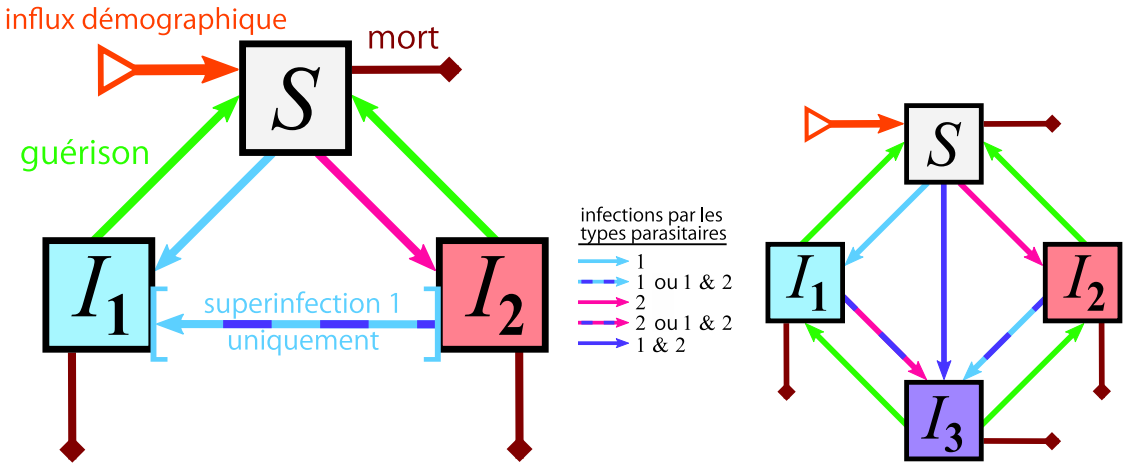

FIGURE 2.ω.1. – Déclinaison du modèle SIS selon trois des patrons d'infection dimorphes engendrés par notre modèle.
Selon les paramètres de la dynamique intra-hôte, la dynamique épidémiologique, ici inscrite dans le cadre SIS, présente des altérations qualitatives. **1)** diagramme de gauche (sans la flèche entre crochets) : deux compartiments simplement infectés sans transition directe entre eux, **priorinfection**. **2)** diagramme de gauche (avec la flèche entre crochets) : deux compartiments simplement infectés avec remplacement possible du type 2 par le type 1, **superinfection 1**. **3)** diagramme de droite : deux compartiments simplement infectés et un compartiment doublement infecté, **coinfection**.

3 Dynamique inter-hôte

3.α. Prologue

Les deux précédents chapitres ont mis en évidence la diversité des dynamiques parasitaires au sein des hôtes et la nécessité de leur prise en compte dans la caractérisation de l'épidémiologie des parasites polymorphes. Néanmoins, ces travaux se sont bornés à seulement deux types de parasites. Il s'avère que la modélisation des infections multiples dans le cas général, *i.e.* sans limite du nombre de types considérés, se heurte à plusieurs difficultés théoriques qui justifient, selon METCALF *et al.* (2015), son appartenance aux cinq défis actuels de l'épidémiologie évolutive.

Une difficulté d'ordre général est engendrée par la croissance géométrique du nombre de combinaisons de types parasitaires avec le polymorphisme. En effet, avec $n \in \mathbb{N}$ types parasitaires circulants, 2^n classes d'hôtes, caractérisées par la combinaison de types parasitaires infectant, sont (théoriquement) possibles. Ainsi, pour un polymorphisme potentiellement réaliste (l'Homme peut être simultanément infecté par une dizaine de souches de *Plasmodium falciparum* (JULIANO *et al.*, 2010), tandis que circulent plusieurs dizaines de types d'HPV (DE OLIVEIRA *et al.*, 2015)), la dimensionnalité de l'espace des états est très grande (le nombre de variables du système dynamique modélisant l'épidémiologie est au moins d'un ordre de grandeur supérieur à celui des modèles classiques monomorphes tels qu'au chapitre 0). Il en va de même avec l'espace des paramètres, puisque pour toute classe d'hôte de rang r (où r désigne le nombre de parasites infectants), $2^r - 1$ taux de transmissions sont à définir, un pour chaque inoculum (ensemble de propagules transmises à chaque contact inter-hôte) que cette classe peut produire. Soulignons au passage que la richesse des dynamiques observables est potentiellement élevée, et la résolution analytique du système inconcevable (KUCHARSKI *et al.*, 2016).

L'origine et le devenir des inocula constituent en outre des questions ouvertes. En effet, rares sont les systèmes hôte-parasite pour lesquels la taille des inocula et leur diversité est quantifiée avec précision (mais voir par exemple SALAZAR-GONZALEZ *et al.* (2009) dans le cas du VIH). Par taille des inocula, nous entendons le nombre de parasites effectivement transmis d'un hôte à l'autre par contact (aérosols inclus). *A minima,* des estimations larges de doses infectieuses (SCHMID-HEMPEL & FRANK, 2007), *i.e.* le plus petit nombre d'individus parasites nécessaires à l'initiation d'une infection, confirment que les populations intra-hôtes de microparasites atteignent, après infection, des tailles

supérieures de plusieurs ordres de grandeur à leur taille initiale. Considérant des microparasites empruntant un même canal de transmission, il est légitime de se demander si les hôtes infectés par plusieurs types parasitaires peuvent en transmettre un seul ou plusieurs à la fois. Plus exactement, le modèle épidémiologique nécessite de connaître, pour chacune des classes d'hôtes, la distribution multinomiale des classes d'inocula (équivalent des classes d'hôtes pour la diversité qualitative des ensembles de propagules).

Enfin, la dépendance à la croissance intra-hôte des taux épidémiologiques canoniques – à savoir le taux de transmission, le taux de guérison ainsi que la virulence – est elle aussi méconnue. Si la virulence totale subie par l'hôte semble augmenter avec le polymorphisme de l'infection (Griffiths *et al.*, 2011), il est en revanche impossible d'extrapoler une fonction liant explicitement la virulence subie à la charge parasitaire, tant les données sont limitées. Le problème est encore plus prégnant dans le cas de la transmission et la guérison. Un hôte infecté par plusieurs types parasitaires transmet-il plus de propagules qu'un autre infecté par un seul type parasitaire ? Quel est l'effet de la compétition inter-typique sur le taux de transmission total (une inhibition mutuelle pourrait diminuer la charge parasitaire totale par rapport aux infections simples) ? Une charge parasitaire élevée promeut-elle la réponse immunitaire ou au contraire l'inhibe-t-elle ? Les hôtes guérissent-ils de plusieurs types parasitaires à la fois ? Toute tentative de modélisation ne peut donc qu'être une suggestion qu'il conviendra de discuter à la lumière d'apports empiriques futurs.

Dans le présent chapitre, nous présentons une approche originale de la modélisation des infections multiples dans la mesure où, pour la première fois, la croissance intra-hôte est explicite [*] et affecte la dynamique épidémiologique dans laquelle elle est emboîtée [†]. Cette influence apparaît qualitative : l'issue de la croissance intra-hôte détermine l'ensemble des classes d'hôtes possibles et les transitions de l'une à l'autre par infection et guérison. Mais l'influence de la croissance intra-hôte sur la dynamique inter-hôte est aussi quantitative : les charges parasitaires à l'équilibre sont les arguments des fonctions déterminant les taux épidémiologiques [‡].

En termes d'application, le modèle épidémiologique présenté ci-après constitue une base de travail adaptée à l'étude quantitative des maladies infectieuses non vectorielles, polymorphes et chroniques (ou en général à courte durée d'incubation relativement à la durée de l'infection). Citons dans ce cas celles causées par les parasites HIV, HPV, Rotavirus, *Haemophilus influenzae*, *Mycobacterium tuberculosis*, *Neisseria gonorrhoeae* chez l'Homme ou le TMV chez certaines angiospermes.

∗. Le modèle intra-hôte présenté ici est l'extension à n types parasitaires de celui étudié au chapitre 2. Les hypothèses inédites portant sur certains paramètres ($\rho_i > 0, \sigma_{i,i} = 0, m_{i,i} < 0$) ne contraignent en réalité que les simulations de la Figure 3.5.1.

†. À noter que le modèle inter-hôte peut aisément s'adapter à d'autres formulations du modèle intra-hôte.

‡. Une attention toute particulière a été accordée à la recherche d'une fonction modélisant le taux de transmission telle que la somme totale des taux d'émission de chaque inoculum soit égale pour toutes les classes d'hôtes infectés, voir preuve en annexe 3.d.1.

Des interactions intra-hôte à la compétition épidémiologique : un modèle général pour les infections multiples

Mircea T. SOFONEA, Samuel ALIZON, Yannis MICHALAKIS

Résumé

De nombreux hôtes sont infectés par plusieurs génotypes de parasites à la fois. Dans ces hôtes co-infectés, les différentes interactions qu'entretiennent les parasites sont à l'origine d'une diversité de dynamiques intra-hôtes qui rend difficile la prédiction de l'expression et de l'évolution de la virulence. Ces infections multiples génèrent en outre une diversité combinatoire de chemins de cotransmission au niveau de la population d'hôtes, laquelle complique l'épidémiologie et peut aboutir à des issues non triviales. Nous introduisons un nouveau modèle pour les infections multiples dans lequel les hôtes peuvent être infectés par un nombre quelconque de génotypes parasitaires et potentiellement coexister dans la population. Dans notre modèle, les parasites affectent mutuellement leur croissance intra-hôte par des interactions densité-dépendantes et au moyen de biens communs et de produits de méchanceté. Ces interactions intra-hôte déterminent virulence(s), taux de guérison et taux de transmissions, lesquels sont ensuite intégrés dans un réseau de transmission. Nous utilisons des solutions analytiques et des simulations numériques pour étudier les rétro-actions épidémiologiques dans les populations d'hôtes infectés par plusieurs génotypes parasitaires. Enfin, nous discutons des perspectives générales au sujet des infections multiples.

Mots-clés :

épidémiologie, coinfection, superinfection, nombre de reproduction de base, bien commun, méchanceté

From within host interactions to epidemiological competition: a general model for multiple infections

Mircea T. Sofonea, Samuel Alizon, Yannis Michalakis

Abstract

Many hosts are infected by several parasite genotypes at a time. In these coinfected hosts parasites can interact in various ways thus creating diverse within-host dynamics, making it difficult to predict the expression and the evolution of virulence. Moreover, multiple infections generate a combinatorial diversity of cotransmission routes at the host population level, which complicates the epidemiology and may lead to non-trivial outcomes. We introduce a new model for multiple infections, which allows any number of parasite genotypes to infect hosts and potentially coexist in the population. In our model, parasites affect one another's within-host growth directly through density dependent interactions and indirectly by means of public goods and spite. These within-host interactions determine virulence, recovery and transmission rates, which are then integrated in a transmission network. We use analytical solutions and numerical simulations to investigate epidemiological feedbacks in host populations infected by several parasite genotypes. Finally we discuss general perspectives on multiple infections.

Keywords: epidemiology; coinfection; superinfection; basic reproduction number; public goods; spite

Citation: Sofonea MT, Alizon S, Michalakis Y. 2017. From within-host interactions to epidemiological competition: a general model for multiple infections. *Philosophical Transactions of the Royal Society B: Biological Sciences*. **370:** 20140303.
doi: 10.1098/rstb.2014.0303

3.1. Introduction

There is increasing evidence that multiple parasite strains or species infecting the same host is a common context of parasitism in the wild (Petney & Andrews, 1998; Lord *et al.*, 1999; Juliano *et al.*, 2010; Balmer & Tanner, 2011). These coinfections occur for several host-parasite interactions that range from bacteria infected by bacteriophage viruses to animals or plants infected by viruses, bacteria or worms (Raso *et al.*, 2004; Bentwich *et al.*, 1999). In addition to being a major concern in public health, human and veterinary medicine and phytopathology, coinfections are also a challenging subject for ecology and evolution. In a coinfected host, the different strains or species of parasites (hereafter referred to as 'genotypes') can interact in various ways (Brown & Grenfell, 2001; Mideo, 2009; Kümmerli & Brown, 2010). For instance some symbiont bacteria produce siderophores that harvest iron for the whole microbiota (West & Buckling, 2003), whereas others produce bacteriocins that break down the membrane of other bacterial species (Riley & Wertz, 2002). Such processes generate diverse within-host dynamics that make it difficult to predict the evolution or even sometimes the expression of the 'overall virulence' (Choisy & de Roode, 2010; Alizon *et al.*, 2013), i.e. the additional host mortality rate in the coinfected host. Moreover, considering multiple infections at the host population level generates a combinatorial diversity of (co)transmission routes, which complicates the epidemiology. This can lead to non-trivial outcomes of epidemics involving multiple genotypes.

The unpredictable outcome of the within-host interactions between parasites and the combinatorial complexity of the cotransmissions are probably the two main reasons why the vast majority of epidemiological models still leans on classical SIR models (Kermack & McKendrick, 1932; Anderson & May, 1982) which consider only one parasite genotype infecting a population of hosts. Models allowing for several genotypes are often restricted to two strains (Levin & Pimentel, 1981; van Baalen & Sabelis, 1995) or arbitrarily choose between a superinfection pattern (Levin & Pimentel, 1981; Nowak & May, 1994) and a coinfection pattern (van Baalen & Sabelis, 1995; May & Nowak, 1995; Choisy & de Roode, 2010). In superinfections, parasite genotypes cannot coexist within the host and one always one that outcompetes the others. In coinfections, within-host coexistence is made possible but these models usually rely on strong assumptions such as no within-host interactions (May & Nowak, 1995), fixed relatedness (Brown *et al.*, 2002), or epidemiological equivalence between genotypes (Lion, 2013).

Epidemiological and biological observations render the state of the art of modelling multiple infections unsatisfying. For instance, it is obvious that dividing the reality between coinfections (always coexistence) and superinfection (never coexistence) is oversimplifying. In several pathogens, for instance, coexistence can be only transitory and one of the genotypes can eventually exclude the others, as shown in the case of rodent malaria (de Roode *et al.*, 2005a). Furthermore, arbitrarily limiting the number of genotypes per host to two is oversimplifying, as shown e.g. in the case of human malaria (Juliano *et al.*, 2010). A final unsatisfying model limitation is the one that parasites only interact through one type of process. Yet, it is known that bacteria for instance can simultaneously compete for host resources, produce public goods and bacteriocins (Garbutt *et al.*, 2011).

Here we develop a new model for multiple infections, which captures many kinds of within-host outcomes, while allowing for an arbitrary number of parasite genotypes. We based our approach on nesting the within-host processes into the between-host epidemiology. Nested models have already been investigated in epidemiology to study multiple infections, either by modelling exploitation competition through host resource use (Bre-

mermann & Pickering, 1983), or immune cell infection dynamics by viruses (Boldin & Diekmann, 2008; Alizon & van Baalen, 2008). However, existing nested models (reviewed by Mideo et al. 2008 (Mideo *et al.*, 2008)) often ignore several within-host processes, such as within-host parasite interactions, and force the outcome of infection (superinfection or coinfection). By explicitly allowing parasite genotypes to affect one another's growth inside the host in more than one way, for instance through the production of public goods, spite, competition for host resources or interactions with the host immune system, we do not need to make assumptions such as superinfection or coinfection: such states appear as outcomes of the within host interactions. We then use these within-host interactions to define infection, recovery and death rates, allowing for partial cotransmission (i.e. we do not impose constraints on which genotype combination an infected host transmits) and numerically simulate epidemics.

We show that relaxing assumptions commonly made leads to rich and complex behaviour of the epidemics, because of epidemiological feedbacks. Such feedbacks could not be captured by previous models based solely on within-host dynamics (Brown *et al.*, 2002) because they failed to integrate the between-host level. Here we also propose a methodology to capture these feedbacks when estimating the basic reproduction number, that is the number of secondary infections caused by an infected host in a fully susceptible host population during its entire period of infectiousness (Anderson & May, 1991).

3.2. Within-host dynamics

The first challenging step is to model the within-host growth of an arbitrary number of unrelated genotypes by taking into account several processes. Indeed, current models typically, though not always, only involve a single process and/or at most 2 genotypes. To this end, we assume that the parasite load of each genotype follows a quadratic ordinary differential equation inspired by the classical framework of population dynamics (Verhulst, 1838). Besides regular reproduction rate and density-dependent feedback, we allow the growth of parasite loads to be affected by molecules produced by the parasites: public goods and spite. We present the equations and main assumptions before solving the system at steady state.

We consider an arbitrary number $n \in \mathbb{N}^\star$ of parasite genotypes which are not necessarily related nor from the same species (all the notations used thereafter are summarised in appendix 3.a). Each genotype is defined by a set of within-host traits, which are assumed to be constant (no plasticity). We denote $\mathcal{G} := [\![1;n]\!]$ the set of parasite genotypes (where $:=$ means 'equals by definition'). We wish to model the variation with time t of the parasite load vector $\mathbf{x} := (X_k(t))_{k\in\mathcal{G}}$ in a host coinfected by all n genotypes.

3.2.1. Public production dynamics

Parasites such as symbiotic bacteria can produce and secrete molecules in the (within-host) environment (Alizon *et al.*, 2013). Because any genotype can be affected by molecules produced by another genotype, we refer to these as public productions (PP). PP can have positive effects on the growth of the receiver. This is the case for siderophores (Neilands, 1995) and more generally, what we refer to as public goods (PG) (Kümmerli & Brown, 2010). PP can also be detrimental to the receiver as in the case for bacteriocins (Riley & Wertz, 2002) and we refer to this as spite (Gardner *et al.*, 2004). We assume each genotype can produce at most one type of PG and one type of spite, implying there are $2n$ concentrations of molecules that also vary with time, respectively $\mathbf{g} := (G_k(t))_{k\in\mathcal{G}}$ for PG and $\mathbf{z} := (Z_k(t))_{k\in\mathcal{G}}$ for spite. We assume that PP are produced by the parasites at a constant rate, independently of the current PP, and are cleared by hosts in a non-specific but concentration-dependent way at a standard clearing rate v. Overall, the dynamics of the PP concentrations follow

$$\begin{cases} \frac{\mathrm{d}}{\mathrm{d}t}\mathbf{g} = v(\mathbf{U}.\mathbf{x} - \mathbf{g}), \\ \frac{\mathrm{d}}{\mathrm{d}t}\mathbf{z} = v(\mathbf{V}.\mathbf{x} - \mathbf{z}), \end{cases} \tag{3.2.1}$$

where $\mathbf{U} := \mathrm{diag}(u_i)_{i\in\mathcal{G}}$ and $\mathbf{V} := \mathrm{diag}(v_i)_{i\in\mathcal{G}}$ are the diagonal matrices of PP production rates standardised by v.

3.2.2. Parasite load dynamics

PG increase parasite growth rate, while spite molecules decrease it. We assume these effects depend linearly on the molecule concentrations and that there is no heterogeneity in these concentrations. One type of PP can have different effects depending on the genotype of the receiver. We can define the matrix of PG effects on growth rate $\mathbf{\Gamma} := \left(\gamma_{k,j}\right)_{(k,j)\in\mathcal{G}^2}$ where $\gamma_{k,j} > 0$ is the effet of the PG type produced by genotype j on the growth of genotype k. Likewise, $\mathbf{\Sigma} := \left(\sigma_{k,j}\right)_{(k,j)\in\mathcal{G}^2}$ is the matrix of spite effects on growth rate where $\sigma_{k,j} > 0$ is the effect (in absolute value) of the spite type produced by genotype j on the growth rate of genotype k if $k \neq j$. We assume a genotype is not affected by its own spite type (that is $\sigma_{k,k} = 0$).

In addition to these PP secreted within the host, we group all the other genotype-to-genotype interactions into $\mathbf{H} \coloneqq \left(\eta_{k,j}\right)_{(k,j)\in\mathcal{G}^2}$ called the matrix of density-dependent effects, where $\eta_{k,j} \in \mathbb{R}$ is the density-dependent effect of genotype j on the growth rate of genotype k. These density-dependent effects could reflect competition for host resources, indirect interactions through the elicitation of the host immune system or any other within host process through which parasites could interact. Notice that $\boldsymbol{\Gamma}$, $\boldsymbol{\Sigma}$ and $\mathbf{H}$ are not necessarily symmetrical.

Finally, with $\boldsymbol{\varrho} \coloneqq \left(\varrho_k\right)_{k\in\mathcal{G}}$ being the basic growth rate vector, the parasite load vector $\mathbf{x}$ satisfies the following ordinary nonlinear differential equation

$$\frac{\mathrm{d}}{\mathrm{d}t}\mathbf{x} = \left(\boldsymbol{\varrho} + \boldsymbol{\Gamma}.\mathbf{g} - \boldsymbol{\Sigma}.\mathbf{z} + \mathbf{H}.\mathbf{x}\right) \odot \mathbf{x}, \tag{3.2.2}$$

where $\odot$ denotes the HADAMARD (element-wise) matrix product. Since the basic growth rate takes place in the only linear term of (3.2.2), it actually captures non only the rate at which a parasite genotype would grow at first if isolated but also the cost of public good and spite productions.

The within-host dynamics are summarised in Figure 3.2.1. Note that the total number of parameters for this part of the model is $3n^2 + 2n + 1$.

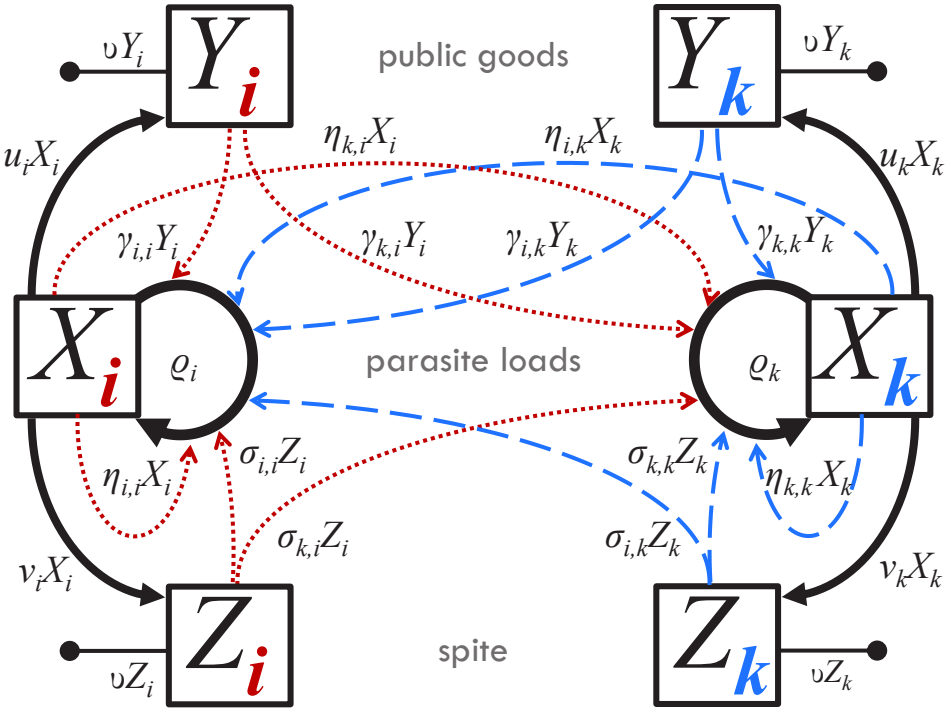

Figure 3.2.1. – Within-host flow diagram for two different genotypes i and k.
Plain arrows represent PP flows while dot-ended arrows represent public production clearance flows. Dotted arrows, respectively dashed arrows, are *per capita* growth rate modulation effects generated by genotype $\boldsymbol{i}$ parasites, respectively by genotype $\boldsymbol{k}$ parasites. Public goods ($G_{\boldsymbol{i}}$ and $G_{\boldsymbol{k}}$) increase the growth of all genotypes ($X_{\boldsymbol{i}}$ and $X_{\boldsymbol{k}}$), while spite ($Z_{\boldsymbol{i}}$ and $Z_{\boldsymbol{k}}$) only harms the other genotype.

3.2.3. Steady-state

These within-host dynamics are complex and, as explained in the next section, we will often need to summarise them using their steady state. We denote by $\widehat{.}$ a steady-state value of a variable. The steady-state vectors $\widehat{\mathbf{x}}$, $\widehat{\mathbf{g}}$ and $\widehat{\mathbf{z}}$ cancel out in equations (3.2.1), thus leading to two equalities

$$\begin{cases} \widehat{\mathbf{g}} = \mathbf{U}.\widehat{\mathbf{x}}, \\ \widehat{\mathbf{z}} = \mathbf{V}.\widehat{\mathbf{x}}. \end{cases} \tag{3.2.3}$$

Therefore a within-host equilibrium is fully determined by the parasite load vector $\widehat{\mathbf{x}}$.

If we assume, for the moment, that the values of $\widehat{\mathbf{x}}$ are non zero, setting (3.2.2) to 0 and using (3.2.3), it is straightforward that the only steady state parasite load vectors are the ones that satisfy

$$\mathbf{M}.\widehat{\mathbf{x}} = \boldsymbol{\rho}, \tag{3.2.4}$$

where $\mathbf{M}$ is the constant matrix sum

$$\mathbf{M} \coloneqq \boldsymbol{\Gamma}.\mathbf{U} - \boldsymbol{\Sigma}.\mathbf{V} + \mathbf{H}, \tag{3.2.5}$$

thereafter called *interaction matrix*.

Usually, and even more so for a random set of parameter values, $\mathbf{M}$ is not singular, which imples that $\widehat{\mathbf{x}}$ is unique and analytically found as

$$\widehat{\mathbf{x}} = -\mathbf{M}^{-1}.\boldsymbol{\rho}. \tag{3.2.6}$$

In the special case where the determinant of $\mathbf{M}$ is 0, equation (3.2.4) has an infinite number of solutions and there is no other option than to integrate numerically the within-host system ((3.2.1),(3.2.2)) to find $\lim_{t\to\infty} \mathbf{x}(t)$ (the generalized Moore-Penrose inverse matrix $\mathbf{M}^{+}$ does not necessarily match with the attractor coordinates). This problem can however be bypassed with small changes in the parameter values.

Let us now relax our assumption of non zero values of $\widehat{\mathbf{x}}$. This makes sense when a particular genotype did not take part in the inoculation of the host, implying that its parasite load is equal to 0. We then consider a partial combination of genotypes, that is to say any proper subset $\boldsymbol{i}$ of $\mathcal{G}$. The rows of equation (3.2.2) associated with the genotypes that do not belong to $\boldsymbol{i}$ are tautological at steady-state and therefore are removed. The new set of equations we obtain satisfies the assumption of non zero steady state values. The solution of equation (3.2.6) restricted to the rows that belong to $\boldsymbol{i}$ is the unique steady-state parasite load associated to the partial combination of genotypes $\boldsymbol{i}$ which we denote $\widehat{\mathbf{x}_{\boldsymbol{i}}}$ (see proof in appendix 3.b.1).

3.3. Linking the within and between-host levels

To eventually make inferences at the between-host level, we need to somehow simplify the within-host dynamics. In this part we introduce the class concept, which gives an epidemiological meaning to partial combinations of genotypes. We also nest within-host outcomes into the between host dynamics based on the assumption that the within-host steady-state is quickly reached. Put differently, we impose a time scale separation between the two levels. This assumption is commonly used in nested models (Mideo *et al.*, 2008) but here we show that it cannot be satisfied in the case of unlimited within-host growth and present a way of handling this situation via what we call *ultrainfection*.

3.3.1. Host and inoculum classes

We define a class as any combination of genotypes. Since there are $\mathcal{G}$ genotypes, there are $\wp(\mathcal{G})$ classes, which is the power set of $\mathcal{G}$. Mathematically, a class is any element $\boldsymbol{i}$ of $\wp(\mathcal{G})$. We call *susceptible* a host infected by no genotype (the class of which is the empty set $\emptyset$). We call *singly infected host* a host infected by only one genotype and *coinfected host* a host infected by at least two different genotypes. We call *rank* of a given class $\boldsymbol{i}$ the number of genotypes that belong to $\boldsymbol{i}$, that is $n_{\boldsymbol{i}} \coloneqq \mathrm{card}\boldsymbol{i}$. For computational purposes, it is useful to order these classes which is why we introduce a binary labelling operator in appendix 3.c.1.

Once a host is infected by a genotype combination, it may transmit any subset of its coinfecting genotypes. We call *inoculum* a combination of genotypes transmitted by an infected host. The set of all possible inocula is also $\wp(\mathcal{G})$. We assume that hosts infected by the same genotype combination are identical in every point. We also make no difference between inocula containing the same genotype combination, even if they originate from hosts infected by different genotype combinations.

3.3.2. Ultrainfection and constraints on susceptible and single infection classes

The susceptible state, is unstable if parasites grow in a singly infected host, i.e. if $\varrho_k > 0$, which we will assume from now on (the proof is shown in appendix (3.c.3) and involves the expression of the within-host jacobian matrix calculated in appendix (3.c.2)). As a consequence, no infection can end by the extinction of all genotypes: either the within-host dynamics reach a steady state, or at least one parasite load goes to infinity. In order to avoid the latter case (because it is not compatible with the time scale separation assumption), we invoke two modelling assumptions from the between-host dynamics, namely

1. death rates of infected hosts are proportional to the total parasite load,
2. the size of the host population is constant.

Following these assumptions, if a host is infected by an inoculum that causes an infinite parasite growth at the within-host level, its death rate is infinite (1.); it thus dies instantaneously upon infection and is replaced by a susceptible host (2.). To picture this, one can think of a singly infected host that would become infected by another parasite genotype which facilitates the growth of the first genotype, and *vice versa*, such that both parasite loads increase endlessly. If we assume that this process is much faster than the transmission process and that very high parasite loads eventually lead to host death, the host will die before infecting another host and is thus epidemiologically irrelevant. We

call this case *ultrainfection* since it cannot be considered within the superinfection and coinfection frameworks.

The drawback of allowing ultrainfection is that some parameter sets might result in genotypes that do not reach a steady state in any class, such that the between-host dynamics would be in fact governed by an effective number of genotypes n' smaller than n. To avoid these "shadow genotypes", one solution is to force the steady state in single infections to be both positive and stable. When a susceptible is infected by only one genotype, let us say k, the infected steady state parasite load is then $\widehat{x_{\{k\},k}}$ and its value is given by (3.2.6) applied for $n = 1$,

$$\widehat{x_{\{k\},k}} = -\frac{\varrho_k}{\eta_{k,k} + \gamma_{k,k} u_k} =: x_k^\circ, \tag{3.3.1}$$

given $\varrho_k > 0$, the single infection parasite load is positive and stable if and only if (for the proof of the stability see (3.c.4))

$$\eta_{k,k} < -\gamma_{k,k} u_k. \tag{3.3.2}$$

Since the effect of PG on self and the PG production rate are both assumed to be positive, this implies that the self density-dependent effect is negative ($\eta_{k,k} < 0$). One can interpret $\frac{1}{\eta_{k,k}}$ as the carrying capacity of (3.2.2). Inequality (3.3.2) will be checked for all parameter sets used thereafter.

3.3.3. Biological and epidemiological coinfection classes

When at least two genotypes coinfect the same host, finding the steady state reached by the system is a mathematical challenge for several reasons:

1. the number of possible steady states is an exponential function of the class rank,
2. the stability of a steady state cannot be analytically deduced from the parameters in the general case,
3. several steady states can be biologically meaningful at the same time, i.e. positive and stable (found with numerically computed eigenvalues),
4. the nonlinearity of the system causes unpredictability of the output given the initial conditions.

This leaves us with no other option than to numerically simulate higher rank infection events as follows.

First, we have to withdraw from the analysis all the host classes for which the associated (unique) steady state is not biologically meaningful. We thus say that an infected class is *biological* if its unique steady state is both positive and stable. Even though it is unstable and zero valued, the susceptible class is a biological class too. We denote the set of biological classes by $\mathcal{B} \subset \wp\left(\mathcal{G}\right)$. Note that the set of inocula arising from hosts that belong to $\mathcal{B}$ can be greater than $\mathcal{B}$ itself (high rank coinfections may stabilise the system). For instance, let k be a genotype absent from class $\boldsymbol{i}$ and let $\boldsymbol{i} \cup \{k\}$ be a biological class. If genotype k is such that it stabilises the within-host dynamics in a host of class $\boldsymbol{i} \cup \{k\}$ (by limiting the growth of highly spite producing genotypes for example), $\boldsymbol{i}$ may not be a biological host class even though $\boldsymbol{i}$ is a possible inoculum because it can be produced by biological class $\boldsymbol{i} \cup \{k\}$ hosts.

A class may be biologically meaningful but epidemiologically meaningless if no infection event leads to it. For this reason, we define the infection operator ϕ which has two arguments, the receiver host class $\boldsymbol{r}$ and the inoculum class $\boldsymbol{p}$. $\phi(\boldsymbol{r}, \boldsymbol{p})$ is the output class, that is the class into which a host from class $\boldsymbol{r}$ turns if it is infected by an inoculum from class $\boldsymbol{p}$. In terms of system dynamics theory, $\phi(\boldsymbol{r}, \boldsymbol{p})$ is the class associated to

the potentially new steady state the within-host system reaches after the perturbation corresponding to the inoculation. We show in the appendix 3.c.6 that non steady-state attractors can be avoided if the self density-dependent effects $\eta_{k,k}$ are negative and strong enough and if public production rates u_k and v_k are small enough. Note that $\phi(\boldsymbol{r},\boldsymbol{p})$ can be the empty set because ultrainfection is allowed for coinfected classes.

A biological infected class $\boldsymbol{i}$ is said to be *epidemiological* if it can appear during an epidemic, that is if there is at least one infection event involving two biological classes that leads to it. More formally, class $\boldsymbol{i}$ is epidemiological if there is a couple of biological classes $(\boldsymbol{r},\boldsymbol{d}) \in \mathcal{B}^2$, $\boldsymbol{r}$ being the receiver host class and $\boldsymbol{d}$ the donor host class, such that there exists an inoculum class $\boldsymbol{p}$ of $\boldsymbol{d}$ that satisfies $\phi(\boldsymbol{r},\boldsymbol{p}) = \boldsymbol{i}$. As an exception, the susceptible class is also epidemiological. The set of epidemiological classes is denoted by $\mathcal{E}$ (and $\mathcal{E}^\star$ if the susceptible class is excluded).

If a class is not epidemiological, then there is no infection event (not even by infecting susceptible hosts) to renew these hosts that inevitably recover or die, even if initially present. After some time, this non epidemiological compartment has completely vanished with no other consequence than having delayed an initial input of susceptibles. For this reason, we only consider epidemiological classes in the between-host dynamics of our model.

For formal definitions of $\mathcal{B}$, ϕ, and $\mathcal{E}$ see 3.c.5.

3.4. Between-host dynamics

In this part we use the steady state parasite loads and the host and inoculum class framework previously introduced to define the compartments and the flow rates of a deterministic between-host dynamical system. This system is conceived as an extended SIS model with sequential recovery in a randomly mixed population of constant size, which is a common framework in modelling of infectious diseases (Choisy & de Roode, 2010). However, unlike previous models where transmission is also sequential (that is only one genotype at a time) (Lion, 2013), this model allows for partial cotransmission, that is the possibility for any host class to transmit any subset of genotypes it is coinfected with. A consequence of this is that suceptibles can directly turn into coinfected hosts. Assuming also that the overall transmission rate is constant, the appropriate infection rate for partial cotransmission is given hereafter.

3.4.1. Infected hosts dynamics

Due to the time scale separation, infected hosts from the same class have the same parasite loads. Each host class is then considered as a compartment characterised by its proper time-dependent density $I_{\boldsymbol{i}}$. Notice the index-set notation analogous to the one used in Andreasen *et al.* (1997) for cross-immunity. These at most 2^n host class densities define the density vector $\mathbf{y} := (I_{\boldsymbol{i}})_{\boldsymbol{i}\in\mathcal{E}}$.

Infection events are due to uniformly random encounters between two hosts of different classes. The donor host can infect the receiver host with any class of inoculum it may generate (any non empty subset of its class), independently of the parasite genotypes the receiver is already infected by.

Recovery is allowed for every infected host class but only sequentially, which means that a given host can only recover from one parasite genotype at a time. Moreover, it does not provide any immunization. The between-host part of our model can therefore be seen as a generalization to multiple infections of the classical Susceptible-Infected-Susceptible model (Kermack & McKendrick, 1927).

Given all these assumptions, the density of any infected host i satisfies the following autonomous nonlinear ODE, where $\beta_{\boldsymbol{a},\boldsymbol{b},\boldsymbol{c}}$ refer to infection flows, $\theta_{\boldsymbol{a},\boldsymbol{b}}$ to recovery flows and $\mu_{\boldsymbol{a}}$ to death flows:

$$\frac{\mathrm{d}I_{\boldsymbol{i}}}{\mathrm{d}t} = \sum_{(\boldsymbol{r},\boldsymbol{d})\in(\mathcal{E}\setminus\{\boldsymbol{i}\})\times\mathcal{E}^\star} \beta_{\boldsymbol{r},\boldsymbol{d},\boldsymbol{i}} I_{\boldsymbol{r}} I_{\boldsymbol{d}} + \sum_{\boldsymbol{d}\in\mathcal{E}} \theta_{\boldsymbol{d},\boldsymbol{i}} I_{\boldsymbol{d}} - \left(\sum_{(\boldsymbol{d},\boldsymbol{\ell})\in\mathcal{E}^\star\times(\mathcal{E}\setminus\{\boldsymbol{i}\})} \beta_{\boldsymbol{i},\boldsymbol{d},\boldsymbol{\ell}} I_{\boldsymbol{d}} + \sum_{\boldsymbol{\ell}\in\mathcal{E}\setminus\{\boldsymbol{i}\}} \theta_{\boldsymbol{i},\boldsymbol{\ell}} + \mu_{\boldsymbol{i}} \right) I_{\boldsymbol{i}}, \tag{3.4.1}$$

the five right side terms respectively correspond to

1. the infection input flow, by which donor hosts $\boldsymbol{d}$ infect receiver hosts $\boldsymbol{r}$ which become hosts $\boldsymbol{i}$,
2. the recovery input flow, by which hosts $\boldsymbol{d}$ lose one genotype and become hosts $\boldsymbol{i}$,
3. the infection output flow, by which donor hosts $\boldsymbol{d}$ infect receiver hosts $\boldsymbol{i}$ which become hosts $\boldsymbol{\ell}$,
4. the recovery output flow, by which where hosts $\boldsymbol{i}$ lose one genotype and become hosts $\boldsymbol{\ell}$,
5. the mortality output flow, by which where hosts $\boldsymbol{i}$ die.

3.4.2. Susceptible host dynamics

We assume a constant host population size ($s^\circ > 0$). Susceptible hosts density may decrease through infection and may increase through recovery or dead infected hosts replacement. Overall, S satisfies the following ODE:

$$\frac{\mathrm{d}S}{\mathrm{d}t} = \sum_{\boldsymbol{d}\in\mathcal{L}^\star} \mu_{\boldsymbol{d}} I_{\boldsymbol{d}} + \sum_{(\boldsymbol{r},\boldsymbol{d})\in\mathcal{L}^{\star 2}} \beta_{\boldsymbol{r},\boldsymbol{d},\emptyset} I_{\boldsymbol{r}} I_{\boldsymbol{d}} + \sum_{\boldsymbol{d}\in\mathcal{L}^\star} \theta_{\boldsymbol{d},\emptyset} I_d - \sum_{(\boldsymbol{d},\boldsymbol{\ell})\in\boldsymbol{E}^{\star 2}} \beta_{\emptyset,\boldsymbol{d},\boldsymbol{\ell}} I_{\boldsymbol{d}} S, \tag{3.4.2}$$

where the second term corresponds to the ultrainfection input flow.

3.4.3. Modelling the epidemiological events

Making explicit the infection, recovery and death rates used in (3.4.1) and (3.4.2) is the key step of the nesting (Mideo *et al.*, 2008). Here we include the within-host outcome into between-host dynamics through the dependance of the epidemiological events on the steady-state parasite loads. From now on, $x_{\boldsymbol{i},k}$ denotes the within-host steady-state parasite load of genotype k in host class $\boldsymbol{i}$ (the hat is omitted to avoid confusion with between-host steady-state).

We use constants to characterise the overall rate of each event type, that is infection (β), recovery (θ), and death (μ). For instance, doubling β will double the rate at which infection events occur, for a given host density vector $\mathbf{y}$. β, θ and μ are the only epidemiological parameters.

3.4.3.1. Infection rates

We assume that all infected hosts have the same overall transmission rate, equal to β, the constant transmission factor. This is motivated by two reasons. The first one is that the inoculum dose cannot affect the outcome of the infection because of the within-host dynamics determinism; further, we assume that the total parasite load does not affect the contact rate of infected hosts with other hosts. The second reason to keep the transmission rate constant is to make sure that if higher parasite loads, leading to higher host death rate, are selected, this will be because of within-host competition and not because of a transmission advantage. We thus avoid imposing a trade-off relationship between virulence and transmission. We model transmission by independent random drawing of each genotype within each inoculum, using frequencies (that is relative parasite loads) as proxies for probabilities of being drawn.

The rate at which a receiver host $\boldsymbol{r}$ turns into a host $\boldsymbol{i}$ through infection by a donor $\boldsymbol{d}$ is given by

$$\beta_{\boldsymbol{r},\boldsymbol{d},\boldsymbol{i}} \coloneqq \beta \sum_{\substack{\boldsymbol{p}\in\wp(\boldsymbol{d}) \\ \phi(\boldsymbol{r},\boldsymbol{p})=\boldsymbol{i}}} |\boldsymbol{p}| \prod_{k\in\boldsymbol{p}} \frac{x_{\boldsymbol{d},k}}{\sum_{\ell\in\boldsymbol{d}} x_{\boldsymbol{d},\ell}} \prod_{k\in\boldsymbol{d}\setminus\boldsymbol{p}} \left(1 - \frac{x_{\boldsymbol{d},k}}{\sum_{\ell\in\boldsymbol{d}} x_{\boldsymbol{d},\ell}}\right), \tag{3.4.3}$$

where

1. β is the constant infection factor,
2. $\sum_{\substack{\boldsymbol{p}\in\wp(\boldsymbol{d}) \\ \phi(\boldsymbol{r},\boldsymbol{p})=\boldsymbol{i}}}$ is the sum over all possible inocula of host $\boldsymbol{d}$ that turn host $\boldsymbol{r}$ into host $\boldsymbol{i}$,
3. $|\boldsymbol{p}|$ is the rank of the inoculum class (number of genotypes),
4. $\prod_{k\in\boldsymbol{p}} \frac{x_{\boldsymbol{d},k}}{\sum_{\ell\in\boldsymbol{d}} x_{\boldsymbol{d},\ell}}$ is the product of genotype frequencies in $\boldsymbol{d}$ over all genotypes of $\boldsymbol{p}$,

5. $\prod_{k\in\boldsymbol{d}\setminus\boldsymbol{p}}\left(1-\frac{x_{\boldsymbol{d},k}}{\sum_{\ell\in\boldsymbol{d}}x_{\boldsymbol{d},\ell}}\right)$ is conversely the product of the complementary frequencies over the remaining genotypes of $\boldsymbol{d}$.

Importantly, $\beta_{\boldsymbol{r},\boldsymbol{d},\boldsymbol{i}}$ is an infection rate and not a transmission rate, as it quantifies the flow between two host compartments due to infection. In models that consider only one kind of host that can be infected, S, and only one kind of infected host (I), there is only one infection rate, β (and βSI is the infection flow) (Anderson & May, 1982). This infection rate is also the transmission rate because there is only one host class that can be infected (S) and because infection always leads to the same host class (I). The infection rate - transmission rate equality still holds in more complex models with several infected host types if genotypes are transmitted one at a time (Alizon, 2013a; Lion, 2013). In our model of transmission however, donor hosts can cotransmit any subset of their coinfecting genotype combination while receiver hosts may not be affected by such contacts or may be affected differently according to within-host parameters. Infection flows are thus unpredictable here because they depend, through the infection operator ϕ, on the outcomes of the within-host dynamics, which determine how steady-state parasite loads are affected by contamination of new genotypes. Because ODEs (3.4.1) and (3.4.2) only describe flows between compartments, $\beta_{\boldsymbol{r},\boldsymbol{d},\boldsymbol{i}}$ refers to infection rates and not to more intuitive transmission rates.

Nonetheless, it is possible to make an interpretation of the transmission process based on the definition of $\beta_{\boldsymbol{r},\boldsymbol{d},\boldsymbol{i}}$. To do so, one should consider that transmission is a process that does not depend on the outcome of the contamination (which becomes an infection event only if the receiver host class changes). In other words, if we denote by $\beta_{\boldsymbol{d}}$ the overall transmission rate of infected host class $\boldsymbol{d}$, $\beta_{\boldsymbol{r},\boldsymbol{d},\boldsymbol{i}}$ gives $\beta_{\boldsymbol{d}}$ when ignoring the condition $\phi(\boldsymbol{r},\boldsymbol{p})=\boldsymbol{i}$ under the sum or when assuming that all the inocula classes $\boldsymbol{p}$ of $\boldsymbol{d}$ are epidemiological.

In the case we assume that all the inocula classes of the donor host class $\boldsymbol{d}$ are epidemiological, $\phi(\emptyset,\boldsymbol{p})=\boldsymbol{p}$ for all $\boldsymbol{p}\in\wp(\boldsymbol{d})^\star$ and $\beta_{\boldsymbol{d}}$ is measured as the overall transmission rate to a susceptible, that is

$$\beta_{\boldsymbol{d}}=\sum_{\boldsymbol{p}\in\wp(\boldsymbol{d})^\star}\beta_{\emptyset,\boldsymbol{d},\boldsymbol{p}}=\beta\sum_{\boldsymbol{p}\in\wp(\boldsymbol{d})}|\boldsymbol{p}|\prod_{k\in\boldsymbol{p}}\frac{x_{\boldsymbol{d},k}}{\sum_{\ell\in\boldsymbol{d}}x_{\boldsymbol{d},\ell}}\prod_{k\in\boldsymbol{d}\setminus\boldsymbol{p}}\left(1-\frac{x_{\boldsymbol{d},k}}{\sum_{\ell\in\boldsymbol{d}}x_{\boldsymbol{d},\ell}}\right).$$

Subsequently, it is possible to define the rate at which a given genotype k is transmitted by hosts from class $\boldsymbol{d}$. We denote this rate $\beta_{\boldsymbol{d},k}$. We show in the appendix 3.d.1 that

$$\forall\boldsymbol{d}\in\mathcal{E}^\star,\beta_{\boldsymbol{d}}\quad=\quad\beta,\tag{3.4.4}$$

as expected, but also that

$$\forall\boldsymbol{d}\in\mathcal{E}^\star,\forall k\in\boldsymbol{d},\beta_{\boldsymbol{d},k}=\beta\frac{x_{\boldsymbol{d},k}}{\sum_{\ell\in\boldsymbol{d}}x_{\boldsymbol{d},\ell}}\left(2-\frac{x_{\boldsymbol{d},k}}{\sum_{\ell\in\boldsymbol{d}}x_{\boldsymbol{d},\ell}}\right).\tag{3.4.5}$$

As a consequence, the transmission rate of a host does not depend either on the total parasite load nor on the number of infecting genotypes. A higher parasite load thus confers no transmission advantage in single infections for a given genotype. Higher relative parasite loads do confer an advantage in coinfections because the probability that each genotype is transmitted depends on its frequency. Transmission rates of coinfected hosts

thus reflect the outcome of the within-host dynamics.

3.4.3.2. Recovery rates

Recovery rates are the rate at which hosts $\boldsymbol{d}$ turn into hosts $\boldsymbol{i}$ through recovery,

$$\theta_{\boldsymbol{d},\boldsymbol{i}} \coloneqq \theta \sum_{\substack{k\in\boldsymbol{d} \\ \phi(\varnothing,\boldsymbol{d}\setminus\{k\})=\boldsymbol{i}}} 1, \tag{3.4.6}$$

where

1. θ is the constant recovery factor,
2. $\sum_{\substack{k\in\boldsymbol{d} \\ \phi(\varnothing,\boldsymbol{d}\setminus\{k\})=\boldsymbol{i}}} 1$ is the number of genotypes of $\boldsymbol{d}$ that can reach class $\boldsymbol{i}$ through a recovery event.

Note that the condition $\phi(\varnothing,\boldsymbol{d}\setminus\{k\})=\boldsymbol{i}$ implies that $\boldsymbol{i}$ is an epidemiological class.

For a given couple of host classes $(\boldsymbol{d},\boldsymbol{i})\in\mathcal{E}^\star\times\mathcal{E}$, recovery is thus interpreted as a constant rate θ multiplied by the number of ways a class $\boldsymbol{d}$ host can recover and turn into a class $\boldsymbol{i}$ host, which is also the number of genotypes the recovery from which leads the parasite loads to the steady state $\widehat{\mathbf{x}_{\boldsymbol{i}}}$. This number is greater than one if and only if several genotypes cannot survive in the coinfection without the presence of each other.

The total recovery rate of a given infected host class $\boldsymbol{d}$ is $|\boldsymbol{d}|\theta$ since recovering from a genotype always leads to another host class.

3.4.3.3. Death rates

The death rates are given as the sum over all parasite loads times a constant death factor,

$$\mu_{\boldsymbol{i}} \coloneqq \mu\sum_{k\in\boldsymbol{d}} x_{\boldsymbol{d},k}. \tag{3.4.7}$$

Death rates are assumed to be linear functions of the total parasite load: the higher the parasite load a host carries, the more rapidly it dies. Total parasite load can therefore be used as a proxy for virulence.

3.4.4. Synthesis

The following master equation captures the between-host dynamics:

$$\frac{\mathrm{d}}{\mathrm{d}t}\mathbf{y} = \mathbf{\Phi}.(\mathbf{y}\otimes\mathbf{y}) - (\mathbf{\Psi}.\mathbf{y})\odot\mathbf{y} + (\mathbf{\Xi}-\mathbf{\Theta}-\mathbf{\Delta}).\mathbf{y}, \tag{3.4.8}$$

where $\mathbf{\Phi}$ is the infection input flow matrix, $\mathbf{\Psi}$ is the infection output flow matrix, $\mathbf{\Xi}$ is the recovery input flow matrix, $\mathbf{\Theta}$ is the recovery output flow matrix and $\mathbf{\Delta}$ is the death matrix. There is no general expression for these matrices because their structure depends on the way classes are ordered. For an explicit definition of these matrices according to the labelling we use for computing the model, see 3.d.2.

Although (3.4.8) cannot be solved analytically it is a useful expression of the between-host dynamics that allows for fast computing.

Between-host dynamics are summarised in Figure 3.4.1.

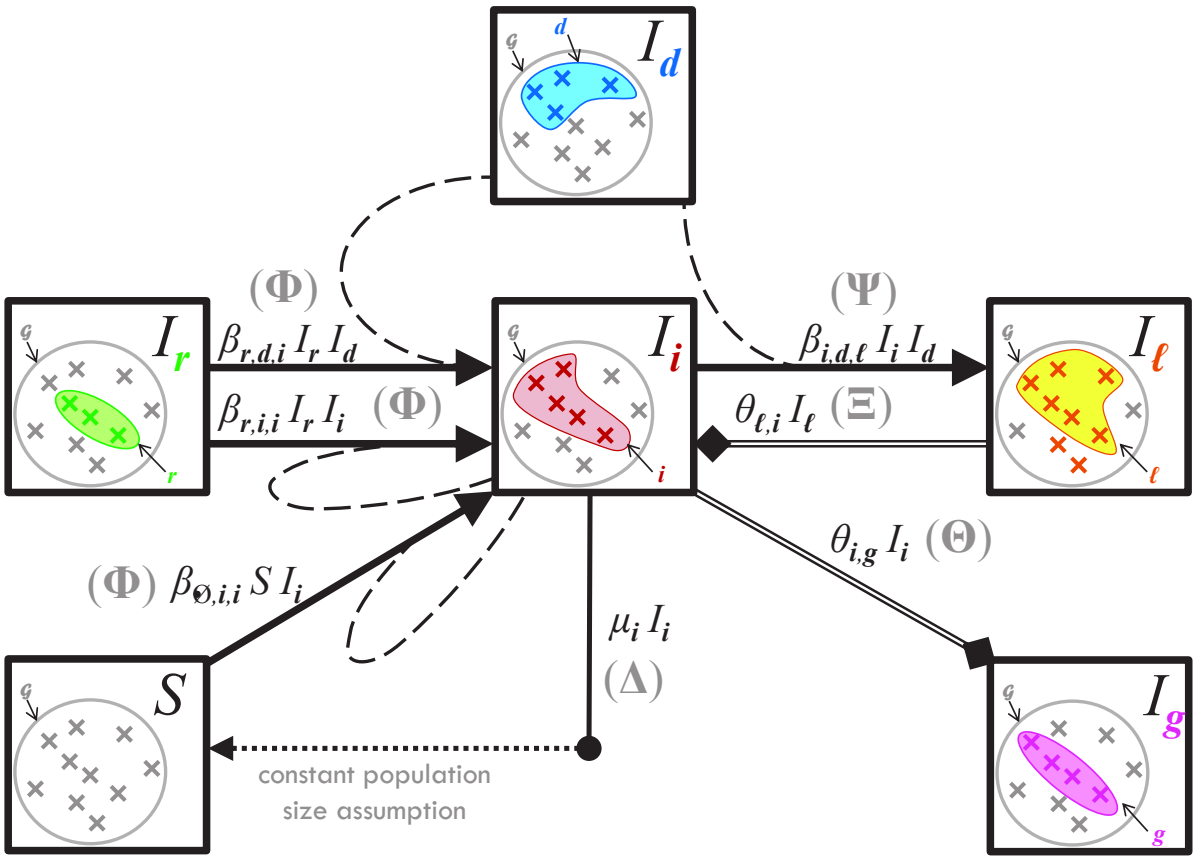

Figure 3.4.1. – Between-host flow diagram focused on host class $\boldsymbol{i}$, represented here as a set of 5 out of $n = 10$ genotypes. Not all the flows involving $I_{\boldsymbol{i}}$ are shown but each type of event is shown at least once. The rates are given as they appear in the ODE satisfied by $I_{\boldsymbol{i}}$. The matrix through which each flow is introduced into the master equation is shown in brackets. The solid filled triangle-ended arrows stand for infection flows and are joined by dashed lines that indicate the donor. The solid hollow square-ended arrows stand for recovery flows. While a host can be infected by several genotypes simultaneously, it recovers only from one genotype at a time. The dot-ended arrow followed by a dotted arrow represents the death flow that leads to the susceptible compartment, as a consequence of the constant population size assumption.

3.5. Basic reproduction numbers and epidemiological feedback

The basic reproduction number, denoted by $\mathcal{R}_0$, is the most widely used parameter in epidemiological modelling (Kermack & McKendrick, 1932; Anderson & May, 1979; Alizon, 2013a). $\mathcal{R}_0$ is defined as the expected number of secondary infections produced by a single infected individual during its entire period of infectiousness in a fully susceptible population (Diekmann *et al.*, 1990; Anderson & May, 1991; Diekmann & Heesterbeek, 2000). Hence, it is often interpreted as the fitness of the parasite (Anderson & May, 1982; Alizon *et al.*, 2009; Alizon & Michalakis, 2015) or as the inverse of the minimum proportion of vaccinated hosts required to eradicate an infectious disease (Diekmann & Heesterbeek, 2000). More generally, $\mathcal{R}_0$ corresponds to the epidemiological threshold above which the endemic state is always reached (i.e. when $\mathcal{R}_0 > 1$).

The latest and most general method to determine the basic reproduction number relies on the asymptotic instability of the disease free equilibrium (van den Driessche & Watmough, 2002; Hurford *et al.*, 2010), that is to say $\mathcal{R}_0$ greater than 1 if and only if the between-host steady state where there are only susceptibles is unstable. This method, called 'next-generation', is usually convenient because it does not require finding the infected steady state densities. On the other hand, it may not provide any information on the proportion of susceptible or infected hosts at the infected steady state. According to the instability of the 'disease free equilibrium', the 'next-generation basic reproduction number' of our model is

$$\mathcal{R}_0^{\mathrm{I}} = \beta s^\circ \max_{\boldsymbol{i}\in\mathcal{E}^\star} \left(\left(\theta n_{\boldsymbol{i}} + \mu x_{\boldsymbol{i},\bullet}\right)^{-1} \sum_{\substack{\boldsymbol{p}\in\wp(\boldsymbol{i}) \\ \phi(\emptyset,\boldsymbol{p})=\boldsymbol{i}}} |\boldsymbol{p}| \prod_{k\in\boldsymbol{p}} \frac{x_{\boldsymbol{i},k}}{x_{\boldsymbol{i},\bullet}} \prod_{k\in\boldsymbol{d}\setminus\boldsymbol{p}} \left(1 - \frac{x_{\boldsymbol{i},k}}{x_{\boldsymbol{i},\bullet}}\right) \right), \tag{3.5.1}$$

where $\bullet$ stands for the sum over the given index (see proof in 3.e.1).

Other methods calculate $\mathcal{R}_0$ via the positivity condition of the infected steady state density (Heffernan *et al.*, 2005; Roberts, 2007). In this case $\mathcal{R}_0$ is simply the inverse of the proportion of the remaining susceptibles (Dietz & Schenzle, 1985). If we call J the sum of the infected hosts densities, we have

$$\widehat{S} + \widehat{J} = s^\circ,$$

which gives the following 'endemic basic reproduction number'

$$\widehat{J} > 0 \Longleftrightarrow \mathcal{R}_0^{\mathrm{II}} := \frac{s^\circ}{\widehat{S}} > 1. \tag{3.5.2}$$

This quantity, which is more specific to our model, can also be written as a function of the steady-state marginal arithmetic means of infection, recovery and death rates, as

$$\mathcal{R}_0^{\mathrm{II}} = \frac{\left|\mathcal{E}^\star\right| \overline{\overline{\beta_{\emptyset,\bullet,\bullet}}} s^\circ}{\overline{\theta_{\bullet,\emptyset}} + \overline{\mu_\bullet}}, \tag{3.5.3}$$

where the marginal arithmetic means over one and two indices are respectively denoted by $\overline{y_{\bullet,j}} := \sum_i y_{i,j} f_i$ and $\overline{\overline{y_{\bullet,\bullet}}} := \sum_j \overline{y_{\bullet,j}} f_j$ (see proof in 3.e.2).

These two basic reproduction numbers share two important features.

First, like the basic reproduction number of simple models (such as SIS and SIR),

they are the ratio of a transmission factor in a fully susceptible host population over a sum of recovery and death rates. This is classically interpreted as the expected number of secondary infected hosts at the beginning of an epidemic, where there is only one infected host (as the transmission rate is multiplied by the infected host life expectancy).

Second, $\mathcal{R}_0 > 1$ means that there is at least one infected compartment that is non zero at steady state. This does not provide any information, however, on which host class and parasite genotype has reached this steady state.

Conversely, the definition of the infection, recovery and death rates involved in the basic reproduction number differs between these definitions. The next-generation basic reproduction number ($\mathcal{R}_0^{\mathrm{I}}$) is determined by the within-host parameters of the genotype that maximises the quantity. Therefore a change in epidemiological parameters does not affect this basic reproduction number since such changes do not affect the class of the maximising genotype. In the endemic basic reproduction number ($\mathcal{R}_0^{\mathrm{II}}$), however, the involved rates are arithmetic means that depend on the distribution of host class frequencies at steady state. Therefore it is possible for $\mathcal{R}_0^{\mathrm{II}}$ to show complex behaviours when epidemiological parameters vary.

Because between-host dynamics are nonlinear, changes in epidemiological parameters that determine the rates of epidemiological events can cause non trivial modifications of the steady state. These are often referred to as epidemiological feedbacks (Alizon *et al.*, 2013). We prove in the appendix 3.e.3 that the endemic basic reproduction number can capture these while the next-generation basic reproduction number cannot. This is also illustrated in Figure 3.5.1.

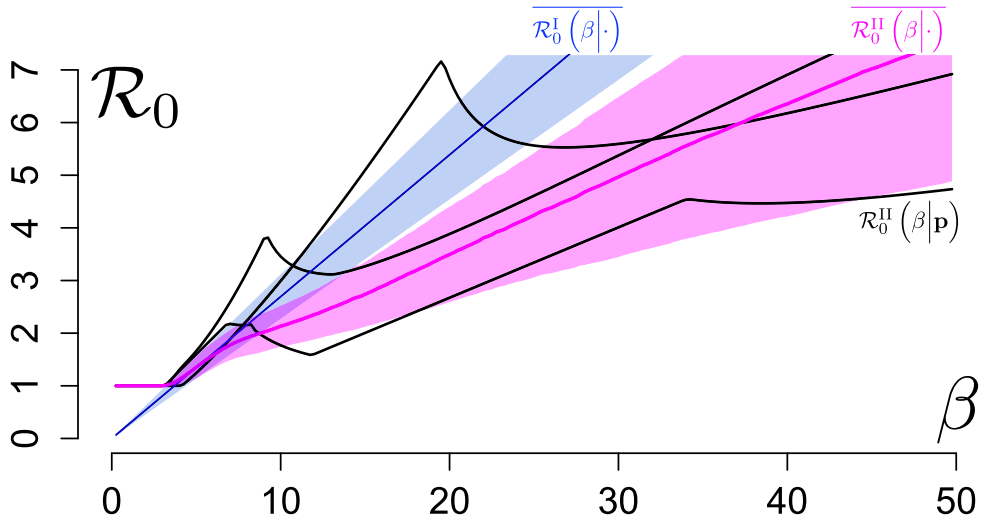

Figure 3.5.1. – Apprehending epidemiological feedbacks through the endemic basic reproduction number.

Considering five parasite genotypes ($n = 5$), 300 within-host parameter sets were randomly generated from the same uniform distributions (see below) and 200 epidemic simulations were ran with each parameter set with a different constant transmission factor β ranging from 0 to 50, the constant recovery and death factors being fixed ($\mu = 5$ and $\theta = 3$). The initial number of infected hosts was set to $10^{-3}s^{\circ}$, equally distributed to all the epidemiological host classes. Both basic reproduction numbers were calculated according to (3.5.1) and (3.5.2) for each run. $\mathcal{R}_0^{\mathrm{II}}$ was also numerically derived twice with respect to β. Over all parameter sets and all values of β, the standard deviation of $\left|\frac{\partial^2 \mathcal{R}_0^{\mathrm{II}}}{\partial \beta^2}\right|$ is about 0.11 and the maximum is about 3,94. The figure shows the mean of $\mathcal{R}_0^{\mathrm{I}}$ (thin solid line) and $\mathcal{R}_0^{\mathrm{II}}$ (thick solid line) as a function of β over the 300 parameter sets, along their standard deviation (respectively the light blue area and the pink area). The $\mathcal{R}_0^{\mathrm{II}}$ of three particular parameter sets (black lines) are also given as examples of strong epidemiological feedbacks. The within-host parameters were drawn in the standard uniform distribution $\mathcal{U}(0,1)$, excepted for $\eta_{ij}, i \neq j$, drawn in $\mathcal{U}(-1,1)$ and $\eta_{i,i}$ was calculated as $-\frac{\varrho_i}{x_i^{\circ}} - \gamma_{i,i}u_i$ with x_i° drawn in $\mathcal{U}(0,1)$. The standard clearing rate v was fixed to 1.

Our simulations in Fig. 3.5.1 show that $\mathcal{R}_0^{\mathrm{II}}$ is a nonlinear function of intermediate values of β (even after averaging over hundreds of parameter sets), confirming that it captures epidemiological feedbacks. Moreover, individual parameter combination (dotted lines) often exhibit local minima of $\mathcal{R}_0^{\mathrm{II}}$. Therefore, any increase or decrease in β starting from this minimum will increase the steady state total prevalence of infection. This means that public health interventions that decrease transmission could increase disease spread or, conversely, that factors increasing contact rate between hosts could slow down disease spread. This unexpected effect is correlated with genotypic diversity since the median of $\min\left(\frac{\mathrm{d}\mathcal{R}_0^{\mathrm{II}}}{\mathrm{d}\beta}\right)$ is -3.33×10^{-2} for the $n = 5$ results shown in Figure 3.5.1 and -1.05×10^{-5} in similar simulations done for $n = 2$ (not shown).

To understand the phenomenon that leads to the non-linearities in $\mathcal{R}_0^{\mathrm{II}}$, it helps to consider the case of two genotypes that can coinfect the same host. When β is hardly large enough for $\mathcal{R}_0^{\mathrm{II}}$ (and $\mathcal{R}_0^{\mathrm{I}}$) to be greater than one, the genotype with the lowest para-

site load in single infections is the only one that becomes endemic. The second genotype is epidemiologically cleared because it kills hosts faster, such that its proper basic reproduction number is lower than one (recall that transmission does not increase in parasite load). When β is large enough to compensate for the higher death rate induced by the second genotype, this genotype also spreads in the host population. Susceptible hosts are turned into singly-infected hosts at first, but since the two genotypes can coinfect the same host, both singly-infected host classes infect one another and become coinfected hosts. Nonlinearities can then appear if the total parasite load of the coinfected host is greater than the parasite load of the singly-infected. Indeed, part of the singly-infected hosts become coinfected and then die more rapidly than if they had remained singly infected, so the basic reproduction number $\mathcal{R}_0^{\mathrm{II}}$ decreases, even if β has increased. Note that our model shows coexistence of parasite genotypes not over the evolutionary time scale between singly infected hsots as showed in previous sutdies Pugliese (2002); Boldin & Diekmann (2008), but over the epidemic time scale with the persistence of coinfected hosts.

An analoguous reasoning can be done in case of superinfection. As above, the genotype with the highest parasite load in single infections spreads in the population already infected by the first genotype only if β is large enough so it compensates the higher death rate of its singly-infected hosts. Nonlinearities can then appear if the second genotype superinfects the infected hosts infected by the first genotypes. Part of the latter hosts becomes infected by the second genotype and dies more rapidly than if it had remained infected by the first genotype. Again $\mathcal{R}_0^{\mathrm{II}}$ decreases, even though β has increased.

If nonlinearity is possible for only two genotypes, it is even more favoured for a higher number of genotypes because the infection patterns can be a combination of superinfections and coinfections, thus multiplying the sources of nonlinearity.

3.6. Discussion

There is a crying lack of general models for multiple infections. The few exceptions that allow for more than two parasite genotypes rely on very stringent assumptions (May & Nowak, 1995; Lion, 2013). Here, we introduce a novel model with many potentialities. Above all, it can include any number of unrelated different parasite genotypes whereas the vast majority of existing models are restricted to a single monomorphic parasite, or few related parasites. Our model also brings new features to infectious diseases modelling.

The first feature is the explicit modelling of diverse within-host dynamics, where the host plays the role of an isolated constant ecosystem in which parasites grow. As in population dynamics (Verhulst, 1838) and multispecies ecological models (Lotka, 1925; Volterra, 1928), the growth rate of each parasite genotype is affected by its own density and the density of the other genotypes. Public productions (public goods and spite) are also taken into account through their own proper dynamics. Along with parasite-load dependent effects, public productions enrich the diversity of within-host dynamics and outcomes. Although public goods and spite have already been integrated in within-host dynamics (Brown *et al.*, 2002; West & Buckling, 2003; Buckling & Brockhurst, 2008), they have never been included together and linked with an epidemiological model, while it is known that some parasites can produce both public goods and spite with epidemiological consequences (Garbutt *et al.*, 2011). Our model can also integrate additional interactions, especially competition for host resources, host immune response and cross immunity through the parasite-load dependent effects.

Nested dynamics have already been tackled (Mideo *et al.*, 2008; Choisy & de Roode, 2010), but have never been generalised to several within-host interactions and for more than two parasite genotypes. This flexibility generates a great diversity of infection patterns which increases exponentially, as the number of parasite combinations, with the number of considered genotypes.

In particular, linking the two levels allows us to identify a biological scenario that the superinfection and the coinfection hypotheses fail to capture. This occurs when genotype combinations are unstable and cause unlimited growth. Indeed, while several genotypes can grow inside the host (as in coinfections), the host may vanish at the host population level (as in superinfections) because of infinite death rate. We call such pattern ultrainfection.

A second new feature is the set of definitions of biological and epidemiological classes for host and inocula. These definitions allow us to build functions to go beyond the classical superinfection - coinfection dichotomy (Nowak & May, 1994; May & Nowak, 1995) which has proved to be problematic (Alizon & van Baalen, 2008). A final original feature of the between-host part of the model allows for partial cotransmission, that is an infected host can infect another host with any subset of its coinfecting genotypes combination, unlike the other multiple infection models that assume sequential (one genotype at a time) or all-or-nothing transmission (but see Alizon (2013b)).

Epidemiological feedbacks drive between-host outcomes (Alizon, 2013a) and selective pressures (Alizon *et al.*, 2013). Despite the complexity of our model, we show that it is possible to capture these feedbacks through the endemic basic reproduction number. As shown in figure 3, in some situations the basic reproduction number, and thus disease prevalence, can increase even if the (constant) transmission factor decreases, because of the multiplicity of genotypes. This effect is missed by methods that are based on next-generation basic reproduction number (Anderson & May, 1983) because it is equal to the endemic basic reproduction number when only one genotype is considered (see appendix

3.e.4). Overlooking parasite genotypic diversity can therefore have major consequences, since quarantine measures could for instance increase disease spread instead of preventing it. Overall, we argue that accounting for parasite genotypic diversity and using the endemic basic reproduction number to study epidemiological feedbacks is key to controlling infectious diseases.

Since this is the first analysis of this multi-strain multiple infection model, we had to make some simplifying assumptions. Some of these, such as the time scales separation, are constitutive of the model but others could be alleviated or modified. In particular, the assumptions linking within-host steady state variables (population sizes) to epidemiological parameters (transmission rate, virulence and recovery rate) can be changed without affecting the between-host master equation. This is important as these assumptions are likely to depend on the biological system considered. Here, we assumed the transmission rate to be constant, which has the advantage that the only selective pressure allowing the persistence of virulent parasites has to come from the within-host level. Further extensions of this model could consider a link between parasite load and transmission rate. However, earlier models have shown that further assumptions would then be needed because if both virulence and transmission rates are linear functions of parasite load, natural selection will always favour the strains with the highest possible level of virulence (Alizon & van Baalen, 2005). One possibility could be to focus on a biological system where these relationships have been parameterised such as HIV in humans (Fraser *et al.*, 2007), myxomatosis in rabbits (Dwyer *et al.*, 1990), *Ophryocystis elektroscirrha* in monarch butterflies (de Roode *et al.*, 2008) or the cauliflower mosaic virus in turnips (Doumayrou *et al.*, 2013).

The between-host dynamics used here are also based on simplifying assumptions that may not be suitable for all host-parasite systems: time scale separation, random mixing, host homogeneity, lack of immunization and constant population size, range from the strongest and hardest to adapt from the given equations to the weakest and easy to relax.

Finally, a direct application of this model has to do with parameter inference. Indeed, for many diseases we have detailed epidemiological data on the prevalence of coinfections that include combinatorial diversity (for instance in the case of human papillomavirus (Garland *et al.*, 2009)). Such data, possibly combined with information on within-host processes, could allow us to compare between models and estimate parameters.

Overall, our model opens new perspectives for investigating the evolution of parasite traits such as virulence and public goods and spite production rates in multiple infections owing to its capacity of handling the combinatorial complexity of cotransmissions and epidemiological feedbacks.

Appendix

3.a. Notations

notation	$\in$	type	meaning
		mathematical objets	
sets and associated notations			
$\mathbb{N},\mathbb{Z}$		set	of natural numbers, integers
$\mathbb{Q},\mathbb{R},\mathbb{C}$		division ring	of rationals, real, complex numbers
$\in,\notin$			belongs to, does not belong to
$\ni,\not\ni$			contains, does not contain
$\mathfrak{M}$		set	of matrices (including vectors)
$\mathcal{A}$		set	of applications
$\wp$		set	power set
$.^\star$		set	without 0 or the empty set
$[\![m;p]\!]$		set	$[m;p]\cap\mathbb{N}$
$\lvert.\rvert$		cardinality	number of elements of a set
$\setminus$		operator	set-theoretic difference
$\aleph_0$		cardinality	of the natural numbers ($\aleph_0 := \lvert\mathbb{N}\rvert$)
$\max_I, \min_I$		element	the biggest, the smallest, of a set indexed by I
elementary notations			
$:=$			equal by definition
a	$\mathbb{R}$	scalar	constant
A	$\mathcal{A}(\mathbb{R})$	scalar	time-dependent variable
$\boldsymbol{a}$	$\wp(\mathbb{N})$	set	subset of $\mathbb{N}$
$\mathbf{a}$	$\mathfrak{M}(\mathbb{R})$	vector	(may be line or colum vector)
$\mathbf{A}$	$\mathfrak{M}(\mathbb{R})$	matrix	
$\Re$	$\mathbb{R}$	scalar	real part of a complex number
$\mathbb{I}_{\{A\}}$	$\{0;1\}$	variable	dummy variable of condition A
$\delta_{i,j}$	$\mathcal{A}\left(\mathbb{R}^2,\{0;1\}\right)$	number	KRONECKER's delta, 1 if $i=j$, null otherwise
$\mathbf{0}_m$	$\mathfrak{M}_{1,m}(\mathbb{R})$	vector	m-dimensional null vector, $\begin{pmatrix}0 & 0 & \cdots & 0\end{pmatrix}_m$
$\mathbf{1}_m$	$\mathfrak{M}_{1,m}(\mathbb{R})$	vector	m-dimensional unit vector, $\begin{pmatrix}1 & 1 & \cdots & 1\end{pmatrix}_m$
$\mathbf{e}_i^{(m)}$	$\mathfrak{M}_{1,m}(\mathbb{R})$	vector	i-th vector of the $\mathbb{R}^m$ standard basis
$\mathbf{0}_{m,p}$	$\mathfrak{M}_{m,p}(\mathbb{R})$	matrix	$m\times p$ zero matrix
$\mathbf{I}_m$	$\mathfrak{M}_{m,m}(\mathbb{R})$	matrix	$m\times m$ identity matrix
$\mathbf{J}$	$\mathfrak{M}(\mathbb{R})$	matrix	jacobian matrix
Sp	$\mathbb{C}$	set	spectrum of a square matrix
s	$\mathbb{R}$	set	spectral bound of a square matrix
ρ	$\mathbb{R}$	set	spectral radius of a square matrix

Table 3.a.1. – List of the notations used in the text and in the appendix, with remarks

notation	∈	type	meaning
arithmetical operations			
$\lfloor . \rfloor$			floor function
mod_m			modulo operation, $m \in \mathbb{Z}, \mathrm{mod}_m(a) = c \iff a \equiv c\,[m]$
$\cdot_{i_1,\ldots,i_{k-1},\bullet,i_{k+1},\ldots}$			sum over the k-th index
$\overline{\cdot_{i_1,\ldots,i_{k-1},\bullet,i_{k+1},\ldots}}$			marginal arithmetic mean over the k-th index
$\overline{\overline{\cdot_{i_1,\ldots,i_{k-1},\bullet,i_{k+1},\ldots,i_{\ell-1},\bullet,i_{\ell+1},\ldots}}}$			marginal arithmetic mean over the k-th and ℓ-th indices
analytical objects			
$\frac{\mathrm{d}}{\mathrm{d}t}$			derivative with respect to time
$\widehat{\cdot}$			steady-state value of a variable (constant solution of an ODE)
ε	$\mathbb{R}$	quantity	negligible, $\lvert\varepsilon\rvert \ll 1$
C^k		property	for a function to have $k \in \mathbb{N}$ continuous derivatives
matrix operations			
.		product	standard matrix product, scalar product
$\odot$		product	HADAMARD product (termwise product), $(\mathbf{A},\mathbf{B}) \in \mathfrak{M}^2_{\ell,c} \Longrightarrow \mathbf{A} \odot \mathbf{B} = \left(a_{ij} c_{ij}\right)_{(i,j) \in [\![1;\ell]\!] \times [\![1;c]\!]}$
$\otimes$		product	de KRONECKER (outer product) $\mathbf{A} \in \mathfrak{M}_{\ell,c}, \mathbf{B} \in \mathfrak{M}_{p,q} \Longrightarrow \mathbf{A} \otimes \mathbf{B} = \left(a_{ij}\mathbf{B}\right)_{(i,j) \in [\![1;\ell]\!] \times [\![1;c]\!]} \in \mathfrak{M}_{\ell p, cq}$
$\mathbf{T}$		operator	transpose matrix
vec		operator	vectorized matrix, $\mathbf{A} \in \mathfrak{M}_{\ell,c} \iff \mathrm{vec}(\mathbf{A}) = \left(a_{\mathrm{mod}_c(i)+1, \left\lfloor \frac{i}{c} \right\rfloor + 1}\right)_{i \in [\![1;\ell c]\!]}$
diag		operator	diagonalized matrix, $\mathbf{v} \in \mathfrak{M}_{1,c} \iff \mathrm{diag}(\mathbf{v}) = \left(\delta_{i,j}\mathbf{v}_i\right)_{(i,j) \in [\![1;c^2]\!]}$
det		operator	square matrix determinant
dimensions			
$\#_{\mathrm{p}}$			parasite load
$\#_{\mathrm{h}}$			host density
c			concentration of public production molecules
t			time
modelling objects			
t	$\mathbb{R}_+$		time
n	$\mathbb{N}^\star$	number	of parasite genotypes
$\mathcal{G} = [\![1;n]\!]$		set	of genotypes
$\mathcal{R}$	$\mathbb{R}_+$	number	basic reproductive number
$\circ$			single infection state (within-host level) or disease-free state (between-host level)

notation	$\in$	dimension	type	meaning
within-host				
$\mathbf{x} = (X_k)$	$\mathfrak{M}_{n,1}(\mathbb{R}_+)$	$\#_{\mathrm{p}}$	vector	parasite loads
$\mathbf{g} = (G_k)$	$\mathfrak{M}_{n,1}(\mathbb{R}_+)$	c	scalar	public good concentration
$\mathbf{z} = (Z_k)$	$\mathfrak{M}_{n,1}(\mathbb{R}_+)$	c	vector	spite concentrations
$\mathbf{U} = \mathrm{diag}(u_k)$	$\mathfrak{M}_n(\mathbb{R}_+)$	$\mathrm{c}.\#_{\mathrm{p}}^{-1}$	vector	public good production rates
$\mathbf{V} = \mathrm{diag}(v_k)$	$\mathfrak{M}_n(\mathbb{R}_+)$	$\mathrm{c}.\#_{\mathrm{p}}^{-1}$	matrix	spite production rates
$\mathbf{\Gamma} = (\gamma_{k,\ell})$	$\mathfrak{M}_n(\mathbb{R}_+)$	$\mathrm{c}^{-1}.\mathrm{t}^{-1}$	vector	public good effects on growth rate
$\mathbf{\Sigma} = (\sigma_{k,\ell})$	$\mathfrak{M}_n(\mathbb{R}_-)$	$\mathrm{c}^{-1}.\mathrm{t}^{-1}$	matrix	spite effects on growth rate
$\mathbf{H} = (\eta_{k,\ell})$	$\mathfrak{M}_n(\mathbb{R})$	$\#_{\mathrm{p}}^{-1}.\mathrm{t}^{-1}$	matrix	binary interactions
$\boldsymbol{\varrho} = (\varrho_k)$	$\mathfrak{M}_{n,1}(\mathbb{R}_+)$	t^{-1}	vector	basal growth rates
υ	$\mathbb{R}_+^\star$	t^{-1}	scalar	standard clearing rate
P_k	$\mathbb{R}$	t^{-1}	scalar	malthusian growth rate
class handling				
$\wp(\mathcal{G})$	$\wp(\mathbb{N})$		set	host and inoculum classes
$\boldsymbol{i}$	$\wp(\mathcal{G})$		set	host or inoculum class
$\mathcal{C}$	$\mathcal{A}(\wp(\mathcal{G}), [\![0; 2^n - 1]\!])$		operator	class labelling
$c_{i,k}$	$\{0;1\}$		coefficient	presence
$\mathbf{c}_i$	$\{0;1\}^n$		vector	presence
i	$[\![0; 2^n - 1]\!]$		label	of host or inoculum class $\boldsymbol{i} = \mathcal{C}^{-1}(i)$
$\mathcal{B}$	$\wp(\mathcal{G})$		set	biological classes
$\mathcal{E}$	$\wp(\mathcal{G})$		set	epidemiological classes
ϕ	$\mathcal{A}(\mathcal{B}^2, \mathcal{B})$	1	operator	infection operator
ς	$\mathcal{A}(\wp(\mathcal{G}), \{0,1\})$	1	operator	stability indicator
between host				
$\beta_{\boldsymbol{r},\boldsymbol{d},\boldsymbol{i}}$	$\mathbb{R}_+^\star$	$\#_{\mathrm{h}}^{-2}.\mathrm{t}^{-1}$	scalar	transmission rate
β	$\mathbb{R}_+^\star$	$\#_{\mathrm{h}}^{-1}.\mathrm{t}^{-1}$	scalar	constant transmission factor
$\theta_{d,i}$	$\mathbb{R}_+^\star$	$\#_{\mathrm{h}}^{-1}.\mathrm{t}^{-1}$	scalar	recovery rate
θ	$\mathbb{R}_+^\star$	$\#_{\mathrm{h}}^{-1}.\mathrm{t}^{-1}$	scalar	constant recovery factor
μ_i	$\mathbb{R}_+^\star$	$\#_p^{-1}.\#_{\mathrm{h}}^{-1}.\mathrm{t}^{-1}$	scalar	death rate
μ	$\mathbb{R}_+^\star$	$\#_{\mathrm{p}}^{-1}.\#_{\mathrm{h}}^{-1}.\mathrm{t}^{-1}$	scalar	constant death factor
s°	$\mathbb{R}_+^\star$	$\#_{\mathrm{h}}$	scalar	constant total population size
S	$\mathbb{R}_+$	$\#_{\mathrm{h}}$	scalar	susceptible density
$\mathbf{y} = (I_i)$	$\mathfrak{M}_{n,1}(\mathbb{R}_+)$	$\#_{\mathrm{h}}$	vector	host densities ($I_0 \equiv S$)
$\mathbf{X} = (x_{i,j})$	$\mathfrak{M}_{n,2^n}(\mathbb{R}_+)$	$\#_{\mathrm{p}}$	matrix	within-host steady state parasite loads
$\mathbf{\Psi}$	$\mathfrak{M}_{2^n,2^n}(\mathbb{R})$	$\#_{\mathrm{h}}^{-2}.\mathrm{t}^{-1}$	matrix	infection output rates
$\mathbf{\Phi}$	$\mathfrak{M}_{2^n,2^{2n}}(\mathbb{R})$	$\#_{\mathrm{h}}^{-2}.\mathrm{t}^{-1}$	matrix	infection input rates
$\mathbf{\Theta}$	$\mathfrak{M}_{2^n,2^n}(\mathbb{R})$	$\#_{\mathrm{h}}^{-1}.\mathrm{t}^{-1}$	matrix	recovery output rates
$\mathbf{\Xi}$	$\mathfrak{M}_{2^n,2^n}(\mathbb{R})$	$\#_{\mathrm{h}}^{-1}.\mathrm{t}^{-1}$	matrix	recovery input rates
$\mathbf{\Delta}$	$\mathfrak{M}_{2^n,2^n}(\mathbb{R})$	$\#_{\mathrm{h}}^{-1}.\mathrm{t}^{-1}$	matrix	death output rates (input for susceptibles)

3.b. Within-host dynamics

3.b.1. Partial genotype combination steady-state

Here we show that there is a unique steady-state parasite load associated to a partial combination of genotypes. Let $\boldsymbol{i}$ be the set of genotypes with non zero parasite loads at steady state (for a given set of initial conditions),

$$\boldsymbol{i} := \left\{k \in \mathcal{G} : \widehat{X_k} \neq 0\right\},$$

and $\widehat{\mathbf{x}_{\boldsymbol{i}}}$ the steady state parasite load vector associated to $\boldsymbol{i}$. Therefore, the elements of $\widehat{\mathbf{x}_{\boldsymbol{i}}}$ the index of which do not belong to $\boldsymbol{i}$ are 0. This gives

$$\begin{aligned} \forall j \in \mathcal{G} \setminus \boldsymbol{i}, \qquad & \widehat{X_j} := 0, \\ (3.2.3) \quad & \widehat{G_j} = 0, \widehat{Z_j} = 0, \\ (3.2.2) \quad & 0 = \widehat{X_j}(\mathbf{M}.\widehat{\mathbf{x}_{\boldsymbol{i}}})_j = 0, \end{aligned}$$

where $\mathbf{M} =: \left(m_{k,j}\right)_{(k,j)\in\mathcal{G}^2}$ is the square matrix of steady-state interactions. In order to solve (3.2.2) at steady state, it is necessary to extract these tautological rows. If $\mathbf{M}_{\boldsymbol{i}}$ is a sub-matrix and $\boldsymbol{\varrho}_{\boldsymbol{i}}$ a sub-vector defined as

$$\mathbf{M}_{\boldsymbol{i}} := \left(m_{k,\ell}\right)_{(k,\ell)\in\boldsymbol{i}^2}, \boldsymbol{\varrho}_{\boldsymbol{i}} := \left(\varrho_k\right)_{k\in\boldsymbol{i}},$$

then the elements of $\widehat{\mathbf{x}_{\boldsymbol{i}}}$ are given by

$$\widehat{X_k} = \begin{cases} 0, & k \notin \boldsymbol{i}, \\ -\left(\mathbf{M}_{\boldsymbol{i}}^{-1}.\boldsymbol{\varrho}_{\boldsymbol{i}}\right)_k, & k \in \boldsymbol{i}. \end{cases} \tag{3.b.1}$$

Since $\mathbf{M}$ is a constant matrix, the elements of $\widehat{\mathbf{x}_{\boldsymbol{i}}}$ do not depend on the initial conditions of the within-host system. As a consequence, there is only one steady state parasite load vector for each partial genotype combination.

3.c. Linking the within and between-host levels

3.c.1. Class labelling

As explained in the main text, labelling the class is a computational requirement to model and simulating parasite dynamics. For n different parasite genotypes, there exist exactly $\left|\wp\left(\mathcal{G}\right)\right| = 2^n$ different host and inoculum classes.We introduce the following labelling operator:

$$\mathcal{C}(\boldsymbol{i}) \coloneqq \sum_{k=1}^{n} \mathbb{I}_{\{k\in\boldsymbol{i}\}} 2^{k-1},$$

where the set $\boldsymbol{i} \subset \mathcal{G}$ is a class and $\mathbb{I}_{\mathsf{A}}$ the indicator function which equals 1 if A is true and 0 otherwise.

The label of the susceptible class, which is uninfected, is then

$$\mathcal{C}(\emptyset) = \sum_{k=1}^{n} \mathbb{I}_{\{k\in\emptyset\}} 2^{k-1} = \sum_{k=1}^{n} 0 \times 2^{k-1} = 0.$$

The label of the class which contains all the n genotypes is

$$\mathcal{C}\left(\mathcal{G}\right) = \mathcal{C}(\llbracket 1;n \rrbracket) = \sum_{k=1}^{n} \mathbb{I}_{\{k\in\llbracket 1;n\rrbracket\}} 2^{k-1} = \sum_{k=1}^{n} 2^{k-1} = 1 \times \frac{1-2^n}{1-2} = 2^n - 1.$$

Since $\forall \boldsymbol{i} \subset \mathcal{G}, \forall k \in \mathcal{G}, \mathbb{I}_{\{k\in\mathcal{G}\}} \geq \mathbb{I}_{\{k\in\boldsymbol{i}\}}$, all the labels range from 0 to 2^{n-1} and we use $\llbracket 0;2^n-1 \rrbracket$ to index $\wp\left(\mathcal{G}\right)$.

$\mathcal{C}$ is a labelling function if and only it is bijective. To prove so, let us study the following function

$$\begin{aligned} f : \llbracket 0;2^n-1 \rrbracket &\longrightarrow \wp\left(\mathcal{G}\right), \\ i &\longmapsto f(i) \coloneqq \left\{ k \in \mathcal{G} : \mathrm{mod}_2 \left\lfloor \frac{i}{2^{k-1}} \right\rfloor = 1 \right\}. \end{aligned}$$

Let us consider an arbitrary label $i \in \llbracket 0;2^n-1 \rrbracket$. Because $\llbracket 0;2^n-1 \rrbracket \subset \mathbb{N}$, and because any natural number can be written using the binary numeral system, there is a sequence of $\left(a_j\right)_{j\in\mathbb{N}} \in \{0;1\}^{\mathbb{N}}$, which is constantly equal to 0 after a certain rank N, and which corresponds to the digits of i in the binary numeral system (0 or 1), such that

$i = (\ldots 0 \ldots 0 a_N a_{N-1} \ldots a_1 a_0)_2 = \sum_{j=0}^{\infty} a_j 2^j$. Then, for any $k \in \mathcal{G}$, we have

$$\begin{aligned}
\mathrm{mod}_2 \left\lfloor \frac{i}{2^{k-1}} \right\rfloor &:= \left\lfloor \frac{i}{2^{k-1}} \right\rfloor - 2 \left\lfloor \frac{\frac{i}{2^{k-1}}}{2} \right\rfloor, \\
&= \left\lfloor \frac{\sum_{j=1}^{\infty} a_j 2^{j-1}}{2^{k-1}} \right\rfloor - 2 \left\lfloor \frac{\sum_{j=1}^{\infty} a_j 2^{j-1}}{2^k} \right\rfloor, \\
&= \left\lfloor \underbrace{\frac{1}{2^k} \sum_{j=1}^{k-1} \left(a_j 2^j\right)}_{<1 \ (*)} + \sum_{j=k}^{\infty} \left(a_j 2^{j-k}\right) \right\rfloor - 2 \left\lfloor \underbrace{\sum_{j=1}^{k} \left(a_j 2^{j-k-1}\right)}_{<1} + \sum_{j=k+1}^{\infty} \left(a_j 2^{j-k-1}\right) \right\rfloor, \\
&= \sum_{j=k}^{\infty} \left(a_j 2^{j-k}\right) - 2 \sum_{j=k+1}^{\infty} \left(a_j 2^{j-k-1}\right), \\
&= a_k,
\end{aligned}$$

where $(*)$ is justified by the well-known sum $\sum_{j=0}^{\infty} \frac{1}{2^j} = 2$.

Finally, by identifying i to the label of a class $\boldsymbol{i}$, $i := \mathcal{C}(\boldsymbol{i})$, we have $a_k = \mathbb{I}_{\{k \in \boldsymbol{i}\}}$ and $f(i) = \{k \in \mathcal{G} : a_k = 1\} = \{k \in \mathcal{G} : \mathbb{I}_{\{k \in \boldsymbol{i}\}} = 1\} = \{k \in \mathcal{G} : k \in \boldsymbol{i}\} = \{k \in \boldsymbol{i}\} = \boldsymbol{i}$. So f is the inverse function of $\mathcal{C}$. We have proved that $\mathcal{C}$ is bijective and that its inverse function, which is also bijective, is $\mathcal{C}^{-1} : i \mapsto \left\{k \in \mathcal{G} : \mathrm{mod}_2 \left\lfloor \frac{i}{2^{k-1}} \right\rfloor = 1\right\}$.

Therefore it is possible to know if a genotype belongs to a class directly from the label of the latter. This is done by calculating the following presence coefficient for each couple $(i,k) \in [\![0; 2^n - 1]\!] \times [\![1; n]\!]$,

$$c_{i,k} = \mathrm{mod}_2 \left\lfloor \frac{i}{2^{j-1}} \right\rfloor = \mathbb{I}_{\{k \in \mathcal{C}^{-1}(i)\}},$$

which is 1 if genotype k belongs to host class i. As a consequence of this definition, we have

$$i = \sum_{k \in \mathcal{G}} c_{i,k} 2^{k-1}.$$

The presence vector $\mathbf{c}_i := \left(c_{i,k}\right)_{k \in \mathcal{G}}$ is then the vector of the presence coefficients for all genotypes in a given class. The presence vector is useful for calculating class ranks. For a given class with label i, its rank denoted n_i, that is the number of genotypes it contains, is

$$n_i = \mathbf{c}_i . \mathbf{1}_n^{\mathbf{T}},$$

where $\mathbf{1}_n$ is the unity vector of $\mathbb{R}_n$.

Thereafter, light class indices (such as i) refer to labelled classes and bold class indices (such as $\boldsymbol{i}$) refer to the associated set-theoretic classes. Class-related functions can indifferently be applied to both forms owing to the bijectivity of $\mathcal{C}$.

3.c.2. Within-host jacobian matrix

We need to calculate the within-host jacobian matrix $\mathbf{J}_{\mathrm{w}}$ in order to determine the stability of the steady states. $\mathbf{J}_{\mathrm{w}}$ is the $3n \times 3n$ matrix given by the following general

formula

$$\mathbf{J}_{\mathrm{w}} := \left(\frac{\partial}{\partial W_j}\left(\frac{\mathrm{d}W_k}{\mathrm{d}t}\right)\right)_{(k,j)\in[\![1;3n]\!]^2} \text{ where } W_k = \begin{cases} X_k, & k \in [\![1;n]\!], \\ G_{k-n}, & k \in [\![n+1;2n]\!], \\ Z_{k-2n}, & k \in [\![2n+1;3n]\!], \end{cases}$$

which can be split into nine $n \times n$ submatrices as follows

$$\mathbf{J}_{\mathrm{w}} = \begin{pmatrix} \mathbf{J}_{X,X} & \mathbf{J}_{X,G} & \mathbf{J}_{X,Z} \\ \mathbf{J}_{G,X} & \mathbf{J}_{G,G} & \mathbf{J}_{G,Z} \\ \mathbf{J}_{Z,X} & \mathbf{J}_{Z,G} & \mathbf{J}_{Z,Z} \end{pmatrix}.$$

Let us calculate $\frac{\partial}{\partial X_j}\left(\frac{\mathrm{d}X_k}{\mathrm{d}t}\right)$,

$$\begin{aligned} \frac{\partial}{\partial X_j}\left(\frac{\mathrm{d}X_k}{\mathrm{d}t}\right) &= \frac{\partial}{\partial X_j}\left(\left(\varrho_k + \sum_{\ell\in\mathcal{G}} \gamma_{k,\ell} G_\ell - \sum_{\ell\in\mathcal{G}} \sigma_{k,\ell} Z_\ell + \sum_{\ell\in\mathcal{G}} \eta_{k,\ell} X_\ell\right) X_k\right), \\ \text{if } j \neq k, &= \eta_{k,j} X_k, \\ \text{if } j = k, &= \varrho_k + \sum_{\ell\in\mathcal{G}} \gamma_{k,\ell} G_\ell - \sum_{\ell\in\mathcal{G}} \sigma_{k,\ell} Z_\ell + \sum_{\ell\in\mathcal{G}} \eta_{k,\ell} X_\ell + \eta_{k,k} X_k, \end{aligned}$$

so

$$\mathbf{J}_{X,X} = \mathrm{diag}\left(\boldsymbol{\varrho} + \boldsymbol{\Gamma}.\mathbf{g} - \boldsymbol{\Sigma}.\mathbf{z} + \mathbf{H}.\mathbf{x}\right) + \mathbf{H} \odot (\mathbf{x}.\mathbf{1}_n).$$

Let us calculate $\frac{\partial}{\partial G_j}\left(\frac{\mathrm{d}X_k}{\mathrm{d}t}\right)$,

$$\begin{aligned} \frac{\partial}{\partial G_j}\left(\frac{\mathrm{d}X_k}{\mathrm{d}t}\right) &= \frac{\partial}{\partial G_j}\left(\left(\varrho_k + \sum_{\ell\in\mathcal{G}} \gamma_{k,\ell} G_\ell - \sum_{\ell\in\mathcal{G}} \sigma_{k,\ell} Z_\ell + \sum_{\ell\in\mathcal{G}} \eta_{k,\ell} X_\ell\right) X_k\right), \\ &= \gamma_{k,j} X_k, \end{aligned}$$

so

$$\mathbf{J}_{X,G} = \boldsymbol{\Gamma} \odot (\mathbf{x}.\mathbf{1}_n).$$

Let us calculate $\frac{\partial}{\partial Z_j}\left(\frac{\mathrm{d}X_k}{\mathrm{d}t}\right)$,

$$\begin{aligned} \frac{\partial}{\partial Z_j}\left(\frac{\mathrm{d}X_k}{\mathrm{d}t}\right) &= \frac{\partial}{\partial Z_j}\left(\left(\varrho_k + \sum_{\ell\in\mathcal{G}} \gamma_{k,\ell} G_\ell - \sum_{\ell\in\mathcal{G}} \sigma_{k,\ell} Z_\ell + \sum_{\ell\in\mathcal{G}} \eta_{k,\ell} X_\ell\right) X_k\right), \\ \text{if } j \neq k, &= -\sigma_{k,j} X_k, \\ \text{if } j = k, &= 0 \qquad (\text{because } \sigma_{k,k} = 0), \end{aligned}$$

so

$$\mathbf{J}_{X,Z} = -\boldsymbol{\Sigma} \odot (\mathbf{x}.\mathbf{1}_n).$$

Let us calculate $\frac{\partial}{\partial X_j}\left(\frac{\mathrm{d}G_k}{\mathrm{d}t}\right)$,

$$\begin{aligned} \frac{\partial}{\partial X_j}\left(\frac{\mathrm{d}G_k}{\mathrm{d}t}\right) &= \frac{\partial}{\partial X_j}(\upsilon(u_k X_k - G_k)) \\ \text{if } j \neq k, &= 0, \\ \text{if } j = k, &= \upsilon u_j, \end{aligned}$$

so

$$\mathbf{J}_{G,X} = v\mathbf{U}.$$

Let us calculate $\frac{\partial}{\partial Z_j}\left(\frac{\mathrm{d}G_k}{\mathrm{d}t}\right)$,

$$\begin{aligned}\frac{\partial}{\partial Z_j}\left(\frac{\mathrm{d}G_k}{\mathrm{d}t}\right) &= \frac{\partial}{\partial Z_j}(v(u_k X_k - G_k)),\\ &= 0,\end{aligned}$$

so

$$\mathbf{J}_{G,Z} = \mathbf{0}_{n,n}.$$

Let us calculate $\frac{\partial}{\partial G_j}\left(\frac{\mathrm{d}G_k}{\mathrm{d}t}\right)$,

$$\begin{aligned}\frac{\partial}{\partial G_j}\left(\frac{\mathrm{d}G_k}{\mathrm{d}t}\right) &= \frac{\partial}{\partial G_j}(v(u_k X_k - G_k)),\\ \text{if } j \neq k, &= 0,\\ \text{if } j = k, &= -v,\end{aligned}$$

so

$$\mathbf{J}_{G,G} = -v\mathbf{I}_n.$$

Let us calculate $\frac{\partial}{\partial X_j}\left(\frac{\mathrm{d}Z_k}{\mathrm{d}t}\right)$,

$$\begin{aligned}\frac{\partial}{\partial X_j}\left(\frac{\mathrm{d}Z_k}{\mathrm{d}t}\right) &= \frac{\partial}{\partial X_j}(v(v_k X_k - Z_k)),\\ \text{if } j \neq k, &= 0,\\ \text{if } j = k, &= vv_k,\end{aligned}$$

so

$$\mathbf{J}_{Z,X} = v\mathbf{V}$$

Let us calculate $\frac{\partial}{\partial Z_j}\left(\frac{\mathrm{d}Z_k}{\mathrm{d}t}\right)$,

$$\begin{aligned}\frac{\partial}{\partial Z_j}\left(\frac{\mathrm{d}Z_k}{\mathrm{d}t}\right) &= \frac{\partial}{\partial Z_j}(v(v_k X_k - Z_k)),\\ \text{if } j \neq k, &= 0,\\ \text{if } j = k, &= -v,\end{aligned}$$

so

$$\mathbf{J}_{Z,Z} = -v\mathbf{I}_n.$$

Let us calculate $\frac{\partial}{\partial G_j}\left(\frac{\mathrm{d}Z_k}{\mathrm{d}t}\right)$,

$$\begin{aligned}\frac{\partial}{\partial G_j}\left(\frac{\mathrm{d}Z_k}{\mathrm{d}t}\right) &= \frac{\partial}{\partial G_j}(v(v_k X_k - Z_k)),\\ &= 0,\end{aligned}$$

so

$$\mathbf{J}_{Z,G} = \mathbf{0}_{n,n}.$$

$\mathbf{J}_{\mathrm{w}}$ can then be written as the following bloc matrix:

$$\mathbf{J}_{\mathrm{w}}(\mathbf{x},\mathbf{g},\mathbf{z}) = \begin{pmatrix} \mathrm{diag}\left(\boldsymbol{\rho}+\boldsymbol{\Gamma}.\mathbf{g}-\boldsymbol{\Sigma}.\mathbf{z}+\mathbf{H}.\mathbf{x}\right)+\mathbf{H}\odot(\mathbf{x}.\mathbf{1}_n) & \boldsymbol{\Gamma}\odot(\mathbf{x}.\mathbf{1}_n) & -\boldsymbol{\Sigma}\odot(\mathbf{x}.\mathbf{1}_n) \\ \upsilon\mathbf{U} & -\upsilon\mathbf{I}_n & \mathbf{0}_{n,n} \\ \upsilon\mathbf{V} & \mathbf{0}_{n,n} & -\upsilon\mathbf{I}_n \end{pmatrix}.$$

Finally, in a steady state $\left(\widehat{\mathbf{x}},\widehat{\mathbf{g}},\widehat{\mathbf{z}}\right)$ with non zero values of $\widehat{\mathbf{x}}$, it follows from (3.2.6) that

$$\mathbf{J}_{\mathrm{w}}\left(\widehat{\mathbf{x}},\widehat{\mathbf{g}},\widehat{\mathbf{z}}\right) = \begin{pmatrix} \mathbf{H}\odot(\widehat{\mathbf{x}}.\mathbf{1}_n) & \boldsymbol{\Gamma}\odot(\widehat{\mathbf{x}}.\mathbf{1}_n) & -\boldsymbol{\Sigma}\odot(\widehat{\mathbf{x}}.\mathbf{1}_n) \\ \upsilon\mathbf{U} & -\upsilon\mathbf{I}_n & \mathbf{0}_{n,n} \\ \upsilon\mathbf{V} & \mathbf{0}_{n,n} & -\upsilon\mathbf{I}_n \end{pmatrix}.$$

3.c.3. Susceptible state instability

In an uninfected host, $\mathbf{x}=\mathbf{g}=\mathbf{z}=\mathbf{0}_n^{\mathbf{T}}$. Therefore the within susceptible host jacobian matrix is

$$\mathbf{J}_{\mathrm{w}}^{\circ} = \begin{pmatrix} \mathrm{diag}\left(\boldsymbol{\rho}\right) & \mathbf{0}_{n,n} & \mathbf{0}_{n,n} \\ \upsilon\mathbf{U} & -\upsilon\mathbf{I}_n & \mathbf{0}_{n,n} \\ \upsilon\mathbf{V} & \mathbf{0}_{n,n} & -\upsilon\mathbf{I}_n \end{pmatrix},$$

which is a real-valued upper triangular matrix. Its eigenvalues are straightforward $\mathrm{Sp}\left(\mathbf{J}_{\mathrm{w}}^{\circ}\right) = \left\{\rho_1,\ldots,\rho_n,-\upsilon\right\}$. Since we assume that any considered genotype grows when alone within a host, i.e. $\rho_k > 0$, the susceptible state is unstable for any $n \in \mathbb{N}^{\star}$.

3.c.4. Single infection state stability

Assuming $\varrho > 0$ makes the susceptible state unstable. Assuming $\eta+\gamma u < 0$ makes the single infection steady state positive. The stability of the latter still needs to be proved. The jacobian matrix within singly infected host is the following 3×3 matrix

$$\mathbf{J}_{\mathrm{w}}(X,G,Z) = \begin{pmatrix} \varrho+\gamma G+2\eta X & \gamma X & 0 \\ \upsilon u & -\upsilon & 0 \\ \upsilon v & 0 & -\upsilon \end{pmatrix},$$

where the indices are not shown for the sake of simplicity. Note that σ does not appear, for we assume that no genotype is affected by the spite it produces.

At steady state, we have $\varrho+\gamma\widehat{G}+2\eta\widehat{X} = \varrho-\gamma u\left(\frac{\varrho}{\eta+\gamma u}\right)-2\eta\left(\frac{\varrho}{\eta+\gamma u}\right) = -\frac{\varrho\eta}{\eta+\gamma u}$, so

$$\mathbf{J}_{\mathrm{w}}\left(x_k^{\circ}(1,u_k,v_k)\right) = \begin{pmatrix} \frac{-\varrho\eta}{\eta+\gamma u} & \frac{-\varrho\gamma}{\eta+\gamma u} & 0 \\ \upsilon u & -\upsilon & 0 \\ \upsilon v & 0 & -\upsilon \end{pmatrix},$$

the eigenvalues of which ares the roots of the following determinant

$$\begin{aligned}
\left|\mathbf{J}_{\mathrm{w}}\left(x_k^{\circ}(1,u_k,v_k)\right)-\lambda I_3\right| &= \begin{vmatrix} \frac{-\varrho\eta}{\eta+\gamma u}-\lambda & \frac{-\varrho\gamma}{\eta+\gamma u} & 0 \\ \upsilon u & -\upsilon-\lambda & 0 \\ \upsilon\upsilon & 0 & -\upsilon-\lambda \end{vmatrix}, \\
&= -(\upsilon+\lambda)^2\left(\frac{\varrho\eta}{\eta+\gamma u}+\lambda\right)-(\upsilon+\lambda)\frac{\varrho\gamma}{\eta+\gamma u}\upsilon u, \\
&= -(\upsilon+\lambda)\left((\upsilon+\lambda)\left(\frac{\varrho\eta}{\eta+\gamma u}+\lambda\right)+\frac{\upsilon\varrho\gamma u}{\eta+\gamma u}\right), \\
&= -(\upsilon+\lambda)\left(\lambda^2+\left(\upsilon+\frac{\varrho\eta}{\eta+\gamma u}\right)\lambda+\varrho\upsilon\right).
\end{aligned}$$

A first obvious eigenvalue is $\lambda_0 = -\upsilon < 0$. The remaining two are the roots of the following polynomial

$$\lambda^2+\left(\upsilon+\frac{\varrho\eta}{\eta+\gamma u}\right)\lambda+\varrho\upsilon=0,$$

the discriminant of which is

$$\begin{aligned}
\Delta &= \left(\upsilon+\frac{\varrho\eta}{\eta+\gamma u}\right)^2-4\varrho\upsilon, \\
&= \upsilon^2-\frac{2\varrho\upsilon\left(2\gamma u+\eta\right)}{\eta+\gamma u}+\left(\frac{\varrho\eta}{\eta+\gamma u}\right)^2, \\
&= \left(\upsilon-\frac{\varrho\eta}{\eta+\gamma u}\right)^2-\frac{4\varrho\upsilon\gamma u}{\eta+\gamma u}.
\end{aligned}$$

Owing to the previous assumptions, $\Delta > 0$, and the eigenvalues are the following real real numbers

$$\lambda_{1,2} = -\frac{1}{2}\left(\upsilon+\frac{\varrho\eta}{\eta+\gamma u}\pm\sqrt{\left(\upsilon+\frac{\varrho\eta}{\eta+\gamma u}\right)^2-4\varrho\upsilon}\right)<0.$$

These eigenvalues are both negative, implying the single infection steady state stable.

3.c.5. Biological, epidemiological classes and infection, stability operators

As explained in the main text, labelling the class is a computational requirement to model and simulating parasite dynamics. The set of biological classes $\mathcal{B}$ is formally defined as

$$\mathcal{B} \coloneqq \left\{\boldsymbol{i}\in\wp\left(\mathcal{G}\right)^{\star} : \forall k\in\boldsymbol{i}, \widehat{\mathbf{x}_{\boldsymbol{i}}}>0 \wedge \max\left(\Re\left(\mathrm{Sp}\left(\mathbf{J}_{\mathrm{w}}\left(\left(\mathbf{I}_n,\mathbf{U},\mathbf{V}\right).\widehat{\mathbf{x}_{\boldsymbol{i}}}\right)\right)\right)\right)<0\right\}\cup\{\emptyset\},$$

where $\mathbf{J}_{\mathrm{w}}$ is here the $3|\boldsymbol{i}|\times 3|\boldsymbol{i}|$ jacobian matrix obtained by removing the lines and columns related to genotypes absent from $\boldsymbol{i}$ and $\max\left(\Re\left(\mathrm{Sp}\left(\mathbf{J}_{\mathrm{w}}\left(\left(\mathbf{I}_{\mathrm{n}},\mathbf{U},\mathbf{V}\right).\widehat{\mathbf{x}_{\boldsymbol{i}}}\right)\right)\right)\right)$ refers to the greatest real part among its eigenvalues.

Consider now a host belonging to class $\boldsymbol{r}\in\boldsymbol{B}$ the parasite loads of which have reached the biologically meaningful within-host steady state $\widehat{\mathbf{x}_{\boldsymbol{r}}}$, that is to say positive and stable. Let us further assume that this host is infected by a class $\boldsymbol{p}$ inoculum. We call $\left(\mathbf{x}^{(\boldsymbol{r},\boldsymbol{p})},\mathbf{g}^{(\boldsymbol{r},\boldsymbol{p})},\mathbf{z}^{(\boldsymbol{r},\boldsymbol{p})}\right)(t)$ the dynamical system that corresponds to this infection event, defined by its initial condition $\left(\mathbf{x}^{(\boldsymbol{r},\boldsymbol{p})},\mathbf{g}^{(\boldsymbol{r},\boldsymbol{p})},\mathbf{z}^{(\boldsymbol{r},\boldsymbol{p})}\right)(0) \coloneqq \left(\widehat{\mathbf{x}_{\boldsymbol{r}}}+\varepsilon\left\|\widehat{\mathbf{x}_{\boldsymbol{r}}}\right\|\mathbf{c}_{\boldsymbol{p}},\widehat{\mathbf{g}_{\boldsymbol{r}}},\widehat{\mathbf{z}_{\boldsymbol{r}}}\right)$, where $0<\varepsilon\ll$

1 is the inoculation factor.

Given this modelling of infection events, the output class is found through the infection operator defined as

$$\phi(\boldsymbol{r},\boldsymbol{p}) := \begin{cases} \min\limits_{\boldsymbol{i}\in\boldsymbol{B}} \left\| \lim\limits_{t\to\infty} \mathbf{x}^{(\boldsymbol{r},\boldsymbol{p})}(t) - \widehat{\mathbf{x}_{\boldsymbol{i}}} \right\|, & \left\| \lim\limits_{t\to\infty} \mathbf{x}^{(\boldsymbol{r},\boldsymbol{p})}(t) \right\| < \infty, \\ 0, & \text{otherwise.} \end{cases}$$

This definition of ϕ holds only if $\mathbf{x}^{(\boldsymbol{r},\boldsymbol{p})}$ has a finite limit when $t \to \infty$. If the limit is infinite, then ϕ is 0 because of our definition of the ultrainfection pattern (see below). If there is no finite nor infinite limit (this occurs when the attractor is not a fixed point), then ϕ must be adapted depending on the behaviour of the system, the use of the model and additionnal assumptions. As alternative definitions of ϕ, one can think of fixing a finite time for within-host dynamics, that is

$$0 < T < \infty, \phi(\boldsymbol{r},\boldsymbol{p}) := \mathbb{I}_{\left\{ \sup\limits_{t\in[0,T]} \mathbf{x}^{(\boldsymbol{r},\boldsymbol{p})}(t) < \infty \right\}} \min_{\boldsymbol{i}\in\boldsymbol{B}} \left\| \lim_{t\to T} \mathbf{x}^{(\boldsymbol{r},\boldsymbol{p})}(t) - \widehat{\mathbf{x}_{\boldsymbol{i}}} \right\|,$$

or averaging over a period or an long amount of time, as in

$$0 < T < \infty, \phi(\boldsymbol{r},\boldsymbol{p}) := \mathbb{I}_{\left\{ \sup\limits_{t\in[0,2T]} \mathbf{x}^{(\boldsymbol{r},\boldsymbol{p})}(t) < \infty \right\}} \min_{\boldsymbol{i}\in\boldsymbol{B}} \left\| \frac{1}{T} \int_{T}^{2T} \mathbf{x}^{(\boldsymbol{r},\boldsymbol{p})}(t)\,\mathrm{d}t - \widehat{\mathbf{x}_{\boldsymbol{i}}} \right\|.$$

Finally, in case of chaos, one should pay attention to the inoculation factor which can greatly influence the output. In the next subsection (3.c.6) we give a sufficient condition for $\lim\limits_{t\to\infty} \mathbf{x}^{(\boldsymbol{r},\boldsymbol{p})}(t)$ to always be a steady-state $\widehat{\mathbf{x}_{\boldsymbol{i}}}$ with $\boldsymbol{i} \in \mathcal{B}$, so the first definition of ϕ holds.

Ultrainfection happens when the growth of at least one genotype is not bounded. Recall that ultrainfection relies on three assumptions:

1. time scale separation between the two levels of dynamics, that is to say at within-host level all hosts of a given class have the same class show the same parasite loads and these are at steady-state,
2. host mortality rate is an increasing non bounded function of total parasite load,
3. constant population size.

Then the set of epidemiological class $\mathcal{E}$ is defined as

$$\mathcal{E} := \left\{ \boldsymbol{i} \in \mathcal{B} : \exists (\boldsymbol{r},\boldsymbol{d}) \in \mathcal{B}^2, \exists \boldsymbol{p} \subset \boldsymbol{d}, \phi(\boldsymbol{r},\boldsymbol{p}) = \boldsymbol{i} \right\} \cup \{\emptyset\}.$$

The stability operator ς, used thereafter in the labelled form of between-host rates, is simply defined as

$$\forall i \in [\![0; 2^n - 1]\!], \varsigma(i) := \mathbb{I}_{\{\mathcal{C}^{-1}(i)\in\mathcal{E}\}}.$$

3.c.6. A sufficient condition for global asymptotic stability

In this subsection we use a Lyapunov function (Wiggins, 2003) to derive a sufficient condition for within-host steady states to be globally asymptotically stable so that non fixed point attractors are avoided. The derivation is inspired from previous works on generalized competitive Lotka-Volterra systems such as Goh (1977); Takeuchi (1996).

The set of biological infected classes

$$\mathcal{B}^\star := \left\{ \boldsymbol{i} \in \wp\left(\mathcal{G}\right)^\star : \forall k \in \boldsymbol{i}, \widehat{\mathbf{x}_{\boldsymbol{i}}} > 0, \max(\Re(\mathrm{Sp}(\mathbf{J}_{\mathrm{w}}((\mathbf{I}_n, \mathbf{U}, \mathbf{V}).\widehat{\mathbf{x}_{\boldsymbol{i}}})))) < 0 \right\}$$

is characterized by its feasibility, that is the positivity of the steady state parasite loads, and by its local asymptotic stability, provided by the negativity of the real part of all eigenvalues of the jacobian matrix evaluated at the steady state (Wiggins, 2003). A steady state is said to be locally asymptotically stable (LAS) if there is a neighbourhood of the steady state where any trajectory starting from it will converge infinitely close to the steady state as time goes to infinity. However, this neighbourhood may be very limited and its boundary difficult to estimate. Thus, local asymptotic stability does not guarantee that any feasible trajectory will get infinitely close to the steady state. The trajectory may be trapped in other attractors that are not a fixed point but a finite set of points, a limit cycle or even strange attractors. The only way to make sure that any trajectory that starts with positive initial conditions will not be trapped by other attractors than steady states is to make these steady states globally asymptotically stable (GAS) (Wiggins, 2003).

Let us consider $\boldsymbol{i} \in \mathcal{B}^\star$ a biological class and assume that that the steady state $\widehat{\mathbf{w}_{\boldsymbol{i}}} = \begin{pmatrix} \widehat{\mathbf{x}_{\boldsymbol{i}}} \\ \widehat{\mathbf{g}_{\boldsymbol{i}}} \\ \widehat{\mathbf{z}_{\boldsymbol{i}}} \end{pmatrix}$, with $\widehat{x_{\boldsymbol{i},k}} > 0, \forall k \in \boldsymbol{i}$, is LAS in $(\mathbb{R}_+)^{3n}$. Even though this last condition is more restrictive than $\widehat{\mathbf{w}_{\boldsymbol{i}}}$ being LAS in $(\mathbb{R}_+)^{3|\boldsymbol{i}|}$ (it is straightforward that $\widehat{\mathbf{w}_{\boldsymbol{i}}}$ LAS in $(\mathbb{R}_+)^{3n} \Longrightarrow \widehat{\mathbf{w}_{\boldsymbol{i}}}$ LAS in $(\mathbb{R}_+)^{3|\boldsymbol{i}|}$), we use it for the sake of simplicity. Indeed, since n and $\boldsymbol{i}$ are arbitrary, the following result can be applied to any nonempty subset of $\mathcal{G}$ without any loss of generality.

First of all, we note that $(\mathbb{R}_+)^{3n}$ is a positively invariant set, that is any trajectory starting in $(\mathbb{R}_+)^{3n}$ remains in $(\mathbb{R}_+)^{3n}$ (Wiggins, 2003). This can be intuitively shown as follows. The time derivative in (3.2.1) and (3.2.2) are respectively linear and bilinear, and therefore continuous; therefore $X_k(t)$ cannot become negative without taking the value 0 beforehand. But since X_k is a common factor in (3.2.2), it will remain 0 from then on. Similarly, $G_k(t)$ cannot become negative without taking the value 0 beforehand. Due to the previous argument, it then follows that $\frac{\mathrm{d}}{\mathrm{d}t}G_k(t) = u_k X_k \geq 0$ and the same applies to $Z_k(t)$. This allows us to define a Lyapunov function on $(\mathbb{R}_+)^{3n}$ (see below).

Let $\mathbf{w} = \begin{pmatrix} \mathbf{x} \\ \mathbf{g} \\ \mathbf{z} \end{pmatrix}$ be the variable vector and $\Omega_{\boldsymbol{i}}$ be the following subset of $(\mathbb{R}_+)^{3n}$:

$$\Omega_{\boldsymbol{i}} := \left\{ \mathbf{w} \in (\mathbb{R}_+)^{3n} : \forall k \in \boldsymbol{i}, X_k > 0 \right\}.$$

The usual way of proving that a steady state is GAS on a given set is to prove the existence of a Lyapunov function that satisfies certain definiteness properties on the set (Wiggins, 2003). Here, $\widehat{\mathbf{w}_{\boldsymbol{i}}}$ is globally asymptotically stable on $\Omega_{\boldsymbol{i}}$ if there is a C^1 function $V_{\boldsymbol{i}} : (\mathbb{R}_+)^{3n} \to \mathbb{R}$ such that

1. $V_{\boldsymbol{i}}(\widehat{\mathbf{w}_{\boldsymbol{i}}}) = 0$,
2. $\forall \mathbf{w} \in \Omega_{\boldsymbol{i}} \setminus \{\widehat{\mathbf{w}_{\boldsymbol{i}}}\}, V_{\boldsymbol{i}}(\mathbf{w}) > 0$,
3. $\frac{\mathrm{d}}{\mathrm{d}t} V_{\boldsymbol{i}}(\widehat{\mathbf{w}_{\boldsymbol{i}}}) = 0$,
4. $\forall \mathbf{w} \in \Omega_{\boldsymbol{i}} \setminus \{\widehat{\mathbf{w}_{\boldsymbol{i}}}\}, \frac{\mathrm{d}}{\mathrm{d}t} V_{\boldsymbol{i}}(\mathbf{w}) < 0$.

We now present a sufficient condition on within-host parameters for this function to exist.

We now consider the function $V_{\boldsymbol{i}}$ defined as

$$V_{\boldsymbol{i}}(\mathbf{w}) := \sum_{k \in \boldsymbol{i}} q_{\mathrm{x},k} \left(X_k - \widehat{x_{\boldsymbol{i},k}} - \widehat{x_{\boldsymbol{i},k}} \log\left(\frac{X_k}{\widehat{x_{\boldsymbol{i},k}}} \right) \right) + \sum_{k \in \mathcal{G} \setminus \boldsymbol{i}} q_{\mathrm{x},k} X_k + \frac{1}{2\upsilon} \sum_{k \in \mathcal{G}} q_{\mathrm{g},k} \left(G_k - \widehat{g_{\boldsymbol{i},k}} \right)^2 + q_{\mathrm{z},k} \left(Z_k - \widehat{z_{\boldsymbol{i},k}} \right)^2, \tag{3.c.1}$$

where $\forall k \in \mathcal{G}, \left(q_{\mathrm{x},k}, q_{\mathrm{g},k}, q_{\mathrm{z},k}\right) \in \left(\mathbb{R}_+^\star\right)^3$, and $\forall k \notin \boldsymbol{i}, \widehat{g_{\boldsymbol{i},k}} = \widehat{z_{\boldsymbol{i},k}} = \widehat{x_{\boldsymbol{i},k}} = 0$ by definition.

$V_{\boldsymbol{i}}$ is C^1 on Ω because it is a sum of elementary single variable functions which are C^1 on $\mathbb{R}_+$ except the logarithm that applies to $X_k, k \in \boldsymbol{i}$ and is C^1 on $\mathbb{R}_+^\star$.

The first sum of $V_{\boldsymbol{i}}$ in (3.c.1) involves terms of the form $f(x) \coloneqq x - a - a(\log x - \log a)$, with $a > 0$. Given that the first derivative of f is $f'(x) = 1 - \frac{a}{x}$ and its second derivative is $f''(x) = \frac{a}{x^2} > 0$, it follows that the $\underset{\mathbb{R}_+^\star}{\operatorname{argmin}}(f) = a$ and $\underset{\mathbb{R}_+^\star}{\min}(f) = 0$. Thus, and since $V_{\boldsymbol{i}}$ is a separable function in each component of $\mathbf{w}$ and $q_{\mathrm{x},k}, q_{\mathrm{g},k}, q_{\mathrm{z},k}$ and υ are positive constants, it is straightforward that

$$\begin{cases} \forall \mathbf{w} \in \Omega \setminus \{\widehat{\mathbf{w}_{\boldsymbol{i}}}\}, V_{\boldsymbol{i}}(\mathbf{w}) > 0, \\ V_{\boldsymbol{i}}(\widehat{\mathbf{w}_{\boldsymbol{i}}}) = 0. \end{cases}$$

Properties 1 and 2 of the Lyapunov function are satisfied.

Let us now calculate the time derivative of $V_{\boldsymbol{i}}$ with the help of the following notation of the malthusian growth rate $\mathrm{P}_k(\mathbf{w})$ that satisfies

$$\frac{\mathrm{d}}{\mathrm{d}t} X_k = \mathrm{P}_k(\mathbf{w}) X_k,$$

hence

$$\mathrm{P}_k(\mathbf{w}) \coloneqq \varrho_k + \sum_{\ell \in \mathcal{G}} \gamma_{k,\ell} G_\ell - \sigma_{k,\ell} Z_\ell + \eta_{k,\ell} X_\ell,$$

so the time derivative of $V_{\boldsymbol{i}}$ is

$$\begin{aligned} \frac{\mathrm{d}}{\mathrm{d}t} V_{\boldsymbol{i}}(\mathbf{w}) &= \sum_{k \in \boldsymbol{i}} q_{\mathrm{x},k} \left(\mathrm{P}_k(\mathbf{w}) X_k - \widehat{x_{\boldsymbol{i},k}} \frac{\mathrm{P}_k(\mathbf{w}) X_k}{X_k} \right) + \sum_{k \in \mathcal{G} \setminus \boldsymbol{i}} q_{\mathrm{x},k} \mathrm{P}_k(\mathbf{w}) X_k \\ &\quad + \sum_{k \in \mathcal{G}} q_{\mathrm{g},k} (u_k X_k - G_k) \left(G_k - \widehat{g_{\boldsymbol{i},k}} \right) + q_{\mathrm{z},k} (v_k X_k - Z_k) \left(Z_k - \widehat{z_{\boldsymbol{i},k}} \right). \end{aligned}$$

Given that $\forall k \notin \boldsymbol{i}, \widehat{x_{\boldsymbol{i},k}} = 0$, it follows that

$$\frac{\mathrm{d}}{\mathrm{d}t} V_{\boldsymbol{i}}(\mathbf{w}) = \sum_{k \in \mathcal{G}} q_{\mathrm{x},k} \mathrm{P}_k(\mathbf{w}) \left(X_k - \widehat{x_{\boldsymbol{i},k}} \right) + q_{\mathrm{g},k} (u_k X_k - G_k) \left(G_k - \widehat{g_{\boldsymbol{i},k}} \right) + q_{\mathrm{z},k} (v_k X_k - Z_k) \left(Z_k - \widehat{z_{\boldsymbol{i},k}} \right).$$

It is straightforward that $\frac{\mathrm{d}}{\mathrm{d}t} V_{\boldsymbol{i}}(\widehat{\mathbf{w}_{\boldsymbol{i}}}) = 0$, that is property 3 is satisfied. The following calculations are then made to find a sufficient condition for property 4.

From (3.2.3) and (3.b.1), we have that $\forall k \in \boldsymbol{i}$, $\mathrm{P}_k(\widehat{\mathbf{w}_{\boldsymbol{i}}}) = 0$, which gives

$$\varrho_k = -\sum_{\ell \in \mathcal{G}} \gamma_{k,\ell} \widehat{g_{\boldsymbol{i},\ell}} + \sigma_{k,\ell} \widehat{z_{\boldsymbol{i},\ell}} - \eta_{k,\ell} \widehat{x_{\boldsymbol{i},\ell}},$$

thus $\forall k \in \boldsymbol{i}$,

$$\mathrm{P}_k(\mathbf{w}) = \sum_{\ell \in \mathcal{G}} \gamma_{k,\ell} \left(G_\ell - \widehat{g_{\boldsymbol{i},\ell}} \right) - \sigma_{k,\ell} \left(Z_\ell - \widehat{z_{\boldsymbol{i},k}} \right) + \eta_{k,\ell} \left(X_\ell - \widehat{x_{\boldsymbol{i},k}} \right).$$

Note now that $\forall k \notin \boldsymbol{i}$, the following equality holds

$$\begin{aligned} \mathrm{P}_k(\mathbf{w}) &= \sum_{\ell \in \mathcal{G}} \gamma_{k,\ell} \left(G_\ell - \widehat{g_{\boldsymbol{i},\ell}} \right) - \sigma_{k,\ell} \left(Z_\ell - \widehat{z_{\boldsymbol{i},k}} \right) + \eta_{k,\ell} \left(X_\ell - \widehat{x_{\boldsymbol{i},k}} \right) + \varrho_k + \sum_{\ell \in \mathcal{G}} \gamma_{k,\ell} \widehat{g_{\boldsymbol{i},\ell}} - \sigma_{k,\ell} \widehat{z_{\boldsymbol{i},\ell}} + \eta_{k,\ell} \widehat{x_{\boldsymbol{i},\ell}}. \\ &= \sum_{\ell \in \mathcal{G}} \gamma_{k,\ell} \left(G_\ell - \widehat{g_{\boldsymbol{i},\ell}} \right) - \sigma_{k,\ell} \left(Z_\ell - \widehat{z_{\boldsymbol{i},k}} \right) + \eta_{k,\ell} \left(X_\ell - \widehat{x_{\boldsymbol{i},k}} \right) + \mathrm{P}_k(\widehat{\mathbf{w}_{\boldsymbol{i}}}). \end{aligned}$$

Moreover, note that $\forall k \in \mathcal{G}$, $u_k X_k - G_k$ can be written as

$$\begin{aligned} u_k X_k - G_k &= u_k X_k - u_k \widehat{x_{\boldsymbol{i},k}} + u_k \widehat{x_{\boldsymbol{i},k}} - G_k, \\ &= u_k \left(X_k - \widehat{x_{\boldsymbol{i},k}}\right) - \left(G_k - \widehat{g_{\boldsymbol{i},k}}\right), \end{aligned}$$

and the same holds for $v_k X_k - Z_k$

$$v_k X_k - Z_k = v_k \left(X_k - \widehat{x_{\boldsymbol{i},k}}\right) - \left(Z_k - \widehat{z_{\boldsymbol{i},k}}\right).$$

Therefore, the time derivative of $V_{\boldsymbol{i}}$ can be written as

$$\begin{aligned} \frac{\mathrm{d}}{\mathrm{d}t} V_{\boldsymbol{i}}(\mathbf{w}) &= \sum_{k \in \mathcal{G}} \sum_{\ell \in \mathcal{G}} q_{\mathrm{x},k} \left(\gamma_{k,\ell} \left(G_\ell - \widehat{g_{\boldsymbol{i},\ell}}\right) - \sigma_{k,\ell} \left(Z_\ell - \widehat{z_{\boldsymbol{i},k}}\right) + \eta_{k,\ell} \left(X_\ell - \widehat{x_{\boldsymbol{i},k}}\right)\right) \left(X_k - \widehat{x_{\boldsymbol{i},k}}\right) \\ &\quad + \sum_{k \in \mathcal{G}} q_{\mathrm{g},k} u_k \left(X_k - \widehat{x_{\boldsymbol{i},k}}\right) \left(G_k - \widehat{g_{\boldsymbol{i},k}}\right) - q_{\mathrm{g},k} \left(G_k - \widehat{g_{\boldsymbol{i},k}}\right)^2 \\ &\quad + q_{\mathrm{z},k} v_k \left(X_k - \widehat{x_{\boldsymbol{i},k}}\right) \left(Z_k - \widehat{z_{\boldsymbol{i},k}}\right) - q_{\mathrm{z},k} \left(Z_k - \widehat{z_{\boldsymbol{i},k}}\right)^2 \\ &\quad + \sum_{k \in \mathcal{G} \setminus \boldsymbol{i}} q_{\mathrm{x},k} \mathrm{P}_k(\widehat{\mathbf{w}_{\boldsymbol{i}}}) X_k. \end{aligned}$$

Then, because $\widehat{\mathbf{w}_{\boldsymbol{i}}}$ is assumed to be LAS, we can apply the following theorem by Takeuchi (1996),

$$\forall N \in \mathbb{N}^\star, \begin{cases} \frac{\mathrm{d}}{\mathrm{d}t}\mathbf{w} = \mathbf{f}(\mathbf{w}) \odot \mathbf{w}, \\ \mathbf{f} : \mathbb{R}^N \to \mathbb{R}^N \text{ is } C^1, \\ \widehat{\mathbf{w}} \text{ is LAS}, \end{cases} \implies \mathbf{f}(\widehat{\mathbf{w}}) \in (\mathbb{R}_-)^N.$$

Hence, $\sum_{k \in \mathcal{G} \setminus \boldsymbol{i}} q_{\mathrm{x},k} \mathrm{P}_k(\widehat{\mathbf{w}_{\boldsymbol{i}}}) X_k \leq 0$ so we have

$$\begin{aligned} \frac{\mathrm{d}}{\mathrm{d}t} V_{\boldsymbol{i}}(\mathbf{w}) &\leq \sum_{k \in \mathcal{G}} \Big(q_{\mathrm{g},k} u_k \left(X_k - \widehat{x_{\boldsymbol{i},k}}\right) \left(G_k - \widehat{g_{\boldsymbol{i},k}}\right) - q_{\mathrm{g},k} \left(G_k - \widehat{g_{\boldsymbol{i},k}}\right)^2 \\ &\quad + q_{\mathrm{z},k} v_k \left(X_k - \widehat{x_{\boldsymbol{i},k}}\right) \left(Z_k - \widehat{z_{\boldsymbol{i},k}}\right) - q_{\mathrm{z},k} \left(Z_k - \widehat{z_{\boldsymbol{i},k}}\right)^2 \\ &\quad \sum_{\ell \in \mathcal{G}} \left(q_{\mathrm{x},k} \gamma_{k,\ell} \left(G_\ell - \widehat{g_{\boldsymbol{i},\ell}}\right) \left(X_k - \widehat{x_{\boldsymbol{i},k}}\right) - q_{\mathrm{x},k} \sigma_{k,\ell} \left(Z_\ell - \widehat{z_{\boldsymbol{i},k}}\right) \left(X_k - \widehat{x_{\boldsymbol{i},k}}\right) \right. \\ &\quad \left. + q_{\mathrm{x},k} \eta_{k,\ell} \left(X_\ell - \widehat{x_{\boldsymbol{i},k}}\right) \left(X_k - \widehat{x_{\boldsymbol{i},k}}\right)\right)\Big). \end{aligned} \tag{3.c.2}$$

If we use now generalized variable notations W_k and $\widehat{w_{\boldsymbol{i},k}}$ such that

$$\forall k \in \overline{\mathcal{G}}, \begin{cases} W_k \coloneqq \mathbb{I}_{\{k \in [\![1;n]\!]\}} X_k + \mathbb{I}_{\{k \in [\![n+1;2n]\!]\}} G_k + \mathbb{I}_{\{k \in [\![2n+1;3n]\!]\}} Z_k, \\ \widehat{w_{\boldsymbol{i},k}} \coloneqq \mathbb{I}_{\{k \in [\![1;n]\!]\}} \widehat{x_{\boldsymbol{i},k}} + \mathbb{I}_{\{k \in [\![n+1;2n]\!]\}} \widehat{g_{\boldsymbol{i},k}} + \mathbb{I}_{\{k \in [\![2n+1;3n]\!]\}} \widehat{z_{\boldsymbol{i},k}}, \end{cases}$$

where $\overline{\mathcal{G}} \coloneqq [\![1;3n]\!]$. Similarly, we define

$$\forall k \in \overline{\mathcal{G}}, q_k \coloneqq \mathbb{I}_{\{k \in [\![1;n]\!]\}} q_{\mathrm{x},k} + \mathbb{I}_{\{k \in [\![n+1;2n]\!]\}} q_{\mathrm{g},k} + \mathbb{I}_{\{k \in [\![2n+1;3n]\!]\}} q_{\mathrm{z},k}.$$

Using these notations, we can now see that

$$\frac{\mathrm{d}}{\mathrm{d}t} V_{\boldsymbol{i}}(\mathbf{w}) \leq \sum_{(k,\ell) \in \overline{\mathcal{G}}^2} q_k a_{k,\ell} \left(W_k - \widehat{w_{\boldsymbol{i},k}}\right) \left(W_\ell - \widehat{w_{\boldsymbol{i},\ell}}\right) = \frac{1}{2} (\mathbf{w} - \widehat{\mathbf{w}_{\boldsymbol{i}}})^{\mathbf{T}} \left(\mathbf{Q}.\mathbf{A} + \mathbf{A}^{\mathbf{T}}.\mathbf{Q}\right) (\mathbf{w} - \widehat{\mathbf{w}_{\boldsymbol{i}}}), \tag{3.c.3}$$

where $\mathbf{Q} = \mathrm{diag}(q_k)_{k\in\overline{\mathcal{G}}}$ and $\mathbf{A} := \left(a_{k,\ell}\right)_{(k,\ell)\in\overline{\mathcal{G}}^2}$. By comparing (3.c.2) and (3.c.3), it follows that $\mathbf{A}$ is the following matrix of within-host parameters

$$\mathbf{A} = \begin{pmatrix} \mathbf{H} & \mathbf{\Gamma} & -\mathbf{\Sigma} \\ \mathbf{U} & -\mathbf{I}_n & \mathbf{0}_{n,n} \\ \mathbf{V} & \mathbf{0}_{n,n} & -\mathbf{I}_n \end{pmatrix}. \tag{3.c.4}$$

From (3.c.3), it follows that property 4 is satisfied if and only if there exists a positive diagonal matrix $\mathbf{Q} \in \mathfrak{M}_{3n,3n}\left(\mathbb{R}_+^\star\right)$ such that $\mathbf{Q}.\mathbf{A} + \mathbf{A}^\mathbf{T}.\mathbf{Q}$ is negative definite.

We finally use a theorem from Berman & Plemmons (1979) that states $\forall N \in \mathbb{N}^\star, \forall \mathbf{A} = \left(a_{i,j}\right)_{(i,j)\in[\![1;N]\!]^2} \in \mathfrak{M}_{N,N}(\mathbb{R})$,

$$\exists \mathbf{d} = (d_i)_{i\in[\![1;N]\!]} \in \left(\mathbb{R}_+^\star\right)^N : \forall k \in [\![1;N]\!], -d_i a_{i,i} > \sum_{j\in[\![1;N]\!]\setminus\{i\}} \left|a_{i,j}\right| d_j$$
$$\Longrightarrow \exists \mathbf{Q} \in \mathfrak{M}_{N,N}\left(\mathbb{R}_+^\star\right) \text{ diagonal} : \mathbf{Q}.\mathbf{A} + \mathbf{A}^\mathbf{T}.\mathbf{Q} \text{ is negative definite.}$$

The premise of this theorem is called strict row diagonal dominance. Then, a sufficient condition for property 4 to be satisfied is the following by setting $\mathbf{d} = \mathbf{1}_n$ for instance,

$$\forall k \in \overline{\mathcal{G}}, a_{k,k} < -\sum_{\ell\in\overline{\mathcal{G}}\setminus\{i\}} \left|a_{k,\ell}\right| < 0,$$

that is to say, by (3.c.4),

$$\forall k \in \mathcal{G}, \begin{cases} \eta_{k,k} & < -\sum\limits_{\ell\in\mathcal{G}\setminus\{k\}} \left|\eta_{k,\ell}\right| - \sum\limits_{\ell\in\mathcal{G}} \gamma_{k,\ell} + \sigma_{k,\ell} < 0, \\ 0 < u_k & < 1, \\ 0 < v_k & < 1. \end{cases} \tag{3.c.5}$$

We have thus proved that if $\widehat{\mathbf{w_i}}$ is a LAS steady state in $(\mathbb{R}_+)^{3n}$ and the within-host parameters satisfy (3.c.5), then $\widehat{\mathbf{w_i}}$ is GAS in $\Omega_{\boldsymbol{i}}$, that is $\mathbf{w}(0) \in \Omega_{\boldsymbol{i}} \Longrightarrow \lim\limits_{t\to\infty} \mathbf{w}(t) = \widehat{\mathbf{w_i}}$.

3.d. Between host level

3.d.1. Transmission rates properties

Hereafter we provide a proof of the two transmission rate properties which are (3.4.4), the overall transmission rate is constant whatever the host class, and (3.4.5), which gives the transmission rate of a given genotype from a given host class. For the sake of simplicity, the proof is provided for an abstract finite set instead of a set of parasite genotypes.

Let Ω be a finite set such that

$$\Omega = \{\omega_1, \omega_2, \ldots, \omega_{|\Omega|}\}, |\Omega| < \aleph_0.$$

We define an arbitrary measure μ on Ω as follows

1. $\mu \in \mathcal{A}(\Omega, [0;1])$,
2. $\mu(\emptyset) = 0$,
3. $\mu(\Omega) = 1$,
4. $\forall \omega \in \Omega, 0 < \mu(\{\omega\}) < 1$,
5. $\forall \mathcal{P} \in \wp(\Omega), \mu(\mathcal{P}) = \sum_{\omega \in \mathcal{P}} \mu(\{\omega\})$.

One can see μ as an elementary probability associated to Ω. As a consequence of points 3. and 5. of this definition, we have

$$\sum_{\omega \in \Omega} \mu(\{\omega\}) \overset{5.}{=} \mu(\Omega) \overset{3.}{=} 1. \tag{3.d.1}$$

Next, we introduce the operator $F_{.,.}$ that is a function of a couple of disjoint subsets of Ω,

$$\forall (\mathcal{P}, \mathcal{Q}) \in \wp(\Omega)^2 : \mathcal{P} \cap \mathcal{Q} = \emptyset, F_{\mathcal{P},\mathcal{Q}} \coloneqq \prod_{\omega \in \mathcal{P}} \mu(\{\omega\}) \prod_{\omega \in \mathcal{Q}} \big(1 - \mu(\{\omega\})\big).$$

This operator is the product over all the measures of each element of its first subset argument and the complementary measures of each element of its second subset argument. It has the following properties

6. $\forall \alpha \in \Omega, F_{\{\alpha\},\emptyset} = \mu(\{\alpha\})$,
7. $\forall \alpha \in \Omega, F_{\emptyset,\{\alpha\}} = 1 - \mu(\{\alpha\})$,
8. $\forall \alpha \in \Omega, F_{\{\alpha\},\emptyset} + F_{\emptyset,\{\alpha\}} = 1$,
9. $\forall (\mathcal{P}, \mathcal{Q}, \mathcal{R}, \mathcal{S}) \in \wp(\Omega)^4$ mutually disjoint, $F_{\mathcal{P},\mathcal{Q}} F_{\mathcal{R},\mathcal{S}} = F_{\mathcal{P}\cup\mathcal{R},\mathcal{Q}\cup\mathcal{S}}$,
10. $\forall \alpha \in \Omega, \forall (\mathcal{P}, \mathcal{Q}) \in \wp(\Omega \setminus \{\alpha\})^2 : \mathcal{P} \cap \mathcal{Q} = \emptyset, F_{\mathcal{P},\mathcal{Q}} = F_{\mathcal{P}\cup\{\alpha\},\mathcal{Q}} + F_{\mathcal{P},\mathcal{Q}\cup\{\alpha\}}$.

Let us prove them all.

The proof of property 6. is the following

$$\begin{aligned} \forall \alpha \in \Omega, F_{\{\alpha\},\emptyset}, &\coloneqq \prod_{\omega \in \{\alpha\}} \mu(\{\omega\}) \prod_{\omega \in \emptyset} \big(1 - \mu(\{\omega\})\big), \\ &= \mu(\{\alpha\}) \times 1, \\ &= \mu(\{\alpha\}), \end{aligned}$$

since the empty product is the neutral element of multiplication, that is one, such for $\forall x \in \mathbb{R}^\star, x^0 = 1$.

Similarly, the proof of property 7. is

$$\begin{aligned}\forall \alpha \in \Omega, F_{\emptyset,\{\alpha\}}, &:= \prod_{\omega\in\emptyset}\mu(\{\omega\})\prod_{\omega\in\{\alpha\}}\big(1-\mu(\{\omega\})\big)\\ &= 1\times\big(1-\mu(\{\alpha\})\big),\\ &= 1-\mu(\{\alpha\}).\end{aligned}$$

The proof of property 8. is straightforward from the previous two

$$\begin{aligned}\forall \alpha \in \Omega, F_{\{\alpha\},\emptyset}+F_{\emptyset,\{\alpha\}} &\overset{6.\text{ and }7.}{=} \mu(\{\alpha\})+\big(1-\mu(\{\alpha\})\big),\\ &= 1.\end{aligned}$$

To prove property 9., let $\mathcal{P},\mathcal{Q},\mathcal{R},\mathcal{S}$ a family of four mutually disjoint subsets of Ω, then

$$\begin{aligned}F_{\mathcal{P},\mathcal{Q}}F_{\mathcal{R},\mathcal{S}} &:= \left(\prod_{\omega\in\mathcal{P}}\mu(\{\omega\})\prod_{\omega\in\mathcal{Q}}\big(1-\mu(\{\omega\})\big)\right)\left(\prod_{\omega\in\mathcal{R}}\mu(\{\omega\})\prod_{\omega\in\mathcal{S}}\big(1-\mu(\{\omega\})\big)\right),\\ &= \prod_{\omega\in\mathcal{P}\cup\mathcal{R}}\mu(\{\omega\})\prod_{\omega\in\mathcal{Q}\cup\mathcal{S}}\big(1-\mu(\{\omega\})\big),\\ &=: F_{\mathcal{P}\cup\mathcal{R},\mathcal{Q}\cup\mathcal{S}}.\end{aligned}$$

Finally, to prove property 10., let α be an element of Ω and $\mathcal{P},\mathcal{Q}$ two disjoint susbets of $\Omega\setminus\{\alpha\}$, that is none of them contains α. Using properties 8. and 9. we have

$$\begin{aligned}F_{\mathcal{P},\mathcal{Q}} &\overset{8.}{=} \big(F_{\{\alpha\},\emptyset}+F_{\emptyset,\{\alpha\}}\big)F_{\mathcal{P},\mathcal{Q}},\\ &= F_{\{\alpha\},\emptyset}F_{\mathcal{P},\mathcal{Q}}+F_{\emptyset,\{\alpha\}}F_{\mathcal{P},\mathcal{Q}},\\ &\overset{9.}{=} F_{\mathcal{P}\cup\{\alpha\},\mathcal{Q}}+F_{\mathcal{P},\mathcal{Q}\cup\{\alpha\}}.\end{aligned}$$

Let us now do the following calculation starting from $F_{\{\omega_1\},\emptyset}$ and using $|\Omega|-1$ times property 8,

$$\begin{aligned}F_{\{\omega_1\},\emptyset} &\overset{8.}{=} F_{\{\omega_1\},\emptyset}\big(F_{\{\omega_2\},\emptyset}+F_{\emptyset,\{\omega_2\}}\big)\big(F_{\{\omega_3\},\emptyset}+F_{\emptyset,\{\omega_3\}}\big)\ldots\Big(F_{\{\omega_{|\Omega|}\},\emptyset}+F_{\emptyset,\{\omega_{|\Omega|}\}}\Big),\\ &= F_{\{\omega_1\},\emptyset}\left(\sum_{\mathcal{P}\in\wp(\Omega\setminus\{\omega_1\})}\prod_{\omega\in\mathcal{P}}F_{\{\omega\},\emptyset}\prod_{\omega\in(\Omega\setminus\{\omega_1\})\setminus\mathcal{P}}F_{\emptyset,\{\omega\}}\right),\\ &\overset{9.}{=} F_{\{\omega_1\},\emptyset}\left(\sum_{\mathcal{P}\in\wp(\Omega\setminus\{\omega_1\})}F_{\mathcal{P},\emptyset}F_{\emptyset,(\Omega\setminus\{\omega_1\})\setminus\mathcal{P}}\right),\\ &\overset{9.}{=} F_{\{\omega_1\},\emptyset}\left(\sum_{\mathcal{P}\in\wp(\Omega\setminus\{\omega_1\})}F_{\mathcal{P},(\Omega\setminus\{\omega_1\})\setminus\mathcal{P}}\right),\end{aligned}$$

by noticing that each term of the expansion contains either $F_{\{\omega_k\},\emptyset}$ or $F_{\emptyset,\{\omega_k\}}$, for a given ω of $\Omega\setminus\{\omega_1\}$. Each term of the expansion is then a unique partition $(\mathcal{P},(\Omega\setminus\{\omega_1\})\setminus\mathcal{P})$ of $\Omega\setminus\{\omega_1\}$, whence the sum index.

Including $F_{\{\omega_1\},\emptyset}$ in the sum, we have

$$\begin{aligned} F_{\{\omega_1\},\emptyset} &= \sum_{\mathcal{P}\in\wp(\Omega\setminus\{\omega_1\})} F_{\{\omega_1\},\emptyset}F_{\mathcal{P},(\Omega\setminus\{\omega_1\})\setminus\mathcal{P}}, \\ &\overset{9.}{=} \sum_{\mathcal{P}\in\wp(\Omega\setminus\{\omega_1\})} F_{\mathcal{P}\cup\{\omega_1\},(\Omega\setminus\{\omega_1\})\setminus\mathcal{P}}, \\ &= \sum_{\substack{\mathcal{P}\in\wp(\Omega)\\ \mathcal{P}\ni\omega_1}} F_{\mathcal{P},\Omega\setminus\mathcal{P}}. \end{aligned}$$

The same calculation can be done for each ω of Ω. The following equality holds

$$\forall\omega\in\Omega, F_{\{\omega\},\emptyset} = \sum_{\substack{\mathcal{P}\in\wp(\Omega)\\ \mathcal{P}\ni\omega}} F_{\mathcal{P},\Omega\setminus\mathcal{P}}. \tag{3.d.2}$$

Let us now do the following calculation

$$\begin{aligned} 1 &\overset{(3.d.1)}{=} \sum_{\omega\in\Omega}\mu(\{\omega\}), \\ &\overset{6.}{=} \sum_{\omega\in\Omega} F_{\{\omega\},\emptyset}, \\ &\overset{(3.d.2)}{=} \sum_{\omega\in\Omega}\sum_{\substack{\mathcal{P}\in\wp(\Omega)\\ \mathcal{P}\ni\omega}} F_{\mathcal{P},\Omega\setminus\mathcal{P}}, \\ &= \sum_{\mathcal{P}\in\wp(\Omega)}\sum_{\omega\in\mathcal{P}} F_{\mathcal{P},\Omega\setminus\mathcal{P}}, \\ &= \sum_{\mathcal{P}\in\wp(\Omega)} F_{\mathcal{P},\Omega\setminus\mathcal{P}}\sum_{\omega\in\mathcal{P}} 1, \\ &= \sum_{\mathcal{P}\in\wp(\Omega)} F_{\mathcal{P},\Omega\setminus\mathcal{P}}|\mathcal{P}|. \end{aligned}$$

Thus we proved that

$$\sum_{\mathcal{P}\in\wp(\Omega)} |\mathcal{P}|F_{\mathcal{P},\Omega\setminus\mathcal{P}} = 1. \tag{3.d.3}$$

Let us now reversely apply the previous argument to the sum $\sum_{\mathcal{P}\in\wp(\Omega\setminus\{\alpha\})} |\mathcal{P}|F_{\mathcal{P},(\Omega\setminus\{\alpha\})\setminus\mathcal{P}}$, $\forall\alpha\in\Omega$ (note that Ω is replaced by $\Omega\setminus\{\alpha\}$). We have

$$\begin{aligned} \sum_{\mathcal{P}\in\wp(\Omega\setminus\{\alpha\})} |\mathcal{P}|F_{\mathcal{P},(\Omega\setminus\{\alpha\})\setminus\mathcal{P}} &= \sum_{\omega\in\Omega\setminus\{\alpha\}}\sum_{\substack{\mathcal{P}\in\wp(\Omega\setminus\{\alpha\})\\ \mathcal{P}\ni\omega}} F_{\mathcal{P},(\Omega\setminus\{\alpha\})\setminus\mathcal{P}}, \\ &\overset{(3.d.2)}{=} \sum_{\omega\in\Omega\setminus\{\alpha\}} F_{\{\omega\},\emptyset}, \\ &\overset{6.}{=} \sum_{\omega\in\Omega\setminus\{\alpha\}}\mu(\{\omega\}), \\ &= \sum_{\omega\in\Omega}\mu(\{\omega\}) - \mu(\{\alpha\}), \\ &\overset{(3.d.1)}{=} 1-\mu(\{\alpha\}). \end{aligned} \tag{3.d.4}$$

It is then straightforward that

$$\begin{aligned}
\sum_{\substack{\mathcal{P}\in\wp(\Omega)\\ \mathcal{P}\not\ni\alpha}} |\mathcal{P}| F_{\mathcal{P},\Omega\setminus\mathcal{P}} &\overset{9.}{=} \sum_{\mathcal{P}\in\wp(\Omega\setminus\{\alpha\})} |\mathcal{P}| F_{\emptyset,\{\alpha\}} F_{\mathcal{P},(\Omega\setminus\{\alpha\})\setminus\mathcal{P}} \\
&= F_{\emptyset,\{\omega_1\}} \left(\sum_{\mathcal{P}\in\wp(\Omega\setminus\{\alpha\})} |\mathcal{P}| F_{\mathcal{P},(\Omega\setminus\{\alpha\})\setminus\mathcal{P}} \right), \\
&\overset{7.\text{ and }(3.\text{d}.4)}{=} \big(1-\mu(\{\alpha\})\big)\big(1-\mu(\{\alpha\})\big),
\end{aligned}$$

that is

$$\forall \alpha \in \Omega, \sum_{\substack{\mathcal{P}\in\wp(\Omega)\\ \mathcal{P}\not\ni\alpha}} |\mathcal{P}| F_{\mathcal{P},\Omega\setminus\mathcal{P}} = \big(1-\mu(\{\alpha\})\big)^2. \tag{3.d.5}$$

Finally, we have $\forall \alpha \in \Omega$,

$$\begin{aligned}
\sum_{\substack{\mathcal{P}\in\wp(\Omega)\\ \mathcal{P}\ni\alpha}} |\mathcal{P}| F_{\mathcal{P},\Omega\setminus\mathcal{P}} &\overset{10.}{=} \sum_{\substack{\mathcal{P}\in\wp(\Omega)\\ \mathcal{P}\ni\alpha}} |\mathcal{P}| \big(F_{\mathcal{P}\setminus\{\alpha\},\Omega\setminus\mathcal{P}} - F_{\mathcal{P}\setminus\{\alpha\},\{\Omega\setminus\mathcal{P}\}\cup\{\alpha\}}\big), \\
&= \sum_{\substack{\mathcal{P}\in\wp(\Omega)\\ \mathcal{P}\ni\alpha}} |\mathcal{P}| F_{\mathcal{P}\setminus\{\alpha\},\Omega\setminus\mathcal{P}} - \sum_{\substack{\mathcal{P}\in\wp(\Omega)\\ \mathcal{P}\ni\alpha}} |\mathcal{P}| F_{\mathcal{P}\setminus\{\alpha\},\{\Omega\setminus\mathcal{P}\}\cup\{\alpha\}}, \\
&= \sum_{\mathcal{P}\in\wp(\Omega)} |\mathcal{P}| F_{\mathcal{P},\Omega\setminus\mathcal{P}} - \sum_{\substack{\mathcal{P}\in\wp(\Omega)\\ \mathcal{P}\not\ni\alpha}} |\mathcal{P}| F_{\mathcal{P},\{\Omega\setminus\mathcal{P}\}}, \\
&\overset{(3.\text{d}.3)\text{ and }(3.\text{d}.5)}{=} 1-\big(1-\mu(\{\alpha\})\big)^2, \\
&= 1-1+2\mu(\{\alpha\})-\mu(\{\alpha\})^2, \\
&= \mu(\{\alpha\})\big(2-\mu(\{\alpha\})\big).
\end{aligned} \tag{3.d.6}$$

Now, by identifying Ω to host class $\boldsymbol{d}$, ω_k to genotypes, $\mu(\{\omega_k\})$ to genotypes frequencies $\frac{x_{\boldsymbol{d},k}}{\sum_{\ell\in\boldsymbol{d}} x_{\boldsymbol{d},\ell}}$, it is straightforward that (3.d.3) implies (3.4.4) and (3.d.6) implies (3.4.5).

The curve of $\beta_{\boldsymbol{d},k}$ as a function of $x_{\boldsymbol{d},k}$ is given in Figure 3.d.1.

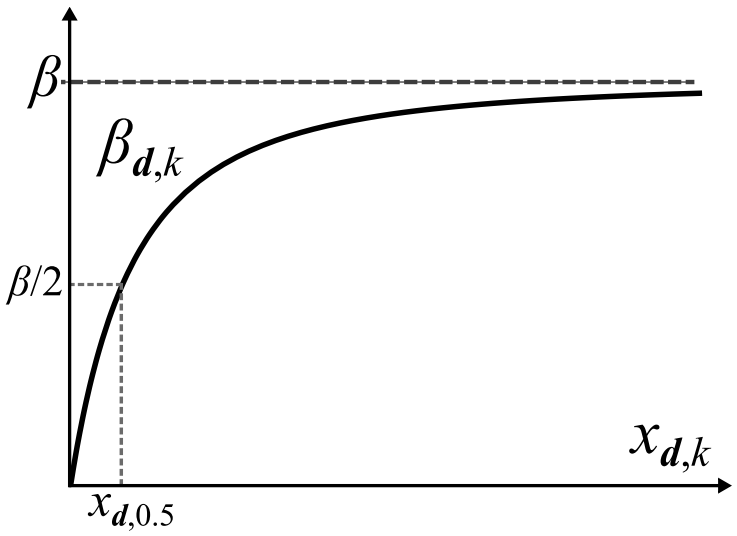

Figure 3.d.1. – Transmission rate of genotype k from hosts $\boldsymbol{d}$ as a function of the parasite load of genotype k
(the parasite loads of the other genotypes being fixed), for $|\boldsymbol{d}| \geq 2$.

The plateau corresponds to the overall transmission rate β, and is the limit of genotype k transmission rate when its frequency goes to 1, that is

$$\begin{aligned}\lim_{x_{\boldsymbol{d},k}\to\infty}\beta_{\boldsymbol{d},k} &= \lim_{x_{\boldsymbol{d},k}\to\infty}\beta\frac{x_{\boldsymbol{d},k}}{\sum\limits_{\ell\in\boldsymbol{d}}x_{\boldsymbol{d},\ell}}\left(2-\frac{x_{\boldsymbol{d},k}}{\sum\limits_{\ell\in\boldsymbol{d}}x_{\boldsymbol{d},\ell}}\right),\\ &= \beta\lim_{x_{\boldsymbol{d},k}\to\infty}\frac{1}{1+\sum\limits_{\ell\in\boldsymbol{d}\setminus\{k\}}\frac{x_{\boldsymbol{d},\ell}}{x_{\boldsymbol{d},k}}}\left(2-\frac{x_{\boldsymbol{d},k}}{x_{\boldsymbol{d},k}\left(1+\sum\limits_{\ell\in\boldsymbol{d}\setminus\{k\}}\frac{x_{\boldsymbol{d},\ell}}{x_{\boldsymbol{d},k}}\right)}\right),\\ &= \beta.\end{aligned}$$

However, the transmission rate of genotype k reaches half of the overall transmission rate relatively quickly. Indeed, if we denote $x_{\boldsymbol{d},0.5}$ the parasite load that satisfies the following equation

$$\beta\frac{x_{\boldsymbol{d},0.5}}{\sum\limits_{\ell\in\boldsymbol{d}}x_{\boldsymbol{d},\ell}}\left(2-\frac{x_{\boldsymbol{d},0.5}}{\sum\limits_{\ell\in\boldsymbol{d}}x_{\boldsymbol{d},\ell}}\right)=\frac{\beta}{2},$$

we have

$$\left(\frac{x_{\boldsymbol{d},0.5}}{\sum\limits_{\ell\in\boldsymbol{d}}x_{\boldsymbol{d},\ell}}\right)^2-2\frac{x_{\boldsymbol{d},0.5}}{\sum\limits_{\ell\in\boldsymbol{d}}x_{\boldsymbol{d},\ell}}+\frac{1}{2}=0.$$

The discriminant of this polynomial is $\Delta=2$ so its only root lying in $[0;1]$ is

$$\frac{x_{\boldsymbol{d},0.5}}{\sum\limits_{\ell\in\boldsymbol{d}}x_{\boldsymbol{d},\ell}}=\frac{+2-\sqrt{2}}{2}=1-\frac{\sqrt{2}}{2}\approx 29\,\%.$$

If we denote by $\overline{\boldsymbol{x}_{\boldsymbol{d},\circ}}$ the average parasite load of the $|\boldsymbol{d}|-1$ other genotypes in $\boldsymbol{d}$, the half overall transmission parasite load $x_{\boldsymbol{d},0.5}$ is

$$\begin{aligned}x_{\boldsymbol{d},0.5} &= \left(1-\frac{\sqrt{2}}{2}\right)\left(x_{\boldsymbol{d},0.5}+(|\boldsymbol{d}|-1)\overline{x_{\boldsymbol{d},\circ}}\right),\\ &= \frac{1-\frac{\sqrt{2}}{2}}{\frac{\sqrt{2}}{2}}(|\boldsymbol{d}|-1)\overline{x_{\boldsymbol{d},\circ}},\\ &= \left(\sqrt{2}-1\right)(|\boldsymbol{d}|-1)\overline{x_{\boldsymbol{d},\circ}},\end{aligned}$$

where $\sqrt{2}-1\approx 41\%$. A numerical application shows that $x_{\boldsymbol{d},0.5}$ is smaller than $\overline{\boldsymbol{x}_{\boldsymbol{d},\circ}}$ only in bi- and tri-infected hosts.

The main result of this calculation is that whatever the rank of the coinfected host class (provided that $|\boldsymbol{d}|\geq 2$), a given genotype is involved in at least half of the transmissions if its frequency is higher than about 29% (reminding us that the sum of the parasite transmission rates can be greater than the overall transmission rate because of shared inoculas).

3.d.2. Labelled forms of between-host equations

Based on the labelling previously defined, we present here the labelled alternative forms of the equations and rates written in the set-theoretic form in the main text. We also detail the master equation matrices, for readers interested in computing the model. Thereafter $\delta_{a,b}$ refers to the KRONECKER's delta, which is 1 if $a = b$ and 0 otherwise.

3.d.2.1. Between-host ODEs

The labelled form of the between-host ODEs is the following

$$\begin{cases} \frac{\mathrm{d}I_i}{\mathrm{d}t} &= \sum\limits_{r=0}^{2^n-1}\sum\limits_{d=0}^{2^n-1}\beta_{r,d,i}I_rI_d + \sum\limits_{d=0}^{2^n-1}\theta_{d,i}I_d - \left(\sum\limits_{d=0}^{2^n-1}\sum\limits_{\ell=0}^{2^n-1}\beta_{i,d,\ell}I_d + \sum\limits_{\ell=0}^{2^n-1}\theta_{i,\ell} + \mu_i\right)I_i, \\ \frac{\mathrm{d}S}{\mathrm{d}t} &= \sum\limits_{d=0}^{2^n-1}\mu_dI_d + \sum\limits_{r=0}^{2^n-1}\sum\limits_{d=0}^{2^n-1}\beta_{r,d,0}I_rI_d + \sum\limits_{d=0}^{2^n-1}\theta_{d,0}I_d - \sum\limits_{d=0}^{2^n-1}\sum\limits_{\ell=0}^{2^n-1}\beta_{0,d,\ell}I_dS. \end{cases}$$

3.d.2.2. Infection rates

The labelled form of the infection rates is the following

$$\beta_{r,d,i} \coloneqq \beta\varsigma(r)\varsigma(d)\varsigma(i)\left(1-\delta_{r,i}\right)\sum_{p=0}^{2^n-1}\left(\min_{k\in[\![1;n]\!]}\left(\delta_{c_{d,k},c_{d,k}+c_{p,k}-c_{d,k}c_{p,k}}\right)\delta_{i,\phi(r,p)}n_p \prod_{k=1}^{n}\frac{\left(2\delta_{c_{p,k},1}-1\right)x_{d,k}+\left(1-\delta_{c_{p,k},1}\right)\sum\limits_{\ell=1}^{n}x_{d,\ell}}{\sum\limits_{\ell=1}^{n}x_{d,\ell}}\right),$$

where

1. β is the constant transmission factor,
2. $\varsigma(r)\varsigma(d)\varsigma(i)$ cancels out if one of the three involved classes is not epidemiological,
3. $\left(1-\delta_{r,i}\right)$ cancels out if the infection event is trivial (the receiver class is already the output),
4. $\sum\limits_{p=0}^{2^n-1}$ is the sum over all inocula,
5. $\min\limits_{k\in[\![1;n]\!]}\left(\delta_{c_{d,k},c_{d,k}+c_{p,k}-c_{d,k}c_{p,k}}\right)$ cancels out whenever a genotype belongs to p but not to d (ensuring that inoculum p can be produced by donor host d),
6. $\delta_{i,\phi(r,p)}$ cancels out whenever host class r does not turn into host class i when infected by inoculum class p,
7. n_p is the rank of the inoculum class,
8. $\prod\limits_{k=1}^{n}$ is the product over all genotypes (nested in the inocula),
9. $\frac{\left(2\delta_{c_{p,k},1}-1\right)x_{d,k}+\left(1-\delta_{c_{p,k},1}\right)\sum\limits_{\ell=1}^{n}x_{d,\ell}}{\sum\limits_{\ell=1}^{n}x_{d,\ell}}$ is the product of frequencies and complementary frequencies over all genotypes of d depending on the presence or absence in p.

3.d.2.3. Recovery rates

The labelled form of the recovery rates is the following

$$\theta_{d,i} \coloneqq \theta\varsigma(d)\left(1-\delta_{d,i}\right)\sum_{k=1}^{n}\delta_{i,\phi\left(0,c_{d,k}\left(d-2^{k-1}\right)\right)},$$

where

1. θ is the constant recovery factor,
2. $\varsigma(d)$ cancels out if the recovering class is not epidemiologically meaningful,
3. $\left(1-\delta_{r,i}\right)$ cancels out if the recovery event is trivial (the recovering class is already the output),
4. $\sum_{k=1}^{n}$ is the sum over all genotypes,
5. $\delta_{i,\phi\left(0,c_{d,k}\left(d-2^{k-1}\right)\right)}$ cancels out whenever host class d does not turn into host class i when losing genotype k.

3.d.2.4. Death rate

The labelled form of the death rates is the following

$$\mu_i \coloneqq \mu\sum_{k=1}^{n}x_{d,k}.$$

3.d.2.5. Master equation matrices

Recall that the master equation of between-host dynamics is:

$$\frac{\mathrm{d}}{\mathrm{d}t}\mathbf{y} = \mathbf{\Phi}.(\mathbf{y}\otimes\mathbf{y}) - (\mathbf{\Psi}.\mathbf{y})\odot\mathbf{y} + (\mathbf{\Xi}-\mathbf{\Theta}-\mathbf{\Delta}).\mathbf{y}.$$

The expression of each matrix are the following:

$$\begin{cases}
\mathbf{\Phi} \coloneqq \left(\beta_{\mathfrak{r}(j),\mathfrak{d}(j),i}\right)_{(i,j)\in[\![0;2^n-1]\!]\times[\![0;2^{2n}-1]\!]}, \\
\mathfrak{r}(j) \coloneqq \left\lfloor\frac{j}{2^n}\right\rfloor, \quad \mathfrak{d}(j) \coloneqq \mathrm{mod}_{2^n}(j), \\
\mathbf{\Psi} \coloneqq \left(\sum_{\ell=0}^{2^n-1}\beta_{i,j,\ell}\right)_{(i,j)\in[\![0;2^n-1]\!]^2}, \\
\mathbf{\Xi} \coloneqq \left(\theta_{i,j}\right)_{(i,j)\in[\![0;2^n-1]\!]^2}, \\
\mathbf{\Theta} \coloneqq \left(\delta_{i,j}\sum_{\ell=0}^{2^n-1}\theta_{i,\ell}\right)_{(i,j)\in[\![0;2^n-1]\!]^2}, \\
\mathbf{\Delta} \coloneqq \left(\left(\delta_{i,j}\left(1-\delta_{i,0}\right)-\delta_{i,0}\right)\mu_j\right)_{(i,j)\in[\![0;2^n-1]\!]^2}.
\end{cases}$$

Note that the $\mathbf{\Phi}$ matrix has a nested structure (donor host classes are nested into receiver host classes) that requires arithmetical calculation on indices, whence the $\mathfrak{r}$ and $\mathfrak{d}$ functions.

3.e. Basic reproduction numbers calculation

3.e.1. Next-generation basic reproduction number

The next-generation basic reproduction number, $\mathcal{R}_0^{\mathrm{I}}$, is derived from the susceptible steady state instability. First, we need to calculate the between infected hosts jacobian matrix, denoted by $\mathbf{J}_{\mathrm{b}}$, the elements of which are found through the following partial derivative

$$\begin{aligned}\frac{\partial}{\partial I_{\boldsymbol{j}}}\left(\frac{\mathrm{d}I_{\boldsymbol{i}}}{\mathrm{d}t}\right) &= \sum_{(\boldsymbol{r},\boldsymbol{d})\in(\mathcal{E}\setminus\{\boldsymbol{i}\})\times\mathcal{E}^\star}\beta_{\boldsymbol{r},\boldsymbol{d},\boldsymbol{i}}\frac{\partial I_{\boldsymbol{r}}I_{\boldsymbol{d}}}{\partial I_{\boldsymbol{j}}}\\ &\quad+\sum_{\boldsymbol{d}\in\mathcal{E}}\theta_{\boldsymbol{d},\boldsymbol{i}}\frac{\partial I_{\boldsymbol{d}}}{\partial I_{\boldsymbol{j}}}-\frac{\partial}{\partial I_{\boldsymbol{j}}}\left(\left(\sum_{(\boldsymbol{d},\boldsymbol{\ell})\in\mathcal{E}^\star\times(\mathcal{E}\setminus\{\boldsymbol{i}\})}\beta_{\boldsymbol{i},\boldsymbol{d},\boldsymbol{\ell}}I_{\boldsymbol{d}}+\sum_{\boldsymbol{\ell}\in\mathcal{E}\setminus\{\boldsymbol{i}\}}\theta_{\boldsymbol{i},\boldsymbol{\ell}}+\mu_{\boldsymbol{i}}\right)I_{\boldsymbol{i}}\right),\\ &= \sum_{\boldsymbol{r}\in\mathcal{E}\setminus\{\boldsymbol{i}\}}\beta_{\boldsymbol{r},\boldsymbol{j},\boldsymbol{i}}I_{\boldsymbol{r}}+\sum_{\boldsymbol{d}\in\mathcal{E}^\star}\beta_{\boldsymbol{j},\boldsymbol{d},\boldsymbol{i}}I_{\boldsymbol{d}}+\theta_{\boldsymbol{j},\boldsymbol{i}}-I_{\boldsymbol{i}}\sum_{\boldsymbol{\ell}\in(\mathcal{E}\setminus\{\boldsymbol{i}\})}\beta_{\boldsymbol{i},\boldsymbol{j},\boldsymbol{\ell}}\\ &\quad-\left(\sum_{(\boldsymbol{d},\boldsymbol{\ell})\in\mathcal{E}^\star\times(\mathcal{E}\setminus\{\boldsymbol{i}\})}\beta_{\boldsymbol{i},\boldsymbol{d},\boldsymbol{\ell}}I_{\boldsymbol{d}}+\sum_{\boldsymbol{\ell}\in\mathcal{E}\setminus\{\boldsymbol{i}\}}\theta_{\boldsymbol{i},\boldsymbol{\ell}}+\mu_{\boldsymbol{i}}\right)\frac{\partial I_{\boldsymbol{i}}}{\partial I_{\boldsymbol{j}}},\end{aligned}$$

where we used the fact that $\beta_{\boldsymbol{j},\boldsymbol{j},\boldsymbol{i}}=0$ since self class infection does not turn into another host class.

If $\boldsymbol{i}\neq\boldsymbol{j}$, we have

$$\frac{\partial}{\partial I_{\boldsymbol{j}}}\left(\frac{\mathrm{d}I_{\boldsymbol{i}}}{\mathrm{d}t}\right)=\sum_{\boldsymbol{r}\in\mathcal{E}\setminus\{\boldsymbol{i}\}}\beta_{\boldsymbol{r},\boldsymbol{j},\boldsymbol{i}}I_{\boldsymbol{r}}+\sum_{\boldsymbol{d}\in\mathcal{E}^\star}\beta_{\boldsymbol{j},\boldsymbol{d},\boldsymbol{i}}I_{\boldsymbol{d}}+\theta_{\boldsymbol{j},\boldsymbol{i}}-I_{\boldsymbol{i}}\sum_{\boldsymbol{\ell}\in(\mathcal{E}\setminus\{\boldsymbol{i}\})}\beta_{\boldsymbol{i},\boldsymbol{j},\boldsymbol{\ell}},$$

and if $\boldsymbol{i}=\boldsymbol{j}$,

$$\begin{aligned}\frac{\partial}{\partial I_{\boldsymbol{i}}}\left(\frac{\mathrm{d}I_{\boldsymbol{i}}}{\mathrm{d}t}\right) &= \sum_{\boldsymbol{r}\in\mathcal{E}\setminus\{\boldsymbol{i}\}}\beta_{\boldsymbol{r},\boldsymbol{i},\boldsymbol{i}}I_{\boldsymbol{r}}+\sum_{\boldsymbol{d}\in\mathcal{E}^\star}\beta_{\boldsymbol{i},\boldsymbol{d},\boldsymbol{i}}I_{\boldsymbol{d}}+\theta_{\boldsymbol{i},\boldsymbol{i}}-I_{\boldsymbol{i}}\sum_{\boldsymbol{\ell}\in(\mathcal{E}\setminus\{\boldsymbol{i}\})}\beta_{\boldsymbol{i},\boldsymbol{i},\boldsymbol{\ell}}\\ &\quad-\left(\sum_{(\boldsymbol{d},\boldsymbol{\ell})\in\mathcal{E}^\star\times(\mathcal{E}\setminus\{\boldsymbol{i}\})}\beta_{\boldsymbol{i},\boldsymbol{d},\boldsymbol{\ell}}I_{\boldsymbol{d}}+\sum_{\boldsymbol{\ell}\in\mathcal{E}\setminus\{\boldsymbol{i}\}}\theta_{\boldsymbol{i},\boldsymbol{\ell}}+\mu_{\boldsymbol{i}}\right),\\ &= \sum_{\boldsymbol{r}\in\mathcal{E}\setminus\{\boldsymbol{i}\}}\beta_{\boldsymbol{r},\boldsymbol{i},\boldsymbol{i}}I_{\boldsymbol{r}}-\sum_{(\boldsymbol{d},\boldsymbol{\ell})\in\mathcal{E}^\star\times(\mathcal{E}\setminus\{\boldsymbol{i}\})}\beta_{\boldsymbol{i},\boldsymbol{d},\boldsymbol{\ell}}I_{\boldsymbol{d}}-\sum_{\boldsymbol{\ell}\in\mathcal{E}\setminus\{\boldsymbol{i}\}}\theta_{\boldsymbol{i},\boldsymbol{\ell}}-\mu_{\boldsymbol{i}},\end{aligned}$$

where we used the fact that $\beta_{\boldsymbol{i},\boldsymbol{i},\boldsymbol{\ell}}=0$ (see above), and $\beta_{\boldsymbol{i},\boldsymbol{d},\boldsymbol{i}}=0$ and $\theta_{\boldsymbol{i},\boldsymbol{i}}=0$ both because these events do not correspond to a flow between compartments.

In a fully susceptible host population, that is to say when $\forall\boldsymbol{i}\in\mathcal{E}^\star, I_{\boldsymbol{i}}=0$ and $I_\emptyset=S=s^\circ$, the expression are simplified as

$$\frac{\partial}{\partial I_{\boldsymbol{j}}}\left(\frac{\mathrm{d}I_{\boldsymbol{i}}}{\mathrm{d}t}\right)=\begin{cases}\beta_{\emptyset,\boldsymbol{j},\boldsymbol{i}}s^\circ+\theta_{\boldsymbol{j},\boldsymbol{i}}, & \boldsymbol{i}\neq\boldsymbol{j},\\ \beta_{\emptyset,\boldsymbol{j},\boldsymbol{i}}s^\circ-\theta_{\boldsymbol{i},\bullet}-\mu_{\boldsymbol{i}}, & \boldsymbol{i}=\boldsymbol{j},\end{cases}$$

and the between infected hosts jacobian matrix evaluated at susceptible steady state can be written as

$$\mathbf{J}_{\mathrm{b}}\left(\mathbf{0}_{|\mathcal{E}^\star|}\right)=\left(\beta_{\emptyset,\boldsymbol{j},\boldsymbol{i}}s^\circ+\left(1-\mathbb{I}_{\{\boldsymbol{i}=\boldsymbol{j}\}}\right)\theta_{\boldsymbol{j},\boldsymbol{i}}-\mathbb{I}_{\{\boldsymbol{i}=\boldsymbol{j}\}}\left(\theta_{\boldsymbol{i},\bullet}+\mu_{\boldsymbol{i}}\right)\right)_{(\boldsymbol{i},\boldsymbol{j})\in\mathcal{E}^{\star 2}},$$

where $\bullet$ stands for the sum over the given index. Note that at this point there is still no need to order the classes (the diagonal holds whatever the order).

The next-generation theorem, as given in Hurford *et al.* (2010), is the following

equivalence

$$\forall (\mathbf{F},\mathbf{V}) \in \mathfrak{M}(\mathbb{R}) \times GL_n(\mathbb{R}), \begin{cases} \mathbf{J} = \mathbf{F} - \mathbf{V}, \\ \mathbf{F} \geq 0, \\ s(-\mathbf{V}) < 0, \\ \mathbf{V}^{-1} \geq 0, \end{cases} \iff \left(\mathrm{s}(\mathbf{J}) \lesseqgtr 0 \Leftrightarrow \rho\left(\mathbf{F}.\mathbf{V}^{-1}\right) \lesseqgtr 1 \right),$$

where the spectral bound is defined as $\mathrm{s}(\mathbf{M}) := \max\{\Re(\lambda_i), \lambda_i \in \mathrm{Sp}(\mathbf{M})\}$ and the spectral radius as $\rho(\mathbf{M}) := \max\{|\lambda_i|, \lambda_i \in \mathrm{Sp}(\mathbf{M})\}$.

In our case, the following matrices satisfy the assumptions of the next-generation theorem,

$$\begin{aligned} \mathbf{F} &:= \left(\beta_{\emptyset,\boldsymbol{j},\boldsymbol{i}} s^\circ + \left(1 - \mathbb{I}_{\{\boldsymbol{i}=\boldsymbol{j}\}}\right)\theta_{\boldsymbol{j},\boldsymbol{i}}\right)_{(\boldsymbol{i},\boldsymbol{j})\in\mathcal{E}^{\star 2}}, \\ \mathbf{V} &:= \left(\mathbb{I}_{\{\boldsymbol{i}=\boldsymbol{j}\}}\left(\theta_{\boldsymbol{i},\bullet} + \mu_{\boldsymbol{i}}\right)\right)_{(\boldsymbol{i},\boldsymbol{j})\in\mathcal{E}^{\star 2}}. \end{aligned}$$

$\mathbf{V}$ is diagonal, so its inverse is directly

$$\mathbf{V}^{-1} = \left(\frac{\delta_{\boldsymbol{i},\boldsymbol{j}}}{\theta_{\boldsymbol{i},\bullet} + \mu_{\boldsymbol{i}}}\right)_{(\boldsymbol{i},\boldsymbol{j})\in\mathcal{E}^{\star 2}},$$

and the product of $\mathbf{F}$ with $\mathbf{V}^{-1}$ is

$$\mathbf{F}.\mathbf{V}^{-1} = \left(\frac{\beta_{\emptyset,\boldsymbol{j},\boldsymbol{i}} s^\circ}{\theta_{\boldsymbol{j},\bullet} + \mu_{\boldsymbol{j}}}\right)_{(\boldsymbol{i},\boldsymbol{j})\in\mathcal{E}^{\star 2}}.$$

A straightforward calculation of the spectrum of $\mathbf{F}.\mathbf{V}^{-1}$ requires to order the classes. To do so we use the labelling previously defined and replace bold indices by light indices with no loss of information. In this case, $\beta_{\emptyset,\boldsymbol{j},\boldsymbol{i}}$ becomes $\beta_{0,j,i}$ with $(i,j) \in [\![0; 2^n - 1]\!]^2$. Therefore we have $\beta_{0,j,i} = 0$ for all $j < i$.

Indeed, if a susceptible is infected by a donor j, the resulting class i can only contain genotypes that donor j already has. Using the presence coefficients, we have

$$\begin{aligned} \forall k \in \mathcal{G}, c_{i,k} &\leq c_{j,k}, \\ c_{i,k} 2^{k-1} &\leq c_{j,k} 2^{k-1}, \end{aligned}$$

then by summing over all k, it follows that $i < j$, from the presence coefficient property (see 3.c.1).

The inequality $i < j$ is a necessary condition for the event 'turning a susceptible into a host i through infection by j' to occur. As a consequence, such an event does not occur if $j > i$, leading to $\beta_{\emptyset,j,i} = 0$ in this case. Thus, $\mathbf{F}.\mathbf{V}^{-1}$ is a triangular matrix the eigenvalues of which are its diagonal terms

$$\mathrm{Sp} = \left\{\frac{\beta_{\emptyset,\boldsymbol{i},\boldsymbol{i}} s^\circ}{\theta_{\boldsymbol{i},\bullet} + \mu_{\boldsymbol{i}}}\right\}_{\boldsymbol{i}\in\mathcal{E}^\star}.$$

Following the next-generation theorem, the basic reproduction number according to this method is then

$$\mathcal{R}_0^{\mathrm{I}} = \max_{\boldsymbol{i}\in\mathcal{E}^\star}\left(\frac{\beta_{\emptyset,\boldsymbol{i},\boldsymbol{i}} s^\circ}{\theta_{\boldsymbol{i},\bullet} + \mu_{\boldsymbol{i}}}\right).$$

Explicitation of the infection, recovery and death rates finally gives

$$\frac{\beta_{\emptyset,\boldsymbol{i},\boldsymbol{i}}s^\circ}{\theta_{\boldsymbol{i},\bullet}+\mu_{\boldsymbol{i}}} = \beta s^\circ \left(|\boldsymbol{i}|\theta+\mu x_{\boldsymbol{i},\bullet}\right)^{-1} \sum_{\substack{\boldsymbol{p}\in\wp(\boldsymbol{i})\\ \phi(\emptyset,\boldsymbol{p})=\boldsymbol{i}}} |\boldsymbol{p}| \prod_{k\in\boldsymbol{p}} \frac{x_{\boldsymbol{i},k}}{x_{\boldsymbol{i},\bullet}} \prod_{k\in\boldsymbol{d}\setminus\boldsymbol{p}} \left(1-\frac{x_{\boldsymbol{i},k}}{x_{\boldsymbol{i},\bullet}}\right).$$

3.e.2. Endemic basic reproduction number

An epidemic reaches an endemic state if and only if the sum of the infected host densities is positive at steady state. Such a condition is an alternative definition of the basic reproduction number, which we note $\mathcal{R}_0^{\mathrm{II}}$. Let us call J the sum of the infected host densities, $J \coloneqq \sum_{\boldsymbol{i}\in\mathcal{E}^\star} I_{\boldsymbol{i}}$. The time derivative of J is then

$$\begin{aligned}\frac{\mathrm{d}J}{\mathrm{d}t} = \sum_{\boldsymbol{i}\in\mathcal{E}^\star}\frac{\mathrm{d}I_{\boldsymbol{i}}}{\mathrm{d}t} &= S\sum_{\boldsymbol{i}\in\mathcal{E}^\star}\sum_{\boldsymbol{d}\in\mathcal{E}^\star}\beta_{\emptyset,\boldsymbol{d},\boldsymbol{i}}I_{\boldsymbol{d}} - \sum_{\boldsymbol{i}\in\mathcal{E}^\star} I_{\boldsymbol{i}}\sum_{\boldsymbol{d}\in\mathcal{E}^\star}\beta_{\boldsymbol{i},\boldsymbol{d},\emptyset}I_{\boldsymbol{d}} - \sum_{\boldsymbol{i}\in\mathcal{E}^\star}\theta_{\boldsymbol{i},\emptyset}I_{\boldsymbol{i}} - \sum_{\boldsymbol{i}\in\mathcal{E}^\star}\mu_{\boldsymbol{i}}I_{\boldsymbol{i}},\\ &= J\left(S\sum_{\boldsymbol{i}\in\mathcal{E}^\star}\sum_{\boldsymbol{d}\in\mathcal{E}^\star}\beta_{\emptyset,\boldsymbol{d},\boldsymbol{i}}\frac{I_{\boldsymbol{d}}}{J} - \sum_{\boldsymbol{i}\in\mathcal{E}^\star} I_{\boldsymbol{i}}\sum_{\boldsymbol{d}\in\mathcal{E}^\star}\beta_{\boldsymbol{i},\boldsymbol{d},\emptyset}\frac{I_{\boldsymbol{d}}}{J} - \sum_{\boldsymbol{i}\in\mathcal{E}^\star}\theta_{\boldsymbol{i},\emptyset}\frac{I_{\boldsymbol{i}}}{J} - \sum_{\boldsymbol{i}\in\mathcal{E}^\star}\mu_{\boldsymbol{i}}\frac{I_{\boldsymbol{i}}}{J}\right).\end{aligned}$$

We used here both the fact that the derivative is linear and that the only flows that come or leave the infected compartment J as a whole are the ones related to the susceptibles, that is infection of the susceptibles, ultrainfection, recovery to the susceptibles and deaths. The last expression is written such that infection, recovery and death rates can be seen as weighted by the frequency of the associated hosts (for a given index). Using the marginal arithmetic mean notation, as in $\overline{y_{\bullet,j}} \coloneqq \sum_i y_{i,j}f_i$, we get at steady state

$$\widehat{J}\left(\widehat{S}\sum_{\boldsymbol{i}\in\mathcal{E}^\star}\overline{\beta_{\emptyset,\bullet,\boldsymbol{i}}} - \sum_{\boldsymbol{i}\in\mathcal{E}^\star}\widehat{I}_{\boldsymbol{i}}\overline{\beta_{\boldsymbol{i},\bullet,\emptyset}} - \overline{\theta_{\bullet,\emptyset}} - \overline{\mu_\bullet}\right) = 0. \tag{3.e.1}$$

Because infection flows are quadratic, another sum can be performed for the infection-related terms. While the second sum in (3.e.1) is straightforward, it is worth pointing out that in the first one, sums over the third index of $\beta_{\boldsymbol{a},\boldsymbol{b},\boldsymbol{c}}$ do not need to be weighted since the overall infection flow does not depend on the density of the outcoming class of the infections (the total infection flow is given by the formula $\sum_{\boldsymbol{a}}\sum_{\boldsymbol{b}}\beta_{\boldsymbol{a},\boldsymbol{b},\boldsymbol{c}}I_{\boldsymbol{a}}I_{\boldsymbol{b}}$) but only on their number, which is $\left|\mathcal{E}^\star\right|$. Assuming that $\widehat{J}\neq 0$, we have

$$\left|\mathcal{E}^\star\right|\overline{\overline{\beta_{\emptyset,\bullet,\bullet}}}\widehat{S} - \overline{\overline{\beta_{\bullet,\bullet,\emptyset}}}\widehat{J} - \overline{\theta_{\bullet,\emptyset}} - \overline{\mu_\bullet} = 0.$$

Then, by using the fact that the population size is constant, that is $\widehat{S}+\widehat{J}=s^\circ$, it follows that

$$\widehat{J} = \frac{\left|\mathcal{E}^\star\right|\overline{\overline{\beta_{\emptyset,\bullet,\bullet}}}s^\circ - \overline{\theta_{\bullet,\emptyset}} - \overline{\mu_\bullet}}{|\mathcal{E}^\star|\overline{\overline{\beta_{\emptyset,\bullet,\bullet}}} + \overline{\overline{\beta_{\bullet,\bullet,\emptyset}}}}, \tag{3.e.2}$$

and this steady-state density is positive if and only if the following quantity, which defines $\mathcal{R}_0^{\mathrm{II}}$, is greater than one,

$$\mathcal{R}_0^{\mathrm{II}} = \frac{\left|\mathcal{E}^\star\right|\overline{\overline{\beta_{\emptyset,\bullet,\bullet}}}s^\circ}{\overline{\theta_{\bullet,\emptyset}}+\overline{\mu_\bullet}}.$$

Note that the three marginal arithmetic means involved in the latter formula depend on the densities of infected hosts at steady-state so they cannot be calculated directly from the parameters.

3.e.3. Epidemiological feedback sensitiviy

In order to see that the basic reproduction numbers can capture the epidemiological feedback, we arbitrarily decide to derive them twice with respect to the constant transmission factor β, as if it were a variable. If the second derivative is 0, the basic reproduction number responds linearly to a change in epidemiological parameters, and hence cannot capture epidemiological feedbacks.

The next-generation basic reproduction number gives

$$\frac{\partial \mathcal{R}_0^{\mathrm{I}}}{\partial \beta} = s^\circ \max_{\boldsymbol{i}\in\mathcal{E}^\star}\left(\left(|\boldsymbol{i}|\theta+\mu x_{\boldsymbol{i},\bullet}\right)^{-1} \sum_{\substack{\boldsymbol{p}\in\wp(\boldsymbol{i})\\ \phi(\emptyset,\boldsymbol{p})=\boldsymbol{i}}} |\boldsymbol{p}| \prod_{k\in\boldsymbol{p}} \frac{x_{\boldsymbol{i},k}}{x_{\boldsymbol{i},\bullet}} \prod_{k\in\boldsymbol{d}\setminus\boldsymbol{p}} \left(1-\frac{x_{\boldsymbol{i},k}}{x_{\boldsymbol{i},\bullet}}\right)\right),$$

then

$$\frac{\partial^2 \mathcal{R}_0^{\mathrm{I}}}{\partial \beta^2} = 0.$$

$\mathcal{R}_0^{\mathrm{I}}$ cannot capture epidemiological feedbacks in any case.

The endemic basic reproduction number gives

$$\frac{\partial \mathcal{R}_0^{\mathrm{II}}}{\partial \beta} = \left|\mathcal{E}^\star\right| s^\circ \left(\frac{1}{\overline{\overline{\theta_{\bullet,\emptyset}}+\overline{\mu_\bullet}}} \frac{\partial \overline{\overline{\beta_{\emptyset,\bullet,\bullet}}}}{\partial \beta} + \overline{\overline{\beta_{\emptyset,\bullet,\bullet}}} \frac{\partial}{\partial \beta}\left(\frac{1}{\overline{\overline{\theta_{\bullet,\emptyset}}+\overline{\mu_\bullet}}}\right)\right).$$

Under the assumption of $\frac{\partial \widehat{I}_{\boldsymbol{i}}}{\partial \beta} = 0$, we have

$$\frac{\partial \mathcal{R}_0^{\mathrm{II}}}{\partial \beta} = \frac{\left|\mathcal{E}^\star\right| s^\circ}{\overline{\overline{\theta_{\bullet,\emptyset}}+\overline{\mu_\bullet}}} \frac{\overline{\overline{\beta_{\emptyset,\bullet,\bullet}}}}{\beta},$$

and

$$\begin{aligned}
\frac{\partial^2 \mathcal{R}_0^{\mathrm{II}}}{\partial \beta^2} &= \frac{\left|\mathcal{E}^\star\right| s^\circ}{\overline{\overline{\theta_{\bullet,\emptyset}}+\overline{\mu_\bullet}}} \left(\frac{\partial}{\partial \beta}\left(\frac{\overline{\overline{\beta_{\emptyset,\bullet,\bullet}}}}{\beta}\right)\right),\\
&= \frac{\left|\mathcal{E}^\star\right| s^\circ}{\overline{\overline{\theta_{\bullet,\emptyset}}+\overline{\mu_\bullet}}} \left(\frac{\overline{\overline{\beta_{\emptyset,\bullet,\bullet}}}}{\beta^2} - \frac{\overline{\overline{\beta_{\emptyset,\bullet,\bullet}}}}{\beta^2}\right),\\
&= 0.
\end{aligned}$$

The contraposition of this result is

$$\frac{\partial^2 \mathcal{R}_0^{\mathrm{II}}}{\partial \beta^2} \neq 0 \Longrightarrow \frac{\partial \widehat{I}_{\boldsymbol{i}}}{\partial \beta} \neq 0.$$

In other words, if we observe a non zero second derivative of $\mathcal{R}_0^{\mathrm{II}}$ with respect to β in certain cases, $\mathcal{R}_0^{\mathrm{II}}$ does capture the epidemiological feedback.

3.e.4. Basic reproduction numbers for $n = 1$

Let us consider only one parasite genotype ($n = 1$), arbitrary denoted 1. Because of assumption (3.3.2), {1} is an epidemiological host class, carrying $x_{\{1\},1} > 0$ units of parasite load.

The between-host dynamics are at their simplest form because there are only two compartments, S and $I_{\{1\}}$. The ODE the latter satisfies is sufficient to characterize these dynamics because of the constant population size assumption $S + I_{\{1\}} = s^\circ$. We have

$$\frac{\mathrm{d}I_{\{1\}}}{\mathrm{d}t} = \beta_{\emptyset,\{1\},\{1\}} S I_{\{1\}} - \theta_{\{1\},\emptyset} I_{\{1\}} - \mu_{\{1\}} I_{\{1\}},$$

and, by explicitating infection, recovery and death rates, we get

$$\begin{aligned} \frac{\mathrm{d}I_{\{1\}}}{\mathrm{d}t} &= \beta S I_{\{1\}} - \theta I_{\{1\}} - \mu x_{\{1\},1} I_{\{1\}}, \\ &= \left(\beta\left(s^\circ - I_{\{1\}}\right) - \theta - \mu x_{\{1\},1}\right) I_{\{1\}}. \end{aligned} \tag{3.e.3}$$

The jacobian matrix of the system is reduced to a single quantity, which is

$$\frac{\partial}{\partial I_{\{1\}}}\left(\frac{\mathrm{d}I_{\{1\}}}{\mathrm{d}t}\right) = -2\beta I_{\{1\}} + \beta s^\circ - \theta - \mu x_{\{1\},1}.$$

The next-generation basic reproduction number $\mathcal{R}_0^{\mathrm{I}}$ is defined from the condition that this quantity evaluated at the disease-free equilibrium, that is $I_{\{1\}}(0) = 0$, is positive (unstable equilibrium), whence

$$\frac{\partial}{\partial I_{\{1\}}}\left(\frac{\mathrm{d}I_{\{1\}}}{\mathrm{d}t}\right)(0) > 0 \Longleftrightarrow \mathcal{R}_0^{\mathrm{I}} > 1, \mathcal{R}_0^{\mathrm{I}} = \frac{\beta s^\circ}{\theta + \mu x_{\{1\},1}}.$$

On the contrary, the endemic basic reproduction number involves the endemic steady-state value of $I_{\{1\}}$. At the endemic steady-state, $\frac{\mathrm{d}I_{\{1\}}}{\mathrm{d}t} = 0$ and $\widehat{I_{\{1\}}} \neq 0$, (3.e.3) then gives

$$\begin{aligned} \beta\left(s^\circ - \widehat{I_{\{1\}}}\right) - \theta - \mu x_{\{1\},1} &= 0, \\ \widehat{I_{\{1\}}} &= s^\circ - \frac{\theta + \mu x_{\{1\},1}}{\beta}, \end{aligned}$$

and the endemic basic reproduction number is defined from the condition that this quantity is positive, whence

$$\widehat{I_{\{1\}}} > 0 \Longleftrightarrow \mathcal{R}_0^{\mathrm{II}} > 1, \mathcal{R}_0^{\mathrm{II}} = \frac{\beta s^\circ}{\theta + \mu x_{\{1\},1}}.$$

We have proved that for $n = 1$ the two methods lead to the same basic reproduction number,

$$\mathcal{R}_0^{\mathrm{I}} = \mathcal{R}_0^{\mathrm{II}}.$$

3.ω. Épilogue

La prise de décision en santé publique s'appuie, entre autres, sur les prédictions engendrées par l'épidémiologie mathématique (Heesterbeek *et al.*, 2015). Plus précisément, et quel que soit le modèle considéré, il s'agit d'exprimer un descripteur pertinent vis-à-vis de la question posée, *i.e.* une quantité fonction des paramètres – que les données épidémiologiques permettent d'estimer – qui synthétise en un scalaire un aspect étudié du comportement du système.

L'objectif de la prévention est la réduction de l'incidence d'une épidémie. Par définition, cela revient à minimiser le nombre de reproduction de base ($\mathcal{R}_0$ mais noté $\mathcal{R}_0^{\mathrm{I}}$ dans ce chapitre) (Anderson & May, 1981; Diekmann *et al.*, 1990). Le contrôle vise quant à lui la réduction de la prévalence d'une endémie, donc la minimisation de la quantité $s^\circ/\widehat{S}$ (où s° est la taille totale de la population avant le début de l'épidémie [*] et $\widehat{S}$ la densité de susceptibles une fois l'endémie établie).

Tandis que le calcul de $\mathcal{R}_0^{\mathrm{I}}$ repose sur la dynamique initiale de propagation de la maladie dans une population totalement susceptible (voir l'introduction i), celui de $s^\circ/\widehat{S}$ requiert l'intégration jusqu'à l'équilibre épidémiologique. Néanmoins, parce que ces deux descripteurs présentent des expressions identiques pour des paradigmes comme le modèle SIS (voir Figure i.2.1), il y a une tentation à étendre l'usage du nombre de reproduction de base à l'étude du contrôle (ce rapprochement justifie en outre la notation malheureuse $\mathcal{R}_0^{\mathrm{II}}$ et l'appellation fautive de *nombre de reproduction de base endémique* attribuées à $s^\circ/\widehat{S}$ dans le présent chapitre). Or, pour des dynamiques plus complexes que celles du modèle SIS, les descripteurs $\mathcal{R}_0^{\mathrm{I}}$ et $s^\circ/\widehat{S}$ ne sont plus égaux, le second capturant les rétro-actions épidémiologiques qui échappent au premier (Roberts, 2007; Metz *et al.*, 2008; Lion & Metz, 2017). Une illustration remarquable de cette distinction est la possible bifurcation rétrograde qui rend caduque le seuil $\mathcal{R}_0 = 1$ dans une perspective de contrôle partant de l'équilibre endémique (Hadeler & Van den Driessche, 1997), voir la Figure 3.ω.1.

∗. L'implication du facteur s° doit être vue comme une normalisation qui rend le seuil de $s^\circ/\widehat{S}$ visé par le contrôle égal à l'unité, à l'instar de la prévention et $\mathcal{R}_0^{\mathrm{I}}$.

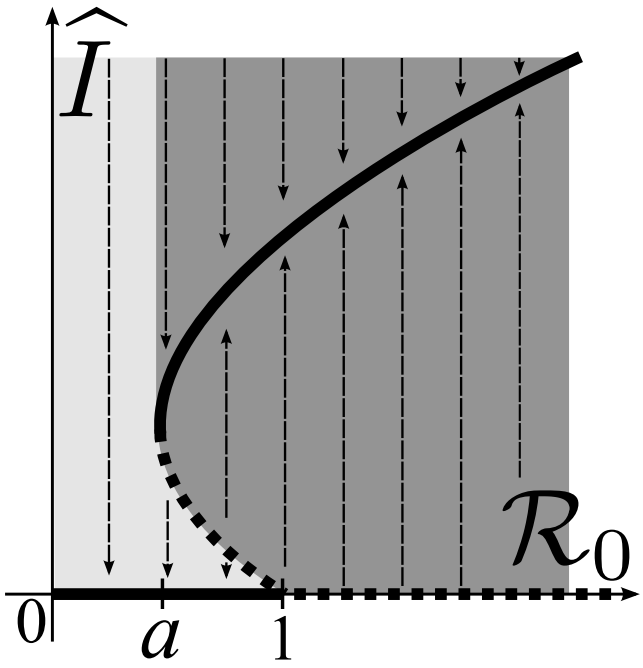

FIGURE 3.ω.1. – Principe de la bifurcation rétrograde
Certains modèles plus complexes que les modèles SIS peuvent présenter une zone de bistabilité pour des valeurs de $\mathcal{R}_0$ inférieures à 1 (ici, entre a et 1). Ainsi, l'éradication d'une maladie infectieuse endémique n'est pas nécessairement atteinte pour un nombre de reproduction de base abaissé à 1. Les courbes grasses et pointillées indiquent les valeurs de $\widehat{I}$ associées à un équilibre localement asymptotiquement stable et instable, respectivement. Les flèches indiquent le sens de convergence des solutions $I(t)$ à $\mathcal{R}_0$ fixé. D'après BRAUER (2004).

Avec le présent modèle, nous avons montré que les infections multiples font partie de ces conditions qui mettent à mal l'égalité entre $\mathcal{R}_0^{\mathrm{I}}$ et $s^\circ/\widehat{S}$. Le nombre de reproduction de base est ainsi un mauvais descripteur pour le contrôle des infections multiples, comme le montre la Figure 3.ω.2 sur l'exemple du contrôle de la transmission. Dans cette figure, la diminution du facteur de transmission β (lecture de droite à gauche des courbes) mime une intervention de santé publique dans une population où circule un parasite endémique polymorphe. *A contrario* du nombre de reproduction de base, la fonction $s^\circ/\widehat{S}$ de β présente une non-linéarité plus ou moins prononcée selon les jeux de paramètres représentant les traits des 5 types parasitaires simulés, un polymorphisme qui ne manque pas d'engendrer des rétro-actions épidémiologiques.

Néanmoins, il est remarquable d'observer que cette non-linéarité ne requiert pas un système de grande dimension car un dimorphisme parasitaire et trois classes d'hôtes uniquement suffit à la faire apparaître. La Figure 3.ω.2 montre ainsi comment une baisse généralisée de la transmission peut conduire, contre-intuitivement, à l'augmentation de la prévalence d'une maladie infectieuse portée par deux types parasitaires en superinfection (voir la légende pour une explication détaillée).

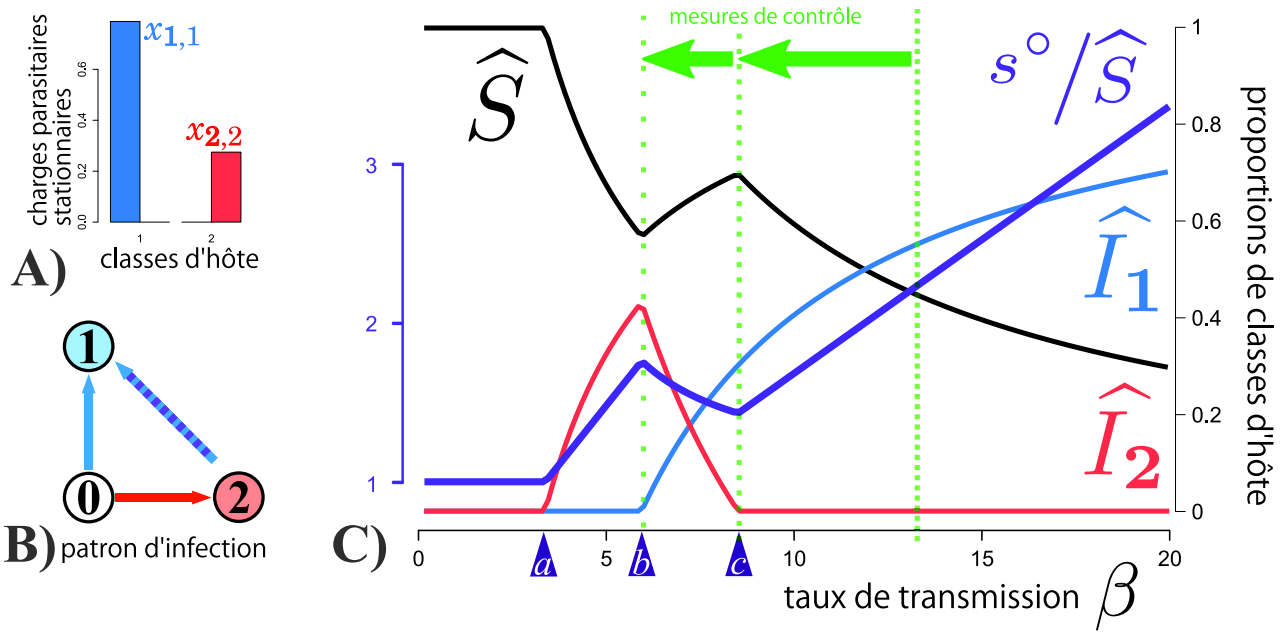

FIGURE 3.ω.2. – Impact épidémiologique de la superinfection.
Soient deux types parasitaires ($n = 2$) numérotés 1 (en bleu) et 2 (en rose). **A)** Charges parasitaires stationnaires des deux types parasitaires dans leur infection simple respective ($x_{1,1}$ et $x_{2,2}$). Le type 1 est ainsi plus virulent que le type 2. **B)** Patron d'infection effectif : le type 1 superinfecte le type 2. **C)** Variations des densités d'hôtes à l'équilibre $\widehat{S}, \widehat{I_1}, \widehat{I_2}$ (échelle de droite) et du descripteur $s^\circ/\widehat{S}$ (ou *nombre de reproduction de base endémique* $\mathcal{R}_0^{\mathrm{II}}$, échelle de gauche) en fonction du taux de transmission β supposé identique entre types parasitaires. Les triangles violets indiquent des valeurs remarquables de β. Tant que $\beta < a$, aucun parasite ne circule car la transmission est trop faible. Pour $a < \beta < b$, la transmission est suffisamment élevée pour propager le type 2 dans la population d'hôtes – la densité d'hôtes non infectés à l'équilibre $\widehat{S}$ diminue – mais pas le type 1 car sa virulence est plus importante. Pour $b < \beta < c$, la transmission compense la virulence du type 1, qui se propage à son tour, en remplaçant, par superinfection, le type 2 dans certains individus infectés. Les infections par le type 1 entraînant une mort plus rapide que celles par le type 2, le nombre de reproduction de base endémique baisse. Cette baisse prend fin pour $\beta = c$, où la superinfection de 2 par 1 est systématique : le type 2 ne peut plus se propager. Au-delà, la prévalence augmente du seul fait de plus forte transmission du type 1. En regardant à présent la baisse du taux de transmission β comme l'effet de mesures de contrôle (p.ex. recommandations hygiéniques, quarantaine imparfaite), il apparaît que s'il existe un polymorphisme parasitaire latent, comme ici sous la forme d'une superinfection qui ne s'exprime épidémiologiquement que dans la gamme $\beta \in [b, c]$, alors le contrôle peut, contre-intuitivement, augmenter la prévalence des infections en permettant à des types superinfectés et moins virulents de se propager.

III

Des réponses et de nouvelles questions

4 Nécessaire virulence des infections multiples

4.α. Prologue

Par essence, tout processus (micro-)évolutif repose sur un différentiel de reproduction (plus précisément de contribution génétique à la génération suivante). Dans le cas des parasites, ce différentiel réside tout particulièrement dans l'étape limitante de leur cycle de vie : la transmission d'un hôte à l'autre (Alizon & Michalakis, 2015). Or, nous avons montré à la fin du précédent chapitre que la connaissance du patron d'infection confère une clé de lecture aux rétro-actions épidémiologiques qui rendent la dynamique inter-hôte non triviale en contexte d'infections multiples. Il apparaît ainsi judicieux de placer la typologie des patrons d'infection au cœur de l'étude ultime du présent travail – l'influence des infections multiples sur l'évolution de la virulence.

Dans cette dernière tâche (le chapitre δ n'étant qu'un épilogue hypertrophié), nous réinvestissons des éléments de modélisation et des résultats théoriques des précédents chapitre* dans la construction d'une approche intégrée de l'évolution de la virulence. Si nous nous référons en premier lieu à la version la plus générale du modèle de croissance intra-hôte pour deux types parasitaires du chapitre 1, nous nous ramenons *de facto* à sa version réduite aux équations classiques de Lotka-Volterra. Cette simplification, soutenue par un argument de séparation des échelles de temps, nous permet d'assigner à chaque région de l'espace des paramètres un des patrons d'infection décrits au chapitre 2. L'ensemble de ces patrons d'infections s'expriment épidémiologiquement dans une formulation plus générale du modèle inter-hôte employé au chapitre 3. Pour finir, le niveau de dynamique le plus distal, l'évolution du parasite, est examinée à la lueur de l'analyse d'invasion introduite à l'occasion du chapitre 0.

*. Le contenu du supplément méthodologique (annexes 4.b à 4.e), dont l'objectif est de rendre le chapitre auto-suffisant sur ce plan, apparaîtra ainsi familier au lecteur des précédents chapitres.

Pourquoi les infections multiples favorisent les parasites virulents

Mircea T. Sofonea, Samuel Alizon, Yannis Michalakis

Résumé

La plupart des modèles théoriques employés pour appréhender la dynamique épidémiologique ou évolutive des interactions hôte-parasite font l'hypothèse du monomorphisme du parasite. Or, nous savons aujourd'hui que plusieurs souches/espèces (et simplement types, par la suite) de parasites circulent au sein des populations naturelles d'hôtes. Ce polymorphisme parasitaire, au sens large, peut même être retrouvé au sein d'un même hôte, dans lequel les différents types parasitaires peuvent interagir de diverses façons et ainsi interférer avec leur transmission et donc leur évolution. Cette complexité combinatoire et dynamique explique le manque d'une prédiction unitaire en ce qui concerne l'évolution de la virulence dans de tels contextes d'infections multiples. Visant à déterminer une tendance générale à l'évolution de la virulence, nous modélisons chaque niveau de dynamique sur lequel l'évolution parasitaire repose. En particulier, nous étudions explicitement les interactions et les issues de la compétition intra-hôte, la dynamique épidémiologique et l'invasibilité évolutive. En prenant le cas des infections chroniques dimorphes dues à des micro-parasites à transmission horizontale, nous appliquons conjointement une approche de systèmes dynamiques et d'événements aléatoires à cette dynamique emboîtée afin d'explorer les issues évolutives. En utilisant la typologie des patrons d'infection introduite au chapitre précédent, nous montrons analytiquement que la survie de parasites mutants phénotypiquement proches de leur ancêtre résident ne dépend pas de leur virulence mais seulement du patron d'infection qu'ils entretiennent avec lui. Ce résultat nous permet alors d'identifier un biais évolutif d'augmentation de la virulence. Nous expliquons cette augmentation de la virulence moyenne sur le long terme par l'avantage compétitif conféré par les mutations associées à des augmentations du taux de croissance. Ce cadre de modélisation est une première étape dans la réconciliation des prédictions contradictoires de l'évolution de la virulence obtenues par des modèles distincts.

Mots-clés : superinfection, coinfection, infections multiples, compétition intra-hôte, épidémiologie, patron d'infection, évolution de la virulence

Why multiple infections favour virulent parasites

Mircea T. Sofonea, Samuel Alizon, Yannis Michalakis

Abstract

It is now a fact that several strains/species (hereafter types) of parasites circulate in natural host populations. Parasite polymorphism can even occur within the same host, where distinct parasite types can interact in various ways. This can affect their transmission and, therefore, their evolution. We still lack general predictions regarding the evolution, in such multiple infection contexts, of virulence – the infection-induced host mortality, essentially because its emanation from within-host growth was often ignored so far. Here, we explicitly investigate within-host interactions, within-host competition outcomes, epidemiological dynamics and evolutionary invasibility using a formalism as general as possible. Focusing on chronic dimorphic infections caused by horizontally-transmitted microparasites, we apply both dynamical systems and probabilistic approaches to this bottom-up sequence of dynamics to explore the evolutionary outcomes. We show that within-host growth traits are under strong selective pressure and when small mutations affect them, most of the surviving mutants are more virulent than their resident. We thus identify a robust and unavoidable selection bias towards higher virulence.

Keywords: superinfection; coinfection; multiple infections; within-host competition; epidemiology; infection pattern; virulence evolution

4.1. Introduction

Virulence has been an intriguing paradox since parasites that reduce the lifetime of their host concomitantly reduce their opportunities to be transmitted and thus one would expect them to be counter-selected (Smith, 1887; Méthot, 2012). Adaptive evolution of virulence has been reviewed several times (Dieckmann, 2002; Alizon & Michalakis, 2015; Cressler *et al.*, 2015) and one can distinguish three main reasons to why parasites may harm their hosts: 1) virulence trades off with other features of the parasite's life cycle (transmission, recovery, free stage persistence) (Anderson & May, 1982; Gandon, 1998; Alizon, 2008; Alizon *et al.*, 2009; Alizon & Michalakis, 2011), 2) virulence is associated with within-host competitiveness (Alizon *et al.*, 2013) and 3) virulence is the by-product of 'short-sighted' within-host evolution (Levin & Bull, 1994). Notice that each of these explanations is self-contained but they are not mutually exclusive.

The fact that virulence may be driven by the competition between parasites seems relevant as it is now well established that a diversity of parasite types (species, strains, genotypes) share the same host population (Petney & Andrews, 1998; Lord *et al.*, 1999; Juliano *et al.*, 2010; Rigaud *et al.*, 2010; Balmer & Tanner, 2011). When several types of parasites circulate in the same host population, they not only compete for susceptible hosts to infect but they also compete within the host for limiting resources (Mideo, 2009). When simultaneously inside the same host, parasite interactions, may they be direct or indirect, positive or negative, within the same type or between types (Bashey, 2015), can make coexistence impossible, as in any ecological community (Barabás *et al.*, 2016). This subsequent diversity of within-host outcomes (Sofonea *et al.*, 2017b) amplifies the richness of the epidemiological dynamics governed by transmission, recovery and death of the thus numerous classes of hosts (Sofonea *et al.*, 2015; Kucharski *et al.*, 2016). Besides, within-host coexistence of several parasite types can modulate the rate at which a host dies from the multiple infection with respect to single infections (Griffiths *et al.*, 2011). It follows that the virulence undergone by a multiply infected host has to be distinguished from the virulence of a parasite, usually revealed in single infections (de Roode *et al.*, 2005b).

The first evolutionary epidemiological models accounting for parasite polymorphism exposed an evolutionary increase of virulence comparable to the selfish tendency to over-exploit a common good, as in any tragedy of the commons (Levin & Pimentel, 1981; Bremermann & Pickering, 1983; Nowak & May, 1994; van Baalen & Sabelis, 1995; May & Nowak, 1995; Frank, 1996). The generality of this conclusion has however been challenged by later models that assumed host exploitation to rely on a collective action (such as public good production or parasite load limitation) which tends to decrease parasite virulence (Brown, 1999; Brown *et al.*, 2002; West & Buckling, 2003). These results were in turn contradicted when accounting for trade-offs and epidemiological feedbacks (Alizon & Lion, 2011). This in the end reveals that, up to now, theoretical research on the consequences of multiple infections has failed to provide a unified answer to the selective pressure parasite virulence undergoes. This is at least partly explained by the tendency to increase the complexity of the model from the top (Alizon, 2013a) while keeping within-host dynamics, and therefore how virulence arises, unaddressed (but see Alizon & van Baalen (2005)).

Because of their challenging analysis, the within-host dynamics have been ignored or oversimplified by an impressive majority of evolutionary epidemiological models involving at least two parasite types (Alizon, 2013a; Cressler *et al.*, 2015). More precisely, most of these models arbitrarily forced all growth outcomes inside multiply inoculated hosts to result either to the dominance of a unique type (Levin & Pimentel, 1981) or to

the coexistence of all inoculated types (Bremermann & Pickering, 1983). The first case is known as superinfection and corresponds to the fast competitive exclusion of all parasite types that are less competitive than the surviving parasite type. Competitiveness is almost always assumed to be positively correlated with virulence, which is both limiting and arguable (Sofonea *et al.*, 2017b). The second case is known as coinfection and corresponds to stable (or meta-stable) coexistence between all inoculated parasite types the transmission rates of which are often assumed to be identical to that of single infections, which is also limiting and arguable (Sofonea *et al.*, 2017b). Although Nowak and May acknowledged these two cases might be biologically extreme, they claimed "to bracket the reality of polymorphic parasites" (May & Nowak, 1995). It eventually became common in the literature that the epidemiology of any biological system with multiple infections lies somewhere in a continuum between super and coinfection e.g. (Mosquera & Adler, 1998; Boldin & Diekmann, 2008; Alizon, 2013a). Our previous work has shown, however, that explicitly considering within-host dynamics reveals a diversity of within-host outcomes (Sofonea *et al.*, 2017b), questioning the relevance of imposing within-host outcomes when investigating the evolution of parasite traits.

Finding a general trend in virulence evolution with multiple infections thus requires constructing a new framework based on the parasite growth traits (Cressler *et al.*, 2015). By means of bottom-up emergence and dynamical nesting, this approach should be able to capture, and weight, a diversity of multiple infection scenarios so far separated or ignored. In a previous work (Sofonea *et al.*, 2017b), we introduced and detailed, both formally and biologically, the notion of infection pattern which captures the within-host outcomes of all sets of parasite types. Intuitively, an infection pattern is the way each parasite type behaves – i.e. either survives or vanishes – in presence of any combination of other parasite types (including when the focal type is alone).

First, this notion generalizes the super/coinfection dichotomy. We indeed showed that even with only two parasites, there can be more than a hundred of these patterns. Interestingly, several of the patterns we uncovered theoretically have been known in the empirical literature for decades and cannot be modelled as any mixture of super and coinfection. This is for example the case when the first inoculated type always outcompetes the second one, as for the mutual exclusion of phages in *E. coli* (Delbrück, 1945), a pattern we referred to as priorinfection (Sofonea *et al.*, 2017b). Second, infection patterns allows us to root the epidemiological network and transmission routes in the within-host dynamics while relaxing the assumption that links competitiveness to virulence.

In the present article we take advantage of the previously introduced infection pattern typology for dimorphic infections (Sofonea *et al.*, 2017b) to investigate how mutations on parasite growth traits affect the average virulence of the parasite meta-population (i.e. at the between-host level) through nesting a classical two-species competitive Lotka-Volterra model for within-host dynamics into into an extended version of the Susceptible-Infected-Susceptible (*SIS*) model developed in (Sofonea *et al.*, 2015). The integrated principle of this bottom-up approach is exposed in Figure 4.1.1. We finally interpret the results as an evolutionary force that acts on parasite virulence, examining the effects of both small and large mutations.

We provide in the appendix the full description and analysis of the models (Supplementary Methods part) and some more technical results (Supplementary Results part).

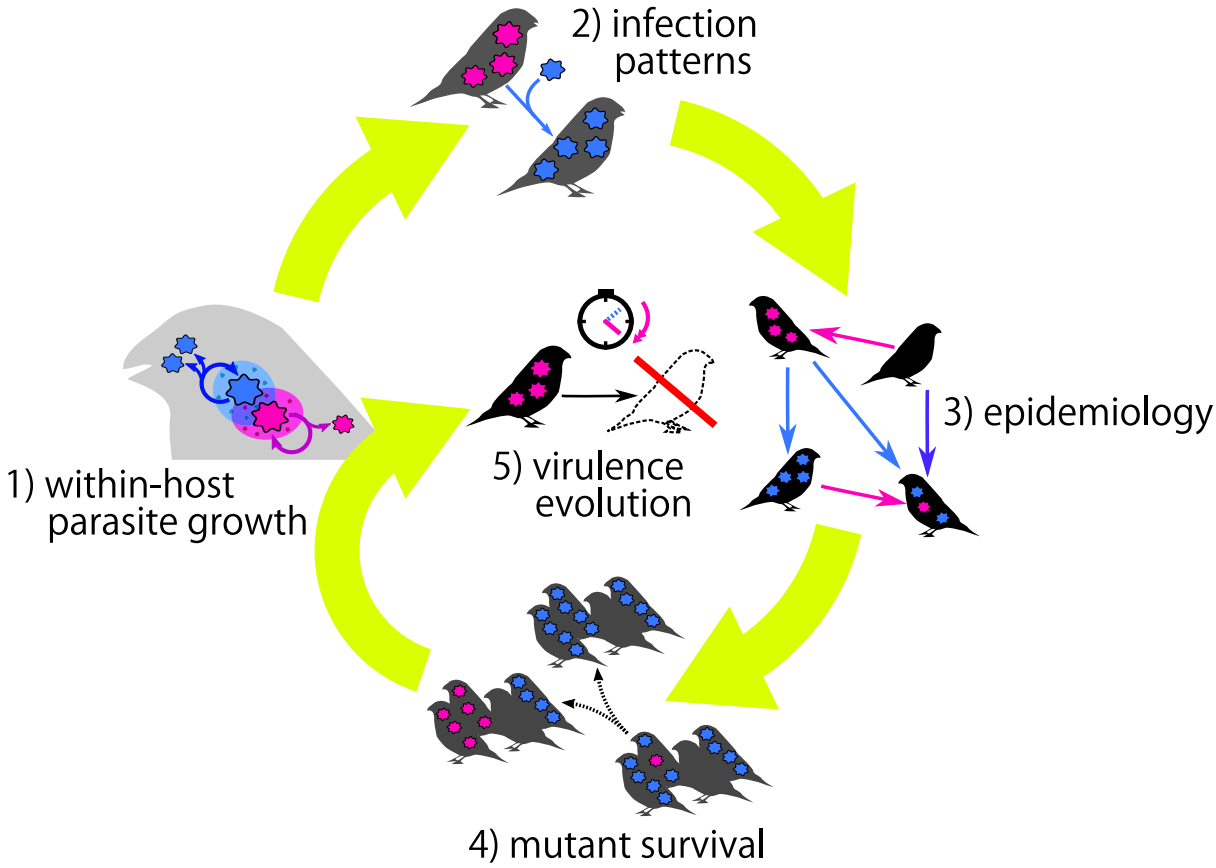

Figure 4.1.1. – Overview of the bottom-up framework used to address virulence evolution.

This figure illustrates the general approach used in this work that involves three dynamical levels: the within-host dynamics (which also includes secreted compounds kinetics) (step 1), the between-host dynamics (step 3) and the evolutionary dynamics (step 5). Each of these three levels is characterized by a proper model respectively inspired from the competitive Lotka-Volterra equations , the SIS model and general probability theory. They are nested one into the other by two key theoretical linkages: the infection pattern typology (step 2) projects the within-host growth outcomes into epidemiology while mutant survival (step 4) deducts from the epidemiology the result on virulence evolution, the goal of our study viewed through the prism of parasite growth traits (hence the last arrow's detour). See references in main text.

4.2. The model

4.2.1. Within-host dynamics

The parasite population dynamics that take place within a host are assumed to be governed by the interactions between parasites individuals. After inoculation, the growth of each parasite type population depends on the parasite load of both types but also on the concentrations of secreted compounds in the medium that can originate from the parasites or the hosts. We refer to compounds that positively affect parasite growth as public goods, e.g. siderophores for bacteria (West & Buckling, 2003) or replication enzymes for viruses (Huang & Baltimore, 1970). Those with a negative effect are either parasite spite such as bacteriocins (Gardner *et al.*, 2004) in bacteria and entry receptor down regulators (Nethe *et al.*, 2005) in viruses, or host defense molecules induced by the infection, e.g. lactoferrin and siderocalin (Skaar, 2010). We thus do not regard within-host parasite growth as a simple exploitative competition but we allow for interference competition, apparent competition and cooperation as well (Read & Taylor, 2001; Cressler *et al.*, 2015).

These diffusible compounds are assumed to be renewable, which is the case of any enzyme and known for siderophores (Neilands, 1995), lactoferrin (Farnaud & Evans, 2003), some bacteriocins (Riley & Chavan, 2007). They are also assumed to be mostly removed from the medium through parasite unrelated processes such as self-denaturation, dilution or host immunity. If one of these two conditions is met, a time scale separation between compound kinetics and parasite replication holds and the parasite within-host dynamics can be reduced to a classical competitive Lotka-Volterra model (Lotka, 1925; Volterra, 1928) illustrated in Figure 4.2.1 for the dimorphic case to which we restrict our approach (the full model and the proof of the reduction are provided appendix 4.b.1). Labelling the parasite types 1 and 2, the within-host dynamics only depends on six parameters: the intrinsic growth rates, ϱ_1, ϱ_2, that quantify the speed at which each parasite individual would reproduce if completely isolated, the self interaction traits, $m_{1,1}, m_{2,2}$, that quantify the strength of intra-type competition, and the cross interaction traits, $m_{1,2}, m_{2,1}$, that quantify the strength of inter-type competition. Note that from the point of view of a given type, let us say 1, both $m_{1,1}$ and $m_{1,2}$ capture the competitive pressure experienced by 1 while $m_{2,1}$ captures its competitiveness. These interpretations can likewise be given in cooperation terms.

The within-host system possesses four equilibria (appendix 4.b.2) – one uninfected, two singly infected and one doubly infected. Each of them corresponds to a host class, which we define as the set of parasite types that chronically infect a host. Besides recovery addressed below, hosts may change class owing to inoculation challenges.

In order to assess the consequence of an inoculation, we investigate the feasibility and the stability of each fixed point given the inoculated parasite types (see appendix 4.b.3 for details). Figure 4.2.2 shows the within-host growth of the two parasite types when sequentially inoculated in the same host, according to four different parameter sets. As already pointed in Sofonea *et al.* (2017b), these results illustrate that our simple within-host model can generate a diversity of within-host outcomes such as type replacement (**A**), stationary coexistence (**B**), infection burst (**C**) and mutual exclusion (**D**). Notice that only the first two cases are addressed by the super/co-infection dichotomy (Nowak & Sigmund, 2002).

Figure 4.2.1. – Within-host model.
The load of parasite type 1 (X_1) varies according to its instantaneous growth rate, which is the sum of its intrinsic growth rate ϱ_1, intra-type interaction effect $m_{1,1}X_1$ and inter-type interaction effect $m_{2,1}X_2$, where X_2 denotes the load of parasite type 2. The same holds symmetrically for parasite type 2, but notice that the cross interaction traits are not necessarily symmetric ($m_{1,2} \neq m_{2,1}$), even though they are shared traits (as signified by their colors). More generally, the four interaction traits $m_{i,j}$ capture density-dependent, beneficial and detrimental compounds and host environment mediation effects.

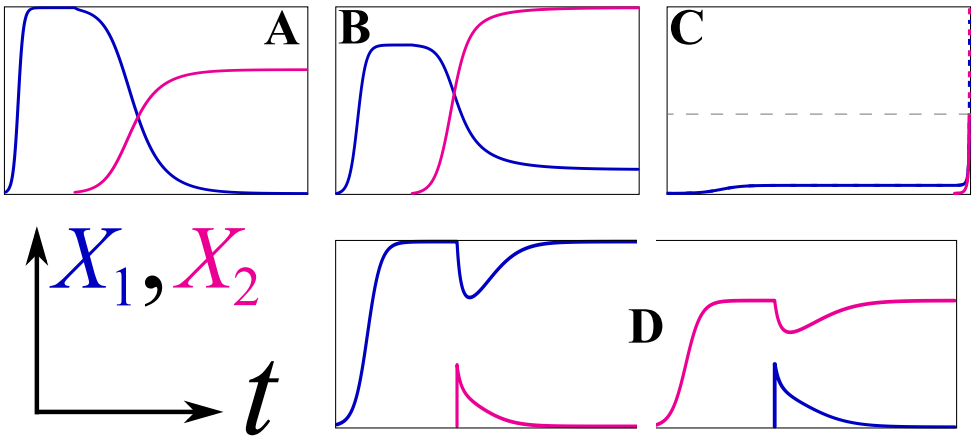

Figure 4.2.2. – Examples of inoculation outcomes.
Four representative outcomes generated by the within host model are shown in terms of parasite loads through time, $(X_1, X_2)(t)$. In all panels, parasite type 1 is first inoculated alone in the host and its load reaches a plateau, the value of which is equal in the four parameter sets for the sake of comparison). Few time units later, the second parasite type is inoculated. **A**) Type replacement: parasite type 2 grows and outcompetes parasite type 1 (notice that it reaches a lower plateau but this is not necessary). **B**) Stationary coexistence: both parasite types reach stationarity (notice that parasite type 1 then reaches another plateau). **C**) Infection burst: once together, the two parasite types' growth explode and therefore exceeds the load threshold above which an acute host immune response is triggered (here arbitrarily set to ten times the stationary parasite load of parasite type 1 and denoted by the dashed line). **D**) Mutual exclusion, even inoculated at high dose, parasite type 2 fails to grow and rapidly vanishes while parasite type 1 recovers its plateau (left sub-panel). Inverting the inoculation order shows the opposite outcome (right sub-panel). The parameter sets used for numerical integration are given in appendix 4.b.1.

4.2.2. Infection patterns

The space of within-host traits can be split into regions that share the same within-host outcomes for each inoculation challenge. These regions are called infection patterns and have been thoroughly discussed in Sofonea *et al.* (2017b), both abstractly (see the mapping formalism in the appendix therein) and biologically (hence the associated terminology and biological examples). The present model generates seven non trivial infection patterns illustrated in Figure 4.2.3 (see proof in appendix 4.c). These patterns have already been exposed in Sofonea *et al.* (2017b), where biological support and references are provided. Besides the aforementioned superinfection and coinfection patterns, we emphasize on priorinfection, where the two kinds of single infections are possible but none of the parasite types can take over a host already infected by the other, and latinfection, where one parasite type is absent from all within-host outcomes (although it can be transiently observed).

It is worth noticing moreover that, unlike previous models that assume that the most virulent type can take over any infected host (Levin & Pimentel, 1981; Nowak & May, 1994), our model is more general and allows competitive exclusion by the less virulent type, provided that virulence is an increasing function of parasite load (see appendix 4.d.3), as empirical studies on various host-parasite systems suggest (Ebert & Mangin, 1997; Kover & Schaal, 2002; de Roode *et al.*, 2008; Fraser *et al.*, 2014; Sy *et al.*, 2014). More generally, this reminds that assuming a unique infection pattern while investigating the space of within-host growth traits can lead to erroneous interpretations.

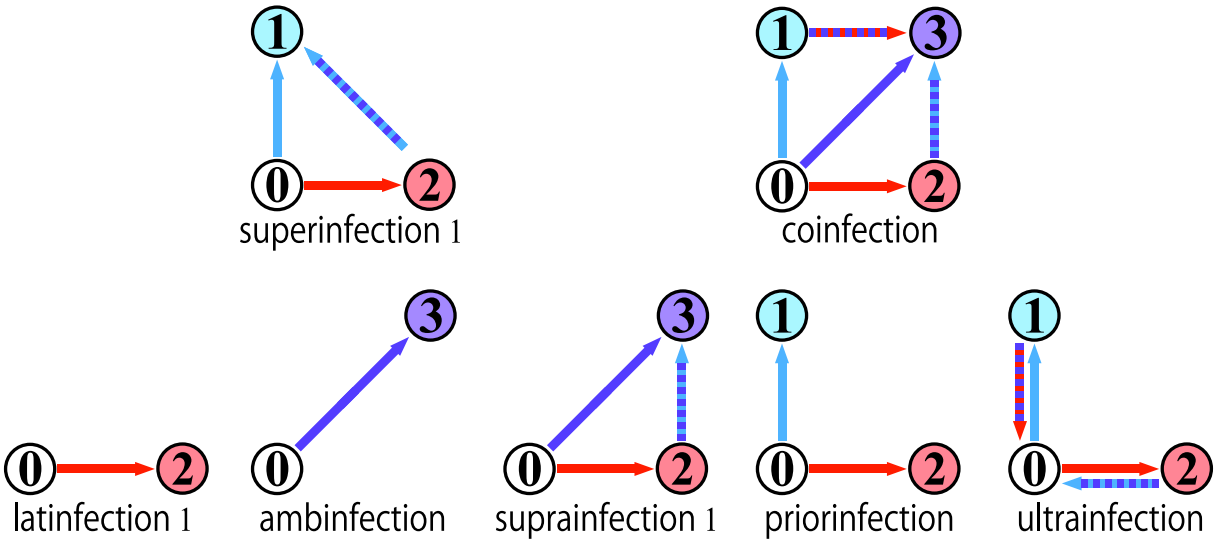

Figure 4.2.3. – Infection patterns.
Graphical representation and names of the seven non trivial infection patterns generated by the within-host model. We only provide one example of asymmetric patterns for which a distinct twin can be obtained by swapping the type labels and their name is followed by 1. Circled labels represent host classes and arrows transitions between host classes through a specified inoculation. Full blue arrows represent inocula of type 1 alone, full red arrows represent inocula of type 2 alone, full purple arrows represent inocula of both types, blue and purple dashed arrows represent inocula of type 1 and possibly type 2, and red and purple dashed arrows represent inocula of type 2 and possibly type 1. For the sake of clarity, inoculation challenges that do not produce any host class transition are not shown. (More details on graphical conventions and naming of infection patterns are available in Sofonea *et al.* (2017b).)

4.2.3. Between-host dynamics

Accounting for parasite polymorphism in epidemiology is a challenge both in terms of modeling and biological interpretation (Metcalf *et al.*, 2015). Indeed, the number of host compartments increases exponentially with the number of parasite types if all type combinations are allowed to coinfect (Sofonea *et al.*, 2015; Kucharski *et al.*, 2016). For the sake of both biological intelligibility and mathematical tractability, we adapt the classical Susceptible-Infected-Susceptible (SIS) model (Keeling & Rohani, 2008) to parasite dimorphism. We however endow this model with very general features.

Here, the functions that govern host demography, with respect to host densities, and epidemiological rates (transmission, virulence and recovery), with respect to parasite load, only have to satisfy minor and common assumptions (e.g. transmission does not decrease with parasite load). Importantly, these functions are otherwise left unspecified, that is we do not assign them any analytical expression. We emphasize on the fact that this guarantees a great generality of the subsequent results which will therefore be valid for a diversity of demographic dynamics and physiological responses hence also preventing them from structural sensitivity (Wood & Thomas, 1999; Fussmann & Blasius, 2005).

Besides, we allow the doubly infected hosts to transmit the three possible kinds of inocula (1 alone, 2 alone and 1 & 2) and, in addition to recovery, all compartment transitions are possible so that the model captures all infection patterns previously introduced. The flow diagram and more information about the model are given in Figure 4.2.4. The associated equations and the analysis of the model are provided in appendix 4.d.

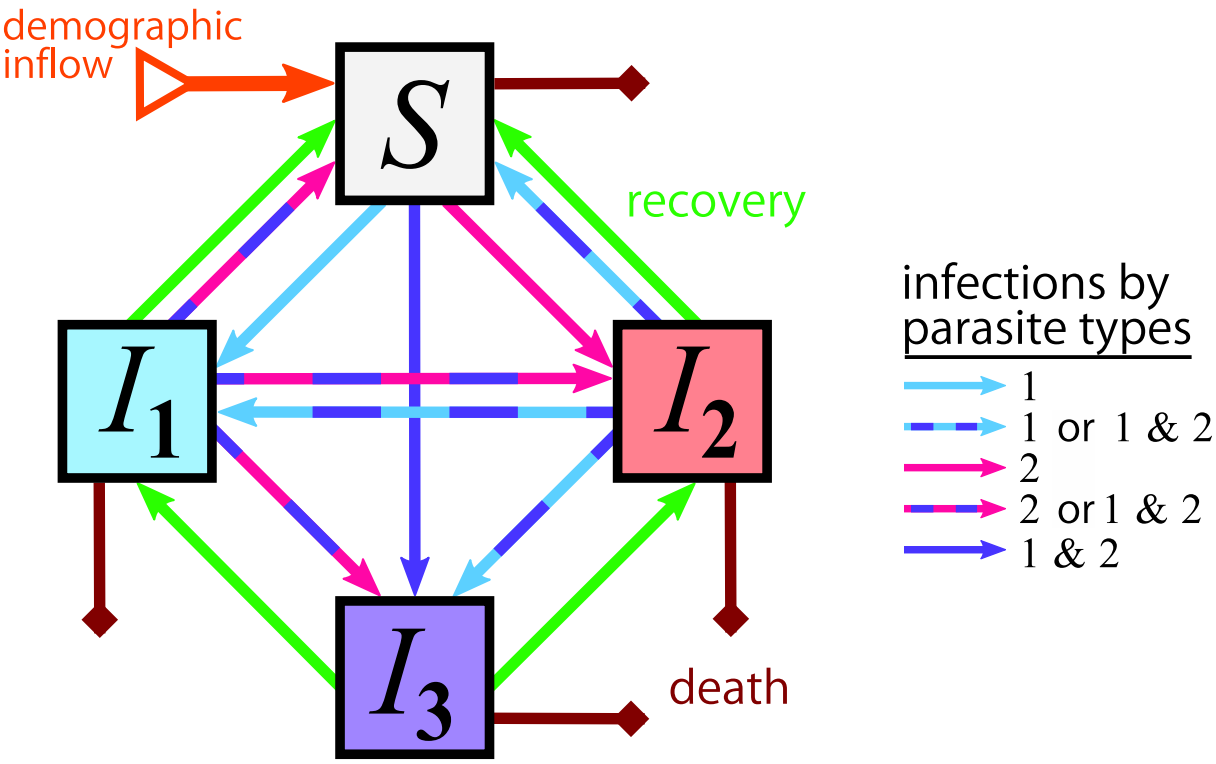

Figure 4.2.4. – Flow diagram of the generic SIS model with parasite dimorphism. The between-host dynamics characterize the density of four host compartments (boxes) through time, namely the susceptible hosts S, the hosts singly infected by parasite type 1 I_1, the hosts singly infected by parasite type 2 I_2 and the doubly infected hosts. Parasite transmission is assumed to be purely horizontal so all new hosts (offspring or immigrants) are susceptible (orange arrow). Hosts change compartment either through infection (blue, pink, purple and mixed arrows) or through recovery (green arrows). Infections result from transmission of one or both parasite types from both singly or doubly infected hosts. Recovery is possible one parasite at a time. Finally, mortality (deep red arrows) affects all host compartments but at different rates: natural mortality is shared but virulence, that is additional mortality due to infection, can differ among infected host compartments.

4.2.4. Mutational setting

Virulence originates from the parasite ability to grow within a host. It can therefore be seen through the prism of stationary parasite load (as, for instance, in FRASER *et al.* (2014)), which is the combination of two within-host growth traits: intrinsic growth rate and self interaction.

Let us consider that a monomorphic parasite is already circulating in a host population (not necessarily at epidemiological equilibrium) and, among its offspring, one mutant individual possesses traits that differ from those of its resident ancestor. Regarding the ancestor and its mutant as respectively parasite types 1 and 2, we write $\rho_2 = \rho_1 + R$ and $m_{i,j} = m_{1,1} + M_{i,j}$ where R and $M_{i,j}$ are random variables. The greatest standard deviation of these random variables hereafter serves as a proxy for the overall mutational effect.

In the following, we focus on mutants that differ only slightly from their ancestor as it allows us to fully characterize its survival in spite of the model's generality, while being a usual assumption in theoretical evolutionary biology (TAYLOR, 1989; GERITZ *et al.*, 1998). To do so, we examine a diversity of mutational settings we distinguish according to two complementary properties: the mutational distribution – that governs the spreading shape of the probabilities with which the mutant traits take their values (i.e. the laws of R and $M_{i,j}$) – and the mutational scenario – that governs the dominance and correlations between mutant traits. We hereafter verbally expose a simplified view of these settings but see appendix 4.e for their mathematical formulation.

In order to capture a large range of mutational processes, we consider three different mutational distributions, a) the fixed step distribution, i.e. mutations that, in first approximation, add or subtract with equal probabilities the same quantity to the ancestor trait value, b) the Gaussian distribution, where the mutant trait values are normally distributed around those of the ancestor (WOLF *et al.*, 2007), and c) the generic distribution, that is any probability distribution symmetrically distributed around the ancestor trait values. The fixed step and generic mutational distributions are treated analytically while the Gaussian mutational distribution is used for numerical confirmations (and larger mutation effects, see below).

As for the mutational scenarios, we consider the cases where #1 - the mutation results in a change in intrinsic growth rate, #2 - the mutation mainly lies in the interaction traits, #3 - the mutation independently affects all four traits simultaneously in comparable absolute value (we call it the unconstrained, or free, scenario), #4 - the traits are strongly traded-off, e.g. an increase in intrinsic growth rates necessarily increases the competitive pressure undergone by the mutant and lowers its competitiveness.

We can now implement these mutational settings into the previously developed bottom-up approach, from within-host interactions to epidemiological dynamics and investigate the proportion of mutants that survive with respect to their virulence, which is the support of virulence evolution. The endpoint results of this analysis are the proportions of surviving mutants that are more virulent than their ancestor obtained under all combinations of mutational distributions and mutational scenarios (see subsection 4.3.1 below).

For the sake of completeness, we also extend our investigations to large mutation effects. Because they raise analytical difficulties, we limit ourselves to numerical simulations of only one, but representative, case: the Gaussian mutational distribution under the free mutation scenario (#3) (see subsection 4.3.2 below).

4.3. Results

4.3.1. Small mutations

If mutations have a small phenotypic effect, it is easy to show that under any of the mutation settings described above, exactly one half of the generated mutants are more virulent than their ancestor. Besides, the only infection patterns that emerge are superinfections, coinfection and priorinfection. Following the next-generation method (VAN DEN DRIESSCHE & WATMOUGH, 2002; HURFORD *et al.*, 2010), we derive the invasion fitness of the mutant the sign of which is, at least partially, governed by the infection pattern. Hence, we show that a mutant can survive, in spite of its ancestor's anteriority in the host population, only when, within one doubly inoculated host, it always excludes its ancestor (superinfection 2), coexists with it (coinfection) or when the the mutant and its ancestor exclude each other according to the anteriority inside the host. More precisely, all mutants that establish a superinfection 2 or a coinfection survive whatever their virulence. In contrast, the survival of the mutants involved in a priorinfection depends on virulence, as the sign of the invasion fitness changes according to the shape of the epidemiological trade-offs that govern their capacity to spread among hosts, usually quantified by the basic reproduction number $\mathcal{R}_0$(DIEKMANN *et al.*, 1990). Consequently, under priorinfection, the mutants that survive are either those that are more virulent than their ancestor; if $\mathcal{R}_0$ increases with virulence, or, those less virulent if $\mathcal{R}_0$ decreases with virulence. Investigating whether $\mathcal{R}_0$ increases or decreases with virulence is exactly equivalent to investigating whether the resident's virulence is located on an ascending or a descending slope of the unidimensional $\mathcal{R}_0$ landscape with respect to virulence. Since we do not investigate any particular mutant nor any particular $\mathcal{R}_0$ landscape we make the neutral assumption that the direction of the slope on which the resident's virulence is located has as equal chances to be ascending or descending. Hence, because half of the mutations increase virulence, it results that half of the mutants involved in priorinfection survive in the end. If a mutant establishes any other pattern (essentially superinfection 1, but this holds for latinfection 2 and ultrainfection as well), it always goes extinct. The results about how infection patterns affect the mutant's probability of survival are summarized in Table 4.3.1.

infection pattern	superinfection 2	coinfection	priorinfection	other patterns
probability that the mutant survives given the infection pattern	1	1	½	0

Table 4.3.1. – Mutant survival according to infection pattern.

Intuitively, the mutants that possess both properties of higher virulence and survival are a minority. However, when we focus on the proportion of more virulent mutants among the surviving mutants, by combining results from Table 4.3.1, the frequency of each infection pattern and their statistical association with virulence (see appendix 4.f) , we find that more virulent mutants always constitute the majority of surviving mutants. This observed selection bias towards higher virulence is supported by all combinations of investigated mutational distributions and mutational scenarios, as shown in Figure 4.3.1, where all analytical values or numerical estimates of the proportion of more virulent mutants among surviving mutants lie in the right half side of the gradient.

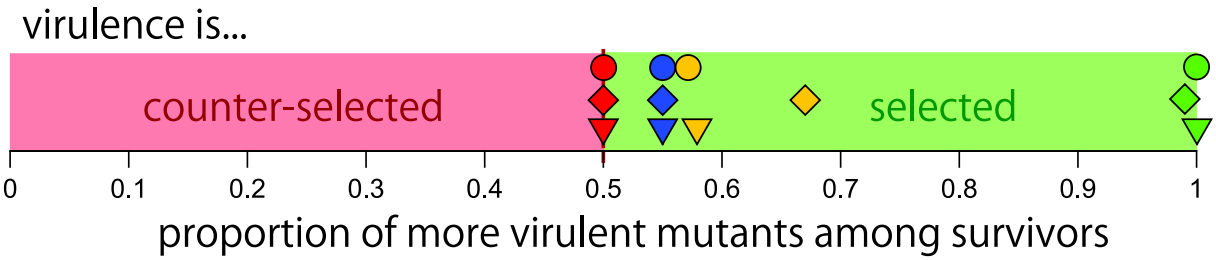

Figure 4.3.1. – Virulence selection bias in several mutational settings.
The horizontal position of the triangles, circles and rhombi gives the proportion of surviving mutants that are more virulent than their ancestor when the mutational distribution is a fixed step, generic and Gaussian respectively. The results are analytical for the first two distributions and numerical for the third (10^5 simulations for each mutational setting). Colors denote the mutational scenario: fully constrained in red, competition-driven in blue, unconstrained in orange and growth-driven in green Since the solution in the generic distribution of unconstrained mutation is not unique, only a lower boundary is shown. The effect of the epidemiological trade-off is neutralized by averaging over a distribution of resident virulence assumed symmetric with respect to the epidemiologically optimal virulence.

Although the precise results rely on tedious calculations (exposed in appendix 4.f), it is possible to qualitatively approach this apparently robust virulence selection bias by means of a marginal simplification of the mutational setting and elementary geometry, as provided in Figure 4.3.2. A simplified interpretation of the results would state that, on one hand, a higher virulence is achieved through faster growth and greater self cooperation compared to the respective ancestor's traits. On the other hand, a mutant survives through faster growth and competition escape. Most mutants that grow faster are also more virulent, while those who escape their ancestor's competition can nonetheless present a greater self cooperation which makes some of them more virulent as well. In the end, a surviving mutant is statistically more likely to present virulence-increasing traits.

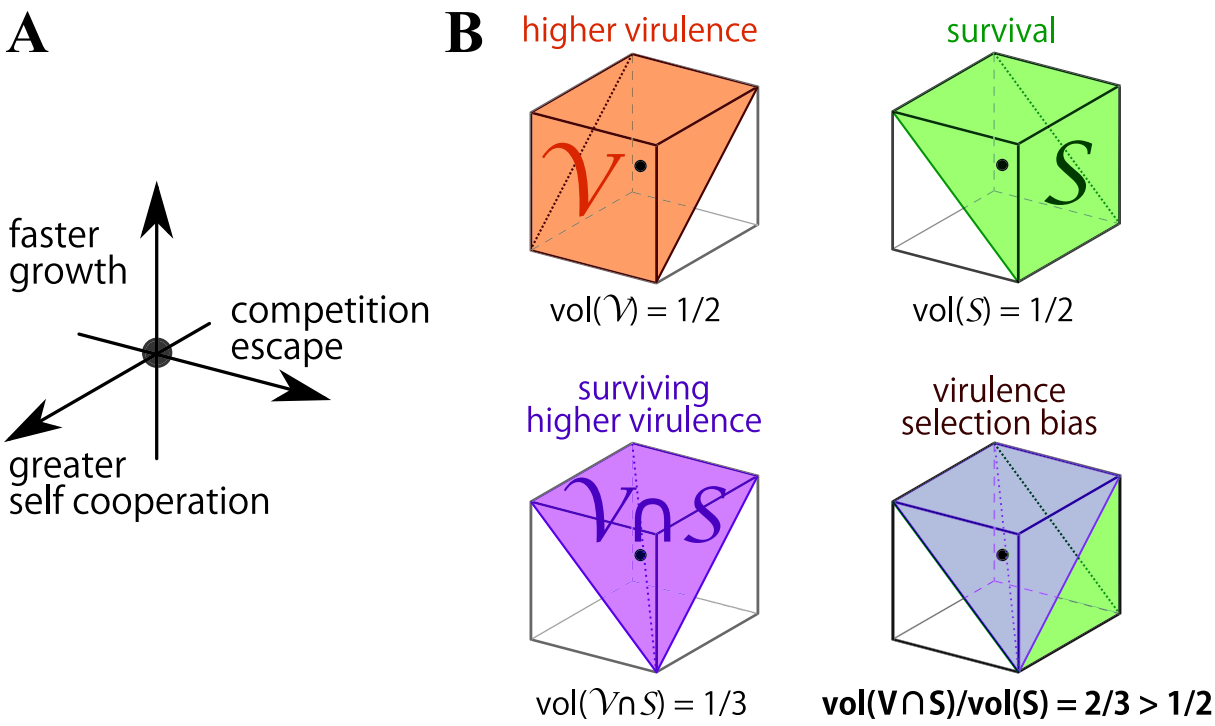

Figure 4.3.2. – Geometrical explanation of the virulence selection bias.
Leaving aside the competition pressure undergone by the resident, which does not qualitatively affect the final result, we can project the space of unconstrained mutations (scenario #3) into an arbitrarily bound cube. Each axis corresponds to the mutational deviation of a within-host trait value, as depicted on the diagram **A**. More precisely, i) the competition undergone by the mutant with itself decreases along the x-axis ($m_{2,2} - m_{1,1}$) – or equivalently the self cooperation increases, ii) the competition undergone by the mutant from its ancestor decreases along the y-axis ($m_{2,1} - m_{1,1}$) and iii) its the intrinsic growth rate increases along the z-axis ($\varrho_2 - \varrho_1$). **B)** Mutants with higher virulence than their ancestor grow faster or compete less with themselves (region $\mathcal{V}$), but only mutants that grow faster or experience less competition from their ancestor survive (region $\mathcal{S}$). Each of these two regions occupies half of the volume (vol) of the cube. Their intersection $\mathcal{V} \cap \mathcal{S}$ occupies ⅓ of the cube, which represents ⅔ of the volume of $\mathcal{S}$. Therefore, more than half of the surviving mutants are more virulent than their ancestor. Note that this explanation is also easily applicable to growth-driven (scenario #1) and competition-driven mutations (#2) by projecting over the vertical axis or the middle horizontal plane respectively. Traded-off mutations (scenario #4) cannot however be looked at this way.

4.3.2. Large mutations

Numerical simulations under Gaussian mutational distribution and the free mutational scenario not only confirm the previous results (on the left hand side of the graphs in Figure 4.3.3**A** and **B**), but they also provide insight to the consequences of larger mutation effects over the epidemiology and evolution of the parasite (on the right hand side).

First but not surprisingly, latinfection 2, suprainfection 2 and ultrainfection occur more frequently when mutations get larger (Figure 4.3.3**A**), as predicted by analytical calculations. We even remark that more than two thirds (ca. 68%) of very large mutations produce the latinfection 2 pattern. This has important consequences on mutant survival since, whatever its epidemiological rates, no mutant can survive if it undergoes

latinfection. Actually, latinfection 2 is the only pattern under which we can exactly assess mutant survival under large mutations. This is the meaning of curve *c* in Figure 4.3.3**B**: it represents the upper bound of the mutant survival probability, that is the sum of the probabilities of all infection patterns but latinfection 2 as if they were all allowing for mutant survival (which is nonetheless very unlikely). We can also extrapolate the survival probability from the infection pattern distribution assuming that infection patterns resulted in or prevented mutant survival in a similar way to the small mutations scenario (i.e. all superinfecting, all coinfecting , half of priorinfecting and none of superinfected or ultrainfecting mutants survive (see appendices 4.f.3 and 4.f.5)). Because we have no basis from which to extrapolate mutant survival under suprainfection 2, we consider the two extreme cases: either all suprainfecting mutants survive (curve *d* in Figure4.3.3**B**), or none of them survives (curve *e*). These two extrapolated boundaries suggest that mutant survival is likely to lie approximately halfway between 0 and curve *c* (ca. 0.2).

Virulence (orange curve) is a ground (i.e. unextrapolated) output of the simulations and interestingly, while small mutations produce equal numbers of mutants with higher virulence or lower virulence with respect to their ancestor under all investigated mutational distributions and mutational scenarios, the probability that a mutant is more virulent than its ancestor dramatically drops as mutations become larger and saturates at a relatively low value (ca. 0.13). This results from the predominance of latinfection 2 in large mutational outcomes, and marginally the appearance of suprainfection 2, the two infection patterns in which mutants are avirulent by definition.

Virulence selection bias (brown curves), that is the proportion of surviving mutants which are more virulent than their ancestor relative to the proportion of surviving mutants, is found by combining the virulence mutational outcomes to the aforementioned extrapolated survival (curve *a* excludes suprainfecting mutants from survival while curve *b* includes them). Of course, the decrease in mutant survival does not affect as much virulence selection bias since the surviving mutants might be very rare but all virulent. We nonetheless observe that the virulence selection bias decreases and steps below the one half probability line when mutation effects become very large.

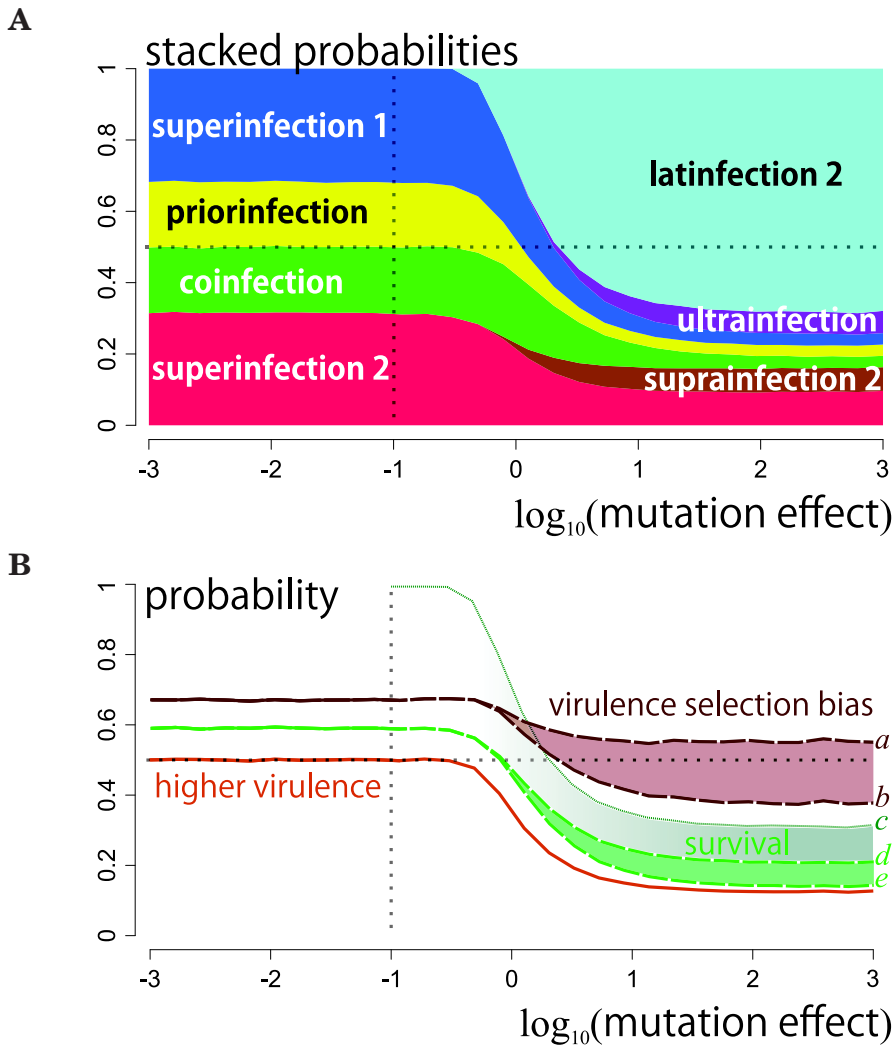

Figure 4.3.3. – Mutant virulence and survival under large mutational effects.
These results are based on numerical simulations under the following mutational setting: the mutational distributions are assumed Gaussian and follow the free mutation scenario, i.e. no correlation between within-host growth traits and equal standard deviation across traits, here called the mutational effect. For 30 mutational effect values ranging from 10^{-3} to 10^{3}, we simulated 10^{5} independent (and separate) mutations of the same resident (with no loss of generality). For each of these $3 \cdot 10^{6}$ mutations, we registered the induced infection pattern and compared its virulence to that of the resident. In both panels, the x-axis corresponds to the order of magnitude of the mutational effect, while the y-axis corresponds to probabilities, either stacked (panel **A**) or independent (panel **B**). The vertical dotted line separates the domain of small mutations (on the left), from the one of large mutations (on the right), arbitrarily set at one order of magnitude below the resident's traits absolute values. The horizontal dotted line indicates the one half probability, $y = 1/2$.
A) Probability distribution of the infection patterns induced by the mutation according to the mutational effect. **B**) Probabilities that a mutation increases virulence (orange curve), mutant survival (green curves: upper bound (*c*), high (*d*) and low (*e*) extrapolations) and virulence selection bias (brown curves: high (*a*) and low (*b*) extrapolations) as functions of the mutational effect. The solid curves (or curve portions) correspond to certain data, either ground simulation outputs or outputs combined with applicable analytical results. The dashed curve portions, lying in the large mutation side of the graph, correspond to simulation outputs combined with extrapolated analytical results from the small mutational setting. See text for more details.

4.4. Discussion

The idea that virulence could be driven by within-host competition naturally arose with the first theoretical models accounting for parasite polymorphism (Levin & Pimentel, 1981; Bremermann & Pickering, 1983; Nowak & May, 1994; May & Nowak, 1995), which is now known to be the rule of natural infections (Petney & Andrews, 1998; Read & Taylor, 2001; Balmer & Tanner, 2011). While some empirical evidence suggest an evolutionary increase of virulence due to a positive correlation with competitiveness (de Roode *et al.*, 2005b; Bell *et al.*, 2006), several experimental systems have shown that within-host parasite polymorphism would counter-select virulence instead (Turner & Chao, 1999; Garbutt *et al.*, 2011; Pollitt *et al.*, 2014), as predicted by alternative models (Frank, 1992; Brown & Grenfell, 2001; Brown *et al.*, 2002; Brown, 1999; Gardner *et al.*, 2004). These works highlight the fact that when infection relies on a collective action (such as public goods production) then lower virulent strains are favored.

Many subsequent studies tried to find a unified answer to the evolution of virulence in a multiple infection context but they are usually based on strong assumptions or lack one essential dynamical level (either within or between host dynamics), as we detail below. Following the specifications that a relevant approach to this issue has to satisfy Cressler *et al.* (2015), we developed a nested model based on Sofonea *et al.* (2015) with explicit within-host dynamics, between-host dynamics and several possible mutational settings. We paid special attention to the generality of the possible patterns each of these processes can generate. In particular, we used the infection pattern typology exposed in a previous work (Sofonea *et al.*, 2017b), that is the coupling between inoculation challenges and parasite growth outcomes, to avoid any arbitrary assumptions on the within-host outcomes and epidemiological trade-offs.

First, we show that while quite simple within-host dynamics can generate seven infection patterns, only three of them matter if mutational effects are small. These patterns are superinfection, coinfection and priorinfection (note by the way that the well-known super/co-infection dichotomy misses here an evolutionary relevant pattern). This may explain why the four other patterns are marginal in nature (but see Sofonea *et al.* (2017b)). Second, and importantly, we show that most of the mutants able to survive are more virulent than their ancestor. We establish the robustness of this result by examining several distributions of mutational effects, including generic distributions, and various mutational scenarios, including differential variance and unfavorable genetic constraints (competitiveness coming with a cost, as spiteful compounds for instance (Gardner *et al.*, 2004)). We therefore conclude that if polymorphism (of within-host growth traits) can emerge, then this inevitably increases the mean virulence of the parasite species.

In addition, we observed that large mutations are mostly deleterious. This provides an *a posteriori* support to our focus on small mutations since within-host growth traits appear to be, according to the model, under a strong selective pressure which denotes important developmental constraints. Further, large mutations contribute considerably less to the emergence of more virulent mutants (about three times less under the Figure 4.3.3 setting (unshown result)) and the virulence selection bias seems to be reduced. This may be explained by the fact that the vast majority of large mutations fail to produce virulent mutants which compensates the ground virulence selection bias. This question is however left open as more specific investigations on large mutations are required.

To our knowledge, our framework is the first to capture virulence evolution in multiple infections while 1) explicitly accounting for dynamics ranging from the molecular kinetics to epidemiological persistence, thus making virulence emerge from within-host

growth traits, 2) allowing for several infection patterns, single and co-transmissions simultaneously, recovery, multi-dimensional mutations and 3) not specifying any link between virulence and competitiveness nor any epidemiological trade-off, 4) addressing the evolutionary outcome through weighting all possible mutations instead of considering the fate of one more virulent mutant alone and 5) being analytically tractable.

The present model captures several infection patterns with one set of equations instead of using distinct models for each pattern (Nowak & Sigmund, 2002), or deriving them from limit cases (Mosquera & Adler, 1998), or artificially mixing them (Boldin & Diekmann, 2008). The within-host outcomes completely rely on explicit population dynamics of the parasites and not any trait defined at a higher organization level such as virulence (Levin & Pimentel, 1981; Nowak & May, 1994). In particular, parasite competitiveness results from cross interaction traits that do not affect the virulence level. A parasite type can therefore be indifferently invaded and outcompeted by a more virulent and a less virulent type (see Figure 4.2.2A). This independence of competitive ability and virulence contrasts with most models (Frank, 1992, 1994; Bonhoeffer & Nowak, 1994; May & Nowak, 1994; Nowak & May, 1994; Frank, 1996; Gandon, 1998; Boldin & Diekmann, 2008).

Here, unlike Mosquera & Adler (1998), double infections originate from actual stable within-host dynamics. Unlike in May & Nowak (1995), they may indifferently affect transmission or not while the trend on virulence evolution is not affected by the co-transmission probability, as opposed to Alizon (2013b). While cooperation is allowed through cross interactions or potential increase in overall transmission in double infections, polymorphism implies increased virulence. This contrasts with earlier studies (Brown *et al.*, 2002; West & Buckling, 2003) in which polymorphism (or low relatedness) decreases virulence. Nonetheless it has been shown that the results of these models can be inverted by considering the between-host level which they lack (Alizon & Lion, 2011). Note however that this requires assuming some trade-offs not needed here.

One can legitimately then wonder what drives the necessity of increased virulence that emerges in our model. We highlight (see appendix 4.f.4) that a phenotypically close mutant survives in the host population in which already circulates its ancestor if it can prevent the host it infects from secondary infections by its ancestor and/or if it can grow within hosts already infected by its ancestor (which can persist or vanish). If the mutant can only protect its host, we have priorinfection. If it can only grow in hosts infected by the resident, we have coinfection. When the mutant is able to do both, it superinfects its ancestor. Coinfection guarantees the survival of the mutant since it can grow in all hosts. In the case of priorinfection, there is only a single 'resource' (uninfected hosts) so the mutant will persist in the host population only if the infections it causes are epidemiologically fitter than those caused by the resident (which depends on their transmission, virulence and recovery rates). Hence, a majority of surviving mutants are either superinfecting or coinfecting their ancestor. Since these two infection patterns require the ability to grow within already infected hosts, these mutants necessarily present a faster intrinsic growth or escape their ancestor's competitive pressure. Faster intrinsic growth is one of the two features of higher virulence – the other being greater self cooperation. Consequently, either mutants survive exclusively because of their faster intrinsic growth and they are more virulent, either they survive because they undergo less competition from their ancestor while they present greater self cooperation or faster intrinsic growth, which makes them more virulent as well. In the end, the probability that a surviving mutant is more virulent is at least of one half (and up to one), while only half of the mutants ever produced are more virulent than their ancestor. This result holds independently of whether the parasite's intrinsic growth trades off with competition escape.

Coming back to the adaptive explanation of virulence, we are prone to thinking that this systematic selection bias towards higher virulence answers this question by unifying reasons 2 and 3: in multiple infections, virulence results from a mixture of selection for competitiveness – actually competition escape ability – and as a by-product of local selection for faster within host growth or greater self cooperation. As pointed out by Levin & Pimentel (1981), this induces a short-sighted evolution as more virulent mutants survive even if their traits do not lead to epidemiological optimality, thus leading to an unavoidable degree of maladaptation. It is then legitimate to wonder where this increasing virulence will lead the parasite species, e.g. towards a stable polymorphism asymmetrically distributed towards higher virulence or a never-ending increase of virulence. This model is unable to address these long-term dynamics, however at some point epidemiological constraints will possibly limit this increase and/or the host will possibly develop resistance or tolerance.

As a counterpart of the model's generality, knowing that the mutant survives does not give us any insight on the survival of the resident. We claim that this does not affect the result since, whether the ancestor survives or not, the mean virulence in the parasite population increases in any case. It is however a main perspective of future work to generalize the framework to an unbounded and varying polymorphism. This task does not seem analytically tractable but specifying the functions undetermined so far based on documented experimental systems, as recommended by Cressler *et al.* (2015) sounds promising. Accounting for spatial structure, host heterogeneity and host evolution would certainly modulate the present result.

Appendix

4.a. Mathematical notations

Throughout this appendix we use several notations which are worth clarifying.

To distinguish notations from mathematical results, we always introduce notations using the defining equality $:=$ (the colon being on the side of the introduced notation), while $\equiv$ states equivalence between objects.

We use the Iverson brackets for denoting statement-dependent binary functions, that is for any statement s, $[\mathrm{s}] = 1$ if s is true and 0 otherwise.

Classical logical operators such as negation $\neg$ ("not"), disjunction $\vee$ (inclusive "or") and conjunction $\wedge$ ("and") are used.

$\succ, \succeq$ are used as the entrywise equivalent of greater than and greater than or equal to. $\odot$ stands for the entrywise (Hadamard) product.

$\mathbb{R}^\star$ denotes the set of real numbers without 0 while $\mathbb{R}_+, \mathbb{R}_-$ denote the set of non-negative and non-positive real numbers respectively.

$A^\complement$ denotes the absolute complement of a set A.

Since we consider two parasite types (labelled 1 and 2), we often have to deal with label-dependent quantities or objects for which the general form can be advantageously given using dummy indices. Therefore, unless stated otherwise, i represents 1 and 2 while k respectively represents 2 and 1. j may be used along i for the four couples of $\{1,2\} \times \{1,2\}$. This convention is sometimes briefly reminded as $i = 1,2, k = 2$, and $j = 1,2$. It also holds for the corresponding bold labels $\boldsymbol{i}, \boldsymbol{k}, \boldsymbol{j}$ that refer to hosts or inocula.

Supplementary methods

4.b. Within-host dynamics

In this section we expose and investigate the stationary dynamics model for the within-host parasite growth.

4.b.1. Full model and dynamical reduction

Let us consider two parasite types labeled 1 and 2 that grow within the same host. Their respective loads, denoted by $X_i(t) \in \mathbb{R}_+, i = 1,2$, vary in "parasite time" $t \in \mathbb{R}_+$ according to several within-host mechanisms:

1. Intrinsic growth: it is quantified by the rate $\varrho_i \in \mathbb{R}$, which can be negative if the parasite type is unable to initiate an infection alone.
2. Self density dependence: this effect emerges from interactions between individuals that belong to the same type and is quantified by $\eta_{i,i} \in \mathbb{R}$. In particular, this rate is negative if the parasite population undergoes intra-type inhibition.
3. Cross density dependence: this effect is defined as the consequences of the inter-type interactions and is quantified by $\eta_{i,k} \in \mathbb{R}$.
4. Diffusible compounds, especially molecules, that modulate the parasite's growth, according to their time-varying concentration $Y_p(t) \in \mathbb{R}_+$ and their respective effect $\gamma_{i,p} \in \mathbb{R}$ on parasite type i's growth. These compounds are likely to be directly produced by one or both parasite types and depending on their qualitative effect (i.e. the sign of $\gamma_{i,p}$), they may be considered as public goods or spite products, with respect to one or both types (see main text for examples and references). One can also consider that some of them are produced by the host itself owing to immuno-physiological processes induced by the infection (e.g. iron-binding and siderophore-binding proteins, antimicrobial peptides, complement proteins, ...). These compounds thus capture part of the apparent competition between parasite types. Whether they are parasite or host secretions, these compounds are likely to be produced at rates that are proportional to parasite loads through a positive factor denoted by $u_{i,p} \in \mathbb{R}_+$. (Note that $u_{i,p} = 0$ if parasite type i does not contribute to compound p production.) We moreover assume that these compounds are mostly removed from the medium through processes that are not related to their activity, such as self-denaturation, host degradation, dilution – which is the case of a large class of secreted molecules namely those with a renewable activity such as enzymes and more specifically siderophores, bacteriocins, lactoferrin (references are given in the main text). Their clearance is therefore proportional to their concentration through a positive factor denoted by $v_p > 0$.

In the end, the within-host growth of the two parasite types conforms to the following set of ODEs, with $p = 1,2,\ldots,p_{\max}$, $i = 1,2$, $k = 2,1$,

$$\begin{cases} \frac{\mathrm{d}X_i}{\mathrm{d}t}(t) &= \left(\varrho_i + \eta_{i,i}X_i(t) + \eta_{i,k}X_k(t) + \sum\limits_p \gamma_{i,p}Y_p(t)\right)X_i(t), \\ \epsilon\frac{\mathrm{d}Y_p}{\mathrm{d}t}(t) &= u_{1,p}X_1(t) + u_{2,p}X_2(t) - v_pY_p(t), \end{cases} \tag{4.b.1}$$

where ϵ is a kinetics parameter that quantifies the time scale difference between the rather fast processes related to the compounds turn-over and the rather slow processes related to parasite replication. Assuming that this parameter is small, $0 < \epsilon \ll 1$, allows

us to see (4.b.1) as a fast-slow system (where the Y_ps and the X_is are respectively the fast and slow variables) and apply to it the suitable geometric singular perturbation theory exposed in KUEHN (2015).

Setting $\epsilon = 0$ transforms (4.b.1) into the slow subsystem with the algebraic constraint

$$u_{1,p}X_1 + u_{2,p}X_2 - v_pY_p = 0, \tag{4.b.2}$$

which restricts the associated slow flow to the critical manifold

$$C_0 = \left\{ \left(X_1, X_2, Y_1, \ldots, Y_p\right) \in \mathbb{R}_+^{p+2} : \forall p \in \{1, \ldots, p_{\max}\}, Y_p = \frac{1}{v_p}\left(u_{1,p}X_1 + u_{2,p}X_2\right) \right\}, \tag{4.b.3}$$

which is smooth, normally hyperbolic and attracting everywhere since $\frac{\partial}{\partial Y_{p'}}\left(\frac{\mathrm{d}Y_p}{\mathrm{d}t}\right) = -\left[p' = p\right] v_p$. By applying the Fenichel-Tikhonov theorem to (4.b.1), we know that there exists a slow manifold C_ϵ nearby C_0, which is attracting with respect to the Y_ps as well and on which the flow converges to the slow flow as $\epsilon \to 0$.

Hence, for ϵ sufficiently small, we can approximate the long-term behaviour of (4.b.1) by the one of the so-called reduced problem

$$\frac{\mathrm{d}X_i}{\mathrm{d}t} = \left(\varrho_i + \eta_{i,i}X_i + \eta_{i,k}X_k + \sum_p \gamma_{i,p}y_p\right) X_i,$$

where the y_ps satisfy the algebraic constraint of the critical manifold, giving

$$\eta_{i,i}X_i + \eta_{i,k}X_k + \sum_p \gamma_{i,p}y_p = \left(\eta_{i,i} + \sum_p \frac{\gamma_{i,p}u_{i,p}}{v_p}\right) X_i + \left(\eta_{i,k} + \sum_p \frac{\gamma_{i,p}u_{k,p}}{v_p}\right) X_k.$$

We denote by $m_{i,j}$ these sums of parameters that captures all the direct and indirect interactions effects, such that, for $i, j = 1, 2$,

$$m_{i,j} \coloneqq \eta_{i,j} + \sum_p \frac{\gamma_{i,p}u_{j,p}}{v_p}, \tag{4.b.4}$$

Then, the initial full model (4.b.1) that contains $2+p$ variables and $4p+6$ parameters can be advantageously simplified to a classical dimorphic Lotka-Volterra system containing 6 parameters:

$$\frac{\mathrm{d}X_1}{\mathrm{d}t} = \left(\varrho_1 + m_{1,1}X_1 + m_{1,2}X_2\right) X_1, \qquad \frac{\mathrm{d}X_2}{\mathrm{d}t} = \left(\varrho_2 + m_{2,1}X_1 + m_{2,2}X_2\right) X_2. \tag{4.b.5}$$

Note that, in general, $m_{1,2} \neq m_{2,1}$. Hence, depending on the values of the $\left(m_{1,2}, m_{2,1}\right) \in (\mathbb{R})^2$ couple, model (4.b.5) encompasses all major kinds of ecological interactions BEGON *et al.* (2005) that could occur between the two parasite types.

Simulations in Figure 4.2.2 result from numerical integration of ODEs (4.b.5) with the following parameter sets: **A)** $\varrho_1 = 9, \varrho_2 = 8, m_{1,1} = -3, m_{1,2} = -5, m_{2,1} = -2, m_{2,2} = -4$ – **B)** $\varrho_1 = 9, \varrho_2 = 8, m_{1,1} = -3, m_{1,2} = -2, m_{2,1} = -1, m_{2,2} = -4$ – **C)** $\varrho_1 = \varrho_2 = 9, m_{1,1} = m_{2,2} = -3, m_{1,2} = 9, m_{2,1} = 10$ – **D)** $\varrho_1 = 9, \varrho_2 = 8, m_{1,1} = -3, m_{1,2} = -6, m_{2,1} = m_{2,2} = -4$.

4.b.2. Fixed point determination

First, let us rewrite (4.b.5) in the vectorial form,

$$\frac{\mathrm{d}}{\mathrm{d}t}\mathbf{x} = \left(\boldsymbol{\varrho} + \mathbf{M}\mathbf{x}\right) \odot \mathbf{x} =: \mathbf{f}(\mathbf{x}), \tag{4.b.6}$$

where

$$\mathbf{x} \equiv (X_1, X_2), \boldsymbol{\varrho} \equiv \left(\varrho_1, \varrho_2\right), \mathbf{M} \equiv \begin{bmatrix} m_{1,1} & m_{1,2} \\ m_{2,1} & m_{2,2} \end{bmatrix}.$$

The within-host fixed points (also known as equilibria, steady states, stationary solutions) are therefore solutions of $\mathbf{f}(\mathbf{x}) = \mathbf{0}$. Because of the entrywise product, we first have to address the cases in which at least one component of $\mathbf{x}$ is zero. It is trivial that the nullity of both parasite loads constitutes a fixed point and we naturally qualify it susceptible. Now, if we set $X_2 = 0$ but $X_1 \neq 0$, $\frac{\mathrm{d}X_1}{\mathrm{d}t}$ cancels out for $X_1 = -\frac{\varrho_1}{m_{1,1}}$. We hereafter call this quantity the *s*tationary parasite *l*oad in *s*ingle infection 1 (SLS 1) and denote it by $x_{\mathbf{1},1}$ (note that the bold first label stands for the host class – see below section 4.c.1 – and the second for the parasite type). Likewise, the SLS 2 $X_2 = -\frac{\varrho_2}{m_{2,2}} =: x_{\mathbf{2},2}$ cancels $\frac{\mathrm{d}X_2}{\mathrm{d}t}$ when $X_1 = 0$. These two fixed points thus correspond to the single infection by each parasite type.

Finally, considering non-zero values of X_1 and X_2 brings us to solve $\boldsymbol{\varrho} + \mathbf{M}\mathbf{x} = \mathbf{0}$. This linear system has a unique solution if and only if $\mathbf{M}$ is non-singular, that is $\det\mathbf{M} = m_{1,1}m_{2,2} - m_{1,2}m_{2,1} \neq 0$. But since the subset in which $m_{1,1}m_{2,2} = m_{1,2}m_{2,1}$ is of measure zero in the parameter space, it is biologically irrelevant and so not addressed here. The double infection fixed point it thus given by $\mathbf{x} = -\mathbf{M}^{-1}\boldsymbol{\varrho}$ the entries of which are of the form

$$x_{\mathbf{3},i} := \frac{m_{i,k}\varrho_k - m_{k,k}\varrho_i}{m_{1,1}m_{2,2} - m_{1,2}m_{2,1}} =: \frac{b_i}{\det\mathbf{M}},$$

with $i = 1,2, k = 2,1$ and b_i a further useful shorthand for $m_{i,k}\varrho_k - m_{k,k}\varrho_i$.

System (4.b.5) thus possesses four fixed points, the terminology, the notation and the values of which are gathered in Table 4.b.1.

fixed point	notation	stationary parasite load	
		type 1	type 2
susceptible	$\mathbf{0}$	0	0
single infection 1	$\widehat{\mathbf{x}}_{\mathbf{1}}$	$-\frac{\varrho_1}{m_{1,1}} =: x_{\mathbf{1},1}$	0
single infection 2	$\widehat{\mathbf{x}}_{\mathbf{2}}$	0	$-\frac{\varrho_2}{m_{2,2}} =: x_{\mathbf{2},2}$
double infection	$\widehat{\mathbf{x}}_{\mathbf{3}}$	$\frac{b_1}{\det\mathbf{M}} =: x_{\mathbf{3},1}$	$\frac{b_2}{\det\mathbf{M}} =: x_{\mathbf{3},2}$

Table 4.b.1. – The four within-host dynamics fixed points.

4.b.3. Stability analysis and growth attractors

Apart from parameter set regions of measure zero which we do not consider, system (4.b.5) either converges to one of the fixed points listed above (Table 4.b.1), either explodes (see appendix D of Sofonea *et al.* (2017b)) (note the planar Lotka-Volterra system shows no isolated periodic orbit (Hofbauer & Sigmund, 1998)). We therefore address here the local asymptotic stability of fixed points (see Wiggins (2003) for definitions).

It is nonetheless worth noticing that the long-term behavior of system (4.b.5) depends on the initially inoculated parasite types. Indeed, if only parasite 1 has been inoculated

into the host, then the dynamics are restricted to the line $\mathcal{X}_{\mathbf{1}} \coloneqq \mathbb{R}_+ \times \{0\}$ which we call the single inoculation space 1, and therefore cannot converge towards other fixed points than the susceptible one, $\mathbf{0}$, and the single infection 1 one, $\widehat{\mathbf{x}}_{\mathbf{1}}$. The same holds for parasite type 2 with respect to $\mathcal{X}_{\mathbf{2}} \coloneqq \{0\} \times \mathbb{R}_+$, that only contains $\mathbf{0}$ and $\widehat{\mathbf{x}}_{\mathbf{2}}$. Obviously, the doubly infection fixed point $\widehat{\mathbf{x}}_{\mathbf{3}}$ can be reached only if both parasite types are inoculated, then the dynamics take place in the double inoculation space $\mathcal{X}_{\mathbf{3}} \coloneqq \mathbb{R}_+^2$ (which, as well as $\mathcal{X}_{\boldsymbol{i}}, \boldsymbol{i} = \mathbf{1}, \mathbf{2}$, is positively invariant (Hofbauer & Sigmund, 1998)).

We define the growth attractor of an inoculation space $\mathcal{X}_{\boldsymbol{h}}, \boldsymbol{h} = \mathbf{1}, \mathbf{2}, \mathbf{3}$ as the set $\mathfrak{A}(\mathcal{X}_{\boldsymbol{h}})$ of fixed points of (4.b.5) that are both feasible (i.e. non-negative) and locally asymptotically stable:

$$\mathfrak{A}(\mathcal{X}_{\boldsymbol{h}}) \coloneqq \left\{ \mathbf{x} \in \mathcal{X} : (\mathbf{f}(\mathbf{x}) = \mathbf{0}) \wedge (\mathbf{x} \geq 0) \wedge \left(\max_{\lambda \in \mathrm{Sp}(\mathbf{J}_{\mathrm{w},\boldsymbol{h}}(\mathbf{x}))} \mathrm{Re}(\lambda) < 0 \right) \right\}, \tag{4.b.7}$$

where local stability is achieved by the negativity of the greatest real part of all eigenvalues of the Jacobian matrix of system (4.b.5) evaluated at the given fixed point (Re denotes the real part, $\mathbf{J}_{\mathrm{w},\boldsymbol{h}}$ the Jacobian matrix of (4.b.5) restricted to $\mathcal{X}_{\boldsymbol{h}}$ and Sp the spectrum of a square matrix). Biologically, $\mathfrak{A}(\mathcal{X}_{\boldsymbol{h}})$ contains all stationary growth outcomes given the inoculated types (indicated by label $\boldsymbol{h}$). From the above, it is straightforward that $\mathfrak{A}(\mathcal{X}_{\boldsymbol{i}}) \subset \{\mathbf{0}, \widehat{\mathbf{x}}_{\boldsymbol{i}}\}$ and $\mathfrak{A}(\mathcal{X}_{\mathbf{3}}) \subset \{\mathbf{0}, \widehat{\mathbf{x}}_{\mathbf{1}}, \widehat{\mathbf{x}}_{\mathbf{2}}, \widehat{\mathbf{x}}_{\mathbf{3}}\}$. Notice however that the growth attractors may also be empty, thus characterizing the explosion of the parasite loads.

The feasibility conditions are trivially derived from the stationary parasite load values given in Table 4.b.1. As for the local asymptotic stability, the Jacobian matrix in single infections is simply $\mathbf{J}_{\mathrm{w},\boldsymbol{i}} \coloneqq \frac{\partial}{\partial X_i}\left(\frac{\mathrm{d}X_i}{\mathrm{d}t}\right)\Big|_{X_2=0} = \varrho_i + 2m_{i,i}X_i$ which equals ϱ_i in $\mathbf{0}$ and $-\varrho_i$ in $\widehat{\mathbf{x}}_{\boldsymbol{i}}$. In double infections, the Jacobian matrix is

$$\mathbf{J}_{\mathrm{w},\mathbf{3}} \coloneqq \frac{\partial \begin{bmatrix} \frac{\mathrm{d}X_1}{\mathrm{d}t} & \frac{\mathrm{d}X_2}{\mathrm{d}t} \end{bmatrix}}{\partial \begin{bmatrix} X_1 & X_2 \end{bmatrix}} = \begin{bmatrix} \varrho_1 + 2m_{1,1}X_1 + m_{1,2}X_2 & m_{1,2}X_1 \\ m_{2,1}X_2 & \varrho_2 + m_{2,1}X_1 + 2m_{2,2}X_2 \end{bmatrix},$$

which respectively equals

$$\mathrm{diag}\left(\varrho_1, \varrho_2\right) \text{ in } \mathbf{0}, \begin{bmatrix} -\varrho_1 & -m_{1,2}\frac{\varrho_1}{m_{1,1}} \\ 0 & -\frac{b_2}{m_{1,1}} \end{bmatrix} \text{ in } \widehat{\mathbf{x}}_{\mathbf{1}} \text{ and } \begin{bmatrix} -\frac{b_1}{m_{2,2}} & 0 \\ -m_{2,1}\frac{\varrho_2}{m_{2,2}} & -\varrho_2 \end{bmatrix} \text{ in } \widehat{\mathbf{x}}_{\mathbf{2}},$$

the spectrum of these three matrices being their diagonal terms.

Finally $\mathbf{J}_{\mathrm{w},\mathbf{3}}$ evaluated at $\widehat{\mathbf{x}}_{\mathbf{3}}$ equals

$$\frac{1}{\det \mathbf{M}} \begin{bmatrix} m_{1,1}b_1 & m_{1,2}b_1 \\ m_{2,1}b_2 & m_{2,2}b_2 \end{bmatrix},$$

which, from classical algebra, has negative real part eigenvalues if and only if $\frac{b_1 b_2}{\det \mathbf{M}} > 0$ and $c \coloneqq m_{11}b_1 + m_{2,2}b_2 < 0$.

The parameter conditions for a fixed point to be a growth attractor of a given inoculation space are therefore the combination of the feasibility conditions and the local stability conditions. These synthetic conditions are provided for each combination of fixed point and inoculation space in Table 4.b.2.

$\mathbf{x} \in \mathfrak{A}(\mathcal{X})$ iff	$\mathcal{X}_{\boldsymbol{i}}$ (single inoculation space $\boldsymbol{i}$)	$\mathcal{X}_{\mathbf{3}}$ (double inoculation space)
$\mathbf{0}$	$\varrho_i < 0$	$\left(\varrho_1 < 0\right) \wedge \left(\varrho_2 < 0\right)$
$\widehat{\mathbf{x}}_{\boldsymbol{i}}$	$\left(\varrho_i > 0\right) \wedge \left(m_{i,i} < 0\right)$	$\left(\varrho_i > 0\right) \wedge \left(m_{i,i} < 0\right) \wedge \left(b_k < 0\right)$
$\widehat{\mathbf{x}}_{\mathbf{3}}$	impossible	$(\det\mathbf{M} > 0) \wedge (b_1 > 0) \wedge (b_2 > 0) \wedge (c < 0)$

Table 4.b.2. – Growth attractor conditions of the fixed points according to the inoculation space.
This table gives the sufficient and necessary conditions on the parameters for each fixed point (in rows) to be a growth attractor of each inoculation space (in columns). For instance, the uninfected fixed point is a growth attractor (i.e. is feasible and locally stable) in the doubly inoculated space if and only if $\left(\varrho_1 < 0\right) \wedge \left(\varrho_2 < 0\right)$.

A close look to Table 4.b.2 yields the three major compatibility rules of growth attractors, namely

$$\begin{cases} \mathbf{0} \in \mathfrak{A}(\mathcal{X}_{\mathbf{3}}) \Rightarrow (\mathbf{0} \in \mathfrak{A}(\mathcal{X}_{\mathbf{1}}) \cap \mathfrak{A}(\mathcal{X}_{\mathbf{2}})) \wedge (\{\widehat{\mathbf{x}}_{\mathbf{1}}, \widehat{\mathbf{x}}_{\mathbf{2}}\} \not\supseteq \mathfrak{A}(\mathcal{X}_{\mathbf{3}})), \\ \widehat{\mathbf{x}}_{\boldsymbol{i}} \in \mathfrak{A}(\mathcal{X}_{\mathbf{3}}) \Rightarrow \widehat{\mathbf{x}}_{\boldsymbol{i}} \in \mathfrak{A}(\mathcal{X}_{\boldsymbol{i}}), \\ \widehat{\mathbf{x}}_{\mathbf{3}} \in \mathfrak{A}(\mathcal{X}_{\mathbf{3}}) \Rightarrow (\{\widehat{\mathbf{x}}_{\mathbf{1}}, \widehat{\mathbf{x}}_{\mathbf{2}}\} \not\supseteq \mathfrak{A}(\mathcal{X}_{\mathbf{3}})). \end{cases} \tag{4.b.8}$$

Actually, these rules underpin biological trivialities. The first one states that if the parasite types cannot grow together then they cannot grow alone and none outcompetes the other. The second rule states that if one parasite type can outcompete the other type then it can grow alone. The third rule states that if within-host coexistence is possible then no parasite type outcompetes the other.

Importantly, one should keep in mind that degenerated cases associated to fixed point superposition (e.g. $\mathbf{0} = \widehat{\mathbf{x}}_{\mathbf{1}}$ if $\varrho_1 = 0$) or non hyperbolic fixed points (e.g. $b_1 = 0$) are not addressed here since they occur on a set of measure zero and that they are structurally unstable, hence not biologically relevant (Goh, 1977; Barabás *et al.*, 2016).

4.c. Infection patterns

In this section we develop a suitable formalism for linking the within-host outcomes to epidemiology, essentially by introducing the notions of inoculation outcome map and infection patterns.

4.c.1. Classes and inoculation outcome map

From the host point of view, each of the fixed points previously determined correspond to a distinct chronic infection status, that is the parasite types that persists within it. In the following between-host dynamics part of the present work, we assume that hosts which share the same infection status are epidemiologically equivalent, and so we group them into classes. We thus label by $\mathbf{0},\mathbf{1},\mathbf{2}$ and $\mathbf{3}$ these host classes that respectively correspond to hosts that are uninfected, singly infected by parasite type 1, singly infected by parasite type 2 and doubly infected. Likewise, we define inoculum classes as the set of parasite types carried by an inoculum (here meant as the set of parasite propagules emitted by infected hosts): $\mathbf{1},\mathbf{2}$ and $\mathbf{3}$ respectively denote inocula containing parasite type 1 alone, parasite type 2 alone and both parasite types.

Aside from recovery that is assumed unconditioned by within-host growth (if not induced by it in the case of the below described ultrainfection pattern) and addressed in the between-host dynamics section, hosts change class owing to inoculation events. Indeed, if a host is inoculated with a new parasite type and if the fixed point associated with the initial host class is not a growth attractor in the new inoculation space, then the parasite loads depart from this fixed point and eventually either reach a new growth attractor or explode (see appendix D in Sofonea *et al.* (2017b) for a proof of such a behavior).

It is then possible to formalize host class transitions by the means of a bivariate discrete map we call inoculation outcome map. An inoculation outcome map ϕ is defined such that $\phi(\boldsymbol{h},\boldsymbol{q})$ is the host class outcome of the inoculation challenge of a class $\boldsymbol{h}$ host by a class $\boldsymbol{q}$ inoculum. But not all parameter sets allow to consider all host classes and all inoculum classes – the corresponding fixed point may not be a growth attractor – then some values of ϕ are undefined and denoted by $\emptyset$ hereafter. The inoculation map is thus a partial map on $\{\mathbf{0},\mathbf{1},\mathbf{2},\mathbf{3}\}\times\{\mathbf{1},\mathbf{2},\mathbf{3}\}$ with values on $\{\mathbf{0},\mathbf{1},\mathbf{2},\mathbf{3}\}$ (i.e. it allows, but not necessarily, some domain elements to have no assigned image).

Although their domain comprises twelve elements, the relevant information of inoculation maps is reducible to only five key values. Indeed, if one reasonably assumes that, when it comes to microparasites, the inoculum size is several orders of magnitude smaller than the infection parasite load, the re-inoculation of an already infecting type should not affect the within-host outcome: thus $\phi(\boldsymbol{i},\boldsymbol{i})=\boldsymbol{i}$ and $\phi(\boldsymbol{i},\mathbf{3})=\phi(\boldsymbol{i},\boldsymbol{k})$ for $\boldsymbol{i}=1,2,\boldsymbol{k}=2,1$ on one hand, and $\phi(\mathbf{3},\boldsymbol{q})=\mathbf{3}$ for $\boldsymbol{q}=\mathbf{1},\mathbf{2},\mathbf{3}$ on the other hand. The five key values of ϕ are therefore $\phi(\mathbf{0},\mathbf{1}),\phi(\mathbf{0},\mathbf{2}),\phi(\mathbf{0},\mathbf{3}),\phi(\mathbf{1},\mathbf{2})$ and $\phi(\mathbf{2},\mathbf{1})$.

4.c.2. Linking inoculation outcome map to growth attractors

Although inoculation outcome maps can be abstractly conceived *per se* (see appendix A in Sofonea *et al.* (2017b)), we here apply this formalism to the long term dynamics of model (4.b.5), which is the first step of nesting within-host into between-host dynamics. To do so, we associate to each key value of ϕ the growth attractor configuration required for the inoculation challenge to end as specified. The translation of the inoculation map into growth attractor terms is essentially based on the instability of the fixed point associated to the initial host class (first argument of ϕ) and the feasibility and stability of the

host outcome class (value of ϕ). However, one should remember that rules (4.b.8) apply and that ϕ not being defined for a given couple (it then values $\emptyset$) is conditioned to the whole epidemiological system inability to generate either the host or the inoculum class. The resulting configurations are given in Table 4.c.1.

$\phi(\boldsymbol{h},\boldsymbol{j})$ $=\boldsymbol{h}'$ iff	$\phi(\mathbf{0},\boldsymbol{i})$	$\phi(\mathbf{0},\mathbf{3})$	$\phi(\boldsymbol{i},\boldsymbol{k})$
$\emptyset$	$(\widehat{\mathbf{x}}_{\boldsymbol{i}} \notin \mathfrak{A}(\mathcal{X}_{\boldsymbol{i}})) \wedge (\widehat{\mathbf{x}}_{\mathbf{3}} \notin \mathfrak{A}(\mathcal{X}_{\mathbf{3}}))$	$\widehat{\mathbf{x}}_{\mathbf{3}} \notin \mathfrak{A}(\mathcal{X}_{\mathbf{3}})$	$(\widehat{\mathbf{x}}_{\boldsymbol{i}} \notin \mathfrak{A}(\mathcal{X}_{\boldsymbol{i}})) \vee ((\widehat{\mathbf{x}}_{\boldsymbol{k}} \notin \mathfrak{A}(\mathcal{X}_{\mathbf{3}})) \wedge (\widehat{\mathbf{x}}_{\mathbf{3}} \notin \mathfrak{A}(\mathcal{X}_{\mathbf{3}})))$
$\mathbf{0}$	$(\widehat{\mathbf{x}}_{\boldsymbol{i}} \notin \mathfrak{A}(\mathcal{X}_{\boldsymbol{i}})) \wedge (\widehat{\mathbf{x}}_{\mathbf{3}} \in \mathfrak{A}(\mathcal{X}_{\mathbf{3}}))$	impossible	$(\mathfrak{A}(\mathcal{X}_{\mathbf{3}}) = \emptyset) \wedge (\widehat{\mathbf{x}}_{\boldsymbol{i}} \in \mathfrak{A}(\mathcal{X}_{\boldsymbol{i}})) \wedge (\widehat{\mathbf{x}}_{\boldsymbol{k}} \in \mathfrak{A}(\mathcal{X}_{\boldsymbol{k}}))$
$\boldsymbol{i}$	$\widehat{\mathbf{x}}_{\boldsymbol{i}} \in \mathfrak{A}(\mathcal{X}_{\boldsymbol{i}})$	impossible	$(\widehat{\mathbf{x}}_{\boldsymbol{i}} \in \mathfrak{A}(\mathcal{X}_{\mathbf{3}})) \wedge (\widehat{\mathbf{x}}_{\boldsymbol{k}} \in \mathfrak{A}(\mathcal{X}_{\boldsymbol{k}}))$
$\boldsymbol{k}$	impossible	impossible	$(\widehat{\mathbf{x}}_{\boldsymbol{i}} \in \mathfrak{A}(\mathcal{X}_{\boldsymbol{i}})) \wedge (\widehat{\mathbf{x}}_{\boldsymbol{k}} \in \mathfrak{A}(\mathcal{X}_{\mathbf{3}}))$
$\mathbf{3}$	impossible	$\widehat{\mathbf{x}}_{\mathbf{3}} \in \mathfrak{A}(\mathcal{X}_{\mathbf{3}})$	$(\widehat{\mathbf{x}}_{\boldsymbol{i}} \in \mathfrak{A}(\mathcal{X}_{\boldsymbol{i}})) \wedge (\widehat{\mathbf{x}}_{\boldsymbol{k}} \in \mathfrak{A}(\mathcal{X}_{\boldsymbol{k}})) \wedge \widehat{\mathbf{x}}_{\mathbf{3}} \in \mathfrak{A}(\mathcal{X}_{\mathbf{3}})$

Table 4.c.1. – Growth attractor configurations and inoculation map values.
For each key host - inoculum class couple (in column), the growth attractors are characterized according to the inoculation outcome map value (in row). Notice that the "impossible" values in the first column are due to the fact that single inoculation of one type cannot lead to the infection by the other type nor to double inoculation. As for the "impossible" values in the second column – the doubly inoculated susceptible host – they are due to the fact that if they were true, then double infection could not be reached in the epidemiological system, following rules (4.b.8), and so no double inoculum class could be generated, which contradicts the premise.

4.c.3. Infection patterns and condition table

Let $\mathscr{U}$ be the parameter space of (4.b.5), $\mathscr{U} := \{(\varrho_1, \varrho_2, m_{1,1}, m_{1,2}, m_{2,1}, m_{2,2}) \in \mathbb{R}^6\}$, the generic element of which is a parameter set hereafter denoted by $\mathbf{u}$. From subsection 4.b.3, the datum of $\mathbf{u}$ fully determines the growth attractors of the three inoculation spaces. From 4.c.1, this in turn fully determines the inoculation outcome map. Hence, the parameter space $\mathscr{U}$ can be partitioned into non zero measure regions defined as the collection of parameter sets that share the same growth attractors and the same inoculation outcome map. And because the inoculation outcome map characterizes the epidemiology generated by the within-host dynamics, in terms of host classes and infection routes, these regions are called infection patterns.

For instance, let us consider all parameter sets $\mathbf{u}$ that satisfy $(\varrho_i > 0) \wedge (m_{i,i} < 0) \wedge (b_i > 0) \wedge (\det\mathbf{M} > 0) \wedge (c < 0)$ for all $i = 1,2$. It then follows from Table 4.b.2 that $\mathfrak{A}(\mathcal{X}_{\boldsymbol{i}}) = \widehat{\mathbf{x}}_{\boldsymbol{i}}, \boldsymbol{i} = 1,2$ and $\mathfrak{A}(\mathcal{X}_{\mathbf{3}}) = \widehat{\mathbf{x}}_{\mathbf{3}}$. Therefore, it follows from Table 4.c.2 that $\phi(\mathbf{0},\boldsymbol{i}) = \boldsymbol{i}, \boldsymbol{i} = \mathbf{1},\mathbf{2}$, $\phi(\mathbf{0},\mathbf{3}) = \mathbf{3}$ and $\phi(\mathbf{1},\mathbf{2}) = \phi(\mathbf{2},\mathbf{1}) = \mathbf{3}$. In other words, the algebraic conditions on $\mathbf{u}$ characterize the existence of both single infections and the double infection. All these parameter sets thus define the region of $\mathscr{U}$ in which the subsequent infection pattern is the one known as coinfection. The exhaustive exploration of all compatible combinations of algebraic conditions listed in Table 4.b.2, or, likewise, of all compatible growth attractor combinations, results in the identification of 11 infection patterns, with three pairs of "twin" patterns (i.e. they are equivalent by type label swap). These infection patterns are the same as those highlighted by the model of higher dimension investigated in Sofonea *et al.* (2017b) (as it takes explicitly into account two public goods and two spite products) and ergo use the same terminology as suggested and supported by the biological background discussed therein. Table 4.c.2 summarizes both the identification of the infection patterns and the correspondence between them, the growth attractors and the

algebraic conditions that partition the parameter space $\mathscr{U}$.

Let us denote by $\mathfrak{A}_{\text{ip}}(\mathcal{X})$, ϕ_{ip} and Cond_{ip} respectively the growth attractors (of a given inoculation space $\mathcal{X}$), the inoculation outcome map and the algebraic conditions with respect to infection pattern ip according to 4.c.2. Therefore, the region of the parameter space related to infection pattern ip can be defined under three equivalent points of view as follows:

$$\mathscr{P}_{\text{ip}} := \{\mathbf{u} = \left(\varrho_i, m_{i,j}\right)_{i,j=1,2} \in \mathbb{R}^6 : \begin{cases} & \forall (\boldsymbol{h},\boldsymbol{j}) \in \{(\mathbf{0},\mathbf{1}),(\mathbf{0},\mathbf{2}),(\mathbf{0},\mathbf{3}),(\mathbf{1},\mathbf{2}),(\mathbf{2},\mathbf{1})\}, \phi(\boldsymbol{h},\boldsymbol{j}) = \phi_{\text{ip}}(\boldsymbol{h},\boldsymbol{j}), \\ \text{or} & \forall \boldsymbol{h} \in \{\mathbf{1},\mathbf{2},\mathbf{3}\}, \mathfrak{A}(\mathcal{X}_{\boldsymbol{h}}) = \mathfrak{A}_{\text{ip}}(\mathcal{X}_{\boldsymbol{h}}), \\ \text{or} & \text{Cond}_{\text{ip}} \end{cases} \} \qquad (4.c.1)$$

growth attractors ($\mathfrak{A}_{\text{ip}}$)			inoculation outcome map (ϕ_{ip})					infection pattern
$\mathfrak{A}(\mathcal{X}_{\boldsymbol{i}})$	$\mathfrak{A}(\mathcal{X}_{\boldsymbol{k}})$	$\mathfrak{A}(\mathcal{X}_{\mathbf{3}})$	$\phi(\mathbf{0},\boldsymbol{i})$	$\phi(\mathbf{0},\boldsymbol{k})$	$\phi(\mathbf{0},\mathbf{3})$	$\phi(\boldsymbol{i},\boldsymbol{k})$	$\phi(\boldsymbol{k},\boldsymbol{i})$	
$\{\mathbf{0}\}$ or $\emptyset$	$\{\mathbf{0}\}$ or $\emptyset$	$\{\mathbf{0}\}$ or $\emptyset$ or $\{\mathbf{0},\widehat{\mathbf{x}}_3\}$	$\emptyset$	$\emptyset$	$\emptyset$	$\emptyset$	$\emptyset$	**no infection** (no)
		$\{\widehat{\mathbf{x}}_3\}$	$\mathbf{0}$	$\mathbf{0}$	$\mathbf{3}$	$\emptyset$	$\emptyset$	**ambinfection** (ab)
$\{\widehat{\mathbf{x}}_{\boldsymbol{i}}\}$		$\{\widehat{\mathbf{x}}_{\boldsymbol{i}}\}$ or $\emptyset$	$\boldsymbol{i}$	$\emptyset$	$\emptyset$	$\emptyset$	$\emptyset$	**latinfection** k (la_k)
		$\{\widehat{\mathbf{x}}_3\}$	$\boldsymbol{i}$	$\mathbf{0}$	$\mathbf{3}$	$\mathbf{3}$	$\emptyset$	**suprainfection** k (sa_k)
	$\{\widehat{\mathbf{x}}_{\boldsymbol{k}}\}$	$\emptyset$	$\boldsymbol{i}$	$\boldsymbol{k}$	$\emptyset$	$\mathbf{0}$	$\mathbf{0}$	**ultrainfection** (ut)
		$\{\widehat{\mathbf{x}}_{\boldsymbol{i}}\}$	$\boldsymbol{i}$	$\boldsymbol{k}$	$\emptyset$	$\boldsymbol{i}$	$\boldsymbol{i}$	**superinfection** i (se_i)
		$\{\widehat{\mathbf{x}}_{\mathbf{1}},\widehat{\mathbf{x}}_{\mathbf{2}}\}$	$\boldsymbol{i}$	$\boldsymbol{k}$	$\emptyset$	$\boldsymbol{i}$	$\boldsymbol{k}$	**priorinfection** (pr)
		$\{\widehat{\mathbf{x}}_3\}$	$\boldsymbol{i}$	$\boldsymbol{k}$	$\mathbf{3}$	$\mathbf{3}$	$\mathbf{3}$	**coinfection** (co)

infection pattern	parameter conditions (Cond_{ip})							
	ϱ_i	$m_{i,i}$	ϱ_k	$m_{k,k}$	b_i	b_k	$\det\mathbf{M}$	c
no infection (no)	$\neg(+,-)$		$\neg(+,-)$		$\neg(+,+,+,-)$			
ambinfection (ab)	$\neg(+,-)$		$\neg(+,-)$		$+$	$+$	$+$	$-$
latinfection k (la_k)	$+$	$-$	$\neg(+,-)$		$\neg(+,+,+,-)$			
suprainfection k (sa_k)	$+$	$-$	$\neg(+,-)$		$+$	$+$	$+$	$-$
ultrainfection (ut)	$+$	$-$	$+$	$-$	$+$	$+$	$\neg(+,-)$	
superinfection i (se_i)	$+$	$-$	$+$	$-$	$+$	-	$\top$	
priorinfection (pr)	$+$	$-$	$+$	$-$	$-$	$-$	$\top$	
coinfection (co)	$+$	$-$	$+$	$-$	$+$	$+$	$+$	$-$

Table 4.c.2. – Infection patterns and corresponding growth attractors, inoculation outcome map and parameter conditions.
The upper table establishes the exhaustive list of infection patterns starting from the compatible sets of growth attractors $\mathfrak{A}$ of the three inoculation spaces, from which results the key values inoculation outcome map ϕ. Each row is then an infection pattern, the identification and the name of which arises from the biological interpretation of its corresponding map (but see Sofonea *et al.* (2017b) for more details on infection pattern identification and terminology). Sufficient and necessary conditions on parameters for each pattern to occur are derived from the growth attractor conditions, Table 4.c.2, and are given in the lower table. $\emptyset$ stands for undefined value of the map and results from the impossibility of the epidemiological system to produce the host class and/or the inoculum class arguments of the partial map (no corresponding growth attractor). $+$ and $-$ stand for positiveness and negativeness. $\neg(\cdot)$ denotes the logical negation here meaning that the condition is satisfied for all sign combinations but the one in brackets. $\top$ denotes the logical tautology and here means that the condition is satisfied for all sign combinations. The one or two letters into brackets next to the infection pattern names are the corresponding labels that will be used henceforward.

4.d. Between-host dynamics

In this section, we first expose the generic version of the between-host dynamics and how within-host dynamics are nested into them. We then investigate the disease free and monomorphic endemic equilibria.

4.d.1. Generic dimorphic SIS model

For the sake of both biological intelligibility and mathematical tractability, we model the between-host dynamics of parasite dimorphism using the Susceptible-Infected-Susceptible (SIS) framework (Keeling & Rohani, 2008). We first leave aside the diversity of infection patterns to describe the most generic version of the model independently of the within-host parameters. The epidemiological model contains four host compartments, each being represented by its density, namely $S, I_{\mathbf{1}}, I_{\mathbf{2}}$ and $I_{\mathbf{3}}$ that vary with "host time" $\tau \in \mathbb{R}_+$. These respectively identify with host classes **0** (uninfected), **1** (singly infected by parasite type 1), **2** (*id.* for type 2) and **3** (doubly infected).

We assume parasite transmission to be horizontal and density-dependent, which is a common epidemiological setting (Keeling & Rohani, 2008). Hosts are thus born susceptible and the S compartment receives an undetermined inflow Λ (this also holds for immigrants). A given host is then exposed to inoculation by a non already infecting parasite type $\boldsymbol{i}$ at a rate called force of infection (van Baalen & Sabelis, 1995) and denoted by $B_{\boldsymbol{i}}$. The force of infection of parasite type $\boldsymbol{i}$ alone is the sum of two transmission contributions: that from the singly infected hosts $I_{\boldsymbol{i}}$ and that from the doubly infected hosts $I_{\mathbf{3}}$ and is equal to $B_{\boldsymbol{i}} \coloneqq \beta_{\boldsymbol{i},\boldsymbol{i}} I_{\boldsymbol{i}} + \beta_{\mathbf{3},\boldsymbol{i}} I_{\mathbf{3}}$, where $\beta_{\boldsymbol{h},\boldsymbol{i}}$ is the transmission rate of monomorphic class $\boldsymbol{i}$ inocula by class $\boldsymbol{h}$ hosts, $\boldsymbol{i} = \mathbf{1},\mathbf{2}, \boldsymbol{h} = \boldsymbol{i},\mathbf{3}$. Likewise, the force of infection of the two parasite types together is $B_{\mathbf{3}} \coloneqq \beta_{\mathbf{3},\mathbf{3}} I_{\mathbf{3}}$. Importantly, if a single infected host is susceptible to the other parasite type, then dimorphic inocula do contribute to the secondary infection of these hosts in addition to the monomorphic inocula containing the other type.

A natural mortality rate $\mu > 0$ affects all hosts, while each infected host class undergoes an additional mortality rate due to infection, i.e. virulence, denoted by $\alpha_{\boldsymbol{h}}, \boldsymbol{h} = \mathbf{1},\mathbf{2},\mathbf{3}$. We allow for recovery of infected hosts one parasite at a time and a class $\boldsymbol{h} = \mathbf{1},\mathbf{2},\mathbf{3}$ recovers from parasite type $i = 1,2$ it is infected with at a rate $\theta_{\boldsymbol{h},i}$. To shorten the equations, we gather these three processes (natural mortality, virulence and recovery) into one term we call elimination and quantify by the rate $\zeta_{\boldsymbol{h}} \coloneqq \mu + \alpha_{\boldsymbol{h}} + \theta_{\boldsymbol{h},1} + \theta_{\boldsymbol{h},2}$ (with the convention that $\theta_{\boldsymbol{h},i} = 0$ if class $\boldsymbol{h}$ hosts are not infected by parasite type i).

Provided that the within-host dynamics are fast enough compared to the epidemiology (see next subsection), each inoculation challenge leads to the outcome determined by the within-host parameter set. Thus, not all inoculation outcomes, and therefore not all transmission routes, are simultaneously possible. To acknowledge for the diversity of infection patterns and nevertheless present a generic formulation of the described between-host dynamics, we weight the transmission terms by the following binary factor $\Phi_{\boldsymbol{h},\boldsymbol{q},\boldsymbol{h}'} \coloneqq \left[\phi(\boldsymbol{h},\boldsymbol{q}) = \boldsymbol{h}'\right]$, which cancels the term if the inoculation of a class $\boldsymbol{h}$ host by a class $\boldsymbol{q}$ inoculum does not generate a class $\boldsymbol{h}'$ host, and equals 1 if it does. (Notice the implicit convention that statements involving undefined values of ϕ are always false.)

In the end, the between-host dynamics follows the ensuing set of ODEs, with $\boldsymbol{i} = \mathbf{1}, \mathbf{2}$,

$$\begin{cases} \frac{\mathrm{d}S}{\mathrm{d}\tau} &= \Lambda + \theta_{\mathbf{1},1} I_{\mathbf{1}} + \theta_{\mathbf{2},2} I_{\mathbf{2}} + \Phi_{\mathbf{1},\mathbf{2},\mathbf{0}} (B_{\mathbf{2}} + B_{\mathbf{3}}) I_{\mathbf{1}} + \Phi_{\mathbf{2},\mathbf{1},\mathbf{0}} (B_{\mathbf{1}} + B_{\mathbf{3}}) I_{\mathbf{2}} \\ &\quad - \big(\Phi_{\mathbf{0},\mathbf{1},\mathbf{1}} B_{\mathbf{1}} + \Phi_{\mathbf{0},\mathbf{0},\mathbf{2}} B_{\mathbf{2}} + \big(1 - \Phi_{\mathbf{0},\mathbf{3},\mathbf{0}}\big) B_{\mathbf{3}}\big) S - \mu S, \\ \frac{\mathrm{d}I_{\boldsymbol{i}}}{\mathrm{d}\tau} &= \big(\Phi_{\mathbf{0},\boldsymbol{i},\boldsymbol{i}} B_{\boldsymbol{i}} + \Phi_{\mathbf{0},\mathbf{3},\boldsymbol{i}} B_{\mathbf{3}}\big) S + \Phi_{\boldsymbol{k},\boldsymbol{i},\boldsymbol{i}} (B_{\boldsymbol{i}} + B_{\mathbf{3}}) I_{\boldsymbol{k}} + \theta_{\mathbf{3},k} I_{\mathbf{3}} \\ &\quad - \big(1 - \Phi_{\boldsymbol{i},\boldsymbol{k},\boldsymbol{i}}\big) (B_{\boldsymbol{k}} + B_{\mathbf{3}}) I_{\boldsymbol{i}} - \zeta_{\boldsymbol{i}} I_{\boldsymbol{i}}, \\ \frac{\mathrm{d}I_{\mathbf{3}}}{\mathrm{d}\tau} &= \Phi_{\mathbf{0},\mathbf{3},\mathbf{3}} B_{\mathbf{3}} S + \Phi_{\mathbf{1},\mathbf{2},\mathbf{3}} (B_{\mathbf{2}} + B_{\mathbf{3}}) I_{\mathbf{1}} + \Phi_{\mathbf{2},\mathbf{1},\mathbf{3}} (B_{\mathbf{1}} + B_{\mathbf{3}}) I_{\mathbf{2}} - \zeta_{\mathbf{3}} I_{\mathbf{3}}, \end{cases} \tag{4.d.1}$$

recalling that $B_{\boldsymbol{i}} \coloneqq \beta_{\boldsymbol{i},\boldsymbol{i}} I_{\boldsymbol{i}} + \beta_{\mathbf{3},\boldsymbol{i}} I_{\mathbf{3}}$ and $B_{\mathbf{3}} \coloneqq \beta_{\mathbf{3},\mathbf{3}} I_{\mathbf{3}}$.

4.d.2. Epidemiological rates (un)specification

Considering that, especially in the case of microparasites, parasite populations grow faster within the host than they transmit between the hosts ($t \ll \tau$), we assume a time scale separation between the two dynamical levels. This leads us to use the within-host parasite load in each host at their stationary values at any moment of the between-host dynamics, in the same way we used the steady values of the compound kinetics in equation (4.b.1).

Owing to this time scale separation, all hosts from the same compartment harbor the same constant parasite loads for each type, namely the corresponding class stationary load value. This makes all hosts belonging to the same compartment epidemiologically equivalent. Yet, the parasite loads of a host instantaneously change to those of another compartment as soon it undergoes a new infection.

Importantly, within-host dynamics do not only shape the transmission routes in (4.d.1) by canceling the terms that do not match with the subsequent infection pattern, but also affect all epidemiological rates but natural mortality and demography. We indeed assume the parasite load of an infected host directly impacts its transmission ability, its life expectancy and its recovery potential. Formally, we allow the epidemiological rates $\beta_{\boldsymbol{h},\boldsymbol{q}}, \alpha_{\boldsymbol{h}}, \theta_{\boldsymbol{h},i}$ (hence $\zeta_{\boldsymbol{h}}$ as well) to be smooth functions of $\widehat{\mathbf{x}}_{\boldsymbol{h}}$. Importantly, we do not specify the dependence between these rates and the stationary parasite loads, provided that they are respectively non-decreasing, increasing and non-decreasing functions of the total parasite load. In particular, we do not specify any particular shape such as satiation, which would characterize a trade-off (Anderson & May, 1981).

As for demography, the inflow Λ is left undetermined. It can be a positive constant as well as a non-negative function of all host densities (e.g. capturing host density-dependence or balancing deaths such that the host population is stationary). A cost of this generality in terms of host demography is that it is not possible to express the non trivial fixed points of (4.d.1) as closed form stationary solutions.

Notice that the notations $\beta_{\boldsymbol{h},\boldsymbol{q}}(\widehat{\mathbf{x}}_{\boldsymbol{h}}), \alpha_{\boldsymbol{h}}(\widehat{\mathbf{x}}_{\boldsymbol{h}}), \theta_{\boldsymbol{h},i}(\widehat{\mathbf{x}}_{\boldsymbol{h}}), \zeta_{\boldsymbol{h}}(\widehat{\mathbf{x}}_{\boldsymbol{h}}), \Lambda(S, I_{\mathbf{1}}, I_{\mathbf{2}}, I_{\mathbf{3}})$ are hereafter usually implied.

4.d.3. Linking virulence to parasite load

Let x be the stationary parasite load in single infection (SLS) of a given parasite type and $\alpha : x \mapsto \alpha(x)$ a function that maps its SLS to its virulence. If virulence is directly or indirectly due to host exploitation by the parasite, then it is assumed that α is an increasing differentiable function of SLS ($\frac{\mathrm{d}\alpha}{\mathrm{d}x} > 0$) over a relevant range.

Let x' be the other parasite type's SLS and α' its proper virulence function. If the infection physiopathology of the two parasite types are similar, then we can consider that

$\alpha'(x) = \alpha(x)$ and $\frac{\mathrm{d}\alpha'}{\mathrm{d}x} = q\frac{\mathrm{d}\alpha}{\mathrm{d}x}$, where $q > 0$. The first equality follows from the fact that it is unlikely that virulence would vary drastically without any variation in SLS. The second equality models the change in virulence function as a change of slope, which is a first-order approximation given the previous equality – the positivity of the factor follows from the assumption that virulence should increase with parasite load. Therefore, we have

$$\alpha'\left(x'\right) = \alpha'\left(x + \left(x' - x\right)\right) \approx \alpha'(x) + \left(x' - x\right)\frac{\mathrm{d}\alpha'}{\mathrm{d}x}(x) = \alpha(x) + \left(x' - x\right)q\frac{\mathrm{d}\alpha}{\mathrm{d}x}(x),$$

hence $\alpha'\left(x'\right) > \alpha(x) \iff \left(x' - x\right)q\frac{\mathrm{d}\alpha}{\mathrm{d}x}(x) > 0 \iff x' > x$ since both q and $\frac{\mathrm{d}\alpha}{\mathrm{d}x}(x)$ are positive.

To conclude, under our assumptions, virulence and parasite load can be indifferently considered as the same biological quantity for which the hierarchies are preserved.

Note that in double infections, hosts would experience an overall virulence calculated as the sum of the virulence of both types evaluated at their respective stationary parasite loads in double infection. But this is not used to define parasite virulence since double infected hosts may not exist and virulence in double infections does not only reflect the traits of each parasite type but is also modulated by the interactions with the other type.

4.d.4. Disease free equilibrium

If the host population is not exposed to any parasite, then system (4.d.1) reduces to the simple ODE $\frac{\mathrm{d}S}{\mathrm{d}\tau} = \Lambda - \mu S$, the fixed points of which are solutions of $\Lambda(S) = \mu S$. We assume that this equation has a unique positive solution $\overset{\circ}{S} > 0$ called the disease free equilibrium (DFE) of the host population (van den Driessche & Watmough, 2002).

The DFE is the host demographical endpoint only if it is stable while $S = 0$ is unstable. The between-host Jacobian matrix restricted to susceptible hosts being $\mathbf{J}_{\mathrm{b},(\mathbf{0})} \coloneqq \frac{\partial}{\partial S}\left(\frac{\mathrm{d}S}{\mathrm{d}\tau}\right) = \frac{\partial\Lambda}{\partial S} - \mu$, this is equivalent to

$$\left(\frac{\partial\Lambda}{\partial S}(0,0,0,0) > \mu\right) \wedge \left(\frac{\partial\Lambda}{\partial S}\left(\overset{\circ}{S},0,0,0\right) < \mu\right), \tag{4.d.2}$$

which is hereafter assumed.

4.d.5. Monomorphic endemic equilibrium

Let us now consider that a demographically stable host population, i.e. being at the DFE, is challenged with one parasite type. Let it be parasite type 1 without loss of generality. System (4.d.1) thus reduces to the monomorphic SIS model

$$\begin{cases} \frac{\mathrm{d}S}{\mathrm{d}\tau} &= \Lambda + \theta_{\mathbf{1},1}I_{\mathbf{1}} - \Phi_{\mathbf{0},\mathbf{1},1}\beta_{\mathbf{1},1}I_{\mathbf{1}}S - \mu S, \\ \frac{\mathrm{d}I_{\mathbf{1}}}{\mathrm{d}\tau} &= \Phi_{\mathbf{0},\mathbf{1},1}\beta_{\mathbf{1},1}I_{\mathbf{1}}S - \zeta_{\mathbf{1}}I_{\mathbf{1}}. \end{cases} \tag{4.d.3}$$

This parasite spreads into the host population if and only if the DFE $\left(\overset{\circ}{S},0\right)$ is unstable (Diekmann *et al.*, 1990). This requires to calculate the monomorphic between-host Jacobian matrix

$$\mathbf{J}_{\mathrm{b},(\mathbf{0},\mathbf{1})} = \begin{bmatrix} \frac{\partial\Lambda}{\partial S} - \Phi_{\mathbf{0},\mathbf{1},1}\beta_{\mathbf{1},1}I_{\mathbf{1}} - \mu & \frac{\partial\Lambda}{\partial I_{\mathbf{1}}} + \theta_{\mathbf{1},1} - \Phi_{\mathbf{0},\mathbf{1},1}\beta_{\mathbf{1},1}S \\ \Phi_{\mathbf{0},\mathbf{1},1}\beta_{\mathbf{1},1}I_{\mathbf{1}} & \Phi_{\mathbf{0},\mathbf{1},1}\beta_{\mathbf{1},1}S - \zeta_{\mathbf{1}} \end{bmatrix},$$

to evaluate it at the DFE, that is

$$\mathbf{J}_{\mathrm{b},(\mathbf{0},\mathbf{1})}\left(\mathring{S},0\right)=\begin{bmatrix}\frac{\partial\Lambda}{\partial S}\left(\mathring{S},0,0,0\right)-\mu & \frac{\partial\Lambda}{\partial I_{\mathbf{1}}}\left(\mathring{S},0,0,0\right)+\theta_{\mathbf{1},1}-\Phi_{\mathbf{0},\mathbf{1},\mathbf{1}}\beta_{\mathbf{1},\mathbf{1}}\mathring{S}\\ 0 & \Phi_{\mathbf{0},\mathbf{1},\mathbf{1}}\beta_{\mathbf{1},\mathbf{1}}\mathring{S}-\zeta_{\mathbf{1}}\end{bmatrix},$$

and condition at least one of its eigenvalues to have its real part positive. From the previous subsection, it follows that this condition is equivalent to

$$\frac{\Phi_{\mathbf{0},\mathbf{1},\mathbf{1}}\beta_{\mathbf{1},\mathbf{1}}\mathring{S}}{\zeta_{\mathbf{1}}}>1, \tag{4.d.4}$$

which defines the basic reproduction number of parasite type 1 (Diekmann *et al.*, 1990). It is obvious that this condition constrains the within-host traits of parasite type 1 to be such that $\Phi_{\mathbf{0},\mathbf{1},\mathbf{1}}\neq 0$ i.e. $\phi(\mathbf{0},\mathbf{1})=\mathbf{1}$. From Table 4.c.2, this happens if and only if

$$\left(\rho_1>0\right)\wedge\left(m_{1,1}<0\right), \tag{4.d.5}$$

which corresponds to the parasite ability to chronically infect a host alone. In the following, we only consider parasites that satisfy these conditions and let $\Phi_{\mathbf{0},\mathbf{1},\mathbf{1}}=1$.

Once the parasite spreads, the epidemiological system may converge towards and even reach a monomorphic endemic equilibrium 1 (MEE1) denoted by $\left(\widetilde{S},\widetilde{I_{\mathbf{1}}}\right)$ provided that it is feasible and stable. Canceling the time derivative with respect to the singly infected density in (4.d.3) results in the key equality

$$\beta_{\mathbf{1},\mathbf{1}}\widetilde{S}=\zeta_{\mathbf{1}}, \tag{4.d.6}$$

which also characterizes the stationary density of susceptible hosts at the MEE1.

It is however not possible to find the closed form of $\widetilde{I_{\mathbf{1}}}$ since Λ is undetermined. We can only acknowledge that it is the positive solution, assumed unique, of $\Lambda\left(\frac{\beta_{\mathbf{1},\mathbf{1}}}{\zeta_{\mathbf{1}}},\widetilde{I_{\mathbf{1}}},0,0\right)-\left(\mu+\alpha_{\mathbf{1}}\right)\widetilde{I_{\mathbf{1}}}-\mu\frac{\beta_{\mathbf{1},\mathbf{1}}}{\zeta_{\mathbf{1}}}=0$.

It is moreover possible to show that, if feasible, the MEE1 is likely to be stable since the monomorphic between-host Jacobian matrix $\mathbf{J}_{\mathrm{b},(\mathbf{0},\mathbf{1})}$ evaluated at the MEE1 is

$$\mathbf{J}_{\mathrm{b},(\mathbf{0},\mathbf{1})}\left(\widetilde{S},\widetilde{I_{\mathbf{1}}}\right)=\begin{bmatrix}\frac{\partial\Lambda}{\partial S}\left(\widetilde{S},\widetilde{I_{\mathbf{1}}},0,0\right)-\beta_{\mathbf{1},\mathbf{1}}\widetilde{I_{\mathbf{1}}}-\mu & \frac{\partial\Lambda}{\partial I_{\mathbf{1}}}\left(\widetilde{S},\widetilde{I_{\mathbf{1}}},0,0\right)-\mu-\alpha_{\mathbf{1}}\\ \beta_{\mathbf{1},\mathbf{1}}\widetilde{I_{\mathbf{1}}} & 0\end{bmatrix},$$

the eigenvalues of which are, if real,

$$\frac{1}{2}\left(\frac{\partial\Lambda}{\partial S}\left(\widetilde{S},\widetilde{I_{\mathbf{1}}},0,0\right)-\beta_{\mathbf{1},\mathbf{1}}\widetilde{I_{\mathbf{1}}}-\mu\right.$$
$$\left.\pm\sqrt{\left(\frac{\partial\Lambda}{\partial S}\left(\widetilde{S},\widetilde{I_{\mathbf{1}}},0,0\right)-\beta_{\mathbf{1},\mathbf{1}}\widetilde{I_{\mathbf{1}}}-\mu\right)^2+4\left(\frac{\partial\Lambda}{\partial I_{\mathbf{1}}}\left(\widetilde{S},\widetilde{I_{\mathbf{1}}},0,0\right)-\mu-\alpha_{\mathbf{1}}\right)\beta_{\mathbf{1},\mathbf{1}}\widetilde{I_{\mathbf{1}}}}\right).$$

Now, if the values $\frac{\partial\Lambda}{\partial S}\left(\widetilde{S},\widetilde{I_{\mathbf{1}}},0,0\right)$ and $\frac{\partial\Lambda}{\partial I_{\mathbf{1}}}\left(\widetilde{S},\widetilde{I_{\mathbf{1}}},0,0\right)$ are not too large compared to $\frac{\partial\Lambda}{\partial S}\left(\mathring{S},0,0,0\right)$, which is reasonable if the parasite does not drive the host population close to extinction, then given inequality (4.d.2), $\frac{\partial\Lambda}{\partial S}\left(\widetilde{S},\widetilde{I_{\mathbf{1}}},0,0\right)<\mu+\beta_{\mathbf{1},\mathbf{1}}\widetilde{I_{\mathbf{1}}}$ and $\frac{\partial\Lambda}{\partial I_{\mathbf{1}}}\left(\widetilde{S},\widetilde{I_{\mathbf{1}}},0,0\right)<\mu+\alpha_{\mathbf{1}}$ is satisfied for a large range of Λ functions we hereafter assume. It is then straightforward that both eigenvalues are negative. Note that the same result holds if the eigen-

values have an imaginary part.

4.d.6. Second type survival

For the sake of simplicity, let us here assume that parasite type 1 is now established in the host population hence called the "resident" (but note this assumption will be later slightly relaxed). The host densities are those of the MEE1, which implies $\left(\varrho_1, -m_{1,1}\right) \succ 0$ and $\widetilde{S} = \frac{\zeta_1}{\beta_{1,1}}$ (relations(4.d.5) and (4.d.6)).

If a second parasite type is introduced in the host population, its prevalence, which is initially very low, increases if and only if the MEE1 is unstable in the full dimorphic system (4.d.1) (VAN DEN DRIESSCHE & WATMOUGH, 2002). Because the MEE1 is assumed to be unique and because the DFE is unstable in presence of the first parasite type 1 (see previous subsection), the instability of the MEE1 in the dimorphic system is equivalent to the second parasite type surviving, may it remain alone (in that case the dimorphism is unstable and the system may converge towards a MEE2) or co-circulate with parasite type 1 (the dimorphism is stable at the host population level even if within-host coexistence is impossible).

Following the next-generation method (VAN DEN DRIESSCHE & WATMOUGH, 2002; HURFORD *et al.*, 2010), this condition is related to the sign of the invasion fitness W, which is the greatest real part of the eigenvalues of the Jacobian matrix of the system evaluated at the MEE1, denoted by $\mathbf{J}_{\mathrm{b},(\mathbf{0},\mathbf{1},\mathbf{2},\mathbf{3})}\left(\widetilde{S}, \widetilde{I_1}, 0, 0\right)$. A close look at system (4.d.1) shows that for $\boldsymbol{a} = \mathbf{2},\mathbf{3}$, $\frac{\partial}{\partial I_{\boldsymbol{a}}}\left(\frac{\mathrm{d}S}{\mathrm{d}\tau}\right) = \frac{\partial}{\partial I_{\boldsymbol{a}}}\left(\frac{\mathrm{d}I_1}{\mathrm{d}\tau}\right) = 0$ at the MEE1. Consequently this matrix is a lower block triangular matrix of the form

$$\mathbf{J}_{\mathrm{b},(\mathbf{0},\mathbf{1},\mathbf{2},\mathbf{3})}\left(\widetilde{S}, \widetilde{I_1}, 0, 0\right) = \begin{bmatrix} \mathbf{J}_{\mathrm{b},(\mathbf{0},\mathbf{1})}\left(\widetilde{S}, \widetilde{I_1}\right) & * \\ \mathbf{0}_{2,2} & \mathbf{J}_{\mathrm{b},(\mathbf{2},\mathbf{3})}\left(\widetilde{S}, \widetilde{I_1}, 0, 0\right) \end{bmatrix},$$

the eigenvalues of which are those of the two diagonal 2×2 matrices. Since the MEE1 is assumed to be reached and stable in the absence of parasite type 2, all its eigenvalues have negative real parts (see previous subsection). The invasibility conditions thus only concern the matrix $\mathbf{J}_{\mathrm{b},(\mathbf{2},\mathbf{3})} := \partial\begin{bmatrix}\frac{\mathrm{d}I_2}{\mathrm{d}\tau} & \frac{\mathrm{d}I_3}{\mathrm{d}\tau}\end{bmatrix}/\partial\begin{bmatrix}I_2 & I_3\end{bmatrix}$ which is the Jacobian submatrix related to the compartments of hosts infected by the second parasite type,

$$\mathbf{J}_{\mathrm{b},(\mathbf{2},\mathbf{3})} = \begin{bmatrix} \left(\Phi_{\mathbf{0},\mathbf{2},\mathbf{2}}S + \Phi_{\mathbf{1},\mathbf{2},\mathbf{2}}I_1\right)\beta_{\mathbf{2},\mathbf{2}} & \left(\Phi_{\mathbf{0},\mathbf{2},\mathbf{2}}\beta_{\mathbf{3},\mathbf{2}} + \Phi_{\mathbf{0},\mathbf{3},\mathbf{2}}\beta_{\mathbf{3},\mathbf{3}}\right)S + \Phi_{\mathbf{1},\mathbf{2},\mathbf{2}}\left(\beta_{\mathbf{3},\mathbf{2}} + \beta_{\mathbf{3},\mathbf{3}}\right)I_1 \\ -\left(1 - \Phi_{\mathbf{2},\mathbf{1},\mathbf{2}}\right)(B_1 + B_3) - \zeta_{\mathbf{2}} & +\theta_{\mathbf{3},1} - \left(1 - \Phi_{\mathbf{2},\mathbf{1},\mathbf{2}}\right)\left(\beta_{\mathbf{3},\mathbf{1}} + \beta_{\mathbf{3},\mathbf{3}}\right)I_2 \\ \Phi_{\mathbf{1},\mathbf{2},\mathbf{3}}\beta_{\mathbf{2},\mathbf{2}}I_1 + \Phi_{\mathbf{2},\mathbf{1},\mathbf{3}}(B_1 + B_3) & \Phi_{\mathbf{0},\mathbf{3},\mathbf{3}}\beta_{\mathbf{3},\mathbf{3}}S + \Phi_{\mathbf{1},\mathbf{2},\mathbf{3}}\left(\beta_{\mathbf{3},\mathbf{2}} + \beta_{\mathbf{3},\mathbf{3}}\right)I_1 \\ & +\Phi_{\mathbf{2},\mathbf{1},\mathbf{3}}\left(\beta_{\mathbf{3},\mathbf{1}} + \beta_{\mathbf{3},\mathbf{3}}\right)I_2 - \zeta_{\mathbf{3}} \end{bmatrix},$$

evaluated at $\left(\widetilde{S}, \widetilde{I_1}, 0, 0\right)$, which gives a matrix we denote $\mathbf{J}_{\mathrm{inv}}$ from now on,

$$\mathbf{J}_{\mathrm{inv}} = \begin{bmatrix} \left(\Phi_{\mathbf{0},\mathbf{2},\mathbf{2}}\widetilde{S} + \Phi_{\mathbf{1},\mathbf{2},\mathbf{2}}\widetilde{I_1}\right)\beta_{\mathbf{2},\mathbf{2}} & \left(\Phi_{\mathbf{0},\mathbf{2},\mathbf{2}}\beta_{\mathbf{3},\mathbf{2}} + \Phi_{\mathbf{0},\mathbf{3},\mathbf{2}}\beta_{\mathbf{3},\mathbf{3}}\right)\widetilde{S} \\ -\left(1 - \Phi_{\mathbf{2},\mathbf{1},\mathbf{2}}\right)\beta_{1,1}\widetilde{I_1} - \zeta_{\mathbf{2}} & +\Phi_{\mathbf{1},\mathbf{2},\mathbf{2}}\left(\beta_{\mathbf{3},\mathbf{2}} + \beta_{\mathbf{3},\mathbf{3}}\right)\widetilde{I_1} + \theta_{\mathbf{3},1} \\ \left(\Phi_{\mathbf{1},\mathbf{2},\mathbf{3}}\beta_{\mathbf{2},\mathbf{2}} + \Phi_{\mathbf{2},\mathbf{1},\mathbf{3}}\beta_{1,1}\right)\widetilde{I_1} & \Phi_{\mathbf{0},\mathbf{3},\mathbf{3}}\beta_{\mathbf{3},\mathbf{3}}\widetilde{S} + \Phi_{\mathbf{1},\mathbf{2},\mathbf{3}}\left(\beta_{\mathbf{3},\mathbf{2}} + \beta_{\mathbf{3},\mathbf{3}}\right)\widetilde{I_1} - \zeta_{\mathbf{3}} \end{bmatrix}. \tag{4.d.7}$$

However, it is not worth at this point to provide the closed form expression of the eigenvalues of this matrix, since the entries will simplify along with the infection pattern determination. We nevertheless emphasize on the main result of this subsection: the second type survives in the host population at the monormophic endemic equilibrium if and only if

$$W := \max\{\mathrm{Re}(\lambda), \lambda \in \mathrm{Sp}(\mathbf{J}_{\mathrm{inv}})\} > 0. \tag{4.d.8}$$

In addition, it is reasonable to admit that, following the course of parasite 1 epidemic towards the MEE1, S globally (i.e. on the long run) decreases from $\overset{\circ}{S}$ to $\widetilde{S}$, while I_1 globally increases from 0 to $\widetilde{I_1}$. Therefore, there exists a neighborhood of epidemiological states (S, I_1) close to the MEE1 such that (4.d.8) is satisfied under the same conditions as the MEE1.

4.e. Mutational setting

From now on, we consider that parasite type 2 is a mutant of the resident parasite type 1. Following the previous section, we seek an expression for the invasion fitness W of the second parasite type in a host population endemically infected by the resident parasite type 1. This expression should be a function of within-host parasite traits. The generality of the epidemiological model (4.d.1) prevents us from finding such a closed form expression for all couples of parasite types (this is because the functions $\beta_{\boldsymbol{h},\boldsymbol{q}}(\widehat{\mathbf{x}}_{\boldsymbol{h}}), \theta_{\boldsymbol{h},i}(\widehat{\mathbf{x}}_{\boldsymbol{h}}), \zeta_{\boldsymbol{h}}(\widehat{\mathbf{x}}_{\boldsymbol{h}}), \Lambda(S, I_{\mathbf{1}}, I_{\mathbf{2}}, I_{\mathbf{3}})$ are left undetermined).

Analytical progress is however possible by assuming that the second parasite type is phenotypically similar to the resident. This covers the cases where the second parasite type is a close mutant of the resident, i.e. when the mutational effects on growth traits are small (this is later justified by the fact that large mutations are more likely to be deleterious, see later subsection 4.f.3 and main text 4.3.2). From now on we will thus call parasite type 2 the "mutant" and the resident its "ancestor".

4.e.1. Mutation formalisation

We know from the study of the MEE1 that the resident traits are such that it can infect alone: its intrinsic growth rate is positive, $\varrho_1 > 0$, and its self interaction effect is negative, $m_{1,1} < 0$ (inequalities (4.d.5)). Since these two quantities do not have the same unit (the first is a rate, while the second is a rate per load), we can set from now on $\varrho_1 = 1$ and $m_{1,1} = -1$, without loss of generality.

Intuitively, the mutant traits ϱ_2 and $m_{2,2}$ have values that are close to ϱ_1 and $m_{1,1}$. However, to fully determine the dimorphic within-host dynamics, we also need the values of the cross interaction effects, $m_{1,2}$ and $m_{2,1}$. These two shared traits involve the mutant's physiology and ecology. Indeed, from the mutant perspective, $m_{1,2}$ is the ability to interfere with the ancestor's growth (e.g. the quality of the public goods it produces) while $m_{2,1}$ is the ability to take advantage of or to escape from the ancestor's activity (e.g. counter the effect of spite molecules). Consequently, one can see $m_{1,2}$ and $m_{2,1}$ as the between-type modifications of the initial within-type interaction effect $m_{1,1}$ hence we hereafter they share the same order of magnitude as the self interaction effects.

Let us now decompose the four trait values that emanate from the phenotypic mutation as the sum of the ancestor trait value from which the mutant derives (either $\varrho_1 = +1$ or $m_{1,1} = -1$) and a random part that captures the mutation. The first term is constant and, unless otherwise stated, dominates the second. With $(i,j) = (1,2),(2,1),(2,2)$ (hereafter always implied), this can be written as

$$\begin{cases} \varrho_2 & := +1 + \varepsilon\sigma, \\ m_{i,j} & := -1 + \nu_{i,j}\sigma, \end{cases} \tag{4.e.1}$$

where $\varepsilon, \nu_{1,2}, \nu_{2,1}$ and $\nu_{2,2}$ are the real mutational random variables (MRVs, specified below) and $\sigma \geq 0$ the scaling factor that captures the greatest standard deviation among mutational deviations and is from now on called the mutational effect. The mutational effect is hereafter assumed small, $\sigma \ll 1$ (except in numerical simulations of Figure 4.3.3 that investigate large mutations) while $\sigma = 0$ corresponds to the case where a mutation does not modify the phenotype.

Another scaling factor, $\kappa \geq 0$, implicitly lies in the standard deviation of each MRV. Indeed, we assume that the standard deviation of ε on one hand, and the standard deviations of $\nu_{1,2}, \nu_{2,1}$ and $\nu_{2,2}$ on the other hand, are proportional to $\min(1,\kappa)$ and $\min\left(1,\kappa^{-1}\right)$ respectively. Hence, κ scales the magnitude ratio of the mutations affecting the intrinsic

growth rate with respect to those affecting the interactions traits. Modulating κ allows us to consider the case where mutations differently modify these two trait categories (see the further subsection 4.e.3 about mutational scenarios).

Since there is no acknowledged universal pattern of mutational effects over parasite demographics traits, we further examine three kinds of probability laws for the MRVs that we call the mutational distributions. And as mutations only slightly affect the within-host growth trait values, their distribution on the increasing side, in terms of trait values, are not likely to differ much from their distribution on the decreasing side. Hence, we assume the underlying probability density function (PDF) to be symmetric with respect to zero. Moreover, in order to be compatible with the small mutational effect assumption, most of the mass should be concentrated between -1 and 1.

4.e.2. Mutational distributions

4.e.2.1. Fixed step mutational distribution

The fixed step mutational distribution is characterized by the fact that its support is discrete which allows us to easily derive qualitative results in spite of biological realism.

Under the fixed step mutational distribution, the MRVs are assumed to satisfy

$$\begin{cases} \varepsilon & = \min(1,\kappa) \sum_{q=0}^{Q} \varepsilon_q \sigma^q, \\ \nu_{i,j} & = \min\left(1,\kappa^{-1}\right) \sum_{q=0}^{Q} \nu_{i,j,q} \sigma^q, \end{cases} \tag{4.e.2}$$

where Q is a potentially large integer. For all $q \in \{0,\dots,Q\}$, ε_q and $\nu_{i,j,q}$ are identically distributed discrete random variables that equal either $+1$ or -1 each with probability $1/2$ (this is known as the Rademacher distribution).

As σ is considered small, (4.e.2) can be rewritten as

$$\begin{cases} \varepsilon & = \min(1,\kappa)\varepsilon_0 + o(\sigma), \\ \nu_{i,j} & = \min\left(1,\kappa^{-1}\right)\nu_{i,j,0} + o(\sigma), \end{cases} \tag{4.e.3}$$

where the Landau's little-o notation $o(\sigma)$ denotes any function which divided by σ tends to 0 when σ goes to 0, *i.e.* $f(\sigma) = o(\sigma) \iff \frac{f(\sigma)}{\sigma} \underset{\sigma\to 0}{\longrightarrow} 0$. Note that even their notation is the same, the $o(\sigma)$ terms can differ from one trait to another – they only share the same asymptotic behavior.

One can thus see ε_0 and $\nu_{i,j,0}$ as the leading terms of the MRVs. They capture the direction of the mutation: either an increase or a decrease with respect to the ancestor's value. Indeed, it is straightforward that the sign of ε and $\nu_{i,j}$ are those of ε_0 and $\nu_{i,j,0}$ respectively, hence their denomination of 'mutational directions'. Note that ε_0 and the $\nu_{i,j,0}$s may not be independent. On the contrary, the other ε_q and $\nu_{i,j,q}$, for $q \in \{1,\dots,Q\}$, are assumed to be mutually independent and also independent from ε_0 and the $\nu_{i,j,0}$s. This property captures the noisiness of the mutations.

Subsequent properties of the mutations are carried by sums of mutational deviations we call mutational sums (namely b_1, b_2 and d, see further subsection 4.f.4). The sign of such mutational sums may then not be only determined by those of ε_0 and the $\nu_{i,j,0}$s as their sum can cancel out with non zero probability if $\kappa = 1$ (which will be implied towards the end of the following calculations). In this case, the sign moves on to the next term of

the bigger sum and so on, as illustrated below for $\varepsilon + \nu_{i,j}$,

$$\varepsilon + \nu_{i,j} = \underbrace{\varepsilon_0 + \nu_{i,j,0}}_{=0} + \left(\varepsilon_1 + \nu_{i,j,1}\right)\sigma + \underbrace{\left(\varepsilon_2 + \nu_{i,j,2}\right)\sigma^2 + \ldots + \left(\varepsilon_L + \nu_{i,j,L}\right)\sigma^Q}_{=o(\sigma)},$$

which likewise holds for sums between $\nu_{i,j}$s.

Actually, we can calculate, using the independence property, that

$$\begin{aligned}\mathbb{P}\left[\varepsilon + \nu_{i,j} > 0\right] &= \sum_{q=0}^{Q} \mathbb{P}\left[\varepsilon_q = \nu_{i,j,q}\right]\left(\prod_{\ell=0}^{q-1} \mathbb{P}\left[\varepsilon_\ell = -\nu_{i,j,\ell}\right]\right), \\ &= \frac{1}{4}\sum_{q=0}^{Q} \frac{1}{2^q}, \\ &= \frac{1}{2}\left(1 - \frac{1}{2^{Q+1}}\right),\end{aligned}$$

which likewise holds for $\mathbb{P}\left[\varepsilon + \nu_{i,j} < 0\right]$.

It results that a mutational sum is strictly signed with a probability close to 1 if Q is large, and that we can reasonably partition the cases where their leading terms sum to 0 as half of positive cases and half of negative cases.

4.e.2.2. Generic mutational distribution

Seeking for generality, we also examine the case where the mutational distribution has no particular form except that the associated probability density function (PDF) is symmetric with respect to 0, hence called generic.

Let us first introduce the cumulative distribution function (CDF) F. As any CDF, F satisfies $F(-\infty) = 0$ and $F(\infty) = 1$. Its (potentially distributional) derivative is the PDF denoted by f , $\frac{\mathrm{d}F}{\mathrm{d}a} = f > 0$. The symmetry assumption constrains f to satisfy $f(a) = f(-a)$ for any real number a. Note that this implies that $F(0) = 1/2$ (i.e. the median of the mutational distribution is 0). To insure compatibility with small mutation effects, $F(-1)$ and $1 - F(1)$ are both negligible compared to $F(1) - F(-1)$.

We state that the MRVs follow generic mutational distributions when they can take any real number value $a \in \mathbb{R}$ according to the corresponding CDFs $F_\varepsilon(a) \coloneqq \mathbb{P}[\varepsilon \leq a]$ and $F_{\nu_{i,j}}(a) \coloneqq \mathbb{P}\left[\nu_{i,j} \leq a\right]$ such that

$$\begin{cases} F_\varepsilon(a) & = F\left(\frac{a}{\min(1,\kappa)}\right), \\ F_{\nu_{i,j}}(a) & = F\left(\frac{a}{\min\left(1,\kappa^{-1}\right)}\right), \end{cases} \tag{4.e.4}$$

for all $a \in \mathbb{R}$.

Condition (4.e.4) has two strong implications we here only expose for ε though they analogously apply to the $\nu_{i,j}$ as well (by simply substituting κ by κ^{-1}). On one hand, F_ε identifies with F for all $\kappa \geq 1$. On the other hand, the distribution of ε concentrates to 0 as κ goes to 0 and equals 0 in the limit $\kappa = 0$. Indeed,

$$F_\varepsilon(a) = F\left(\frac{a}{\min(1,\kappa)}\right) \underset{\kappa \to 0}{\longrightarrow} \begin{cases} F(\infty) = 1, & \text{if } a > 0, \\ F(0) = \frac{1}{2}, & \text{if } a = 0, \\ F(-\infty) = 0, & \text{if } a < 0, \end{cases}$$

that is $F_\varepsilon(a) \underset{\kappa \to 0}{\longrightarrow} [a > 0]$, which is the Heaviside step function (defined with the half-

maximum convention).

4.e.2.3. Gaussian mutational distribution

The Gaussian mutational distribution is used as numerical confirmation of the analytical results obtained with the two previous distributions and is in particular used to investigate the consequences of larger mutation effects. We say the MRVs follow a Gaussian mutational distribution when $\varepsilon \sim \mathcal{N}(0, \min(1,\kappa))$ and $\nu_{i,j} \sim \mathcal{N}\left(0, \min\left(1,\kappa^{-1}\right)\right)$.

The results shown in Figure 4.3.1 and Table 4.f.7 were obtained from 10^5 simulations with $\sigma = 0.1$ and $\kappa = 0.1, 1$ and 10 according to the mutational scenario (see below). The results shown in Figure 4.3.3 were obtained from 10^5 simulations for 30 values of σ ranging from 10^{-3} to 10^3 uniformly spaced in the decadic logarithmic scale and $\kappa = 1$.

4.e.3. Mutational scenarios

The mutational distributions defined by (4.e.1) have two main degrees of freedom. The first one is the scale parameter κ that governs which trait category – either intrinsic growth or interactions – is predominantly affected by the phenotypic mutation. In particular, when $\kappa \gg 1$, mutations are mostly driven by a change in intrinsic grow rate, while $0 \leq \kappa \ll 1$ corresponds to mutations that mainly impact the interaction effects. If $\kappa \approx 1$, mutations affect the four trait values comparably.

The other degree of freedom resides in the stochastic dependence between the MRVs which can significantly impact the mutational outcome in terms of trait correlations.

We take advantage of this modularity to identify four biologically relevant mutational scenarios. The first two scenarios investigate predominance of mutations through extreme values of κ, while the last two explore physiological constraints through the dependence between the MRVs. Each of these scenarios will be referred to by its number.

4.e.3.1. Scenario #1: instrinsic growth-driven mutations

Scenario #1 is characterized by $\kappa \gg 1$ so that the overall effect of the mutation is mainly driven by the effect on the intrinsic growth rate. Hence it is unnecessary to specify any dependence between mutational directions. Practically, this allows us to neglect $\nu_{i,j}$ when summed with ε, i.e. $\varepsilon \pm \nu_{i,j} \approx \varepsilon$.

4.e.3.2. Scenario #2: interaction driven mutations

On the contrary, scenario #2 is characterized by $0 < \kappa \ll 1$ so that the overall effect of the mutation is mainly driven by the effect on the self and cross interactions. Practically, this allows us to neglect ε when summed with $\nu_{i,j}$, i.e. $\nu_{i,j} \pm \varepsilon \approx \nu_{i,j}$. Independence between $\nu_{i,j}$s is assumed here.

4.e.3.3. Scenario #3: free mutations

Scenario #3 is characterized by $\kappa = 1$ so that the four mutant traits deviate comparably from their ancestor traits and no MRV is negligible compared to any other. Further, we assume mutual independence between all MRVs. This is the most 'neutral' (and diverse) scenario.

4.e.3.4. Scenario #4: traded-off mutations

Scenario #4 also assumes that $\kappa = 1$ but with the additional assumption that the mutational directions are linked. We here assume that there is a strong trade-off between intrinsic growth rate and interaction effects. The idea is that any increase in intrinsic growth rate is costly in terms of competitive ability. Concretely, if a mutant grows faster than its resident, the mutant undergoes a stronger competitive pressure from both itself and its ancestor while the ancestor undergoes a weaker competition from its mutant. This rule also applies the other way and can then be seen as a niche separation.

Since perfect correlations (and anti-correlations) are biologically unlikely, we decided to keep a mutational background randomness and, for this scenario only, we imposed

$$\varepsilon_0 = \nu_{1,2,0} = -\nu_{2,1,0} = -\nu_{2,2,0},$$

under the fixed step mutational distribution (which contains the noisiness of higher order MRVs), and

$$\varepsilon = \nu_{1,2} + \iota_{1,2}\sigma = -\nu_{2,1} + \iota_{2,1}\sigma = -\nu_{2,2} + \iota_{2,2}\sigma,$$

under the generic and Gaussian mutational distributions, where the $\iota_{i,j}$ are MRVs following $\mathcal{N}\left(0,\sigma'\right)$ (with $\sigma' = 10^{-3}$ in the simulations).

Supplementary results

4.f. Evolutionary outcomes

This part of the appendix finally integrates all previous 'supplementary methods' sections with the aim to investigate mutant survival according to all possible infection patterns and the consequences on virulence evolution under all previously defined mutational settings. Hence, the next pages not only contain the methods that lead to the main text results but also relevant intermediate and additional results along with the full version of the final results. Note that, throughout this section, mutations are assumed small.

4.f.1. Mutation and stationary parasite loads

Following our bottom-up approach, the proximal consequences of mutation are the ones on parasite loads. For the sake of simplicity denote by x the stationary parasite load in single infection of resident parasite 1 (SLS1), which, from previous conventions, is simply

$$x = x_{\mathbf{1},1} := -\frac{\varrho_1}{m_{1,1}} = 1,$$

and by x' the one of the mutant, which given the mutational setting, is

$$x' = x_{\mathbf{2},2} := -\frac{\varrho_2}{m_{2,2}} = -\frac{1+\varepsilon\sigma}{-1+\nu_{2,2}\sigma}.$$

Since σ is small, this can be approximated by

$$x' \approx (1+\varepsilon\sigma)\left(1+\nu_{2,2}\sigma\right) \approx 1+\left(\varepsilon+\nu_{2,2}\right)\sigma, \tag{4.f.1}$$

by neglecting terms proportional to σ^2 and it is straightforward that $x' \underset{\sigma\to 0}{\longrightarrow} x$. At neutrality, the SLS are equal.

As for double infections, we denote by ξ and ξ' the stationary parasite loads of the resident and the mutant respectively in doubly infected hosts. Let us remark that the total stationary parasite load in a double infection is

$$\begin{aligned}
\xi+\xi' &= x_{\mathbf{3},1}+x_{\mathbf{3},2},\\
&= \frac{m_{1,2}\varrho_2 - m_{2,2}\varrho_1 + m_{2,1}\varrho_1 - m_{1,1}\varrho_2}{m_{1,1}m_{2,2}-m_{1,2}m_{2,1}},\\
&= \frac{\left(-1+\nu_{1,2}\sigma\right)(1+\varepsilon\sigma)-\left(-1+\nu_{2,2}\sigma\right)+\left(-1+\nu_{2,1}\sigma\right)+(1+\varepsilon\sigma)}{-\left(-1+\nu_{2,2}\sigma\right)-\left(-1+\nu_{1,2}\sigma\right)\left(-1+\nu_{2,1}\sigma\right)},\\
&= \frac{\left(\nu_{1,2}+\nu_{2,1}-\nu_{2,2}\right)\sigma+\varepsilon\nu_{1,2}\sigma^2}{\left(\nu_{1,2}+\nu_{2,1}-\nu_{2,2}\right)\sigma-\nu_{1,2}\nu_{2,1}\sigma^2},\\
&\approx 1.
\end{aligned}$$

In conclusion, when the mutational effect is small, the two parasite types share the same carrying capacity as in single infections instead of increasing the total parasite load – which is, in passing, a classical assumption regarding microparasitic infections, that here emerges from the mutational setting. Since the mutant is identical to the resident

at neutrality we have

$$\xi = \xi' = \frac{1}{2} = \frac{x}{2}. \tag{4.f.2}$$

4.f.2. Epidemiological rates at neutrality

The transmission rates $\beta_{\boldsymbol{h},\boldsymbol{q}}$, the virulences $\alpha_{\boldsymbol{h}}$ and the recovery rates $\theta_{\boldsymbol{h},i}$ are assumed to be smooth functions of the parasite loads associated with host class $\boldsymbol{h}$. Furthermore, they are assumed to be respectively non-decreasing, increasing and non-decreasing (see subsection 4.d.2). Within the mutational framework, we assume that the functions that underlie the rates are as well smoothly impacted by the mutation. Formally, we assume their convergence towards those of the resident as the mutation effect goes to zero, that is $\left(\beta_{\mathbf{2},\mathbf{2}}, \alpha_{\mathbf{2}}, \theta_{\mathbf{2},2}\right) \underset{\sigma \to 0}{\longrightarrow} \left(\beta_{\mathbf{1},\mathbf{1}}, \alpha_{\mathbf{1}}, \theta_{\mathbf{1},1}\right)$ for any SLS argument in the neighborhood of x.

Given the results on stationary parasite loads showed in the previous subsection, the epidemiological rates related to mutant single infections are equal to those of the resident at neutrality, the notation of which can be simplified into

$$\begin{cases} \beta_{\mathbf{2},\mathbf{2}}\left(x_{\mathbf{2},2}\right) & = \beta_{\mathbf{1},\mathbf{1}}\left(x_{\mathbf{1},1}\right) =: \beta, \\ \alpha_{\mathbf{2}}\left(x_{\mathbf{2},2}\right) & = \alpha_{\mathbf{1}}\left(x_{\mathbf{1},1}\right) =: \alpha, \\ \theta_{\mathbf{2},2}\left(x_{\mathbf{2},2}\right) & = \theta_{\mathbf{1},1}\left(x_{\mathbf{1},1}\right) =: \theta. \end{cases} \tag{4.f.3}$$

Therefore, the elimination rate $\zeta_{\mathbf{2}}\left(x_{\mathbf{2},2}\right) := \mu + \alpha_{\mathbf{2}}\left(x_{\mathbf{2},2}\right) + \theta_{\mathbf{2},2}\left(x_{\mathbf{2},2}\right)$ equals $\zeta_{\mathbf{1}}\left(x_{\mathbf{1},1}\right) =: \zeta$ at neutrality.

Regarding the epidemiological rates related to double infections, we know from (4.f.2) that, at neutrality, the overall stationary parasite load is identical to that in single infections. Hence, it is reasonable to assume that the overall transmission rate, the overall virulence and the overall recovery rate, which are all functions of the overall stationary parasite load, are also identical to those in single infections, i.e.

$$\begin{cases} \left(\beta_{\mathbf{3},\mathbf{1}} + \beta_{\mathbf{3},\mathbf{2}} + \beta_{\mathbf{3},\mathbf{3}}\right)\left(\frac{x}{2} + \frac{x}{2}\right) & = \beta, \\ \alpha_{\mathbf{3}}\left(\frac{x}{2} + \frac{x}{2}\right) & = \alpha, \\ \left(\theta_{\mathbf{3},1} + \theta_{\mathbf{3},2}\right)\left(\frac{x}{2} + \frac{x}{2}\right) & = \theta. \end{cases} \tag{4.f.4}$$

Let us now introduce the co-transmission proportion $\varsigma \in [0,1]$, which is the probability for an inoculum generated by a doubly infected host to be dimorphic (i.e. to carry both the resident and the mutant). Formally, we have

$$\beta_{\mathbf{3},\mathbf{3}} = \varsigma\beta, \tag{4.f.5}$$

Equality (4.f.2) also shows that, at neutrality, the resident and the mutant are present in the same proportions within doubly infected hosts. Consequently, they equitably share the remaining transmission rates, that is the part related to the monomorphic inocula, resulting in

$$\beta_{\mathbf{3},\mathbf{1}}\left(\frac{x}{2}\right) = \beta_{\mathbf{3},\mathbf{2}}\left(\frac{x}{2}\right) = \frac{1-\varsigma}{2}\beta. \tag{4.f.6}$$

Analogously, the resident and the mutant equitably share half of the overall transmission, leading to

$$\theta_{\mathbf{3},i}\left(\frac{x}{2}, \frac{x}{2}\right) = \frac{\theta}{2}, i = 1,2, \tag{4.f.7}$$

thus the elimination rate is likewise invariant at neutrality,

$$\zeta_{\mathbf{3}} \coloneqq \mu + \alpha_{\mathbf{3}} + \left(\theta_{\mathbf{3},1} + \theta_{\mathbf{3},2}\right) = \mu + \alpha + \theta = \zeta. \tag{4.f.8}$$

4.f.3. Infection patterns and mutant survival

In subsection 4.d.6 we have shown that a new parasite type survives in a host population in which already circulates a monomorphic parasite if and only if the real part of all eigenvalues of matrix $\mathbf{J}_{\text{inv}}$ are negative. Assuming that the new parasite type is phenotypically close to the resident now allows us to greatly simplify the entries of this matrix despite its inceptive generality.

By denoting by u the endemic prevalence of the resident parasite, $u \coloneqq \widetilde{I_{\mathbf{1}}}/\left(\widetilde{S} + \widetilde{I_{\mathbf{1}}}\right) \in (0,1)$, and applying equalities (4.d.6) and (4.f.3)-(4.f.8) to (4.d.7), it follows that the sign of the eigenvalues of $\mathbf{J}_{\text{inv}}$ are the same as those of the following matrix

$$\left(\left(\widetilde{S} + \widetilde{I_{\mathbf{1}}}\right)\beta\right)^{-1}\mathbf{J}_{\text{inv}} = \begin{bmatrix} \left(\Phi_{\mathbf{0},\mathbf{2},\mathbf{2}} - 1\right)(1-u) & \left(\frac{1-\varsigma}{2}\Phi_{\mathbf{0},\mathbf{2},\mathbf{2}} + \varsigma\Phi_{\mathbf{0},\mathbf{3},\mathbf{2}}\right)(1-u) \\ -\left(1 - \Phi_{\mathbf{2},\mathbf{1},\mathbf{2}} - \Phi_{\mathbf{1},\mathbf{2},\mathbf{2}}\right)u & \quad + \frac{1+\varsigma}{2}\Phi_{\mathbf{1},\mathbf{2},\mathbf{2}}u + \frac{\theta}{2\left(\widetilde{S}+\widetilde{I_{\mathbf{1}}}\right)\beta} \\ \left(\Phi_{\mathbf{1},\mathbf{2},\mathbf{3}} + \Phi_{\mathbf{2},\mathbf{1},\mathbf{3}}\right)u & \frac{1+\varsigma}{2}\Phi_{\mathbf{1},\mathbf{2},\mathbf{3}}u \\ & \quad -(1-\varsigma)(1-u)\Phi_{\mathbf{0},\mathbf{3},\mathbf{3}} \end{bmatrix}, \tag{4.f.9}$$

when the mutational effect is infinitesimally small (so that the neutrality equalities hold).

The sign of the invasion fitness W has now to be determined by specifying the binary variables $\Phi_{\boldsymbol{h},\boldsymbol{q},\boldsymbol{h}'}$. Biologically, this means that the mutant survival strongly depends on the infection pattern in which the mutation drives the resident - mutant couple (in fact in the case of priorinfection only, non infection pattern factors are also involved as shown below). Hereafter, we consider all 11 infection patterns (see subsection 4.c.3) and proceed by pooling them according to their compatibility with the epidemiology, the mutational setting and the subsequent methodology to evaluate the sign of W.

4.f.3.1. Incompatible infection patterns

4.f.3.1.1. Epidemiological incompatibility: no infection, latinfection 1, ambinfection, suprainfection 1

The present investigation relies on a pre-existing resident parasite able to infect alone. We therefore ignore the four infection patterns that violate condition (4.d.5). These are the no infection, latinfection 1, ambinfection and suprainfection 1 patterns.

4.f.3.1.2. Mutational incompatiblity: latinfection 2, suprainfection 2

The mutant is assumed to be phenotypically close to the resident. In particular, we assume that the mutational effect is smaller than the resident trait values in absolute value. The signs ofϱ_2 and $m_{2,2}$ are therefore unlikely to differ from those of their resident equivalent (ϱ_1 and $m_{1,1}$), which makes the latinfection 2 and the suprainfection 2 patterns improbable (and hence neglected here).

Notice however that these two patterns only produce avirulent mutants since the mutant fails to infect alone ($x' = 0$). Without an explicit expression of epidemiological rates related to double infection, it is impossible to determine the mutant survival in suprainfection 2. On the contrary, it is straightforward that the mutant never survives in latinfection 2, and this holds for any mutational effect.

4.f.3.2. Without double infection: superinfections, ultrainfection, priorinfection

Among the infection patterns that allow for a MEE1 and arise with small mutational effects, four of them exclude double infections, namely superinfections 1 and 2, ultrainfection and priorinfection. Discarding the entries related to the double infected host density in $\mathbf{J}_{\text{inv}}$ reduces it to its first diagonal term $\lambda_1 := \left(\Phi_{\mathbf{0},\mathbf{2},\mathbf{2}} - 1\right)(1-u) - \left(1 - \Phi_{\mathbf{2},\mathbf{1},\mathbf{2}} - \Phi_{\mathbf{1},\mathbf{2},\mathbf{2}}\right)u$, which is trivially its eigenvalue as well.

4.f.3.2.1. superinfection 1 and ultrainfection

Both superinfection 1 and ultrainfection are characterized by $\phi(\mathbf{0},\mathbf{2}) = \mathbf{2}, \phi(\mathbf{2},\mathbf{1}) \neq \mathbf{2}$ and $\phi(\mathbf{1},\mathbf{2}) \neq 2$. Therefore, $\lambda_1 = -u < 0$ since u is a prevalence. The invasion fitness is zero at neutrality and all mutants similar to the resident go extinct within these infection patterns.

4.f.3.2.2. superinfection 2

By definition, $\phi(\mathbf{0},\mathbf{2}) = \mathbf{2}, \phi(\mathbf{2},\mathbf{1}) = \mathbf{2}$ and $\phi(\mathbf{1},\mathbf{2}) = \mathbf{2}$ in superinfection 2. It results that $\lambda_1 = u > 0$ so the invasion fitness is positive at neutrality and all mutants in a close neighborhood of the resident survive in this pattern.

4.f.3.2.3. priorinfection

By definition, $\phi(\mathbf{0},\mathbf{2}) = \mathbf{2}, \phi(\mathbf{2},\mathbf{1}) = \mathbf{2}$ and $\phi(\mathbf{1},\mathbf{2}) = \mathbf{1}$ in priorinfection. It results that $\lambda_1 = 0$. Since the invasion fitness cancels out at neutrality, we need to calculate the selection gradient with respect to the SLS, that is, from (4.d.7),

$$\frac{\partial W}{\partial x'}(x,x) = \widetilde{S}\frac{\mathrm{d}\beta_{\mathbf{2},\mathbf{2}}}{\mathrm{d}x'}(x) - \frac{\mathrm{d}\alpha_{\mathbf{2}}}{\mathrm{d}x'}(x) - \frac{\mathrm{d}\theta_{\mathbf{2},2}}{\mathrm{d}x'}(x).$$

This gradient is unknown without explicit expressions for the transmission, virulence an recovery rates.

However, it is worth noticing that unless the resident exactly possesses an epidemiologically singular SLS x such that $W(x,x)$ is a local extremum, we have $\frac{\partial W}{\partial x'}(x,x) \neq 0$. Since we assume that the fitness landscape is not degenerated (i.e. completely flat), the set of epidemiologically singular SLS is of measure zero in the parameter space hence we can state that $\frac{\partial W}{\partial x'}(x,x) \neq 0$ almost everywhere (a. e.).

Consequently, the selection gradient is either positive or negative a. e. If $\frac{\partial W}{\partial x'}(x,x) > 0$, then only mutants that are more virulent than their resident (in a close neighborhood) can survive. Reciprocally, if $\frac{\partial W}{\partial x'}(x,x) < 0$, only the mutants that are less virulent than their resident survive. Figure 4.f.1 illustrates this fact.

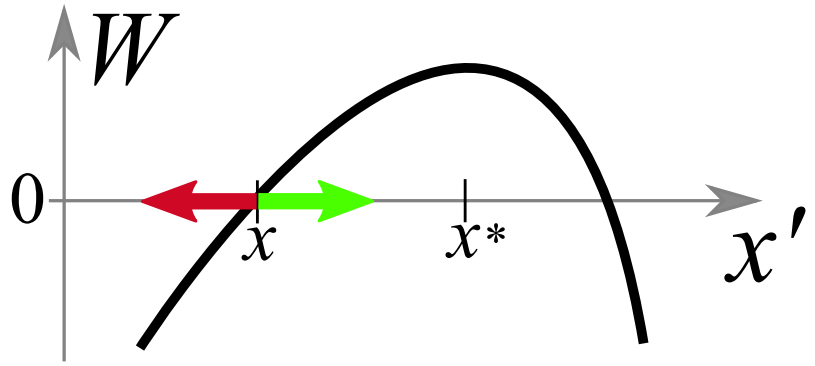

Figure 4.f.1. – Mutant survival in priorinfection.
Since the invasion fitness cancels W at neutrality, the non neutral mutant survives depending on its SLS x'. The selection gradient, that is the slope of the invasion fitness at neutrality $x' = x$, determines which side of the possible SLS invades. This can also be seen as the relative position of the resident SLS x with respect to the optimal SLS x^*. The green arrow denotes the range of mutant SLS that ensures survival while the red arrow denotes the range of mutant SLS that prevent any mutant to invade.

4.f.3.3. With double infection: coinfection

Unlike the other patterns, coinfection preserves the two host compartments infected by the mutant, and so matrix $\mathbf{J}_{\text{inv}}$ remains a 2×2 matrix. By specifying the $\Phi_{\boldsymbol{h},\boldsymbol{q},\boldsymbol{h}'}$ notations in (4.f.9), it follows that

$$2\left(\left(\widetilde{S}+\widetilde{I_1}\right)\beta\right)^{-1}\mathbf{J}_{\text{inv}} = \begin{bmatrix} -2u & (1-\varsigma)(1-u)+\frac{\theta}{(\widetilde{S}+\widetilde{I_1})\beta} \\ 4u & 3u+2\varsigma-\varsigma u-2 \end{bmatrix}.$$

The rightmost eigenvalue of this matrix is given by the formula

$$\lambda_2 = \frac{1}{2}\left(j_{1,1}+j_{2,2}+\sqrt{4j_{1,2}j_{2,1}+\left(j_{1,1}-j_{2,2}\right)^2}\right),$$

where the $j_{a,b}$'s denote the entries of the matrix . Then, we have

$$j_{1,1}+j_{2,2} \;=\; u+2\varsigma-\varsigma u-2 = -(1-\varsigma)(2-u) < 0,$$

and

$$j_{1,1}-j_{2,2} \;=\; -5u-2\varsigma+\varsigma u+2 = -\left(j_{1,1}+j_{2,2}\right)-4u,$$

thus

$$\left(j_{1,1}-j_{2,2}\right)^2 = \left(j_{1,1}+j_{2,2}\right)^2 - 8(1-\varsigma)(2-u)u + 16u^2,$$

while

$$4j_{1,2}j_{2,1} = 16\left((1-\varsigma)(1-u)+\frac{2\theta}{\left(\widetilde{S}+\widetilde{I_1}\right)\beta}\right)u \geq 16(1-\varsigma)(1-u)u,$$

therefore

$$\begin{aligned} 4j_{1,2}j_{2,1}+\left(j_{1,1}-j_{2,2}\right)^2 &\geq \left(j_{1,1}+j_{2,2}\right)^2 + 8(2(1-\varsigma)(1-u)+2u-(1-\varsigma)(2-u))u, \\ &\geq \left(j_{1,1}+j_{2,2}\right)^2 + 8(1+\varsigma)u^2, \end{aligned}$$

which results in

$$\lambda_2 \geq \frac{1}{2}\left(j_{1,1}+j_{2,2}+\left|j_{1,1}+j_{2,2}\right|\right)=0.$$

This proves that the invasion fitness is positive at neutrality and that all mutants in a close neighborhood of the resident survive if in coinfection.

4.f.3.4. Conclusion

Among the 11 infection patterns, only five of them are compatible with both the epidemiology and the mutational setting and we focus on them from now on. These patterns are the two superinfections, ultrainfection, priorinfection and coinfection. Only superinfection 2, priorinfection and coinfection allow for mutant survival.

4.f.4. Evolutionary epidemiological random events

In the previous subsection, we showed that the infection patterns govern the survival of the mutant. To estimate the overall chance for a mutant to survive, we now need to estimate the probability of each infection pattern to occur subsequent to a mutational event.

First, let us remind that eight within-host trait values determine the infection patterns: the sign of $\rho_1, m_{1,1}, \rho_2, m_{2,2}, b_1, b_2, \det\mathbf{M}$, and c (see subsections 4.b.2, 4.b.3 and Table 4.c.2). We already know that ρ_1 and $m_{1,1}$ are necessarily positive and negative respectively, because of the resident's epidemiology (inequality (4.d.5)). Since the mutational effect σ is small, the same result holds for ρ_2 and $m_{2,2}$ (see paragraph 4.f.3.1.2).

Let us now rewrite the positiveness of $b_1, b_2, \det\mathbf{M}$ and c according to the mutational setting (4.e.1):

$$\begin{aligned} b_1 &:= m_{1,2}\rho_2 - m_{2,2}\rho_1, \\ &\approx \left(-1+\nu_{1,2}\sigma\right)(1+\varepsilon\sigma)-\left(-1+\nu_{2,2}\sigma\right), \\ &\approx \left(\nu_{1,2}-\nu_{2,2}-\varepsilon\right)\sigma. \end{aligned}$$

Hence, since $\sigma > 0$,

$$b_1 > 0 \Longleftrightarrow \nu_{1,2}-\nu_{2,2}-\varepsilon > 0. \tag{4.f.10}$$

Likewise,

$$\begin{aligned} b_2 &:= m_{2,1}\rho_1 - m_{1,1}\rho_2, \\ &\approx \left(-1+\nu_{2,1}\sigma\right)-(-1)(1+\varepsilon\sigma), \\ &\approx \left(\varepsilon+\nu_{2,1}\right)\sigma, \end{aligned}$$

hence

$$b_2 > 0 \Longleftrightarrow \varepsilon+\nu_{2,1} > 0. \tag{4.f.11}$$

As for $\det\mathbf{M}$ and c, we have

$$\begin{aligned} \det\mathbf{M} &:= m_{1,1}m_{2,2} - m_{1,2}m_{2,1}, \\ &\approx -\left(-1+\nu_{2,2}\sigma\right)-\left(-1+\nu_{1,2}\sigma\right)\left(-1+\nu_{2,1}\sigma\right), \\ &\approx \left(\nu_{1,2}+\nu_{2,1}-\nu_{2,2}\right)\sigma, \end{aligned}$$

and

$$\begin{aligned} c &:= m_{1,1}b_1 + m_{2,2}b_2, \\ &\approx -1\left(\nu_{1,2} - \nu_{2,2} - \varepsilon\right)\sigma + \left(-1 + \nu_{2,2}\sigma\right)\left(\varepsilon + \nu_{2,1}\right)\sigma, \\ &\approx \left(\nu_{2,2} - \nu_{1,2} - \nu_{2,1}\right)\sigma. \end{aligned}$$

It then follows that

$$\det\mathbf{M} > 0 \Longleftrightarrow c < 0 \Longleftrightarrow \nu_{1,2} + \nu_{2,1} - \nu_{2,2} > 0. \tag{4.f.12}$$

Now, let us remark from (4.f.10)-(4.f.12) that

$$\begin{cases} b_1 > 0 \\ b_2 > 0 \end{cases} \Longleftrightarrow \begin{cases} \nu_{1,2} - \nu_{2,2} > \varepsilon \\ \varepsilon > -\nu_{2,1} \end{cases} \Longrightarrow \nu_{1,2} - \nu_{2,2} > -\nu_{2,1} \Longleftrightarrow \det\mathbf{M} > 0 \Longleftrightarrow c < 0.$$

A close look to the condition table 4.c.2 indicates that the previous result makes the ultrainfection pattern *de facto* impossible. It also allows us to characterize the remaining four patterns implied by the mutation using only two inequalities. Consequently, the four events Se_1, Se_2, Pr and Co, achieved when the mutation results in superinfection 1, superinfection 2, priorinfection and coinfection respectively, can be defined as

$$\begin{cases} Se_1 & := \{b_1 > 0\} \cap \{b_2 < 0\}, \\ Se_2 & := \{b_1 < 0\} \cap \{b_2 > 0\}, \\ Pr & := \{b_1 < 0\} \cap \{b_2 < 0\}, \\ Co & := \{b_1 > 0\} \cap \{b_2 > 0\}. \end{cases} \tag{4.f.13}$$

These events are all pairwise incompatible and form a partition of the mutational universe Ω (less a negligible subset),

$$\Omega = Se_1 \cup Se_2 \cup Pr \cup Co. \tag{4.f.14}$$

Since we are interested in virulence evolution, we investigate the mutational outcome under which the mutant is more virulent than its ancestor. As we use the SLS as the proxy for virulence (see subsection 4.d.3), the mutant is more virulent than its resident if and only if $d := x' - x > 0$ which, from equality (4.f.1), is equivalent to

$$d > 0 \Longleftrightarrow \varepsilon + \nu_{2,2} > 0. \tag{4.f.15}$$

We denote by Δ the event achieved when the mutant is more virulent than the resident, that is

$$\Delta := \{d > 0\}. \tag{4.f.16}$$

Note that quantities b_1, b_2 and d are sums of two or three mutational deviations. Hereafter, we refer to them as mutational sums.

Finally, we introduce Ψ, which is the event achieved when the mutant survives, that is

$$\Psi := \{W > 0\}. \tag{4.f.17}$$

In the previous subsection, we showed that all mutants in superinfection 2 and coinfection survive, meaning that

$$Se_2 \subset \Psi \text{ and } Co \subset \Psi.$$

As for priorinfection, only the fraction of mutants the SLS of which are on the side

determined by the selection gradient (greater than the resident's SLS if the selection gradient is positive, and smaller if negative) survive.

Introducing Υ, the event achieved by the positiveness of the selection gradient, that is

$$\Upsilon := \left\{ \frac{\partial W}{\partial x'}(x,x) > 0 \right\}, \tag{4.f.18}$$

it follows that

$$(Pr \cap \Upsilon \cap \Delta) \subset \Psi \text{ and } \left(Pr \cap \Upsilon^{\complement} \cap \Delta^{\complement}\right) \subset \Psi.$$

This finally allows us to write Ψ as a the following union

$$\Psi = Se_2 \cup Co \cup \left(Pr \cap \left((\Upsilon \cap \Delta) \cup \left(\Upsilon^{\complement} \cap \Delta^{\complement}\right)\right)\right). \tag{4.f.19}$$

Note that since Pr and Δ solely depend on the mutational outcome and since Υ solely depends on the resident's virulence and the epidemiological constrains, Υ is independent from Pr and Δ.

4.f.5. Virulence selection bias formula

The proportion of surviving mutants that are more virulent than their ancestor is the conditional probability $\mathbb{P}[\Delta|\Psi]$. Given the results and definitions of subsection 4.f.4 and applying elementary set and probability theories, it follows that

$$\begin{aligned} \mathbb{P}[\Delta|\Psi] &:= \frac{\mathbb{P}[\Delta \cap \Psi]}{\mathbb{P}[\Psi]}, \\ &= \frac{\mathbb{P}[\Delta \cap Se_2] + \mathbb{P}[\Delta \cap Co] + \mathbb{P}[\Upsilon]\mathbb{P}[\Delta \cap Pr]}{\mathbb{P}[Se_2] + \mathbb{P}[Co] + \mathbb{P}[\Upsilon]\mathbb{P}[\Delta \cap Pr] + (1 - \mathbb{P}[\Upsilon])(\mathbb{P}[Pr] - \mathbb{P}[\Delta \cap Pr])}. \end{aligned} \tag{4.f.20}$$

The numerator of this fraction is the decomposition of the probability that the mutant is more virulent than its ancestor and also survives, which occurs with probability 1 under either superinfection 2 or coinfection, probability $\mathbb{P}[\Upsilon]$ in priorinfection and never occurs for all other infection patterns. The denominator is the decomposition of the probability that the mutant survives, regardless of its virulence, hence including all cases of superinfection 2, coinfection and the priorinfection cases where the virulence order matches the sign of the selection gradient.

Unless the mutational effect distribution itself tends to produce more virulent mutants (which it does not, for small mutation effects, as checked further), $\mathbb{P}[\Delta|\Psi] \neq 1/2$ denotes a selection bias towards virulence.

$\mathbb{P}[\Upsilon]$ is an unknown factor one can regard as follows: if the resident's virulence is smaller than the epidemiologically optimal virulence, then $\mathbb{P}[\Upsilon] = 1$. On the contrary, it the resident's virulence is greater than the epidemiologically optimal virulence, $\mathbb{P}[\Upsilon] = 0$. In the absence of any information about the selection gradient, or at least about the relative position of the resident's virulence with respect to the epidemiologically optimal virulence, one can neutralize the effect of the epidemiological trade-offs over mutant survival by averaging these two extreme values, which naturally leads to $\mathbb{P}[\Upsilon] = 1/2$. We use this neutral value in the main text results but, for the sake of completeness, we also consider the cases $\mathbb{P}[\Upsilon] = 0$ and 1 in our following analysis.

In addition, formula (4.f.20) shows that virulence selection bias requires 6 unknown values to be computed.

4.f.6. Fixed step mutational distribution screening

In this subsection, we exhaustively list all possible combinations of fixed step mutational directions for each scenario and apply their proper assumptions (Tables 4.f.1 to 4.f.4). Each combination determines the sign of the b_1, b_2 and d mutational sum values. The infection pattern is consequently determined by b_1 and b_2 (see subsection 4.f.4). The weight of each combination is given and is divided by 2 each time the half-partitioning rule exposed at the end of subsection 4.e.2.1 is applied. The signs+ and − denote the values of the mutational directions (+1 or −1 respectively) and the sign of the mutational sum values.

The following tables are further used to calculate the relevant quantities linking virulence and survival in Table 4.f.5.

4.f.6.1. Scenario #1: intrinsic growth driven mutations

ε_0	b_1	b_2	ip	d	weight
−	+	−	se_1	−	1
+	−	+	se_2	+	1

Table 4.f.1. – Evolutionary outcome screening of scenario #1 (intrinsic growth driven mutations).
See text for details.

4.f.6.2. Scenario #2: interaction driven mutations

$\nu_{1,2,0}$	$\nu_{2,1,0}$	$\nu_{2,2,0}$	b_1	b_2	ip	d	weight
−	−	−	+	−	se_1	−	½
			−		pr		½
−	−	+	−	−	pr	+	1
−	+	−	+	+	co	−	½
			−		se_2		½
−	+	+	−	+	se_2	+	1
+	−	−	+	−	se_1	−	1
+	−	+	+	−	se_1	+	½
			−		pr		½
+	+	−	+	+	co	−	1
+	+	+	+	+	co	+	½
			−		se_2		½

Table 4.f.2. – Evolutionary outcome screening of scenario #2 (interaction driven mutations).
See text for details.

4.f.6.3. Scenario #3: free mutations

ε_0	$\nu_{1,2,0}$	$\nu_{2,1,0}$	$\nu_{2,2,0}$	b_1	b_2	ip	d	weight
−	−	−	−	+	−	se_1	−	1
−	−	−	+	−	−	pr	+	1/2
							−	1/2
−	−	+	−	+	+	co	−	1/2
					−	se_1		1/2
−	−	+	+	−	+	se_2	+	1/4
							−	1/4
					−	pr	+	1/4
							−	1/4
−	+	−	−	+	−	se_1	−	1
−	+	−	+	+	−	se_1	+	1/2
							−	1/2
−	+	+	−	+	+	co	−	1/2
					−	se_1		1/2
−	+	+	+	+	+	co	+	1/4
							−	1/4
					−	se_1	+	1/4
							−	1/4
+	−	−	−	−	+	se_2	+	1/4
							−	1/4
					−	pr	+	1/4
							−	1/4
+	−	−	+	−	+	se_2	+	1/2
					−	pr		1/2
+	−	+	−	−	+	se_2	+	1/2
							−	1/2
+	−	+	+	−	+	se_2	+	1
+	+	−	−	+	+	co	+	1/4
							−	1/4
					−	se_1	+	1/4
							−	1/4
+	+	−	+	−	+	se_2	+	1/2
					−	pr		1/2
+	+	+	−	+	+	co	+	1/2
							−	1/2
+	+	+	+	−	+	se_2	+	1

Table 4.f.3. – Evolutionary outcome screening of scenario #3 (free mutations). See text for details.

4.f.6.4. Scenario #4: mutations governed by a trade-off

ε_0	$\nu_{1,2,0}$	$\nu_{2,1,0}$	$\nu_{2,2,0}$	b_1	b_2	ip	d	weight
−	−	+	+	−	+	se_2	+	1/4
							−	1/4
					−	pr	+	1/4
							−	1/4
+	+	−	−	+	+	co	+	1/4
							−	1/4
					−	se_1	+	1/4
							−	1/4

Table 4.f.4. – Evolutionary outcome screening of scenario #4 (traded off mutations).
See text for details.

4.f.6.5. Screening synthesis

probability of		scenario			
		#1	#2	#3	#4
superinfection 1,	$\mathbb{P}[Se_1]$	1/2	1/4	5/16	1/4
virulence increasing mutation and superinfection 1,	$\mathbb{P}[\Delta \cap Se_1]$	0	1/16	1/16	1/8
superinfection 2,	$\mathbb{P}[Se_2]$	1/2	1/4	5/16	1/4
virulence increasing mutation and superinfection 2,	$\mathbb{P}[\Delta \cap Se_2]$	1/2	3/16	4/16	1/8
coinfection,	$\mathbb{P}[Co]$	0	1/4	3/16	1/4
virulence increasing mutation and coinfection,	$\mathbb{P}[\Delta \cap Co]$	0	1/16	1/16	1/8
priorinfection	$\mathbb{P}[Pr]$	0	1/4	3/16	1/4
virulence increasing mutation and priorinfection,	$\mathbb{P}[\Delta \cap Pr]$	0	3/16	2/16	1/8
virulence increasing mutation,	$\mathbb{P}[\Delta]$	1/2	1/2	1/2	1/2

Table 4.f.5. – Fixed step mutational distribution screening synthesis.
For each scenario, the probability of each event to occur is given by counting each matching weighted combination in Tables 4.f.1 to 4.f.4. The probability of increasing virulence mutations is given to show that mutation is unbiased with respect to virulence.

4.f.7. Generic mutational distribution screening

Here, we analogously calculate the relevant quantities involved in equation (4.f.20) under the generic mutational distribution.

4.f.7.1. Scenarios #1, #2 and #3

We first address the most general case, namely scenario #3. The results for scenarios #1 and #2 are likewise calculated by simply replacing f by the Dirac delta function

for the neglected variable(s). For the sake of consistency, we use the same dummy variables w, x, y and z to designate the values over which we integrate the PDF of $\varepsilon, \nu_{1,2}, \nu_{2,1}$ and $\nu_{2,2}$, respectively. The dummy variable ω is introduced each time we integrate by substitution, with $\omega := -w$. We thus have that

$$\begin{aligned}
\mathbb{P}[Se_2] + \mathbb{P}[Co] &= \mathbb{P}[\{b_2 > 0\}], \\
&= \int\int\int\int_{\mathbb{R}^4} [y > -w] f(w) f(x) f(y) f(z) \mathrm{d}w \mathrm{d}x \mathrm{d}y \mathrm{d}z, \\
&= \int_{\mathbb{R}} (1 - F(-w)) f(w) f \mathrm{d}w, \\
&= 1 + \int_{\infty}^{-\infty} F(\omega) f(-\omega) \mathrm{d}\omega, \\
&= 1 - \left[\frac{F^2(\omega)}{2} \right]_{-\infty}^{\infty}, \\
&= 1/2,
\end{aligned}$$

which holds for scenarios #1 and #2 as well.

$$\begin{aligned}
\mathbb{P}[\Delta \cap Se_2] + \mathbb{P}[\Delta \cap Co] &= \mathbb{P}[\{d > 0\} \cap \{b_2 > 0\}], \\
&= \int\int\int\int_{\mathbb{R}^4} [z > -w][y > -w] f(w) f(x) f(y) f(z) \mathrm{d}w \mathrm{d}x \mathrm{d}y \mathrm{d}z, \\
&= \int_{\mathbb{R}} (1 - F(-w))^2 f(w) f \mathrm{d}w, \\
&= 1 + 2\int_{\infty}^{-\infty} F(\omega) f(-\omega) \mathrm{d}\omega - \int_{\infty}^{-\infty} F^3(\omega) f(-\omega) \mathrm{d}\omega, \\
&= \left[\frac{F^3(\omega)}{3} \right]_{-\infty}^{\infty}, \\
&= 1/3,
\end{aligned}$$

while this sum equals ½ in scenario #1 and ¼ in scenario #2.

$$\begin{aligned}
\mathbb{P}[Pr] &= \int\int\int\int_{\mathbb{R}^4} [b_1 < 0][b_2 < 0] f(w) f(x) f(y) f(z) \mathrm{d}w \mathrm{d}x \mathrm{d}y \mathrm{d}z, \\
&= \int\int_{\mathbb{R}^2} \left(\int_{\mathbb{R}} [x < w + z] f(x) \mathrm{d}x \right) \left(\int_{\mathbb{R}} [y < -w] f(y) \mathrm{d}y \right) f(w) f(y) \mathrm{d}w \mathrm{d}z, \\
&= \int_{\mathbb{R}} \left(\int_{\mathbb{R}} F(w + z) f(z) \mathrm{d}z \right) F(-w) f(w) \mathrm{d}w,
\end{aligned}$$

and since it is not possible to continue the integration without any further knowledge on F, we seek for a lower and an upper boundary of this integral. We first notice that since F is an increasing function between 0 and 1, we have that

$$\begin{cases}
0 \leq F(w + z) \leq F(z), & \text{when } w < 0, \\
F(z) \leq F(w + z) \leq 1, & \text{when } w > 0,
\end{cases}$$

thus, on one hand,

$$\begin{aligned}\mathbb{P}[Pr] &\geq \int_{\mathbb{R}} [w>0]\left(\int_{\mathbb{R}} F(z)f(z)\mathrm{d}z\right)F(-w)f(w)\mathrm{d}w,\\ &= \left[\frac{F^2(z)}{2}\right]_{-\infty}^{\infty}\left(-\int_{\infty}^{-\infty}[\omega<0]F(\omega)f(-\omega)\mathrm{d}\omega\right),\\ &= \frac{1}{2}\left[\frac{F^2(\omega)}{2}\right]_{-\infty}^{0},\\ &= 1/16,\end{aligned}$$

and on the other hand,

$$\begin{aligned}\mathbb{P}[Pr] \leq& \int_{\mathbb{R}} [w<0]\left(\int_{\mathbb{R}} F(z)f(z)\mathrm{d}z\right)F(-w)f(w)\mathrm{d}w\\ &+\int_{\mathbb{R}}[w>0]F(-w)f(w)\mathrm{d}w,\\ &= \frac{1}{2}\left(-\int_{\infty}^{-\infty}[\omega>0]F(\omega)f(-\omega)\mathrm{d}\omega\right)\\ &+\left(-\int_{\infty}^{-\infty}[\omega<0]F(\omega)f(-\omega)\mathrm{d}\omega\right),\\ &= \frac{1}{2}\left[\frac{F^2(\omega)}{2}\right]_{0}^{\infty}+\left[\frac{F^2(\omega)}{2}\right]_{-\infty}^{0},\\ &= 5/16.\end{aligned}$$

In scenarios #1 and #2, $\mathbb{P}[Pr]$ equals 0 and 1/4 respectively.
Moreover, we have that

$$\begin{aligned}\mathbb{P}[\Delta\cap Pr] &= \int\int\int\int_{\mathbb{R}^4}[d>0][b_1<0][b_2<0]f(w)f(x)f(y)f(z)\mathrm{d}w\mathrm{d}x\mathrm{d}y\mathrm{d}z,\\ &= \int\int\int\int_{\mathbb{R}^4}[z>-w][z>x-w][y<-w]f(w)f(x)f(y)f(z)\mathrm{d}w\mathrm{d}x\mathrm{d}y\mathrm{d}z,\\ &= \int\int\int_{\mathbb{R}^3}[z>-w][x<0]F(-w)f(w)f(x)f(z)\mathrm{d}w\mathrm{d}x\mathrm{d}z\\ &\quad+\int\int\int_{\mathbb{R}^3}[z>x-w][x>0]F(-w)f(w)f(x)f(z)\mathrm{d}w\mathrm{d}x\mathrm{d}z,\\ &= \frac{1}{2}\int\int_{\mathbb{R}^2}[z>-w]F(-w)f(w)f(z)\mathrm{d}w\mathrm{d}z\\ &\quad+\int\int_{\mathbb{R}^2}[x>0](1-F(x-w))F(-w)f(w)f(x)\mathrm{d}w\mathrm{d}x,\end{aligned}$$

Let us address the first integral,

$$\begin{aligned}\frac{1}{2}\int\int_{\mathbb{R}^2}[z>-w]F(-w)f(w)f(z)\mathrm{d}w\mathrm{d}z &= \frac{1}{2}\int_{\mathbb{R}}(1-F(-w))F(-w)f(w)\mathrm{d}w,\\ &= \frac{1}{2}\left(\int_{\infty}^{-\infty}F(\omega)f(-\omega)\mathrm{d}\omega+\int_{\infty}^{-\infty}F^2(\omega)f(-\omega)\mathrm{d}\omega\right),\\ &= \frac{1}{2}\left(\left[\frac{F^2(\omega)}{2}\right]_{-\infty}^{\infty}-\left[\frac{F^3(\omega)}{3}\right]_{-\infty}^{\infty}\right),\\ &= \frac{1}{12}.\end{aligned}$$

The second integral can be bounded as previously, noticing that, when $x > 0$,

$$0 \leq 1 - F(x-w) \leq 1 - F(-w),$$

hence $\mathbb{P}[\Delta \cap Pr] \geq \frac{1}{12}$ and

$$\begin{aligned}\mathbb{P}[\Delta \cap Pr] &\leq \frac{1}{12} + \int\int_{\mathbb{R}^2} [x > 0](1 - F(-w))F(-w)f(w)f(x)\mathrm{d}w\mathrm{d}x,\\ &= \frac{1}{12} + \frac{1}{2}\int_{\mathbb{R}} (1 - F(-w))F(-w)f(w)\mathrm{d}w,\\ &= \frac{1}{8}.\end{aligned}$$

In scenarios #1 and #2, $\mathbb{P}[\Delta \cap Pr]$ equals 0 and 3⁄16 respectively.

4.f.7.2. Scenario #4

In scenario #4, the RMVs are constrained as $\varepsilon = \nu_{1,2} + \iota_{1,2}\sigma = -\nu_{2,1} + \iota_{2,1}\sigma = -\nu_{2,2} + \iota_{2,2}\sigma$. Using the fact that $\sigma \ll 1$, the mutational sums simplify the same way as in the corresponding fixed step case (Table 4.f.4) and because the $\iota_{i,j}$s are mutually independent and independent from ε as well, the multiple integrals simplify in products of simple integrals, which straightforwardly result in the values given in Table 4.f.6.

4.f.7.3. Screening synthesis

One can straightforwardly show that $\mathbb{P}[\Delta] = 1⁄2$ in all four scenarios. Table 4.f.6 sums up these results.

scenarios	#1	#2	#3	#4
$\mathbb{P}[Se_2] + \mathbb{P}[Co]$	1⁄2	1⁄2	1⁄2	1⁄2
$\mathbb{P}[\Delta \cap Se_2] + \mathbb{P}[\Delta \cap Co]$	1⁄2	1⁄4	1⁄3	1⁄4
$\mathbb{P}[Pr]$	0	1⁄4	[1⁄16, 5⁄16]	1⁄4
$\mathbb{P}[\Delta \cap Pr]$	0	3⁄16	[1⁄12, 1⁄8]	1⁄8
$\mathbb{P}[\Delta]$	1⁄2	1⁄2	1⁄2	1⁄2

Table 4.f.6. – Generic mutational distribution distribution screening synthesis.

Applying equation (4.f.20), the values of $\mathbb{P}[\Delta|\Psi]$ given in Table 4.f.7 for scenario #3 simply result from the analysis of the function

$$g_z(x,y) = \frac{\frac{1}{3} + zy}{\frac{1}{2} + zy + (1-z)(x-y)},$$

for $z = 0, 1⁄2, 1$ and $x \in [1⁄16, 5⁄16], y \in [1⁄12, 1⁄8], y \leq x$.

4.f.8. Synthesis of virulence selection bias results

Table 4.f.7 below compiles all the values of virulence selection bias ($\mathbb{P}[\Delta|\Psi]$) obtained by applying equation (4.f.20) to all screening (for fixed step, Table 4.f.5, and generic mutational distributions, Table 4.f.6) or simulation results (Gaussian mutational distributions, see subsection for parametrization 4.e.2.3) for each mutational scenario and examining the three relevant values of $\mathbb{P}[\Upsilon]$.

mutational distribution	$\mathbb{P}[\Upsilon]$	mutational scenarios			
		#1	#2	#3	#4
Fixed step (analytical)	0	1	$4/9 \approx 0.44$	$5/9 \approx 0.56$	$2/5 = 0.4$
	$1/2$	1	$11/20 = 0.55$	$11/19 \approx 0.58$	$1/2 = 0.5$
	1	1	$7/11 \approx 0.64$	$6/10 = 0.6$	$3/5 = 0.6$
Gaussian (numerical)	0	0.99	0.45	0.60	0.40
	$1/2$	0.99	0.55	0.67	0.50
	1	0.99	0.63	0.73	0.60
Generic (analytical)	0	1	$4/9 \approx 0.44$	$[16/35 \approx 0.46, 2/3 \approx 0.67]$	$2/5 = 0.4$
	$1/2$	1	$11/20 = 0.55$	$[4/7 \approx 0.57, 19/27 \approx 0.70]$	$1/2 = 0.5$
	1	1	$7/11 \approx 0.64$	$[5/7 \approx 0.71, 11/15 \approx 0.73]$	$3/5 = 0.6$

Table 4.f.7. – Virulence selection bias values $\mathbb{P}[\Delta|\Psi]$ for the four mutational scenarios, three values of $\mathbb{P}[\Upsilon]$ and three mutational effect distributions.
Approximated values (introduced by $\approx$) are two-digits rounded.

4.ω. Épilogue

La discussion et l'extension des résultats de ce chapitre forment le chapitre à part entière suivant.

δ De la mutation à l'adaptation

$\delta.\alpha$. Prologue

Dans le précédent chapitre, nous avons montré que si une lignée parasitaire mutante apparaît et se maintient au sein d'une population d'hôtes initialement infectée par un parasite monomorphe, alors elle est probablement plus virulente que l'ancêtre dont elle est issue. Selon ce résultat, la virulence moyenne de la population parasitaire est sujette à une croissance permanente.

La généralité du modèle nous a permis de moyenner la virulence et la survie sur l'ensemble des mutations possibles et ce suivant diverses modalités. En contrepartie, cette même généralité limite la méthode à une seule étape évolutive (une mutation et son éventuelle sélection). Bien qu'utile pour prédire une tendance évolutive à court terme, cette restriction nous empêche en particulier d'étudier l'évolution parasitaire pour des polymorphismes plus élevés (atteints par la survie de mutants successifs sans exclusion de la population d'hôte des types résidents).

Dans ce chapitre, nous présentons une extension computationnelle du précédent modèle qui nous permet de le réitérer et d'envisager l'évolution à plus de deux types parasitaires. Il se trouve que l'écriture de cet algorithme a mis en lumière une question que la méthodologie usuelle d'analyse d'invasion passait sous silence : le contexte d'apparition du mutant, qu'il est nécessaire de préciser dès lors que plusieurs patrons d'infection sont autorisés. La discussion de la localisation du mutant en lien avec sa survie fait ainsi l'objet de la première partie de ce chapitre, dont le résultat sera intégré au cours de la seconde, qui présentent les résultats de l'extension numérique.

δ.1. Note on the mutant's location and fate

Theoretical parasite evolution is often addressed through a classical invasion analysis, which is the eco-evolutionary analogue of the perturbation analysis famous to mechanics. Previously (see chapter 4), and following the next-generation method (Diekmann *et al.*, 1990), we investigated the survival of a given mutant type by introducing, in a host population in which a resident type already circulates, a negligible density of any of the possible host classes containing the mutant type. Despite of its commonness, this perturbation approach may skip an important step: does the mutation actually lead to any of the mutant-infected host class used to trigger the mutant epidemic?

Indeed, a mutant parasite involved in a priorinfection pattern (Sofonea *et al.*, 2017b) immediately vanishes if it appears in a host already infected by its ancestor. This kind of mutant can spread and persist in the host population later on only if it appears within an ancestor-deprived inoculum that contaminates a susceptible host. I then appears that the fate of a mutant parasite type does not only depend on its trait values (and the ones of its ancestor), but also of its initial location. Therefore, within the field of evolutionary epidemiology, a biologically realistic invasion analysis – may it be for model analysis or individual-based simulations – should rely on the replacement of a single host individual. The class of this host should be carefully addressed either through an explicit assumption or through the estimation of the probability distribution over mutation-carrying classes. On the contrary, most evolutionary epidemiological models implicitly place the mutant parasite alone in an inoculum transmitted to a susceptible host (van Baalen & Sabelis (1995); Dieckmann (2002); Alizon & Lion (2011) but see exceptions in Coombs *et al.* (2007); Boldin & Diekmann (2008)). This mathematical simplification can nonetheless be partially explained by the lack of empirical knowledge on inoculum production, inoculum sizes and inoculum diversity.

In the following, we try to conceive a simple formalization of the links between mutation and inoculum sampling in microparasites before implementing it in a partly individual based iterative version of the previous model design for investigating long-term virulence evolution with an unbounded polymorphism level. From now on, we only consider multicellular hosts chronically infected by microparasites. Unless they establish on their host's external surface, microparasites usually migrate from the inoculation point to specific host organ(s), tissue(s) or cell(s) in order to reproduce (this is called tropism or motility, see Leggett *et al.* (2017)) and from there to other host parts in order to be transmitted. Let us discretize a host into a large but finite number of $m \in \mathbb{N}^\star$ microsites, which we here define a microsite as the smallest host volume in which one parasite individual can dwell. This formal representation encompasses a variety of micro-environments that may differ in terms of biological properties and volume measures. We therefore allow for a distorted discretization of the overall available host volume so that all microsites have the same probability to be occupied by one parasite individual (otherwise they are empty). We assume that $z \in \mathbb{N}^\star$ of the m microsites are involved in inoculum production and constitute what we call the transmission zone, that is the leaking of some host volume out in the environment (e.g. cough droplets or bleeding microlesions). Figure δ.1.1 illustrates this formalization.

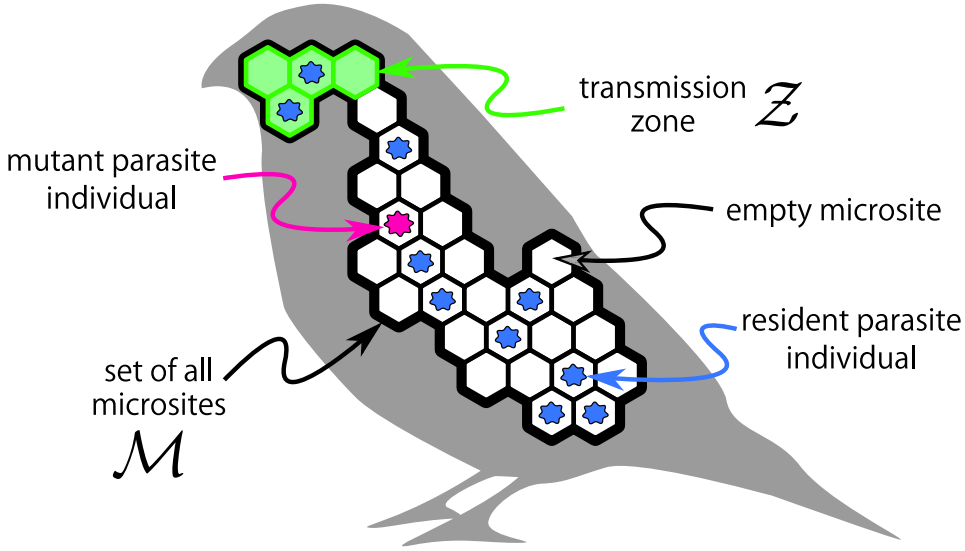

Figure δ.1.1. – Host microsite discretization.
The whole host volume inhabitable by the focal microparasite species is divided into a large number of microsites, each of them being at most occupied by one parasite individual. The set of all microsites is denoted by $\mathcal{M}$, with $\mathrm{Card}\mathcal{M} =: m$. The set of microsites to be transmitted is denoted by $\mathcal{Z}$ and is strictly included in $\mathcal{M}$ ($\mathcal{Z} \subsetneq \mathcal{M}$), and $\mathrm{Card}\mathcal{Z} =: z$. For illustration purposes, the host is here infected by a resident parasite type individuals (in blue), one of which has undergone a mutation (in red) but it cannot be transmitted since it is not located in the transmission zone $\mathcal{Z}$.

Let us denote by $x \in \mathbb{N}^\star$ the number of parasite individuals chronically infecting a host. Since chronic infections do not reach very high parasite loads – except in their last stage whose epidemiological contribution is negligible – and since the host is likely to die long before the parasites colonize it almost entirely, it is reasonable to assume that most microsites are unoccupied, hence $x \ll m$ (here to be understood as $x \leq \frac{m}{10}$). Furthermore, the inoculum transmission of microparasites to another host does not depress the parasite load of the infected host. It is then reasonable to assume that, once the infection is established, the total number of parasites within the host outweighs the maximum number of parasites the host can transmit at once, hence $z \ll x$. Finally, given that typical infective doses consist at least of ten propagules (see Schmid-Hempel & Frank (2007) but note that this number may be smaller for vectorized plant viruses (Moury *et al.*, 2007; Péréfarres *et al.*, 2014)), we have that

$$1 \ll z \ll x \ll m. \tag{δ.1.1}$$

We assume that phenotypic mutations are rare enough so that they do not overlap in time. When such an event occurs, one of the x resident parasite individuals becomes a mutant (see Figure δ.1.1 for illustration). If this single mutant can replicate within the host despite the numerous $(x-1)$ ancestors and if it can grow alone or accompanied by ancestor individuals, the invasion analysis outcome is independent from the spatial history of the mutant. The same holds for mutants unable to grow alone nor accompanied. However, if the mutant is competitively excluded by its ancestor (or other parasites sharing the same host) but is able to grow alone or, conversely, when it requires the ancestor to grow as it cannot alone, then the precise location of the mutant does matter.

By chance, if the mutant individual is located in a transmitted microsite, it soon escapes from the host, potentially with other ancestor individuals. Consequently, its epidemiologically relevant growth will take place in another host. Note that if the mutant can reproduce before being transmitted, it is likely that its progeny is also moving with it. Let p_{h} be the probability that the mutant is not sampled for transmission, i.e. is not located in the transmission zone $\mathcal{Z}$ (see Figure δ.1.1). Instead of considering the parasite individuals in motion over the grid of all microsites $\mathcal{M}$, we can regard their distribution as fixed and randomly choose z microsites out of m to constitute the transmission zone $\mathcal{Z}$. An estimate of p_{h} is then

$$p_{\mathrm{h}} = \left(1-\frac{1}{m}\right)\left(1-\frac{1}{m-1}\right)\cdots\left(1-\frac{1}{m-z+1}\right) \overset{(\delta.1.1)}{\approx} \left(1-\frac{1}{m}\right)^{z},$$

which, according to (δ.1.1), is greater than 99%. Even in this case, one needs to distinguish between monomorphic inocula, when the mutant is alone, and polymorphic inocula, where it is accompanied by ancestor individuals. Given its location in a sampled microsite, the probability p_{m} to be in a monomorphic inoculum is analogously calculated over the $z-1$ remaining microsites and the $x-1$ available ancestor individuals, that is

$$p_{\mathrm{m}} = \left(1-\frac{x-1}{m-1}\right)\left(1-\frac{x-1}{m-2}\right)\cdots\left(1-\frac{x-1}{m-z+1}\right) \overset{(\delta.1.1)}{\approx} \left(1-\frac{x}{m}\right)^{z},$$

which, according to (δ.1.1), is lower than 35%.

Now, let p_{c} denote the probability that an emitted inoculum effectively contaminates a host and f the proportion of hosts infected by an ancestor, that is the ancestor's prevalence. There is little knowledge on the value of p_{c}, that may greatly differ from one biological system to another. However, the fact that the mutant comes from an already infected host implies that $f > 0$.

To sum up, an arising mutant escapes from its ancestor's presence with probability

$$p_{\mathrm{e}} = (1-p_{\mathrm{h}})(1-f)\,p_{\mathrm{m}}p_{\mathrm{c}} < 3.5\times10^{-3},$$

where the upper bound is the highest estimate compatible with our modelling assumptions, setting $m = 10x = 10^2 z = 10^3$. However, realistic data is likely to drive p_{e} to even lower values as HIV infections e.g. are known to contain up to $x = 10^9$ within-host virions (Fraser *et al.*, 2014).

This result nonetheless illustrates that even with very conservative parameters, the probability that transmission changes the fate of a mutant – either by saving it from competitive exclusion by transmitting it alone to a host in which it can grow (priorinfection success) or by preventing it from the required help of its ancestor by isolating it in another host (suprainfection failure) – is very low. In the case of priorinfection, notice moreover than the effective survival probability, which is conditioned by the epidemiological dynamics, is then even lower than the escape probability p_{e}. This result naturally leads to re-evaluate the virulence selection bias estimated in the previous paper since a non negligible part of the priorinfection cases where regarded as leading to mutant survival. Nevertheless, after calculations (not shown here but easily reproducible with the data in appendix 4.f) setting the priorinfection survival to 0, the probability that a surviving mutant is more virulent than its ancestor is still equal or greater than one half. Moreover, the numerical simulations provided in the next section show that virulence can reach an evolutionary quasi-stable level within a much shorter time period than the one expected for such a rare event (either priorinfection success or suprainfection failure) to occur once, according to the highest estimate of p_{e}.

We have thus proved that even if the mutant's initial location can affect its survival, almost all mutants remain within the host they appeared in, together with their ancestor. The parasite micro-evolution therefore relies on the proportion of possible mutations that engender mutant parasite types able to grow along their ancestor. If this proportion is not negligible while a diversity of infection patterns is possible, the major trends of the parasite micro-evolution can be addressed by restricting the investigation to these mutants able to grow within the host they originate and us the latter as the standard epidemiological perturbation.

δ.2. *In silico* long-term virulence evolution

In a previous work, we investigated the evolution of virulence through the survival at the host population level of a mutant arising in a monomorphic parasite meta-population. Averaging over all small mutations according to several mutation settings, we have shown that surviving mutants are more likely to be more virulent than their ancestor. We referred to this as the virulence selection bias since the mutation process itself is unbiased with respect to virulence. Here, virulence is the stationary parasite load in single infections (SLS – which is an appropriate proxy for comparing virulence of closely related parasites if virulence is a strictly increasing function of the SLS). Because of its generality, our approach was analytically tractable over only one mutation step. Consequently, whether the observed virulence selection bias still holds after several rounds of mutations and especially in a higher polymorphism context, was still an open question.

To address virulence evolution on the long term, we have developed an algorithm, illustrated and explained in Figure δ.2.1, that recursively applies the previous model (see chapter 4).

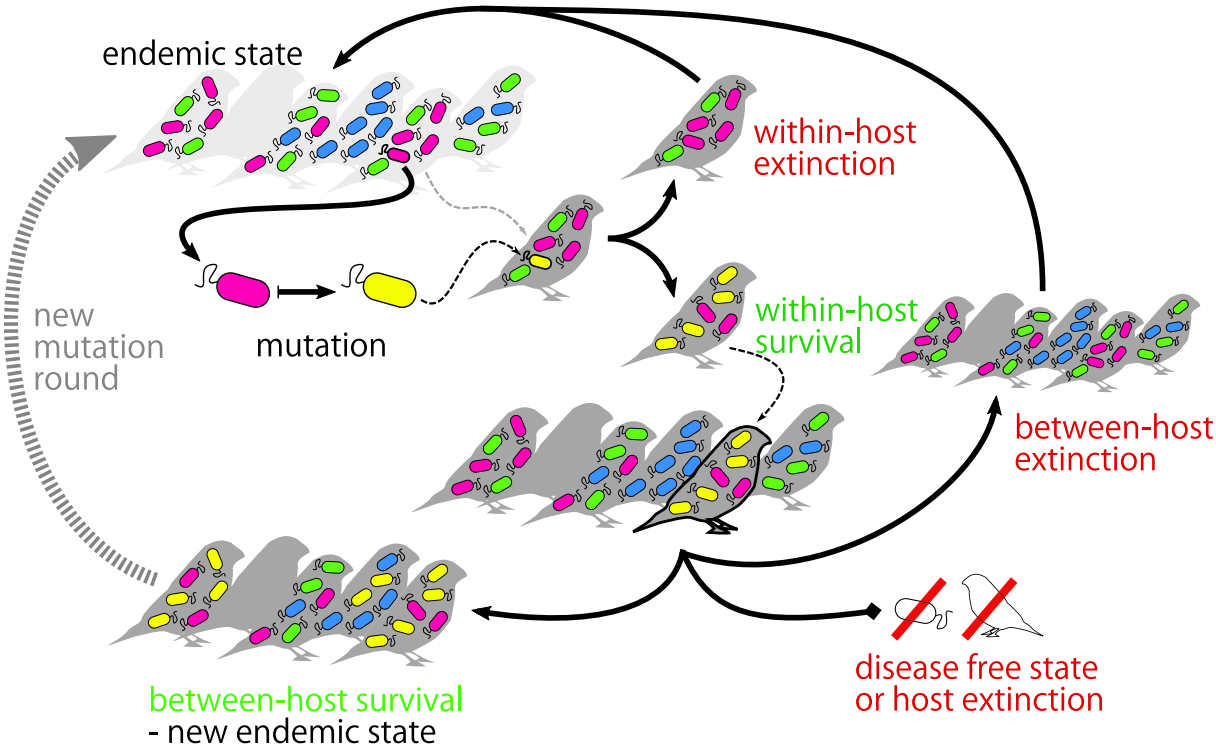

Figure δ.2.1. – Outline of the *in silico* virulence evolution algorithm.
Given a host population at an endemic equilibrium in which circulate one or several parasite types (here depicted in blue, green and pink), one of the infecting parasite individuals mutates within a host and generates a new parasite type (here in yellow). If the mutant survives within the host it appeared in, then its between-host survival is investigated. Between-host survival consists in the long-term persistence of at least one host class that contains the new parasite type. In this case, a new endemic state is determined (other parasite types may go extinct in the process), in which the next mutation will place. Otherwise, if the new parasite type vanishes either at the within-host level or at the between-host level, the next mutation takes place in the unchanged endemic state.

In order to introduce a new mutant over the first one, it is necessary to determine the endpoint of the epidemiological dynamics once the first mutant has spread in the host population (the phenotypic mutations are assumed to be rare enough so that they only arise at endemic equilibria). This requires making explicit the epidemiological functions so far unspecified. Following Sofonea *et al.* (2015), the polymorphic SIS epidemiological dynamics are governed by the derivative of the host class $\boldsymbol{i}$ density ($I_{\boldsymbol{i}}$) with respect to time τ as

$$\begin{aligned}\frac{\mathrm{d}I_{\boldsymbol{i}}}{\mathrm{d}\tau} = &\sum_{\boldsymbol{r}\in\wp(\mathcal{G})\setminus\{\boldsymbol{i}\}}\ \sum_{\boldsymbol{d}\in\wp(\mathcal{G})}\beta_{\boldsymbol{r},\boldsymbol{d},\boldsymbol{i}}I_{\boldsymbol{r}}I_{\boldsymbol{d}} + \sum_{\boldsymbol{u}\in\wp(\mathcal{G})}\theta_{\boldsymbol{u},\boldsymbol{i}}I_{\boldsymbol{u}}\\ &- \sum_{\boldsymbol{v}\in\wp(\mathcal{G})}\ \sum_{\boldsymbol{w}\in\wp(\mathcal{G})\setminus\{\boldsymbol{i}\}}\beta_{\boldsymbol{i},\boldsymbol{v},\boldsymbol{w}}I_{\boldsymbol{v}}I_{\boldsymbol{i}} - \sum_{\boldsymbol{\ell}\in\wp(\mathcal{G})}\theta_{\boldsymbol{i},\boldsymbol{\ell}}I_{\boldsymbol{i}}\\ &-\left(\mu+\alpha_{\boldsymbol{i}}\right)I_{\boldsymbol{i}} + [\boldsymbol{i}=\emptyset]\,\Lambda\left(\sum_{\boldsymbol{i}\in\wp(\mathcal{G})}I_{\boldsymbol{i}}\right),\end{aligned} \tag{δ.2.1}$$

where bold indices denote sets of parasite types, i.e. elements of the power set $\wp(\mathcal{G})$ of the set of parasite type labels $\mathcal{G}=\{1,2,\ldots,n\}$ with n as large as needed. $\beta_{\boldsymbol{r},\boldsymbol{d},\boldsymbol{i}}$ is the rate at which a $\boldsymbol{r}$-class host becomes an $\boldsymbol{i}$-class host through contact with a $\boldsymbol{d}$-class host, $\theta_{\boldsymbol{u},\boldsymbol{i}}$ is the rate at which a $\boldsymbol{u}$-class host recovers to an $\boldsymbol{i}$-class host, μ is the natural mortality rate and $\alpha_{\boldsymbol{i}}$ captures the expressed virulence undergone by $\boldsymbol{i}$-class hosts. The Λ term corresponds to the susceptible host inflow, here assumed to be the logistic function (Verhulst, 1838)

$$\Lambda\left((I_{\boldsymbol{i}})_{\boldsymbol{i}\in\wp(\mathcal{G})}\right) := \left(r - \frac{r-\mu}{\overset{\circ}{S}}\sum_{\boldsymbol{i}\in\wp(\mathcal{G})}I_{\boldsymbol{i}}\right)\sum_{\boldsymbol{i}\in\wp(\mathcal{G})}I_{\boldsymbol{i}},$$

with r the intrinsic growth rate of the host population and $\overset{\circ}{S}$ the host population size at the disease free equilibrium (indeed, in the absence of parasites, $\frac{\mathrm{d}S}{\mathrm{d}t} = \Lambda - \mu S = \left(r-\mu\right)S\left(1-\frac{S}{\overset{\circ}{S}}\right)$ which cancels out for $S=\overset{\circ}{S}>0$). We do not assume any infection-induced fecundity cost nor vertical transmission of the parasite (hence the presence of the $[\boldsymbol{i}=\emptyset]$ binary factor).

The between-host dynamics are parameterized by three kinds of epidemiological namely recovery, transmission and expressed virulence. These are difficult to define because of the limited empirical knowledge on how they relate to within-host processes, which is even more limited when multiple infections are involved. Many alternative formulations could have been used. Nonetheless, the present definitions are simple enough to be regarded as starting points while allowing us to interpret straightforwardly the evolution of parasite virulence by making use of a small set of parameters and by focusing on the impact of within-host interactions without assuming any specific trade-off constraints (see below).

First, we assume that infected hosts can recover from chronically infecting parasites one type at a time with the same rate,

$$\theta_{\boldsymbol{u},\boldsymbol{i}} := \theta\mathrm{Card}\left\{k\in\boldsymbol{u} : \phi(\emptyset,\boldsymbol{u}\setminus\{k\}) = \boldsymbol{i}\right\},$$

where θ is a constant recovery factor and ϕ the inoculation outcome map which captures the infection pattern, i.e. $\phi(\boldsymbol{a},\boldsymbol{b})$ is the host class that results from the inoculation of a $\boldsymbol{b}$-class inoculum in an $\boldsymbol{a}$-class receiver host (see details in Sofonea *et al.* (2017b)). Since we assume within-host dynamics to be very fast compared to epidemiological events, recovery from acute infections is directly embedded in the transmission-related rates.

Unlike recovery, we assume that transmission and expressed virulence depend on the outcome of the within-host dynamics, i.e. the fixed points of the within-host parasite growth assumed to follow the n-species Lotka-Volterra equations

$$\frac{\mathrm{d}X_k}{\mathrm{d}t} = \left(\varrho_k + \sum_{j\in\mathcal{G}} m_{k,j}X_j\right)X_k =: f_k, \tag{δ.2.2}$$

where ϱ_k is the intrinsc growth rate of type k and $m_{k,j}$ is the effect of parasite type j on parasite type k's growth. Hence, $x_{\boldsymbol{d},k}$ is the stationary parasite load of parasite type k in a host chronically infected by all parasite types in the $\boldsymbol{d}$ class (by definition, $x_{\boldsymbol{d},k}$ is zero iff $k \in \boldsymbol{d}$ but $x_{\boldsymbol{d},k}$ may be negative for a given $k \in \boldsymbol{d}$ which hinders the feasilibity of host class $\boldsymbol{d}$).

Transmission is modelled assuming that all infected hosts have the same inoculum emission rate β called the transmission factor. This quantity is then split among all inocula that can emerge from the host class. Put differently, the constant β is the sum of the transmission rates of all inoculum classes a host can produce if each inoculum were infectious. The fractioning is governed by the proportion of each parasite type within the host estimated via their stationary parasite loads $x_{\boldsymbol{d},k}$. It results that the transition rate of an $\boldsymbol{r}$-class receiver host to a focal $\boldsymbol{i}$-class host by contact with a $\boldsymbol{d}$-class donor host is

$$\beta_{\boldsymbol{r},\boldsymbol{d},\boldsymbol{i}} \coloneqq \beta \sum_{\boldsymbol{p}\in\wp(\boldsymbol{d})} \left(\left[\phi(\boldsymbol{r},\boldsymbol{p}) = \boldsymbol{i}\right] \mathrm{Card}\boldsymbol{p} \quad \left(\prod_{k\in\boldsymbol{p}} \frac{x_{\boldsymbol{d},k}}{\sum\limits_{\ell\in\boldsymbol{p}} x_{\boldsymbol{d},\ell}} \right) \quad \left(\prod_{j\in\boldsymbol{d}\setminus\boldsymbol{p}} \left(1 - \frac{x_{\boldsymbol{d},j}}{\sum\limits_{\ell\in\boldsymbol{p}} x_{\boldsymbol{d},\ell}} \right) \right) \right),$$

per capita of both receiver and donor hosts (see properties and associated proofs in Sofonea *et al.* (2015) appendix D.1). Note that when the inoculation of an $\boldsymbol{r}$-class receiver host by a $\boldsymbol{p}$-class inoculum induces an acute infection instead of a chronic infection, a strong immune response is triggered which clears the host from all parasite types (namely $\phi(\boldsymbol{r},\boldsymbol{p}) = \emptyset$).

Expressed virulence (Ebert & Bull, 2008 – or overall virulence for Alizon *et al.*, 2013), is defined as the additional host mortality rate due to infection. Expressed virulence is the result of the biological activity of the parasite individuals within their host. Since each parasite individual takes part in the exploitation of the host, increasing the number of parasite individuals cannot decrease the overall exploitation. Hence, expressed virulence is a non-decreasing function of the overall parasite load. Empirically, a positive correlation has been found between expressed virulence and parasite load in various host-parasite systems (Ebert & Mangin, 1997; Kover & Schaal, 2002; de Roode *et al.*, 2008; Fraser *et al.*, 2014; Sy *et al.*, 2014). For the sake of simplicity, we assume that expressed virulence follows the simplest physiological response – linearity – with respect to the overall stationary parasite load

$$\alpha_{\boldsymbol{i}} \coloneqq \alpha \sum_{k\in\boldsymbol{i}} x_{\boldsymbol{i},k},$$

where α is a constant virulence factor. This definition is undoubtedly not valid for all biological systems and all parasite load values, however the linear approximation holds when the investigated parasite loads fall into a narrow range (which is hereafter the case because the mutation effect is assumed to be small).

Importantly, expressed virulence has to be distinguished from intrinsic parasite virulence – hereafter simply termed virulence. Indeed, a host infected by several parasite types experiences an expressed virulence that results from the inter-type interactions

that modulate the various type parasite loads. Therefore, expressed virulence coincides with virulence only for single infections (since it reflects the growth ability of the parasite type alone). The measure of virulence of any parasite type k is then $\max\{0, \alpha x_{\{k\},k}\}$ since a negative fixed point value $x_{\{k\},k} = -\varrho_k/m_{k,k}$ denotes either a failed or an acute infection, both of them being non virulent with respect to our chronic infection focus.

By definition, an increased virulence shortens the singly infected host lifetime. Virulence therefore decreases parasite fitness through single infections as there is no counter-benefit through recovery or transmission (the rates of which are equal to the constants θ and β respectively). Virulence can then only be selected because of epidemiological advantages provided by multiply inoculated hosts. This setting allows us to focus on the adaptive evolution of virulence solely due to the multiple infection context.

Adaptive evolution proceeds through consecutive mutations, a fraction of which only is selected for. As mentioned in Figure δ.2.1, one parasite individual is (uniformely) picked at random among the whole parasite meta-community (as several parasite types are dispersed in several hosts) and undergoes a phenotypic mutation that affects all its within-host growth traits. These pleiotropic mutations are assumed to be rare, hence the parasite meta-community always has enough time to reach the endemic equilibrium before the next mutation event occurs. Let $\mathcal{G}_k \subset \mathcal{G}$ be the set of extant parasite type labels right before the mutation generating parasite type k occurs (by definition, $k \notin \mathcal{G}_k$). The trait values of the mutant parasite type k are assumed to derive from those of its ancestor $a(k)$ in the following way:

$$\begin{cases} \varrho_k & \coloneqq \varrho_{a(k)} + \sigma\varepsilon_k, \\ m_{k,j} & \coloneqq m_{a(k),j} + \sigma\nu_{k,j}, \quad \forall j \in \mathcal{G}_k, \\ m_{j,k} & \coloneqq m_{j,a(k)} + \sigma\nu_{j,k}, \quad \forall j \in \mathcal{G}_k, \\ m_{k,k} & \coloneqq m_{a(k),a(k)} + \sigma\nu_{k,k}, \end{cases} \tag{δ.2.3}$$

where $\varepsilon_k, \nu_{i,j}, \forall (i,j) \in \left(\mathcal{G}_k \cup \{k\}\right)^2$ are independent random variables identically distributed according to the standard normal distribution $\mathcal{N}(0,1)$ (note that this mutation setting corresponds to the Gaussian scenario #3 in chapter 4).

Our previous one-step result raised two main questions. First, is selection still biased towards higher virulence in higher polymorphisms ($n > 2$)? Second, does the evolutionary increase in virulence persist beyond the point of epidemiological sustainability that is a virulence level so high that the parasite could not spread anymore ($\mathcal{R}_0 < 1$)? Put differently, is there any countering evolutionary force (not trade-off related) that prevents the 'evolutionary suicide' of the parasite population?

To address these questions, we ran numerical simulations of our algorithm starting from a single parasite type the basic reproduction number of which was near the $\mathcal{R}_0 = 1$ threshold. This choice is motivated by the fact that if the evolutionary increase in virulence still holds for several mutation rounds, then parasite lineages should approach the threshold quickly, making the simulation time required to answer our second question shorter.

Rather than aiming at statistical power, and for the sake of clarity, we here adopt a simple qualitative approach and present the results (Figure δ.2.2 to δ.2.9) of 10 independent simulations identically parameterized as follows (importantly, these runs have not been intentionally selected but their representativity has been checked by comparison with ninety other runs). On the within-host side, $\varrho_1 \coloneqq 1, m_{1,1} \coloneqq -1$; on the between-host side $\overset{\circ}{S} \coloneqq 1, r \coloneqq 3, \beta \coloneqq 10, \mu \coloneqq 1, \alpha \coloneqq 4, \theta \coloneqq 3$, making the basic reproduction number of the initial parasite type 1 equal to $\mathcal{R}_{0,1} = \beta\overset{\circ}{S}/\left(\mu + \theta - \alpha\varrho_1/m_{1,1}\right) = 1.25$. As for evolutionary

parameters, the mutation effect is set to be small, $\sigma := 10^{-2}$, and we follow 400 rounds.

Figure δ.2.2 illustrates how parasite trait related plots are depicted throughout the following analysis.. Each horizontal line segment corresponds to a parasite type, from its mutational origin (left end) to its extinction from the meta-community counted in mutation rounds. (Note that mutational time is different from the actual physical time since the epidemiological system reaches the endemic equilibrium before the next mutation arises – in particular, the between-mutation duration is almost zero if the mutant directly goes extinct in the host in which it appeared.) Vertical coordinates indicate trait values (here relative virulence). Vertical line segments indicate the ancestor-mutant filiation. Therefore, the topology of the resulting graph is equivalent to the phylogenetic tree of the parasite types. In Figure δ.2.2, we highlight some remarkable evolutionary patterns (see details in the legend). In this simulation, we observe that virulence clearly increases during the first sixty mutation rounds and then plateaus before wandering around in no apparent direction.

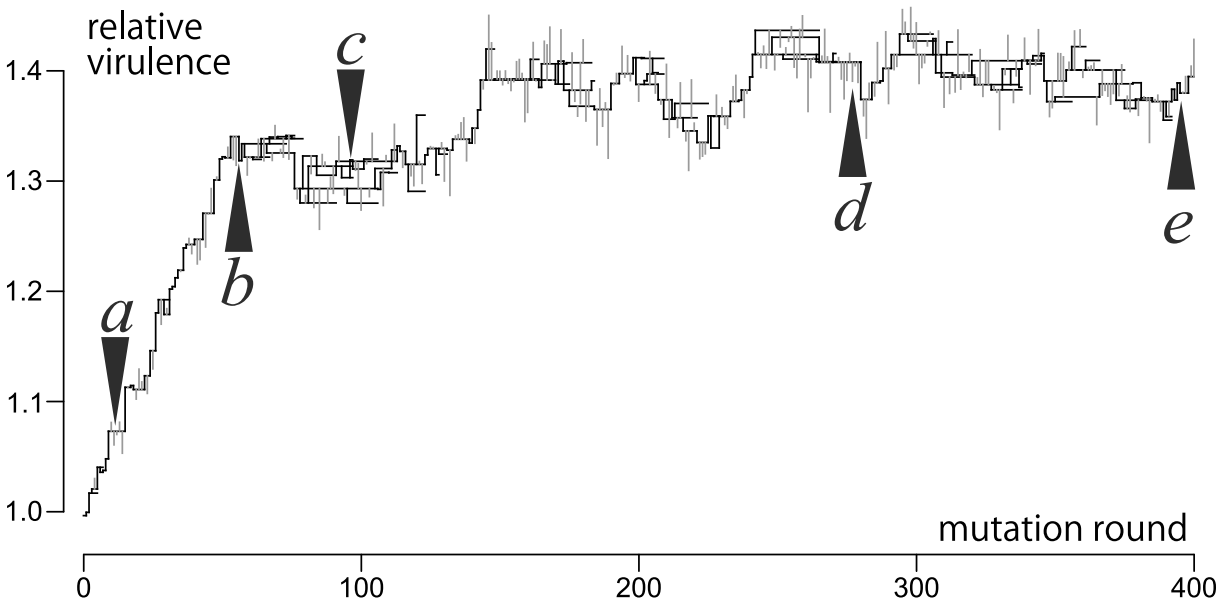

Figure δ.2.2. – Virulence phylogenetics: a commented example.
Virulence evolution of one typical run of the *in silico* evolution algorithm through 400 mutation steps. The x-axis represents the time measured in mutation steps. The y-axis represents the virulence level (normalized by the initial parasite type virulence, i.e. the stationary parasite load in single infection (SLS) $x_{\{k\},k} = -\varrho_k/m_{k,k}$). Each horizontal line segment represents the natural history of a parasite type: it originates from a mutation event at the left end and disappears from the host population at the right-end. The position of the horizontal line segments on the y-axis corresponds to the (relative) virulence level of the parasite types. The vertical line segments connect ancestor types to their mutant types. Overall, the resulting graph is a phylogenetic tree anchored in both mutational time and virulence level. Note that the mutants that fail to persist in the host population are depicted by gray vertical line segments. The parameters used are given in the main text.
Remarkable patterns are highlighted by labelled arrows: ***a***) a more virulent mutant replaces its ancestor; ***b***) a less virulent mutant replaces its ancestor; ***c***) complex evolution of a parasite meta-community (up to six types) – the virulence order accross lineages changes several times; ***d***) relatively stable monomorphism (8 consecutive mutants failed to invade); ***e***) oscillating monomorphic evolution – virulence increases then decreases twice by replacement.

This two-phase trend is confirmed by the nine other simulations investigated, as shown in Figure δ.2.3. In all runs, virulence globally increased up to around a hundred mutation rounds and then wandered about a plateau. It is interesting to note that one simulation seems to reach an apparently stable evolutionary equilibrium: the red-colored run shows no surviving mutant for more than 300 mutation rounds, supporting the hypothesis that the five resident parasite types constitute a non invadable meta-community. (Note that this kind of behaviour is not exceptional, and it has been frequently observed.)

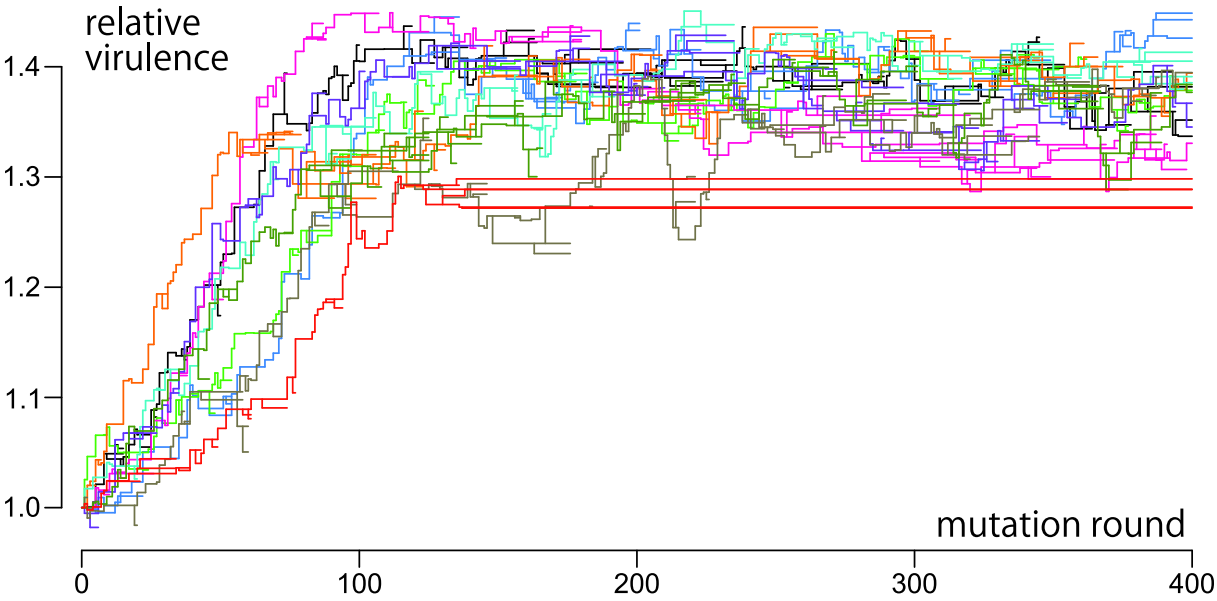

Figure δ.2.3. – Virulence phylogenetics
of 10 identically parameterized independent simulations. See Figure δ.2.2 for the graphical details and the main text for the parameter values. For the sake of clarity, only the parasite types that survive at least one mutation round are depicted.

On the contrary, the parasite type turn-over is sustained in the other runs. Figure δ.2.4 shows that the probability that a mutant survives decreases only slightly in the course of adaptation. The general survival probability calculated over the 400 mutation rounds of the 10 simulations is about 0.37. This value is much lower than that the one analytically derived in the previous chapter under the same conditions (0.5 if priorinfection prevents all mutants from survival, see the appendix). This difference is almost fully explained by the fact that, here; the resident parasite population is not always monomorphic.

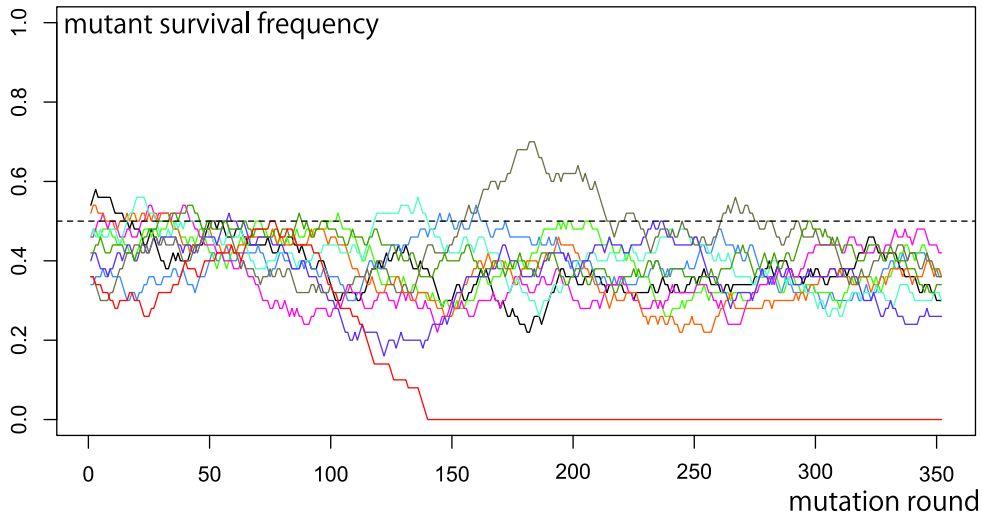

Figure δ.2.4. – Frequency of surviving mutants.
Proportion of arising mutants that survive, at least for one mutation round, in the host population. It is computed as the mean of $\left[\sum_{i \in \varphi(\mathcal{G}_{k+1}) \cap \{k\}} \widehat{I}_i > 0\right]$ averaged over a rolling window of 50 mutation rounds.
(The color code is identical to that of Fig. δ.2.3.)

As shown in Figure δ.2.5, monomorphism is far from being the rule. Averaging over all mutation rounds and runs, 62% of the mutants appear in an already polymorphic meta-community in which the survival probability is considerably lower (ca. 0.32) compared to that observed in the monomorphic cases (ca. 0.44). Interestingly, monomorphic and polymorphic periods alternate (except for the particular red-colored simulation/last row in Figure δ.2.5) but the latter are much more frequent in the second evolutionary phase (ca. 71% of endemic equilibria are polymorphic after the 100^{th} mutation round, but only 34% before). Here, diversity never exceeds seven parasite types circulating at a time.

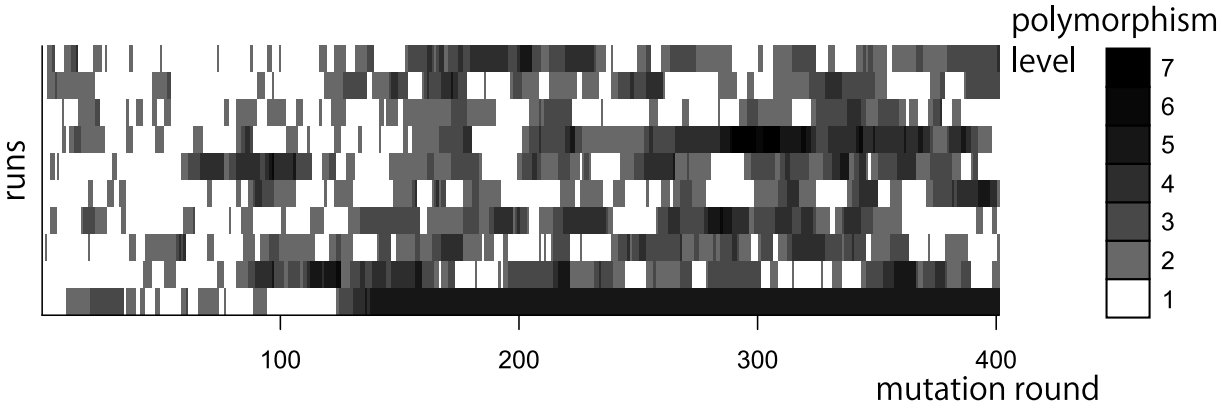

Figure δ.2.5. – Polymorphism level.
For the 10 simulations (in rows), the grayscale indicates at each mutation round how many parasite types have reached the endemic equilibrium. The polymorphism level associated to each shade is given in the right bar. In particular, monomorphism is denoted by white tiles.

Let us now try to understand why virulence initially increases and then stagnates on the evolutionary time scale. We have seen that this cannot be due to an absence of diversity input as new mutants regularly survive and eventually get fixed. It is also not because mutation is biased in terms of virulence: over all mutation rounds and all simulations, the proportion of mutants that are more virulent than their ancestor is about 0.50, as shown in Figure δ.2.6.

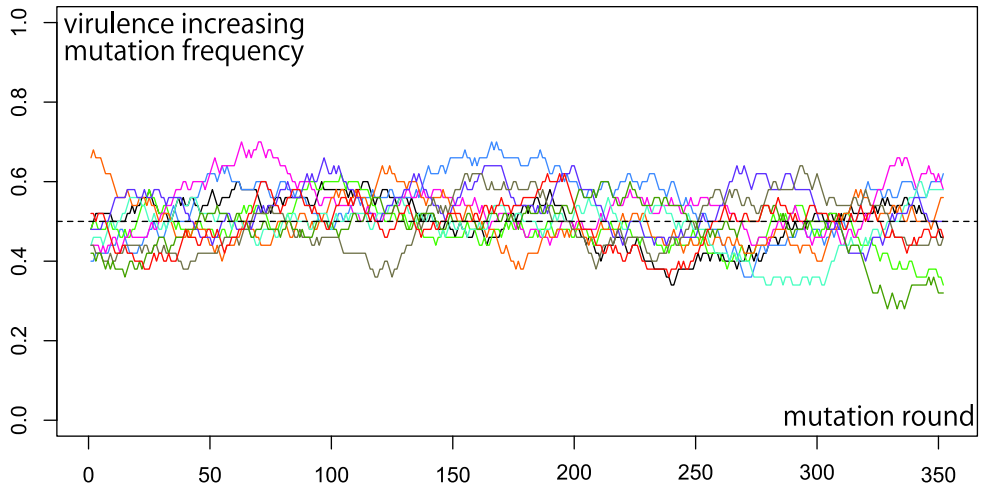

Figure δ.2.6. – Frequency of virulence increasing mutations.
Proportion of mutants including those that fail to persist within or between the hosts that are more virulent than their ancestor. It is computed as the mean of $\left[x_{\{k\},k} > x_{\{a(k)\},a(k)}\right]$ averaged over a rolling window of 50 mutation rounds. Note that this proportion drops to 0 for the red-colored simulation since an evolutionary stable meta-community has been reached.
(The color code is identical to that of Fig. δ.2.3.)

Therefore, the explanation of the two-phase evolution of virulence must lie in the association between survival and virulence, namely the virulence selection bias. In Figure δ.2.7, this bias clearly shows the same slope break visible in Figure δ.2.3 at about 100 mutation rounds. Before this point, a substantial majority (ca. 70%) of the surviving mutants is more virulent than their respective ancestors. After that point, the selection bias drops below 0.55 and slowly decreases through mutational time. On the investigated time scale, virulence evolved towards an almost stable evolutionary value. In adaptive dynamics terms (Geritz *et al.*, 1998; Dieckmann, 2002), this virulence level (ca. 5.50) is a quasi-continuously stable strategy since it attracts evolutionary trajectories that start nearby and its further evolution is limited (he red-colored run is again an exception since the stable meta-community impeded further evolution). The difference with the classical adaptive dynamics framework lies in the fact that several traits are here co-evolving, the number of which varies with the changing polymorphism level.

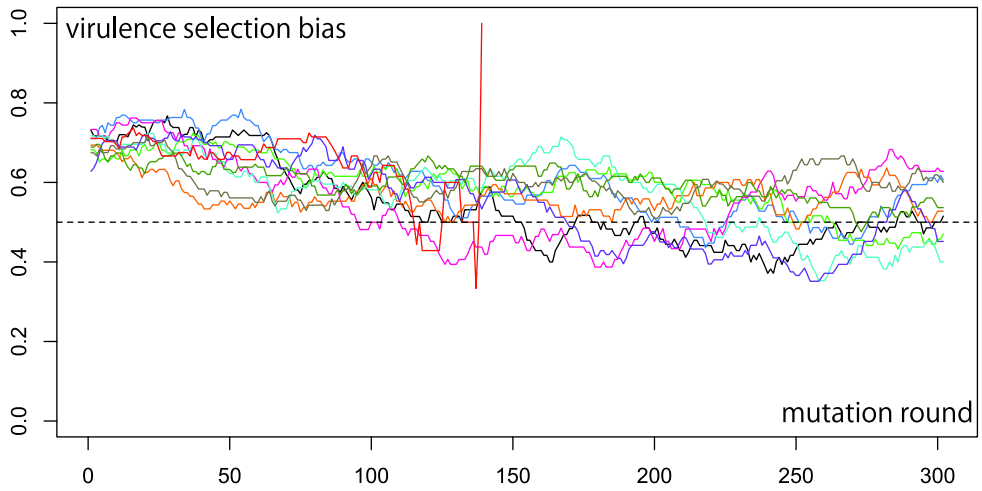

Figure δ.2.7. – Virulence selection bias.
Proportion of mutants that are more virulent than their ancestor among those that survive. It is computed as $\left[x_{\{k\},k} > x_{\{a(k)\},a(k)}\right]$ averaged over all mutation rounds for which $\left[\sum_{\boldsymbol{i}\in\wp(\mathcal{G}_{k+1})\cap\{k\}} \widehat{I}_{\boldsymbol{i}} > 0\right]$ within a rolling window of 100 mutation rounds. Notice that the peak of the red-colored simulation (the last value of the curve is 1) is due to the fact that no mutant survives after that mutation round. (The color code is identical to that of Fig. δ.2.3.)

In our setting, virulence depends on exactly two evolving parasite traits, namely the intrinsic growth rate ϱ_k and the self interaction trait $m_{k,k}$. The resulting virulence is proportional to $-\varrho_k/m_{k,k}$. This quantity is positive if and only if $\varrho_k > 0$ and $m_{k,k} < 0$. Therefore both traits are positively correlated with virulence within these respective ranges. To understand the observed virulence evolution more precisely, it is necessary to look at how these two traits co-evolve. Figure δ.2.8 displays the evolution of these two traits, along with that of the cross-interaction traits (depending on whether the focal type is by the mutant or the resident types). For all four traits, we observe two evolutionary phases, the shift taking place around the 100$^{\text{th}}$ mutation round.

While the shift in the intrinsic growth rate evolution only results in a slower increasing slope, the interaction trait evolution show a non-monotonic behaviour: first increasing and then decreasing. The evolution of the interaction traits appears congruous on the long term.

Self and cross interaction traits experience distinct selective pressures in general but here, these straits are evolutionarily linked because of the recurrent monomorphic phases. As seen in Figure δ.2.5, the parasite population is indeed rarely polymorphic for long periods of time and diversity frequently drops to a single type. When this happens, the self and cross interaction trait values become inevitably close again. This is due to the fact that all these traits derive from the same value, the one of the ancestor's self interaction trait $m_{a(k),a(k)}$ (see the mutation setting δ.2.3 applying to the only other parasite type $j := a(k)$). As a consequence, the evolution of the cross interaction traits follows that of the self interaction trait because of these bottlenecks. (We then do not address the evolution of the cross interaction traits further.)

Having shown that virulence evolution can be understood by the evolution of only two traits, ϱ_k and $m_{k,k}$, the next interpretation of the previous observations requires to bear in mind that an initially rare parasite type k introduced, by inoculation or mutation, in

an already infected $\boldsymbol{d}$-class host ($\boldsymbol{d} \neq \emptyset, k \notin \boldsymbol{d}$) grows if and only if

$$\frac{\partial f_k}{\partial X_k}\left(x_{\boldsymbol{d},1},\ldots,x_{\boldsymbol{d},n}\right) = \varrho_k + \sum_{j\in\boldsymbol{d}} m_{k,j}x_{\boldsymbol{d},j} > 0. \tag{δ.2.4}$$

It results that a surviving mutant k is likely to show a highly positive ϱ_k. But growing within the host in which it appeared does not guarantee the mutant its survival at the between-host level so the mutant must also ensure its transmission to other hosts.

In our model, we have assumed that multiply infected hosts produce the same number of propagules as singly infected hosts, so coinfecting parasite types have to split the overall transmission rate. Besides, the differences in expressed virulence compensate each other on average – some multiply infected host classes experience higher expressed virulences than singly infected hosts (synergistic effect), and other lower (inhibition effect). Each parasite type is then less transmitted from multiply infected hosts than from singly infected hosts. Consequently, a mutant parasite is more likely to reach the next endemic equilibrium if it can prevent secondary infections (which would lead to a decrease in transmission at least, and to a competitive exclusion at worst).

Swapping the type labelling in (δ.2.4), and taking $\boldsymbol{d} := \{k\}$, it follows that a mutant prevents secondary infections if and only if $\varrho_j - m_{j,k}\varrho_k/m_{k,k} < 0$. It results that surviving mutant k is also likely to show a lowly negative $m_{k,k}$. This reasoning explains the first phase of virulence evolution: a rapid increase due to a correlative increase in both the intrinsic growth rate and the self interaction trait. However, this does not hold for the second phase, where $m_{k,k}$ decreases instead of increasing (Fig. δ.2.8**B**).

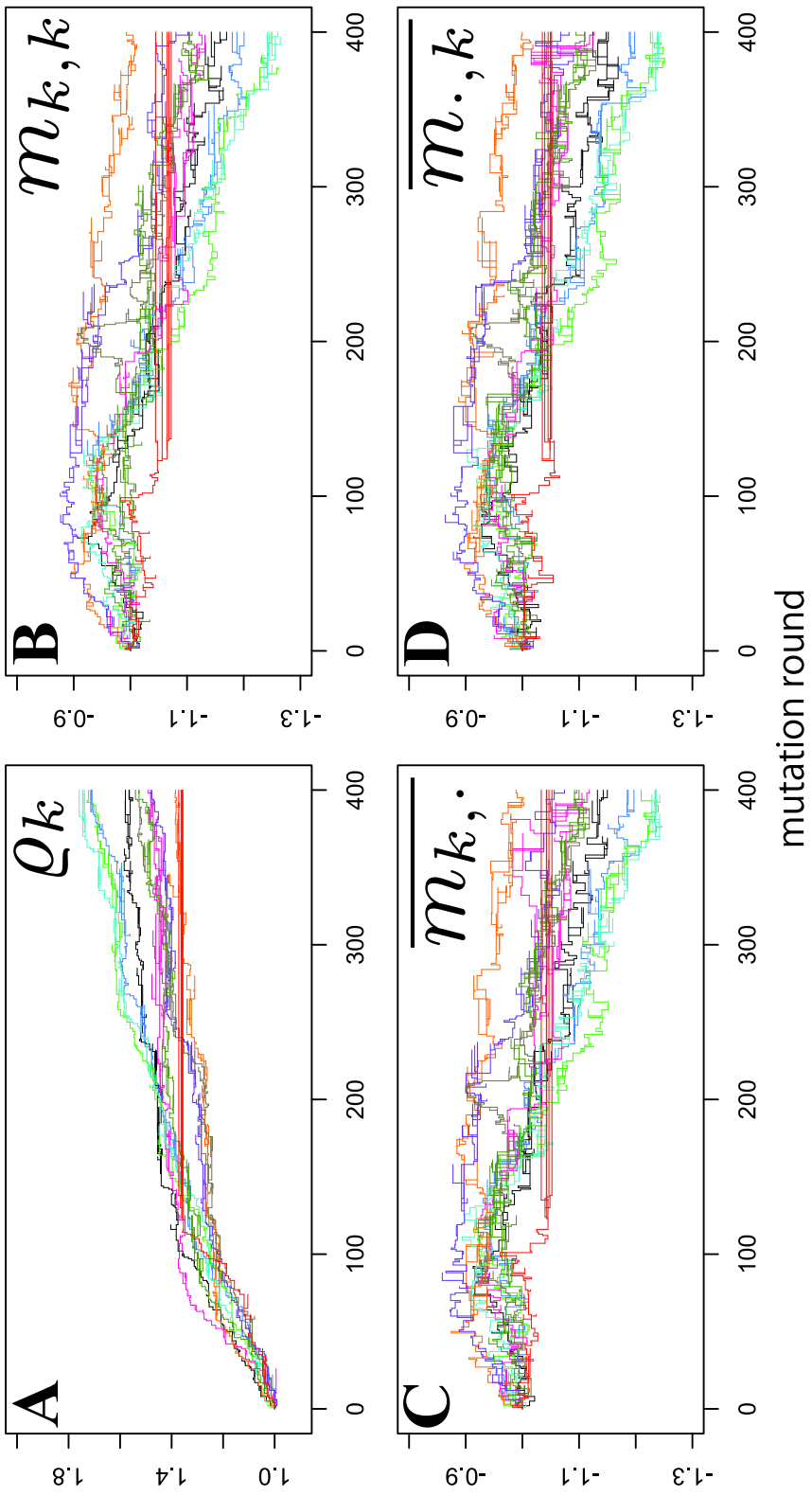

Figure δ.2.8. – Within-host trait phylogenetics.
A) Evolution of the intrinsic growth rate ϱ_k. **B**) Evolution of the self interaction trait $m_{k,k}$. **C**) Evolution of the average interaction undergone by the mutant from the parasite types present at the round the mutation arises, namely $\overline{m_{k,\cdot}} := \left(\mathrm{Card}\,\mathcal{G}_k\right)^{-1} \sum_{j\in\mathcal{G}_k} m_{k,j}$. **D**) Evolution of the average interaction from the mutant experienced by the parasite types present at the round the mutation arises, namely $\overline{m_{\cdot,k}} := \left(\mathrm{Card}\,\mathcal{G}_k\right)^{-1} \sum_{j\in\mathcal{G}_k} m_{j,k}$.
(The color code is identical to that of Fig. δ.2.3.)

By the first evolutionary phase, the parasites have reached a higher virulence level which, importantly, shortens the lifespan of the singly infected hosts. As a result, singly infected hosts are to die from the single infection than to be secondary infected. This can be observed by the decrease in the proportion of infected hosts that are infected by several parasite types simultaneously (Figure δ.2.9). Because rule (δ.2.4) still applies, surviving mutants are still likely to have a higher intrinsic growth rate than their ancestors. This is why the selective pressure on the self interaction trait reverses. The fitness loss due to secondary infections becomes negligible while the lifespan of singly infected hosts approaches the minimum value allowing to persist in the host population. Therefore, only the mutants that have a strong enough self competition (low $m_{k,k} < 0$) to compensate the increase in ϱ_k – that made them succeed in the host in which they appeared – do survive. In the end, virulence remains almost constant and the anti-correlated evolution of ϱ_k and $m_{k,k}$ explains the second phase of the observed virulence evolution (Fig. δ.2.8**B**).

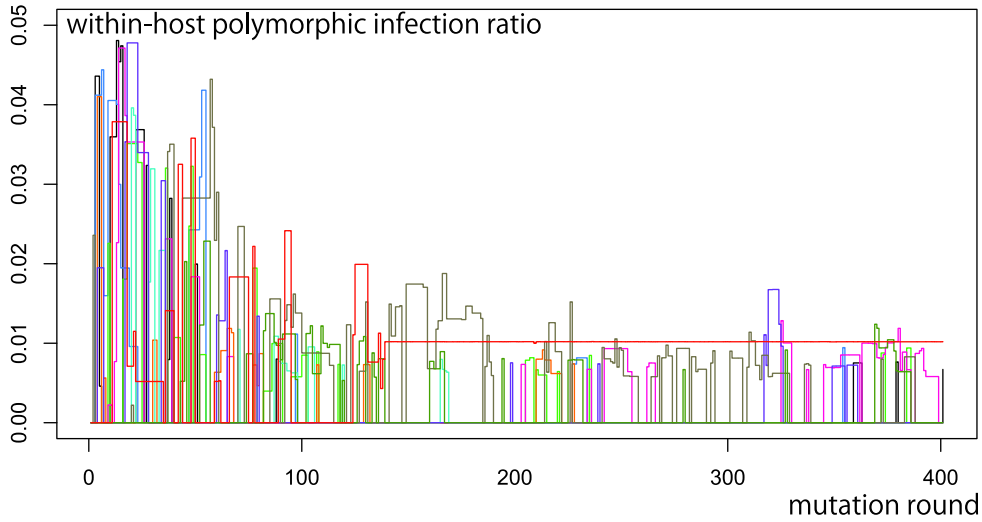

Figure δ.2.9. – Within-host polymorphic infection ratio.
The proportion of hosts infected by more than one parasite type at a given time among all infected hosts, based on their density at the endemic equilibrium, that is $\varpi := 1 - \left(\sum_{k \in \mathcal{G}} \widehat{I_{\{k\}}}\right) / \left(\sum_{\boldsymbol{i} \in \wp(\mathcal{G}), \boldsymbol{i} \neq \emptyset} \widehat{I_{\boldsymbol{i}}}\right)$. The observed values are relatively low because of the low basic reproduction of the initial parasite type itself ($\mathcal{R}_{0,1} = 1.25$). The sawtooth pattern is caused by the monomorphic periods that drive ϖ to 0 by definition.
(The color code is identical to that of Fig. δ.2.3.)

In our model, virulence is a pure cost for parasites in single infections, since it is not correlated with transmission nor with recovery. In the absence of any related trade-off (Levin & Pimentel, 1981; Anderson & May, 1982; Alizon *et al.*, 2009), the basic reproduction number $\mathcal{R}_0$ is a decreasing function of virulence. Had our model been a simple epidemiological setting with generalized mutual exclusion, then $\mathcal{R}_0$ would have followed an optimization principle (Metz *et al.*, 2008; Lion & Metz, 2017), that is mutants with higher $\mathcal{R}_0$ would always replace their ancestor, driving the host population to a minimum density, as in one-resource competition models (Tilman, 1982; Mylius & Diekmann, 1995). In this setting, one would then expect virulence to evolve towards as low as possible values (Smith, 1904; Méthot, 2012). The fact that we observe an increase in virulence proves the role of multiple infections as a driver of virulence evolution, even if multiply infected hosts are not frequent or even possible (as in the superinfection pattern, see previous chapter). Figure δ.2.10 indicates that the basic reproduction number of successive para-

site types actually decreases, confirming that $\mathcal{R}_0$ does not follow an optimization principle in multiple infection contexts. The underlying trait evolution highlighted above explains why $\mathcal{R}_0$ approaches 1 but does not go beyond this threshold, which would have led to the evolutionary suicide of the parasite.

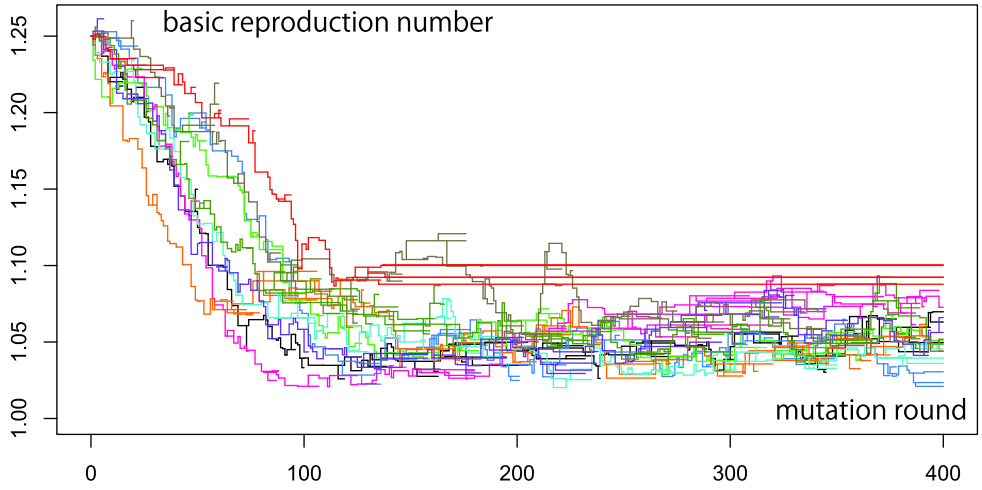

Figure δ.2.10. – Basic reproduction number phylogenetics.
Expected number of secondary infections a host singly infected by each parasite type would cause during its entire infectious period, had the host population been completely susceptible (namely at the disease free equilibrium $(I_{\boldsymbol{i}})_{\boldsymbol{i}\in\wp(\mathcal{G})} = \left(\mathring{S},0,\ldots,0\right)$. It is computed as $\mathcal{R}_{0,k} \coloneqq \beta\mathring{S}/\left(\mu+\theta-\alpha\varrho_k/m_{k,k}\right)$.
(The color code is identical to that of Fig. δ.2.3.)

Finally, it is interesting to observe that while the parasite evolves towards higher virulence, its average impact on the host population actually diminishes. Indeed, the average host mortality plotted in Figure δ.2.11 evolves in a similar way as the basic reproduction number. Of course, infected hosts have a shorter lifespan as virulence evolutionarily increases. However, the evolutionary increase in virulence drives the parasite to spread less, which consequently increases the host population size while decreasing total prevalence, as shown in Figures δ.2.12 and δ.2.13 respectively. Therefore overall, and somehow counter-intuitively, the evolution of virulence, despite its evolutionary increase, turns out to be beneficial for the host population.

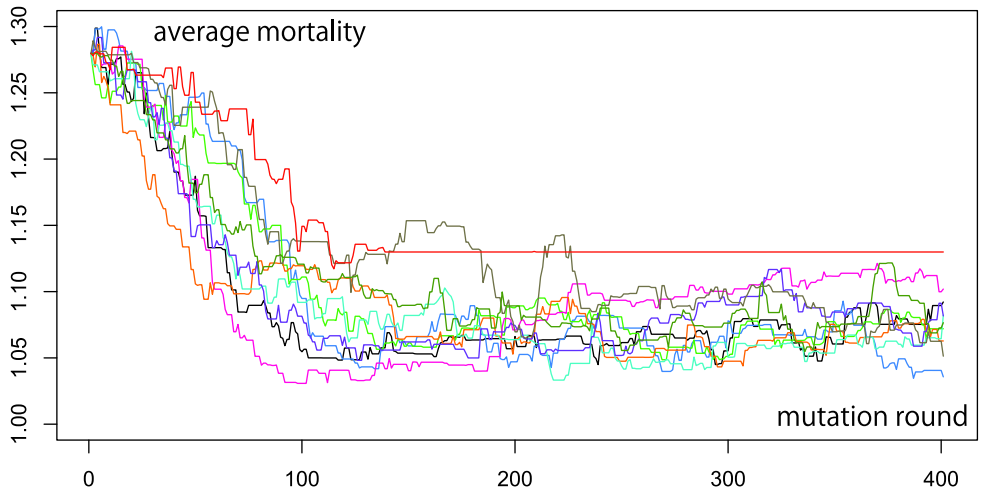

Figure δ.2.11. – Average host mortality.
The average host mortality is the mean rate at which a host dies, may it be infected or susceptible. It is computed as the (constant) natural mortality rate plus the expressed virulence averaged over all host classes according to their density at the endemic equilibrium, namely $\overline{\mu}^H := \mu + \alpha\left(\sum_{\boldsymbol{i}\in\wp(\mathcal{G})} \widehat{I}_{\boldsymbol{i}} \sum_{k\in\mathcal{G}} x_{\boldsymbol{i},k}\right) / \left(\sum_{\boldsymbol{j}\in\wp(\mathcal{G})} \widehat{I}_{\boldsymbol{j}}\right)$ (note that the expressed virulence experienced by susceptible hosts is 0 ($\alpha x_{\emptyset,k} = 0, \forall k \in \mathcal{G}$).
(The color code is identical to that of Fig. δ.2.3.)

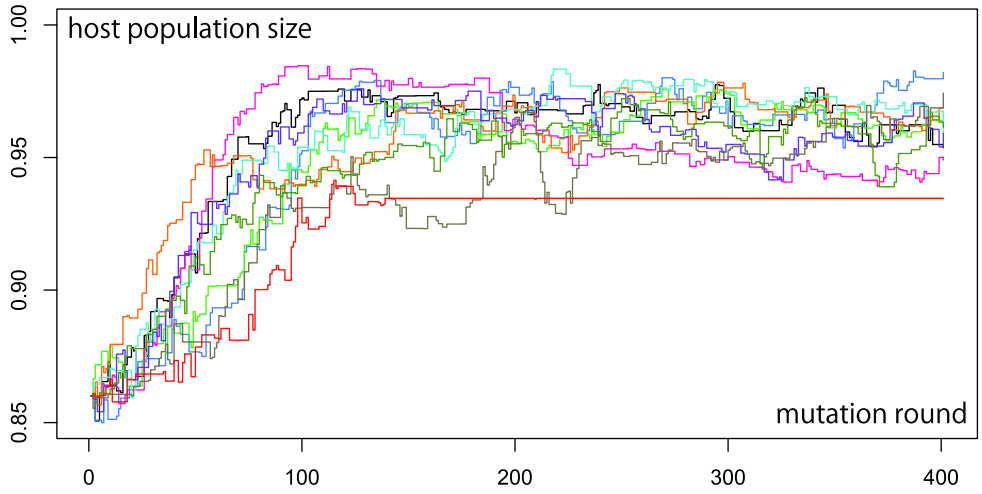

Figure δ.2.12. – Total host population size.
The total host population size is the sum of host densities over all host classes at the endemic equilibrium, namely $\widehat{N} := \sum_{\boldsymbol{i}\in\wp(\mathcal{G})} \widehat{I}_{\boldsymbol{i}}$.
(The color code is identical to that of Fig. δ.2.3.)

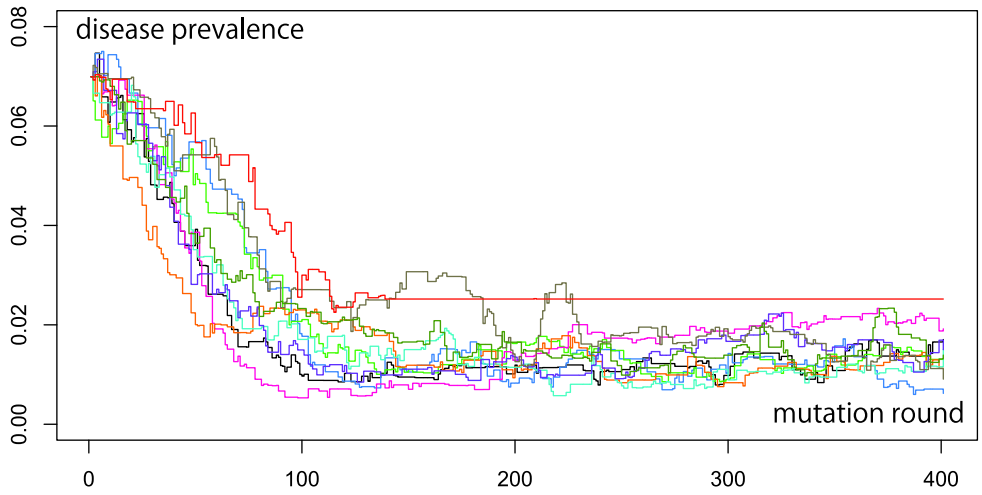

Figure δ.2.13. – Total prevalence.
The total prevalence is the proportion of infected hosts among all hosts. It is computed at the endemic equilibrium as $p = 1 - \widehat{I_\varnothing}/\widehat{N}$.
(The color code is identical to that of Fig. δ.2.3.)

To conclude, this numerical study confirms the selection bias we found in our previous study. The evolutionary increase in virulence, driven by the necessity to escape from the ancestor (and potentially other parasite types) that already infects the host in which the mutant arises, holds for higher polymorphism levels. The adaptive sequence nonetheless avoids evolutionary suicide thanks to an epidemiological feedback that shifts the survival criterion from secondary infection prevention to virulence limitation (interestingly, this emerging evolutionary shift relates to the conditional strategies mentioned by VAN BAALEN & SABELIS (1995) about hypothetical parasite plastic strategy of host exploitation). The resulting apparent impediment of further virulence evolution actually conceals a persisting and gradual evolution of both the intrinsic growth rate and the self interaction trait. This observation reminds that the parasite's growth rate is not a sufficient descriptor of its virulence and might explain why LEGGETT *et al.* (2017) found a negative correlation between growth rate and virulence in human pathogens.

We acknowledge that we have focused here on a single algorithm configuration. Nonetheless, we did consider alternative settings, which we hereafter discuss. Runs starting from higher values of $\mathcal{R}_{0,1}$ result in a monotone, globally constant-slope, increase of virulence and later reach the plateau in a comparable way as the simulations shown previously. Runs with several starting parasite types lead to qualitatively similar results since one parasite lineage took over the host population sooner or later. Runs with larger mutation effects behave more erratically but the two-phase pattern was preserved. Finally, complexifying the within-host model with each parasite type producing one kind of public good and one type of spite (see SOFONEA *et al.* (2015)) does not affect this trend.

Besides evaluating the robustness of these results to other mutation settings – and in particular in the case where monomorphic phases are less frequent such that the interaction traits evolutionarily decorrelate –, future studies should analyze and understand the pattern of interactions that shape the apparent evolutionary stability of parasite metacommunities such as the red-colored simulation pointed out so far.

D Discussion générale

D.1. Contexte

Le parasitisme est une interaction essentielle du monde vivant depuis des centaines de millions d'années (Bassett *et al.*, 2004). Sa manifestation la plus proximale, les maladies infectieuses, demeure un défi de santé publique majeur (Dye, 2014). Mais le parasitisme ne saurait se réduire à un enjeu de recherche appliquée : il constitue un objet d'étude exceptionnellement diversifié tant sur le plan spatial – des interactions moléculaires (Pollitt *et al.*, 2014) aux impacts écosystémiques (Thomas *et al.*, 2005) – que temporel – de la réaction immunitaire (Nazzi *et al.*, 2012) à la co-évolution adaptative (Ebert, 2008) –, phylogénétique – du coucou (Brooke & Davies, 1988) aux virus d'archées (Prangishvili *et al.*, 2006) – en enfin méthodologique – de l'échantillonnage de terrain (Lievens *et al.*, 2016) aux fonctions de Lyapunov (Korobeinikov & Maini, 2004).

Loin de pouvoir aborder l'ensemble des facettes du parasitisme, le présent travail a pour objectif d'apporter un éclairage théorique synthétique et original sur l'épidémiologie et l'évolution des parasites à la lueur de leur polymorphisme, dont la réalité établie (Read & Taylor, 2001) réduit la portée des modèles canoniques reposant sur le monormophisme (Keeling & Rohani, 2008). Ce travail s'inscrit donc dans la vaste et hétérogène démarche de généralisation des modèles d'épidémiologies classique et évolutive initiée il y a déjà plus de trois décennies (Levin & Pimentel, 1981).

L'évolution des parasites reposant sur leur transmission entre les hôtes et cette dernière étant déterminée par leur reproduction au sein des hôtes, l'emboîtement de ces processus (Mideo *et al.*, 2008) aux échelles spatio-temporelles distinctes, nous est apparu comme la fondation indispensable de toute modélisation à prétention généralisatrice, jusqu'ici négligée ou réduite à des hypothèses trop fortes pour en appréhender la diversité biologique observée (Rigaud *et al.*, 2010). Le présent travail s'est donc tout particulièrement attaché à construire, au moyen de méthodes éprouvées par les mathématiques appliquées et de modélisations familières de la biologie théorique, les bases d'un nouveau cadre théorique pour l'épidémiologie évolutive des infections multiples, avant de tenter d'apporter sa contribution à la compréhension scientifique de la virulence parasitaire.

D.2. Synthèse des résultats

Ce travail a mis en avant l'étonnante diversité des ensembles d'issues d'inoculation compatibles (chapitre 2), y compris à partir de dynamiques de croissance parasitaire d'apparence sommaires mais à l'analyse non triviale (chapitre 1). D'une part, il fallait donner un sens et un support biologique à ce « bestiaire » combinatoire (chapitre 2). D'autre part, ces observations devant servir de lien mécanique entre le niveau intra-hôte et le niveau inter-hôte (chapitres 3 et 4), il fallait leur donner une forme manipulable. C'est ce qui a motivé notre définition du patron d'infection (chapitres 2, 3, et 4), qui généralise les infections multiples en s'affranchissant des hypothèses qui conduisaient inéluctablement à l'une ou l'autre des alternatives de l'arbitraire dichotomie super-/coinfection.

La promotion de la typologie des patrons d'infections ici introduite constitue un triple apport pour l'épidémiologie des infections multiples : *i*) la mise à plat d'une terminologie existante confuse, *ii*) l'éclairage de certains systèmes biologiques dont les observations naturalistes ou expérimentales n'avaient pas de support théorique (chapitre 2) et *iii*) l'unification des dynamiques épidémiologiques sous une approche modulable (chapitre 3). Sur le plan évolutif, les patrons identifiés ont permis d'inscrire l'analyse d'invasion de parasites mutants de traits de croissance dans un cadre d'une généralité inédite. Ils sont donc à l'origine du principal résultat du présent travail : la mise en évidence d'une augmentation inévitable de la virulence des parasites, inhérente au polymorphisme (chapitre 4). Cette observation, confirmée numériquement (chapitre δ), fournit un support théorique au rapprochement des virulences collatérale et de compétition et vient enrichir le corpus d'explication évolutive du maintien de la virulence, au même titre que la très documentée virulence de compromis (Alizon *et al.*, 2009) et que la virulence imposée par le cycle de vie telle que montrée dans l'introduction de ce travail (chapitre 0).

D.3. Limites

À l'origine de l'intérêt et de la richesse de la recherche en modélisation en biologie réside la possibilité de faire appel à multitude d'approches issues des sciences formelles (Otto & Day, 2007; Haefner, 2012; Broom & Rychtár, 2013). Ainsi, la construction et l'étude des modèles ici abordés ont modestement emprunté à divers champs des mathématiques : systèmes dynamiques, algèbre linéaire, théorie des jeux, combinatoire, probabilités élémentaires. Les résultats qui en sont issus héritent inéluctablement des contraintes que ces formalismes imposent (citons par exemple la distribution exponentielle des temps d'attente qui sous-tendent les équations différentielles ordinaires employées) et demeurent conditionnés par des hypothèses de travail simplificatrices. Néanmoins, nombre de celles formulées dans de précédents modèles ont été ici levées (au premier rang desquels viennent le patron d'infection imposé et la relation virulence - compétitivité).

Pour s'affranchir des hypothèses simplificatrices restantes, une banale complexification des équations peut suffire, citons notamment l'homogénéité des hôtes, la petite taille des inocula relativement à la charge parasitaire totale, l'absence de délais, de mémoire immunitaire, de vecteur de transmission et la densité-dépendance de celle-ci. D'autres hypothèses requièrent quant à elles, pour être levées, un changement en profondeur des modèles conjointement à l'apport de méthodes mathématiques plus avancées, il s'agit en particulier du déterminisme des dynamiques intra- et inter-hôte, de la chronicité des infections et de la séparation des échelles de temps, de l'absence de spatialisation des hôtes. Le recours aux processus stochastiques et aux équations aux dérivées partielles apparait alors évident. Toutefois, s'affranchir de toutes ces hypothèses simultanément relève de la prouesse technique et ne peut vraisemblablement s'opérer qu'au détriment de la lisibilité, de la compréhension et de l'interprétation du système. De fait, rien ne garantit que l'étude des modèles issus d'une particularisation ou d'une généralisation des modèles ici présentés puisse être menée au même niveau d'aisance que celle de ces derniers, et qu'elle ne se borne pas à des cas-exemples décrits numériquement. Puisqu'aucun modèle ne peut simultanément optimiser son réalisme, son intelligibilité et sa généralité (cf. encadré **[a]** p.29), c'est à la communauté scientifique qu'il revient de s'accorder sur les questions auxquelles il peut apporter des réponses pertinentes, et celles sur lesquelles il n'apporte aucun éclairage, rappelant au passage l'importance de l'énoncé du problème initialement posé.

D.4. Perspectives

Identifiées, les limitations des nos modèles deviennent le point de départ naturel de travaux futurs dont quelques pistes sont présentées ci-après.

D.4.1. Implications de l'hôte

Le grand absent de notre modélisation est sans aucun doute l'hôte. Afin d'isoler les effets imputables à la seule multiplicité des types parasitaires, nous avons jusqu'ici traité les hôtes comme de simples sites d'immigration, reproduction et émigration des parasites, supports passifs (exception faite de la guérison), identiques et constants. Or l'interaction parasite-hôte est une relation bilatérale. L'immunité de l'hôte peut être modifiée suite à l'infection et la guérison par un type de parasite et prévenir une infection ultérieure par ce même type (mémoire immunitaire), voire un type antigéniquement proche (immunité croisée). L'intégration de l'historique immunitaire au contexte d'infections multiples conduit à des modèles dont l'analyse n'est pas aisée (Andreasen *et al.*, 1997). Dans ce cas, étudier l'épidémiologie sous le prisme du statut infectieux adjoint de l'hypothèse selon laquelle l'immunité croisée réduit la contagiosité (plutôt que la susceptibilité) permet de réduire la dimensionnalité des modèles et ainsi d'en faciliter l'étude, comme par exemple dans le cas du virus de la grippe (Ballesteros *et al.*, 2009). Lorsque l'immunité adaptative n'est plus une composante négligeable du système épidémiologique, il est intuitif de s'attendre à ce que la virulence évolue vers des valeurs intermédiaires, dans la mesure où s'affrontent deux pressions de sélection opposées : la réduction des hôtes immunologiquement susceptibles favorise les parasites qui les exploitent avec prudence tandis que l'exclusion par compétition apparente bénéficie aux parasites plus virulents activant le système immunitaire (Bashey, 2015). En outre, l'immunité n'est pas la seule fonction physiologique de l'hôte modulée par les parasites : l'investissement dans la reproduction est un trait d'histoire de vie connu pour être anticipé en cas d'infection (Agnew *et al.*, 2000). Malgré tout, la composante stérilisante de la virulence, de même que la morbidité, est souvent ignorée dans les modèles, du fait des rétro-actions épidémiologiques complexes qu'elle induit via la démographie de l'hôte, rétro-actions dont l'intensité est notamment amplifiée par la structure spatiale et les infections multiples (Abbate *et al.*, 2015).

Si nous n'avons d'ailleurs pas abordé l'évolution des hôtes, c'est qu'elle est le plus souvent négligeable devant celle du parasite, à l'image des épidémies à EBOV – un virus émergent, qui plus est à ARN, infectant un mammifère au temps de gestation parmi les plus élevés de sa classe. L'évolution de l'hôte est d'autant plus évidente que son cycle de vie est court ou sa taille de population faible (Buckling & Rainey, 2002). Pour de grandes échelles de temps, l'évolution de l'hôte peut, entre autres, être approchée par l'étude comparative des phylogénies (Manceau *et al.*, 2016). Les adaptations du parasite modifient les pressions de sélection pesant sur l'hôte et réciproquement : l'hôte et le parasite co-évoluent (Ebert, 2008). Cette « course aux armements » à laquelle ils se livrent au fil des générations constitue l'illustration canonique de l'hypothèse de la Reine Rouge (Van Valen, 1973), qui postule que les pressions de sélection régissant l'évolution des entités biologiques sont essentiellement d'ordre biotique et résident en particulier dans les interactions, directes comme indirectes, qu'ils entretiennent mutuellement. En particulier, l'adaptation des hôtes à l'infection endémique du parasite tend à abaisser les charges parasitaires et la virulence que les hôtes au cours des générations d'hôtes. De fait, on distingue la résistance, lorsque la diminution concerne conjointement la charge parasitaire et la virulence (la baisse de la seconde étant due à celle de la première), de la tolérance, qui correspond à une baisse de virulence à charge parasitaire constante.

L'étude théorique de l'évolution de ces deux traits, partagés entre l'hôte et le parasite au même titre que la virulence elle-même, a souvent été menée du point de vue de l'hôte (Little *et al.*, 2010). Or, si l'on considère au contraire le déterminisme parasitaire de ces traits (on peut imaginer la résistance comme la faculté opposée à l'échappement immunitaire), de nouvelles questions relatives à l'évolution des infections multiples émergent. La première étant : au sein d'un hôte coinfecté, les résistances et tolérances de chacun des types parasitaires s'additionnent-elles ? Comment distinguer par ailleurs la résistance totale des effets de la compétition intra-hôte sur les charges parasitaires ? Comment la virulence des parasites évolue-t-elle si la tolérance propre de chaque type varie tandis que la virulence totale subie par les hôtes co-infectés est liée à la charge parasitaire totale, elle-même modulée par la compétition ? Ces questions illustrent la non trivialité de l'évolution de la virulence lorsque celle-ci est fonction de la résistance et tolérance (la distinction entre ces deux traits étant par ailleurs discutable, comme le suggère les modèles spatialisés de Débarre *et al.* (2012) et Lion & Gandon (2015)).

D.4.2. Symbioses et systèmes d'études

Les parasites ne sont pas les seuls micro-organismes vivant au sein des hôtes. Nombreux sont ceux, en premier lieu les animaux possédant un tube digestif, qui hébergent naturellement des bactéries commensales ou mutualistes, aussi appelées symbiotes. Chez l'Homme, le nombre de ces bactéries est au moins du même ordre de grandeur que celui de cellules eucaryotes (Sender *et al.*, 2016). Or il est désormais bien établi que ces bactéries jouent un rôle actif dans la susceptibilité des hôtes aux infections et modulent la virulence de celles-ci (Mouton *et al.*, 2004; Murall *et al.*, 2017). Remplacer un des types parasitaires dans les modèles ici présentés par une espèce symbiotique serait le premier pas vers la prise en compte de cette composante de l'hôte dans l'évolution de la virulence des parasites. On peut s'attendre, en première approximation, à ce que cette dernière évolue selon sa corrélation avec les traits qui permettent au parasite d'exclure ou du moins de diminuer l'effet anti-parasitaire du symbiote, au moins jusqu'au point où la présence symbiote devient bénéfique pour le parasite (par rétro-action épidémiologique, via la valeur sélective de l'hôte).

Les communautés microbiotiques sont les équivalents symbiotiques des infections multiples. Elles constituent du reste un sujet de recherche majeur. La faible diversité de son microbiote lorsqu'élevée en laboratoire – une dizaine d'espèces bactériennes (Staubach *et al.*, 2013) – fait de *Drosophila melanogaster*, déjà organisme modèle en génétique et embryologie, le système biologique idéal pour étudier expérimentalement la stabilité de telles communautés. Les bactéries étant mutualistes envers l'hôte drosophile, mais pas nécessairement entre elles, de futures études pourront s'attacher à quantifier l'impact des interactions entre espèces bactériennes sur leur croissance. Ces données pourront être interprétées à la lueur du modèle de croissance intra-hôte ici présentée, dans le but de le confirmer, de le modifier, voire de le calibrer afin de réaliser des prédictions sur la variation de la prévalence de chaque espèce bactérienne ou de chaque association d'espèces au cours des générations d'hôtes.

Une autre approche empirique des communautés microbiotiques réside dans l'étude d'un groupe parasite de polymorphisme au contraire très élevé et de pathogénicité à forte variance. C'est le cas, entre autres, des papillomavirus (HPV), dont on recense plus de deux cents types circulant dans les populations humaines (Bzhalava *et al.*, 2015). Les individus infectés le sont souvent par plusieurs types mais la distribution des co-occurrences est loin de suivre des tirages indépendants (Garland *et al.*, 2009), bien qu'il faille corriger pour des effets fondateurs et spatiaux. On peut se demander si des interactions de facilitation ou d'exclusion entres types permettent d'expliquer les patrons de prévalence des

classes d'hôtes (combinaisons de types) et de là tenter de prédire les variations au long cours des prévalences de chaque type et l'évolution de la virulence du HPV, enjeux de santé publique étant donné l'oncogénicité du virus. Le modèle général d'infections multiples ici présenté permet à ce titre de tester des hypothèses biologiques sous-tendues par des structures différentes du modèle ajusté sur des données cliniques. L'intégration de données longitudinales de charges virales et les données transversales de prévalence permettraient d'inférer les coefficients de la matrice d'interaction des types de papillomavirus, et sur cette base, réaliser des prédictions épidémiologiques et évolutives sur un polymorphisme viral documenté, et d'intérêt sanitaire majeur.

Notons que ces questions peuvent aussi être abordée sous l'angle des méta-communautés (Wilson, 1992; Leibold *et al.*, 2004), constituant ainsi un terrain de convergence privilégié entre l'épidémiologie et cette frange de l'écologie (Kuris *et al.*, 1980; Pedersen & Fenton, 2007; Mihaljevic, 2012; Seabloom *et al.*, 2015).

D.4.3. Vecteurs

Tous les modèles présentés jusqu'ici ont supposé une transmission du parasite par contact direct, d'hôte à hôte – sous-entendu de la même espèce. Il ne s'agit pas de l'unique mode de transmission horizontale. En effet, certains parasites, dits hétéroxènes, présentent un cycle de vie comportant non pas une espèce d'hôte mais deux, l'une étant appelé vecteur[*]. Ces parasites sont par ailleurs loin d'être négligeables sur le plan sanitaire : il s'agit, entre autres, des agents du paludisme, de la maladie du sommeil, de la dengue, du Chikungunya ou du récent Zika. La transmission vectorielle requiert une modélisation adaptée qui modifie naturellement l'expression de la valeur sélective du parasite (Champagne *et al.*, 2016), qui reflète le cycle de vie, à l'image des trois voies de transmission du virus Ebola (chapitre 0). *A fortiori* dans le cas des parasites transmis par des vecteurs, les rétro-actions épidémiologiques sont nécessairement plus complexes (puisque les deux hôtes ont leur propre démographie, par c qu'ils sont différemment affectés par la stratégie d'exploitation du parasite (Day, 2002)) et de nouveaux compromis évolutifs peuvent intervenir (p.ex. une corrélation négative entre la croissance au sein de l'hôte intermédiaire *vs* au sein de l'hôte définitif). L'épidémie de Chikungunya qu'a connu la Réunion en 2006 est ainsi un cas remarquable de sauvetage évolutif (Gonzalez *et al.*, 2013) que le virus doit à une mutation unique lui ayant permis de mieux exploiter son vecteur, le moustique tigre *Aedes albopictus* (Schuffenecker *et al.*, 2006; Hartfield & Alizon, 2014).

Intégrer le polymorphisme dans un tel contexte représente donc un nouveau défi, et peu nombreux sont les travaux s'y étant attaqué à ce jour. L'enjeu réside principalement dans la prise en compte de l'effet amplificateur du polymorphisme parasitaire que peut représenter la déconnexion des hôtes en deux espèces dynamiquement indépendantes.

∗. En écologie, le vecteur est l'hôte dans lequel la fécondation n'a pas lieu : il est dit intermédiaire tandis que l'autre est qualifié de définitif. En médecine au contraire, le vecteur est nécessairement l'espèce non focale de la discipline (donc l'espèce autre que l'Homme ou l'animal domestique considéré), quand bien même la reproduction y aurait lieu. Le cas du paludisme, pour lequel l'Homme est le vecteur écologique et non le moustique anophèle, est un exemple de cette confusion.

D.5. Conclusion

Sans que cela soit une surprise, le présent travail montre à quel point modéliser une diversité de processus à l'œuvre dans une diversité de systèmes, que d'aucuns pourraient qualifier de complexes, n'est pas chose aisée. Cette difficulté est par ailleurs amplifiée par notre quête de généralité, laquelle nous prive de la réduction de nombreux degrés de liberté que la calibration expérimentale d'un système biologique spécifié aurait pu entraîner. Cette particularisation facilite l'étude (comme le montrent, du reste, les investigations numériques ciblées du chapitre 0) et constitue l'étape charnière vers la validation des prédictions théoriques (Cressler *et al.*, 2015). Néanmoins, les cadres de travail abstraits et généraux, parce qu'ils présentent une remarquable capacité à faire émerger des concepts, parce que leur interprétation ne repose pas sur des inductions cavalières et parce que leur portée se veut embrasser l'ensemble du vivant – ainsi que l'exige le nom même de la discipline (Lamarck, 1809) –, demeurent encore une nécessité pour la recherche en biologie.

Bibliographie

Aaskov, J., Buzacott, K., Thu, H. M., Lowry, K. & Holmes, E. C. 2006, Long-term transmission of defective RNA viruses in humans and Aedes mosquitoes, *Science*, vol.311, n° 5758, p. 236–238. 137, 139

Abbate, J. L., Kada, S. & Lion, S. 2015, Beyond mortality : Sterility as a neglected component of parasite virulence, *PLOS Pathogens*, vol.11, n° 12, p.e1005 229. 310

Abbate, J. L., Murall, C. L., Richner, H. & Althaus, C. L. 2016, Potential Impact of Sexual Transmission on Ebola Virus Epidemiology : Sierra Leone as a Case Study, *PLOS Neglected Tropical Diseasese*, vol.10, n° 5, p.1–15. 50, 52, 53, 66, 75

Abedon, S. T. 2013, Are archaeons incapable of being parasites or have we simply failed to notice ?, *BioEssays*, vol.35, n° 6, p.501–501. 25

Agnew, P., Koella, J. C. & Michalakis, Y. 2000, Host life history responses to parasitism, *Microbes and Infection*, vol.2, n° 8, p.891–896. 310

Ali, H., Dumbuya, B., Hynie, M., Idahosa, P., Keil, R. & Perkins, P. 2016, The Social and Political Dimensions of the Ebola Response : Global Inequality, Climate Change, and Infectious Disease, dans *Climate Change and Health : Improving Resilience and Reducing Risks*, édité par W. Leal Filho, M. U. Azeiteiro & F. Alves, Springer International Publishing, Switzerland, p.151–169. 62

Alizon, S. 2008, Transmission-recovery trade-offs to study parasite evolution, *The American Naturalist*, vol.172, n° 3, p.E113–E121. 230

Alizon, S. 2013a, Co-infection and super-infection models in evolutionary epidemiology, *Interface Focus*, vol.3, n° 6, p.20130 031. 39, 88, 185, 188, 192, 230, 231

Alizon, S. 2013b, Parasite co-transmission and the evolutionary epidemiology of virulence, *Evolution*, vol.67, n° 4, p.921–933. 192, 245

Alizon, S. & van Baalen, M. 2005, Emergence of a convex trade-off between transmission and virulence, *The American Naturalist*, vol.165, n° 6, p.E155–E167. 39, 53, 61, 88, 193, 230

Alizon, S. & van Baalen, M. 2008, Multiple infections, immune dynamics, and the evolution of virulence, *The American Naturalist*, vol.172, n° 4, p.E150–E168. 121, 136, 176, 192

Alizon, S., Hurford, A., Mideo, N. & van Baalen, M. 2009, Virulence evolution and the trade-off hypothesis : history, current state of affairs and the future, *Journal of Evolutionary Biology*, vol.22, p.245–259. 36, 39, 188, 230, 302, 308

ALIZON, S. & LION, S. 2011, Within-host parasite cooperation and the evolution of virulence, *Proceedings of the Royal Society B : Biological Sciences*, vol. 278, n° 1725, p. 3738–3747. 84, 90, 92, 103, 121, 136, 230, 245, 286

ALIZON, S. & MICHALAKIS, Y. 2011, The transmission-virulence trade-off and superinfection : comments to smith, *Evolution*, vol. 65, n° 12, p. 3633–3638. 230

ALIZON, S. & MICHALAKIS, Y. 2015, Adaptive virulence evolution : the good old fitness-based approach, *Trends in Ecology & Evolution*, vol. in press. 38, 39, 49, 52, 62, 188, 227, 230

ALIZON, S., DE ROODE, J. C. & MICHALAKIS, Y. 2013, Multiple infections and the evolution of virulence, *Ecology Letters*, vol. 16, n° 4, p. 556–567. 36, 40, 84, 88, 121, 137, 175, 177, 189, 192, 230, 292

ALIZON, S., VON WYL, V., STADLER, T., KOUYOS, R. D., YERLY, S., HIRSCHEL, B., BÖNI, J., SHAH, C., KLIMKAIT, T., FURRER, H., RAUCH, A., VERNAZZA, P., BERNASCONI, E., BATTEGAY, M., BÜRGISSER, P., TELENTI, A., GÜNTHARD, H. F., BONHOEFFER, S. & THE SWISS HIV COHORT STUDY. 2010, Phylogenetic approach reveals that virus genotype largely determines HIV set-point viral load, *PLOS Pathogens.*, vol. 6, n° 9, p. e1001 123. 62

ALLEN, L. J. & BURGIN, A. M. 2000, Comparison of deterministic and stochastic SIS and SIR models in discrete time, *Mathematical Biosciences*, vol. 163, n° 1, p. 1–33. 33

ALTER, M. J. 2006, Epidemiology of viral hepatitis and HIV co-infection, *Journal of Hepatology*, vol. 44, p. S6–S9. 83

ANDERSON, R. & MAY, R. 1982, Coevolution of hosts and parasites, *Parasitology*, vol. 85, n° 02, p. 411–426. 39, 175, 185, 188, 230, 302

ANDERSON, R. & MAY, R. 1983, Vaccination against rubella and measles : quantitative investigations of different policies, *Journal of Hygiene*, vol. 90, n° 02, p. 259–325. 33, 192

ANDERSON, R. M. & MAY, R. M. 1979, Population biology of infectious diseases : Part I, *Nature*, vol. 280, n° 280, p. 361–7. 38, 188

ANDERSON, R. M. & MAY, R. M. 1981, The Population Dynamics of Microparasites and Their Invertebrate Hosts, *Philosophical Transactions of the Royal Society B : Biological Sciences*, vol. 291, n° 1054, p. 451–524. 33, 55, 221, 258

ANDERSON, R. M. & MAY, R. M. 1985, Vaccination and herd immunity, *Nature*, vol. 318, p. 28. 31

ANDERSON, R. M. & MAY, R. M. 1991, *Infectious diseases of humans*, vol. 1, Oxford University Press. 176, 188

ANDREASEN, V., LIN, J. & LEVIN, S. A. 1997, The dynamics of cocirculating influenza strains conferring partial cross-immunity, *Journal of Mathematical Biology*, vol. 35, n° 7, p. 825–842. 183, 310

ANTIA, R., LEVIN, B. R. & MAY, R. M. 1994, Within-host population dynamics and the evolution and maintenance of microparasite virulence, *The American Naturalist*, p. 457–472. 131

ANTIA, R., YATES, A. & DE ROODE, J. C. 2008, The dynamics of acute malaria infections. I. Effect of the parasite's red blood cell preference, *Proceedings of the Royal Society B : Biological Sciences*, vol. 275, n° 1641, p. 1449–1458. 86

VAN BAALEN, M. & SABELIS, M. W. 1995, The dynamics of multiple infection and the evolution of virulence, *The American Naturalist*, p. 881–910. 39, 83, 88, 91, 120, 121, 136, 175, 230, 257, 286, 305

Bacaër, N. 2011, *A short history of mathematical population dynamics*, Springer Science & Business Media. 31

Bae, T., Baba, T., Hiramatsu, K. & Schneewind, O. 2006, Prophages of Staphylococcus aureus Newman and their contribution to virulence, *Molecular Microbiology*, vol.62, n° 4, p.1035–1047. 88

Bailly, A. 1895, *Dictionnaire grec-français*, Hachette. 25

Ballesteros, S., Vergu, E. & Cazelles, B. 2009, Influenza A gradual and epochal evolution : insights from simple models, *PLOS ONE*, vol.4, n° 10, p.e7426. 310

Balmer, O. & Tanner, M. 2011, Prevalence and implications of multiple-strain infections, *The Lancet Infectious Diseases*, vol.11, n° 11, p.868–878. 83, 84, 120, 175, 230, 244

Barabás, G., Michalska-Smith, M. J. & Allesina, S. 2016, The Effect of Intra- and Interspecific Competition on Coexistence in Multispecies Communities, *The American Naturalist*, vol. 188, n° 1, p.E1–E12. 87, 99, 101, 110, 113, 230, 252

Bashey, F. 2015, Within-host competitive interactions as a mechanism for the maintenance of parasite diversity, *Philosophical Transactions of the Royal Society B : Biological Sciences*, vol. 370, n° 1675. 84, 85, 86, 88, 93, 101, 110, 127, 230, 310

Bassett, M. G., Popov, L. E. & Holmer, L. E. 2004, The oldest-known metazoan parasite ?, *Journal of Paleontology*, vol.78, n° 6, p.1214–1216. 307

Battilani, M., Balboni, A., Ustulin, M., Giunti, M., Scagliarini, A. & Prosperi, S. 2011, Genetic complexity and multiple infections with more Parvovirus species in naturally infected cats, *Veterinary Research*, vol.42, n° 1, p.43. 84, 120

Bausch, D. G., Towner, J. S., Dowell, S. F., Kaducu, F., Lukwiya, M., Sanchez, A., Nichol, S. T., Ksiazek, T. G. & Rollin, P. E. 2007, Assessment of the risk of Ebola virus transmission from bodily fluids and fomites, *Journal of Infectious Diseases*, vol.196, n° Supplement 2, p.S142–S147. 49

Begon, M., Townsend, C. R. & Harper, J. L. 2005, *From individuals to ecosystems*, Blackwell Publishers Hoboken. 26, 101, 249

Bell, A. S., De Roode, J. C., Sim, D. & Read, A. F. 2006, Within-host competition in genetically diverse malaria infections : parasite virulence and competitive success, *Evolution*, vol.60, n° 7, p.1358–1371. 88, 244

Bennett, J. E., Dolin, R. & Blaser, M. J. 2014, *Mandell, Douglas, and Bennett's principles and practice of infectious diseases*, Elsevier Health Sciences. 26

Bentwich, Z., Kalinkovich, A., Weisman, Z., Borkow, G., Beyers, N. & Beyers, A. D. 1999, Can eradication of helminthic infections change the face of AIDS and tuberculosis ?, *Immunology Today*, vol.20, n° 11, p.485–487. 175

Berman, A. & Plemmons, R. J. 1979, Nonnegative matrices, *The Mathematical Sciences, Classics in Applied Mathematics*, vol.9. 108, 208

Berngruber, T. W., Froissart, R., Choisy, M. & Gandon, S. 2013, Evolution of virulence in emerging epidemics, *PLOS Pathogens.*, vol.9, n° 3, p.e1003 209. 59

Bernoulli, D. 1760, Essai d'une nouvelle analyse de la mortalité causée par la petite Vérole, et des avantages de l'Inoculation pour la prévenir, *Histoire de l'Académie Royale des Sciences avec les Mémoires de Mathématique et de Physique*, p.1–45. 31

Boldin, B. & Diekmann, O. 2008, Superinfections can induce evolutionarily stable coexistence of pathogens, *Journal of Mathematical Biology*, vol.56, n° 5, p.635–672. 121, 176, 191, 231, 245, 286

Bonhoeffer, S. & Nowak, M. A. 1994, Mutation and the evolution of virulence, *Proceedings of the Royal Society B : Biological Sciences*, vol.258, n° 1352, p.133–140. 245

Boots, M. & Sasaki, A. 1999, 'Small worlds' and the evolution of virulence : infection occurs locally and at a distance, *Proceedings of the Royal Society B : Biological Sciences*, vol. 266, p. 1933–1938. 62

Bose, J., Kloesener, M. H. & Schulte, R. D. 2016, Multiple-genotype infections and their complex effect on virulence, *Zoology*, vol.119, n° 4, p.339–349. 84

Brauer, F. 2004, Backward bifurcations in simple vaccination models, *Journal of Mathematical Analysis and Applications*, vol.298, n° 2, p.418–431. 33, 222

Breman, J. & Arita, I. 1980, The confirmation and maintenance of smallpox eradication., *The New England Journal of Medicine*, vol.303, n° 22, p.1263. 28

Bremermann, H. J. & Pickering, J. 1983, A game-theoretical model of parasite virulence, *Journal of Theoretical Biology*, vol.100, n° 3, p.411–426. 39, 88, 91, 128, 175, 230, 231, 244

Briddon, R. & Stanley, J. 2006, Subviral agents associated with plant single-stranded DNA viruses, *Virology*, vol.344, n° 1, p.198–210. 139

Brogden, K. A., Guthmiller, J. M. & Taylor, C. E. 2005, Human polymicrobial infections, *The Lancet*, vol.365, n° 9455, p.253–255. 84, 120

Brooke, M. d. L. & Davies, N. 1988, Egg mimicry by cuckoos Cuculus canorus in relation to discrimination by hosts, *Nature*, vol.335, n° 6191, p.630–632. 307

Broom, M. & Rychtár, J. 2013, *Game-theoretical models in biology*, CRC Press. 309

Brown, S. 1999, Cooperation and conflict in host–manipulating parasites, *Proceedings of the Royal Society B : Biological Sciences*, vol.266, n° 1431, p.1899–1904. 84, 92, 230, 244

Brown, S. P. & Grenfell, B. T. 2001, An unlikely partnership : parasites, concomitant immunity and host defence, *Proceedings of the Royal Society B : Biological Sciences*, vol.268, n° 1485, p.2543–2549. 175, 244

Brown, S. P., Hochberg, M. E. & Grenfell, B. T. 2002, Does multiple infection select for raised virulence ?, *Trends in Microbiology*, vol.10, n° 9, p.401–405. 85, 86, 88, 89, 92, 120, 122, 128, 175, 176, 192, 230, 244, 245

Bryan, C. P. 1930, *The Papyrus Ebers*, Geoffrey Bles, London. 26

Buckling, A. & Brockhurst, M. 2008, Kin selection and the evolution of virulence, *Heredity*, vol.100, n° 5, p.484–488. 128, 192

Buckling, A. & Rainey, P. B. 2002, Antagonistic coevolution between a bacterium and a bacteriophage, *Proceedings of the Royal Society B : Biological Sciences*, vol.269, n° 1494, p.931–936. 310

Bundy, D., Chandiwana, S., Homeida, M., Yoon, S. & Mott, K. 1991, The epidemiological implications of a multiple-infection approach to the control of human helminth infections, *Transactions of the Royal Society of Tropical Medicine and Hygiene*, vol.85, n° 2, p.274–276. 120

Bzhalava, D., Eklund, C. & Dillner, J. 2015, International standardization and classification of human papillomavirus types, *Virology*, vol. 476, p. 341–344. 311

Canguilhem, G. 1966, *Le normal et le pathologique*, Presses Universitaires de France, Paris. 26

Cao, H., Kanki, P., Sankalé, J.-L., Dieng-Sarr, A., Mazzara, G. P., Kalams, S. A., Korber, B., MBoup, S. & Walker, B. D. 1997, Cytotoxic T-lymphocyte cross-reactivity among different human immunodeficiency virus type 1 clades : implications for vaccine development., *Journal of Virology*, vol. 71, n° 11, p. 8615–8623. 86

Carius, H. J., Little, T. J. & Ebert, D. 2001, Genetic variation in a host-parasite association : potential for coevolution and frequency-dependent selection, *Evolution*, vol. 55, n° 6, p. 1136–1145. 36

Cassle, S. E., Landrau-Giovannetti, N., Farina, L. L., Leone, A., Wellehan Jr, J. F., Stacy, N. I., Thompson, P., Herring, H., Mase-Guthrie, B., Blas-Machado, U. *et al.*. 2016, Coinfection by Cetacean morbillivirus and Aspergillus fumigatus in a juvenile bottlenose dolphin (Tursiops truncatus) in the Gulf of Mexico, *Journal of Veterinary Diagnostic Investigation*, vol. 28, n° 6, p. 729–734. 84

CDC. 2016, *Outbreaks Chronology : Ebola Virus Disease*, Center for Disease Control and Prevention. 45

Champagne, C., Salthouse, D. G., Paul, R., Cao-Lormeau, V.-M., Roche, B. & Cazelles, B. 2016, Structure in the variability of the basic reproductive number (R0) for Zika epidemics in the Pacific islands, *eLife*, vol. 5, p. e19 874. 33, 39, 312

Chan, M. 2014, Ebola Virus Disease in West Africa - No Early End to the Outbreak, *The New England Journal of Medicine*, vol. 371, n° 13, p. 1183–1185. 49, 50

Charnov, E. L. 1976, Optimal foraging, the marginal value theorem, *Theoretical Topulation Biology*, vol. 9, n° 2, p. 129–136. 39

Chen, Y.-D., Liu, M.-Y., Yu, W.-L., Li, J.-Q., Dai, Q., Zhou, Z.-Q. & Tisminetzky, S. G. 2003, Mix-infections with different genotypes of HCV and with HCV plus other hepatitis viruses in patients with hepatitis C in China, *World Journal of Gastroenterology*, vol. 9, n° 5, p. 984–992. 84, 120

Choisy, M. & de Roode, J. C. 2010, Mixed infections and the evolution of virulence : effects of resource competition, parasite plasticity, and impaired host immunity, *The American Naturalist*, vol. 175, n° 5, p. E105–E118. 175, 183, 192

CIA. 2016, *The World Factbook*, Central Intelligence Agency. URL `https://www.cia.gov/library/publications/the-world-factbook/geos/sl.html`. 51, 52

Collet, P., Méléard, S. & Metz, J. A. 2013, A rigorous model study of the adaptive dynamics of Mendelian diploids, *Journal of Mathematical Biology*, p. 1–39. 41

Combes, C. 2001, *Parasitism : the ecology and evolution of intimate interactions*, University of Chicago Press, Chicago and London. 120

Combes, C. 2010, *L'art d'être parasite : les associations du vivant*, Flammarion. 25, 83

Coombs, D., Gilchrist, M. A. & Ball, C. L. 2007, Evaluating the importance of within-and between-host selection pressures on the evolution of chronic pathogens, *Theoretical Population Biology*, vol. 72, n° 4, p. 576–591. 121, 286

Cornelis, G. R., Boland, A., Boyd, A. P., Geuijen, C., Iriarte, M., Neyt, C., Sory, M.-P. & Stainier, I. 1998, The virulence plasmid of Yersinia, an antihost genome, *Microbiology and Molecular Biology Reviews*, vol. 62, n° 4, p. 1315–1352. 140

Costerton, J. W., Stewart, P. S. & Greenberg, E. P. 1999, Bacterial biofilms : a common cause of persistent infections, *Science*, vol. 284, n° 5418, p. 1318–1322. 85

Cousineau, S. V. & Alizon, S. 2014, Parasite evolution in response to sex-based host heterogeneity in resistance and tolerance, *Journal of Evolutionary Biology*, vol. 27, n° 12, p. 2753–66. 62

Cox, F. 2001, Concomitant infections, parasites and immune responses, *Parasitology*, vol. 122, n° S1, p. S23–S38. 83, 84, 86, 120

Cox, F. E. 2002, History of human parasitology, *Clinical Microbiology Reviews*, vol. 15, n° 4, p. 595–612. 26

Coyte, K. Z., Schluter, J. & Foster, K. R. 2015, The ecology of the microbiome : Networks, competition, and stability, *Science*, vol. 350, n° 6261, p. 663–666. 99, 101, 113, 127

Cressler, C. E., McLeod, D. V., Rozins, C., Van Den Hoogen, J. & Day, T. 2015, The adaptive evolution of virulence : a review of theoretical predictions and empirical tests, *Parasitology*, vol. 143, p. 915–930. 36, 84, 88, 93, 230, 231, 233, 244, 246, 313

Crowe, S. J., Maenner, M. J., Kuah, S., Erickson, B. R., Coffee, M., Knust, B., Klena, J., Foday, J., Hertz, D., Hermans, V. *et al.*. 2016, Prognostic indicators for Ebola patient survival, *Emerging Infectious Diseases*, vol. 22, n° 2, p. 217. 53, 62

Damasio, G. A., Pereira, L. A., Moreira, S. D., Duarte dos Santos, C. N., Dalla-Costa, L. M. & Raboni, S. M. 2015, Does virus–bacteria coinfection increase the clinical severity of acute respiratory infection ?, *Journal of Medical Virology*. 84, 120

Darwin, C. 1859, *On the origin of species by means of natural selection – or the preservation of favoured races in the struggle for line*, 1re éd., John Murray, 1859. 27

Dawkins, R. 1999, *The extended phenotype : The long reach of the gene*, Oxford University Press. 36

Day, T. 2002, The evolution of virulence in vector-borne and directly transmitted parasites, *Theoretical Population Biology*, vol. 62, n° 2, p. 199–213. 312

Day, T. 2003, Virulence evolution and the timing of disease life-history events, *Trends in Ecology & Evolution*, vol. 18, n° 3, p. 113–118. 49

Day, T., Alizon, S. & Mideo, N. 2011, Bridging scales in the evolution of infectious disease life histories : theory, *Evolution*, vol. 65, n° 12, p. 3448–3461. 168

Day, T. & Gandon, S. 2006, Insights from Price's equation into evolutionary, *Disease evolution : models, concepts, and data analyses*, vol. 71, p. 23. 54

Day, T. & Proulx, S. R. 2004, A general theory for the evolutionary dynamics of virulence, *The American Naturalist*, vol. 163, n° 4, p. E40–E63. 54, 59

De Meeûs, T. & Renaud, F. 2002, Parasites within the new phylogeny of eukaryotes, *Trends in Parasitology*, vol. 18, n° 6, p. 247–251. 25, 36

Dean, D., Minard, P., Murrell, K. & Vannier, W. 1978, Resistance of mice to secondary infection with Schistosoma mansoni. II. Evidence for a correlation between egg deposition and work elimination., *The American journal of tropical medicine and Hygiene*, vol. 27, n° 5, p. 957–965. 121

Débarre, F., Lion, S., Van Baalen, M. & Gandon, S. 2012, Evolution of host life-history traits in a spatially structured host-parasite system, *The American Naturalist*, vol.179, n° 1, p.52–63. 311

Deen, G. F., Knust, B., Broutet, N., Sesay, F. R., Formenty, P., Ross, C., Thorson, A. E., Massaquoi, T. A., Marrinan, J. E., Ervin, E. *et al.*. 2015, Ebola RNA persistence in semen of Ebola virus disease survivors – preliminary report, *The New England Journal of Medicine*. 50

Delbrück, M. 1945, Interference Between Bacterial Viruses : III. The Mutual Exclusion Effect and the Depressor Effect1, 2, *Journal of Bacteriology*, vol.50, n° 2, p.151. 87, 120, 138, 141, 231

Demaerschalck, I., Messaoud, A. B., De Kesel, M., Hoyois, B., Lobet, Y., Hoet, P., Bigaignon, G., Bollen, A. & Godfroid, E. 1995, Simultaneous presence of different Borrelia burgdorferi genospecies in biological fluids of Lyme disease patients., *Journal of Clinical Microbiology*, vol.33, n° 3, p.602–608. 84, 120

Dieckmann, U. 2002, Adaptive dynamics of pathogen-host interactions, dans *Adaptive dynamics of infectious diseases : In pursuit of virulence management*, édité par U. Dieckmann, J. A. J. Metz, M. W. Sabelis & K. Sigmund, chap. 4, Cambridge University Press, p.39–59. 38, 39, 42, 43, 69, 230, 286, 298

Diekmann, O. 2004, A beginner's guide to adaptive dynamics, *Banach Center Publications*, vol.63, p.47–86. 43

Diekmann, O. & Heesterbeek, J. 2000, *Mathematical epidemiology of infectious diseases : model building, analysis, and interpretation*, Wiley, New York. 188

Diekmann, O., Heesterbeek, J. & Metz, J. A. 1990, On the definition and the computation of the basic reproduction ratio R 0 in models for infectious diseases in heterogeneous populations, *Journal of Mathematical Biology*, vol.28, n° 4, p.365–382. 33, 35, 52, 54, 68, 188, 221, 239, 259, 260, 286

Dietz, K. 1993, The estimation of the basic reproduction number for infectious diseases, *Statistical Methods in Medical Research*, vol.2, n° 1, p.23–41. 33

Dietz, K. & Heesterbeek, J. 2002, Daniel Bernoulli's epidemiological model revisited, *Mathematical Biosciences*, vol.180, n° 1, p.1–21. 31

Dietz, K. & Schenzle, D. 1985, Proportionate mixing models for age-dependent infection transmission, *Journal of Mathematical Biology*, vol.22, n° 1, p.117–120. 188

Dobson, A., Cotter, P. D., Ross, R. P. & Hill, C. 2012, Bacteriocin production : a probiotic trait ?, *Applied and Environmental Microbiology*, vol.78, n° 1, p.1–6. 102

Dormans, J., Burger, M., Aguilar, D., HERNANDEZ-PANDO, R., Kremer, K., Roholl, P., Arend, S. & Van Soolingen, D. 2004, Correlation of virulence, lung pathology, bacterial load and delayed type hypersensitivity responses after infection with different Mycobacterium tuberculosis genotypes in a BALB/c mouse model, *Clinical & Experimental Immunology*, vol. 137, n° 3, p.460–468. 93

Doumayrou, J., Avellan, A., Froissart, R. & Michalakis, Y. 2013, An experimental test of the transmission-virulence trade-off hypothesis in a plant virus, *Evolution*, vol. 67, n° 2, p. 477–486. 36, 39, 193

van den Driessche, P. & Watmough, J. 2002, Reproduction numbers and sub-threshold endemic equilibria for compartmental models of disease transmission, *Mathematical Biosciences*, vol.180, n° 1, p.29–48. 33, 35, 188, 239, 259, 261

DWYER, G. 1994, Density dependence and spatial structure in the dynamics of insect pathogens, *The American Naturalist*, vol. 143, n° 4, p. 533–562. 87

DWYER, G., LEVIN, S. A. & BUTTEL, L. 1990, A simulation model of the population dynamics and evolution of myxomatosis, *Ecological Monographs*, p. 423–447. 193

DYE, C. 2014, After 2015 : infectious diseases in a new era of health and development, *Philosophical Transactions of the Royal Society B : Biological Sciences*, vol. 369, n° 1645. 28, 307

EBERT, D. 2008, Host–parasite coevolution : insights from the Daphnia–parasite model system, *Current Opinion in Microbiology*, vol. 11, n° 3, p. 290–301. 307, 310

EBERT, D. & BULL, J. J. 2008, The evolution and expression of virulence, *Evolution in health and disease*, vol. 2, p. 153–167. 292

EBERT, D. & MANGIN, K. L. 1997, The influence of host demography on the evolution of virulence of a microsporidian gut parasite, *Evolution*, p. 1828–1837. 235, 292

EGGO, R., WATSON, C., CAMACHO, A., KUCHARSKI, A., FUNK, S. & EDMUNDS, W. 2015, Duration of Ebola virus RNA persistence in semen of survivors : population-level estimates and projections, *Euro Surveillance*, vol. 20, n° 48. 49

ESHEL, I. 1983, Evolutionary and continuous stability, *Journal of Theoretical Biology*, vol. 103, n° 1, p. 99–111. 43

EWALD, P. 1988, Cultural vectors, virulence, and the emergence of evolutionary epidemiology, *Oxford Surveys in Evolutionary Biology (UK)*. 38

EZANNO, P., VERGU, E., LANGLAIS, M. & GILOT-FROMONT, E. 2012, Modelling the dynamics of host-parasite interactions : basic principles, dans *New Frontiers of Molecular Epidemiology of Infectious Diseases*, Springer, p. 79–101. 30, 33

FARNAUD, S. & EVANS, R. W. 2003, Lactoferrin – a multifunctional protein with antimicrobial properties, *Molecular Immunology*, vol. 40, n° 7, p. 395–405. 233

FELDMANN, H. & GEISBERT, T. W. 2011, Ebola haemorrhagic fever, *The Lancet*, vol. 377, n° 9768, p. 849–862. 50, 61

FENNER, F. 1983, The Florey Lecture, 1983 : biological control, as exemplified by smallpox eradication and myxomatosis, *Proceedings of the Royal Society B : Biological Sciences*, vol. 218, n° 1212, p. 259–285. 37

FERGUSON, H. & READ, A. 2002, Genetic and environmental determinants of malaria parasite virulence in mosquitoes, *Proceedings of the Royal Society B : Biological Sciences*, vol. 269, n° 1497, p. 1217–1224. 36, 37

FERRIÈRE, R. & LEGENDRE, S. 2013, Eco-evolutionary feedbacks, adaptive dynamics and evolutionary rescue theory, *Philosophical Transactions of the Royal Society B : Biological Sciences*, vol. 368, n° 1610, p. 20120 081. 91

FISHER, R. A. 1930, *The genetical theory of natural selection*, Oxford University Press. 27, 38, 41

FRADA, M., PROBERT, I., ALLEN, M. J., WILSON, W. H. & DE VARGAS, C. 2008, The "Cheshire Cat" escape strategy of the coccolithophore Emiliania huxleyi in response to viral infection, *Proceedings of the National Academy of Sciences of the United States of America*, vol. 105, n° 41, p. 15 944–15 949. 27

FRANCKI, R. 1985, Plant virus satellites, *Annual Reviews in Microbiology*, vol. 39, n° 1, p. 151–174. 87, 139

FRANK, S. A. 1992, A kin selection model for the evolution of virulence, *Proceedings of the Royal Society B : Biological Sciences*, vol.250, n° 1329, p.195–197. 88, 244, 245

FRANK, S. A. 1994, Kin selection and virulence in the evolution of protocells and parasites, *Proceedings of the Royal Society B : Biological Sciences*, vol.258, p.153–161. 88, 90, 245

FRANK, S. A. 1996, Models of parasite virulence, *Quarterly Review of Biology*, p.37–78. 88, 90, 91, 230, 245

FRASER, C., HOLLINGSWORTH, T. D., CHAPMAN, R., DE WOLF, F. & HANAGE, W. P. 2007, Variation in HIV-1 set-point viral load : epidemiological analysis and an evolutionary hypothesis, *Proceedings of the National Academy of Sciences of the United States of America*, vol.104, n° 44, p.17 441–17 446. 39, 93, 193

FRASER, C., LYTHGOE, K., LEVENTHAL, G. E., SHIRREFF, G., HOLLINGSWORTH, T. D., ALIZON, S. & BONHOEFFER, S. 2014, Virulence and pathogenesis of HIV-1 infection : an evolutionary perspective, *Science*, vol.343, n° 6177, p.1243 727. 37, 52, 235, 238, 288, 292

FROISSART, R., WILKE, C. O., MONTVILLE, R., REMOLD, S. K., CHAO, L. & TURNER, P. E. 2004, Co-infection weakens selection against epistatic mutations in RNA viruses, *Genetics*, vol. 168, n° 1, p.9–19. 139

FUSSMANN, G. F. & BLASIUS, B. 2005, Community response to enrichment is highly sensitive to model structure, *Biology Letters*, vol.1, n° 1, p.9–12. 236

GAGNEUX, S. 2012, Host-pathogen coevolution in human tuberculosis, *Philosophical Transactions of the Royal Society B : Biological Sciences*, vol.367, n° 1590, p.850–859. 49

GANDON, S. 1998, The curse of the pharoah hypothesis, *Proceedings of the Royal Society B : Biological Sciences*, vol.265, n° 1405, p.1545–1552. 89, 91, 137, 230, 245

GANDON, S., HOCHBERG, M. E., HOLT, R. D. & DAY, T. 2013, What limits the evolutionary emergence of pathogens ?, *Philosophical Transactions of the Royal Society B : Biological Sciences*, vol. 368, p.20120 086. 55

GANDON, S. & MICHALAKIS, Y. 2002, Multiple Infection and Its Consequences for Virulence Management, dans *Adaptive dynamics of infectious diseases : In pursuit of virulence management*, édité par U. Dieckmann, J. A. J. Metz, M. W. Sabelis & K. Sigmund, chap. 11, Cambridge University Press, p.150–164. 88, 90

GARBUTT, J., BONSALL, M. B., WRIGHT, D. J. & RAYMOND, B. 2011, Antagonistic competition moderates virulence in Bacillus thuringiensis, *Ecology Letters*, vol.14, n° 8, p.765–772. 175, 192, 244

GARDNER, A., WEST, S. A. & BUCKLING, A. 2004, Bacteriocins, spite and virulence, *Proceedings of the Royal Society B : Biological Sciences*, vol.271, n° 1547, p.1529–1535. 85, 86, 88, 128, 177, 233, 244

GARLAND, S. M., STEBEN, M., SINGS, H. L., JAMES, M., LU, S., RAILKAR, R., BARR, E., HAUPT, R. M. & JOURA, E. A. 2009, Natural history of genital warts : analysis of the placebo arm of 2 randomized phase III trials of a quadrivalent human papillomavirus (types 6, 11, 16, and 18) vaccine, *Journal of Infectious Diseases*, vol.199, n° 6, p.805–814. 120, 193, 311

GERITZ, S., GYLLENBERG, M., JACOBS, F. & PARVINEN, K. 2002, Invasion dynamics and attractor inheritance, *Journal of Mathematical Biology*, vol.44, n° 6, p.548–560. 43

GERITZ, S. A. H., KISDI, E., MESZENA, G. & METZ, J. A. J. 1998, Evolutionarily singular strategies and the adaptative growth and branching of the evolutionary tree, *Evolutionary Ecology*, vol.12, p.35–57. 42, 43, 53, 73, 101, 102, 142, 238, 298

GHOUL, M., WEST, S. A., MCCORKELL, F. A., LEE, Z.-B., BRUCE, J. B. & GRIFFIN, A. S. 2016, Pyoverdin cheats fail to invade bacterial populations in stationary phase, *Journal of Evolutionary Biology*. 101

GILCHRIST, M. A. & COOMBS, D. 2006, Evolution of virulence : interdependence, constraints, and selection using nested models, *Theoretical Population Biology*, vol.69, n° 2, p.145–153. 131

GLENDINNING, P. 1994, *Stability, instability and chaos : an introduction to the theory of nonlinear differential equations*, vol.11, Cambridge University Press. 34

GOH, B. S. 1977, Global stability in many-species systems, *The American Naturalist*, p.135–143. 99, 101, 107, 204, 252

GONZALEZ, A., RONCE, O., FERRIÈRE, R. & HOCHBERG, M. E. 2013, Evolutionary rescue : an emerging focus at the intersection between ecology and evolution, *Philosophical Transactions of the Royal Society B : Biological Sciences*, vol.368, n° 1610. 312

GORMAN, S., HARVEY, N. L., MORO, D., LLOYD, M. L., VOIGT, V., SMITH, L. M., LAWSON, M. A. & SHELLAM, G. R. 2006, Mixed infection with multiple strains of murine cytomegalovirus occurs following simultaneous or sequential infection of immunocompetent mice, *Journal of General Virology*, vol.87, n° 5, p.1123–1132. 121

GOUYON, P. & HENRY, J. 1998, Précis de génétique des populations, *ÉditionS Masson, Paris*. 38

GOUYON, P.-H., HENRY, J.-P. & ARNOULD, J. 1996, *Les avatars du gène*, Belin, Paris. 83

GRAFEN, A. 2015, Biological fitness and the fundamental theorem of natural selection, *The American Naturalist*, vol.186, n° 1, p.1–14. 41

GRAHAM, A. L., ALLEN, J. E. & READ, A. F. 2005, Evolutionary causes and consequences of immunopathology, *Annual Review of Ecology, Evolution, and Systematics*, vol.36, p.373–397. 40

GRIFFITHS, E. C., PEDERSEN, A. B., FENTON, A. & PETCHEY, O. L. 2011, The nature and consequences of coinfection in humans, *Journal of Infection*, vol.63, n° 3, p.200–206. 84, 172, 230

GROBMAN, D. M. 1959, Homeomorphism of systems of differential equations, *Doklady Akademii Nauk SSSR*, vol.128, n° 5, p.880–881. 35, 101

GROSS, C. P. & SEPKOWITZ, K. A. 1998, The myth of the medical breakthrough : smallpox, vaccination, and Jenner reconsidered, *International Journal of Infectious Diseases*, vol.3, n° 1, p.54–60. 31

HADELER, K. P. & VAN DEN DRIESSCHE, P. 1997, Backward bifurcation in epidemic control, *Mathematical Biosciences*, vol.146, n° 1, p.15–35. 33, 221

HAEFNER, J. W. 2012, *Modeling biological systems : principles and applications*, Springer Science & Business Media. 29, 309

HALE, T. L. 1991, Genetic basis of virulence in Shigella species., *Microbiological Reviews*, vol.55, n° 2, p.206–224. 37

HAMILTON, W., BISARO, D., COUTTS, R. H. & BUCK, K. 1983, Demonstration of the bipartite nature of the genome of a single-stranded DNA plant virus by infection with the cloned DNA components, *Nucleic Acids Research*, vol.11, n° 21, p.7387–7396. 140

HARDIN, G. *et al.*. 1968, The tragedy of the commons, *Science*, vol.162, n° 3859, p.1243–1248. 91

HARRIES, A. D., MAHER, D. & GRAHAM, S. 2004, *TB/HIV : a clinical manual*, World Health Organization. 84, 137

HARTFIELD, M. & ALIZON, S. 2014, Epidemiological feedbacks affect evolutionary emergence of pathogens, *The American Naturalist*, vol.183, n° 4, p.E105–E117. 312

HARTMAN, P. 1960, A lemma in the theory of structural stability of differential equations, *Proceedings of the American Mathematical Society*, vol.11, n° 4, p.610–620. 35, 101

HAWASS, Z., GAD, Y. Z., ISMAIL, S., KHAIRAT, R., FATHALLA, D., HASAN, N., AHMED, A., ELLEITHY, H., BALL, M., GABALLAH, F. *et al.*. 2010, Ancestry and pathology in King Tutankhamun's family, *The Journal of the American Medical Association*, vol.303, n° 7, p.638–647. 37

HAYS, J. N. 2005, *Epidemics and pandemics : their impacts on human history*, Abc-clio. 28, 37

HÉBERT-DUFRESNE, L. & ALTHOUSE, B. M. 2015, Complex dynamics of synergistic coinfections on realistically clustered networks, *Proceedings of the National Academy of Sciences of the United States of America*, vol.112, n° 33, p.10 551–10 556. 142

HEESTERBEEK, H., ANDERSON, R. M., ANDREASEN, V., BANSAL, S., DE ANGELIS, D., DYE, C., EAMES, K. T., EDMUNDS, W. J., FROST, S. D., FUNK, S. *et al.*. 2015, Modeling infectious disease dynamics in the complex landscape of global health, *Science*, vol.347, n° 6227, p.aaa4339. 33, 221

HEESTERBEEK, J. A. P. 2002, A brief history of R 0 and a recipe for its calculation, *Acta Biotheoretica*, vol.50, n° 3, p.189–204. 33

HEFFERNAN, J., SMITH, R. & WAHL, L. 2005, Perspectives on the basic reproductive ratio, *Journal of the Royal Society Interface*, vol.2, n° 4, p.281–293. 188

HEINO, M., METZ, J. A. & KAITALA, V. 1998, The enigma of frequency-dependent selection, *Trends in Ecology & Evolution*, vol.13, n° 9, p.367–370. 29

HELLARD, E., FOUCHET, D., VAVRE, F. & PONTIER, D. 2015, Parasite–Parasite Interactions in the Wild : How To Detect Them ?, *Trends in Parasitology*, vol.31, n° 12, p.640–652. 84, 85, 86, 93, 101

HERBECK, J. T., MÜLLER, V., MAUST, B. S., LEDERGERBER, B., TORTI, C., DI GIAMBENEDETTO, S., GRAS, L., GÜNTHARD, H. F., JACOBSON, L. P., MULLINS, J. I. & GOTTLIEB, G. S. 2012, Is the virulence of HIV changing ? A meta-analysis of trends in prognostic markers of HIV disease progression and transmission, *AIDS*, vol.26, n° 2, p.193. 49

HERNÁNDEZ-BERMEJO, B. & FAIRÉN, V. 1997, Lotka-Volterra representation of general nonlinear systems, *Mathematical Biosciences*, vol.140, n° 1, p.1–32. 101

HETHCOTE, H. W. 2000, The mathematics of infectious diseases, *SIAM Review*, vol.42, n° 4, p. 599–653. 33

HIRSCH, M. & SMALE, S. 1974, *Differential Equations, Dynamical Systems, and Linear Algebra*, Academic Press, New York and London. 34, 35

HOFBAUER, J. & SIGMUND, K. 1990, Adaptive dynamics and evolutionary stability, *Applied Mathematics Letters*, vol.3, n° 4, p.75–79. 101

HOFBAUER, J. & SIGMUND, K. 1998, *Evolutionary games and population dynamics*, Cambridge University Press. 41, 99, 250, 251

HOOD, M. 2003, Dynamics of multiple infection and within-host competition by the anther-smut pathogen, *The American Naturalist*, vol.162, n° 1, p.122–133. 121

Hou, Z., Lisena, B., Pireddu, M., Zanolin, F., Ahmad, S. & Stamova, I. M. 2013, *Lotka-Volterra and related systems : recent developments in population dynamics*, vol. 2, Walter de Gruyter. 99

Huang, A. S. & Baltimore, D. 1970, Defective viral particles and viral disease processes, *Nature*, vol.226, p.325–327. 139, 233

Huber, H., Hohn, M. J., Rachel, R., Fuchs, T., Wimmer, V. C. & Stetter, K. O. 2002, A new phylum of Archaea represented by a nanosized hyperthermophilic symbiont, *Nature*, vol. 417, n° 6884, p.63–67. 25

Hughes, S. A., Wedemeyer, H. & Harrison, P. M. 2011, Hepatitis delta virus, *The Lancet*, vol.378, n° 9785, p.73–85. 121, 139

Hull, R. 2013, *Plant Virology*, Academic Press, New York and London. 28, 84, 139

Hurford, A., Cownden, D. & Day, T. 2010, Next-generation tools for evolutionary invasion analyses, *Journal of the Royal Society Interface*. 33, 35, 54, 68, 188, 216, 239, 261

Jones, D. S., Podolsky, S. H. & Greene, J. A. 2012, The burden of disease and the changing task of medicine, *The New England Journal of Medicine*, vol.366, n° 25, p.2333–2338. 28

Jones, K. E., Patel, N. G., Levy, M. A., Storeygard, A., Balk, D., Gittleman, J. L. & Daszak, P. 2008, Global trends in emerging infectious diseases, *Nature*, vol. 451, n° 7181, p. 990–993. 28

Juliano, J. J., Porter, K., Mwapasa, V., Sem, R., Rogers, W. O., Ariey, F., Wongsrichanalai, C., Read, A. F. & Meshnick, S. R. 2010, Exposing malaria in-host diversity and estimating population diversity by capture-recapture using massively parallel pyrosequencing, *Proceedings of the National Academy of Sciences of the United States of America*, vol.107, n° 46, p.20 138–20 143. 83, 120, 141, 171, 175, 230

Keeling, M. J. & Rohani, P. 2008, *Modeling infectious diseases in humans and animals*, Princeton University Press. 27, 29, 32, 33, 50, 83, 236, 257, 307

Kell, A. M., Wargo, A. R. & Kurath, G. 2013, The role of virulence in in vivo superinfection fitness of the vertebrate RNA virus infectious hematopoietic necrosis virus, *Journal of Virology*, vol.87, n° 14, p.8145–8157. 93

Kermack, W. & McKendrick, A. 1927, Contributions to the mathematical theory of epidermics, part 1, *Proceedings of the Royal Society A : Mathematical, Physical and Engineering Science*. 31, 183

Kermack, W. O. & McKendrick, A. G. 1932, Contributions to the mathematical theory of epidemics, part 2, *Proceedings of the Royal Society A : Mathematical, Physical and Engineering Science*, vol.138, n° 834, p.55–83. 31, 121, 175, 188

Kilpatrick, A. M., Briggs, C. J. & Daszak, P. 2010, The ecology and impact of chytridiomycosis : an emerging disease of amphibians, *Trends in Ecology & Evolution*, vol.25, n° 2, p.109–118. 26

Kinnula, H., Mappes, J. & Sundberg, L.-R. 2017, Coinfection outcome in an opportunistic pathogen depends on the inter-strain interactions, *BMC Evolutionary Biology*, vol.17, n° 1, p.77. 93

Kiple, K. F. 1993, *The Cambridge world history of human disease*, Cambridge University Press. 28

KÖHLER, T., BUCKLING, A. & VAN DELDEN, C. 2009, Cooperation and virulence of clinical Pseudomonas aeruginosa populations, *Proceedings of the National Academy of Sciences of the United States of America*, vol.106, n° 15, p.6339–6344. 88

KOROBEINIKOV, A. & MAINI, P. K. 2004, A Lyapunov function and global properties for SIR and SEIR epidemiological models with nonlinear incidence, *Mathematical Biosciences and Engineering*, vol.1, n° 1, p.57–60. 307

KOVER, P. X. & SCHAAL, B. A. 2002, Genetic variation for disease resistance and tolerance among Arabidopsis thaliana accessions, *Proceedings of the National Academy of Sciences of the United States of America*, vol.99, n° 17, p.11 270–11 274. 235, 292

KRUPOVIC, M. & CVIRKAITE-KRUPOVIC, V. 2011, Virophages or satellite viruses ?, *Nature Reviews Microbiology*, vol.9, n° 11, p.762–763. 139

KUCHARSKI, A. J., ANDREASEN, V. & GOG, J. R. 2016, Capturing the dynamics of pathogens with many strains, *Journal of Mathematical Biology*, vol.72, n° 1, p.1–24. 171, 230, 236

KUEHN, C. 2015, *Multiple time scale dynamics*, vol.191, Springer. 35, 249

KÜMMERLI, R. & BROWN, S. P. 2010, Molecular and regulatory properties of a public good shape the evolution of cooperation, *Proceedings of the National Academy of Sciences of the United States of America*, vol.107, n° 44, p.18 921–18 926. 175, 177

KUPFERSCHMIDT, K. 2014, Imagining Ebola's next move, *Science*, vol. 346, n° 6206, p. 151–152. 49, 61

KURIS, A. M., BLAUSTEIN, A. R. & ALIO, J. J. 1980, Hosts as islands, *The American Naturalist*, vol.116, n° 4, p.570–586. 312

KURIS, A. M., HECHINGER, R. F., SHAW, J. C., WHITNEY, K. L., AGUIRRE-MACEDO, L., BOCH, C. A., DOBSON, A. P., DUNHAM, E. J., FREDENSBORG, B. L., HUSPENI, T. C. *et al.*. 2008, Ecosystem energetic implications of parasite and free-living biomass in three estuaries, *Nature*, vol.454, n° 7203, p.515–518. 26

KWIATKOWSKI, D. & NOWAK, M. 1991, Periodic and chaotic host-parasite interactions in human malaria., *Proceedings of the National Academy of Sciences of the United States of America*, vol.88, n° 12, p.5111–5113. 37

LA SCOLA, B., DESNUES, C., PAGNIER, I., ROBERT, C., BARRASSI, L., FOURNOUS, G., MERCHAT, M., SUZAN-MONTI, M., FORTERRE, P., KOONIN, E. *et al.*. 2008, The virophage as a unique parasite of the giant mimivirus, *Nature*, vol.455, n° 7209, p.100–104. 25

DE LA VEGA, M.-A., STEIN, D. & KOBINGER, G. P. 2015, Ebolavirus evolution : past and present, *PLOS Pathogens*, vol.11, n° 11, p.e1005 221. 49

LAMARCK, J. 1809, *Philosophie Zoologique*, Muséeum d'Histoire Naturelle (Jardin des Plantes). 27, 313

LAMBERT, A. 2010, Population genetics, ecology and the size of populations, *Journal of Mathematical Biology*, vol.60, n° 3, p.469. 93

LANCASTRE, F., VIANEY-LIAUD, M., COUTRIS, G., BOLOGNINI-TRENEY, J., MOUGEOT, G. & OUAGHLISSI, J. 1989, Resistance to desiccation of Biomphalaria glabrata adults by polyinfection of Schistosoma mansoni miracidia, *Memórias do Instituto Oswaldo Cruz, Rio de Janeiro*, vol.84, n° 2, p.205–212. 84, 120

LEANDER, R., GOFF, W., MURPHY, C. & PULIDO, S. 2016, Modelling Ebola within a community, *Epidemiology and Infection*, p.1–9. 50, 53

LEDERBERG, J. 2000, Infectious history, *Science*, vol.288, n° 5464, p.287–293. 26

LEGGETT, H. C., CORNWALLIS, C. K., BUCKLING, A. & WEST, S. A. 2017, Growth rate, transmission mode and virulence in human pathogens, *Philosophical Transactions of the Royal Society B : Biological Sciences*, vol.372, n° 1719, p.20160 094. 286, 305

LEGRAND, J., GRAIS, R. F., BOELLE, P.-Y., VALLERON, A. J. & FLAHAULT, A. 2007, Understanding the dynamics of Ebola epidemics, *Epidemiol Infect*, vol.135, n° 4, p.610–21. 50

LEIBOLD, M. A., HOLYOAK, M., MOUQUET, N., AMARASEKARE, P., CHASE, J., HOOPES, M., HOLT, R., SHURIN, J., LAW, R., TILMAN, D. *et al.*. 2004, The metacommunity concept : a framework for multi-scale community ecology, *Ecology Letters*, vol.7, n° 7, p.601–613. 312

LEIMAR, O. 2009, Multidimensional convergence stability, *Evolutionary Ecology Research*, vol.11, n° 2, p.191–208. 42

LENORMAND, T., RODE, N., CHEVIN, L.-M. & ROUSSET, F. 2016, Valeur sélective : définitions, enjeux et mesures, dans *Biologie Évolutive*, chap. 15, De Boeck, p.655–675. 36

LENSKI, R. E., ROSE, M. R., SIMPSON, S. C. & TADLER, S. C. 1991, Long-term experimental evolution in Escherichia coli. I. Adaptation and divergence during 2,000 generations, *The American Naturalist*, vol.138, n° 6, p.1315–1341. 37

LEROY, E. M., BAIZE, S., VOLCHKOV, V. E., FISHER-HOCH, S. P., GEORGES-COURBOT, M.-C., LANSOUD-SOUKATE, J., CAPRON, M., DEBRÉ, P., GEORGES, A. J. & MCCORMICK, J. B. 2000, Human asymptomatic Ebola infection and strong inflammatory response, *The Lancet*, vol.355, n° 9222, p.2210–2215. 55, 62

LEROY, E. M., KUMULUNGUI, B., POURRUT, X., ROUQUET, P., HASSANIN, A., YABA, P., DÉLICAT, A., PAWESKA, J. T., GONZALEZ, J.-P. & SWANEPOEL, R. 2005, Fruit bats as reservoirs of Ebola virus, *Nature*, vol.438, n° 7068, p.575–576. 49

LEVIN, B. R. & BULL, J. J. 1994, Short-sighted evolution and the virulence of pathogenic microorganisms, *Trends in Microbiology*, vol.2, n° 3, p.76–81. 40, 230

LEVIN, S. & PIMENTEL, D. 1981, Selection of intermediate rates of increase in parasite-host systems, *The American Naturalist*, p.308–315. 39, 88, 91, 93, 121, 175, 230, 235, 244, 245, 246, 302, 307

LI, X.-Y., PIETSCHKE, C., FRAUNE, S., ALTROCK, P. M., BOSCH, T. C. & TRAULSEN, A. 2015, Which games are growing bacterial populations playing ?, *Journal of The Royal Society Interface*, vol.12, n° 108, p.20150 121. 114, 126

LIEVENS, E. J., HENRIQUES, G. J., MICHALAKIS, Y. & LENORMAND, T. 2016, Maladaptive sex ratio adjustment in the invasive brine shrimp Artemia franciscana, *Current Biology*, vol. 26, n° 11, p.1463–1467. 307

LINNÉ, C. V. 1735, *Systema naturæ, sive regna tria naturæ systematice proposita per classes, ordines, genera, & species.*, 1re éd., Lugduni Batavorum. (Haak). 26

LION, S. 2013, Multiple infections, kin selection and the evolutionary epidemiology of parasite traits, *Journal of Evolutionary Biology*, vol.26, n° 10, p.2107–2122. 91, 136, 137, 175, 183, 185, 192

LION, S. 2017, Theoretical approaches in evolutionary ecology : environmental feedback as a unifying perspective, *In prep.* 42

LION, S. & VAN BAALEN, M. 2008, Self-structuring in spatial evolutionary ecology, *Ecology Letters*, vol.11, n° 3, p.277–295. 62

Lion, S. & Boots, M. 2010, Are parasites 'prudent' in space ?, *Ecology Letters*, vol. 13, n° 10, p. 1245–1255. 62

Lion, S. & Gandon, S. 2015, Evolution of spatially structured host-parasite interactions, *Journal of Evolutionary Biology*, vol. 28, n° 1, p. 10–28. 311

Lion, S. & Gandon, S. 2016, Spatial evolutionary epidemiology of spreading epidemics, *Proceedings of the Royal Society B : Biological Sciences*, vol. 283, n° 1841, p. 20161 170. 41

Lion, S. & Metz, J. A. J. 2017, Do parasites dream of R0, *In prep.* 221, 302

Lipsitch, M. & Nowak, M. A. 1995, The evolution of virulence in sexually transmitted HIV/AIDS, *Journal of Theoretical Biology*, vol. 174, n° 4, p. 427–440. 89

Little, T. J., Shuker, D. M., Colegrave, N., Day, T. & Graham, A. L. 2010, The coevolution of virulence : tolerance in perspective, *PLOS Pathogens*, vol. 6, n° 9, p. e1001 006. 311

Littré, É. 1839, Oeuvres Complètes d'Hippocrate, *JB Baillière, Paris*. 26

Lobry, C., Sari, T. & Touhami, S. 1998, On Tykhonov's theorem for convergence of solutions of slow and fast systems, *Electronic Journal of Differential Equations*, vol. 1998, n° 19, p. 1–22. 35

Lord, C., Barnard, B., Day, K., Hargrove, J., McNamara, J., Paul, R., Trenholme, K. & Woolhouse, M. 1999, Aggregation and distribution of strains in microparasites, *Philosophical Transactions of the Royal Society B : Biological Sciences*, vol. 354, n° 1384, p. 799–807. 83, 120, 175, 230

Lotka, A. J. 1925, *Elements of physical biology*, Wiliams and Wilkins. 99, 101, 127, 192, 233

Lozano, R., Naghavi, M., Foreman, K., Lim, S., Shibuya, K., Aboyans, V., Abraham, J., Adair, T., Aggarwal, R., Ahn, S. Y. *et al.*. 2013, Global and regional mortality from 235 causes of death for 20 age groups in 1990 and 2010 : a systematic analysis for the Global Burden of Disease Study 2010, *The Lancet*, vol. 380, n° 9859, p. 2095–2128. 27, 28

Lyapunov, A. M. 1992, The general problem of the stability of motion, *International Journal of Control*, vol. 55, n° 3, p. 531–534. 35, 101, 107

Lycett, S. J., Bodewes, R., Pohlmann, A., Banks, J., Bányai, K., Boni, M. F., Bouwstra, R. & Lu, L. 2016, Role for migratory wild birds in the global spread of avian influenza H5N8, *Science*, vol. 354, n° 6309, p. 213–217. 28

Lysenko, E. S., Ratner, A. J., Nelson, A. L. & Weiser, J. N. 2005, The role of innate immune responses in the outcome of interspecies competition for colonization of mucosal surfaces, *PLOS Pathogens*, vol. 1, n° 1, p. e1. 86

MacArthur, R. & Levins, R. 1967, The limiting similarity, convergence, and divergence of coexisting species, *The American Naturalist*, p. 377–385. 137

Manceau, M., Lambert, A. & Morlon, H. 2016, A unifying comparative phylogenetic framework including traits coevolving across interacting lineages, *Systematic Biology*, p. syw115. 38, 310

Mangin, K., Lipsitch, M. & Ebert, D. 1995, Virulence and transmission modes of two microsporidia in Daphnia magna, *Parasitology*, vol. 111, n° 02, p. 133–142. 89

Masel, J. & Trotter, M. V. 2010, Robustness and evolvability, *Trends in Genetics*, vol. 26, n° 9, p. 406–414. 30

MATE, S. E., KUGELMAN, J. R., NYENSWAH, T. G., LADNER, J. T., WILEY, M. R., CORDIER-LASSALLE, T., CHRISTIE, A., SCHROTH, G. P., GROSS, S. M., DAVIES-WAYNE, G. J. *et al.*. 2015, Molecular evidence of sexual transmission of Ebola virus, *The New England Journal of Medicine*, vol.373, n° 25, p.2448–2454. 50

MAY, R. M. 1972, Will a large complex system be stable ?, *Nature*, vol.238, p.413–414. 99

MAY, R. M. 2004, Uses and Abuses of Mathematics in Biology, *Science*, vol.303, n° 5659, p.790–793. 29

MAY, R. M. & ANDERSON, R. M. 1979, Population biology of infectious diseases : Part II, *Nature*, vol.280, n° 5722, p.455–461. 27

MAY, R. M. & ANDERSON, R. M. 1983, Parasite-host co-evolution, dans *Coevolution*, Sunderland, MA : Sinauer, p.186–206. 37

MAY, R. M. & NOWAK, M. A. 1994, Superinfection, metapopulation dynamics, and the evolution of diversity, *Journal of Theoretical Biology*, vol.170, n° 1, p.95–114. 245

MAY, R. M. & NOWAK, M. A. 1995, Coinfection and the evolution of parasite virulence, *Proceedings of the Royal Society B : Biological Sciences*, vol.261, n° 1361, p.209–215. 88, 91, 121, 122, 136, 175, 192, 230, 231, 244, 245

MAYNARD SMITH, J. 1982, *Evolution and the Theory of Games*, Cambridge University Press. 43, 102

MAYNARD SMITH, J., BURIAN, R., KAUFFMAN, S., ALBERCH, P., CAMPBELL, J., GOODWIN, B., LANDE, R., RAUP, D. & WOLPERT, L. 1985, Developmental constraints and evolution : a perspective from the Mountain Lake conference on development and evolution, *The Quarterly Review of Biology*, vol.60, n° 3, p.265–287. 38

MAYNARD SMITH, J. & PRICE, G. R. 1973, The Logic of Animal Conflict, *Nature*, vol.246, p.15. 43

MCCALLUM, H., BARLOW, N. & HONE, J. 2001, How should pathogen transmission be modelled ?, *Trends in Ecology & Evolution*, vol.16, n° 6, p.295–300. 31, 101

MCCOY, K. D., BOULINIER, T., CHARDINE, J. W., DANCHIN, E. & MICHALAKIS, Y. 1999, Dispersal and distribution of the tick Ixodes uriae within and among seabird host populations : the need for a population genetic approach, *The Journal of Parasitology*, p.196–202. 27

MCKENDRICK, A. 1926, Applications of mathematics to medical problems, *Proceedings of the Edinburgh Mathematical Society*, vol.44, p.98–130. 31

METCALF, C., BIRGER, R., FUNK, S., KOUYOS, R., LLOYD-SMITH, J. & JANSEN, V. 2015, Five challenges in evolution and infectious diseases, *Epidemics*, vol.10, p.40–44. 171, 236

MÉTHOT, P.-O. 2012, Why do parasites harm their host ? On the origin and legacy of Theobald Smith's 'law of declining virulence' – 1900-1980, *History and Philosophy of the Life Sciences*, vol.34, n° 4, p.561–601. 27, 37, 49, 230, 302

METZ, J. A. J., MYLIUS, S. D. & DIEKMANN, O. 2008, When Does Evolution Optimize ?, *Evolutionary Ecology Research*, vol.10, p.629–654. 39, 221, 302

METZ, J. A. J., STAŇKOVÁ, K. & JOHANSSON, J. 2016, The canonical equation of adaptive dynamics for life histories : from fitness-returns to selection gradients and Pontryagin's maximum principle, *Journal of Mathematical Biology*, vol.72, n° 4, p.1125–1152. 101

MICHALAKIS, Y., OLIVIERI, I., RENAUD, F. & RAYMOND, M. 1992, Pleiotropic action of parasites : how to be good for the host, *Trends in Ecology & Evolution*, vol.7, n° 2, p.59–62. 36

MIDEO, N. 2009, Parasite adaptations to within-host competition, *Trends in Parasitology*, vol.25, n° 6, p.261–268. 85, 101, 122, 175, 230

MIDEO, N., ALIZON, S. & DAY, T. 2008, Linking within- and between-host dynamics in the evolutionary epidemiology of infectious diseases, *Trends in Ecology & Evolution*, vol. 23, n° 9, p. 511–517. 127, 128, 131, 168, 176, 180, 184, 192, 307

MIHALJEVIC, J. R. 2012, Linking metacommunity theory and symbiont evolutionary ecology, *Trends in Ecology & Evolution*, vol.27, n° 6, p.323–329. 87, 312

MILLER, L. H., BARUCH, D. I., MARSH, K. & DOUMBO, O. K. 2002, The pathogenic basis of malaria, *Nature*, vol.415, n° 6872, p.673–679. 36

MILLER, M. B. & BASSLER, B. L. 2001, Quorum sensing in bacteria, *Annual Reviews in Microbiology*, vol.55, n° 1, p.165–199. 86

MILLER, M. R., WHITE, A. & BOOTS, M. 2006, The evolution of parasites in response to tolerance in their hosts : the good, the bad, and apparent commensalism, *Evolution*, vol.60, n° 5, p.945–56. 62

MILLER, R. 1989, Dqr, spinning and treatment of guinea worm in P. Ebers 875, *The Journal of Egyptian Archaeology*, p.249–254. 26

MOORE, J. W. 1898, Pneumonia : a multiple infection, *Dublin Journal of Medical Science*, vol. 105, n° 1, p.47–60. 84, 120

MOSQUERA, J. & ADLER, F. R. 1998, Evolution of virulence : a unified framework for coinfection and superinfection, *Journal of Theoretical Biology*, vol.195, n° 3, p.293–313. 136, 231, 245

MOUGI, A. & KONDOH, M. 2012, Diversity of interaction types and ecological community stability, *Science*, vol.337, n° 6092, p.349–351. 127

MOURY, B., FABRE, F. & SENOUSSI, R. 2007, Estimation of the number of virus particles transmitted by an insect vector, *Proceedings of the National Academy of Sciences of the United States of America*, vol.104, n° 45, p.17 891–17 896. 287

MOUTON, L., DEDEINE, F., HENRI, H., BOULÉTREAU, M., PROFIZI, N. & VAVRE, F. 2004, Virulence, multiple infections and regulation of symbiotic population in the Wolbachia-Asobara tabida symbiosis, *Genetics*, vol.168, n° 1, p.181–189. 311

MURALL, C., ABBATE, J., TOUZEL, M. P., ALLEN-VERCOE, E., ALIZON, S., FROISSART, R. & MCCANN, K. 2017, Invasions of Host-Associated Microbiome Networks, *Advances in Ecological Research*. 311

MURRAY, J. 2001, *Mathematical Biology I. An introduction*, 3e éd., Springer-Verlag Berlin Heidelberg. 99

MYLIUS, S. D. & DIEKMANN, O. 1995, On evolutionarily stable life histories, optimization and the need to be specific about density dependence, *Oikos*, p.218–224. 302

NATHAN, C. 2015, From transient infection to chronic disease, *Science*, vol.350, n° 6257, p.161–161. 36

NAZZI, F., BROWN, S. P., ANNOSCIA, D., DEL PICCOLO, F., DI PRISCO, G., VARRICCHIO, P., DELLA VEDOVA, G., CATTONARO, F., CAPRIO, E. & PENNACCHIO, F. 2012, Synergistic parasite-pathogen interactions mediated by host immunity can drive the collapse of honeybee colonies, *PLOS Pathogens*, vol.8, n° 6, p.e1002 735. 138, 307

NEE, S. 2000, Mutualism, parasitism and competition in the evolution of coviruses, *Philosophical Transactions of the Royal Society B : Biological Sciences*, vol.355, n° 1403, p.1607–1613. 139

NEILANDS, J. 1995, Siderophores : structure and function of microbial iron transport compounds, *Journal of Biological Chemistry*, vol.270, n° 45, p.26 723–26 726. 101, 127, 128, 177, 233

NETHE, M., BERKHOUT, B. & VAN DER KUYL, A. C. 2005, Retroviral superinfection resistance, *Retrovirology*, vol.2, n° 1, p.52. 86, 233

NOWAK, M. A. & MAY, R. M. 1994, Superinfection and the evolution of parasite virulence, *Proceedings of the Royal Society B : Biological Sciences*, vol.255, n° 1342, p.81–89. 88, 89, 91, 93, 120, 121, 122, 137, 175, 192, 230, 235, 244, 245

NOWAK, M. A. & SIGMUND, K. 2002, Super-and coinfection : the two extremes, dans *Adaptive dynamics of infectious diseases : In pursuit of virulence management*, édité par U. Dieckmann, J. A. J. Metz, M. W. Sabelis & K. Sigmund, chap. 9, Cambridge University Press, p.39–59. 233, 245

NYENSWAH, T. G., KATEH, F., BAWO, L., MASSAQUOI, M., GBANYAN, M., FALLAH, M., NAGBE, T. K., KARSOR, K. K., WESSEH, C. S., SIEH, S. *et al.*. 2016, Ebola and its control in Liberia, 2014-2015, *Emerging Infectious Diseases*, vol.22, n° 2, p.169. 50, 52, 75

O'KEEFE, K. J. & ANTONOVICS, J. 2002, Playing by different rules : the evolution of virulence in sterilizing pathogens, *The American Naturalist*, vol.159, n° 6, p.597–605. 36

DE OLIVEIRA, C. M., BRAVO, I. G., E SOUZA, N. C. S., GENTA, M. L. N. D., FREGNANI, J. H. T. G., TACLA, M., CARVALHO, J. P., LONGATTO-FILHO, A. & LEVI, J. E. 2015, High-level of viral genomic diversity in cervical cancers : A Brazilian study on human papillomavirus type 16, *Infection, Genetics and Evolution*, vol.34, p.44 – 51. 84, 171

OSTERHOLM, M. T., MOORE, K. A., KELLEY, N. S., BROSSEAU, L. M., WONG, G., MURPHY, F. A., PETERS, C. J., LEDUC, J. W., RUSSELL, P. K., VAN HERP, M. *et al.*. 2015, Transmission of Ebola viruses : what we know and what we do not know, *MBio*, vol.6, n° 2, p.e00 137–15. 53

OTTO, S. P. & DAY, T. 2007, *A biologist's guide to mathematical modeling in ecology and evolution*, vol.13, Princeton University Press. 54, 309

OVAA, W., BITTER, W., WEISBEEK, P. & KOSTER, M. 1995, Multiple outer membrane receptors for uptake of ferric pseudobactins inPseudomonas putida WCS358, *Molecular and General Genetics*, vol.248, n° 6, p.735–743. 127

OWEN, J. A., PUNT, J., STRANFORD, S. A. *et al.*. 2013, *Kuby immunology*, WH Freeman New York. 26, 85

PAGE, K. M. & NOWAK, M. A. 2002, Unifying evolutionary dynamics, *Journal of Theoretical Biology*, vol.219, n° 1, p.93–98. 41

PEDERSEN, A. B. & FENTON, A. 2007, Emphasizing the ecology in parasite community ecology, *Trends in Ecology & Evolution*, vol.22, n° 3, p.133–139. 84, 312

PENN, D. J., DAMJANOVICH, K. & POTTS, W. K. 2002, MHC heterozygosity confers a selective advantage against multiple-strain infections, *Proceedings of the National Academy of Sciences of the United States of America*, vol.99, n° 17, p.11 260–11 264. 84, 120

PEPIN, K. M., LAMBETH, K. & HANLEY, K. A. 2008, Asymmetric competitive suppression between strains of dengue virus, *BMC Microbiology*, vol.8, n° 1, p.28. 87

PEPPER, J. W. & ROSENFELD, S. 2012, The emerging medical ecology of the human gut microbiome, *Trends in Ecology & Evolution*, vol.27, n° 7, p.381–384. 101

Péréfarres, F., Thébaud, G., Lefeuvre, P., Chiroleu, F., Rimbaud, L., Hoareau, M. & Reynaud, B. 2014, Frequency-dependent assistance as a way out of competitive exclusion between two strains of an emerging virus, *Proceedings of the Royal Society B : Biological Sciences*, vol.281, n° 1781, p.20133374. 87, 137, 141, 287

Perelson, A. S., Neumann, A. U., Markowitz, M., Leonard, J. M. & Ho, D. D. 1996, HIV-1 Dynamics in Vivo : Virion Clearance Rate, Infected Cell Life-Span, and Viral Generation Time, *Science*, vol.271, p.0–15. 37

Petney, T. N. & Andrews, R. H. 1998, Multiparasite communities in animals and humans : frequency, structure and pathogenic significance, *International Journal for Parasitology*, vol.28, n° 3, p.377–393. 83, 120, 175, 230, 244

Pigliucci, M. 2008, Is evolvability evolvable ?, *Nature Reviews Genetics*, vol.9, n° 1, p.75–82. 29

van der Plank, J. 1963, Plant diseases : epidemics and control., *Plant diseases : epidemics and control*. 28, 84, 120

Pollitt, E. J., West, S. A., Crusz, S. A., Burton-Chellew, M. N. & Diggle, S. P. 2014, Cooperation, quorum sensing, and evolution of virulence in Staphylococcus aureus, *Infection and Immunity*, vol.82, n° 3, p.1045–1051. 40, 84, 88, 93, 244, 307

Poulin, R. & Combes, C. 1999, The concept of virulence : interpretations and implications, *Parasitology Today*, vol.15, n° 12, p.474–475. 36

Power, R. A., Parkhill, J. & de Oliveira, T. 2017, Microbial genome-wide association studies : lessons from human GWAS, *Nat Rev Genet*, vol.18, n° 1, p.41–50. 62

Pradeu, T. & Carosella, E. D. 2006, The self model and the conception of biological identity in immunology, *Biology and Philosophy*, vol.21, n° 2, p.235–252. 26

Prangishvili, D., Forterre, P. & Garrett, R. A. 2006, Viruses of the Archaea : a unifying view, *Nature Reviews Microbiology*, vol.4, n° 11, p.837–848. 307

Prescott, J., Bushmaker, T., Fischer, R., Miazgowicz, K., Judson, S. & Munster, V. J. 2015, Postmortem stability of Ebola virus, *Emerg Infect Dis*, vol.21, n° 5, p.856–9. 51, 52

Price, G. R. *et al.*. 1970, Selection and covariance., *Nature*, vol.227, p.520–521. 41

Price, P. W. 1980, *Evolutionary biology of parasites*, vol.15, Princeton University Press. 26, 36

Pugliese, A. 2002, On the evolutionary coexistence of parasite strains, *Mathematical Biosciences*, vol.177, p.355–375. 191

Pullan, R. & Brooker, S. 2008, The health impact of polyparasitism in humans : are we underestimating the burden of parasitic diseases ?, *Parasitology*, vol.135, n° 07, p.783–794. 84

R Core Team. 2013, *R : A Language and Environment for Statistical Computing*, R Foundation for Statistical Computing, Vienna, Austria. 11, 134

Råberg, L., de Roode, J. C., Bell, A. S., Stamou, P., Gray, D. & Read, A. F. 2006, The role of immune-mediated apparent competition in genetically diverse malaria infections, *The American Naturalist*, vol.168, n° 1, p.41–53. 86

Radomyos, P., Radomyos, B. & Tungtrongchitr, A. 1994, Multi-infection with helminths in adults from northeast Thailand as determined by post-treatment fecal examination of adult worms., *Tropical medicine and parasitology : official organ of Deutsche Tropenmedizinische Gesellschaft and of Deutsche Gesellschaft fur Technische Zusammenarbeit (GTZ)*, vol.45, n° 2, p.133–135. 84, 120

Rahme, L. G., Stevens, E. J., Wolfort, S. F., Shao, J. *et al.*. 1995, Common virulence factors for bacterial pathogenicity in plants and animals, *Science*, vol. 268, n° 5219, p. 1899. 36, 37

Raso, G., Luginbühl, A., Adjoua, C. A., Tian-Bi, N. T., Silué, K. D., Matthys, B., Vounatsou, P., Wang, Y., Dumas, M.-E., Holmes, E. *et al.*. 2004, Multiple parasite infections and their relationship to self-reported morbidity in a community of rural Côte d'Ivoire, *International Journal of Epidemiology*, vol. 33, n° 5, p. 1092–1102. 175

Ratcliff, F., Harrison, B. D. & Baulcombe, D. C. 1997, A similarity between viral defense and gene silencing in plants, *Science*, vol. 276, n° 5318, p. 1558–1560. 87

Ratcliff, F. G., MacFarlane, S. A. & Baulcombe, D. C. 1999, Gene silencing without DNA : RNA-mediated cross-protection between viruses, *The Plant Cell*, vol. 11, n° 7, p. 1207–1215. 138

Rath, C. M. & Dorrestein, P. C. 2012, The bacterial chemical repertoire mediates metabolic exchange within gut microbiomes, *Current Opinion in Microbiology*, vol. 15, n° 2, p. 147–154. 102

Ravigné, V. & Blanquart, F. 2017, A new hypothesis to explain Ebola's high virulence, *Peer Community in Evolutionary Biology*, p. 100 022. 11, 48

Read, A. F. 1994, The evolution of virulence, *Trends in Microbioly*, vol. 2, n° 3, p. 73–76. 36, 137

Read, A. F. & Taylor, L. H. 2001, The ecology of genetically diverse infections, *Science*, vol. 292, n° 5519, p. 1099–1102. 84, 120, 233, 244, 307

Reddy, M. N., Dungdung, R., Valliyott, L. & Pilankatta, R. 2017, Occurrence of concurrent infections with multiple serotypes of dengue viruses during 2013–2015 in northern Kerala, India, *PeerJ*, vol. 5, p. e2970. 84

Restif, O. 2009, Evolutionary epidemiology 20 years on : challenges and prospects, *Infection, Genetics and Evolution*, vol. 9, n° 1, p. 108–123. 38

Rigaud, T., Perrot-Minnot, M.-J. & Brown, M. J. 2010, Parasite and host assemblages : embracing the reality will improve our knowledge of parasite transmission and virulence, *Proceedings of the Royal Society B : Biological Sciences*, vol. 277, n° 1701, p. 3693–3702. 84, 120, 121, 230, 307

Riley, M. A. & Chavan, M. A. 2007, *Bacteriocins*, Springer-Verlag Berlin Heidelberg. 85, 101, 127, 128, 233

Riley, M. A. & Gordon, D. M. 1999, The ecological role of bacteriocins in bacterial competition, *Trends in Microbiology*, vol. 7, n° 3, p. 129–133. 88

Riley, M. A. & Wertz, J. E. 2002, Bacteriocins : evolution, ecology, and application, *Annual Reviews in Microbiology*, vol. 56, n° 1, p. 117–137. 84, 127, 175, 177

Roberts, M. 2007, The pluses and minuses of R0, *Journal of the Royal Society Interface*, vol. 4, n° 16, p. 949–961. 33, 188, 221

Roberts, M. & Heesterbeek, J. 2003, A new method for estimating the effort required to control an infectious disease, *Proceedings of the Royal Society B : Biological Sciences*, vol. 270, n° 1522, p. 1359–1364. 33

Ronce, O. 2007, How does it feel to be like a rolling stone ? Ten questions about dispersal evolution, *Annual Review of Ecology, Evolution, and Systematics*, vol. 38, p. 231–253. 87

de Roode, J. C., Culleton, R., Cheesman, S. J., Carter, R. & Read, A. F. 2004, Host heterogeneity is a determinant of competitive exclusion or coexistence in genetically diverse malaria infections, *Proceedings of the Royal Society B : Biological Sciences*, vol. 271, n° 1543, p. 1073–1080. 138

DE ROODE, J. C., HELINSKI, M. E., ANWAR, M. A. & READ, A. F. 2005a, Dynamics of multiple infection and within-host competition in genetically diverse malaria infections, *The American Naturalist*, vol.166, n° 5, p.531–542. 87, 138, 175

DE ROODE, J. C., PANSINI, R., CHEESMAN, S. J., HELINSKI, M. E., HUIJBEN, S., WARGO, A. R., BELL, A. S., CHAN, B. H., WALLIKER, D. & READ, A. F. 2005b, Virulence and competitive ability in genetically diverse malaria infections, *Proceedings of the National Academy of Sciences of the United States of America*, vol.102, n° 21, p.7624–7628. 36, 40, 88, 89, 93, 230, 244

DE ROODE, J. C., YATES, A. J. & ALTIZER, S. 2008, Virulence-transmission trade-offs and population divergence in virulence in a naturally occurring butterfly parasite, *Proceedings of the National Academy of Sciences of the United States of America*, vol.105, n° 21, p.7489–7494. 39, 93, 193, 235, 292

ROOSSINCK, M. J. 2012, Plant virus metagenomics : biodiversity and ecology, *Annual Review of Genetics*, vol.46, p.359–369. 84, 137

ROSS, R. 1911, *The prevention of malaria*, John Murray ; London. 31

ROUSSARIE, R. & ROUX, J. 2014, *Des équations différentielles aux systèmes dynamiques*, EDP Sciences. 34

RYNKIEWICZ, E. C., BROWN, J., TUFTS, D. M., HUANG, C.-I., KAMPEN, H., BENT, S. J., FISH, D. & DIUK-WASSER, M. A. 2017, Closely-related Borrelia burgdorferi (sensu stricto) strains exhibit similar fitness in single infections and asymmetric competition in multiple infections, *Parasites & Vectors*, vol.10, n° 1, p.64. 87

SAEED, M., ZAFAR, Y., RANDLES, J. W. & REZAIAN, M. A. 2007, A monopartite begomovirus-associated DNA β satellite substitutes for the DNA B of a bipartite begomovirus to permit systemic infection, *Journal of General Virology*, vol.88, n° 10, p.2881–2889. 121, 136

SALAZAR-GONZALEZ, J. F., SALAZAR, M. G., KEELE, B. F., LEARN, G. H., GIORGI, E. E., LI, H., DECKER, J. M., WANG, S., BAALWA, J., KRAUS, M. H. *et al.*. 2009, Genetic identity, biological phenotype, and evolutionary pathways of transmitted/founder viruses in acute and early HIV-1 infection, *Journal of Experimental Medicine*, vol.206, n° 6, p.1273–1289. 171

SANZ, A. I., FRAILE, A., GARCIA-ARENAL, F., ZHOU, X., ROBINSON, D. J., KHALID, S., BUTT, T. & HARRISON, B. D. 2000, Multiple infection, recombination and genome relationships among begomovirus isolates found in cotton and other plants in Pakistan, *Journal of General Virology*, vol.81, n° 7, p.1839–1849. 84

SCHALL, J. J. 1992, Parasite-mediated competition in Anolis lizards, *Oecologia*, vol. 92, n° 1, p. 58–64. 26

SCHMID HEMPEL, P. 2011, *Evolutionary parasitology : the integrated study of infections, immunology, ecology, and genetics*, 574.5249 S2, Oxford University Press. 27, 37, 39

SCHMID-HEMPEL, P. & FRANK, S. A. 2007, Pathogenesis, virulence, and infective dose, *PLOS Pathogensens*, vol.3, n° 10, p.e147. 171, 287

SCHUFFENECKER, I., ITEMAN, I., MICHAULT, A., MURRI, S., FRANGEUL, L., VANEY, M.-C., LAVENIR, R., PARDIGON, N., REYNES, J.-M., PETTINELLI, F. *et al.*. 2006, Genome microevolution of chikungunya viruses causing the Indian Ocean outbreak, *PLOS Medicine*, vol.3, n° 7, p.e263. 312

SEABLOOM, E. W., BORER, E. T., GROSS, K., KENDIG, A. E., LACROIX, C., MITCHELL, C. E., MORDECAI, E. A. & POWER, A. G. 2015, The community ecology of pathogens : coinfection, coexistence and community composition, *Ecology Letters*, vol.18, n° 4, p.401–415. 312

Seilacher, A. 1970, Arbeitskonzept zur Konstruktions-Morphologie, *Lethaia*, vol. 3, n° 4, p. 393–396. 38

Sender, R., Fuchs, S. & Milo, R. 2016, Revised estimates for the number of human and bacteria cells in the body, *PLOS Biology*, vol. 14, n° 8, p. e1002 533. 311

Servedio, M. R., Brandvain, Y., Dhole, S., Fitzpatrick, C. L., Goldberg, E. E., Stern, C. A., Van Cleve, J. & Yeh, D. J. 2014, Not just a theory—the utility of mathematical models in evolutionary biology, *PLOS Biology*, vol. 12, n° 12, p. e1002 017. 30

Shaner, G., Stromberg, E. L., Lacy, G. H., Barker, K. R. & Pirone, T. P. 1992, Nomenclature and concepts of pathogenicity and virulence, *Annual Review of Phytopathology*, vol. 30, n° 1, p. 47–66. 36

Sharma, S., Mohan, A. & Kadhiravan, T. 2005, HIV-TB co-infection : epidemiology, diagnosis & management, *Indian Journal of Medical Research*, vol. 121, n° 4, p. 550. 83

Sheward, D. J., Ntale, R., Garrett, N. J., Woodman, Z. L., Karim, S. S. A. & Williamson, C. 2015, HIV-1 superinfection resembles primary infection, *Journal of Infectious Diseases*, p. jiv136. 120, 121

Shou, W., Bergstrom, C. T., Chakraborty, A. K. & Skinner, F. K. 2015, Theory, models and biology, *eLife*, vol. 4, p. e07 158. 30

Sicard, A., Michalakis, Y., Gutiérrez, S. & Blanc, S. 2016, The Strange Lifestyle of Multipartite Viruses, *PLOS Pathogens*, vol. 12, n° 11, p. e1005 819. 27

Silver, L. L. 2011, Challenges of antibacterial discovery, *Clinical Microbiology Reviews*, vol. 24, n° 1, p. 71–109. 28

Simonyi, E. & Kaszás, M. 1968, Method for the dynamic analysis of nonlinear systems, *Chemical Engineering*, vol. 12, n° 4, p. 314–324. 34, 105, 154

Skaar, E. P. 2010, The battle for iron between bacterial pathogens and their vertebrate hosts, *PLOS Pathogens*, vol. 6, n° 8, p. e1000 949. 101, 233

Sélosse, M.-A. & Gouyon, P.-H. 2011, Les mots de la biologie sont-ils bien choisis ?, *Pour la Science*, vol. 399, p. 14–15. 36

Smith, R. L. & Smith, T. M. 2012, *Elements of Ecology*, 8e éd., Pearson Education. 86

Smith, T. 1887, Parasitic bacteria and their relation to saprophytes, *The American Naturalist*, vol. 21, n° 1, p. 1–9. 37, 230

Smith, T. 1904, Some problems in the life history of pathogenic microorganisms, *Science*, p. 817–832. 302

Sobarzo, A., Ochayon, D. E., Lutwama, J. J., Balinandi, S., Guttman, O., Marks, R. S., Kuehne, A. I., Dye, J. M., Yavelsky, V., Lewis, E. C. *et al.*. 2013, Persistent immune responses after Ebola virus infection, *The New England Journal of Medicine*, vol. 369, n° 5, p. 492–493. 50

Soetaert, K., Petzoldt, T. & Setzer, R. W. 2010, Solving Differential Equations in R : Package deSolve, *Journal of Statistical Software*, vol. 33, n° 9, p. 1–25. 134

Sofonea, M. T., Aldakak, L., Boullosa, L. F. & Alizon, S. 2017a, Can Ebola Virus evolve to be less virulent in humans ?, *bioRxiv*, p. 108 589. 11

Sofonea, M. T., Alizon, S. & Michalakis, Y. 2015, From within-host interactions to epidemiological competition : a general model for multiple infections, *Philosophical Transactions of the Royal Society B : Biological Sciences*, vol.370, n° 1675. 11, 127, 128, 135, 141, 145, 230, 231, 236, 244, 291, 292, 305

Sofonea, M. T., Alizon, S. & Michalakis, Y. 2017b, Exposing the diversity of multiple infection patterns, *Journal of Theoretical Biology*, vol.419, p.278 – 289. 11, 230, 231, 233, 235, 244, 250, 253, 254, 256, 286, 291

Spellberg, B. & Taylor-Blake, B. 2013, On the exoneration of Dr. William H. Stewart : debunking an urban legend, *Infectious Diseases of Poverty*, vol.2, n° 1, p.3. 28

Spicknall, I. H., Foxman, B., Marrs, C. F. & Eisenberg, J. N. 2013, A modeling framework for the evolution and spread of antibiotic resistance : literature review and model categorization, *American Journal of Epidemiology*, vol.178, n° 4, p.508–520. 168

Staubach, F., Baines, J. F., Künzel, S., Bik, E. M. & Petrov, D. A. 2013, Host species and environmental effects on bacterial communities associated with Drosophila in the laboratory and in the natural environment, *PLOS ONE*, vol.8, n° 8, p.e70 749. 311

Stoica, P. & Söderström, T. 1982, On the parsimony principle, *International Journal of Control*, vol.36, n° 3, p.409–418. 29

Suttle, C. A. 2007, Marine viruses—major players in the global ecosystem, *Nature Reviews Microbiology*, vol.5, n° 10, p.801–812. 27

Svennungsen, T. O. & Kisdi, E. 2009, Evolutionary branching of virulence in a single infection model, *Journal of Theoretical Biology*, vol.257, p.408–418. 61

Sy, V. E., Agnew, P., Sidobre, C. & Michalakis, Y. 2014, Reduced survival and reproductive success generates selection pressure for the dengue mosquito Aedes aegypti to evolve resistance against infection by the microsporidian parasite Vavraia culicis, *Evolutionary Applications*, vol.7, n° 4, p.468–479. 235, 292

Syller, J. & Grupa, A. 2015, Antagonistic within-host interactions between plant viruses : molecular basis and impact on viral and host fitness, *Molecular Plant Pathology*. 121, 138

Syverton, J. T. & Berry, G. P. 1947, Multiple virus infection of single host cells, *The Journal of Experimental Medicine*, vol.86, n° 2, p.145–152. 83, 120

Takeuchi, Y. 1996, *Global dynamical properties of Lotka-Volterra systems*, World Scientific. 99, 107, 204, 207

Taylor, L. H., Latham, S. M. & Mark, E. 2001, Risk factors for human disease emergence, *Philosophical Transactions of the Royal Society B : Biological Sciences*, vol.356, n° 1411, p.983–989. 26, 83

Taylor, P. D. 1989, Evolutionary stability in one-parameter models under weak selection, *Theoretical Population Biology*, vol.36, n° 2, p.125–143. 42, 238

Thomas, F., Lefèvre, T. & Raymond, M. 2016, *Biologie évolutive*, 2e éd., De Boeck. 25

Thomas, F., Poulin, R., Guégan, J.-F., Michalakis, Y. & Renaud, F. 2000, Are there pros as well as cons to being parasitized ?, *Parasitology Today*, vol.16, n° 12, p.533–536. 26, 36

Thomas, F., Renaud, F. & Guégan, J.-F. 2005, *Parasitism and ecosystems*, Oxford University Press. 26, 307

THORSON, A., FORMENTY, P., LOFTHOUSE, C. & BROUTET, N. 2016, Systematic review of the literature on viral persistence and sexual transmission from recovered Ebola survivors : evidence and recommendations, *BMJ Open*, vol. 6, n° 1, p. e008 859. 49

TILMAN, D. 1982, *Resource Competition and Community Structure*, Princeton University Press. 87, 302

TIMONEY, J. F., GILLESPIE, J. H., SCOTT, F. W., BARLOUGH, J. E. *et al.*. 1988, *Hagan and Bruner's microbiology and infectious diseases of domestic animals.*, Ed. 8, Cornell University Press. 28

TOWNER, J. S., ROLLIN, P. E., BAUSCH, D. G., SANCHEZ, A., CRARY, S. M., VINCENT, M., LEE, W. F., SPIROPOULOU, C. F., KSIAZEK, T. G., LUKWIYA, M. *et al.*. 2004, Rapid diagnosis of Ebola hemorrhagic fever by reverse transcription-PCR in an outbreak setting and assessment of patient viral load as a predictor of outcome, *Journal of Virology*, vol. 78, n° 8, p. 4330–4341. 53, 62

TSOPELAS, P., SANTINI, A., WINGFIELD, M. J. & WILHELM DE BEER, Z. 2017, Canker stain : a lethal disease destroying iconic plane trees, *Plant Disease*, vol. 101, n° 5, p. 645–658. 28

TURNER, P. E. & CHAO, L. 1998, Sex and the evolution of intrahost competition in RNA virus φ6, *Genetics*, vol. 150, n° 2, p. 523–532.

TURNER, P. E. & CHAO, L. 1999, Prisoner's dilemma in an RNA virus, *Nature*, vol. 398, n° 6726, p. 441–443. 88, 89, 244

URBANOWICZ, R. A., MCCLURE, C. P., SAKUNTABHAI, A., SALL, A. A., KOBINGER, G., MÜLLER, M. A., HOLMES, E. C., REY, F. A., SIMON-LORIERE, E. & BALL, J. K. 2016, Human adaptation of Ebola virus during the West African outbreak, *Cell*, vol. 167, n° 4, p. 1079–1087. 49, 63

UYEKI, T. M., MEHTA, A. K., DAVEY JR, R. T., LIDDELL, A. M., WOLF, T., VETTER, P., SCHMIEDEL, S., GRÜNEWALD, T., JACOBS, M., ARRIBAS, J. R. *et al.*. 2016, Clinical management of Ebola virus disease in the United States and Europe, *The New England Journal of Medicine*, vol. 374, n° 7, p. 636–646. 49, 52

VAN VALEN, L. 1973, A new evolutionary law, *Evolutionary Theory*, vol. 1, p. 1–30. 310

VERHULST, P.-F. 1838, Notice sur la loi que la population suit dans son accroissement, *Correspondance Mathématique et Physique Publiée par A. Quetelet*, vol. 10, p. 113–121. 177, 192, 291

VERMA, M. 2015, Multiple Infections and Cancer : Etiology, Mechanisms and Implications in Cancer Control, dans *Infection and Cancer : Bi-Directorial Interactions*, édité par M. R. Shurin, Y. Thanavala & N. Ismail, Springer International Publishing Switzerland, p. 133–150. 84, 120

VIRGIN, H. W., WHERRY, E. J. & AHMED, R. 2009, Redefining chronic viral infection, *Cell*, vol. 138, n° 1, p. 30–50. 26

VOIT, E. O., MARTENS, H. A. & OMHOLT, S. W. 2015, 150 years of the mass action law, *PLOS Computational Biology*, vol. 11, n° 1, p. e1004 012. 31

VOLTERRA, V. 1928, Variations and fluctuations of the number of individuals in animal species living together, *Journal du Conseil Permanent Internation pour l'Exploration de la Mer*, vol. 3, n° 1, p. 3–51. 99, 101, 127, 192, 233

WAAGE, P. & GULDBERG, C. M. 1986, Studies concerning affinity, *J Chem Educ*, vol. 63, n° 12, p. 1044. 101

WALTER, W. 1998, *Ordinary Differential Equations*, Graduate Texts in Mathematics, Springer New York. 34

WALTHER, B. A. & EWALD, P. W. 2004, Pathogen survival in the external environment and the evolution of virulence, *Biological Reviews*, vol.79, n° 4, p.849–869. 89

WANDERSMAN, C. & DELEPELAIRE, P. 2004, Bacterial iron sources : from siderophores to hemophores, *Annual Review of Microbiology*, vol.58, p.611–647. 85, 101, 127

WEIGLE, J. & DELBRÜCK, M. 1951, Mutual exclusion between an infecting phage and a carried phage, *Journal of Bacteriology*, vol.62, n° 3, p.301. 120

WEITZ, J. S. & DUSHOFF, J. 2015, Modeling post-death transmission of Ebola : challenges for inference and opportunities for control, *Scientific Reports*, vol.5. 49, 50, 52, 53

WEST, S. A. & BUCKLING, A. 2003, Cooperation, virulence and siderophore production in bacterial parasites, *Proceedings of the Royal Society B : Biological Sciences*, vol.270, n° 1510, p.37–44. 88, 92, 175, 192, 230, 233, 245

WEST, S. A., GRIFFIN, A. S. & GARDNER, A. 2007, Social semantics : altruism, cooperation, mutualism, strong reciprocity and group selection, *Journal of Evolutionary Biology*, vol.20, n° 2, p.415–432. 86, 122

WEST, S. A., GRIFFIN, A. S., GARDNER, A. & DIGGLE, S. P. 2006, Social evolution theory for microorganisms, *Nature Reviews Microbiology*, vol.4, n° 8, p.597–607. 86

WHO. 2015, *World health Statistics 2015*, World Health Organization. 28

WHO. 2016a, *Ebola situation report - 30 March 2016*, Wolrd Health Organization. 45, 51

WHO. 2016b, *Ebola virus disease*, Wolrd Health Organization. 45

WHO. 2016c, *Poliomyelitis fact sheet*, Wolrd Health Organization. 28

WHO. 2016d, *Vector-borne diseases*, Wolrd Health Organization. 27

WHO EBOLA RESPONSE TEAM. 2014, Ebola virus disease in West Africa–the first 9 months of the epidemic and forward projections, *The New England Journal of Medicine*, vol.371, n° 16, p. 1481–95. 50, 52, 53, 61, 75

WHO EBOLA RESPONSE TEAM. 2015, West African Ebola epidemic after one year – slowing but not yet under control, *The New England Journal of Medicine*, vol.2015, n° 372, p.584–587. 45, 61

WIGGINS, S. 2003, *Introduction to applied nonlinear dynamical systems and chaos*, vol. 2, Springer-Verlag New York. 31, 34, 204, 205, 250

WILLEY, J. 2008, *Prescott, Harley, and Klein's Microbiology-7th international ed./Joanne M. Willey, Linda M. Sherwood, Christopher J. Woolverton*, McGraw-Hill Higher Education. 25, 120

WILSON, D. S. 1992, Complex interactions in metacommunities, with implications for biodiversity and higher levels of selection, *Ecology*, p.1984–2000. 312

WILSON, K. H. & PERINI, F. 1988, Role of competition for nutrients in suppression of Clostridium difficile by the colonic microflora., *Infection and Immunity*, vol.56, n° 10, p.2610–2614. 85

WINDSOR, D. A. 1998, Controversies in parasitology, Most of the species on Earth are parasites, *International Journal for Parasitology*, vol.28, n° 12, p.1939 – 1941. 26

Wolf, M., Van Doorn, G. S., Leimar, O. & Weissing, F. J. 2007, Life-history trade-offs favour the evolution of animal personalities, *Nature*, vol.447, n° 7144, p.581–584. 238

Wolfe, N. D., Dunavan, C. P. & Diamond, J. 2007, Origins of major human infectious diseases, *Nature*, vol.447, n° 7142, p.279–283. 45

Wolfram Research Inc. 2014, Mathematica, Version 10, Champaign, IL, 2014. 11

Wood, S. N. & Thomas, M. B. 1999, Super–sensitivity to structure in biological models, *Proceedings of the Royal Society B : Biological Sciences*, vol.266, n° 1419, p.565–570. 236

Wylie, K. M., Mihindukulasuriya, K. A., Zhou, Y., Sodergren, E., Storch, G. A. & Weinstock, G. M. 2014, Metagenomic analysis of double-stranded DNA viruses in healthy adults, *BMC Biology*, vol.12, n° 1, p.71. 83

Ybañez, A. P., Ybañez, R. H. D., Yokoyama, N. & Inokuma, H. 2016, Multiple infections of Anaplasma platys variants in Philippine dogs, *Veterinary World*, vol.9, n° 12, p.1456–1460. 84

Zeeman, M. L. 1993, Hopf bifurcations in competitive three-dimensional Lotka–Volterra systems, *Dynamics and Stability of Systems*, vol.8, n° 3, p.189–216. 107, 110

Évolution de la virulence et infections multiples

Mircea T. SOFONEA

Au sein des populations naturelles d'êtres vivants circulent une diversité de parasites, qu'il s'agisse de plusieurs espèces, souches ou plus généralement types. Si certains modèles d'épidémiologie évolutive intègrent déjà le polymorphisme des parasites, rares sont ceux pour lesquels la dynamique épidémiologique dépend de la croissance intra-hôte et des interactions que les parasites entretiennent lorsqu'ils infectent le même hôte. Les complexité combinatoire et dynamique explique pourquoi il n'y a pour l'heure pas de prédiction générale de l'évolution de la virulence dans de tels contextes d'infections multiples. À la recherche d'une tendance générale d'évolution de la virulence, nous modélisons chaque niveau de dynamique sur lequel l'évolution des parasites repose. En particulier, nous étudions explicitement les interactions et l'issue de la compétition au sein des hôtes, les dynamiques épidémiologique et enfin adaptative. Sur l'exemple des infections chroniques causées par des micro-parasites transmis horizontalement, nous employons les approches propres aux systèmes dynamiques et aux probabilités pour emboîter cette suite de dynamiques afin d'en explorer les conséquences évolutives. Nous introduisons notamment le concept de patron d'infection, à savoir l'ensemble des issues intra-hôte associées à chaque configuration d'inoculation et décrivons cinq patrons jusqu'ici non décrits, lesquels échappent à la dichotomie classique entre super- et coinfection. Cette typologie nous permet par la suite d'envisager l'évolution de la virulence dans un cadre général. Nous observons en particulier une inéluctable mais bornée croissance évolutive de la virulence.

Virulence evolution and multiple infections

Mircea T. SOFONEA

Natural populations of living beings are exposed to a diversity of parasites, be they several species, strains or more generally types. While some evolutionary epidemiology models already incorporate parasite polymorphism, few make the connection between between-host dynamics and within-host parasite growth. As parasite polymorphism can even occur within the same host, distinct parasite types can interact in various ways and thus interfere with their transmission and therefore their evolution. The combinatorial and dynamical complexity explains why we still lack general predictions regarding the evolution of virulence in such multiple infection contexts. Seeking for a general trend in virulence evolution, we model each dynamical level on which parasite evolution relies. In particular, we explicitly investigate the within-host interactions and competition outcomes, the epidemiological and adaptive dynamics. Focusing on chronic infections caused by horizontally-transmitted microparasites, we apply both dynamical systems and probabilistic approaches to this nested sequence of dynamics to explore the evolutionary outcomes. We notably define the concept of infection pattern, that is the set of within-host outcomes of all inoculation challenges and identify five yet undescribed patterns that escape from the classical super/coinfection dichotomy. This typology then allows us to address virulence evolution under a general framework. We in particular observe an unavoidable but bounded evolutionary increase in virulence.